Low-Dimensional Contact Geometry

Version Number 0.1, December 2025

John Etnyre

Bülent Tosun

Preface

Contact geometry in dimension 3 has seen rapid growth in the last 30 years, leading to a rich theory with applications to many areas, such as knot theory, the topology of 3 and 4-manifolds, Riemannian geometry, and fluid dynamics. There has also been recent progress in higher-dimensional contact geometry, but the foundations of the theory are still being developed. So except for a few remarks, in this book we will restrict ourselves to low-dimensional contact geometry.

Much of our understanding of low-dimensional contact geometry comes from the study of a special type of surface, called a convex surface. These grew out of Grioux's study of *convex contact structures*, which were originally defined by Eliashberg and Gromov in [**EG91**]. In [**Gir91**], Giroux defined convex surfaces and established many of their fundamental properties. The properties given in [**Gir91**] are what make convex surfaces such a powerful tool in the study of contact 3-manifolds. Another key tool that makes them such a useful tool is the notion of a *bypass*, which was defined by Honda in [**Hon00a**]. With the ideas in these two papers, one can classify contact structures on many simple manifolds, and in some sense, much of this book is an exploration of these two papers and their consequences.

The reason convex surfaces are so useful is that we can cut a contact manifold along convex surfaces until we obtain "simple pieces" (like a ball). We can then understand the contact structure on the simple pieces and try to reassemble the original contact manifold by gluing the simple pieces back together along the convex surfaces. If the surfaces are simple enough, then we can carry out the program to obtain classification results for contact structures on some manifolds and for special knots inside the contact manifolds. expain this more

The book is broken into two parts. In Part I, we restrict to the simplest uses of convex surfaces and bypasses, and also manifolds with the simplest topology. In Part II, we introduce more advanced topics about convex surfaces and bypasses, and also consider manifolds with more complicated topology.

Add details about the content of the book

In several chapters of the book, we adopt an idiosyncratic style. Specifically, certain sections will be broken into two parts, then will have an "executive summary of main results" and "proofs of main results" part. The idea is that the "executive summary of main results" subsection is meant to be a survey of the main results about the topic at hand. Proofs are (mostly) not presented in this subsection as they might detract from a clear picture of the main results and their corollaries, whereas the picture could be obfuscated if the results were interspersed among fairly long proofs. The proofs are then collected in the "proofs of main results" subsection. We hope this makes the presentation helpful as a research reference and as a learning reference.

Prerequisites

The reader is expected to have familiarity with the material in a one-semester course in differential topology and in algebraic topology. Specifically, in differential topology, the reader should not only be familiiar with smooth manifolds and smooth maps (including tangent bundles and local forms for functions with constant rank differentials), but also transversality, flows of vector fields, differential forms, the exterior and Lie derivatives, and de Rham cohomology. This material can be found in most books on differential topology, such as [**GP10**, **Lee13**]. In algebraic topology, the reader should be familiar with the fundamental group, covering spaces, homology, cohomology, and Poincaré duality. A good reference for this material is Chapters 0 through 3 in [**Hat22**].

It would also be helpful if the reader were familiar with locally trivial fiber bundles and characteristic classes, as can be found in [**FF16**, **MS74**]. However, to keep this book as self-contained as possible, we have added much of this material in Appendix A.

Acknowledgments

We thank Rima Chatterjee for useful comments on early drafts of the book. We are grateful to Austin Christian for many helpful comments on an early draft of the book, and in particular for pointing out the two lens spaces that cannot be distinguished using the number of tight contact structures they support as discussed at the end of Example 5.7.3. The first author was partially supported by National Science Foundation grant DMS-2203312 and the Georgia Institute of Technology's Elaine M. Hubbard Distinguished Faculty Award. The second author was supported in part by grants from the National Science Foundation (DMS-2105525 and CAREER DMS 2144363) and the Simons

Foundation (636841 and 2023 Simons Fellowship). He also acknowledges the support of the Charles Simonyi Endowment at the Institute for Advanced Study and Elmore Professorship of the Barefield College of Arts and Sciences at the University of Alabama.

Contents

Part I: Contact structures and convex surfaces

Chapter 1

Introduction to contact geometry in dimension 3

There are many good references for the basic facts about contact geometry, see for example [**Gei08**, **OS04a**]. So in this introduction, we will not try to exhaustively cover the basic results in contact geometry. However, we would like this book to be fairly self-contained, so we will review all the basic definitions and results necessary for the rest of this book. We will give proofs of results that will be used later in the book or give important intuition about the subject and otherwise refer to the existing resources.

In Section 1.1 we give a general discussion of plane fields on a 3-manifold and discuss when they can be tangent to surfaces in the manifold and when they are not, this leads to the definition of a contact structure that is a plane field that is "never tangent to surface along open sets". We then discuss many examples of contact structures. In the following section we discuss "local theorems". These are results that essentially say contact structures are completely determined locally in nice situations. For example, we will prove Darboux's theorem which says that any two contact structures look identical near a point. There are similar results for Legendrian knots (those tangent to the contact planes) and transverse knots (those that are transverse to the contact planes). In Section 1.3 we expand these "local results" to neighborhoods of surfaces in contact manifolds, but in this case, more data is needed to determine the contact structure in a neighborhood of the surface. This extra data is called the characteristic foliation, which is a singular foliation induced on a surface from the contact plane field.

In Section 1.4 we discuss Legendrian and transverse knots. These are fundamental objects in contact geometry and essential to understanding contact structures on manifolds. We will discuss their basic invariants, that is the Thurston-Bennequin invariant

and rotation number of Legendrian knots, and self-linking number for transverse knots, and then how to study them in the standard contact structure on $\mathbb{R}^3$ (and by Darboux's theorem this allows us to study such knots near a point in any contact manifold). We also discuss the Bennequin inequality which bounds the classical invariants of Legendrian and transverse knots, mentioned above, in terms of the Seifert genus of the knot. We then turn to the fact that any smooth knot can be approximated by a Legendrian knot and that we can associate to any Legendrian knot its "transverse push-off" and to any transverse knot many "Legendrian approximations". The section ends with a discussion about the classification of Legendrian knots which will be revisited later in the book.

Section 1.5 is devoted to the existence of contact structures on oriented 3-manifolds. We begin by showing that any oriented 3-manifold admits a contact structure. We then discuss the homotopy classes of oriented plane fields on a 3-manifold and then show that in each homotopy class, there is a contact structure. This means that each oriented 3-manifold admits an infinite number of distinct contact structures. We end the section with a discussion of invariants of oriented plane fields that determine their homotopy class.

In Section 1.6 we introduce a critical dichotomy in contact geometry, this is the tight versus overtwisted dichotomy. A contact structure on a 3-manifold is either overtwisted, which means it contains a special type of disk, or tight. We recall Eliashberg's classification of overtwisted contact structures which says that any homotopy class of plane field admits a unique overtwisted contact structure, we will detail the proof of this result in Chapter 14. We also revisit the Bennequin inequality which characterizes a contact structure as being tight. We then move on to symplectic fillings of a contact manifold and recall that a symplectic fillable contact structure is tight. A special type of symplectic filling is a Stein filling of a contact manifold. We discuss how to construct Stein fillings and use this construction to construct many tight contact structures on lens spaces (we will later show that this is a complete list of tight contact structures on lens spaces) and also show that there can be arbitrarily many tight contact structures in a fixed homotopy class of plane field. We then move on to a brief review of Heegaard Floer homology, which is an invariant of 3-manifolds and knots in them, and define an invariant of contact structures that live in Heegaard Floer homology. This invariant vanishes if the contact structure is overtwisted and so is a good way to prove a contact structure is tight. We also see how to recover the Bennequin inequality from Heegaard Floer theory.

Section 1.7 gives a brief overview of higher dimensional contact geometry. While we will not discuss much about higher dimensional contact manifolds in the book, this section will put the 3-dimensional results in a larger context and highlight differences between the theory in dimension 3 and higher. Specifically, we will discuss differences in the "local" theorems that determine a contact structure near certain submanifolds of

a contact manifold and how the general existence question is quite different in higher dimensions. We will also discuss the tight versus overtwisted dichotomy in higher dimensions as well as symplectic fillability, and see that while there are similarities with dimension 3, there are quite a few differences as well.

In the last section of this chapter, we will discuss the history and applications of contact geometry. We start by discussing some of the first occurrences of contact geometry in geometric optics, thermodynamics, classical mechanics, and partial differential equations. (These occurrences are really precursors to contact geometry. They did not explicitly use contact geometry at the time as contact structures had not been defined yet, but the ideas used are clearly contact geometric in hindsight.) We then move on to discuss a close connection between contact geometry and Riemannian geometry. Specifically, a Riemannian metric determines, and is determined by, the geodesic flow on the unit tangent bundle to a manifold. This flow is conjugate to the Reeb flow (a contact geometric flow) on the unit cotangent bundle (which is a contact manifold). We then discuss connections between contact geometry and fluid mechanics, showing, among other things, that any real analytic solution to the Euler equations for a perfect incompressible fluid on the 3-sphere possesses a close flow line. We then turn to the connection between Riemannian metrics and contact structures again and see how compatible metrics and contact structures can influence each other. We end with a discussion of numerous applications of contact geometry to low-dimensional topology.

1.1. Definitions and first examples

Let M be a closed, oriented 3-dimensional manifold. Contact structures on M are special types of plane fields, so we will begin by discussing plane fields. A *plane field* ξ on a M is a sub-bundle of the tangent bundle of M such that

$$\xi_p = T_pM \cap \xi$$

is a 2-dimensional subspace of T_pM for all $p \in M$. To better understand this idea, it is good to compare it to the more well-known concept of a vector field on a manifold. A vector field is simply a choice of vector in the tangent space of M at each point of M and the vector can change as we move to different points in M (of course we demand that it change in a smooth manner). A plane field is a similar concept, it is a choice of plane in the tangent space of M that changes as we move to different points in M.

Example 1.1.1. We consider several examples of plane fields.

(1) On the manifold $M = \mathbb{R}^3$ consider the plane field

$$\xi = \text{span}\left\{\frac{\partial}{\partial x}, \frac{\partial}{\partial y}\right\}.$$

This constant plane field is shown in Figure 1.1.1.

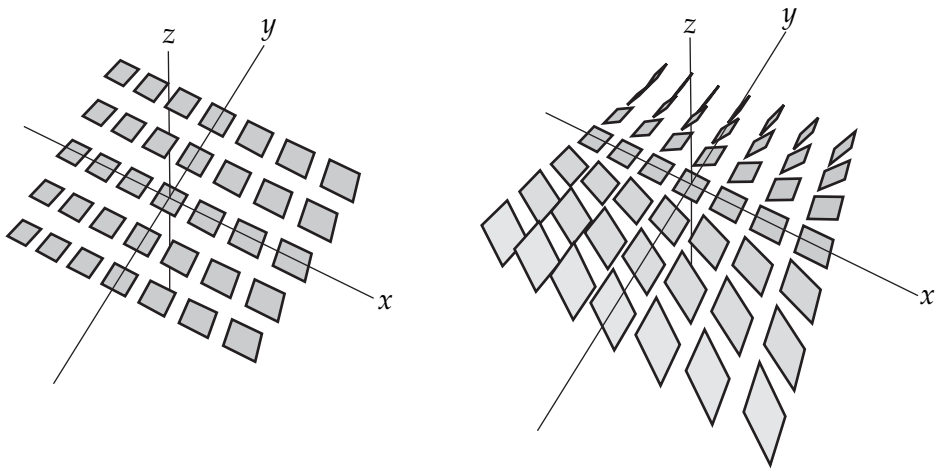

Figure 1.1.1. The plane field on the left is from Example (1) and the plane field on the right is from Example (3). need better pictures!

(2) Consider the manifold $M = \Sigma \times S^1$ where Σ is an orientable surface and the plane field

$$\xi_{(x,\theta)} = T_x\Sigma \subset T_{(x,\theta)}(\Sigma \times S^1).$$

(3) On the manifold $M = \mathbb{R}^3$ consider the plane field

$$\xi = \operatorname{span}\left\{\frac{\partial}{\partial y}, \frac{\partial}{\partial x} + y\frac{\partial}{\partial z}\right\}.$$

This is a non-constant plane field on $\mathbb{R}^3$ and is shown in Figure 1.1.1.

(4) Let α be a 1-form on M so for each $p \in M$ we have that

$$\alpha_p \colon T_pM \to \mathbb{R}$$

is a linear map. We say that α is *non-singular* if α_p is onto $\mathbb{R}$ for all $p \in M$. We will now assume that α is non-singular. In this case for each $p \in M$ we can define the plane

$$\xi_p = \ker \alpha_p$$

and let

$$\xi = \coprod_{p \in M} \xi_p.$$

This is a plane field on M and we write ξ as $\xi = \ker \alpha$. We note that all the previous examples can be described in terms of 1-forms.

(a) For example (1) if we set $\alpha = dz$ then $\xi = \ker \alpha$.
(b) For example (2) if we set $\alpha = d\theta$ then $\xi = \ker \alpha$.
(c) For example (3) if we set $\alpha = dz - y\,dx$ then $\xi = \ker \alpha$.

It is not a coincidence that our examples can be written as the kernel of a 1-form.

Exercise 1.1.2. Show that any plane field can be locally written as the kernel of a 1-form. Here what we mean by "locally written" is that given a plane field ξ on M, for each point $p \in M$ there is an open set U containing p and a 1-form α_U on U such that for each $q \in U$, $\xi_q = \ker \alpha_q$.

Exercise 1.1.3. Show that the following are equivalent:

(1) ξ can be written as the kernel of a 1-form on M

(2) there is a vector field v that is transverse to ξ at all points of M

(3) ξ is orientable.

Hint: Recall that we are assuming that M is orientable. Some of the implications are not true if M is not orientable.

When a plane field ξ has a transverse vector field as in the exercise, we say that the plane field is *transversely orientable* and by the exercise this is equivalent to being orientable.

Convention : We will assume that all of our plane fields are oriented.

It is interesting to consider non-orientable plane fields (and contact structures) but we will not be considering these in this book.

To continue our discussion of plane fields we need the following important theorem. Before stating the theorem we need a few definitions. Given an n-manifold M a *k-plane field*, also known as a *distribution of rank k*, is a subbundle D of the tangent bundle of M with k-dimensional fibers. An *integral submanifold* of D is the image of a one-to-one immersion $f : N \to M$ such that $df(T_xN) = D_{f(x)}$ for all $x \in N$. We say that D is *integrable* if each point $p \in M$ is contained in an integral submanifold of D. Finally, we say that D is *closed under Lie brackets*, this is also known as *involutive*, if given two sections v and w of D, their Lie bracket $[v, w]$ is also a section of D (recall D is a sub-bundle of TM so sections of D are vector fields and hence we can compute their Lie bracket). In other words, $\Gamma(D)$ is a Lie sub-algebra of $\Gamma(TM)$, where $\Gamma(E)$ denotes the space of sections of a bundle E. A smooth integrable plane field defines a *foliation* on a manifold. A foliation $\mathcal{F}$ on a manifold M is a decomposition of the manifold into a union of immersed surfaces such that each point in the manifold has a coordinate chart $\phi\colon U \to V$, where U is an open set in M and V is an open set in $\mathbb{R}^3$ so that the surfaces in the coordinate chart map to constant x_3-hyperplanes where (x_1, x_2, x_3) are coordinates on V. The image of each surface is called a *leaf* of the foliation. (This is actually the definition of a foliation of a 3-manifold by 2-manifolds, but there is a clear generalization for a foliation of an n-manifold by k-manifolds.)

Theorem 1.1.4 (Frobenius Theorem)**.** *Given an n-manifold M and a k-plane field D on M, then*

D is integrable if and only if D is closed under Lie brackets.

It is easy to prove that any integrable distribution is closed under Lie brackets, but the other implication is quite a bit more difficult to establish. You can find a proof of this result in most textbooks on Differential Topology, see for example [**Lee13**, Chapter 19].

Continuing our discussion of plane fields, let ξ be a plane field on the 3-manifolds M that is given as the kernel of a 1-form α. Suppose $v, w \in \Gamma(\xi)$, then clearly $\alpha(v) = 0$, $\alpha(w) = 0$ and $[v, w] \in \Gamma(\xi)$ if and only if $\alpha([v, w]) = 0$. We would like to rephrase this, and to do so we recall from Differential Topology, see [**Lee13**], the formula for the exterior derivative of a 1-form:

$$d\alpha(v, w) = v \cdot \alpha(w) - w \cdot \alpha(v) - \alpha([v, w]),$$

where $v \cdot f$ for a function f and vector field v is the result of applying v, thought of as a derivation on function on M, to f, which of course gives another function on M. Using this formula we see that for $v, w \in \Gamma(\xi)$

$$[v, w] \in \Gamma(\xi) \text{ if and only if } d\alpha(v, w) = 0.$$

Thus

$$\xi \text{ is integrable if and only if } d\alpha|_\xi = 0.$$

Definition 1.1.5. A plane field ξ on a 3-manifold M given as the kernel of a 1-form α is a *foliation* if $d\alpha|_\xi = 0$ and is a *contact structure* if $d\alpha|_\xi$ is never zero. A *contact manifold* is a pair (M, ξ) where M is a manifold and ξ is a contact structure on M.[1]

If $\xi = \ker \alpha$ is a contact structure, then we say that α is a *contact form* for ξ.

Considering our discussion around the Frobenius Theorem, it is easy to see that if ξ is a contact structure then it cannot be tangent to a surface along an open subset of the surface. It is common to define a contact structure on a 3-manifold as a non-integrable plane field.

Continuing to discuss the contact condition we note that $d\alpha|_\xi$ never being zero is equivalent to the fact that for any pair of vectors v, w that span ξ we have $d\alpha(v, w) \neq 0$. Now if we let u be a vector field transverse to ξ, then we clearly see that $\alpha(u)$ is never zero; and thus, for vector fields v and w (locally) spanning ξ

$$\alpha \wedge d\alpha(u, v, w) = \alpha(u) d\alpha(v, w) + \text{terms with } \alpha \text{ evaluated on } v \text{ or } w,$$

[1] It is common to denote the phrase "$d\alpha_\xi$ is never zero" by $d\alpha|_\xi \neq 0$. While this is technically not accurate, this is a common abuse of notation.

and the latter terms must be zero. So if ξ is a contact structure then $\alpha \wedge d\alpha$ is a never zero 3-form on M, that is it is a volume form on M. Thus we have

$$\xi = \ker \alpha \text{ is a contact structure if and only if } \alpha \wedge d\alpha \text{ is never zero.}$$

This is frequently given as the definition of a contact structure, but we see it follows from our geometric definition given above.

Example 1.1.6. We now consider our examples above in light of this discussion.

(1) On the manifold $M = \mathbb{R}^3$ we have the plane field

$$\xi = \operatorname{span}\left\{\frac{\partial}{\partial x}, \frac{\partial}{\partial y}\right\} = \ker \alpha$$

where $\alpha = dz$. Since $d\alpha = d(dz) = 0$ we see that ξ is integrable and defines a foliation. Indeed, $\mathbb{R}^3$ is filled by planes

$$\mathbb{R}^2 \times \{z\}$$

and these planes are tangent to ξ.

(2) On the manifold $M = \Sigma \times S^1$ we have the plane field ξ given as the kernel of $\alpha = d\theta$. Since $d\alpha = d(d\theta) = 0$ we see that ξ is also a foliation. We also see that ξ is tangent to the submanifolds

$$\Sigma \times \{\theta\}$$

and these manifolds fill M.

(3) On the manifold $M = \mathbb{R}^3$ we have the plane field

$$\xi = \operatorname{span}\left\{\frac{\partial}{\partial y}, \frac{\partial}{\partial x} + y\frac{\partial}{\partial z}\right\} = \ker \alpha$$

where $\alpha = dz - y\,dx$. One easily computes

$$\alpha \wedge d\alpha = dx \wedge dy \wedge dz$$

which is a volume form on $\mathbb{R}^3$ and hence ξ is a contact structure on $\mathbb{R}^3$.

Notice that a contact structure ξ can be defined by more than one contact form. Suppose that $\xi = \ker \alpha$ and $\xi = \ker \beta$.

Exercise 1.1.7. Show that there is a non-zero function $f : M \to \mathbb{R}$ such that $\alpha = f\beta$.
Hint: The two linear maps $\alpha_p, \beta_p : T_pM \to \mathbb{R}$ have the same kernel and T_pM is 3-dimensional.

Given a function f from the exercise notice that

$$\begin{aligned}\alpha \wedge d\alpha &= f\beta \wedge d(f\beta) = f\beta \wedge (df \wedge \beta + f\,d\beta)\\ &= -f\,\beta \wedge \beta + f^2\beta \wedge d\beta = f^2\beta \wedge d\beta.\end{aligned}$$

Thus *any* 1-form defining ξ will induce the same orientation on M (recall orientations on a manifold M correspond to equivalence classes of never zero 3-forms, where two such forms are equivalent if one is a positive functional multiple of the other). Recall that M was assumed to be oriented so there is some never zero 3-form Ω on M that defines this orientation. Since $\alpha \wedge d\alpha$ is never zero there is some non-zero function $g\colon M \to \mathbb{R}$ such that

$$\alpha \wedge d\alpha = g\Omega.$$

If $g > 0$ then we write

$$\alpha \wedge d\alpha > 0$$

and say that $\xi = \ker \alpha$ is a *positive contact structure*. If $g < 0$ then we write $\alpha \wedge d\alpha < 0$ and say that ξ is a *negative contact structure*.

Convention: We will assume that all of our contact structures are positive.

So the phrase “contact structure" means “positive contact structure". If we want to study negative contact structures, we will just consider the manifold with the opposite orientation where the contact structure will be positive.

Exercise 1.1.8. Consider a non-transversely oriented contact structure ξ on a 3-manifold M that might or might not be orientable. Recall this means that there is no global 1-form defining ξ, but it can locally be defined by 1-forms. Show that ξ still defines an orientation on M. So non-orientable 3-manifolds cannot admit contact structures.

There is another useful way to determine if a plane field is a contact structure or a foliation that we explore in the following exercises.

Exercise 1.1.9. Give a plane field ξ on a 3-manifold M show that near any point p in M there are coordinates so that ξ is the kernel of a 1-form of the form

$$\alpha = dz - a(x, y, z)\, dx.$$

Moreover, if v is any non-zero section of ξ near p show that the coordinates can be chosen so that v is $\frac{\partial}{\partial y}$.
Hint: Given v choose a disk D transverse to v. Put coordinates (y, z) on D and generate the coordinate system by the flow of v.

Exercise 1.1.10. Given ξ and α as in the previous exercise show that ξ is a positive (negative) contact structure if and only if

$$\frac{\partial a}{\partial y} > 0 \left(\frac{\partial a}{\partial y} < 0 \right).$$

Also show that ξ is a foliation if and only if

$$\frac{\partial a}{\partial y} = 0.$$

These exercises show that a plane field is a positive contact structure if and only if when flowing along a vector field tangent to the plane field the planes rotate in a left-handed fashion and the plane field is a foliation if and only if the plane field is invariant under the flow of any vector field tangent to the plane field.

We will now consider more examples of contact structures.

Example 1.1.11. For these examples we take $M = \mathbb{R}^3$.

(1) Let $\alpha_1 = dz - y\,dx$ and $\xi_1 = \ker \alpha_1$. It is common to call ξ_1 *the standard contact structure on* $\mathbb{R}^3$ and in the rest of the book we will denote it by ξ_{std}.

(2) Let $\alpha_2 = dz + x\,dy - y\,dx$, or in polar coordinates $\alpha_2 = dz + r^2\,d\theta$, and $\xi_2 = \ker \alpha_2$. See Figure 1.1.2. The contact structures ξ_1 and ξ_2 look quite different, but they are in some sense "the same".

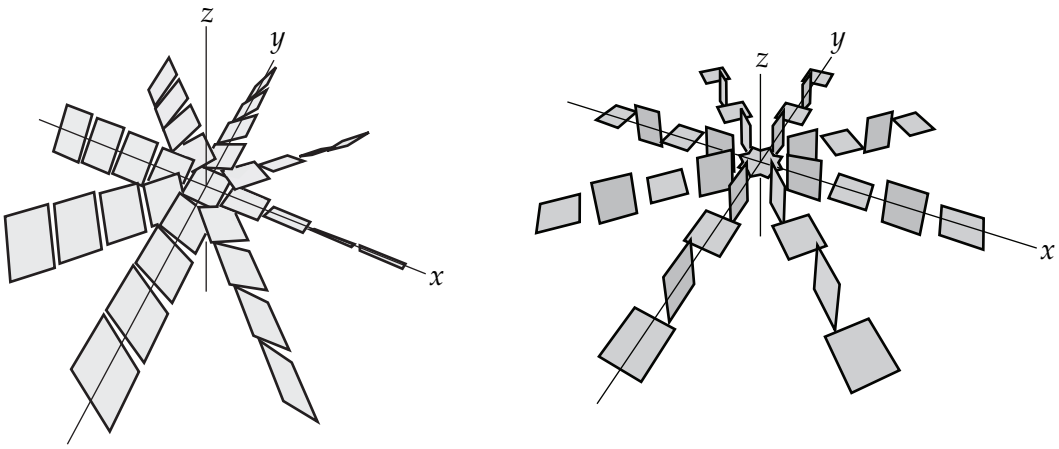

Figure 1.1.2. The plane field on the left is from Example (2) and the plane field on the right is from Example (3). need better pictures!

Definition 1.1.12. Two contact manifolds (M_0, ξ_0) and (M_1, ξ_1) are *contactomorphic* if there is a diffeomorphism $f\colon M_0 \to M_1$ such that $df(\xi_0) = \xi_1$. In terms of contact forms α_i for ξ_i, this condition is equivalent to $f^*\alpha_1 = g\alpha_0$ for some non-zero function $g\colon M_0 \to \mathbb{R}$.

Contactomorphism is the natural equivalence relation on contact manifolds. We can now check that ξ_1 and ξ_2 are contactomorphic. Indeed consider the map

$$f(x, y, z) = \left(\frac{x+y}{2}, \frac{y-x}{2}, z - \frac{xy}{2}\right).$$

Exercise 1.1.13. Show that $f\colon \mathbb{R}^3 \to \mathbb{R}^3$ is a diffeomorphism.

Notice that

$$\begin{aligned} f^*\alpha_2 &= d\left(z - \frac{xy}{2}\right) - \frac{y-x}{2} d\left(\frac{x+y}{2}\right) + \frac{x+y}{2} d\left(\frac{y-x}{2}\right) \\ &= dz - \frac{1}{2}(x\,dy + y\,dx) + \frac{1}{4}(x+y)(dy - dx) - \frac{1}{4}(y-x)(dy + dx) \\ &= dz - y\,dx = \alpha_1. \end{aligned}$$

Thus $df(\xi_1) = \xi_2$ and $(\mathbb{R}^3, \xi_1)$ is contactomorphic to $(\mathbb{R}^3, \xi_2)$.

(3) Let $\alpha_3 = \cos r\, dz + r \sin r\, d\theta$ and $\xi_3 = \ker \alpha_3$. See Figure 1.1.2.

Exercise 1.1.14. Check that ξ_3 is a contact structure.

Exercise 1.1.15. Let $U_a = \{(r, \theta, z) \in \mathbb{R}^3 : r < a\}$.

(a) Show that $(U_a, \xi_3|_{U_a})$ is contactomorphic to $(\mathbb{R}^3, \xi_2)$ for $a \leq \pi$.
Hint: Try to prove this for $a < \pi/2$ first as this is easier. It also might be helpful to read Section 1.3 on characteristic foliations below first.

(b) Show that $(U_a, \xi_3|_{U_a})$ is not contactomorphic to (R^3, ξ_2) for $a > \pi$.
Hint: This is very hard, maybe come back to this after reading Section 1.6.

(4) Let $\alpha_4 = sin(2\pi z)\, dx + \cos(2\pi z)\, dy$ and $\xi_4 = \ker \alpha_4$. See Figure 1.1.3.

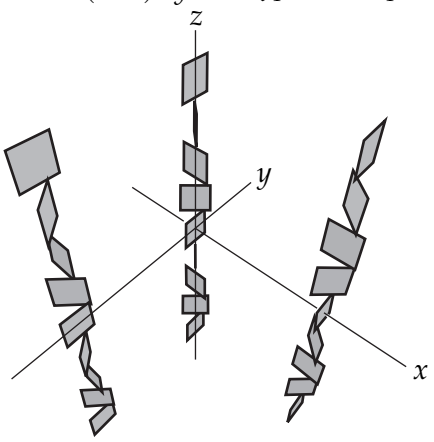

Figure 1.1.3. The plane field is from Example (4). need better pictures!

Exercise 1.1.16. Check that ξ_4 is a contact structure.

Exercise 1.1.17. Show that

$$f(x, y, z) = (z \sin x + y \cos x, z \cos x - y \sin x, x/2\pi)$$

is a contactomorphism from $(\mathbb{R}^3, \xi_1)$ is contactomorphic to $(\mathbb{R}^3, \xi_4)$.

Notice that ξ_3 twists infinitely often and is not contactomorphic to the standard contact structure on $\mathbb{R}^3$ while ξ_4 also twists infinitely often but is contactomorphic to the standard structure. We will see the reason for this in Section 1.6.

Example 1.1.18. In this example, we consider $M = S^3$ thought of as the unit sphere in complex 2-space, $\mathbb{C}^2$. Recall that for any linear space V, the tangent space T_pV can canonically be identified with V. Thus multiplication by i on $\mathbb{C}^2$ induces multiplication by i on all the tangent spaces $T_p\mathbb{C}^2$. We now set

$$\xi_p = T_pS^3 \cap i(T_pS^3)$$

for each $p \in S^3$, that is ξ is the set of complex tangencies to S^3.

We will see that ξ is a contact structure on S^3. To this end, let $(z_1 = x_1 + ix_2, z_2 = x_2 + iy_2)$ be coordinates on $\mathbb{C}^2$ and set

$$f\colon \mathbb{C}^2 \to \mathbb{R}\colon (x_1, y_1, x_2, y_2) \mapsto x_1^2 + y_1^2 + x_2^2 + y_2^2.$$

Clearly 1 is a regular value of f and $S^3 = f^{-1}(1)$. We know that

$$T_{(x_1,y_1,x_2,y_2)}S^3 = \ker df_{(x_1,y_1,x_2,y_2)} = \ker 2(x_1\,dx_1 + y_1\,dy_1 + x_2\,dx_2 + y_2\,dy_2).$$

So $v \in i(T_pS^3)$ if and only if $iv \in T_pS^3$ if and only if $df_p(iv) = 0$. To see what this last condition is we need to understand $df \circ i$. We note that

$$i\frac{\partial}{\partial x_j} = \frac{\partial}{\partial y_j} \text{ and } i\frac{\partial}{\partial y_j} = -\frac{\partial}{\partial x_j}$$

and thus

$$dx_j \circ i\left(\frac{\partial}{\partial x_j}\right) = 0 \text{ and } dx_j \circ i\left(\frac{\partial}{\partial y_j}\right) = -1.$$

Similar further computations lead to the fact that

$$dx_j \circ i = -dy_j \text{ and } dy_j \circ i = dx_j.$$

Thus we see that

$$df \circ i = 2(y_1\,dx_1 - x_1\,dy_1 + y_2\,dx_2 - x_2\,dy_2).$$

So if we set $\alpha = y_1\,dx_1 - x_1\,dy_1 + y_2\,dx_2 - x_2\,dy_2$ then $\alpha_{T^3_S}$ is a 1-form on S^3 defining ξ.

Now notice that

$$d\alpha = -2(dx_1 \wedge dy_1 + dx_2 \wedge dy_2)$$

and so

$$d\alpha \wedge d\alpha = 4\,dx_1 \wedge dy_1 \wedge dx_2 \wedge dy_2$$

which is the standard volume form on $\mathbb{C}^2$. Now let

$$X = \frac{1}{2}\left(x_1\frac{\partial}{\partial x_1} + y_1\frac{\partial}{\partial y_1} + x_2\frac{\partial}{\partial x_2} + y_2\frac{\partial}{\partial y_2}\right)$$

be the radial vector field and notice that it is transverse to S^3 (since $df(X) > 0$). One can now compute that

$$\iota_X d\alpha = \alpha,$$

where $\iota_X d\alpha$ is the contraction of X into the 2-form $d\alpha$, and hence

$$\iota_X(d\alpha \wedge d\alpha) = 2\,\alpha \wedge d\alpha.$$

Now if v_1, v_2, v_3 span the tangent space T_pS^3 then X, v_1, v_2, v_3 span $T_p\mathbb{C}^2$ and hence

$$0 \neq d\alpha \wedge d\alpha(X, v_1, v_2, v_3) = 2\,\alpha \wedge d\alpha(v_1, v_2, v_3),$$

which shows that $\alpha \wedge d\alpha$ is a volume form on S^3. Thus $\xi = \ker \alpha$ is a contact structure as claimed.

This contact structure is called the standard contact structure on S^3 and is usually denoted ξ_{std}. (Even though we use the same notation for the standard contact structure on $\mathbb{R}^3$, the meaning should be clear from the context.)

Exercise 1.1.19. Recall that S^3 is the join of S^1 with S^1. We can see this explicitly by considering the map

$$F\colon\ S^1 \times S^1 \times [0, \pi/2] \to S^3\colon\ (\theta, \phi, t) \mapsto (\cos t(\cos\theta, \sin\theta, 0, 0) + \sin t(0, 0, \cos\phi, \sin\phi)).$$

This is an embedding when restricted to $S^1 \times S^1 \times (0, \pi/2)$ and $S^1 \times S^1 \times \{0, \pi/2\}$ are collapsed to the Hopf link H in S^3. This shows S^3 is the join $S^1 * S^1$. Show the contact form for the standard contact structure on S^3 pulls back to $\cos^2 t\, d\theta + \sin^2 t\, d\phi$ on $T^2 \times (0, \pi/2)$. Notice that this says that on $S^3 - H = S^1 \times S^1 \times (0, \pi/2)$ the standard contact structure is tangent to the $(0, \pi/2)$ factor and the planes rotate from slope ∞ to 0 as one traverses the interval factor.

Exercise 1.1.20. Show that $(S^3 \setminus \{pt\}, \xi|_{S^3\setminus\{pt\}})$ is contactomorphic to $(\mathbb{R}^3, \xi_{std})$.
Hint: This can be challenging, see [**Gei08**] for the details.

The previous example is the first example of a contact structure on a closed 3-manifold. In Section 1.5 we will see that all closed oriented 3-manifolds admit contact structures. But for now, we note a few other simple examples on some closed 3-manifolds.

Exercise 1.1.21. Show that the 3-torus T^3 has a contact structure.
Hint: Recall, one can think of T^3 as $\mathbb{R}^3/\mathbb{Z}^3$, where the integer lattice in $\mathbb{R}^3$ acts by translation. Consider the contact structure ξ_4 above.

Exercise 1.1.22. Construct a contact structure on the lens space $L(p, q)$, where $L(p, q)$ is the manifold obtained from the unit sphere S^3 in $\mathbb{C}^2$ by quotienting out by the $\mathbb{Z}/p\mathbb{Z}$ action generated by $(z_1, z_2) \mapsto (e^{(2\pi i)/p} z_1, e^{(2q\pi i)/p} z_2)$.

We end this section by defining two notions that will be important throughout the book. A knot K in a contact manifold (M, ξ) is called *Legendrian* if it is always tangent to ξ. Legendrian knots are essential to the study of contact manifolds. We will see that we can use them to construct contact manifolds and distinguish contact manifolds. In

addition, they have a very rich and interesting structure. The second notion we need is that of a Reeb vector field.

Exercise 1.1.23. Suppose ω is a skew-symmetric pairing $\mathbb{R}^3 \times \mathbb{R}^3 \to \mathbb{R}$ that is non-zero on some two-dimensional subset of $\mathbb{R}^3$. Show there is a unique line L in $\mathbb{R}^3$ such that for any $v \in L$, $\omega(v, w) = 0$ for all $w \in \mathbb{R}^3$.

From this exercise we know that if α is a contact from defining ξ then there is a unique vector field R_α satisfying $\alpha(R_\alpha) = 1$ and $\iota_{R_\alpha} d\alpha = 0$. This vector field is called a *Reeb vector field* for ξ.

Exercise 1.1.24. Show that the flow of R_α preserves ξ and α. That is the flow gives a family of contactomorphisms of α.

The Reeb vector field is a fundamental object in contact geometry. It is used in many results (for example, see the next section) and its dynamics is extremely rich.

1.2. The local theory

In this section, we will see that contact structures are all "locally the same" in various ways. Most of our theorems will follow from the following result.

Theorem 1.2.1. *Let M be an oriented 3-manifold and N a compact subset of M. Suppose that ξ_0 and ξ_1 are contact structures on M and*

$$\xi_0|_N = \xi_1|_N.$$

Then there is a neighborhood U of N such that the identity map on M is isotopic, relative to N, to a map that is a contactomorphism when restricted to U.

We will prove this theorem later, but first, we examine some of its consequences. We also note that there are higher dimensional analogs of this theorem and its corollaries. We will briefly discuss those in Section 1.7.

Theorem 1.2.2 (Darboux 1882, **[Dar82]**)**.** *Let (M, ξ) be a contact 3-manifold. Every point p in M has a neighborhood U that is contactomorphic to a neighborhood of the origin in $(\mathbb{R}^3, \xi_{std})$.*

Darboux's theorem essentially says that all contact structures look the same near a point. So contact structures do not have interesting local structures (this should be compared with Riemannian geometry, where the curvature is an obstruction to metrics being locally the same). This is an indication that any interesting phenomena in contact geometry should be of a global nature (*i.e.* be related to the global topology of the manifold supporting the contact structure). We also note that given Darboux's theorem we could define a contact structure on a 3-manifold to be a plane field that is locally equivalent to $(\mathbb{R}^3, \xi_{std})$.

Proof. We first claim there is a neighborhood U' of $p \in M$, a neighborhood V' of the origin $\mathbf{0}$ in $\mathbb{R}^3$, and a diffeomorphism

$$\phi\colon U' \to V'$$

taking p to $\mathbf{0}$, the contact hyperplane at p to the one at 0

$$d\phi_p(\xi_p) = (\xi_{std})_{\mathbf{0}}.$$

This may be proven in many ways, one is explored in the following exercise.

Exercise 1.2.3. Find ϕ by first taking any coordinate chart about p that maps p to $\mathbf{0}$, then compose with a linear map of $\mathbb{R}^3$ to make sure the contact plane at p maps to the contact plane at $\mathbf{0}$.

We will give a different proof that ϕ exists that will be useful in future proofs. In particular, we will use the exponential map. More specifically recall [**Pet16**, Proposition 5.5.1] if we fix a metric on a manifold M then there is an exponential map $\exp\colon T_pM \to M$ defined on and a diffeomorphism from a neighborhood of $0 \in T_pM$ to a neighborhood of $p \in M$, and taking 0 to p. In addition, $D\exp_p\colon T_0(T_pM) \to T_pM$ is the identity map (recall there is an obvious identification of the tangent space to a vector space with the vector space). Now choosing any isomorphism from T_pM to $T_{\mathbf{0}}\mathbb{R}^3$ taking a ξ_p to $(\xi_{std})_{\mathbf{0}}$, we can use the exponential map for $\mathbb{R}^3$, the exponential map for M, and the linear isomorphism to construct the claimed diffeomorphism $\phi\colon U' \to V'$.

Let $\xi' = \phi_*\xi$. We have $\xi'_{\mathbf{0}} = (\xi_{std})_{\mathbf{0}}$. Thus Theorem 1.2.1 says there is a neighborhood V'' of $\mathbf{0}$ in V' and an isotopy, fixing $\mathbf{0}$, from the identity map on V'' to f such that on a smaller neighborhood $V \subset V''$ of $\mathbf{0}$ we have

$$f|_V\colon V \to f(V)$$

taking $\xi'|_V$ to $(\xi_{std})|_{f(V)}$. Thus $\phi_U \circ f$ is the desired contactomorphism, where U is the open set $\phi^{-1}(V)$. □

For our next local result, we consider transverse curves. A curve C in a contact manifold (M, ξ) is called a *transverse curve* if T_pC intersects ξ_p transversely for all $p \in C$. A closed transverse curve is called a *transverse knot*.

Theorem 1.2.4. *Any two transverse knots have contactomorphic neighborhoods.*

Proof. Let C_i be a transverse knot in (M_i, ξ_i) for $i = 0, 1$. As in the proof of Darboux's Theorem we only need to find a map from a neighborhood of C_0 to a neighborhood of C_1 such that the contact planes along C_0 are taken to the contact panes along C_1. Once we have such a map we simply apply Theorem 1.2.1 to the ξ_1 and the push-forward of ξ_0 in the neighborhood of C_1. To construct such a map let $f\colon C_0 \to C_1$ be any diffeomorphism from C_0 to C_1. Then choose a bundle map $F\colon T_{C_0}M_0 \to T_{C_1}M_1$ that covers f and sends

ξ_0 to ξ_1. We may now use a normal bundle version of the exponential map, see [**Pet16**, Corollary 5.5.3], to extend f to a neighborhood of C_0. □

Example 1.2.5. Theorem 1.2.4 allows us to write down a standard model for a transverse knot. Consider $\mathbb{R}^3/\sim$ where $(x, y, z) \sim (x, y, z + 1)$ with the contact structure $\xi_{sym} = \ker(dz + r^2\, d\theta)$. The curve $T' = \{(0, 0, z)\} \subset (\mathbb{R}^3/\sim)$ is a transverse knot and hence any transverse knot T in a contact manifold (M, ξ) has a neighborhood N contactomorphic to a neighborhood N' of T' in $(\mathbb{R}^3/\sim, \xi_{sym})$. Moreover, by shrinking this neighborhood we can assume N is contactomorphic to $S_a = \{(r, \theta, z) : r \leq a\}$ for some positive real number a.

Our next local result will concern neighborhoods of Legendrian knots. Recall a knot L in a contact manifold (M, ξ) is called Legendrian if $T_pL \subset \xi_p$ for each $p \in L$.

Theorem 1.2.6. *Any two Legendrian knots have contactomorphic neighborhoods.*

Exercise 1.2.7. Prove this theorem. The proof is essentially the same as the proof of Theorem 1.2.4.

Remark 1.2.8. Note that in the proof of Theorem 1.2.4 we could take *any* diffeomorphism between neighborhoods of transverse knots (that preserve the knots) and isotope it into a contactomorphism on a smaller neighborhood. In particular, there is no preferred framing on a neighborhood of a transverse knot. This is not the case for Legendrian knots! The contact planes give a non-zero section of the normal bundle of a Legendrian knot (recall we are assume our contact structures are transversely oriented). This gives a *framing* of the knot (that is, a trivialization of the normal bundle). Any diffeomorphism of neighborhoods of Legendrian knots that preserves the framing can be isotoped to be a contactomorphism in a neighborhood of the knots. We will discuss this *contact framing* more thoroughly in Section 1.4.

Example 1.2.9. Theorem 1.2.6 allows us to write down a standard model for a Legendrian knot. Consider $\mathbb{R}^3/\sim$ where $(x, y, z) \sim (x + 1, y, z)$ with the contact structure $\xi std = \ker(dz - y\, dx)$. The curve $L' = \{(x, 0, 0)\} \subset (\mathbb{R}^3/\sim)$ is a Legendrian knot and hence any Legendrian knot L in a contact manifold (M, ξ) has a neighborhood N contactomorphic to a neighborhood N' of L' in $(\mathbb{R}^3/\sim, \xi_{std})$. Moreover, by shrinking this neighborhood we can assume N is contactomorphic to $S_a = \{(x, y, z) : y^2 + z^2 \leq a\}$ for some positive real number a.

We now understand contact structures in neighborhoods of points and (special) curves. What about contact structures in the neighborhood of a surface? We have a similar neighborhood theorem, but the details are a little more complicated and interesting, so we defer our discussion of this to the next section.

Moser's method is a way to construct an isotopy from a vector field so that it satisfies certain properties. We will illustrate this in the proof of Gray's theorem.

Theorem 1.2.10 (Gray 1969, [Gra59]). *Let*

$$\xi_t, t \in [0,1],$$

be a family of contact structures on a 3-manifold M. Suppose that $\xi_t = \xi_t'$ outside a compact set $C \subset M$. (That is the contact structures vary on a compact set. If M is compact then we can take $C = M$.) Then there is an isotopy

$$\psi_t \colon M \to M,$$

$t \in [0,1]$, of the identity map such that $\psi_t^* \xi_0 = \xi_t$ and ψ_t is the identity off of C.

It is obvious that an isotopy of M gives is family of contact structures (by pushing forward a fixed contact structure with the isotopy), but Gray's theorem says this is the *only* way to construct a family of contact structures (that vary only on a compact set). One says two contact structures are *isotopic* if there is a 1-parameter family of contact structures interpolating between them. So Gray's theorem essentially says if you have an isotopy of contact structures (fixed outside a compact set) then it is induced from an isotopy of the underlying space. This should be a surprising result, it is saying that given an isotopy occurring in the tangent bundle, it must be induced by an isotopy of the manifold. In general, such results are not true as the following examples show, but the contact condition on the plane field allows us to "integrate the isotopy".

Example 1.2.11. Consider T^3 thought of as $\mathbb{R}^3$ modulo $\mathbb{Z}^3$. Then for a fixed t consider

$$\eta^t_{(x,y,z)} = \operatorname{span}\{\partial_x, \partial_z + t\partial_y\}.$$

Notice that η^t is a plane field for each t and for t a rational number it is tangent to embedded T^2 in T^3 and for t irrational it is tangent to non-compact cylinders $S^1 \times \mathbb{R}$ in T^3. If there was a diffeomorphism $\phi \colon T^3 \to T^3$ taking η^t, for t rational, to η^s, for s irrational, then the diffeomorphism would map a compact torus onto a non-compact cylinder. Since this obviously cannot happen there is no isotopy of T^3 relating the η^t.

Example 1.2.12. We also note that it is essential in Theorem 1.2.10 that the isotopy of the contact structures is constant outside a compact set. Indeed, consider $\mathbb{R}^3$ with the contact structures

$$\xi_{std} = \ker(dz + r^2\, d\theta)$$

and

$$\xi_{ot} = \ker(\cos r\, dz + r \sin r\, d\theta).$$

It is easy to check that these contact structures are isotopic. For example, notice that if

$$\alpha = f(r)\, dz + g(r)\, d\theta$$

for some functions $f, g\colon \mathbb{R} \to \mathbb{R}$ then α describes a contact structure[2] if and only if

$$\alpha \wedge d\alpha = (fg' - gf')\, dr \wedge d\theta \wedge dz$$

is a positive volume form on $\mathbb{R}^3$, and this occurs if and only if

$$fg' - gf' > 0.$$

We can interpret this last condition as saying that the position vector and tangent vector to the curve $r \mapsto (f(r), g(r))$ form a basis for $\mathbb{R}^2$ (that is the position and tangent vectors are not co-linear). Now if for $t \in [0, 1)$ we let $(f_t(r), g_t(r))$ be

$$\begin{cases} (1, r^2) & r \in [0, h(t)] \\ (\cos(r - h(t)), h^2(t) + 2r\sin(r - h(t)) & r \in [h(t), \infty) \end{cases}$$

where $h(t) = \frac{t}{1-t}$, and $(f_1(r), g_1(r)) = (1 + r^2)$, then one can easily check that these 1-forms give an isotopy from $\xi'_{ot} = \ker(\cos r\, dz + 2r \sin r\, d\theta$ to ξ_{std} and ξ'_{ot} is clearly isotopic to ξ_{ot} (prove this if it is not obvious). In Section 1.6 we will see that these contact structures are not contactomorphic and hence there is no isotopy of $\mathbb{R}^3$ relating them.

Before starting the proof of Gray's theorem we need a simple, but essential, preliminary result. To state it we first fix a contact form α on M and R_α its Reeb field. Now set

$$\Omega^1_\alpha = \{ \text{1-forms } \beta \text{ on } M : \beta(R_\alpha) = 0\}.$$

Lemma 1.2.13. *Given a contact manifold (M, ξ) and a contact form α for ξ, there is a one-to-one correspondence*

$$\Gamma(\xi) \to \Omega^1_\alpha(M) : u \mapsto \iota_u d\alpha$$

Proof. Note if we set $(\Lambda^1_\alpha)_x$ to be the elements $\beta \in T^*_x M$ such that $\beta(R_\alpha(x)) = 0$, then this is a 2-dimensional vector space. Now the map

$$(\Lambda^1_\alpha)_x \to \xi_x : v \mapsto \iota_v d\alpha$$

is a linear isomorphism (prove this if it is not clear to you). Thus if we set $\Lambda^1_\alpha = \cup_{x\in M}(\Lambda^1_\alpha)_x$, then $d\alpha$ induces an bundle isomorphism from Λ^1_α to ξ. Thus it also induces a one-to-one correspondence on sections of these bundles. □

We are now ready to move on to the proof of Gray's theorem.

Proof of Theorem 1.2.10. We do not give Gray's original argument here, but instead, we use a technique called Moser's method, also known as Moser's trick. The idea first appeared in [**Mos65**] but has been used in many contexts since then. The idea is to try to find the isotopy $\phi_t\colon M \to M$ as the flow of a time-dependent vector field v_t. One can derive an equation for v_t that will guarantee its flow satisfies the desired properties.

[2] Notice that for α to be a smooth form at 0 we need $g(r)/r \to 0$ as $r \to 0$.

We assume the contact structures ξ_t are all co-oriented.

Exercise 1.2.14. Prove the theorem when the ξ_t are not co-oriented.

Exercise 1.2.15. Show that there is a smoothly varying family of 1-forms α_t such that $\xi_t = \ker \alpha_t$.

We will now determine equations that a vector field v_t must satisfy if its flow ϕ_t will give the isotopy in the theorem. We want the isotopy ϕ_t's to satisfy

$$\phi_t^* \alpha_t = \lambda_t \alpha_0$$

for some functions $\lambda_t \neq 0$. We compute

$$\begin{aligned}
\frac{\partial}{\partial t}(\phi_t^* \alpha_t) &= \lim_{h \to 0} \frac{\phi_{t+h}^* \alpha_{t+h} - \phi_t^* \alpha_t}{h} \\
&= \lim_{h \to 0} \frac{\phi_{t+h}^* \alpha_{t+h} - \phi_{t+h}^* \alpha_t + \phi_{t+h}^* \alpha_t - \phi_t^* \alpha_t}{h} \\
&= \lim_{h \to 0} \phi_{t+h}^* \left(\frac{\alpha_{t+h} - \alpha_t}{h} \right) + \lim_{h \to 0} \frac{\phi_{t+h}^* \alpha_t - \phi_t^* \alpha_t}{h} \\
&= \phi_t^* \left(\frac{d\alpha_t}{dt} \right) + \phi_t^* \mathcal{L}_{v_t} \alpha_t \\
&= \phi_t^* \left(\frac{d\alpha_t}{dt} + \mathcal{L}_{v_t} \alpha_t \right).
\end{aligned}$$

So we want

$$\phi_t^* \left(\frac{d\alpha_t}{dt} + \mathcal{L}_{v_t} \alpha_t \right) = \frac{d\lambda_t}{dt} \alpha_0.$$

But recall $\alpha_0 = \frac{1}{\lambda_t} \phi_t^* \alpha_t$ so

$$\phi_t^* \left(\frac{d\alpha_t}{dt} + \mathcal{L}_{v_t} \alpha_t \right) = \frac{d\lambda_t}{dt} \frac{1}{\lambda_t} \phi_t^* \alpha_t.$$

If we set $h_t = \frac{d}{dt} \left(\log \lambda_t \right) \circ \phi_t^{-1}$, then

$$\phi_t^* \left(\frac{d\alpha_t}{dt} + \mathcal{L}_{v_t} \alpha_t \right) = \phi_t^* \left(h_t \alpha_t \right).$$

Using Cartan's formula for the Lie derivative, $\mathcal{L}_v \alpha = d\iota_v \alpha + \iota_v d\alpha$, see [**Lee13**], we can rewrite this equation as

$$\frac{d\alpha_t}{dt} + \iota_{v_t} d\alpha_t = h_t \alpha_t. \tag{1.2.1}$$

if we look for a vector v_t in $\xi_t = \ker \alpha_t$.

Before we can solve for v_t we need to know what h_t is. Recall the Reeb vector field of α_t is the unique vector field X_t satisfying $\alpha_t(X_t) = 1$ and $\iota_{X_t} d\alpha_t = 0$. If we plug X_t into Equation (1.2.1) we get

$$\frac{d\alpha_t}{dt}(X_t) = h_t.$$

Thus h_t is determined by α_t and Equation (1.2.1) can be written

$$\iota_{v_t} d\alpha_t = h_t \alpha_t - \frac{d\alpha_t}{dt}. \tag{1.2.2}$$

The right-hand side of this equation is a 1-form determined by α_t and satisfies the condition that $\iota_{X_t}\left(h_t\alpha_t - \frac{d\alpha_t}{dt}\right) = 0$.

So, using the notation established before the proof, this 1-form is in $\Omega^1_{\alpha_t}$ and hence by Lemma 1.2.13 we can solve Equation (1.2.2) for v_t. By construction, the flow of v_t will be the desired isotopy.

Finally, where the ξ_t's agree we can choose the α_t to agree and hence $\frac{d\alpha_t}{dt} = 0$. Thus v_t will be zero there. Since the v_t's have compact support their flow exists for all time. In particular, the flow exists from time $t = 0$ to $t = 1$ giving our desired isotopy. □

It is a simple application of Gray's theorem to prove our main Theorem 1.2.1.

Proof of Theorem 1.2.1. Let α_i be contact forms for $\xi_i, i = 0, 1$, that determine the same co-orientation. On N we have $\alpha_0 = f\alpha_1$ for $f \neq 0$ a function on N. Let $\alpha_t = (1-t)\alpha_0 + t\alpha_1$ and $\xi_t = \ker(\alpha_t)$. So $d\alpha_t = (1-t)d\alpha_0 + td\alpha_t$. On N, $d\alpha_0$ and $d\alpha_1$ are both area forms on $\xi_t = \xi_0 = \xi_1$ inducing the same orientation and thus $d\alpha_t$ is also an area from on ξ_t. Hence $d\alpha_t|_{\xi_t} \neq 0$ on a neighborhood U' of N. If we repeat the argument in Gray's theorem we get a vector field v_t in U' whose flow would give the isotopy ψ_t. Since $v_t = 0$ on N, a compact set, there is a sufficiently small neighborhood U'' of N for which the flow of v_t exists for $t \in [0, 1]$ and stays in U'. This gives the desired flow on U''. To extend this to an isotopy on M that gives a contactomorphism near N we use the smooth isotopy extension theorem, see [**Hir76**, Section 8.1].

Exercise 1.2.16. Show that there is a compact set N' that contains N in its interior and is contained in U.

We may now extend our isotopy restricted to N' to an ambient isotopy of M with the desired property on the set U which is the interior of N'. □

We now consider some applications of the Moser trick to Legendrian and transverse knots that we will use below.

We say that L_0 and L_1 are *Legendrian isotopic* if there is a smooth isotopy L_t of L_0 to L_1 such that L_t is always Legendrian. We say they are *contact isotopic*, or *ambient Legendrian isotopic*, if there is an isotopy $\phi_t \colon M \to M$ of contactomorphisms such that ϕ_0 is the

identity on M and $\phi_1(L_0) = L_1$. Finally, we say that L_0 and L_1 are *contactomorphic* if there is a contactomorphism $\phi\colon M \to M$ such that $\phi(L_0) = L_1$. We have similar definitions for transverse knots. That is transverse knots can be *transverse isotopic*, *contact isotopic* (also known as *ambient transverse isotopic*), or *contactomorphic*.

It is clear that L_0 and L_1 being contact isotopic implies that they are both Legendrian isotopic (consider $L_t = \phi_t(L_0)$) and contactomorphic (via ϕ_1). It turns out that being contact isotopic and Legendrian isotopic are equivalent notions.

Lemma 1.2.17. *Let (M, ξ) be a contact manifold. Two Legendrian knots are related by Legendrian isotopy if and only if they are related by ambient contact isotopy.*

Proof. We noted above that contact isotopic implies isotopic. Now assume that $L_t, t \in [0,1]$, is a Legendrian isotopy. By the smooth isotopy extension theorem, see [**Hir76**, Section 8.1], there is an isotopy $\phi_t\colon M \to M, t \in [0,1]$, of M, such that ϕ_0 is the identity on M, and $\phi_t(L_0) = L_t$. Moreover, it is easy to arrange that the ϕ_t may be isotoped so that $\phi_t^*(\xi|_{L_t}) = \xi|_{L_0}$ (note that since ϕ_t is a diffeomorphism we can push-forward or pull-back plane fields). Let $\xi_t = \phi_t^*(\xi)$ This is a one-parameter family of contact structures. with $\xi_t = \xi_0$ along L_0. Thus Gray's theorem implies there is a family of diffeomorphisms ψ_t such that $\psi_t^*(\xi_t) = \xi_0$ and ψ_t is the identity on L_0. Now set $f_t = \phi_t \circ \psi_t$. Note that $f_t^*(\xi_0) = \psi_t^*(\phi_t^*(\xi_0)) = \psi_t^*(\xi_t) = \xi_0$, and so f_t is a contact isotopy and $f_t(L_0) = L_t$. □

Exercise 1.2.18. Prove the analogous theorem for transverse knots.

We now consider a technical result that will be used several times later in the text (see for example Section 1.4 and 6.1).

Lemma 1.2.19. *Let M be a compact 3-manifold on which the space of contact structures isotopic to a fixed contact structure ξ is simply connected (if M has boundary we only consider contact structures that are fixed near ∂M). The classification of Legendrian knots in (M, ξ) up to Legendrian isotopy is equivalent to the classification of Legendrian knots up to contactomorphism isotopic to the identity.*

In Lemma 1.4.1 below, we will see how to apply this lemma to S^3 with its standard contact structure.

Proof. From the previous lemma we see that if two Legendrian knots are Legendrian isotopic then they are contactomorphic by a contactomorphism that is isotopic to the identity. To prove the other implication we assume that L and L' are contactomorphic. That is there is a contactomorphism $\phi\colon M \to M$ that sends L to L' and is smoothly isotopic to the identity. Thus there is an isotopy $\phi_t\colon M \to M$ with $\phi_0 = id_M$ and $\phi_1 = \phi$. Notice that $\xi_t = (\phi_t)_*\xi$ is a loop of contact structures based at ξ. So by hypothesis, there is a map

$$H\colon [0,1] \times [0,1] \to \Xi(\xi)$$

where $\Xi(\xi)$ is the space of contact structures isotopic to ξ, such that $H(t,0) = \xi_t$ and $H(t,1) = H(0,s) = H(1,s) = \xi$. We apply Gray's theorem to $H(t,s)$ for $t \in [0,1]$ and s fixed and notice that as s varies the diffeomorphisms constructed vary smoothly. That is we get a map

$$F\colon [0,1]\times[0,1] \to \mathrm{Diffeo}(M)$$

satisfying $F(0,s) = id_M$, $F(t,1) = id_M$ (since $H(t,1) = \xi$ for all t), and $F(1,s)$ is a contactomorphism of ξ for all s.

Exercise 1.2.20. Show that you can choose α_t such that $\xi_t = \ker \alpha_t$ and $F(t,0) = \phi_t$.

Thus $F(1,s)$ is a contact isotopy from $F(1,1) = id_M$ to $F(1,0) = \phi_1$. □

1.3. Characteristic foliations

In this section we will introduce the characteristic foliation of a surface in a contact manifold. We will see that the contact structure in a neighborhood of the surface is determined by this (singular) foliation. This fundamental concept will be further studied in Chapter 2.

1.3.1. Singular foliations on surfaces. A *singular line field* on a surface Σ is a subset L of the tangent bundle $T\Sigma$ such that at each point $x \in \Sigma$ we have that L_x is either a line or all of $T_x\Sigma$. We call the points x where the latter occurs *singular points* of L. We will be concerned with line fields L that can always be locally spanned by a vector field. That is, for each p in Σ there is a neighborhood U of p and a vector field v such that v is tangent to L where it is non-singular and zero where L is singular. Notice that if v' is any other vector field defining L locally then $v' = fv$ for some non-zero function f. Thus we could define L by choosing a covering $\{U_i\}$ of Σ and vector fields $\{v_i\}$ where v_i is defined only on U_i such that on any overlap $U_i \cap U_j$ the vector fields v_i and v_j are related by some non-zero function as above. Given this, the span of the v_i give L on Σ. We say L is *oriented* if L can be defined by a global vector field on Σ.

Convention: We assume all our singular line fields are orientable.

Notice that since L is given (at least locally, by a vector field) we can look at flow-lines of the vector field. If S is the set of singular points of L, then on $\Sigma - S$ these flow-lines give a foliation. We call this a *singular foliation* on Σ. If the line field is given by the vector field v then we say that v *directs* the singular foliation.

There is another, dual, perspective on singular line fields and singular foliations. Let ω be an area form on Σ. Just as in the proof of Lemma 1.2.13 we see that ω induces an isomorphisms

$$\mathfrak{X}(\Sigma) \to \Omega^1(\Sigma)$$

from vector fields on Σ, denoted by $\mathfrak{X}(\Sigma)$, to 1-forms on Σ, denoted by $\Omega^1(\Sigma)$, by sending the vector field v to $\iota_v\omega$. Thus if v directs the singular foliation, then we get the 1-form $\alpha_v = \iota_v\omega$. Notice that the kernel of α_v defines the singular line field defined by v.

Exercise 1.3.1. Prove this last statement.

Conversely, given a 1-form α on Σ if we let $L = \ker\alpha$, then L is a singular line field that is generated by the unique vector field mapped to α by the above isomorphism.

1.3.2. Characteristic foliations. Let M be a 3–manifold, ξ an oriented contact structure on M, and Σ an oriented surface in M. For each point $p \in \Sigma$ let

$$l_p = \xi_p \cap T_p\Sigma.$$

This gives an oriented singular line field on Σ. That is, at most points of Σ we have a line in $T_p\Sigma$ chosen, and at some points l_p all of $T_p\Sigma$.

Exercise 1.3.2. Show that the set of singular points does not contain a open set.
Hint: If this is true, then you can show that the contact condition is violated. Consider two vectors fields v and w tangent to Σ defined along this open subset. Using the formula $d\alpha(v,w) = v\alpha(w) - w\alpha(v) + \alpha([v,w])$ compute $\alpha \wedge d\alpha$.

At a non-singular point the orientation on the line field l_p comes from intersecting the two oriented planes ξ_p and $T_p\Sigma$ in the oriented 3-space T_pM. Recall this orientation is defined as follows. We say $u \in l_p$ gives the orientation on l_p, if there are vectors $v \in \xi_p$ and $w \in T_p\Sigma$ such that $\{u,v\}$ is an oriented basis for ξ_p, $\{u,w\}$ is an oriented basis for $T_p\Sigma$, and $\{u,v,w\}$ is an oriented basis for T_pM.

From above we know that the singular line field is tangent to a singular foliation of Σ. This singular foliation is called the *characteristic foliation* of Σ and is denoted Σ_ξ. [3]

Example 1.3.3. Consider $\mathbb{R}^3$ with the contact structure $\xi_{sym} = \ker\alpha$ where $\alpha = (dz + r^2\,d\theta)$. Let $f\colon D^2 \to \mathbb{R}^3$ be given by $f(x,y) = (x,y,0)$ where D^2 is the unit disk in $\mathbb{R}^2$. Then

$$f^*\alpha = r^2\,d\theta = x\,dy - y\,dx.$$

It is easy to see that $l_p = \ker f^*\alpha$ so clearly the characteristic foliation is tangent to the line field spanned by $r\frac{\partial}{\partial r}$. See Figure 1.3.4.

Now consider the embedding $g\colon D^2 \to \mathbb{R}^3$ given by $g(x,y) = (x,y,axy)$ where $a > 1$. Then we have

$$g^*\alpha = (a+1)x\,dy + (a-1)y\,dx$$

[3] some authors prefer $\xi\Sigma$.

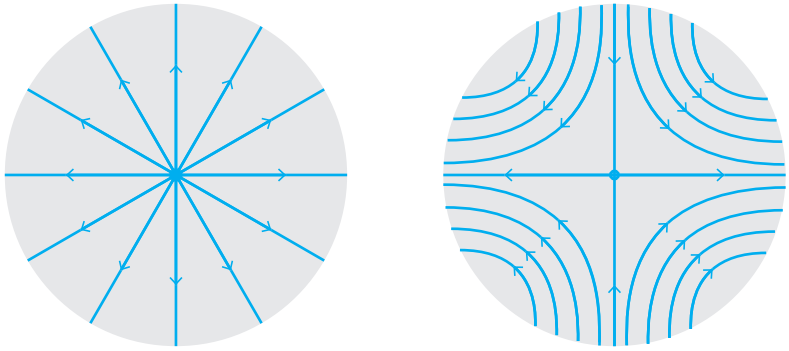

Figure 1.3.4. Characteristic foliations on various embeddings of the disk.

and the characteristic foliation is defined by the flow of the vector field

$$\begin{bmatrix}(a+1)x\\(1-a)y\end{bmatrix}.$$

See Figure 1.3.4. The singularity on the left is called an *elliptic singularity* and also called a *nodal singularity*. The singularity on the right is called a *hyperbolic singularity* and also a *saddle singularity*.

1.3.3. Characteristic foliations and germs of contact structures. The key property of the characteristic foliation of a surface in a contact manifold is that it determines the contact structure in a neighborhood of the surface.

Theorem 1.3.4. *Let (M_i, ξ_i) be a contact manifold and Σ_i an embedded surface for $i = 0, 1$. If there is a diffeomorphism $f\colon \Sigma_0 \to \Sigma_1$ that preserves the characteristic foliation:*

$$f((\Sigma_0)_{\xi_0}) = (\Sigma_1)_{\xi_1},$$

then f may be extended to a contactomorphism in some neighborhood of Σ_0. Moreover, if f was already defined on a neighborhood of Σ_0 then we can isotop f, relative to Σ_0, so as to be a contactomorphism in some (possibly) smaller neighborhood.

For notational convenience, we will prove the following equivalent theorem instead.

Theorem 1.3.5. *Let $\Sigma \subset M$ be an oriented surface in a 3–manifold M. Suppose ξ_0 and ξ_1 are contact structures on M such that*

$$\Sigma_{\xi_0} = \Sigma_{\xi_1}.$$

Then there is a neighborhood U of Σ and an isotopy $\phi_t\colon M \to M$ such that

(1) *ϕ_0 is the identity on M,*

(2) *ϕ_t is fixed on Σ and*

(3) *$\phi_1^*|_U(\xi_0|_U) = \xi_1$.*

Proof. The theorem will follow from Theorem 1.7.4 if we have

$$\xi_0|_\Sigma = \xi_1|_\Sigma,$$

but this does not have to be the case. We shall construct an isotopy of a neighborhood of Σ to achieve this. To this end let $W = \Sigma \times (-\epsilon, \epsilon)$ be a neighborhood of Σ in M. We will denote points in Σ by p and points in $(-\epsilon, \epsilon)$ by s. Our aim is to construct an isotopy $\psi_t, t \in [0,1]$ on a subset of W such that

(1) ψ_t is fixed on Σ,

(2) ψ_0 is the identity on W and

(3) $\psi_1^*(\xi_0(p,0)) = \xi_1(p,0)$.

Once we have found such an isotopy we can extend it arbitrarily to M and apply Theorem 1.7.4 to $\psi_1^*\xi_0$ and ξ_1 to get an isotopy $\Psi_t \colon M \to M$ such that $\Psi_1^*(\psi_1^*\xi_0) = \xi_1$ on a neighborhood of Σ and $\phi_t = \psi_t \circ \Psi_t$ will then be the desired isotopy.

To construct ψ_t we choose contact forms $\alpha_i, i = 0,1$, for our contact structures and write

$$\alpha_i|_\Sigma = \beta_i(p) + f_i(p)\, dt$$

where β_i is a 1–form on Σ and f_i is a function on Σ. As above we have $\Sigma_{\xi_i} = \ker(\beta_i)$ and since $\Sigma_{\xi_0} = \Sigma_{\xi_1}$ there is some positive function $g \colon \Sigma \to \mathbb{R}$ such that $\beta_1 = g\beta_0$.

Exercise 1.3.6. Show that g must be positive.
HINT: Show the only thing to worry about is at the singularities. Write down the contact condition for α_i on Σ and show that when at singularities $\beta_i(p) = 0$ but $d\beta_i(p) \neq 0$.

Now extend g to a non-zero function on all of M and replace α_0 with $g\alpha_0$. We have $\alpha_0|_{T\Sigma} = \alpha_1|_{T\Sigma}$ and $\beta_0 = \beta_1$ which we denote simply β.

Assume for the moment that $f_0 \neq 0$ then $\psi(p,t) = \left(p, \frac{f_1(p)}{f_0(p)}t\right)$ is well–defined. Moreover, if f_1 is also never zero then $\psi \colon W \to M$ is a diffeomorphism onto its image (we might need to shrink the domain of ψ to make sure it is well–defined). We compute $\psi^*\alpha_0 = \alpha_1$ and thus $\psi^*\xi_0 = \xi_1$ so the straight line isotopy from the identity to ψ is the desired isotopy.

In general, f_0 (and f_1) will be zero in some places. Let $\Sigma_\delta = f_0^{-1}(|s| > \delta) \cap f_1^{-1}(|s| > \delta)$. Notice that if p is a singular point $\beta(p) = 0$ so we must have $f_i(p) \neq 0$. Thus if δ is small enough then Σ_δ contains all the singularities of $\Sigma_{\xi_0} = \Sigma_{\xi_1}$. We can define ψ on $\Sigma_{\delta/2}$ as above. Let $\Sigma' = \overline{\Sigma \setminus \Sigma_\delta}$ and $\Sigma'' = \Sigma' \cap \Sigma_{\delta/2}$. Clearly $\Sigma = \Sigma_{\delta/2} \cup \Sigma'$. On Σ' choose a vector field $v = v_\Sigma + \frac{\partial}{\partial s}$ such that $v \in \xi_0$, $v_\Sigma \in T\Sigma$. Note that v is transverse to Σ. Also choose w on Σ' such that $\psi^*v = w$ on Σ'', w is transverse to Σ' and $w \in \xi_1$.

We can write $w = w_\Sigma + h(p)\frac{\partial}{\partial s}$ where $w_\Sigma \in T\Sigma$ and $h(p)$ is some function on Σ''. On Σ'' we have

$$\begin{aligned}\psi^*\left(v_\Sigma + \frac{\partial}{\partial s}\right) &= w_\Sigma + h(p)\frac{\partial}{\partial s} \\ &= v_\Sigma + \frac{f_1(p)}{f_0(p)}\frac{\partial}{\partial s}\end{aligned}$$

since $\psi(p,s) = \left(p, \frac{f_1(p)}{f_0(p)}s\right)$ on Σ''. □

1.3.4. Characteristic foliations and contact structures on neighborhoods of surfaces. In the previous section, we saw that the characteristic foliation on one surface determines the contact structure in some neighborhood of the surface. Here we shall see that a family of foliations on a surface cross interval determines the contact structure on the surface cross interval.

Theorem 1.3.7. *Let $M = \Sigma \times \mathbb{R}$ for a surface Σ. If two contact structures induce the same characteristic foliations on all the surfaces $\Sigma \times \{t\}$, for $t \in \mathbb{R}$, (and are the same in a neighborhood of $\partial\Sigma \times [0,1]$ if $\partial\Sigma \neq \emptyset$) then they are isotopic relative to ∂M.*

Proof. Suppose ξ_0 and ξ_1 are two contact structures on $\Sigma \times \mathbb{R}$ that induces the same characteristic foliations on $\Sigma \times \{t\}$ for all $t \in \mathbb{R}$ and agree near $\partial\Sigma \times R$. Then ξ_i is the kernel of $\alpha_i = \beta_i(t) + u_i(t)\,dt$ where t is the coordinate on $\mathbb{R}$, $\beta_i(t)$ is a 1-form on Σ and $u_i(t)$ is a function on Σ for $i = 0, 1$. Given that the characteristic foliations on all the surfaces $\Sigma \times \{t\}$ are the same we see that there are some non-zero functions $f(t)$ such that $\beta_0(t) = f(t)\beta_1(t)$ (as we argued in the previous section).

Exercise 1.3.8. Show that the f_t vary continuously in t.

So the f_t give a function $F\colon \Sigma \times \mathbb{R} \to \mathbb{R}$ and we can replace α_2 with $(1/F)\alpha_2$, which we still denote α_2 so that $\beta_0 = \beta_1$ which we denote by β. □

1.3.5. Families of surfaces. It will be useful to know that the characteristic foliations on an interval's worth of surface also determine the contact structure up to isotopy. In [Gir00], Giroux refers to this as the *reconstruction lemma*.

Lemma 1.3.9 (Giroux 2000, [Gir00])**.** *Given a surface Σ, consider two contact structures ξ and ξ' on $\Sigma \times [-1,1]$. If the characteristic foliation on $\Sigma_t = \Sigma \times \{t\}$ induced by ξ and ξ' agree for all t, then ξ is isotopic to ξ'.*

In preparation for the proof of this lemma, we consider a contact form on $\Sigma \times [-1,1]$. Such a form can be written

$$\alpha = \beta_t + u_t\,dt,$$

where t is the coordinate on $[-1,1]$ and β_t, respectively u_t, are 1-forms, respectively functions, on Σ depending smoothly on t. The contact condition $\alpha \wedge d\alpha > 0$ is equivalent to

$$u_t\, d\beta_t + \beta_t \wedge \left(du_t + \frac{d\beta_t}{dt} \right) > 0$$

on Σ for all t.

Exercise 1.3.10. Given contact forms $\alpha = \beta_t + u_t\, dt$ and $\alpha' = \beta_t + u_t'\, dt$ show that $\alpha_s = s\alpha + (1-s)\alpha'$ is a contact form for $s \in [0,1]$. That is with the β_t fixed the collection of u_t that define a contact form by the equation above is convex.

Proof of Lemma 1.3.9. Given contact forms α and α' for ξ and ξ', respectively, we can write then as $\alpha = \beta_t + u_t\, dt$ and $\alpha' = \beta_t' + u_t'\, dt$. The fact that the characteristic foliations on the Σ_t induced by ξ and ξ' agree, implies that β_t has the same kernel as β_t'.

Exercise 1.3.11. Verify that the characteristic foliation on Σ induced by ξ is given by the kernel of β_t.

Thus there are non-zero functions $f_t : \Sigma \to \mathbb{R}$ such that $\beta_t' = f_t \beta_t$. Now the contact structure ξ' is also given by the form $\alpha'' = \frac{1}{f_t}(\beta_t' + u_t'\, dt) = \beta_t + \frac{u_t'}{f_t}\, dt$. From the discussion before the proof, we know that there is a 1-parameter family of contact 1-forms $\beta_t + u_t^s\, dt$ interpolating between α and α''. Now, considering the proof of Gray's theorem, Theorem 1.2.10, we know there is a vector field v_s that is tangent to the surfaces Σ_t whose flow (which exists for all time because the flow is tangent to compact surfaces) generates an isotopy taking ξ to ξ'. □

Remark 1.3.12. If ξ and ξ' in the lemma agree near the boundary of $\Sigma \times [-1,1]$ then the isotopy in the theorem can be taken to be fixed in a neighborhood of the boundary.

1.4. Legendrian and transverse knots

Legendrian and transverse knots play a central role in contact geometry. In addition to their rich structure, which we will explore throughout this book, they can be used to construct contact structures and also distinguish them. In this section we will establish some of the basic results concerning these special knots. We begin with the ways in which one can try to classify these knots.

1.4.1. Types of classification. Recall at the end of Section 1.2 we discussed three equivalence relations one can put on Legendrian knots: *Legendrian isotopic*, *abmient Legendrian isotopic* (also konwn as *contact isotopic*), and *contactomorphic*. We have similar definitions for transverse knots. That is transverse knots can be *transverse isotopic*, *contact isotopic* (also known as *ambient transverse isotopic*), or *contactomorphic*.

We also saw in Section 1.2 that L_0 and L_1 being contact isotopic implies that they are both Legendrian isotopic (consider $L_t = \phi_t(L_0)$) and contactomorphic (via ϕ_1) and Lemma 1.2.17 shows that being contact isotopic and Legendrian isotopic are equivalent notions.

Given Lemma 1.2.17 we see that contact isotopy and Legendrian isotopy are the same for Legendrian knots in any contact manifold, and each implies that the Legendrian knots are contactomoprhic. Contactomorphic Legendrian knots need not be Legendrian isotopic, but in some cases this is true. We mention the most relevant case here.

Lemma 1.4.1. *Two Legendrian knots in (S^3, ξ_{std}) or in $(\mathbb{R}^3, \xi_{std})$ are Legendrian isotopic if and only if they are contactomorphic.*

This lemma follows immediately from Lemma 1.2.19 and

Theorem 1.4.2 (Eliashberg 1992, [Eli92])**.** *The space of contact structures $\Xi(\xi_{std})$ on S^3 that are isotopic to the standard contact structure ξ_{std} is simply connected. The same is true for $\Xi(\xi_{std})$ on $\mathbb{R}^3$.*

1.4.2. Classical invariants. Given a Legendrian knot L in a contact manifold (M, ξ), the underlying knot type is an invariant of L. That is if two Legendrian knots are not smoothly isotopic then they are not Legendrian isotopic. There are two other simple, though not quite as obvious, invariants of Legendrian knots up to Legendrian isotopy.

The first is the contact framing, which for null-homologous knots is equivalent to the Thurston-Bennequin invariant. To define this invariant we recall that the normal bundle $\nu(L)$ of a Legendrian knot L is an $\mathbb{R}^2$-bundle over L. This can canonically be identified with a tubular neighborhood of L in M, and we can also think of the tubular neighborhood of L as a disk bundle over L. We will abuse notation and denote all of these by $\nu(L)$, but the meaning should be clear from the context.

Exercise 1.4.3. Since M is oriented show that $\nu(L)$ is trivial.

From the exercise we know that $\nu(L) \cong L \times D^2$. Up to isotopy there are an integers worth of ways to identify $\nu(L)$ with $S^1 \times D^2$ that differ by twisting. More specifically, consider the diffeomorphism

$$\psi_n \colon S^1 \times D^2 \to S^1 \times D^2 \colon (\phi, (r, \theta)) \mapsto (\phi, (r, \theta + n\phi)),$$

where ϕ is the angular coordinate on S^1 and (r, θ) are polar coordinates on D^2. See Figure **??**. Now if $f \colon S^1 \times D^2 \to \nu(L)$ is a trivialization of the normal bundle of L, then $f_n = f \circ \psi_n$ gives other trivializations.

Exercise 1.4.4. Show that these are the only trivializations up to isotopy.

An identification of $\nu(L)$ with $S^1 \times D^2$ is called a *framing* of L.

We note that a non-zero section s of $\nu(L)$ gives a framing of L. One can see this by choosing another section s' of $\nu(L)$ that is independent of s (that is at each point of L, s and s' span the fiber of $\nu(L)$). Given this, we see that

$$\psi\colon\ L \times \mathbb{R}^2 \to \nu(L)\colon\ (x,(a,b)) \mapsto as(x) + bs'(x)$$

is a trivialization.

Now since L is Legendrian it gets a framing by choosing a non-zero vector $s(x)$ in $\xi_x \cap \nu_x(L)$. That is $s(x)$ is an element in the normal bundle that is also in the contact plane. This is called the *contact framing* of L, and is denoted $\mathcal{F}_\xi(L)$.

Exercise 1.4.5. Let R_α be a Reeb vector field for ξ. Show that R_α also gives L a framing and that this framing is the same as the framing defined above.

We now consider knots L that are null-homologous in M.

Exercise 1.4.6. Show that a null-homologous knot L is the boundary of an embedded surface in M. If L is in $\mathbb{R}^3$ or S^3 then give an algorithm to find the surface.
Hint: This can be found in many books on knot theory and 3-manifold topology. See [**Rol76**].

If L is the boundary of a surface Σ, then Σ is called a *Seifert surface* for L. Given Σ there is a framing for L given by a section s of $T\Sigma \cap \nu(L)$. For example, after choosing a metric, one can choose the unit vector normal to L pointing into Σ. This is called the *Seifert framing* of L and is denoted $\mathcal{F}_\Sigma(L)$.

Exercise 1.4.7. Show the Seifert framing is well-defined (that is, it does not depend on the Seifert surface used to define the framing).

Given two framings $\mathcal{F}_1$ and $\mathcal{F}_2$ then we can associate an integer as follows. Notice we have two identifications of $\nu(L)$ with $S^1 \times D^2$

$$S^1 \times D^2 \xrightarrow{\mathcal{F}_1} \nu L \xleftarrow{\mathcal{F}_2} S^1 \times D^2$$

We can now consider $\mathcal{F}_2^{-1} \circ \mathcal{F}_1\colon\ S^1 \times D^2 \to S^1 \times D^2$ which will be isotopic to one of the ψ_n defined above. We say that the difference between $\mathcal{F}_1$ and $\mathcal{F}_2$ is n and write

$$\mathcal{F}_1 - \mathcal{F}_2 = n$$

The *Thurston-Bennequin invariant* of a Legendrian knot L, denoted by $\mathrm{tb}(L)$, is the difference between the contact framing and the Seifert framing:

$$\mathrm{tb}(L) = \mathcal{F}_\xi(L) - \mathcal{F}_\Sigma(L).$$

Exercise 1.4.8. Show that if L_0 and L_1 null-homologous Legendrian knots that are Legendrian isotopic or contactomorphic, then $\mathrm{tb}(L_0) = \mathrm{tb}(L_1)$.

We will also be interested in Legendrian knots L that are on the interior of a surface Σ. Notice that L still inherits a framing from Σ (just as it did from a Seifert surface). We say the *twisting of ξ relative to* Σ is the difference between the contact framing and the Σ framing, and denote it by

$$\mathrm{tw}(L, \Sigma) = \mathcal{F}_\xi - \text{ framing induced by } \Sigma.$$

The last classical invariant of a Legendrian knot is the rotation number. This invariant is defined for oriented null-homologous knots. Suppose that L is an oriented Legendrian knot in (M, ξ) that is the boundary of an oriented surface Σ.

Exercise 1.4.9. Show that any oriented plane field over an oriented surface with boundary is trivial.

So we know that

$$\xi|_\Sigma = \Sigma \times \mathbb{R}^2$$

and this induces a trivialization

$$\xi|_L = L \times \mathbb{R}^2.$$

Exercise 1.4.10. The trivialization $\xi|_\Sigma$ is not unique, but show that the restriction of any such trivialization to $\partial\Sigma$ is unique.

Since L is oriented we can choose a tangent vector $v(x)$ to L at x that points in the direction of the orientation. This gives a section $L \to L \times \mathbb{R}^2$ and hence a map, which we still denote by v, from L to $\mathbb{R}^2$. In particular, we obtain a map $L \to S^1$ given by $x \mapsto v(x)/|v(x)|$ (where $|v(x)|$ is computed with respect to any metric). We define the *rotation number* of L, denoted by $\mathrm{rot}\, L$, to be the degree of this map.

Exercise 1.4.11. Show that if L_0 and L_1 oriented null-homologous Legendrian knots that are Legendrian isotopic or contactomorphic, then $\mathrm{rot}(L_0) = \mathrm{rot}(L_1)$.

One can think of the rotation number in terms of a relative Euler class.

Exercise 1.4.12. Given an oriented Legendrian knot L that bounds a surface Σ, let s be the section of ξ along $\partial\Sigma = L$ that defines the orientation on L. Extend s arbitrarily to a section s' of $\xi|_\Sigma$ so that it is transverse to the zero section. Show that $\mathrm{rot}(L)$ is the signed count of zeros of s'. This is known as the Euler class of $\xi|_\Sigma$ relative to s.

In summary, an oriented, null-homologous, Legendrian knot L has three "classical invariants". Specifically, we have

(1) the smooth knot type of L,

(2) the Thurston-Bennequin invariant of L, and

(3) the rotation number of L.

We will see how to compute these invariants (in certain cases) in the next section.

We now turn to transverse knots. Recall a knot T in a contact manifold (M, ξ) is *transverse* if K is transverse to ξ at each point of K. Recall we are assuming that our contact structures and manifolds are oriented, thus if T is oriented we say it is a *positive transverse knot* if the orientation on T followed by the orientation on ξ induces the orientation on M, otherwise we say that T is a *negative transverse knot*.

Convention: We will assume that all of our transverse knots are positive.

We suppose that T is the boundary of some Seifert surface Σ. As above we know that $\xi|_\Sigma$ is trivial so is bundle isomorphic to $\Sigma \times \mathbb{R}^2$ and we can restrict this trivialization to the boundary to get $\xi|_T = T \times \mathbb{R}^2$. This is a framing on T. The *self-linking number* of T is

$$\mathrm{sl}(T) = \mathrm{link}(T, T')$$

where T' is a push-off of T obtained from the framing above. Much like the rotation number for Legendrian knots, we can think of $\mathrm{sl}(T)$ as a relative Euler class.

Exercise 1.4.13. Given a transverse knot T and surface Σ with $\partial\Sigma = T$ then let s be a vector field along T that is tangent to the characteristic foliation Σ_ξ and pointing out of Σ (note that s is correctly orienting Σ_ξ along $\partial\Sigma$). Show that $\mathrm{sl}(T)$ is the minus of the Euler class of $\xi|_\Sigma$ relative to s. In other words, if we extend s to a section s' of $\xi|_\Sigma$ so that it is transverse to the zero section, then $\mathrm{sl}(T)$ is the minus of the signed count of zeros of s'.

In particular, if Σ_ξ is generic, then it only has elliptic and hyperbolic singularities. Let $e_\pm$ be the number of $\pm$ elliptic singular points in Σ_ξ and $h_\pm$ be the number of $\pm$ hyperbolic singularities. Then

$$\mathrm{sl}(T) = -(e_+ - h_+) + (e_- - h_-).$$

We see that an oriented, null-homologous transverse knot has two classical invariants:

(1) the smooth knot type of T, and

(2) the self-linking number of T.

1.4.3. Legendrian knots in $(\mathbb{R}^3, \xi_{std})$. In this section, we will consider knots in the contact manifold $(\mathbb{R}^3, \xi_{std} = \ker \alpha)$ where $\alpha = dz - y\,dx$. Our main tool to study such knots will be the front projection. The *front projection* is the map

$$\pi\colon\ \mathbb{R}^3 \to \mathbb{R}^3\colon\ (x, y, z) \mapsto (x, z).$$

We will study Legendrian knots by considering their image under this projection. To this end suppose L is a Legendrian knot in $(\mathbb{R}^3, \xi_{std})$. We can parameterize L by a function

$$\psi\colon\ S^1 \to \mathbb{R}^3\colon\ \theta \mapsto (x(\theta), y(\theta), z(\theta)).$$

The knot L being Legendrian is equivalent to $\psi^*\alpha = 0$, which is the same as $(z'(\theta) - y(\theta)x'(\theta))d\theta = 0$ or more simply

$$z'(\theta) - y(\theta)x'(\theta) = 0.$$

Now consider $\pi \circ \psi \colon S^1 \to \mathbb{R}^2$. Where the z-coordinate of this projection can be written as a function of the x-coordinate (that is where $x'(\theta) \neq 0$) we have that

$$\frac{z'(\theta)}{x'(\theta)} = \frac{dz}{dx}(\theta)$$

which implies that

$$y(\theta) = \frac{dz}{dx}(\theta).$$

In other words, the y-coordinate of a Legendrian knot can be recovered as the slope in the front projection (at least where $x'(\theta) \neq 0$).

We now consider the case when $x'(\theta) = 0$. We will first consider the case when the zero of x' is isolated. For convenience, we assume it is $\theta = 0$ where x' is zero. Since $y(\theta)$ is a well-defined smooth function, the limit of $y(\theta)$ as θ goes to 0 exists, and hence $z'(\theta)/x'(\theta)$ is well-defined for $\theta \neq 0$ and the the limit

$$\lim_{\theta \to 0} \frac{z'(\theta)}{x'(\theta)}$$

exists and defines the y-coordinate at $\theta = 0$. Generally the function $x'(\theta)$ will have 0 as a regular value and hence x will be increasing/decreasing before 0 and decreasing/increasing after 0. Thus the picture for the front projection near $\theta = 0$ is as shown in Figure 1.4.5. We note that in order for the limit above to exist, we must have $z'(0) = 0$.

Figure 1.4.5. The front projection of cusps.

Thus for our parameterization to be regular, we must have $y'(0) \neq 0$.

Example 1.4.14. Translating $(x(0), z(0))$ to the origin and assuming that 0 is a regular value of $x'(\theta)$, show that one can re-parameterize the knot so that

$$(x(\theta), y(\theta), z(\theta)) = (a\theta^2, b + \theta, ab\theta^2 + (a2/3)\theta^3)$$

for some constants a and b. Such a curve is called a *semi-cubical cusp*.
Hint: Under the given hypothesis show that the curve can be re-parameterized so that the x and y functions are as stated and then recover the z function from the equation above.

Remark 1.4.15. We note that Legendrian knots could have $x'(0)$ vanishing to higher order and even have the x and z coordinates be constant for some interval of θ values. These will not occur for generic Legendrian knots, but the reader is encouraged to consider the front projection of such knots.

So an immersed curve with cusps in the xz-plane determines a Legendrian knot by setting $y(\theta) = \frac{dz}{dx}(\theta)$.

Example 1.4.16. In Figure 1.4.6 we see two examples of front projections of Legendrian knots.

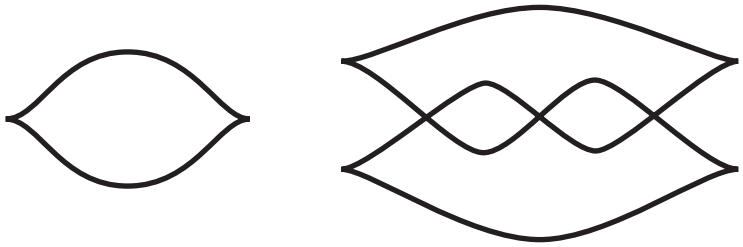

Figure 1.4.6. The front projection of two Legendrian knots.

Knot diagrams usually have crossing information, [**Rol76**], but notice that the diagram on the right in Figure 1.4.6 has no such information. This is because the crossing information is determined by the front projection. In particular, since $y = \frac{dz}{dx}$ we see that the more negative slope must be in front of the more positive slope at any crossing. (Recall, that since we are projecting to the xz-plane, the positive y-direction is going into the the page so that we have a positive orientation on $\mathbb{R}^3$.) We will frequently draw the crossing information in the projection for convenience, but this is not strictly necessary.

We now see how to compute the Thurston-Bennequin invariant and rotation number of knots in $(\mathbb{R}^3, \xi_{std})$. We begin by recalling the definition of the linking number. Given two oriented knots K_0 and K_1 in $\mathbb{R}^3$, let Σ be a Seifert surface for K_0. We define the *linking number* of K_0 and K_1, denoted by $\text{link}(K_0, K_1)$, to be the algebraic intersection between Σ and K_1. We can compute the linking number from a diagram of K_0 and K_1. At a crossing c between K_0 and K_1 in some projection we define the sign of the crossing to be $\epsilon(c)$ as shown in Figure 1.4.7.

Then

$$\text{link}(K_0, K_1) = \frac{1}{2} \sum_c \epsilon(c),$$

where the sum is taken over all crossings c between K_0 and K_1, see [**Rol76**]. It is easy to check that if $\mathcal{F}$ is a framing of a knot K and K' is a push-off of K along the vector field

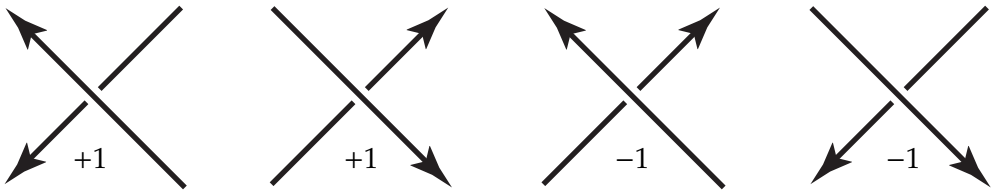

Figure 1.4.7. The signs $\epsilon(c)$ of a crossing in a projection of a knot.

giving the framing, then

$$\mathcal{F} - \text{ Seifert framing } = \text{link}(K, K').$$

Exercise 1.4.17. Verify this claim.

Now if L is a Legendrian knot let L' be the result of pushing L in the direction of the Reeb vector field (which in this case if $\frac{\partial}{\partial z}$). Then

$$\text{tb}(L) = \text{link}(L, L')$$

where we arbitrarily orient L and orient L' in the same direction.

Example 1.4.18. We compute the Thurston-Bennequin invariant of the two knots in the example above. See Figure 1.4.8. Notice that for the knot on the left-hand side, there are

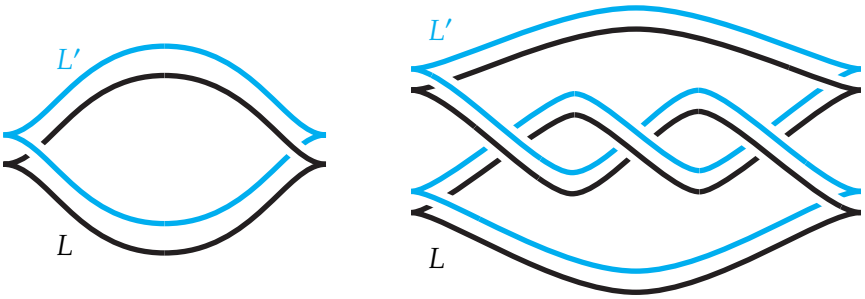

Figure 1.4.8. Computing the Thurston-Bennequin invariant of a Legendrian representative of the right-handed trefoil.

2 crossings coming from the cusps of L. They both contribute a $-$ sign. Thus $\text{tb}(L) = -1$. For the knot on the right-hand side, there are 6 crossings between L and a copy of L pushed up coming from crossings of L. These all have a $+$ sign. There are 4 crossings coming from the cusps of L and they all have a $-$ sign. Thus we see $\text{tb}(L) = 1$.

We can come up with a simpler formula for $\text{tb}(L)$. To do so we define the *writhe* of a diagram D

$$\text{writhe}(K) = \sum_c \epsilon(c)$$

where the sum is taken over all crossings c in the diagram of K and where K is oriented arbitrarily.

Exercise 1.4.19. Given a Legendrian knot L in $(\mathbb{R}^3, \xi_{std})$ show that one can compute the Thurston-Bennequin invariant of L by

$$\mathrm{tb}(L) = \mathrm{writhe}(\pi(L)) - \text{ number of left cusps.}$$

Hint: Consider Example 1.4.18.

Turning to the rotation number notice that $\xi_{std} = \mathrm{span}\left\{\frac{\partial}{\partial y}, \frac{\partial}{\partial x} + y\frac{\partial}{\partial z}\right\}$. So the contact plane field is trivialized by the vectors $\frac{\partial}{\partial y}$ and $\frac{\partial}{\partial x} + y\frac{\partial}{\partial z}$ and this, of course, induces a trivialization on any Seifert surface for a Legendrian knot. So we can compute the rotation number of a Legendrian knot L by counting how many times the oriented tangent vector to the knot passes the line l_y spanned by $\frac{\partial}{\partial y}$ in ξ_{std}. Note, that since the rotation number is a degree, we should only count the number of times the tangent vector passes the ray spanned by $\frac{\partial}{\partial y}$, but we will find it easier to compute the number of times it passes the line and then divide by 2. If the oriented tangent to L passes the line l_y in an anti-clockwise direction, then it contributes a +1 to the degree and if it passes in a clockwise direction, then it will contribute a -1 to the degree.

Exercise 1.4.20. Prove that all the claims above about computing the rotation number are true.

Notice that at points in the front projection of the Legendrian knot L that are not at a cusp, there is always a component of the tangent vector in the x-direction and thus it does not contribute to the degree. If we assume that all the cusps are horizontal (which one can easily see is possible), then each cusp will contribute to a crossing of the tangent vector to L with the line l_y. See Figure 1.4.9. Thus we see that the rotation number of L can be computed by

$$\mathrm{rot}(L) = \frac{1}{2}(D_L - U_L), \tag{1.4.3}$$

where as one traverses the knot in the direction of the orientation, D_L is the number of cusps passed going downwards, and U_L is the number of cusps passes going upwards.

Example 1.4.21. We now consider several examples of Legendrian knots that are smoothly isotopic to the unknot. See Figure 1.4.10. Notice that $\mathrm{tb}(L_1) = \mathrm{tb}(L_2) = -1$ and $\mathrm{tb}(L_3) = \mathrm{tb}(L_4) = \mathrm{tb}(L_5) = -2$, while $\mathrm{rot}(L_1) = \mathrm{rot}(L_2) = 0$ and $-\mathrm{rot}(L_3) = \mathrm{rot}(L_4) = \mathrm{rot}(L_5) = -1$. Thus we see that L_1 and L_2 are not Legendrian isotopic (or contactomorphic) to L_3, L_4, or L_5 since they have distinct Thurston-Bennequin invariants. Similarly, L_3 is not Legendrian isotopic (or contactomorphic) to L_4 or L_5 since they have distinct rotation numbers. But notice that L_1 and L_2 have the same classical invariants as do L_4 and L_5.

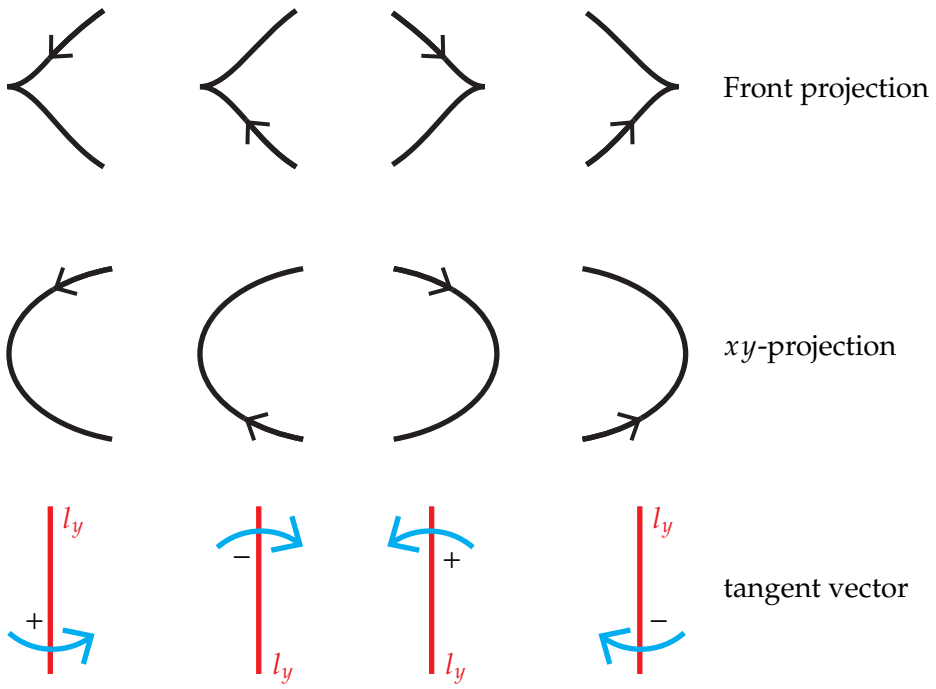

Figure 1.4.9. Cusps in the front projection are shown in the top row. In the second row we see the projection of the cusps to the xy-plane. As ξ_{std} projects isomorphically to the xy-plane and l_y projects to the y-axis, we see in the bottom row the rotation of the oriented tangent vector to L near a cusp.

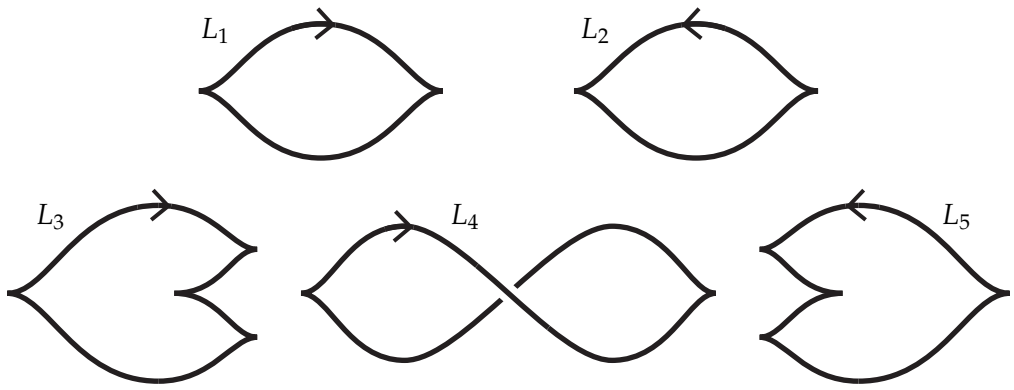

Figure 1.4.10. Legendrian realizations of the unknot.

In the above example, we are left to wonder if L_1 and L_2 are isotopic and similarly for L_4 and L_5. When working with front diagrams of a Legendrian knots we have a sequence of moves that will relate diagrams of the same Legendrian knot.

Theorem 1.4.22 (Świątkowski 1992, [Ś92]). *Two Legendrian knots L_1 and L_2 in $(\mathbb{R}^3, \xi_{std})$ are Legendrian isotopic if and only if their front diagrams are related by a sequence of moves shown in Figure 1.4.11 and ambient isotopies.*

We will not rely on this theorem much in this book and only state it here for reference and to give a few exercises that show it can be difficult to use this theorem to see if two Legendrian knots are Legendrian isotopic. We will prove various classification theorems for Legendrian knots later in this book that will make some of the exercises below trivial. We refer to the original paper cited in the theorem for a proof of this result.

Exercise 1.4.23. Show that L_0 and L_1 from Example 1.4.21 are Legendrian isotopic. Show that L_4 and L_5 from the same example are Legendrian isotopic.

Exercise 1.4.24. Show that the formulas for the Thurston-Bennequin invariant and rotation number of a Legendrian knot in terms of front diagrams are indeed invariants of Legendrian isotopy by using Theorem 1.4.22.

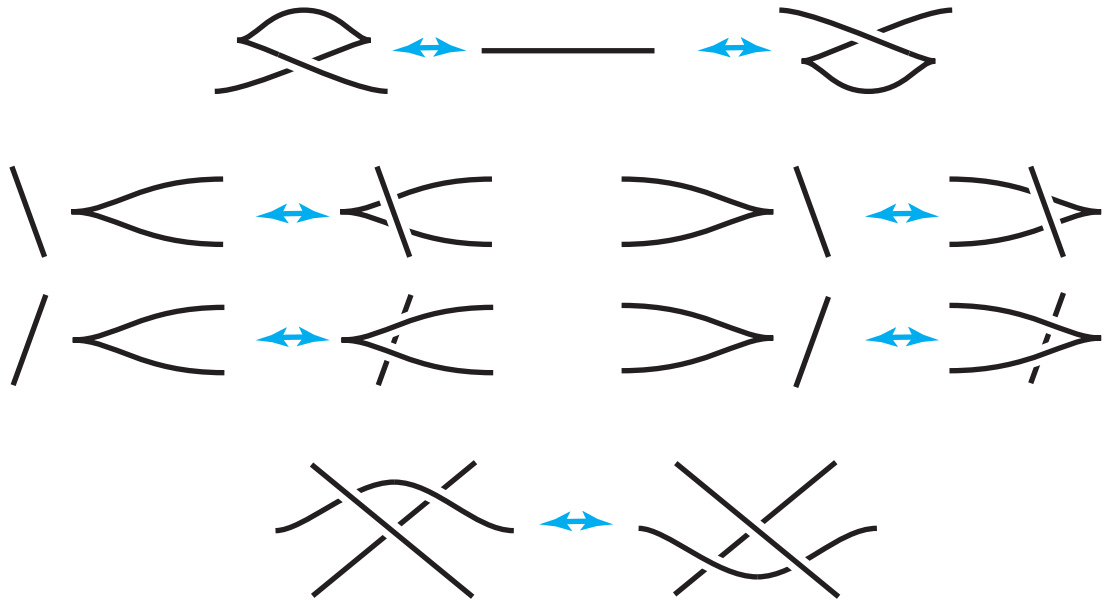

Figure 1.4.11. Legendrian Reidemeister moves. The diagrams indicate a segment of a Legendrian front diagram and one may replace that segment with the indicated segment to obtain an isotopic Legendrian knot. In the top row we see a Type I move, in the middle two rows we see a Type II move, and in the last row is a Type III move.

Exercise 1.4.25. Show that the two front diagrams shown in Figure 1.4.12 are Legendrian isotopic.

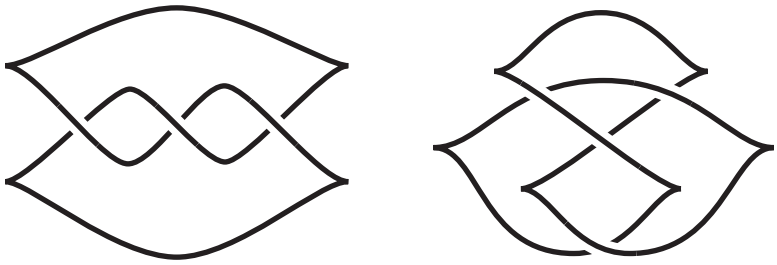

Figure 1.4.12. Two diagrams of Legendrian realizations of the right-handed trefoil.

Given a Legendrian knot L there is an easy way to construct other Legendrian knots in the same knot type as L. Specifically, we define *positive, respectively negative, stabilization* of L by altering the front projection of L as shown in Figure 1.4.13. We will denote the

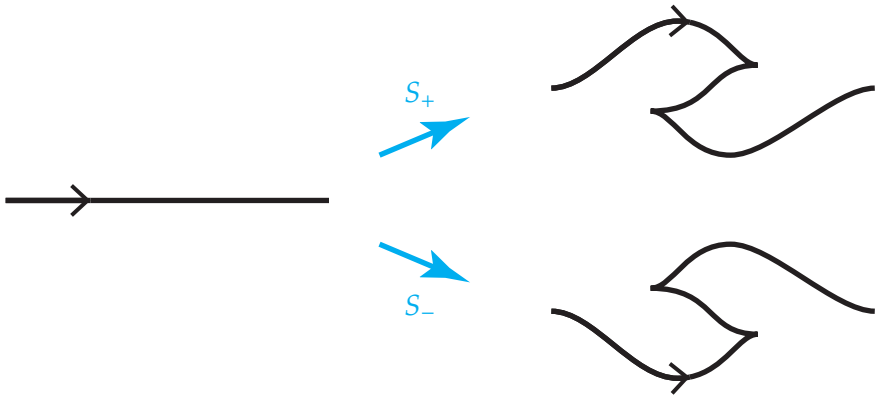

Figure 1.4.13. Positive and negative stabilization of L.

positive stabilization of L by $S_+(L)$ and the negative stabilization by $S_-(L)$.

Exercise 1.4.26. Show that stabilization is well-defined for Legendrian knots in $(\mathbb{R}^3, \xi_{std})$. That is it does not depend on where the stabilization is done on the knot and how large the "zig-zag" is.

It is clear from the figure that the classical invariants of L change as follows under stabilization

$$\mathrm{tb}(S_\pm(L)) = \mathrm{tb}(L) - 1 \text{ and } \mathrm{rot}(S_\pm(L)) = \mathrm{rot}(L) \pm 1.$$

Thus we see that a knot that can be realized by a Legendrian knot (which we will see in the next section is all knots) has infinitely many distinct Legendrian realizations by stabilizing a given one. We can also define stabilizations of Legendrian knots in any contact manifold.

Lemma 1.4.27. *Let L be an oriented Legendrian knot in a contact manifold (M, ξ). Then the positive, respectively negative, stabilization of L is well-defined and we denote it by $S_+(L)$, respectively $S_-(L)$.*

Proof. By Theorem 1.2.6 L in M has a neighborhood N contactomorphic to a neighborhood N' of a Legendrian knot L' in $(\mathbb{R}^3, \xi_{std})$. The stabilization defined above for L' can be carried out inside the neighborhood N' and hence the image of the stabilization in N will be the stabilization of L. □

1.4.4. Legendrian and transverse approximations. In this section we will consider how to approximate smooth knots by Legendrian and transverse knots and also see some relations between Legendrian and transverse knots. We start with transverse push-offs of Legendrian knots.

Lemma 1.4.28. *Any oriented Legendrian knot L is C^∞ close to a positive (respectively negative) transverse knot, denoted L_+ (respectively L_-). Moreover, $L_\pm$ is uniquely determined by the Legendrian isotopy type of L up to transverse isotopy.*

We call L_+ the *(positive) transverse push-off* of L, and similarly for L_-.

Proof. Let $A = S^1 \times [-1, 1]$ be an annulus containing L as $S^1 \times \{0\}$ that is tangent to ξ along L and transverse to ξ elsewhere (it is easy to construct A, see below). The characteristic foliation on A is shown in Figure 1.4.14. We see that $L_\pm = S^1 \times \{\mp\epsilon\}$ is a transverse knot

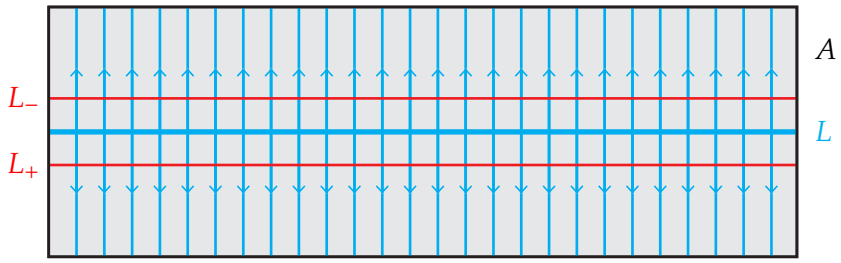

Figure 1.4.14. The positive and negative transverse push-off of L. The annulus A is obtained by identifying the right and left edges of the figure.

and if $L_\pm$ is oriented in the same direction as L then L_+ is a positive transverse knot and L_- is a negative transverse knot. If A' is another such annulus, then note that A and A' are tangent along L. Let $L'_\pm$ be the transverse knots on A'. We can isotope A and A' to agree in a neighborhood of L and this isotopy can be chosen to be disjoint from $L_\pm$ and $L'_\pm$. We now see that we can transversely isotope $L_\pm$ on A into the region where the annuli agree and then further transversely isotop it on A' to agree with $L'_\pm$. Thus the transverse knot $L_\pm$ does not depend, up to transverse isotopy, on the specific annulus chosen to define it. And if L and L' are Legendrian isotopic then we can find an ambient contact isotopy

that will take the annulus for L to one for L' and thus the transverse isotopy class of $L_\pm$ depends only on the Legendrian isotopy class of L.

Recall that any two Legendrian knots have contactomorphic neighborhoods by Theorem 1.2.6. Thus we may assume our Legendrian knot L has a neighborhood N contactomorphic to $S_a = \{(x,y,z) \in \mathbb{R}^3/\sim \, | y^2+z^2 \leq a^2\}$ with the contact structure $\ker(dz - y\,dx)$ and where $(x,y,z) \sim (x+1,y,z)$. Now the annulus $A = \{(x,y,z) \in \mathbb{R}^3/\sim \, | z = 0 \text{ and } y \leq \epsilon\}$ gives the annulus described above. □

One can determine the classical invariant of the transverse push-off of a Legendrian knot from those of the Legedrian knot.

Lemma 1.4.29. *If L is an oriented null-homologous Legendrian knot in a contact manifold (M,ξ), and L_+ is its positive transverse push-off, then*

$$\mathrm{sl}(L_+) = \mathrm{tb}(L) - \mathrm{rot}(L).$$

Proof. Let Σ be a Seifert surface for L. To compute $\mathrm{rot}(L)$ we choose a non-zero vector field t in $\xi|_\Sigma$ and let v be a non-zero vector field along L that agrees with the orientation on L. Then the rotation number of L is simply the twisting of v relative to t in ξ along L. We denote this $\mathrm{rot}(L) = \mathrm{tw}(v,t;\xi)$. Similarly in the normal bundle $\nu(L) \subset TM|_L$ we can choose a non-zero vector field s pointing out of Σ and w a vector field in $\xi|_L$ that is transverse to v and contained in $\nu(L)$. Then the Thurston-Bennequin invariant of L is simply the twisting of w relative to s in $\nu(L)$. That is $\mathrm{tb}(L) = \mathrm{tw}(w,s;\nu(L))$.

Notice that t can be extended to a neighborhood of Σ as a non-zero vector field in ξ. Similarly, v and w can be extended to a neighborhood of L as non-zero vector fields in ξ. Thus we see that we have vector fields t_+, v_+, w_+ in $\xi|_{L_+}$ since L_+ is arbitrarily close to L. Notice that since L_+ is positively transverse then we can identify $\xi|_{L_+}$ and $\nu(L_+)$. Since a framing on a knot induces one on all nearby knots, we have a section s_+ of the normal bundle of L_+ coming from s along L, and hence s_+ is the Seifert framing on L_+. We know that the self-linking number $\mathrm{sl}(L_+)$ is the twisting of t_+ relative to s_+ in $\nu(L_+)$. Thus

$$\begin{aligned}\mathrm{sl}(L_+) &= \mathrm{tw}(t_+,s_+;\nu(L_+)) = \mathrm{tw}(t_+,w_+;\nu(L_+)) + \mathrm{tw}(w_+,s_+;\nu(L_+))\\ &= \mathrm{tw}(t_+,w_+;\xi|_{L_+}) + \mathrm{tw}(w_+,s_+;\nu(L_+))\\ &= \mathrm{tw}(t,w;\xi|_L) + \mathrm{tw}(w,s;\nu(L)) = -\mathrm{rot}(L) + \mathrm{tb}(L).\end{aligned}$$

In the first equality on the third line we note that the twisting of w and v past t is the same. Thus establishing the claimed formula. □

Exercise 1.4.30. Prove that $\mathrm{sl}(L_-) = \mathrm{tb}(L) + \mathrm{rot}(L)$.

To a transverse knot there is not a unique Legendrian associated to it, but it can be approximated by many different Legendrian knots.

Lemma 1.4.31. *If T is a transverse knot then there is a Legendrian knot L such that its positive transverse push-off L_+ is transversely isotopic to T.*

Proof. By Theorem 1.2.4 any transverse knot T has a neighborhood N contactomorphic to a neighborhood N' of the z-axis in $S^1 \times \mathbb{R}^2 = \mathbb{R}^3/\sim$, where $(x, y, z) \sim (x, y, z + 1)$, with the contact structure $\xi = \ker(dz + r^2 d\theta)$. Let $T_a = \{(r, \theta, z) | r = a\}$. There is a k such that for $a < k$ the torus T_a is in N'. Moreover there is an $a < k$ such that $(T_a)_\xi$ is a foliation by curves of slope n for some large negative n. Here "slope n" means that the curve is in the homology class of $[S^1 \times \{p\}] + n[\{q\} \times \partial D^2]$ for some $p \in \partial D^2$ and $q \in S^1$. See Section 4.1 for more on our slope conventions. One may easily check that inside N one may realize any sufficiently negative slope. See Figure 1.4.15. Let L be a leaf in this foliation. Clearly L is Legendrian. Let A be an annulus inside T_a that has one boundary

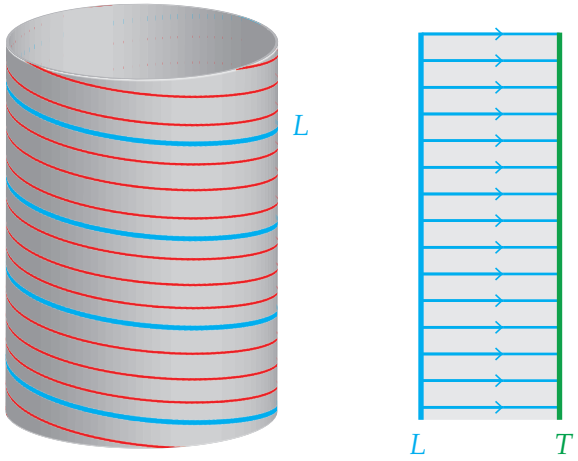

Figure 1.4.15. The torus T_a on the left with one leaf in its characteristic foliations highlighted. On the left is the annulus A that shows T is the transverse push-off of L.

component on L and the other on the z-axis. One may easily check that the foliation is as pictured in Figure 1.4.14. So, by definition, the z-axis which we can think of as T, is the positive transverse push off of L. □

We call a Legendrian L constructed in the proof a *Legendrian approximation* of T.

Exercise 1.4.32. In the proof if L_n is a Legendrian approximation coming from the torus with slope n characteristic foliation and L_{n-1} is the one coming from a torus with slope $n - 1$ characteristic foliation, then show that L_{n-1} is a negative stabilization of L_n.

Remark 1.4.33. In Section 6.1 we will see that L_+ and L'_+ are transversely isotopic if and only if L and L' are related by negative stabilizations. So classifying transverse knots in a knot type is equivalent to classifying Legendrian knots in that knot type up to negative stabilizations.

Lemma 1.4.34. *Any knot (or arc) can be C^0-approximated by a Legendrian knot and a transverse knot.*

Proof. Consider curves on $(\mathbb{R}^3, \xi_{std} = \ker(dz - y\,dx))$. We will begin with an example. Consider a curve C sitting in the $y = 0$ plane and having slope -1. See Figure 1.4.16. If we consider the projection of C to the xz-plane and let C' be the Legendrian curve

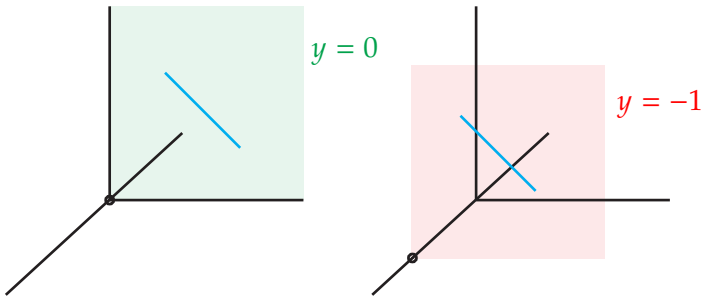

Figure 1.4.16. The smooth curve C sitting in the $y = 0$ plane and the curve C' sitting in the $y = -1$ plane that is the Legendrian lift of C.

with the same projection (we call this the Legendrian lift of the curve on the xz-plane, and obtained by taking the y-coordinate to be the slope of the curve on the xz-plane, see Section 1.4.3), then C' will sit in the $y = -1$ plane. We need to find a curve D_C in the xz-plane whose Legendrian lift is C^0-close to C. We can take D_C to be a curve in a small neighborhood of C that has all of its tangent lines having slopes close to zero. This is done by creating several zig-zags in the curve. See Figure 1.4.17. The Legendrian lift of

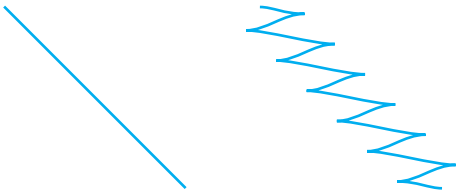

Figure 1.4.17. The smooth curve C sitting in the $y = 0$ plane and the curve D_C in the $y = 0$ plane that lifts to the approximation L_C of C.

D_C, which we denote L_C, is a Legendrian arc that is C^0-close to C. Notice that we do not need to move the endpoints of C to create L_C.

Exercise 1.4.35. Prove that any arc in $\mathbb{R}^3$ can be approximated by a Legendrian arc relative to its endpoints.
Hint: Note that an arc may be subdivided into pieces where the slope of the tangent line to the arc is almost constant. Now slightly generalize the above argument to this setting.

We now consider an arc C in a general contact manifold (M, ξ). Notice that we can cover C by Darboux charts. That is open sets U_i that are contactomorphic to open sets

in $(\mathbb{R}^3, \xi_{std})$. Now C can be subdivided into compact sub-arcs such that each subarc is contained in one of the Darboux charts. Now we can approximate each of these sub-arcs, relative to their endpoints, using the argument above.

Finally, using Lemma 1.4.28 we can also approximate any topological knot by a transverse knot. □

Remark 1.4.36. We will see in Section 6.1 that two Legendrian knots L and L' represent the same topological knot type if and only if they are related by some number of positive and negative stabilizations.

Exercise 1.4.37. Prove the fact in the remark for Legendrian knots in $(\mathbb{R}^3, \xi_{std})$ using front projections.

1.4.5. Classification of Legendrian and transverse knots. We end this section by discussing the classification of Legendrian and transverse knots. Given a smooth knot type $\mathcal{K}$ in a contact manifold (M, ξ) we will denote the set of Legendrian knots realizing the knot type $\mathcal{K}$ by $\mathcal{L}(\mathcal{K})$. (It is common to denote an isotopy class of knots by a fixed representative of that knot type, say K a fixed embedded of S^1 into M. While we will do this as well, for now, we would like to emphasize that we are discussing an isotopy class of embeddings of S^1 by using the notation $\mathcal{K}$.) There is an obvious map

$$\Psi\colon\ \mathcal{L}(\mathcal{K}) \to \mathbb{Z}\times\mathbb{Z}\colon\ L \mapsto (\mathrm{rot}(L), \mathrm{tb}(L)).$$

Classifying Legendrian representatives of $\mathcal{K}$ is equivalent to understanding the image of Ψ, the number of points mapping to a given point in the image, and how two distinct elements in $\mathcal{L}(\mathcal{K})$ mapping to the same point are related by stabilization. The first problem is called the *geography problem* for $\mathcal{K}$ and the second problem is called the *botany problem* for $\mathcal{K}$.

A knot type $\mathcal{K}$ is called *Legendrian simple* if Ψ is injective. Notice that this implies that two Legendrian knots in the knot type are Legendrian isotopic if and only if they have the same rotation numbers and Thurston-Bennequin invariants. In Chapter 6 we will show that the unknot and torus knots are Legendrian simple. It is also known that the figure eight knot is Legendrian simple [**EH01a**]. In Chapter 10 we will see that many cables of torus knots and connected sums are not Legendrian simple. It is also known that negative twist knots are not Legendrian simple [**Che02, EGH00, ENV13**] while positive ones are [**ENV13**].

We now consider a few Legendrian knots in $(\mathbb{R}^3, \xi_{std})$ to get a sense of what the classification of Legendrian knots looks like. We will see much more in Chapters 6 and 10.

Example 1.4.38. Let $\mathcal{U}$ be the knot type of the unknot. Eliashberg and Fraser [**EF98, EF09**] showed that the unknot is Legendrian simple and every Legendrian unknot is a

stabilization of the one shown of the left-hand side of Figure 1.4.6. Thus we see the image of Ψ in this case is shown in Figure 1.4.18.

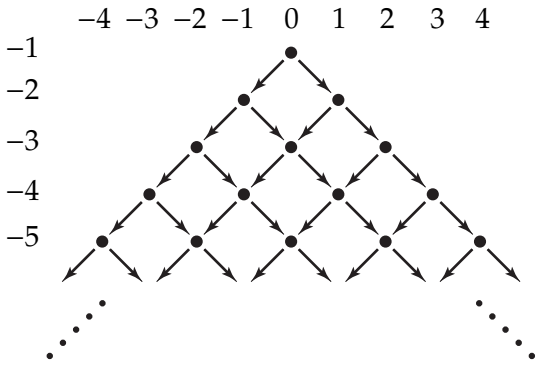

Figure 1.4.18. The image of Ψ for the unknot.

In [**EH01a**], the first author and Honda showed that torus knots were Legendrian simple and classified them. For example, the $(4,-9)$-torus knot has four Legendrian representatives with $\mathrm{tb} = -36$, they have rotation numbers $-5, -3, 3$, and 5. See Figure 1.4.19. All other Legendrian representatives are stabilizations of these. See Figure 1.4.20 for the

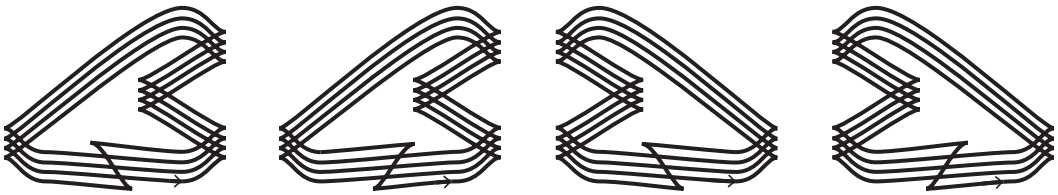

Figure 1.4.19. The four Legendrian $(4,-9)$-torus knots with $tb = -36$. Moving from left to right the rotation numbers are $-5, -3, 3$, and 5.

image of Ψ in this case. See Chapter 6 for notation concerning torus knots, and the classification of Legendrian representatives.

We now consider a non-Legendrian simple knot type. Let $\mathcal{K}$ representatives the $(3,2)$-cable of the right-handed trefoil knot. You can see Legendrian representatives of these knots in Figure 1.4.21 and you can find a general discussion of cables in Section 10.2. In [**EH05**], the first author and Honda classified Legendrian representatives of $\mathcal{K}$ and showed that the image of Ψ for $\mathcal{L}(\mathcal{K})$ is shown in Figure 1.4.22. Notice that some points in $\mathbb{Z}\times\mathbb{Z}$ have more than one representative and that they correspond to rotation numbers and Thurston-Bennequin invariants that are represented by distinct Legendrian knots. Notice that the figure also denotes how Legendrian representatives are related under stabilization. Of course, an arrow pointing to the right is a positive stabilization while an arrow pointing to the left is a negative stabilization. We will see much more about cables of torus knots in Chapter 10.

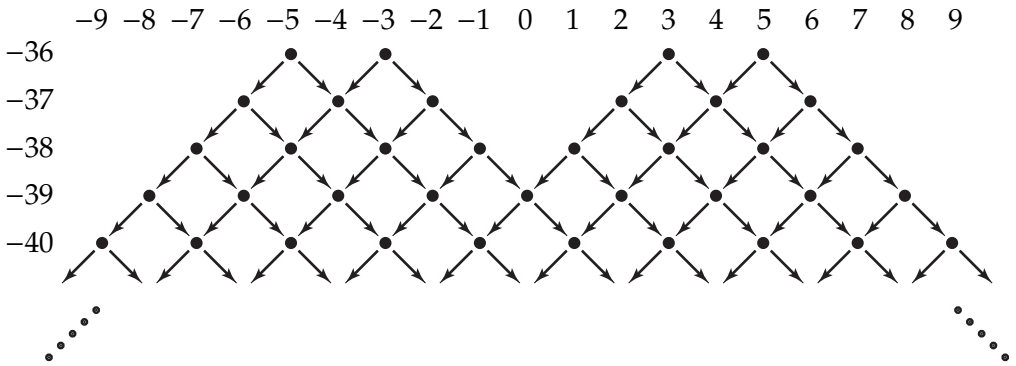

Figure 1.4.20. The image of the map Ψ for the $(4,-9)$-torus knot. The four dots at the top are realized by the Legendrian knots in Figure 1.4.19.

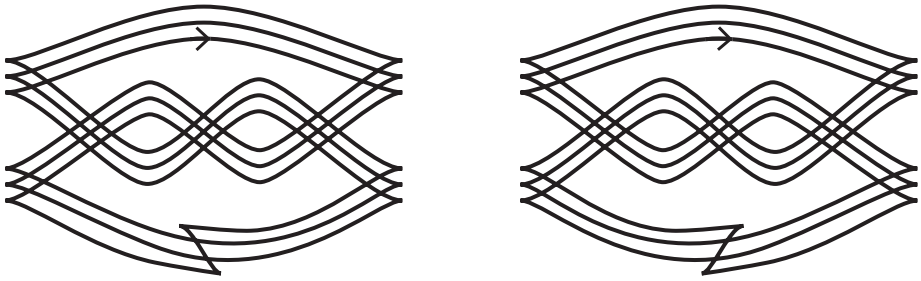

Figure 1.4.21. Two Legendrian knots realizing the $(3,2)$-cables of the right-handed trefoil with tb = 6. The rotation numbers going from left to right are -1 and 1.

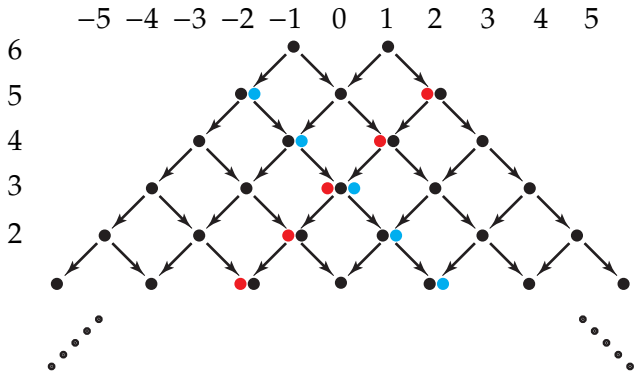

Figure 1.4.22. The image of the map Ψ for the $(3,2)$-cable of the right-handed trefoil.

Given the figures above, the image of Ψ for a given knot type $\mathcal{K}$, along with an indication of the multiplicity of each point and stabilization information is frequently referred to as the *mountain range* of $\mathcal{K}$. The classification of Legendrian representatives is frequently easier to understand by considering the mountain range than by explicitly

stating what all the Legendrian representatives are. We will see such statements in Chapters 6 and 10 and also see how these translate into the easier to understand mountain range. We will also explore general properties of mountain ranges in Section 10.3.

We can study transverse knots in the same way. Given a knot type $\mathcal{K}$ we consider the set of transverse isotopy classes of transverse knots realizing $\mathcal{K}$ and denote this set $\mathcal{T}(\mathcal{K})$. In this case we have a map

$$\Phi\colon\ \mathcal{T}(\mathcal{K}) \to \mathbb{Z}\colon\ T \mapsto \mathrm{sl}(T).$$

We similarly say that a knot type is *transversely simple* if Φ is injective. So two transverse knots in a transversely simple knot type are transversely isotopic if and only if their self-linking numbers are the same.

Example 1.4.39. Recalling from Remark 1.4.33 that the classification of transverse knots is equivalent to the classification of Legendrian knots up to negative stabilization, we see that the unknot and torus knots are transversely simple. In particular, the image of Φ for the unknot is the set of negative odd integers, while the image of Φ for the $(4,-9)$-torus knot is the set of odd integers less than or equal to -31.

We see that the $(3,2)$-cable of the right-handed trefoil is not transversely simple. The image of Φ for this knot type is the set of odd integers less than or equal to 7 and Φ is injective except that there are two transverse knots with self-linking number 3.

Transversely non-simple knots, and the general structure of the classification of transverse knots, will be discussed more in Chapter 10.

1.5. Existence of contact structures on 3-manifolds

In this section we will prove that any orientable closed 3-manifold admits a contact structure. In fact, we will see that in any homotopy class of plane field, we can find a contact structure; so, in particular, such manifolds admit infinitely many distinct contact structures. In Subsection 1.5.1 we will briefly review some facts about Dehn surgery and use that to prove that an orientable closed 3-manifold admits at least one contact structure. In the next subsection we will discuss homotopy classes of plane fields on an orientable 3-manifold and in particular discuss invariants of plane fields Finally, in Subsection 1.5.3 we will prove that every homotopy class of plane field on an orientable 3-manifold contains at least one contact structure.

1.5.1. Constructing contact structures on 3-manifolds. We will construct contact structures through surgery on S^3, thus we begin by reviewing the Dehn surgery construction. We will review more facts about Dehn surgery later in the chapter (and later in the book),

but the reader is referred to [GS99, PS97, Rol76, Sav12] for a more comprehensive discussion of Dehn surgery as well as proofs of the various facts we are using about Dehn surgery.

Given a 3-manifold M and a knot K in M, let $N = S^1 \times D^2$ be a neighborhood of K in M. If α is an embedded curve in $\partial\overline{(M-N)}$ and $f\colon \partial(S^1 \times D^2) \to \partial N \subset \partial\overline{(M-N)}$ is a diffeomorphism sending $\{p\} \times \partial D^2$ to a curve isotopic to α for any point $p \in S^1$, then we say the manifold $M_K(\alpha)$ is obtained from M by *α-Dehn surgery on K* if

$$M_K(\alpha) = (\overline{M-N}) \cup_f (S^1 \times D^2)$$

where $(\overline{M-N}) \cup_f (S^1 \times D^2)$ is the quotient space of $(\overline{M-N}) \cup (S^1 \times D^2)$ obtained by identifying $x \in \partial(S^1 \times D^2)$ with $f(x) \in \overline{M-N}$.

Dehn Surgery Facts. We have the following well-known results about Dehn surgery.

(1) If f_0 and f_1 are two diffeomorphisms $\partial(S^1 \times D^2) \to \partial N \subset \partial\overline{(M-N)}$ that both send $\{p\}\times\partial D^2$ to a curve isotopic to α, then $(\overline{M-N})\cup_{f_0}(S^1\times D^2)$ is diffeomorphic to $(\overline{M-N}) \cup_{f_1} (S^1 \times D^2)$

(2) Any closed oriented 3-manifold can be obtained from S^3 by Dehn surgery on some link.

Exercise 1.5.1. Prove these facts. The second one requires a bit of work, see [Rol76].

We note that $\partial N = T^2$ and there is a non-trivial curve μ in T^2 that bounds a disk in $N \cong S^1 \times D^2$. If K is null-homologous then there is also a curve λ in T^2 that bounds a surface Σ in $\overline{M-N}$.

Exercise 1.5.2. Show that μ and λ can be chosen to intersect exactly once.

If K is not null-homologous, then we can choose a curve λ such that μ and λ intersect once (recall, this is just choosing a framing on K).

The homology classes of μ and λ form a basis for $H_1(T^2) \cong \mathbb{Z} \oplus \mathbb{Z}$. So any embedded simple closed curve α in T^2 has a homology class that can be expressed by $q[\lambda]+p[\mu]$. We will denote the curve α by p/q (with the convention that $1/0 = \infty$). For a more thorough discussion of rational numbers and curves on tori see Section 4.1. Now we can denote $M_K(\alpha)$ by $M_K(p/q)$. For our arguments below, we note that the diffeomorphism f used in the definition of Dehn surgery can be taken to be a linear map (that is, thinking of T^2 as $\mathbb{R}^2/\mathbb{Z}^2$ the diffeomorphism is induced by a linear map on $\mathbb{R}^2$).

For later use, we note several ways one can change a Dehn surgery description of a manifold. See Figure 1.5.23 for the first two of these moves and Figure 1.5.24 for the third. The proof that these moves do not affect the result of Dehn surgery can be found in [Rol76]. The first change one can make is called the *slam-dunk* and is shown on the left of the figure.

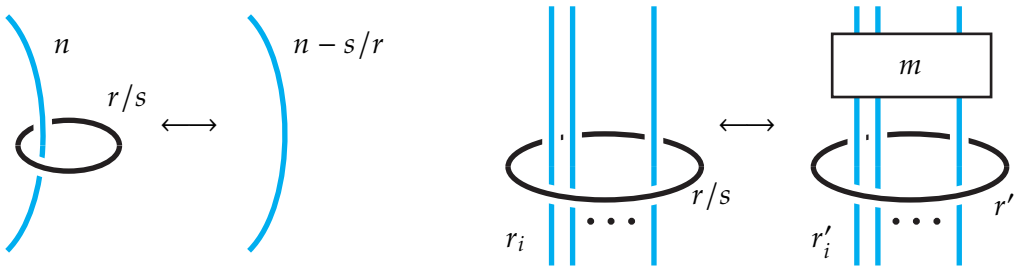

Figure 1.5.23. The slam-dunk move is shown on the left, here n, r, and s are integers. The Rolfsen twist is shown on the right, here m, r, and s are integers and r_i, r_i' are rational numbers. The blue curves correspond to knots $K_1, \dots, K_l$, and each knot can go through the region multiple times. The framing on K_i is r_i. The framings $r_i' = r_i + m(\text{link}(K_i, U))^2$, $r' = r/(s + mr)$, and the box labeled m indicates m full right-handed twists.

Exercise 1.5.3. Use the slam-dunk move to show that any 3-manifold can be obtained from S^3 by Dehn surgery on a link with integer coefficients, that is we do not need to consider general rational Dehn surgery coefficients.

The second change one can make to a surgery description is called a *Rolfsen twist* and is shown on the right-hand side of the figure. The third change is shown in Figure 1.5.24 and is called a handle slide. The figure is schematic in the sense that K_1 and K_2 might

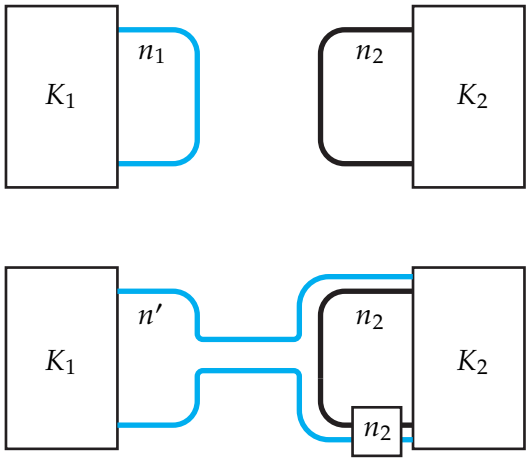

Figure 1.5.24. The top diagram and the bottom diagram represent equivalent surgery diagrams. The n_2 in the box represents n_2 full twists between the blue and the black curves.

link even though that is not shown in the diagram. It is important that both surgery coefficients are integers. The surgery coefficient n' in the figure is

$$n' = n_1 + n_2 \pm \text{link}(K_1, K_2),$$

one must orient K_1 and K_2 to perform this operation and the sign in the formula is + if the orientation on the blue curve in the bottom diagram can be chosen to agree with

the orientation on K_1 and K_2, otherwise the $-$ sign is used. (Note that since link(K_1, K_2) changes sign if we reverse the orientation on one of the components and the sign in the formula changes, then framing n' is actually independent of the chosen orientations.)

We are now ready to bring contact structures into the picture.

Theorem 1.5.4 (Martinet, 1971, [Mar71]). *Any closed, oriented* 3*-manifold has a contact structure*

Proof. Given a closed, oriented 3-manifold M we know from above that it can be realized by Dehn surgery on some link in S^3. We will consider the case where M is Dehn surgery on a knot $S^3_K(p/q)$, but the general case will clearly follow.

First we note that by Lemma 1.4.34 we can isotop K to be a transverse knot in the standard contact structure ξ_{std} on S^3. By Theorem 1.2.4 we know that the transverse knot K has a standard neighborhood. More specifically, if we let $\mathbb{R}^2 \times S^1 = \mathbb{R}^3/\sim$, where $(r, \theta, z) \sim (r, \theta, z + 2\pi)$ with the contact structure $\xi = \ker(\cos r\, dz + r \sin r\, d\theta)$ then $T = \{(0,0)\} \times S^1$ is a transverse curves and K has a neighborhood N contactomorphic to $S_a = \{(r, \theta, z) | r \leq a\}$. We note that ∂S_a has a characteristic foliation of slope $\frac{1}{a} \cot a$ so as a goes from 0 to ∞ the possible slopes of the characteristic foliation trace out all rational numbers (and ∞) infinitely many times.

Now let f be a linear map from $\partial(S^1 \times D^2)$ to $\partial\overline{(S^3 - N)}$ that is used to define $S^3_K(p/q)$. Notice that there is some linear foliation of slope s on T^2 that f will map to the characteristic foliation on $\partial N = \partial S_a$. Notice that there is some $b \in (0, \infty]$ (actually in $(0, \pi]$) so that the characteristic foliation on ∂S_b has slope s. Since the characteristic foliation on a surface determines the contact structure in a neighborhood of the surface by Theorem 1.3.4, we can glue $(S_b, \xi|_{S_b})$ to $(\overline{S^3 - N}, (\xi_{std})|_{\overline{S^3 - N}})$ to obtain a contact structure on M.

To be careful that we have a smooth contact structure on M, one should glue "with overlap". Specifically. Theorem 1.3.4 says that we can extend f and isotop it so that it is a contactomorphism from $S_{b+\epsilon} - S_{b-\epsilon}$ to some open neighborhood of ∂N in S^3. Now we can glue $S_{b+\epsilon}$ to $S^3 - N$ were $S_{b+\epsilon} - S_b$ is glued to a neighborhood of ∂N in $\overline{M - N}$ via the extended f. On the level of the manifold, this is still clearly $S^3_K(p/q)$ but the contact structure induced on the surgered manifold is now smooth. In the future, we will give an argument as in the previous paragraph for constructing contact structures, but one should keep in mind that it is really shorthand for gluing "with an overlap" as just described. □

Exercise 1.5.5. Give a second proof that all closed, oriented 3-manifolds have a contact structure by using the fact that all closed, oriented 3-manifols are covers of S^3 branched over some link. See [Rol76] for the definition of branched cover and this fact.
Hint: Make the branch locus transverse.

Remark 1.5.6. We will give a third method to construct contact structures on 3-manifolds based on open book decompositions in Chapter 12.

Remark 1.5.7. We will see in Sections 6.2 and 12.2, respectively, that *all* contact structures on closed 3-manifolds can be constructed by surgery (a generalization of the one discussed above) and open books decompositions. It is also known that all contact structures can be constructed via branched covering S^3 over a link or knot, see **[Gir02]** and **[Cas13]**, respectively.

We would now like to strengthen this theorem to show that there is a contact structure in any homotopy class of plane field on M, but to do this we first study homotopy classes of plane fields and their invariants.

1.5.2. Homotopy classes of plane fields. In this section we will study the space of plane fields on 3-manifolds. To this end, given a 3-manifold M we define

$$\text{Dist}(M) = \{\text{oriented plane fields in } TM\}.$$

To formally define this space, we let $Gr_k(V)$ be the space of k-planes in the vector space V. One can topologize this just like projective space which is the space of lines in V (that is real projective space is $Gr_1(V)$). Notice that a linear map $L\colon V \to V$ induces a map on $Gr_k(V)$. Recall, that the tangent bundle TM of M is a vector bundle of rank 3 so the transition functions have range $GL(3;\mathbb{R})$ (see Appendix A for recollections about bundles) and thus we can consider the fiber bundle $Gr_2(TM)$ associated to the tangent bundle with fiber $Gr_2(T_xM)$. We call this the *Grassmann bundle of 2-planes in* TM. Now the formal definition of $\text{Dist}(M)$ is the space of sections of $Gr_2(TM)$.

Two plane fields are homotopic if they are connected by a path in $\text{Dist}(M)$. So since our task is to understand the homotopy classes of plane fields on M, we are interested in the path components of $\text{Dist}(M)$ which is commonly denoted

$$\pi_0(\text{Dist}(M)).$$

Our main result about this set is the following.

Proposition 1.5.8. *Given a closed, oriented 3-manifold M, one can fix a trivialization of TM to get a surjective map*

$$F\colon \pi_0(\text{Dist}(M)) \to H_1(M),$$

and for any $x \in H_1(M)$ we have

$$F^{-1}([\gamma]) \cong \mathbb{Z}/(2d(x)\mathbb{Z})$$

where $d(x)$ is the divisibility of x in $H_1(M)$ modulo torsion.

Remark 1.5.9. Notice that $0 \in H_1(M)$ for any manifold M and $d(0) = 0$ so $F^{-1}(0) \cong \mathbb{Z}$. This tells us that $\pi_0(\text{Dist}(M))$ is always an infinite set. So when we show that any homotopy class of plane field contains a contact structure, we will know that there are infinitely many distinct contact structures on any closed, oriented 3-manifold.

We may also use the proposition to see the $\pi_0(\text{Dist}(M))$ is in one-to-one correspondence with $\coprod_{x \in H_1(M)} \mathbb{Z}/(2d(x))\mathbb{Z}$.

There are a few steps in proving this proposition. We begin with a simple observation.

Lemma 1.5.10. *Given an oriented 3-manifold M and a Riemannian metric g on M and set U_gM to be the unit tangent bundle. There is a homeomorphism from sections of U_gM to the space of plane fields on M:*

$$\Psi_g \colon \Gamma(U_gM) \to \text{Dist}(M) \colon v \mapsto v^\perp$$

where $v^\perp$ is the plane field orthogonal to v. Moreover, this homeomorphism is well-defined up to isotopy.

Proof. The map is clearly well-defined given g. Given a plane field ξ there is a unique line field l_ξ orthogonal to ξ and since M and ξ are oriented so is l_ξ. Thus we can choose a unit vector field v in l_ξ that orients l_x. Clearly $\Psi_g(v) = \xi$ so Ψ is onto. Notice that the previous construction gives an inverse map Ψ_g^{-1} to Ψ_g and thus Ψ is a bijection.

Exercise 1.5.11. Review the topology on $\Gamma(U_gT)$ and $\text{Dist}(M)$ and show that Ψ_g and Ψ_g^{-1} are continuous.

Finally, notice that if g_0 and g_1 are two Riemannian metrics on M then $g_t = (1-t)g_0 + tg_1$ is a path of Riemannian metrics on M. There is a natural projection $U_{g_t}M \to U_{g_0}M$ given by sending a unit vector v in $U_{g_t}M$ to $v/|v|$ where $|v|$ is computed with respect to the metric g_0. This projection induces a bundle isomorphism and hence a homeomorphism between of sections of $U_{g_t}M$ and sections of U_{g_0}. Thus Ψ_{g_t} will be an isotopy from Ψ_{g_0} to Ψ_{g_1}. □

It is a well-known fact that the tangent bundle of an oriented 3-manifold M is trivial, see [**Kir89**]. If we fix a trivialization $TM \cong M \times \mathbb{R}^3$, then the unit tangent bundle is $M \times S^2$, and a section of U_gM is determined by a map $M \to S^2$. We denote the homotopy classes of maps from M to S^2 by

$$[M, S^2].$$

From our discussion above, once a trivialization of TM is fixed, we have the equality of sets

$$\pi_0(\text{Dist}(M)) = [M, S^2].$$

The Pontryagin-Thom construction is a way to study homotopy classes of maps from a manifold of any dimension to the k-sphere. We will consider the special case of $[M^3, S^2]$.

See [Mil65b] for the general case. To state the result we first define the framed cobordism group. A framed submanifold of an n-manifold X is pair $(K, \mathcal{F})$, where K is an oriented submanifold of X and $\mathcal{F}$ is a trivialization of its normal bundle. We say $(K_i, \mathcal{F}_i)$, $i = 0, 1$, are framed cobordant if there is a framed manifold $(K', \mathcal{F}')$ of $X \times [0, 1]$ such that

$$(K', \mathcal{F}') \cap (X \times \{i\}) = (K_i, \mathcal{F}_i)$$

and as oriented manifolds $\partial K' = K_1 \cup -K_0$ where $-K_0$ denotes K_0 with the opposite orientation. We denote by $\Omega_1^f(M)$ the set of framed 1-manifolds in M up to framed cobordisms.

Lemma 1.5.12. *For any closed 3-manifold M there is a bijection*

$$[M, S^2] \leftrightarrow \Omega_1^f(M).$$

Proof. Given $\phi\colon M \to S^2$ we can homotop ϕ so that it is transverse to the north pole $n \in S^2$. Let $\gamma = \phi^{-1}(n)$. This is a 1-manifold in M. Moreover, notice that $d\phi_x\colon T_xM \to T_nS^2$ is surjective for all $x \in \gamma$ since ϕ is transverse to n. Thus if we fix a basis v_1, v_2 for T_nS^2, then we can find vector fields $\tilde{v}_1(x), \tilde{v}_2(x)$ along γ so that the vectors are perpendicular to γ (in some Riemannian metric) and $d\phi_x(\tilde{v}_i(x)) = v_i$. It is easy to find these vector fields since $d\phi_x$ restricted to $(T_x\gamma)^\perp$ is an isomorphism onto T_nS^2. Then $\tilde{v}_1(x), \tilde{v}_2(x)$ give a framing $\mathcal{F}$ to γ. Thus we have a map

$$\Psi\colon [M, S^2] \to \Omega_1^f(M)\colon f \mapsto (\gamma, \mathcal{F}).$$

Exercise 1.5.13. Show that Ψ is well-defined. More specifically, show that if ϕ_0 and ϕ_1 are homotopic maps then the associated framed 1-manifolds are framed cobordant.

We now show that Ψ is surjective. To this end let $(\gamma, \mathcal{F})$ be a framed 1-manifold in M. Notice that γ has a neighborhood N that is canonically, up to isotopy, identified with $S^1 \times D^2$ by the framing $\mathcal{F}$. We have the map

$$D^2 \to S^2\colon (r, \theta) \mapsto (\sqrt{1 + (r-1)^2}\cos\theta, \sqrt{1 + (r-1)^2}\sin\theta, r)$$

that maps the interior of D^2 homeomorphically onto $S^2 - \{s\}$ where s is the south pole and maps the boundary of D^2 to s. We can now set $\phi\colon N \to S^2$ to be this map on each D^2 in $S^1 \times D^2 = N$. Now extend ϕ over $M - N$ to be constantly s. Notice that ϕ is smooth on the interior of N and hence we can perturb ϕ to be smooth on all of M so that $M - N$ still maps to a small neighborhood of s and the perturbation was fixed on almost all of N. Thus n is a regular value of ϕ and clearly $\Psi(\phi) = (\gamma, \mathcal{F})$, so Ψ is surjective.

We now show that Ψ is injective. Suppose that $\Psi(\phi_0) = (\gamma_0, \mathcal{F}_0)$ and $\Psi(\phi_1) = (\gamma_1, \mathcal{F}_1)$.

Exercise 1.5.14. Show that if $(\gamma_0, \mathcal{F}_0) = (\gamma_1, \mathcal{F}_1)$. Then ϕ_0 and ϕ_1 are homotopic.

More generally suppose that $(\gamma_0, \mathcal{F}_0)$ is framed cobordant to $(\gamma_1, \mathcal{F}_1)$ via the framed cobordism $(\Sigma, \mathcal{F})$.

Exercise 1.5.15. Construct a homotopy $M \times [0,1] \to S^2$ of ϕ_0 to ϕ_1 using $(\Sigma, \mathcal{F})$.
Hint: From the previous exercise, you can assume that ϕ_i are the maps constructed above associated with $(\gamma_i, \mathcal{F}_i)$. Now the construction of the homotopy is essentially the same as the construction of ϕ form $(\gamma, \mathcal{F})$ above.

Thus $\Psi(\phi_0) = \Psi(\phi_1)$ implies that ϕ_0 is homotopic to ϕ_1 and hence Ψ is injective. □

Remark 1.5.16. Combining Lemmas 1.5.10 and 1.5.12 we see that there is a one-to-one correspondence between $\pi_0(\mathrm{Dist}(M))$ and $\Omega_1^f(M)$ and this correspondence is determined by a trivialization of TM.

We now study $\Omega_1^f(M)$ further. To this end, we consider the set of *cobordism classes* of 1-manifolds in M, denoted by $\Omega_1(M)$. The definition of cobordism classes is the same as framed cobordism classes, except we drop any consideration of the framing. [4]

Lemma 1.5.17. *For any manifold M we have a one-to-one correspondence*

$$\Omega_1(M) \leftrightarrow H_1(M).$$

Proof. Given $\gamma \in \Omega_1(M)$ we can "triangulate" γ, that is write γ as a 1-complex. Thus the inclusion of this 1-complex into M gives a singular 1-cycle in M. That is γ defines a singular homology class $[\gamma] \in H_1(M)$. Now suppose that γ_0 and γ_1 are coborant via a surface $\Sigma \subset M \times [0,1]$. We can triangulate the surface Σ and project this to M. This will give a 2-chain in M. That is an element of the singular 2-chain group $C_2(M)$.

Exercise 1.5.18. Show that $\partial_2 \Sigma = \gamma_1 - \gamma_0$ where $\partial_2 \colon C_2(M) \to C_1(M)$ is the singular boundary map in the definition of singular homology.

Thus we see that γ_0 and γ_1 are homologous and so $[\gamma_0] = [\gamma_1]$ in $H_1(M)$. That is we have shown that the map

$$\Phi \colon \Omega_1(M) \to H_1(M) \colon \gamma \mapsto [\gamma]$$

is well-defined.

It is not hard to see that any $x \in H_1(M)$ is represented by the image of S^1 under some smooth map (recall the abelianization of $\pi_1(M)$ is $H_1(M)$). Thus Φ is clearly surjective.

Now suppose that $\Phi(\gamma_0) = \Phi(\gamma_1)$. Then there is a 2-chain c such that $\partial_2 c = \gamma_1 - \gamma_0$.

Exercise 1.5.19. Show that there is some other 2-chain c' such that c' is the image of a triangulated surface Σ and $\partial_2 c' = \partial_2 c$.

Now let $f \colon \Sigma \to [0,1]$ be a smooth function such that $f^{-1}(i) = \gamma_i$ and i is a regular value for $i = 0, 1$. we now get a map

$$\Sigma \to M \times [0,1] \colon p \mapsto (p, f(p)).$$

[4] One can actually make $\Omega_1(M)$ a group with the operation of disjoint union.

This map can be perturbed, relative to $\partial\Sigma$, to be smooth and self-transverse. This means that the image in $M \times [0,1]$ is an immersed surface with transverse double points.

Exercise 1.5.20. Show that one can "resolve" the double points of this surface to obtain an embedded surface Σ' in $M \times [0,1]$ such that $\Sigma' \cap (M \times \{i\}) = \gamma_i$.
Hint: If you have not seen how to resolve transverse double points, see [GS99].

So Σ' shows that γ_0 is cobordant to γ_1 and hence Φ is injective. □

We are not ready to prove the main result of this section.

Proof of Proposition 1.5.8. There is clearly a map from framed cobordism classes to cobordism classes one gets by forgetting the framing

$$F' \colon \Omega_1^f(M) \to \Omega_1(M) \colon (\gamma, \mathcal{F}) \mapsto \gamma,$$

and using the previous lemma we will consider F' as a map $\Omega_1^f(M) \to H_1(M)$. Moreover, after fixing a trivialization of TM Lemmas 1.5.10 and 1.5.12 give bijection between $\pi_0(\mathrm{Dist}(M))$ and $\Omega_1^f(M)$. We will denote the composition of this bijection with F' above by F. From the discussion above it is clear that F is surjective. So we are left to identify $F^{-1}(x)$ for $x \in H_1(M)$.

Given a homology class $x \in H_1(M)$ let γ be a knot such that $[\gamma] = x$. Fix a framing $\mathcal{F}$ on γ and define the framing $\mathcal{F}_n$ to be the framing of γ obtained from $\mathcal{F}$ by adding n right-handed Dehn twists. We now define a map

$$h \colon \mathbb{Z} \to F^{-1}(x) \colon n \mapsto (\gamma, \mathcal{F}_n).$$

This map is clearly surjective.

Suppose that $h(n) = h(m)$. This means that $(\gamma, \mathcal{F}_n)$ is framed cobordant to $(\gamma, \mathcal{F}_m)$. Denote the framed cobordism by $(\Sigma, \mathcal{F}')$. Thinking of $M \times S^1$ as the quotient space of $M \times [0,1]$ that identifies $M \times \{0\}$ to $M \times \{1\}$ by the identity map on M, we can consider the closed surface T obtained from Σ by identifying $T \cap (M \times \{0\}) = \gamma$ with $T \cap (M \times \{1\}) = \gamma$.

Exercise 1.5.21. Show that the self-intersection of T with itself is $m - n$. Here the self-intersection, denoted $T \cdot T$, is obtained by considering the inclusion $i \colon T \to M \times S^1$ and perturbing it to be transverse to T, then counting the number of intersection points with sign. See [GS99].
Hint: If one has a trivialization of the normal bundle of T then its self-intersection would be 0. The framing $\mathcal{F}'$ frames Σ but does not give a framing to T because it is not the same on $\gamma \subset M \times \{0\}$ and $\gamma \subset M \times \{1\}$. If we take a copy of Σ pushed off of itself with $\mathcal{F}'$ and call it Σ' think how we can make Σ' into a closed surface in $M \times S^1$.

Now let $C = \gamma \times S^1$ in $M \times S^1$. Notice that

$$\begin{aligned} m - n = T \cdot T &= [(T - C) + C] \cdot [(T - C) + C] \\ &= (T - C) \cdot (T - C) + 2(T - C) \cdot C + C \cdot C. \end{aligned}$$

We can take any framing on γ to get a framing on C and thus $C \cdot C = 0$. We now claim that $(T - C) \cdot (T - C) = 0$. Recall that the self-intersection of a surface with itself (or another surface) only depends on the homology class of the surface [GS99]. By the Künneth formula we know that

$$H_2(M \times S^1) = (H_2(M) \otimes H_0(S^1)) \oplus (H_1(M) \otimes H_1(S^1)).$$

Notice that the homology class of $(T - C) \cap (M \times \{pt\})$ in $H_1(M \times S^1)$ is 0 (since it is $x - x$). Thus we see that $T - C \in H_2(M) \otimes H_0(S^1)$ since any nontrivial element in $H_1(M) \otimes H_1(S^1)$ has nontrivial intersection with $M \times \{pt\}$. Thus $T - C$ is homologous to a surface S in M. In $M \times S^1$ we can clearly perturb S to be disjoint from itself and hence $S \cdot S = 0$ which implies the same for $T - C$. We now see that

$$m - n = 2(T - C) \cdot C = 2(T - C) \cdot x$$

since $T - C$ is homologous to a surface S in M and S intersects C in $M \times S^1$ the same way it intersects x in M. Thus we see that if $h(m) = h(n)$ then $m - n$ is divisible by $2d(x)$.

So if $d(x) = 0$ then we see that h is injective and $F^{-1}(x) = \mathbb{Z}$. Now suppose that $d(x) \neq 0$. Let y be a primitive class in $H_1(M)$ such that $x = d(x)y$. By Poincaré duality we know there is a surface α in M such that $y \cdot \alpha = 1$, should we say more... probably so and thus $2x \cdot \alpha = 2d(x)$. Now consider the surface T representing $(\gamma \times S^1) + \alpha$ in $M \times S^1$. Notice we can build T by taking the surface α in $M \times \{pt\}$ and $C = \gamma \times S^1$, which intersect transversely in some points in $M \times \{pt\}$, and resolving the double points. Notice that

$$T \cdot T = 2C \cdot \alpha = 2\gamma \cdot \alpha = 2d(x)$$

Now we can cut $M \times S^1$ along a copy of M (not containing the α used to construct T) to get $M \times [0, 1]$ and inside this manifold T will be cut open to be a surface Σ with $\Sigma \cap (M \times \{i\}) = \gamma$ for $i = 0, 1$. Notice if we fix a framing $\mathcal{F}_n$ on γ then as argued above, we can frame Σ so that it induces $\mathcal{F}_n$ on $\gamma \subset M \times \{0\}$ and $\mathcal{F}_{n+2d(x)}$ on $\gamma \subset M \times \{1\}$. Thus $h\colon \mathbb{Z} \to F^{-1}(x)$ is surjective with kernel $2d(x)\mathbb{Z}$. Thus $F^{-1}(x) \cong \mathbb{Z}/(2d(x)\mathbb{Z})$. □

1.5.3. Contact structures in a given homotopy class of plane field. With our understanding of the set of plane fields on M we are now ready to strengthen Theorem 1.5.4 to show that any homotopy class of plane field contains at least one contact structure. Let $\mathrm{Cont}(M)$ be the subset of $\mathrm{Dist}(M)$ consisting of contact structures on M.

Theorem 1.5.22 (Lutz 1977, [Lut77]). *Given a closed, oriented 3-manifold M, let $i\colon \mathrm{Cont}(M) \to \mathrm{Dist}(M)$ be the inclusion map. Then*

$$i_*\colon \pi_0(\mathrm{Cont}(M)) \to \pi_0(\mathrm{Dist}(M))$$

is surjective. That is every homotopy class of plane field contains a contact structure.

As noted in the previous section we know that this theorem implies that any closed, oriented 3-manifold M admits infinitely many distinct contact structures. We also note that Lutz did not precisely prove this theorem, he showed that a given manifold can admit contact structures in more than one homotopy class of plane field by introducing what we now call a Lutz twist. Since it is not hard to go from the results in his paper to the above theorem, we attribute the result to him.

To prove this theorem, we introduce the notion of a Lutz twist. To do this we consider $\mathbb{R}^2 \times S^1 = \mathbb{R}^3/\sim$, where $(r, \theta, z) \sim (r, \theta, z+2\pi)$ with the contact structure $\xi = \ker(\cos r\, dz + r \sin r\, d\theta)$ that we used in the proof of Theorem 1.5.4. Recall that $T = \{(0,0)\} \times S^1$ is a transverse knot and we have the neighborhoods $S_a = \{(r, \theta, z) | r \leq a\}$ of T such that ∂S_a has a characteristic foliation of slope $r_a = -\frac{1}{a} \cot a$ so as a goes from 0 to π the possible slopes of the characteristic foliation trace out all rational numbers (and ∞). Given a transverse knot K in a contact manifold (M, ξ) we know, by Theorem 1.5.4, that K has a neighborhood N contactomorphic to S_a and we can assume $a \in (0, \pi]$ (by shrinking N if necessary). Notice that there is a unique $b \in (\pi, 2\pi]$ such that S_b and S_a have the same characteristic foliation on their boundaries. See Figure 1.5.25. The contact structure ξ' on

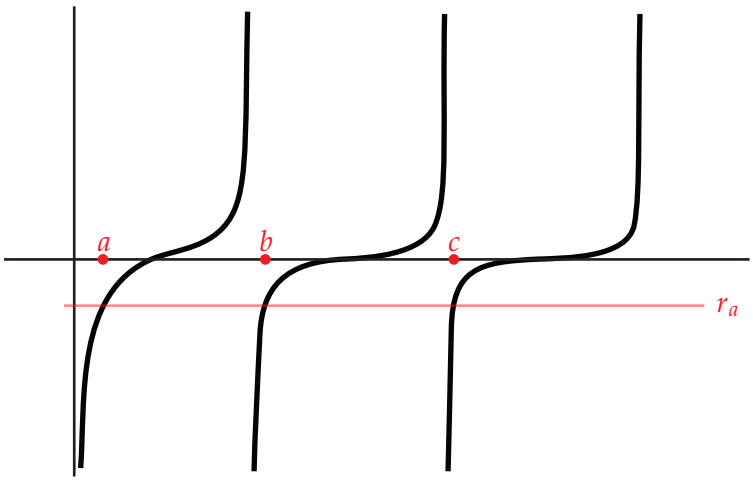

Figure 1.5.25. Graph of $-\frac{1}{x} \cot x$ with the points a, b, and c marked.

M is obtained by removing $S_a = N$ from M and regluing S_b by the identity map (see the proof of Theorem 1.5.4 to guarantee that ξ' is a smooth contact structure) is said to be the result of a *half-Lutz twist* along K in (M, ξ). We also define the *Lutz twist* (or sometimes a *full Lutz twist* in the same manner except instead of gluing in S_b we glue in S_c where c is the unique number in $(2\pi, 3\pi]$ so that the characteristic foliation on ∂S_c is the same as on ∂S_a.

To prove the above theorem we need a few lemmas about Lutz twisting. We first notice that if we fix a trivialization of the tangent space of M then after performing a (half) Lutz twist we still have the same trivialization of TM since doing a Lutz twist smoothly removes a solid torus and reglues it by the identity map, so the resulting manifold is canonically diffeomorphic to M. With this in mind, we have the following results.

Lemma 1.5.23. *Let (M, ξ') be the result of performing a half Lutz twist on a transverse knot K in (M, ξ). Then using the notation from Proposition 1.5.8 we have*

$$F(\xi') = F(\xi) - [K].$$

That is, the first homology class associated with ξ and ξ' differ by $[K]$.

Lemma 1.5.24. *Let (M, ξ') be the result of performing a half Lutz twist on a null-homologous transverse knot K in (M, ξ). If $(\gamma, \mathcal{F})$ is the framed 1-manifold corresponding to ξ by Remark 1.5.16 then $(\gamma, \mathcal{F}_{\mathrm{sl}(K)})$ is the framed manifold associated to ξ' where $\mathcal{F}_n$ is the framing on γ obtained from $\mathcal{F}$ by adding n right-handed twists.*

We will prove these lemmas below, but first, see how they imply our main theorem.

Proof of Theorem 1.5.22. From Theorem 1.5.4 we know there is a contact structure ξ on M. The plane field ξ corresponds to a framed 1-manifold $(\gamma, \mathcal{F})$ by Remark 1.5.16. Now given any framed manifold $(\gamma', \mathcal{F}')$ we need to find a contact structure in the homotopy class of plane field associated with this framed manifold. Let K be a knot realizing the homology class $[\gamma] - [\gamma']$. By Theorem 1.2.4 we can find a transverse knot isotopic to K, we will still call it K. By Lemma 1.5.23 we see that a half-Lutz twist on K will give a contact structure ξ' associated with the framed manifold $(\gamma', \mathcal{F}'')$ for some framing $\mathcal{F}''$ on γ'.

Now in (M, ξ') consider the transverse unknot U in a Darboux ball with $\mathrm{sl}(U) = -1$ and the transverse right-handed trefoil T with $\mathrm{sl}(T) = 1$. According to Lemma 1.5.24 the result of a half-Lutz twist on U or T, respectively, give result in a contact structure ξ'' associated to the framed manifold $(\gamma', \mathcal{F}''_{-1})$, respectively $(\gamma, \mathcal{F}''_1)$. Performing further half-Lutz twists will allow us to find a contact structure realizing any $(\gamma', \mathcal{F}''_n)$ and hence we have a contact structure in the homotopy class of plane field corresponding to the framed manifold $(\gamma', \mathcal{F}')$. □

We now move to the proof of our lemmas about half-Lutz twists.

Proof of Lemma 1.5.23. Using the notation from the proof of Lemma 1.5.12 we fix a trivialization of TM and consider the map from $[M, S^2] \to \Omega^f_1(M)$ (with $[M, S^2]$ identified with $\mathrm{Dist}(M)$ by Lemma 1.5.10 and the following discussion). The contact structure ξ is associated with a map $f\colon M \to S^2$ and we can assume (by isotoping K thourgh transverse knots if necessary) that $f(K) \subset S^2 - \{n\}$. Thus $f(K)$ is homotopic to the constant map

with image the south pole s. We can homotop the trivialization of TM so that $f(K) = s$. Let N be a small neighborhood N of K contactomorphic to S_a for $a \in (0, \pi]$ (for notation see the discussion at the beginning of this section). We can further assume by homotoping the trivialization of TM that $f(\xi|_N) = s$.

Exercise 1.5.25. Prove the last assertion.

As in the definition of half-Lutz twist, let $b \in (\pi, 2\pi]$ be the number such that $(\partial S_b)_\xi = (\partial S_a)_\xi$. If we replace $N = S_a$ in M by S_b and let f_b be the map $M \to S^2$ associated with ξ' the result of a half-Lutz twist on K, then on $S_a \subset S_b$ we see that f' maps this to s. The core of S_b will be mapped to $n \in S^2$ and the rest of $S_b - S_a$ which is $(S^1 \times (0,1]) \times S^1$ will be mapped around $S^2 - \{n\}$. Thus we see that $f_b^{-1} = \gamma \cup -K$. □

To prove Lemma 1.5.24 we need to reconsider our discussion from the previous subsection. Recall from Section 1.5.2 that, once we fixed a trivialization of TM, to ξ we associated a map $f_\xi : M \to S^2$ where S^2 was identified with the unit vectors in $\mathbb{R}^3$ and the framed manifold associated to ξ was $f_\xi^{-1}(n)$, where n is the north pole of S^2 and f was homotoped to be transverse to it. However, S^2 was naturally thought of as the space of oriented planes in $\mathbb{R}^3$, which we now denote by $Gr_2^o(\mathbb{R}^3)$ and is called the *Grassman of oriented 2-planes in* $\mathbb{R}^3$. We identified S^2 with $Gr_2^o(\mathbb{R}^3)$ by sending an oriented plane to the unit vector positively orthogonal to it. So we can think of $[M, S^2]$, which we identified with $\pi_0(\mathrm{Dist}(M))$ earlier in this section, more naturally as $[M, Gr_2^o(\mathbb{R}^3)]$. Now $Gr_2^o(\mathbb{R}^3)$ has a natural oriented vector bundle bundle of rank 2 over it. Specifically, let

$$E_2 = \left\{(P, v) \in Gr_2^o(\mathbb{R}^3) \times \mathbb{R}^3 : v \in P\right\}.$$

We now have a couple of simple observations which we leave as exercises.

Exercise 1.5.26. The bundle E_2 can be naturally identified with TS^2.

Exercise 1.5.27. If $f\colon M \to Gr_2^o(\mathbb{R}^3)$ is the map associated to ξ, then as a vector bundle ξ is isomorphic to the pull-back f^*E_2.

Proof of Lemma 1.5.24. Given the null-homologous transverse knot K in (M, ξ) we know that it bounds a surface Σ. We begin by assuming that Σ is disjoint from γ (recall $(\gamma, \mathcal{F})$ is the framed 1-manifold associated to ξ). From the discussion above, and the fact that S^2 has a vector field that vanishes to order 2 at the north pole n and is otherwise non-vanishing, we can trivialize $T(S^2 - \{n\})$ using this vector field and pull it back to a trivialization of ξ on $M - \gamma$. This gives a trivialization of ξ over Σ, and the framing given by this trivialization relative to the framing coming from Σ is, by definition, the self-linking number of K. Now when we perform a half-Lutz twist to ξ along K to obtain ξ', as in the proof of Lemma 1.5.23, we see that the framed manifold associated to ξ' is $\gamma \cup K$. Moreover, the framing on γ is unchanged and the framing on K is $\mathrm{sl}(K)$. Since K is null-homologous we see that $\gamma \cup K$ is cobordant to γ.

Exercise 1.5.28. Show that under the cobordism mentioned above, the framing on γ is $\mathcal{F}_{\mathrm{sl}(K)}$.

We are left to consider the case when γ intersects Σ. We can assume the intersections are transverse. There are two ways to deal with this case that will be explored in the following exercises.

Exercise 1.5.29. Show that one may homotop to the trivialization of TM so that γ is disjoint from Σ.

Exercise 1.5.30. If $\gamma \cap \Sigma \neq \emptyset$ then the trivialization of $T(S^2 - \{n\})$ does not give a trivialization of ξ over Σ, but we can assume that K and γ are disjoint, so we still have a trivialization of ξ along K. How does this trivialization differ from $\mathrm{sl}(K)$? What framing on γ is framed cobordant to a framing on $\gamma \cup K$.

One may conclude the general case of the lemma from either exercise above. □

We end this section by noting that full-Lutz twists do not affect the homotopy class of the contact structure. As we do not use this in this book we refer the reader to [**Gei08**] for the proof of this fact.

1.5.4. Invariants of plane fields. We know from Section 1.5.2 that there is a one-to-one correspondence between $\pi_0(\mathrm{Dist}(M))$ and $\Omega_1^f(M)$ once a trivialization of TM is fixed. We were able to use that to prove that every homotopy class of plane field contained a contact structure in the previous section. In particular, with a fixed trivialization of TM a complete invariant of the homotopy class of a plane field is given by its associated framed 1-manifold $(\gamma, \mathcal{F})$. But in general, if we have two abstractly diffeomorphic manifolds it is not clear how to relate trivializations of their tangent bundles and so we do not have obvious invariants of plane fields on M. In this section we will remedy this, but to do so we will use several results from bundle theory. The relevant parts of bundle theory necessary for this discussion are reviewed in Appendix A.

The first invariant of a plane field we sill consider is its Euler class, see Section 1.1fix indexing, this should be A.1 for the general definition of Euler class. In our context, we are interested of the Euler class of the contact bundle ξ over M. As ξ is an oriented $\mathbb{R}^2$-bundle over M one can define the Euler class as the Poincaré dual of $\sigma^{-1}(\mathbf{0})$ where σ is a section of ξ that is transverse to the zero section $\mathbf{0}$ of ξ. We denote this by $e(\xi)$ and it is a cohomology class in $H^2(M)$.

We would like to relate $e(\xi)$ to the element in $\Omega_1^f(M)$ that completely characterizes the homotopy type of the plane field ξ. To this end, recall that, once we fixed a trivialization of TM, to ξ we associated a map $f_\xi : M \to S^2$ where S^2 was identified with the unit vectors in $\mathbb{R}^3$ and the framed manifold associated to ξ was $f_\xi^{-1}(n)$, where n is the north

pole of S^2 and f was homotoped to be transverse to it. However, at the end of the last section we say that we can think of S^2 as the space of oriented planes in $\mathbb{R}^3$, which we denoted by $Gr_2^o(\mathbb{R}^3)$. Thus we can think of $[M, S^2]$, which we identified with $\pi_0(\text{Dist}(M))$, more naturally as $[M, Gr_2^o(\mathbb{R}^3)]$. We also saw that $Gr_2^o(\mathbb{R}^3)$ has a natural oriented vector bundle of rank 2 over it. Specifically, let

$$E_2 = \left\{(P, v) \in Gr_2^o(\mathbb{R}^3) \times \mathbb{R}^3 : v \in P\right\}.$$

Finally in the last subsection we saw that E_2 can be naturally identified with TS^2 and if $f\colon M \to Gr_2^o(\mathbb{R}^3)$ is the map associated to ξ, then as a vector bundle ξ is isomorphic to the pull-back f^*E_2.

Given this and the fact that we know that S^2 has a vector field that vanishes to order 2 at the north pole, we see that the Poincaré dual of the Euler class $e(TS^2)$ is $2n$ and hence the Poincaré dual of the Euler class of ξ is $2f^{-1}(n)$. (Recall from Appendix A that characteristic classes, like the Euler class, act naturally under pull-back.) This discussion has established the following result.

Lemma 1.5.31. *Given an oriented 3-manifold M and a fixed trivialization of TM we can associate to an oriented plane field ξ and framed 1-manifold $(\gamma, \mathcal{F})$ as in Lemma 1.5.12 and the discussion before the lemma. We have the following identification*

$$e(\xi) = 2PD[\gamma]$$

where $PD[\gamma]$ is the Poincaré dual of the homology class $[\gamma]$. In particular, the homology class $2[\gamma]$ can be associated to ξ independent of a trivialization of TM.

Unfortunately $2[\gamma]$ does not determine $[\gamma]$ in $H_1(M)$, if $H_1(M)$ has 2-torsion. So $e(\xi)$ does not completely recover the cobordism class of γ. In [**Gom98**], Gompf defined another invariant, the Γ-invariant, that does completely determine the cobordism class of γ. To define this invariant we note that the lemma above implies that $e(\xi)$ is always 2 times some other cohomology class. One can see this in a more direct way as discussed in the next exercise.

Exercise 1.5.32. Let ξ be an oriented plane field on an oriented 3-manifold M. Show that $e(\xi)$ is even (meaning it is 2 times another homology class).
Hint: Notice that $TM = \xi \oplus \mathbb{R}$ and so, as discussed in Appendix 1.3, the Stiefel-Whitney classes satisfy

$$w(TM) = w(\xi) \cup w(\mathbb{R}) = w(\xi).$$

Thus $w_2(\xi) = w_2(TM)$ and since any oriented 3-manifold is spin, see Appendix 1.4, we have $w_2(\xi) = 0$. Finally, we know, see Appendix 1.3, $w_2(\xi)$ is the mod 2 reduction of $e(\xi)$.

Now given an even cohomology class $h \in H^2(M)$ let $G_h = \{[\gamma] \in H_1(M) : 2[\gamma] = PD(h)\}$. We also denote the set of spin structures on M by $\text{Spin}(M)$. The Γ-*invariant* of an

oriented plane field ξ on an oriented 3-manifold M is a map

$$\Gamma_\xi \colon \operatorname{Spin}(M) \to G_{e(\xi)}$$

defined as follows. Given a spin structure $\mathfrak{s}$ on M we know from Appendix 1.4 that $\mathfrak{s}$ induces a trivialization of the tangent bundle of M. Using this trivialization ξ induces a map $\phi_\xi \colon M \to S^2$ as discussed just before Lemma 1.5.12. Homotop ϕ_ξ so that it is transverse to the north pole n of S^2 and let $\Gamma(\xi)(\mathfrak{s}) = \phi_\xi^{-1}(n)$. From the lemma above it is clear that $2\Gamma_\xi(\mathfrak{s})$ is $e(\xi)$ and hence it is in $G_{e(\xi)}$. We begin by noting that Γ_ξ well-defined.

Lemma 1.5.33. *The homology class $\Gamma_\xi(\mathfrak{s})$ does not depend on the trivialization of TM determined by $\mathfrak{s}$ and hence Γ_ξ is well-defined.*

Proof. From Appendix 1.4 we know that $\mathfrak{s}$ determines a unique trivialization of TM over the 2-skeleton of M that can be extended to a trivialization τ of TM over all M, but τ is not uniquely determined by $\mathfrak{s}$. Consider two trivializations τ and τ' of TM that are determined by $\mathfrak{s}$. Any two trivializations of TM differ by a map $M \to SO(3)$ (this is clear as each trivialization is determined by a triple of sections that pointwise give an orthonormal basis for TM, with respect to some Riemannian metric, and hence they differ by an element of $SO(3)$ at each point). Thus if $f \colon M \to SO(3)$ determines the difference between the trivialization of TM given by τ and by τ' then the trivializations of TM give by τ and τ' are related by

$$F \colon M \times \mathbb{R}^3 \to M \times \mathbb{R}^3 \colon (x, v) \mapsto (x, f(x)v).$$

As discussed in Appendix 1.2 we know that the obstruction to homotoping τ to τ' on the 2-skeleton of M is givne by $f^*(\mathbb{1}_2)$ where $\mathbb{1}_2$ is the generator of $H^2(SO(3)) \cong \mathbb{Z}/2\mathbb{Z}$ and since τ and τ' both agree with $\mathfrak{s}$ on the 2-skeleton we see that $f^*(\mathbb{1}_2) = 0$.

Now if $\phi_\tau \colon M \to S^2$ and $\phi_{\tau'} \colon M \to S^2$ are the two maps associated to ξ by the trivializations then consider the maps

$$\Phi_\tau \colon M \to S^2 \times SO(3) \colon p \mapsto (\phi_\tau(p), f(p))$$

and

$$m \colon S^2 \times SO(3) \to S^2 \colon (x, y) \mapsto y \cdot x$$

where $y \cdot x$ means that the matrix y acts on the unit vector $x \in S^2$. Notice that $\phi_{\tau'} = m \circ \Phi_\tau$.

We note that $H^2(S^2 \times SO(3)) \cong H^2(S^2) \oplus H^2(SO(3)) \cong \mathbb{Z} \oplus \mathbb{Z}/2\mathbb{Z}$ and one may easily compute that if $\mathbb{1} \in H^2(S^2)$ is a generator then $m^*(\mathbb{1}) = \mathbb{1} \oplus \mathbb{1}_2$. Thus $\phi_\tau^*,(\mathbb{1}) = \Phi_\tau^* \circ m^*(\mathbb{1}) = \phi_\tau^*(\mathbb{1}) + f^*(\mathbb{1}) = \phi_\tau^*(\mathbb{1})$.

Finally we note that the homology class of a point n in S^2 is Poincaré dual to $\mathbb{1} \in H^2(SO(3))$. Thus $\phi_\tau^{-1}(n)$ is homologous to $\phi_{\tau'}^{-1}(n)$ (see for example [**Bre93**, Chapter IV.11]) and we see that Γ_ξ is well-defined. □

We have the following properties of Γ_ξ.

(1) If $f\colon M \to M'$ is a diffeomorphism and ξ is a plane field on M', then

$$\Gamma_\xi \circ f_* = f_* \circ \Gamma_{f^*\xi}$$

where the first f_* is an identification of the sets $f_* : \mathrm{Spin}(M) \to \mathrm{Spin}(M')$ and the second is the map induced on homology $f_*\colon H_1(M) \to H_1(M')$. That is Γ_ξ is an invariant of ξ that behaves naturally under diffeomorphisms.

(2) We have $\Gamma_\xi = \Gamma_{\xi'}$ if and only if ξ is homotopic to ξ' on the 2-skeleton of M if and only if ξ and ξ' determine the same Spin^c structure on M if and only if in any fixed trivialization τ of TM the 1-homology classes associated to ξ and ξ' by Proposition 1.5.8 are the same.

(3) The group $H^2(M, \mathbb{Z}/2\mathbb{Z}) \cong H_1(M, \mathbb{Z}/2\mathbb{Z})$ acts naturally and transitively on the set $\mathrm{Spin}(M)$, see Appendix 1.4, and on $H_1(M)$ via the long exact sequence in homology corresponding to the short exact sequence $0 \to \mathbb{Z} \to \mathbb{Z} \to \mathbb{Z}/2\mathbb{Z} \to 0$. The map Γ_ξ is equivariant with respect to this action. Thus Γ_ξ is determined by its value on one spin structure.

Exercise 1.5.34. Prove these properties of Γ_ξ (or see [**Gom98**]).

From these properties, we see that Γ_ξ completely recovers the cobordisms class associated to ξ by any trivialization of TM. We are left to see that we can recover the framing as well.

We will define an invariant that recovers this framing for ξ whose Euler class $e(\xi)$ is torsion. There is a more general, and quite a bit more complicated, invariant that works for any ξ, see [**Gom98**], but we will mainly need the simpler invariant so refer the reader to [**Gom98**] for the more general case. We start with a simple observation whose proof can be found in [**Gom98**, Lemma 4.4].

Lemma 1.5.35. *Given an oriented plane field ξ on a closed, oriented 3-manifold M, there is a compact 4-manifolds X that admits an almost complex structure J such that $\partial X = M$ and ξ is the set of complex tangencies to ∂X.*

Given a contact structure ξ on a 3-manifold M let (X, J) be the almost complex manifold with boundary M from Lemma 1.5.35 we then define the d_3-invariant of ξ to be the rational number

$$d_3(\xi) = \frac{1}{4}(c_1^2(J) - 2(\chi(X) - 1) - 3\sigma(X))$$

where $\chi(X)$ is the Euler characteristic of X, $\sigma(X)$ is the signature of X, and c_1 is the Chern class of J. Since X is a manifold with boundary we need to determine what $c_1^2(J)$ really means. To this end, we first recall notice that $TX|_M = \xi \oplus \mathbb{R}^2$ and so when $c_1(J)$ is pulled back to M we see that it equals $c_1(\xi)$ which is simply the Euler class of ξ. Since we are assuming that $e(\xi)$ is torsion we note that $c_1(J)$ on the boundary of X is trivial in cohomology with rational coefficients. Now note that $c_1(J) \in H^2(X)$ which, by Poincaré

duality, is isomorphic to $H_2(X, \partial X)$ denote the image of $c_1(J)$ in $H_2(X, \partial X)$ by c. Consider the portion of the long exact sequence of the pair $(X, \partial X)$

$$\cdots \to H_2(X; \mathbb{Q}) \xrightarrow{i} H_2(X, \partial X; \mathbb{Q}) \xrightarrow{\partial} H_1(\partial X; \mathbb{Q}) \to \cdots .$$

Since we are assuming that $e(\xi) = 0$ in $H^2(M; \mathbb{Q}) \cong H_1(M; \mathbb{Q})$ we see that $\partial c = 0$ and hence by exactness there is some class $c' \in H_2(X; \mathbb{Q})$ for which $i(c') = c$. We can now use the intersection pairing on $H_2(X; \mathbb{Q})$ to compute $c' \cdot c'$. We define $c_1^2(J)$ to be this rational number.

Exercise 1.5.36. Show that $c' \cdot c'$ is the same for any choice of element in $H_2(X; \mathbb{Q})$ that maps to c under i.

In Theorem 6.2.9 we will give a formula for computing $d_3(\xi)$ if ξ is described by a contact surgery diagram.

Lemma 1.5.37. *For an oriented plane field ξ on a closed oriented 3-manifold M, the rational number $d_3(\xi)$ depends only on M and ξ.*

Proof. Given M and ξ, let (X, J) be as in the definition of $d_3(\xi)$ and let (X', J') be an almost complex manifold with $\partial X' = -M$ and the complex tangencies to $\partial X'$ a plane field ξ' homotopic to ξ. Notice that $W = X \cup X'$ is a closed almost complex manifold. Hirzebruch and Hopf [**HH58**] showed that on a closed almost complex manifold one must have

$$c_1^2(W) = 2\chi(W) + 3\sigma(W).$$

We also notice that $\chi(W) = \chi(X) + \chi(X')$ and $\sigma(W) = \sigma(X) + \sigma(X')$.

Exercise 1.5.38. Show that $c_1^2(W) = c_1^2(J) + c_1^2(J')$.

Thus if we set $d_3' = \frac{1}{4}(c_1^2(J') - 2(\chi(X') - 1) - 3\sigma(X'))$ then $d_3(\xi) = -d_3' - 1$ and this is independent of the specific X and J chosen to define $d_3(\xi)$. □

We have the following properties the d_3-invariant.

(1) If $f\colon M \to M'$ is an orientation preserving diffeomorphism then for any plane field ξ on M with torsion Euler class we have $d_3(f_*\xi) = d_3(\xi)$.

(2) If ξ and ξ' are two 2-plane fields on M that have torsion Euler classes are homotopic on the 2-skeleton of M, then they are homotopic on all of M if and only if $d_3(\xi) = d_3(\xi')$.

(3) The number $d_3(\xi)$ is unchanged when the orientation of ξ is changed and changes sign with the orientation on M changes.

Exercise 1.5.39. Prove these properties of $d_3(\xi)$ (or see [**Gom98**]).

maybe we should prove some of these facts and facts for Γ_ξ?

From these properties and those of Γ_ξ we see that Γ_ξ and $d_3(\xi)$ completely determine the homotopy class of ξ (if ξ has torsion Euler class so that $d_3(\xi)$ is well defined.

Remark 1.5.40. The invariant $d_3(\xi)$ has many incarnations in the literature. In [Gom98] Gompf defined the invariant $\theta(\xi)$ that is related to the invariant above by $\theta(\xi) = 4d_3(\xi)-2$ and in some papers the formula for the invariant d_3 does not include the +2. We choose the current convention for the d_3-invariant since it has several nice properties the other definitions do not have. For example, it is an integer if M is an integral homology sphere, it is additive under connected sum, and $-d_3(\xi)$ agrees with the grading on the Heegaard Floer invariant of a contact structure (see Section 1.6.4). Some authors also discuss the Hopf invariant $h(\xi)$ of contact structures ξ on S^3, this is simply $-d_3(\theta)$.

1.6. Tight and overtwisted contact structures

In this section we explore the fundamental dichotomy in contact geometry; specifically, a contact structure can be tight or overtwisted. We will see that overtwisted contact structures are well-understood and determined by algebraic topology while tight contact structures are much more mysterious and are closely connected to the topology of the manifolds that support them.

1.6.1. Tight and overtwisted contact structures. Given a contact manifold (M, ξ) and disk D in M is called an *overtwisted disk*, if the characteristic foliation of D has a unique singularity on its interior, ∂D is a leaf in the characteristic foliation, and the other leaves are asymptotic to the singular point in one direction and ∂D in the other direction. See the drawing on the left-hand side of Figure 1.6.26. We could also define D to be an

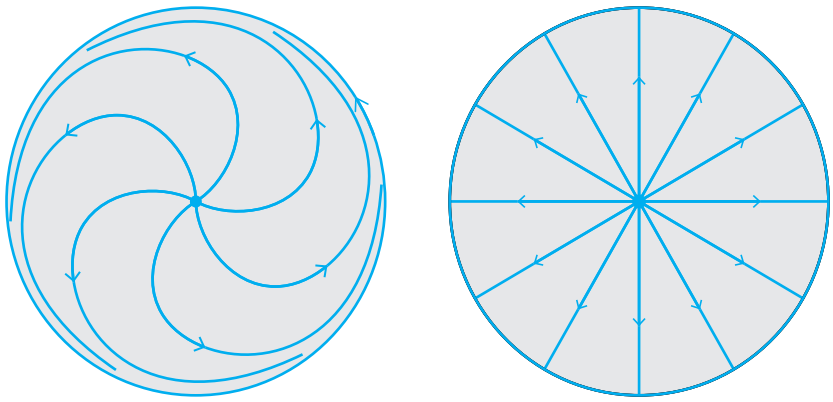

Figure 1.6.26. Two overtwisted disks.

overtwisted disk if the characteristic foliation of D has a unique singularity in its interior,

all points of ∂D are singular points, and the other leaves of the foliation are asymptotic to the interior singularity in one direction and to ∂D in the other direction. See on the right-hand side of Figure 1.6.26.

Exercise 1.6.1. Show that (M, ξ) admits the first type of overtwisted disk if and only if it admits the second type of overtwisted disk.

Given this exercise, we will call either of the above types of disk an overtwisted disk. The contact structure ξ on M is called *overtwisted* if there is an overtwisted disk in (M, ξ), otherwise the contact structure is called *tight*.

We first concentrate on overtwisted contact structures. Let $\mathrm{Cont}_{ot}(M)$ be the subset of all contact structures $\mathrm{Cont}(M)$ consisting of overtwisted contact structures. It is easy to see that, as in the proof of Theorem 1.5.22, that the inclusion map $i\colon\ \mathrm{Cont}_{ot}(M) \to \mathrm{Dist}(M)$ induces a surjection $\pi_0(\mathrm{Cont}_{ot}(M)) \to \pi_0(\mathrm{Dist}(M))$, but we have even more.

Theorem 1.6.2 (Eliashberg 1989, [**Eli89**])**.** *For a closed, oriented* 3*-manifold* M *the inclusion map* $i\colon\ \mathrm{Cont}_{ot}(M) \to \mathrm{Dist}(M)$ *induces a bijection*

$$i\colon\ \pi_0(\mathrm{Cont}_{ot}(M)) \to \pi_0(\mathrm{Dist}(M)).$$

This theorem says that in every homotopy class of plane fields on M there is a unique overtwisted contact structure up to isotopy. Moreover, from Section 1.5.4 we know that we can determine if two plane fields are homotopic using algebraic topological information. So, the classification of overtwisted contact structures on a 3-manifold is well understood, but this also implies that overtwisted contact structures are unlikely to be able to detect any subtle features of a 3-manifold that cannot be seen from the algebraic topology of the manifold. Following work of Huang [**Hua13**], we will use the convex surface theory developed in this book to prove this theorem in Chapter 14, but we note here that the original proof used quite different techniques and proved quite a bit more. To state the more general theorem, we take an embedded disk D in M, fix a singular foliation $\mathcal{F}$ on D that would make D an overtwisted disk (for example, either foliation in Figure 1.6.26) and let $\mathrm{Cont}_D(M)$ be the space of contact structures on M which induces $\mathcal{F}$ as the characteristic foliation on D. Let $p \in D$ be the interior singular point of $\mathcal{F}$ and set $\mathrm{Dist}_D(M)$ be the space of oriented plane fields on M that are tangent to D at p. With all in place we state the following remarkable result *h-principle* due to Eliashberg.

Theorem 1.6.3 (Eliashberg 1989, [**Eli89**])**.** *For a closed, oriented* 3*-manifold* M *the inclusion map* $i\colon\ \mathrm{Cont}_D(M) \to \mathrm{Dist}_D(M)$ *is a weak homotopy equivalence.*

Exercise 1.6.4. Show how Theorem 1.6.2 follows from this theorem.

We now move to a discussion of tight contact structures that will be the main focus of this book. We have seen many overtwisted contact manifolds, but so far have not shown

that there are any tight contact structures. The first result about tight contact manifolds was due to Bennequin (though the terminology of tight and overtwisted did not exist at the time).

Theorem 1.6.5 (Bennequin 1983, [**Ben83**]). *The standard contact structure on S^3 and $\mathbb{R}^3$ is tight.*

This result is fundamental to the subject and can be thought of as the birth of contact topology. One way to see how fundamental a result this is, is to note that it can be proven in a variety of different ways. For example, this theorem was proven by

(1) Bennequin using braid theory [**Ben83**],

(2) Eliashberg and Gromov using holomorphic curves [**Eli90a**, **Gro85**],

(3) Kronheimer and Mrowka using Seiberg-Witten theory [**?**],

(4) Giroux using convex surfaces [**Gir00**], and

(5) Ozsváth and Szabó using Heegaard-Floer theory [**OS05**].

We will give a proof of this result in Chapter 11 based on Giroux's approach. We mention that Bennequin proved that for transverse knots K in the standard contact structure on $\mathbb{R}^3$ we have

$$\mathrm{sl}(K) \leq -\chi(\Sigma)$$

where Σ is any oriented surface in $\mathbb{R}^3$ with boundary K. Notice that, by considering the positive and negative push-off of a Legendrian knot, and using the relation between their classical invariants in Lemma 1.4.29, we also gather that for any Legendrian knot L in the standard contact structure on $\mathbb{R}^3$ we have

$$\mathrm{tb}(L) + |\mathrm{rot}(L)| \leq -\chi(\Sigma).$$

Notice that this allows one to obtain bounds on the minimal genus of a surface with boundary a given knot since $-\chi(\Sigma) = 2g(\Sigma)-1$ where $g(\Sigma)$ is the genus of Σ. Determining the minimal genus of a Seifert surface for a knot has historically been a difficult problem (though with recent advances, in particular with Heegaard Floer theory [**OS04b**, **Ni09**], it is now much more tractable), but we see that contact geometry can give bounds that in some cases are sharp. This observation shows that a tight contact structure (in particular, the standard one on $\mathbb{R}^3$) can "see" subtle features of smooth topology.

It turns out that one can characterize the tightness of a contact structure in terms of the Bennequin inequality as follows.

Theorem 1.6.6. *A contact manifold (M, ξ) is a tight contact manifold if and only if for any Legendrian knot L we have*

$$\mathrm{tb}(L) + |\mathrm{rot}(L)| \leq -\chi(\Sigma)$$

for any orientable surface Σ with boundary L.

We note that one implication in this theorem is clear. If (M, ξ) is overtwisted then it contains an overtwisted disk D with ∂D a Legendrian knot with tb = 0. Thus we see that ∂D violates the inequality. The other implication is the content of Theorem 3.7.5.

In order to give other examples of tight contact manifolds we make a simple observation.

Lemma 1.6.7. *Suppose (M, ξ) is a contact manifold and $\widetilde{M}$ is some covering space of M. If the pull-back of ξ to $\widetilde{M}$ is tight, then so is ξ.*

Proof. Suppose D is an overtwisted disk in (M, ξ), then by the lifting criteria for covering space $i\colon D \to M$ lifts to an embedding of D into $\widetilde{M}$. Since the contact structure on $\widetilde{M}$ is the pull-back of ξ we see that the characteristic foliation on D in $\widetilde{M}$ is the same as the characteristic foliation on D in M. Thus the contact structure pulled-back to $\widetilde{M}$ is overtwisted. □

How contact structures behave under pull-backs to covering spaces is interesting to study. We will call a contact structure ξ on M *universally tight* if its pull-back to the universal cover of M is tight. If the pull-back of ξ to a finite cover of M is overtwisted then we say that ξ is *virtually overtwisted*.

Exercise 1.6.8. Show that a contact structure on a closed 3-manifold is either universally tight or virtually overtwisted, but not both.
Hint: The fundamental group of a 3-manifold is residually finite.

We now see how to construct some universally tight contact structures.

Example 1.6.9. Consider $\widetilde{\xi}_k = \ker(\cos(2k\pi z)\,dx + \sin(2k\pi z)\,dy)$ on $\mathbb{R}^3$. Notice that the diffeomorphisms $\phi_x(x, y, z) = (x + 1, y, z)$, $\phi_y(x, y, z) = (x, y + 1, z)$, and $\phi_z(x, y, z) = (z, y, z + 1)$ all preserve $\widetilde{\xi}_k$. Thus if we look at the quotient of $\mathbb{R}^3$ by the action of $\mathbb{Z}^3$ generated by these diffeomorphisms, which yields the 3-torus T^3, then it inherits a contact structure ξ_k from $\widetilde{\xi}_k$. Since we noted in Exercise 1.1.17 that the $\widetilde{\xi}_1$ is contactomorphic to the standard contact structure on $\mathbb{R}^3$, we see that it is tight. One can similarly show that all the $\widetilde{\xi}_k$ are contactomorphic to the standard contact structure. Hence all the ξ_k on T^3 are tight, and in fact, universally tight.

We will see in Section 5.8 that all the ξ_k on T^3 are pairwise distinct contact structures.

Exercise 1.6.10. Show that all the contact structures ξ_k on T^3 are homotopic as plane fields.

This example shows that tight contact structures behave very differently from overtwisted contact structures. Via Eliashberg's classification theorem, in every homotopy class of plane fields, there is a unique overtwisted contact structure, but for T^3 one homotopy

class contains infinitely many distinct tight contact structures. We will see in Section 3.7 that all but finitely many homotopy classes of plane fields on any fixed 3-manifold contain tight contact structures. In fact, some manifolds do not support tight contact structures at all.

Theorem 1.6.11 (Etnyre and Honda 2001, [**EH01b**])**.** *The Poincaré homology sphere with its opposite orientation does not support a tight contact structure.*

We will define the Poincaré homology sphere and prove this theorem, and a generalization due to Lisca and Stipsicz [**LS07**] in Section 9.8.

Example 1.6.12. We now consider the standard contact structure ξ_{std} on S^3 that comes from complex tangencies to S^3 thought of as the unit sphere in $\mathbb{C}^2$, see Example 1.1.18. Notice if $u \in S^1$ is a unit complex number and $(z_1, z_2) \in S^3$ then $(uz_1, u^k z_2)$ is also in S^3. Now let u_p be a primitive p^{th} root of unity in S^1 and q positive integer relative prime to p. Then the map $S^3 \to S^3\colon\ (z_1, z_2) \mapsto (uz_1, u^q z_2)$ generates a free $\mathbb{Z}/p\mathbb{Z}$ action on S^3. Let $L(p, q)$ denote the quotient space of S^3 by this action. We call $L(p, q)$ a lens space. Since this action is also an action on $\mathbb{C}^2$ that preserves the complex structure, we see that ξ_{std} is invariant under the action and so descends to a contact structure ξ on $L(p, q)$. Thus each lens space has a universally tight contact structure.

We will construct more tight contact structures below, including some virtually overtwisted ones, but we note here that tight contact structures have been classified on many 3-manifolds. The first classification results were due to Eliashberg who showed that there is a unique tight contact structure on S^3 and $S^1 \times S^2$ which follows from his classification of tight contact structures on the 3-ball. We will prove the first two results in Section 5.1 and the latter result in Section 5.0.1. In Chapter 5 we will also classify tight contact structures on lens spaces, 3-torus, solid tori, and thickened tori (given appropriate boundary conditions). In Chapter 9, we will discuss the classification of tight contact structures on torus bundles over the circle, circle bundles over surfaces, and on some small Seifert fibered spaces. These results constitute the majority of current classification results known, but there are a few more. We note that in [**Ghi05b**] Ghiggini classified tight contact structures on Seifert fibered spaces over T^2 with one singular fiber, and in [**Mas08**] classified contact structures with negative twisting on all Seifert fibered spaces except when the base surface is a sphere. The classification on some hyperbolic manifolds was considered in [**CM20**, **HKM03**, **MN23**]. In the first paper, Honda, Kazez, and Matić classified tight contact structures on hyperbolic surface bundles over S^1 with a certain Chern class, in the second paper Conway and Min classified contact structures on most manifolds obtained from surgery on the Figure 8 knot, and in the last paper Min and Nonino classified tight contact structures on many surgeries on the Whitehead link.

1.6.2. Sympletic fillings of contact manifolds. One of the main ways to construct tight contact manifolds is as the boundary of symplectic manifolds. A 2-form ω on a $2n$-dimensional manifold X is called a symplectic form if $d\omega = 0$ and ω^n is a volume form on X, where ω^n means the n-fold wedge product of ω with itself. Note that ω^n orients X and we always use this orientation on X. We call (X, ω) a *symplectic manifold*.

Given a contact 3-manifold (M, ξ) we say (X, ω) is a *weak symplectic filling* of (M, ξ) if $\partial X = M$ (as oriented manifolds), $\omega|_\xi$ is an area form, and X is compact. We also say that (M, ξ) is *weakly fillable* or *weakly symplectically fillable*. Our main interest in fillable contact structures is the following result.

Theorem 1.6.13 (Gromov and Eliashberg, [Eli90a, Gro85]). *If (M, ξ) is a weakly symplectically fillable contact manifold, then ξ is tight.*

We will sketch the proof of this theorem in Appendix B. We note that this theorem immediately proves Theorem 1.6.5 above since $B^4 \subset \mathbb{C}^2$ has symplectic form $\omega = dx_1 \wedge dy_1 + dx_2 \wedge dy_2$ and (B^4, ω) is a weak symplectic filling of (S^3, ξ_{std}).

There are other types of symplectic fillings of a contact manifold. We review two more types of fillings below and refer the reader to the survey article [Etn98] for various others. A symplectic manifold (X, ω) is said to have *convex boundary* if there is a vector field v defined near ∂X, points out of X along ∂X, and satisfies $\mathcal{L}_v \omega = \omega$ (that is the flow of v expands the form ω). Suppose (X, ω) has convex boundary and v is the vector field showing the boundary is convex, then let $\alpha = \iota_v \omega$. We note that α restricted to the boundary is a contact form for ∂X. Indeed, near the boundary $d\iota_v\omega = \omega$ by the convexity condition, and so $\alpha \wedge d\alpha = (\iota_v\omega) \wedge \omega$ is a volume form on ∂X. If (M, ξ) is any contact manifold contactomorphic to $(\partial X, \ker \alpha)$, then we say that (X, ω) is a *strong symplectic filling* of (M, ξ). It is common to refer to a strong symplectic filling as simply a *sympectic filling* and only add the word "strong" when trying to contrast with a weak symplectic filling. It is clear that $\omega = d\alpha$ is positive on $\ker \alpha$ and hence (X, ω) is a weak symplectic filling of $(\partial X, \ker \alpha)$. Thus we see that a strong symplectic filling of a contact manifold is also a weak symplectic filling. We will see in Section 7.3 that strongly symplectically fillable contact structures have some advantages over weakly fillable contact structures. Most notably, they can be used to build symplectic manifolds through cut-and-paste constructions.

Example 1.6.14. Consider $\mathbb{C}^2$ with the symplectic form $\omega = dx_1 \wedge dy_1 + dx_2 \wedge dy_2$. The radial vector field $v = \frac{1}{2}\left(x_1 \frac{\partial}{\partial x_1} + y_1 \frac{\partial}{\partial y_1} + x_2 \frac{\partial}{\partial x_2} + y_2 \frac{\partial}{\partial y_2}\right)$ satisfies $\mathcal{L}_v \omega = \omega$ and is transverse to the unit sphere S^3. Moreover, our discussion in Example 1.1.18 shows that ξ_{std} on S^3 is the kernel of $\iota_v \omega$. Thus the unit ball B^4 is a strong symplectic filling of (S^3, ξ_{std}).

Example 1.6.15. Consider the symplectic manifold $(\mathbb{C} - \{0\}) \times \mathbb{C}$ with symplectic form $dr \wedge d\theta + dx \wedge dy$ where (r, θ) are polar coordinates on $\mathbb{C} - \{0\}$ and (x, y) are Cartesian

coordinates on C. Let $v = (r-1)\frac{\partial}{\partial r} + \frac{1}{2}\left(x\frac{\partial}{\partial x} + y\frac{\partial}{\partial y}\right)$ and $S^1 \times S^2$ be the boundary of a small tubular neighborhood $S^1 \times D^2$ of $S^1 = \{(r, \theta, x, y) | r^2 + x^2 + y^2 < \epsilon^2\}$. Notice that v is transverse to $S^1 \times S^2$ and dilates ω. Thus $(S^1 \times D^3, \omega)$ is a strong symplectic filling of $(S^1 \times S^2, \xi_{std})$ where $\xi_{std} = \ker(\iota_v \omega)$.

Exercise 1.6.16. Try to picture the contact structure ξ_{std} on $S^1 \times S^2$.

We mention one more type of symplectic filling of a contact manifold. Suppose X is a complex manifold and $J\colon TX \to TX$ is the almost complex structure on TX induced from the complex structure on X (that is J is a bundle automorphism that satisfies $J^2 = -\mathrm{id}_{TX}$). Given a function $\phi\colon X \to \mathbb{R}$ we can consider the 1-form $\lambda(v) = -d\phi(Jv)$. We say that ϕ is *J-convex*, which is also called *strictly pluri-subharmonic*, if $d\lambda(v, Jv) > 0$ for all non-zero $v \in TX$. The manifold X is called *Stein* if there exists a J-convex function $\phi\colon X \to \mathbb{R}$ such that ϕ is bounded below and proper (that is the preimage of compact sets is compact). Stein manifolds are important in complex analysis and have several other definitions, but this definition is well-suited to us since $\omega_\phi = -d((d\phi \circ)J)$ is a symplectic form on X.

Exercise 1.6.17. If (X, ϕ) is a Stein manifold and x is a regular value of ϕ, then $M = \phi^{-1}(x)$ is a smooth manifold and $-d\phi \circ J$ is a contact form on M. Moreover, (X, ω_ϕ) is a strong symplectic filling of $(M, \ker d\phi \circ J)$.
Hint: Consider $g_\phi(v, w) = \omega_\phi(v, Jw)$. This is a Riemannian metric on X and the gradient v_ϕ of ϕ with respect to g_ϕ is an expanding vector field for ω_ϕ.

A *Stein domain* is a sub-level set of ϕ for a Stein manifold (X, ϕ) and a contact manifold (M, ξ) is called *Stein fillable* if (M, ξ) is contactomorphic to a regular level set of ϕ. In summary for a contact structure we have;

$$\text{Stein fillable} \implies \text{symplectically fillable} \implies \text{weakly symplectically fillable} \implies \text{tight}.$$

In Section 7.1 we will see that none of the notions of fillability are the same and that none are equivalent to a contact structure being tight.

Exercise 1.6.18. Show that the two examples above of strong fillings of (S^3, ξ_{std}) and $(S^1 \times S^2, \xi_{std})$ are actually Stein fillings.

While it can be difficult to find strong symplectic fillings of contact manifolds, there is a systematic way to construct Stein fillings, and hence tight contact structures, as we will see in the following section.

1.6.3. Constructions of Stein manifolds. There is a simple way to construct Stein manifolds in terms of handle decompositions. To describe this, we review handle decompositions. The reader is referred to [**GS99**] for a thorough discussion of handlebodies.

An n-dimensional k-handle is $h^k = D^k \times D^{n-2}$ where D^l is the l-dimensional unit disk. We define $\partial_- h^k$ to be $(\partial D^k) \times D^{n-k}$ and $\partial_+ h^k$ to be $D^k \times (\partial D^{n-k})$. If X is an n-manifold with boundary and $\phi\colon \partial_- h^k \to \partial X$ is an embedding then we say $X \cup_\phi h^k$ is the result of *attaching a k-handle to X with ϕ* where $X \cup_\phi h^k$ is the quotient space of $X \cup h^k$ where points x in $\partial_- h^k$ are identified with their image $\phi(x)$ in ∂X. See Figure 1.6.27.

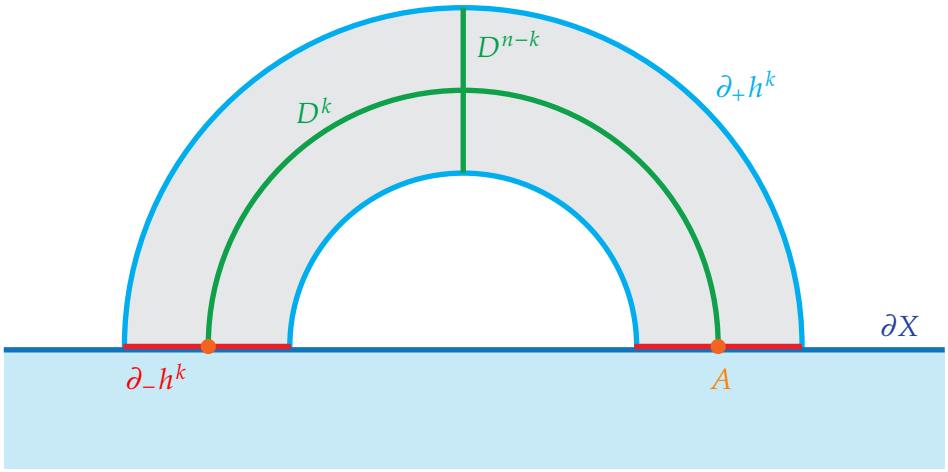

Figure 1.6.27. A k-handle $h^k = D^k \times D^{n-k}$ attached to an n-manifolds X.

Exercise 1.6.19. Show how to put a smooth structure on $X \cup_\phi h^k$. Show that the diffeomorphism type of $X \cup_\phi h^k$ is unchanged if ϕ is changed by an isotopy.

Since we only need to know the isotopy class of ϕ to understand a handle attachment, we will determine what data is needed to fix the isotopy class. To this end, consider $A = (\partial D^k) \times \{p\}$ for some point on the interior of D^{n-k}. We call A the attaching sphere of h^k and its image under ϕ is an embedded S^{k-1} in ∂X. We will also call it a $(k-1)$-knot in ∂X. Notice that the image of $\partial_- h^k$ under ϕ will give a framing to the knot $\phi(A)$. (We discussed framings of an S^1 in a 3-manifolds, but for a general submanifold it is simply a fixed trivialization of the normal bundle.)

Exercise 1.6.20. Show that the isotopy type of the attaching map ϕ is determined by the image of the attaching sphere up to isotopy and the framing on it.

Exercise 1.6.21. Show that if a knotted $(k-1)$-sphere K in ∂X, where X is an n-manifold, with trivial normal bundle, then the set of framings is in one-to-one correspondence with $\pi_{k-1}(O(n-k))$ or if $k > 1$ then also by $\pi_{k-1}(SO(n-k))$.

This last exercise says that one may attach a k-handle to X by identifying a knotted $(k-1)$-sphere in ∂X with a fixed framing. We note that $\partial_- h^0 = \emptyset$, so attaching a 0-handle is the same as taking the disjoint union of X and an n-disk. For a 1-handle the attaching sphere

is S^0 so we must specify two points in ∂X and this is equivalent, up to isotopy, to picking a path component for each point. The framings on a 1-handle are indexed by $\pi_0(O(n-1))$. Thus there are two framings. One may check that one of the framings leads to a non-orientable manifold. So if we wish to attach a 1-handle to an n-manifold so that the result is oriented, we just need to specify two points in ∂X. Lastly, we consider 2-handles. The attaching sphere for a 2-handle is a potentially knotted S^1 and the framings are parameterized by $\pi_1(SO(n-2))$. We will be mainly interested in 4-manifolds, so the framings, in that case, are given by $\pi_1(SO(2)) \cong \mathbb{Z}$ as we noted before. So a 2-handle attached to a 4-manifold is determined by a knot in its 3-manifold boundary and a framing on the knot.

We end our brief discussion of handle attachment by considering the effect on the boundary of a 4-manifold X when a 2-handle is attached. Suppose that $\phi\colon \partial_- h^2 \to \partial X$ is the attaching map for the 2-handle that is determined by a knot K in ∂X and a framing $\mathcal{F}$ on K. Then when h^2 is attached we obtain a manifold X' and $\partial X'$ is obtained from ∂X by removing $\phi(\partial_- h^2)$ (since it will become part of the interior of X') and gluing the torus $\partial_+ h^2$.

Exercise 1.6.22. Show that $\partial X'$ is obtained from ∂X by an α-Dehn surgery on K where α is a curve on the boundary of the neighborhood of K determined by the framing $\mathcal{F}$. In particular, if K is null-homologous then $\partial X'$ is obtained from ∂X by n-Dehn surgery on K where n is the framing on K (here we are using the Seifert framing to define the 0 framing and others are obtained by twisting that framing some integer number of times).

A *handlebody decomposition* of X is a sequence of manifolds $X_0, X_1, \dots, X_k$ where X_0 is the empty set and X_l is obtained from X_{l-1} by attaching a k-handle for some k.

If X is a Stein domain, Eliashberg [**Eli90b**] showed that one may attach a 1-handle to X and the Stein structure can be extended over the new handle. Similarly, if L is a Legendrian knot in ∂X (recall ∂X is a contact manifold) then Eliashberg also showed that one can attach a 2-handle to X with framing one less than the contact framing, that is $\mathrm{tb}(L) - 1$ for a null-homologous knot, and extend the Stein structure of the resulting manifold. Gompf [**Gom98**] examined Stein manifolds further and showed that one could draw a handle diagram for one as shown in Figure 1.6.28 and one can use the formulas for the Thurston-Bennequin invariant and rotation number from Section 1.4.3 for the Legendrian knots in this diagram (even though some of them might not be null-homologous). Combining the work of Eliashberg and Gompf yields the following result.

Theorem 1.6.23 (Eliashberg 1990, [**Eli90b**] and Gompf 1998, [**Gom98**])**.** *An oriented* 4*-manifold X can be given the structure of a Stein domain if and only if it has a handle decomposition with only* 0*,* 1*, and* 2*-handles as shown in Figure 1.6.28 and the* 2*-handles h^2_i are attached to Legendrian knots L_i in the boundary of the union of the* 0 *and* 1*-handles with framing* $\mathrm{tb}(L_i) - 1$.

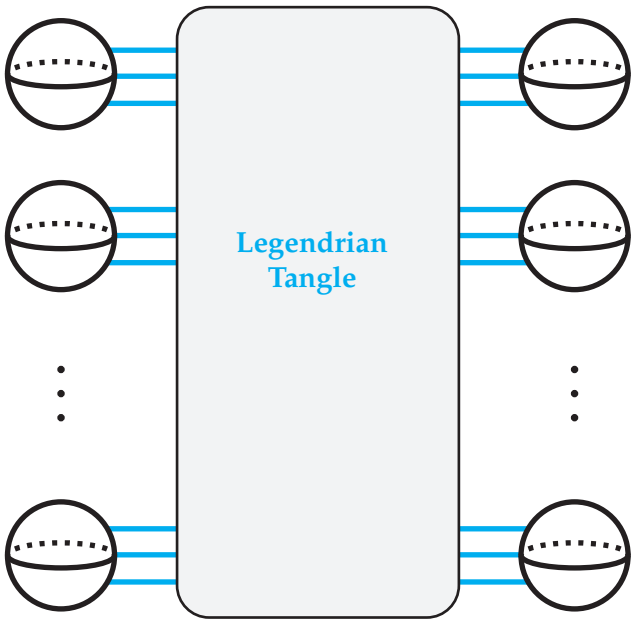

Figure 1.6.28. Handlebody diagram for a Stein manifold. Each pair of 3-balls on a horizontal line is the attaching region for a 1-handle. Legendrian knots are shown in blue.

Moreover, the first Chern class of X evaluated on h_i^2 is

$$\langle c_1(X), h_i \rangle = \text{rot}(L_i).$$

A slightly weaker version of this theorem (for Weinstein manifolds) will be proven in Section 7.4. For this theorem, we note that if X is a handlebody, then the k^{th} cellular chain groups of X are generated by the k-handles of X and hence the k^{th} cellular co-cycles are determined by their values on these handles.

We note that when attaching a 2-handle to a Legendrian knot L as in the theorem, the boundary undergoes a $(\text{tb}(L) - 1)$-Dehn surgery and we have a contact structure on the resulting manifold. More generally given any Legendrian knot L in a contact manifold (M, ξ) we can perform $(\text{tb}(L) - 1)$-Dehn surgery on L, and one can uniquely extend the contact structure on the complement of a neighborhood of L to the surgery torus so that it is tight on that torus. We will prove, and generalize, this in Section 6.2. The new contact manifold formed is said to be obtained from (M, ξ) by *Legendrian surgery on* L. From the theorem above, it is clear that any contact manifold obtained from the standard contact structure on S^3 by Legendrian surgery on some links will be Stein fillable and hence tight. We will use this observation to construct tight contact manifolds below.

We would like to compute the Euler class of the contact structure induced on the boundary of a Stein domain.

Exercise 1.6.24. Show that for a Stein manifold X the complex bundle TX restricted to ∂X splits as $\xi \oplus \mathbb{C}$ where ξ is contact structure induced on ∂X and the trivial bundle $\mathbb{C}$ is spanned by the Reeb vector field.

Thus we see that $c_1(X) = c_1(\xi) + c_1(\mathbb{C}) = c_1(\xi)$. Since the first Chern class of a rank 1 complex bundle is the same as its Euler class, we see that if (M, ξ) is obtained from (S^3, ξ_{std}) by Legendrian surgery on the link $L_1, \dots, L_k$ then the Euler class of ξ is given by

$$e(\xi) = \sum_{i=1}^{k} \text{rot}(L_i) PD([\mu_i]) \tag{1.6.4}$$

where $PD(h)$ means the Poincaré dual of the homology class h and $[\mu_i]$ is the homology class of the meridian μ_i of L_i.

We now construct some more tight contact structures on lens spaces. We defined lens spaces in Examples 1.6.12 but one can also define a lens space $L(p, q)$ as the result of $-\frac{p}{q}$ Dehn surgery on the unknot in S^3.

Exercise 1.6.25. Use the Rolfsen twist discussed in the previous section to show that any non-zero surgery on the unknot is equivalent to surgery on the unknot with surgery coefficient less than or equal to 1.

Example 1.6.26. Legendrian surgery on L_1 in Figure 1.6.29 corresponds to -2 Dehn surgery on the unknot. Thus we have a tight contact structure on $L(2, 1)$ and since the rotation

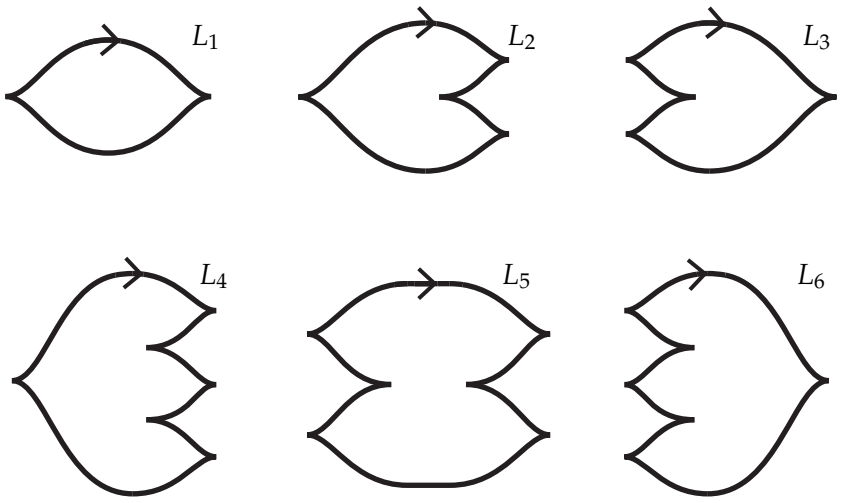

Figure 1.6.29. Legendrian knots L_1 through L_6.

number is 0 we see that its Euler class is 0. Similarly, Legendrian surgery on L_2 or L_3 will yield a tight contact structure on $L(3, 1)$ with the first having Euler class -1 and the

second having Euler class 1. So we see there are (at least) two distinct contact structures on $L(3,1)$. We finally note that Legendrian surgery on L_4, L_5, or L_6 will give tight contact structures on $L(4,1)$ with Euler classes $-2, 0, 2$ respectively. But note that 2 and -2 are the same in $\mathbb{Z}/4Z = H^2(L(4,1))$ so it is not clear at the moment if all three contact structures are different. In Section 6.2 we will see how to compute the Γ invariant and this will distinguish them but we will use a different method below.

For now, we focus on the contact structure ξ on $L(4,1)$ obtained from surgery on L_5. We will use an argument of Gompf [**Gom98**] to see that this contact manifold is virtually overtwisted. Indeed, consider Figure 1.6.30, the blue Legendrian knot L' is a Legendrian

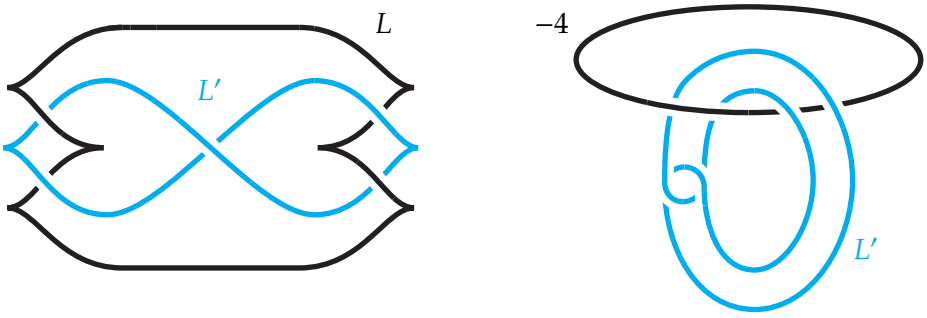

Figure 1.6.30. On the left is the knot L on which we perform Legendrian surgery and L' is a Legendrian knot in the surgered manifold. On the right, the same surgery on L is shown together with a smooth knot isotopic to L'.

knot in $L(4,1)$ with the contact structure induced from Legendrian surgery on L. Notice that L' bounds an immersed disk as can be seen on the left-hand side of the figure.

Exercise 1.6.27. Show that the framing the disk gives to L' is 2 larger than the Seifert framing on L'.

Given the exercise, we note that since $\mathrm{tb}(L') = -2$ the twisting of the contact planes relative to the immersed disk is 0. The fundamental group of $L(4,1)$ is generated by a meridian to L and thus the meridian will unwrap in any cover of $L(4,1)$. So in the 2-fold cover of $L(4,1)$ the immersed disk will lift to two embedded discs (though the disks will intersect each other). Focusing on one disk in the covering space we see that its boundary is a Legendrian knot with $\mathrm{tb} = 0$. That is the disk is an overtwisted disk in the covering space. Thus we see that ξ is indeed virtuatlly overtwisted.

Exercise 1.6.28. Give a criterion for a contact structure constructed by Legendrian surgery on a Legendrian link in (S^3, ξ_{std}) to be virtually overtwisted.
Hint: Consider Legendrian surgery on a Legendrian link that has a component that has been stabilized positively and negatively. Further, consider the meridian to that component. For a general criterion see Proposition 5.1 in [**Gom98**].

To construct distinct contact structures on lens spaces, and other manifolds, we will use the following theorem.

Theorem 1.6.29. *Suppose we have two distinct Stein structures on X build with only one 0-handle and 2-handles. Denote them by J_1 and J_2. If $c_1(J_1) \neq c_1(J_2)$, then the contact structures induced on the boundary of X by these two Stein structures are not isotopic.*

This theorem is a corollary of a result of Lisca and Matić [**LM97**], and we show how this follows from work of Plamenevskaya [**Pla04b**] in Heegaard Floer theory in the next section.

The continued fraction expansion of a rational number $-p/q < -1$ is

$$-p/q = a_0 - \cfrac{1}{a_1 - \cfrac{1}{a_2 \ldots - \cfrac{1}{a_n}}}$$

with $a_i \leq -2$. We will denote this by $r = [a_0, a_1, \ldots, a_n]$ and discuss it more in Section 4.3.

Lemma 1.6.30. *There are at least $|(a_0+1)(a_1+1)\cdots(a_n+1)|$ tight contact structures on $L(p,q)$ where $-p/q = [a_0, \ldots, a_n]$.*

In Section 5.7 we will see that these are all of the tight contact structures.

Proof. The lens space $L(p,q)$ can be obtained by surgery on the unknot, or integer surgery on a chain of unknots using the slam-dunk move (see Figure 1.5.23 and the surrounding text for the slam-dunk move). See Figure 1.6.31. The i^{th} unknot in the chain on the right

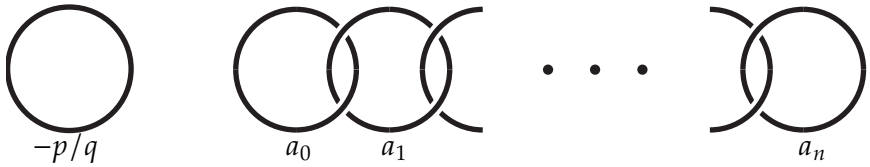

Figure 1.6.31. Two surgery pictures of the lens space $L(p,q)$. The left picture is obtained from the right by a series of slam-dunks starting from the left.

of the figure can be realized by a Legendrian unknot with tb $= a_i + 1$. We can then perform Legendrian surgery on the chain of Legendrian unknots to obtain a tight contact structure on $L(p,q)$ by Theorem 1.6.13. Note that the i^{th} unknot with framing a_i can be realized by a Legendrian unknot in $|a_i + 1|$ ways that are distinguished by their rotation number (one must stabilize the tb $= -1$ Legendrian unknot $|a_i + 2|$ times and as each stabilization can be positive or negative there are $|a_i + 1|$ ways to do this).

Notice that all the distinct Legendrian realizations of the chain have distinct rotation numbers on each component of the chain. Thus by Theorem 1.6.23 the Chern classes

of the Stein manifolds built by attaching 2-handles to these are all different, and thus Theorem 1.6.29 says that all the contact structures are distinct. □

It turns out that all the distinct contact structures constructed on lens spaces are in different homotopy classes of plane fields.

Exercise 1.6.31. If p is odd show that all the Euler classes of contact structures on lens spaces constructed above are distinct. If p is even (and larger than 2) then this is not true, but show that the Γ-invariant is distinct for all distinct contact structures. See Section 6.2 for formulas for the Γ-invariant. Thus each tight contact structure on a lens space is in a different Spin^c structure.

Above we have seen that unlike for overtwisted contact structures, tight contact structures do not exist in any homotopy class of plane field. Another distinction is that there can be multiple distinct contact structures in a fixed Spin^c structure as the next example, which is due to Lisca and Matić [**LM97**], shows.

Example 1.6.32. Let M_n be the manifold obtained from $1/n$ Dehn surgery on the right-handed trefoil. See Figure 1.6.32.

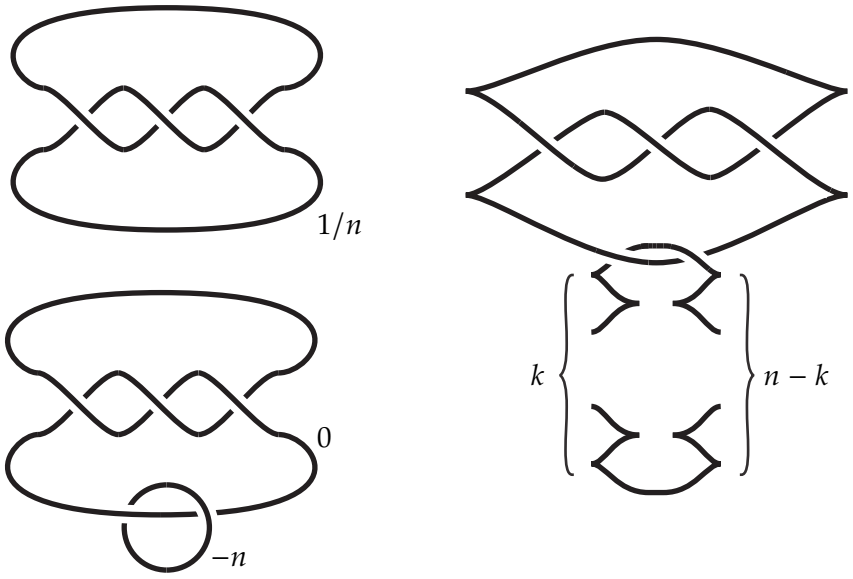

Figure 1.6.32. Two surgery diagrams for the 3-manifold M_n shown on the left. On the right is a Legendrian link on which Legendrian surgery will also produce M_n.

Exercise 1.6.33. Show that M_n has the same homology as S^3.

Using the slam-dunk move on surgery pictures we see that M_n can also be represented by surgery on the two component link in the bottom left of Figure 1.6.32. On the

right of the figure, we see a Legendrian link on which Legendrian surgery will give M_n. Let ξ_k be the contact structures on M_n given by Legendrian surgery on this link. Notice that there are $n-1$ choices for k and the rotation number of the unknot is $n-2k$. Thus the $n-1$ Stein domains constructed using different choices for k will all have distinct Chern classes. Thus the contact structures ξ_k must all be distinct from Theorem 1.6.29.

We now show that all the ξ_k are homotopic as plane fields. We first note that since M_n is a homology sphere the Γ-invariant is the same (indeed zero) for all the contact structures. We can compute the d_3-invariant using the Stein domain, (W_k, J_k), that fills (M_n, ξ_k). We compute that $c_1(J_k) = [n-2k, 0]^T$ and so $c_1^2(J_k) = 0$, the signature $\sigma(W_k) = 0$ and Euler characteristic $\chi(W_k) = 3$ for any k. Thus, their 3-dimensional homotopy invariants are the same; specifically, they are $d_3(\xi_k) = \frac{1}{4}(c_1^2 - 2\chi - 3\sigma + 2) = -1$. As discussed in Section 1.5.4, the Γ-invariant and the d_3-invariant completely determine the homotopy class of a plane field, so all of the ξ_k are homotopic as plane fields.

The above example shows that there can be arbitrarily many different tight contact structures in a fixed homotopy class of plane field. We will see in Section 5.8 that the 3-torus has infinitely many distinct tight contact structures in one homotopy class of plane field.

1.6.4. Heegaard Floer invariants. Heegaard Floer theory consists of a collection of invariants for low-dimensional manifolds. Since its inception, the reach and applicability of this theory in low-dimensional geometry and topology have been truly spectacular. In this section we introduce this theory in its simplest form, and briefly explore its connection to contact geometry. In Appendix C we will provide a more detailed discussion of the theory.

Let M be closed, connected, oriented 3-manifold equipped with a Spin^c structure $\mathfrak{t}$. (See Appendix 1.4 for details Spin^c structures.) With this data in [**OS04d**, **OS04e**] Ozsváth and Szabó introduced the Heegaard Floer homology groups $\widehat{HF}(M,\mathfrak{t})$ and $HF^+(M,\mathfrak{t})$ over $\mathbb{F} = \mathbb{Z}/2\mathbb{Z}$. The group HF^+ has the structure of an $\mathbb{F}[U]$-module where U is a formal variable. Since HF^+ is a $\mathbb{F}[U]$-module, we can think of U as an endomorphism of HF^+. There is a natural long exact sequence in homology connecting those groups as follows

$$\cdots \longrightarrow \widehat{HF}(M,\mathfrak{t}) \longrightarrow HF^+(M,\mathfrak{t}) \xrightarrow{U} HF^+(M,\mathfrak{t}) \longrightarrow \cdots$$

When M is rational homology sphere, or more generally when $c_1(\mathfrak{t})$ is a torsion class, the groups $\widehat{HF}(M,\mathfrak{t})$ and $HF^+(M,\mathfrak{t})$ carry a $\mathbb{Q}$-grading, and they split as

$$HF^o(M,\mathfrak{t}) = \bigoplus_{d\in\mathbb{Q}} HF^o_{(d)}(M,\mathfrak{t}).$$

here HF^o stands for one of $\widehat{HF}$ or HF^+.

Moreover, Heegaard Floer homology is functorial under cobordisms. Namely, for a spin^c cobordism $(W, \mathfrak{s})$ from $(M_1, \mathfrak{t}_1)$ to $(M_2, \mathfrak{t}_2)$, there is a homomorphism

$$F^o_{W,\mathfrak{s}} : HF^o(M_1, \mathfrak{t}_1) \to HF^o(M_2, \mathfrak{t}_2)$$

where $\mathfrak{t}_i = s|_{M_i}$. For contact geometric considerations below, it will be useful to consider the "upside-down cobordism" $\overline{W}$. This is the same W but considered as a cobordism from $-M_2$ to $-M_1$.

Suppose now ξ is a contact structure on M. In [**OS05**], Ozsváth and Szabó defined an element $c \in \widehat{HF}(-M, \mathfrak{t}_\xi)$ which is an isotopy invariant of ξ. Here $\mathfrak{t}_\xi$ is the spin^c structure induced by the plane field ξ. This invariant is called the *contact invariant*. If $c_1(\xi)$ is torsion (for example when M is rational homology sphere), then $c(\xi)$ is a homogeneous element of degree $-d_3(\xi)$. We will denote by $c^+(\xi)$ the image of $c(\xi)$ under the natural map $\widehat{HF}(-M, \mathfrak{t}_\xi) \longrightarrow HF^+(-M, \mathfrak{t}_\xi)$ mentioned in the long exact sequence above.

Heegaard Floer theory and 3-dimensional contact topology have had striking interactions since early 2000, and the contact invariant is at the center of this progress and captures some of the essential features of contact topology. We list some of these.

(1) If (M, ξ) is overtwisted, then $c(\xi) = 0$.

(2) If (M, ξ) is strongly fillable, then $c(\xi) \neq 0$.

(3) $c^+(\xi) \in \ker(U)$.

(4) $c(\xi)$ is natural under Stein cobordism. That is, if $(W, J) : (M_1, \xi_1, \mathfrak{t}_{\xi_1}) \to (M_2, \xi_2, \mathfrak{t}_{\xi_2})$ is a Stein cobordism, then the induced homomorphism $F_{\overline{W},\mathfrak{s}}$ carries $c(\xi_2)$ to $c(\xi_1)$ where $\mathfrak{s}$ is the canonical spin^c structure induced by J.

(5) If (M, ξ) has positive Giroux torsion, then $c(\xi) = 0$. In particular, (M, ξ) is not strongly symplectically fillable. For more on Giroux torsion see Sections 5.8 and 9.3.

The first four items are from the original paper [**OS05**] of Ozsváth and Szabó, and the last one is due to Ghiggini, Honda and Van Horn-Morris [**GHVHM**] (the conclusion that positive Giroux torsion obstructs strong fillability was previously known by work of Gay [**Gay06**]).

Next we focus how the contact class can be used to detect different tight contact structures. This will be achieved by the following results of Plamenevskaya.

Theorem 1.6.34 (Plamenevskaya, 2005, [**Pla04b**]). *Let W be a smooth compact 4-manifold with boundary $M = \partial X$. Let J_1, J_2 be two Stein structures on W that induce spin^c structures $\mathfrak{s}_1$, $\mathfrak{s}_2$ on W and contact structures ξ_1, ξ_2 on M. We puncture W and regard it as a Stein cobordism from S^3 to M. Suppose that $\mathfrak{s}_1|_M = \mathfrak{s}_2|_M$, but the spin^c structures $\mathfrak{s}_1$, $\mathfrak{s}_2$ are not isomorphic. Then*

(1) $F^+_{\overline{W},\mathfrak{s}_i}(c^+(\xi_j)) = 0$ *for* $i \neq j$

(2) $F^+_{\overline{W},\mathfrak{s}_i}(c^+(\xi_i))$ *is a generator of* $HF^+(S^3)$

An immediate and useful consequence of this is the following result.

Corollary 1.6.35. *Let W be a smooth compact 4-manifold with boundary $M = \partial X$. Let J_1, J_2 be two Stein structures on W that induce spin^c structures $\mathfrak{s}_1$, $\mathfrak{s}_2$ on W and contact structures ξ_1, ξ_2 on M. If the spin^c structures are not isomorphic, then the contact invariants $c(\xi_1), c(\xi_2)$ are distinct elements of $\widehat{HF}(-M)$.*

Note that a pair homotopic (as plane fields) contact structures ξ_1 and ξ_2 induces the same spin^c structure $\mathfrak{t}$, and hence the corresponding contact invariants $c(\xi_1), c(\xi_2)$ lie in $HF(-M, \mathfrak{t})$ and have the same grading. The result above says despite this $c(\xi_1)$ and $c(\xi_2)$ can still be different. Here is a concrete example.

Example 1.6.36. Recall M_n is the manifold obtained from $1/n$ Dehn surgery on the right-handed trefoil. A list of $n-1$ Stein fillable contact structures ξ_k was introduced in Example 1.6.32 which are explicitly drawn on the right-hand side of Figure 1.6.32. The handle description there also shows a Stein domain W_n. Various Legendrian surgeries provide Stein structure J_k on W_n which are pairwise non-homotopic. We show that the contact structures ξ_k have distinct contact invariants, and indeed we show that they generate an essential piece of $\widehat{HF}(-M_n)$. To see this, we first claim that one can calculate

$$\widehat{HF}(-M_n) = \mathbb{Z}^n_{(+2)} \oplus \mathbb{Z}^{n-1}_{(+1)}$$

where the subscripts denote the grading. (See Appendix C for this computation.) Also, in the computation above we drop the spin^c structure info since the manifold M_n is an integral homology sphere, and so has a unique spin^c structure.

Recall the grading of a contact structure is calculated via $\mathrm{gr}(c(\xi)) = -d_3(\xi)$. Now as calculated in Example 1.6.32 $d_3(\xi_k) = -1$, and hence $\mathrm{gr}(c(\xi_k)) = 1$. So, for each $k = 1, \cdots, n-1$, the contact class $c(\xi_k)$ lives in $\mathbb{Z}^{n-1}_{(+1)} \subset \widehat{HF}(-M_n)$. Since by Theorem 1.6.34, the $c(\xi_k)$ are pairwise distinct and primitive elements. Thus, we obtain that

$$\widehat{HF}(-M_n)_{(+1)} = \mathbb{Z}^{n-1}_{(+1)} = \mathrm{span}\{c(\xi_1), \cdots, c(\xi_{n-1})\}$$

Next, we examine the contact invariants of tight contact structures on lens spaces constructed in the previous section.

Example 1.6.37. Consider the lens space $L(n,1)$. Following the recipe in the proof of Lemma 1.6.30, one can list $n-1$ Stein fillable contact structures, say ξ_k where $k = 1, \cdots, n-1$, on $L(n,1)$. By using Theorem 1.6.34, we can easily see that the contact invariants $c(\xi_k)$ are non-zero and distinct.they are still linearly independent as they live in groups corresponding to different spin^c structures. One can calculate that $\mathrm{rank}\widehat{HF}(\pm L(n,1)) = n$, and the classes $c(\xi_k)$ are responsible for $n-1$ of these generators. This arguments apply

to a general $L(p,q)$. We already noted this by claiming the contact structures had distinct Γ-invariants, but we can now see this via Heegaard Floer theory too. Indeed, we will verify in Chapter 5 that the spin^c structures induced by the contact structures listed in Lemma 1.6.30, and hence their contact invariants are complete invariants of tight contact structures on $L(p,q)$.

We can significantly expand on the above example. To this end, we recall a crucial class of 3-manifolds, so called L-spaces, which was motivated by the Heegaard Floer homology of lens spaces, and its definition is due to Ozsváth and Szabó.

Definition 1.6.38. A rational homology sphere M is an L-space if $\widehat{HF}(M,\mathfrak{t}) = \mathbb{Z}$ for any $\mathfrak{t} \in \mathrm{Spin}^c(M)$.

We claim the property at the end of the previous example stays true for tight contact structures on all L-spaces that we know (and where the question can be answered). To explain this we consider small Seifert fibered spaces $M = M(e_0; r_1, r_2, r_3)$ where $e_0 \in \mathbb{Z}$ and $r_i \in \mathbb{Q} \cap (0,1)$, given in Figure 1.6.33. It is easy to check that M is a rational homology

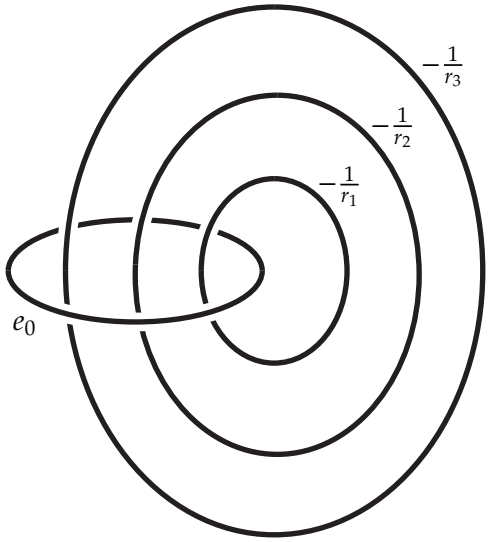

Figure 1.6.33. Surgery diagram for Seifert fibered space $M(e_0; r_1, r_2, r_3)$.

sphere if and only if $e_0 + r_1 + r_2 + r_3 \neq 0$. Among those most are L-spaces. For example, M is an L-space whenever $e_0 \neq -1, -2$, and there are precise criterion [**?**] that certifies M is an L-space for other values of e_0. Combining the results in [**Ghi08**, **GLS06**, **GLS07**, **Mat18**, **Tos20**, **Wu06**] one obtains the following structural result.

Theorem 1.6.39. *Let $M = M(e_0; r_1, r_2, r_3)$ be an L-space. Then two tight contact structures ξ_1 and ξ_2 on M are isotopic if and only if their induced spin^c structures $\mathfrak{t}_{\xi_1}$ and $\mathfrak{t}_{\xi_2}$ are isomorphic if and only if their contact invariants $c(\xi_1)$ and $c(\xi_2)$ are equal.*

In Section 7.1 in Chapter 7 we will study the relationship between various types of symplectic fillings and tightness. Heegaard-Floer homology and the contact invariant will be essential for this discussion.

1.6.5. A Bennequin type bound from Floer homology. Let $K \subset M$ be a smooth knot. Assume that M carries a unique spin^c structure. In [**OS04c**], Ozsváth and Szabó produces the complex $\widehat{CFK}(M,K)$ for the pair (M,K) which comes from $\widehat{CF}(M)$ together with a filtration:

$$\cdots \subset \mathcal{F}_{m-1} \subset \mathcal{F}_m \subset \cdots \subset \widehat{CF}(M)$$

by subcomplexes $\mathcal{F}_m$ such that $\mathcal{F}_m = 0$ for m sufficiently small and $\mathcal{F}_m = \widehat{CF}(M)$ for m sufficiently large. Now for a fixed non-zero element $x \in \widehat{HF}(M)$ one can define an integer-valued invariant $\widehat{\tau}_x(M,K)$ as follows:

$$\widehat{\tau}_x(M,K) = \min\{m \mid x \in \mathrm{Im}(i_m : H_*(\mathcal{F}_m) \to \widehat{HF}(M))\}$$

where i_m is induced by the inclusion $\mathcal{F}_m \subset \widehat{CF}(M)$. If one specializes to a knot $K \subset S^3$, then the construction above gives a well-known invariant $\tau(K) = \widehat{\tau}_\Theta(S^3,K)$ where Θ is the unique non-zero element of $\widehat{HF}(S^3)$. The invariant $\tau(K)$, which was defined by Ozsváth and Szabó [**OS03**] and independently by Rasmussen [**Ras03**], is a concordance invariant. It has a significant geometric content as it is shown in [**OS03**] that $|\tau(K)| \leq g_4(K)$ where $g_4(K)$ is the minimal genus of a surface in B^4 with boundary K. Moreover, it is shown by Plamenevkaya that this invariant captures a Bennequin type bound as follows.

Theorem 1.6.40 (Plamenevskaya 2004, [**Pla04a**]). *For a Legendrian knot $L \subset (S^3, \xi_{std})$*

$$\mathrm{tb}(L) + |\mathrm{rot}(L)| \leq 2\tau(L) - 1$$

This is clearly an improvement over the Bennequin bounds since $\tau(K) \leq g_4(K) \leq g(K)$, where g is the minimal genus of a Seifert surface for K.

1.7. Higher dimensional interlude

While higher dimensional contact manifolds are not the focus of this book, we will now briefly consider them to put out discussion in a broader context and highlight the difference between them and contact structures on 3-manifolds. We begin in the first section with a discussion of basic definitions and see how the "local" theorems differ in higher dimensions. In the following section we will discuss the existence of contact structures on higher dimensional manifolds which is quite different than in dimension 3. Finally, in the last section, we will discuss the tight versus overtwisted dichotomy and its relation to fillability.

1.7.1. Definitions and basic results. A *contact structure on a* $(2n+1)$*-dimensional manifold* M is a distribution ξ of rank $2n$ (that is a hyperplane field) that is *maximally non-integrable*. A more detailed look at the Frobenious Theorem shows that this means that ξ can be given (locally) by a 1-form α such that $\xi = \ker \alpha$ and $\alpha \wedge (d\alpha)^n$ is never zero. Notice in dimension 3 one does not need to say "maximally" non-integrable, but just non-integrable. In higher dimensions, there can be different degrees of non-integrability, but not in dimension 3. Arguing as above, one can easily see that $d\alpha$ at a point p, is a non-degenerate 2-form on ξ_p, that is the pair $(\xi_p, d\alpha_p)$ is a symplectic vector space (this is simply a vector space with a non-degenerate pairing).

Exercise 1.7.1. Show that a symplectic vector space must be even-dimensional. (You can see a proof of this in [**MS98**].)

Thus we see that a contact structure can only exist on an odd-dimensional manifold since the hyperplane must be even-dimensional.

We note that any distribution is at least "partially" integrable. For example, given a distribution, one may take a rank 1 subdistribution which locally is spanned by a vector field, and a vector field can always be integrated to give flow lines which are integral submanifolds of the rank 1 distribution. A careful look at the proof of the Frobenious theorem shows that a distribution of rank $2n$ on a $(2n+1)$-dimensional manifold does have submanifolds of dimension n tangent to it, but if the distribution is a contact structure then it cannot have integral submanifold of dimension larger than n. This is what is meant by "maximally non-integrable". Given a contact manifold (M^{2n+1}, ξ) a submanifold L that is tangent to ξ and of dimension n is called a *Legendrian submanifold*.

Exercise 1.7.2. Recall in Exercise 1.1.8 it was shown that any 3-manifold that admits a contact structure must be orientable. Is this true in higher-dimensional contact manifolds?
Hint: For a $(2n+1)$-manifold consider the parity of n.

We end our discussion of contact structures on all dimensions by considering Reeb vector fields of a contact structure.

Exercise 1.7.3. Given a non-degenerate 2-form ω on $\mathbb{R}^{2n+1}$ (that is ω^n is never zero). Show there is a unique vector field v, up to scale, such that $\iota_v \omega = 0$.

Let (M^{2n+1}, ξ) be a contact manifold and α a contact form for ξ. There is a unique vector field R_α such that

$$\alpha(R_\alpha) = 1 \text{ and } \iota_{R_\alpha}\omega = 0.$$

We call R_α the *Reeb vector field* of α and a *Reeb vector field* for ξ. The Reeb vector field is a fundamental object in contact geometry. The study of its dynamics is a central area of study and we will use it at various points during the rest of the book.

We now consider differences between "local theorems" in dimension 3 and higher. In particular, our main theorem, Theorem 1.2.1, becomes the following.

Theorem 1.7.4. *Let M be an oriented $(2n+1)$–manifold and $N \subset M$ a compact subset of M. Suppose ξ_0 and ξ_1 are contact structures on M such that*

$$\xi_0|_N = \xi_1|_N$$

and there are contact forms α_i for ξ_i such that

$$d\alpha_0|_{\xi_0} = f\, d\alpha_1|_{\xi_1},$$

for some non-zero function f. Then there is a neighborhood U' of N such that the identity map on U' is isotopic, relative to N, to a map that is a contactomorphism when restricted to a smaller neighborhood U of N.

One may easily see that Darboux's theorem is unchanged in higher dimensions as is Theorem 1.2.6 concerning neighborhoods of Legendrian submanifolds. In an $(2n+1)$-dimensional contact manifold one also is interested in *isotropic submanifolds*. These are submanifolds N of M that are tangent to ξ and have dimension less than or equal to n. If the dimension is less than n then there is a similar neighborhood theorem, but there are extra hypotheses. See [**Gei08**].

1.7.2. Existence of contact structures. We now turn to the question of the existence of contact structures on higher dimensional manifolds. In dimension 3 we know that any oriented 3-manifold admits a contact structure, see Theorem 1.5.4, and moreover, every homotopy class of plane field on such a manifold contains a contact structure, see Theorem 1.5.22. This is not true in higher dimensions. There is an obstruction to the existence of a contact structure. Just as in the 3-dimensional case, we will focus on the case of contact structures that are co-orientable, which is given globally as the kernel of a 1-form.

To understand this obstruction, let ξ be a co-orientable contact structure on M^{2n+1} given as the kernel of the 1-form α. Notice that ξ and the span of the Reeb vector field R_α split the tangent bundle

$$TM = \xi \oplus \mathbb{R}.$$

In addition, $d\alpha$ gives ξ the structure of a symplectic bundle. It is well-known, [**MS95**], that any symplectic bundle has a (unique up to homotopy) complex structure. (Recall, a *complex structure* on a bundle $E \to M$ is a bundle map $J\colon E \to E$ such that $J^2 = -id_E$.) Thus ξ has structure group $U(n)$ and hence TM has structure group $U(n) \oplus \mathbf{I}$. See Appendix 1.1 for a reminder about structure groups. We say an *almost contact structure* on M^{2n+1} is a reduction of the structure group of TM to $U(n) \oplus \mathbb{I}$ and two such structures are homotopic if there is a 1-parameter family of reductions connecting them. It is easy to see that this definition is equivalent to the existence of a pair (η, J) where η is a hyperplane field in TM and J is a complex structure on η.

Exercise 1.7.5. Show an almost contact structure on M can equivalently be defined by a pair (α, ω) where α is a non-singular 1-form and ω is a 2-form on M that induces a symplectic structructure on $\eta = \ker \alpha$. Given two such pairs (α, ω) and (α', ω') when do they define homotopic almost contact structures?

Clearly from the discussion above for M to admit a contact structure it must admit an almost contact structure. We observe that there are simple bundle theoretic obstructions to admitting an almost contact structure. For example, notice that given an almost contact structure (η, J) on M we clearly have that the Stiefel-Whitney classes of TM and η agree

$$w_i(TM) = w_i(\eta)$$

since the total Stiefel-Whitney class of the trivial bundle is 1. Moreover, we know that for a complex bundle, the even Stiefel-Whitney classes are the mod 2 reduction of the Chern classes. Thus if, for example, $w_2(M) \in H^2(M; \mathbb{Z}/2\mathbb{Z})$ does not have an integral lift, then M does not admit an almost contact structure and hence it does not admit a contact structure.

Exercise 1.7.6. Show that any oriented 3-manifold admits an almost contact structure and the almost contact structures are in one-to-one correspondence with the homotopy classes of oriented plane fields. (Note that this is why we did not need to discuss almost contact structures in dimension three since for 3-manifolds they are just homotopy classes of oriented plane fields.)

Exercise 1.7.7. Show that an oriented 5-manifold M admits an almost contact structure if and only if $w_2(M)$ admits an integral lift. Moreover, show that two almost contact structures are homotopic if and only if they are homotopic on the 2-skeleton of M. Finally, if $H^2(M; \mathbb{Z})$ has no 2-torsion, then the homotopy type of the almost contact structure is determined by its first Chern class.
Hint: Show that M admitting an almost contact structure is equivalent to there being a section of the $SO(5)/U(2)$ bundle associated to TM and then use the fact that $SO(5)/U(2)$ is homotopy equivalent to $\mathbb{C}P^3$, see [**Gei08**].

Exercise 1.7.8. Show that the simply connected 5-manifold $SU(3)/SO(3)$ does not have an almost contact structure. Should we give a hint?

In general, the existence of almost contact structures in higher dimensions is a purely algebraic topological question [**Mas61**].

So now the real question about the existence of contact structures in higher dimensions is when an almost contact structure on a manifold homotopic, through almost contact structures, to a contact structure.

There is a long history of partial results along these lines. For example in 1991 Geiges [**Gei91**] showed that every almost contact structure on a simply connected 5-manifold is

homotopic to a contact structure and in 1998 Geiges and Thomas [GT98] gave a partial answer for 5-manifolds with $\pi_1 = \mathbb{Z}/2\mathbb{Z}$. In 1993, The case of "highly connected" manifolds in all dimensions was addressed by Geiges [Gei93]. But in general, the existence question remained elusive. For example, up until 2002 it was not known if tori T^{2n+1} for $n > 2$ admitted contact structures! (In 1979 Lutz [Lut79] showed that T^5 admitted a contact structure, but for over 20 years nothing was known about T^7.) In 2002, Bourgeois [Bou02] showed that if M admits a contact structure then so does $M \times T^2$.

The first general result was in 2015 when Casals, Pancholi, and Presas [CPP15] showed that any almost contact structure on a 5-manifold is homotopic to a contact structure. The general existence question was answered in 2015 by Borman, Eliashberg, and Murphy [BEM15]. In that paper they defined a notion of overtwisted contact structures in higher dimensions and showed.

Theorem 1.7.9 (Borman, Eliashberg, and Murphy 2015, [BEM15])**.** *Let (η, J) be an almost contact structure on a manifold M. Then there is a homotopy of (η, J) through almost contact structures to an overtwisted contact structure ξ on M. Moreover, any other contact structure ξ_0 that is homotopic to ξ through almost contact structure and is overtwisted is isotopic to ξ.*

Just as Theorem 1.5.22 did in dimension 3, this theorem completely answers the general existence question in higher dimensions. The theorem parallels Eliashberg's 3-dimensional overtwisted theorem, Theorem 1.6.2. As, for the tight versus overtwisted dichotomy we will see in the next section that there are actually significant differences between dimension 3 and higher.

Before moving on to the next section we briefly discuss the definition of overtwisted contact structures in higher dimensions. The original definition in [BEM15] is somewhat more complicated than the definition in dimension 3 given above, but there are many alternate characterizations of overtwistedness that we now discuss. In [CMP19] Casals, Murphy, and Presas gave several "geometric" interpretations of a contact structure being overtwisted. The simplest criterion for (M^{2n+1}, ξ) being overtwisted is that there is a contact embedding of $(\mathbb{R}^3 \times \mathbb{C}^{n-2}, \ker(\alpha_{ot} + \lambda_{std}))$ where α_{ot} is a contact 1-form for any overtwisted contact structure on $\mathbb{R}^3$, such as the "standard" overtwisted contact structure in Example 1.1.11 (3), and λ_{std} is the Liouville form on $\mathbb{C}^{n-2}$ which in coordinate $(x_1, y_1, \ldots, x_{n-2}, y_{n-2})$ can be expressed by

$$\lambda_{std} = \frac{1}{2}\sum_{i=1}^{n-2}(x_i\, dy_i - y_i\, dx_i).$$

There are several other simple characterizations of overtwisted contact structures, but most involve "loose Legendrian submanifolds" introduced by Murphy in [Mur12] or open book decompositions, which we have not defined yet. So we refer the reader to the paper [CMP19] for more details.

1.7.3. Tight, overtwisted, and fillable contact structures. Just as in dimension 3, we will say a contact structure ξ on a $(2n+1)$-dimensional manifold M is *tight* if it is not overtwisted.

We can use symplectic fillings to produce tight contact structures. Just as in dimension 2 we say a symplectic manifold (X, ω) of dimension $2n+2$ is a *strong symplectic filling* (or just *symplectic filling*) of a contact manifold (M, ξ), if M is the oriented boundary of X and there is a vector field v defined near $\partial X = M$ such that v points out of ∂X, $\mathcal{L}_v \omega = \omega$, and $\iota_v \omega$ restricted to M is a contact form for ξ. There is also a notion of weak symplectic filling in higher dimensions, but it is a bit more complicated than in dimension 3. According to [**MNW13**], we say a symplectic manifold (X, ω) is a *weak symplectic filling* of the contact manifold (M, ξ) if M is the oriented boundary of M and

$$\alpha \wedge d\alpha^k \wedge \omega_\xi^{n-k} > 0$$

for all $k = 0, \dots, n$, where ω_ξ is ω restricted to the contact hyperplanes ξ. In [**MNW13**] it was shown that this definition is equivalent to (M, ξ) being the *tame pseudoconvex boundary* of (X, J) for some almost complex structure on X (that is a complex structure on TX). This means that ξ is the set of J-complex tangencies

$$\xi = TM \cap JTM,$$

$\omega(w, Jw) > 0$ for all non-zero vectors w (we say that J is an ω-*tame* complex structure), and for any 1-form α with kernel ξ we have $d\alpha(w, jw) > 0$ for any non-zero $w \in \xi$. One also says of this last

Exercise 1.7.10. Show a strongly symplectic filling of (M, ξ) is also a weak symplectic filling.

It is much more difficult to show that there are weakly fillable contact structures in high dimensions that cannot be strongly fillable. For such examples, see [**MNW13**]. One may also prove that fillable implies tight in higher dimensions.

Theorem 1.7.11 (Niederkrüger, [**Nie06**])**.** *If (M, ξ) is a weakly symplectically fillable contact manifold, then ξ is tight.*

As a precursor to the notion of overtwisted in higher dimensions Niederkrüger defined the notion of a *plastikstufe* for high-dimensional contact manifolds. This was a particular type of "parameterized" overtwisted disk. He then proved that a contact manifold that contained a plastikstufe could not be symplectically filled. Then in [**BEM15**] it was shown that any overtwisted manifold admits a plastikstufe. Combining these results yields the above theorem.

Recall that in our discussion about symplectic fillability and tightness in the previous section, we noted that, while there are tight contact structures that are not symplectically

fillable, they are relatively rare. In particular, they do not exist on S^3, and if they exist, there are only finitely many of them. In the work of Bowden, Gironella, Moreno, and Zhou we see a striking difference between dimensions 3 and higher.

Theorem 1.7.12 (Bowden, Gironella, Moreno, and Zhou, [BGMZ24]). *If M is a contact manifold of dimension at least 7 that admits a Stein fillable contact structure, then M admits a tight contact structure in the same homotopy class of almost contact structure that is not symplectically fillable. If the dimension of at least 11 and the first Chern class of the contact structure is torsion, then M admits infinitely many distinct tight contact structures that are not symplectically fillable.*

There is an analog to the first part of the theorem when M has dimension 5 if the first Chern class of the contact structure is zero.

This theorem is striking for several reasons. Firstly, it shows that many homotopy classes of almost contact structures contain infinitely many distinct tight contact structures, whereas in dimension 3 there can be at most finitely many. In addition, the result shows that tight, but not strongly fillable contact structures are abundant in higher dimensions, which again is not possible in dimension 3.

1.8. History and applications

1.8.1. Geometric optics. Add section

1.8.2. Thermodynamics. Add section

1.8.3. Classical mechanics. Add section

1.8.4. Jet spaces and partial differential equations. One of the precursors to modern contact geometry is contained in the work of Sophus Lie. In [**?**], Lie introduced the notion of a *berhrungstransformation* in his study of partial differential equations. Even though the notion of a contact structure had not yet been formalized, Lie's berhrungstransformation are contactomorphism, and his work can nicely be described in terms of contact geometry and jet spaces. We explore this idea in this section.

Given any function

$$F\colon \mathbb{R}^{2n+1} \to \mathbb{R}$$

we get a first-order partial differential equation by looking for functions $u\colon \mathbb{R}^n \to \mathbb{R}$ that satisfy

$$F\left(x_1, \dots, x_n, \frac{\partial u}{\partial x_1}, \dots, \frac{\partial u}{\partial x_n}, u\right) = 0 \tag{1.8.5}$$

For example the partial differential equation

$$5\frac{\partial u}{\partial x}\frac{\partial u}{\partial y} - (x^2 - y)\left(\frac{\partial u}{\partial x}\right)^2 = x^2 + y^2 + 3$$

can be written as above where

$$F(x_1, x_2, y_1, y_2, z) = 5y_1y_2 - (x_1^2 - x_2)y_2^2 - x_1^2 - x_2^2 - 3.$$

That is finding a function $u\colon \mathbb{R}^2 \to \mathbb{R}$ satisfying the equation is the same as finding u satisfying $F\left(x, y, \frac{\partial u}{\partial x}, \frac{\partial u}{\partial y}, u\right) = 0$.

To continue our story we need to introduce the jet space of a manifold. This is a natural contact manifold associated with any manifold. If M is an n-manifold then the cotangent bundle T^*M is a $2n$-manifold that has a natural exact symplectic structure. Specifically, there is a unique 1-form λ on T^*M that is characterized by the property that for any 1-form β on M, recall $\beta\colon M \to T^*M$ is a section, we have

$$\beta^*\lambda = \beta.$$

If we choose local coordinates $(q_1, \dots, q_n)$ on some open set U in M, then we get local coordinates $(q_1, \dots, q_n, p_1, \dots, p_n)$ on $T^*U \subset T^*M$. In these coordinates we can write λ as

$$\lambda = \sum_{i=1}^{n} p_i\, dq_i.$$

Exercise 1.8.1. Show that λ exists and that λ has the claimed local expression.

We now define the *jet space of* M, or more precisely the 1-*jet space of* M, to be $J^1(M) = T^*M \oplus \mathbb{R}$. This is an $\mathbb{R}^{n+1}$ bundle over M (the fiber at any point $x \in M$ is $T_x^* \oplus \mathbb{R}$). Let $\pi\colon J^1(M) \to M$ be the bundle projection map. Consider the 1-form

$$\alpha = dt - \lambda$$

where t is the coordinate on $\mathbb{R}$.

Exercise 1.8.2. Show that α is a contact form on $J^1(M)$.
Hint: Check this in local coordinate using the above formula for λ.

We note that $J^1(\mathbb{R}^1)$ is simply $\mathbb{R}^3$ with its standard contact structure from Example 1.1.11(1), and more generally we call the contact structure on $J^1(\mathbb{R}^n)$ the standard contact structure on $\mathbb{R}^{2n+1}$.

Now given a function $f\colon M \to \mathbb{R}$ we can consider its 1-*jet*, $j^1(f)$. This is the section of $J^1(M) \to M$ given by

$$j^1(f)(x) = (df_x, f(x)),$$

that is, the component of $j^1(f)$ in T_x^*M is just the differential of f evaluated at x and the component in $\mathbb{R}$ is just the value of the function $f(x)$. Notice that in local coordinates,

$j^1(f)$ "remembers" the value of f and the value of all its first derivatives. In particular, for functions $f\colon \mathbb{R}^n \to \mathbb{R}$ and $g\colon \mathbb{R}^n \to \mathbb{R}$, the 1-jets of f and g agree at x if and only if their first order Taylor polynomials at x agree. So we can think of $j^1(f)$ as a generalization of the first-order Taylor polynomial of f.

We now note that

$$(j^1(f))^*\alpha = d(f) - df^*\lambda = df - df = 0.$$

Thus the image of $j^1(f)$ is a Legendrian submanifold of $J^1(M)$.

Exercise 1.8.3. Show that a section $\sigma\colon M \to J^1(M)$ parameterizes a Legendrian submanifold if and only if σ is $j^1(f)$ for some function $f\colon M \to \mathbb{R}$.

Returning to partial differential equations, we note that the function $F\colon \mathbb{R}^{2n+1} \to \mathbb{R}$ can be thought of as a function $F\colon J^1(\mathbb{R}) \to \mathbb{R}$. Then from the above discussion, it should be clear that a function $u\colon \mathbb{R}^n \to \mathbb{R}$ is a solution to the partial differential equation given in Equation 1.8.5 if and only if $F \circ j^1(u) = 0$. Thus solving Equation 1.8.5 is equivalent to finding a section $\sigma\colon \mathbb{R}^n \to J^1(\mathbb{R}^n)$ such that

(1) $\sigma(\mathbb{R}^n)$ is Legendrian and

(2) $F \circ \sigma = 0$.

Thus we have turned the analytic problem of solving the Partial Differential Equation 1.8.5 into solving two other problems. The first is geometric while the second is algebraic (if F is an algebraic function). Sophus Lie observed that one could try to use this separation to simplify the problem. Specifically, he noticed that one could look for a contactomorphism ϕ of $J^1(\mathbb{R}^n)$ that simplifies the equation $F \circ \sigma = 0$. If we could solve this "simplified" problem, then we could use ϕ to get a solution of the original problem.

FIND A GOOD EXAMPLE TO DEOMONSTRATE

1.8.5. The unit cotangent bundle and Riemannian geometry. Add section

1.8.6. Fluid dynamics. In [EG00a] the first author and Ghrist introduced the use of contact geometry into the study of fluid dynamics and studied the connection extensively in [EG00b, ?, EG05]. To understand this connection we recall that if v is a time-dependent vector field on a manifold M with a Riemannian metric g, then we say v satisfies the Euler equations for a perfect incompressible fluid if

$$\begin{aligned} \frac{\partial v}{\partial t} + \nabla_v v &= -\nabla p \\ \mathcal{L}_v \mu &= 0. \end{aligned} \tag{1.8.6}$$

where $\nabla_v v$ is the covariant derivative of v along v, p is the "pressure" of the system, μ is a volume form (usually assumed to be associated to g), $\mathcal{L}_v \mu$ is the Lie derivative

of the volume form μ in the direction of v, and ∇p is the gradient of p. The second equation says that v is incompressible (that is preserves volume) and the first equation is a simplification of the Navier-Stokes equation for a perfect (no viscosity) incompressible fluid flow.

We will primarily be concerned with steady solutions to the Euler equations, that is solutions that do not depend on time. Below is a sampling of results that can be proven with contact geometry. First we have the existence of non-singular steady solutions.

Theorem 1.8.4 (Etnyre and Ghrist 2000, [EG00a]). *Every closed oriented 3-manifold admits smooth, steady, nonsingular solutions to the Euler equations for a perfect incompressible fluid.*

Furthermore, every compact domain in $\mathbb{R}^3$ with toroidal boundary components likewise admits such solutions that leave the boundaries invariant.

We can also guarantee certain properties about solutions to the Euler equations. In the theorems below C^ω means *real analytic*.

Theorem 1.8.5 (Etnyre and Ghrist 2000 and 2002, [EG00a, EG02]). *Every C^ω steady solution to the Euler equations for a perfect incompressible fluid on S^3 (in any metric on S^3) possesses a closed flowline. The same is true for flows on the solid torus if the flow is tangent to the boundary.*

To give some perspective on this result we recall the famous Seifert conjecture which asks if every C^k non-zero vector field on S^3 must possess a closed orbit. This conjecture is known to be false for $k = 1$ by Schweitzer [Sch74], for $k = 2$ by Harrison [Har88], for $k = \infty$ by K. Kuperberg [Kup94], and for real-analytic vector fields by G. Kuperberg and K. Kuperberg [KK96]. There is also a C^1 counterexample for volume-preserving fields due to G. Kuperberg [Kup96]. Given these results, one is left to wonder what "regularity" is necessary to force the flow of a vector field to admit a periodic orbit (or does one ever expect a vector field to have a periodic orbit). The theorem above shows that if a vector field is real-analytic and also satisfies the time-independent Euler equations then it must have a closed orbit.

We now turn to the question of what are the possible periodic orbits of a steady fluid flow.

Theorem 1.8.6 (Etnyre and Ghrist 2000, [EG00b]). *For some C^ω Riemannian structure on S^3 (or $\mathbb{R}^3$), there exists a C^ω nonvanishing steady Euler field whose periodic flow lines realize all knot and link types.*

If one is interested in flows with lower regularity, we still have "forcing results". Below we will define *Beltrami fields* these are special steady solutions to the Euler equations.

Theorem 1.8.7 (Etnyre and Ghrist 2001, [EG01]). *There is a computable index I that can be associated with a Beltrami field on a solid torus, and any C^2 or smoother non-vanishing Beltrami*

field on an invariant Riemannian solid torus having nonzero index I possesses a contractible closed orbit.

We note that one can also prove results related to time-dependent solutions to the Euler equations. Here a solution time-independent solution to the Euler equations is, roughly, called "unstable" if when it is (appropriately) perturbed the corresponding solution to the time-dependent Euler equations has unbounded growth in the energy norm (see [EG05] for a more precise definition). Before stating the result, we note, as discussed below, that a vector field that is an eigenfield for the curl operator will be a special case of a Beltrami field and hence a steady solution to the Euler equations.

Theorem 1.8.8 (Etnyre and Ghrist 2005, [EG05])**.** *For a generic set of C^r Riemannian metrics on the 3-torus (for each $2 \leq r < \infty$), all of the curl-eigenfield solutions to the Euler equations (with nonzero eigenvalue) are linearly hydrodynamically unstable in the energy norm.*

To see the connection to contact geometry we will reformulate Equations 1.8.6, using the metric g, in terms of differential forms. Recall there is a one-to-one correspondence between vector fields and 1-forms using the metric g. Specifically, if v is a vector field then $\iota_v g$ is a 1-form, where $\iota_v g$ is the contraction of v into the 2-tensor g. Consulting [AMR88, Section 8.2] we see that

$$\iota_{\nabla_v v} g = \mathcal{L}_v(\iota_v g) + \frac{1}{2} d(\|v\|)^2.$$

Recalling that ∇f for a real-valued function f is the unique vector field that satisfies $\iota_{\nabla f} g = df$, and converting Equations 1.8.6 into 1-forms we have

$$\frac{\partial \iota_v g}{\partial t} + \mathcal{L}_v(\iota_v g) = -d\left(p - \frac{1}{2}\|v\|^2\right).$$

We now recall Cartan's formula [AMR88, Theorem 6.4.8] which says $\mathcal{L}_v = \iota_v d + d\iota_v$ and see the above equation becomes

$$\frac{\partial \iota_v g}{\partial t} + d(\|v\|^2) + \iota_v(d\iota_v g) = -d\left(p - \frac{1}{2}\|v\|^2\right).$$

Simplifying yields

$$\frac{\partial \iota_v g}{\partial t} + \iota_v(d\iota_v g) = -dP \tag{1.8.7}$$

where $P = p + \frac{1}{2}\|v\|^2$ is called the reduced pressure. The particular function P is not important and we will say v satisfies the Euler equations if it satisfies the previous equation and $\mathcal{L}_v \mu = 0$.

Finally, we would like to reformulate this last equation in terms of standard notions from vector calculus generalized to a Riemannian manifold. To this end, we define the

curl of a vector field v with respect to a metric g and volume form μ (again, we usually take μ to be the volume form associated to g) to be the unique vector field $\nabla \times v$ satisfying

$$\iota_{\nabla \times v}\mu = d(\iota_v g)$$

and the cross-product of two vector field v and w to be the unique vector field $v \times w$ that satisfies

$$\iota_{v\times w} g = \iota_v \iota_w \mu.$$

Exercise 1.8.9. If $M = \mathbb{R}^3$, g is the standard flat metric on $\mathbb{R}^3$, and μ is the standard volume form on $\mathbb{R}^3$, then check that the curl of a vector field and the cross-product of vector fields defined above agree with their standard definition in this case.

Exercise 1.8.10. Show that $v \times w$ is orthogonal to v and w.

Now we can rewrite Equation 1.8.7 as

$$\frac{\partial v}{\partial t} + v \times (\nabla \times v) = -\nabla P$$

Recall above we are mainly considering steady solutions to the Euler equations so v does not depend on t. Thus we are concerned with

$$v \times (\nabla \times v) = -\nabla P. \tag{1.8.8}$$

Notice if $\nabla P = 0$ then we must have that v and $\nabla \times v$ are parallel. We call a vector field v a *Beltrami field* if $\nabla \times v = fv$ for some function f and we say the field is a *rotational Beltrami field* if f is never 0. If f is constant then v is a *curl eigenfield*. We will call a vector field *non-singular* if it is never zero.

We call a vector field v on a 3-manifold M *Reeb-like* if there is some contact form α on M and $v = hR_\alpha$ where R_α is the Reeb field for α and h is a positive function (this can equivalently be stated as $\iota_v d\alpha = 0$ and $\alpha(v) > 0$). We are now ready for the main theorem connecting Beltrami fields to contact geometry.

Theorem 1.8.11. *On a Riemannian 3-manifold M a non-singular rotational Beltrami field is a Reeb-like vector field for some contact form on M. Conversely, any never-zero rescaling of a Reeb vector field is a volume-preserving, rotational Beltrami field in some Riemannian metric on M.*

Proof. Suppose that v is a rotational Beltrami field for a metric g on M with volume form μ. Then let $\alpha = \iota_v g$. Notice that the equation $\nabla \times v = fv$ for some f translates into $f\iota_v\mu = d\iota_v g = d\alpha$ and we have

$$\alpha \wedge d\alpha = f(\iota_v g) \wedge \iota_v \mu.$$

At a given point $x \in M$ let u_x, w_x be vectors in T_xM that are orthogonal to $v(x)$ and together with $v(x)$ span $T_x(M)$. Then notice

$$\alpha \wedge d\alpha(v(x), u_x, v_x) = f\|v(x)\|^2 \omega(v(x), u_x, w_x) \neq 0$$

and thus $\alpha \wedge d\alpha$ is a volume form on M. That is α is a contact form and

$$\iota_v d\alpha = f \iota_v \iota_v \omega = 0$$

so v is Reeb-like for α.

Conversely, given a Reeb vector field X on M and positive function f it is not hard to construct a Riemannian metric for which fX is a rotational Beltrami filed. See the next section for this construction. □

Notice that from the previous theorem we see that any Reeb vector field on a 3-manifold will solve the Euler equations for some Riemannian metric on the manifold. This proves Theorem 1.8.4 since we know any oriented 3-manifold admits a contact structure by Theorem 1.5.4.

As for Theorem 1.8.5 we consider the case of a steady (recall, this means time-independent) solution v to the Euler equations on S^3 with some metric. If v has any singular points, then it has flow lines that are constant (hence periodic with any period). We now recall a theorem of Arnold.

Theorem 1.8.12 (Arnold 1966, [**Arn66**])**.** *Let v be a real-analytic steady nonsingular solution to the Euler equations on a closed Riemannian 3-manifold M. If v is not everywhere parallel to its curl, there exists a compact real-analytic subset S in M of codimension 1 or more which splits M into a finite collection of $T^2 \times \mathbb{R}$. Each $T^2 \times \{x\}$ is invariant under the flow of v and the flow is conjugate to a linear flow.*

A sketch of the proof is as follows. Since v satisfies Equation 1.8.8 we know that P is an integral for v. That is the flow lines of v are constrained to lie on level sets of P (since c is orthogonal to ∇P). Since P is real analytic we know that the singular set S (that is the pre-image of all the singular values) must be of codimension at least 1. Now for a point outside of S it sits on a pre-image that is a surface in M and since there is a non-zero vector field on it (that is v) it must be a torus.

Proof of Theorem 1.8.5. We consider the case when the reduced pressure P is not constant. We then have the real-analytic set S from Aronld's theorem. By real analyticity we know S is a Whitney stratified set of codimension at least 1, [**GM88**]. This says that S is the union of compact manifolds of dimension 0, 1, and 2, that come together in simple ways. It is not hard to see that S and its strata are preserved by the flow. If there are no 0 or 1 strata, then S^3 will be foliated by tori but this is not possible.

Exercise 1.8.13. Show that S^3 cannot be foliated by tori.

It is not hard to see that there must be 1-strata and that these will be closed orbits in the flow.

We now need to consider the case when P is contact. As noted above this will imply that $\nabla \times v = fv$ for some function f. If f is non-zero then we can use Theorem 1.8.11 to find a contact structure such that v is a Reeb-like vector field for the contact structure. We now have the desired periodic orbit by a famous theorem of Hofer.

Theorem 1.8.14 (Hofer 1993, [Hof93]). *The flow of any Reeb vector field on S^3 has a closed orbit.*

The proof of this theorem involves pseudo-holomorphic curves and will be sketched in Appendix B.

We are left to consider the case when f is zero at some point of S^3. If f is not constant then we claim that f is an integral of v and hence this case follows just like the case when P was an integral. To see that f is an integral recall that the divergence of v is zero: $d\iota_v\mu = 0$ and so

$$df \wedge \iota_v\mu = d(\iota_{fv}\mu) = d(\iota_{\nabla\times v}\mu) = d(d\iota_v g) = 0.$$

Since $df \wedge \mu$ is a 4-form it must be zero so the above equation is equivalent to $df(v)\mu = 0$; in particular, f is constant on flow lines of v.

We finally consider the case when $f = 0$. Notice that this tells us that the 1-form $\alpha = \iota_v g$ is closed. From our discussion in Section 1.1 we know that the kernel of α defines a foliation on S^3 and v is transverse to this foliation. A theorem of Novikov [Nov65] implies that this foliation must contain a leaf that is a torus, but this contradicts the fact that v is a non-singular volume-preserving flow transverse to the leaves of the foliation. □

add some recent papers building on the above + hydrodynamic instability

1.8.7. More connections to Riemannian geometry. In Section 1.8.5 we saw that the contact geometry of a unit co-tangent bundle was closely related to Riemannian geometry through the geodesic flow. Here we would like to focus on other connections between contact geometry and Riemannian geometry. For context recall that in dimension 3 there is a profound connection between Riemannian geometry and topology as was formalized in Thurston's geometrization conjecture [Thu82], which was established in the early 2000 by Perelman [**?**]. On the other hand, we will see in the next section that there are subtle connections between contact structures and the topology of 3-manifolds. Given these connections, one might expect there to be important connections between contact structure and Riemannian geometry. Here we will discuss some interesting questions in Riemmanian geometry that arise from contact geometry and how a Riemannian metric can influence important properties of a contact structure.

To begin our discussion we assume that the reader is familiar with the basic notation from Riemannian geometry, as can be found in [Pet16], but will briefly recall a few facts

and notation. Given a Riemannian manifold (M, g) one can consider the *exponential map*

$$\exp_p \colon T_pM \to M$$

that sends a vector $v \neq 0$ to $\gamma_v(1)$ where γ_v is the geodesic through p with tangent vector v at p and sends the zero vector $\mathbb{0}$ to p (here $\exp_p$ might not be defined for all $v \in T_pM$, but will be defined for a neighborhood of $\mathbb{0} \in T_pM$). This map is smooth and a diffeomorphism from some open set about $\mathbb{0}$ to an open neighborhood of p. Given a plane $\sigma \subset T_pM$ we let Σ_σ be the image of a neighborhood of $\mathbb{0}$ in σ under the map $\exp_p$. The metric g induces a metric on Σ_σ and we define the *sectional curvature* of σ to be the Gauss curvature of the surface Σ_σ at p its induced metric. We denote this number by $\kappa_p(\sigma)$.

We recall that all the various "curvatures" of (M, g) — such as the curvature tensor, the Ricci curvature, and the scalar curvature — can be computed from κ.

The first hope one might have to relate Riemannian geometry and contact geometry is that the sectional curvature of the contact planes would control something about the contact geometry (like whether the contact structure is tight or overtwisted). This is not the case.

Theorem 1.8.15 (Krouglov 2008, [**Kro08**])**.** *Given any (cooriented) contact structure ξ on a closed 3-manifold M and any strictly negative function f, there is a weakly compatible metric on M such that the sectional curvatures of ξ are given by f. If the Euler class of ξ is zero then any function f may be realized as the sectional curvature of ξ for some metric.*

We will define "weakly compatible metrics" below, but the point of the theorem is that the sectional curvatures of a contact structure cannot tell us anything interesting about the contact structure (even for nice, that is compatible, metrics). The proof of this theorem is done via an explicit local alteration of the metric.

To move forward, we discuss a way to use a metric to determine if a plane field is a contact structure. To this end, let ξ be any plane field and consider the following characterization of ξ being a contact structure.

Exercise 1.8.16. Show that ξ is integrable if and only if the flow of any (possibly local) non-zero vector field tangent to ξ preserves ξ.
Hint: Recall the Frobenius theorem, Theorem 1.1.4.

Now given a Riemannian metric g on M let u and v be (possibly locally defined) sections of ξ that provide an orthonormal basis for ξ and let n be the oriented unit normal to ξ. We would like to measure how much v "twists" as we move along the flow of u. This is given by the quantity

$$g((\phi_{-t})_* v, n)$$

where ϕ_t is the flow of u, and we can extract an angle out of this

$$\theta(t) = \cos^{-1}\left(-\frac{g((\phi_{-t})_* v, n)}{\|(\phi_{-t})_* v\|_g}\right).$$

Notice that for each point $p \in M$ this gives a path of angles. We can now define $\theta'(p)$ to be the derivative of this path at 0. We call $\theta'(p)$ the *instantaneous rotation* of ξ at p.

Exercise 1.8.17. Show that ξ is a (positive) contact structure if and only if θ' is a positive function.

Exercise 1.8.18. Show that θ' only depends on ξ and g (and not the choice of basis u, v).

So we have a quantity θ' that only depends on g and ξ and can tell us if ξ is a contact structure or not! We have the following useful theorem.

Theorem 1.8.19 (Etnyre, Komendarczyk, and Massot 2012, [**EKM12**])**.** *Let g be a Riemannian metric and $\xi = \ker \alpha$ a (positive) contact structure on M. Let R_α be the Reeb vector field associated to α. The following are equivalent.*

(1) *The Reeb vector field R_α is orthogonal to ξ.*

(2) *There is a positive function θ' on M such that $*d\alpha = \theta'\alpha$, where $*d\alpha$ is the Hodge star of the two form $d\alpha$.*

(3) *There is a positive function θ' on M such that*

$$g(u, v) = \frac{\rho}{\theta'}\, d\alpha(u, \phi(v)) + \rho^2\, \alpha(u)\alpha(v),$$

where $\rho = \|R_\alpha\|$, $J\colon \xi \to \xi$ is a complex structure on ξ given by rotation by $\pi/2$, and $\phi\colon TM \to \xi$ is the composition of the projection $TM \to \xi$ along the line field spanned by R_α and J.

Exercise 1.8.20. Prove this theorem.

If g and α satisfy any of the equivalent items in the theorem above we say that g and ξ are *weakly compatible*. If in addition $\|R_\alpha\| = 1$ and θ' is a positive constant then we say that g and ξ are *compatible* (or *strongly compatible*).

In [**CH85**], Chern and Hamilton defined compatibility between a metric and a contact structure as above, but they demanded that $\theta' = 2$. We find the above choice more natural as it allows constant rescaling of the metric (which is quite natural in a Riemannian setting) and also accommodates discrepancies stemming from the different conventions in the definition of the exterior product of differential forms and their impact on the definition of the exterior derivative. Chern and Hamilton were studying various Riemannian geometric conditions associated with compatible metrics. Specifically, they were studying the Webster curvature of compatible metrics. Given a Riemannian metric g on a 3-manifold M and a contact form α with Reeb field R_α we can define the Webster curvature

to be

$$W = \frac{1}{8}(2\kappa(\xi) + \kappa(\xi_1) + \kappa(\xi_2) + 4)$$

where we have, locally, chosen orthonormal vectors v_1 and v_2 that span ξ and ξ_i is the span of R_α and v_i. So W is a "weighted average of sectional curvatures". The main theorem in [CH85] is the following. Check this definition and the conventions in Chern and Hamilton's paper

Theorem 1.8.21 (Chern and Hamilton 1985, [CH85]). *Every contact structure on a closed 3-manifold admits a contact form and a compatible Riemannian metric whose Webster curvature is either a constant less than or equal to 0 or strictly positive.*

This result can be thought of as a contact geometric version of the famous and well-studied Yamabe problem that asks when a manifold admits a metric with constant sectional curvature, see [LP87]. There has been a great deal of further study of the Riemannian geometric properties of metrics compatible with contact structures, see [Bla02][5], but the other direction, namely contact geometric properties of contact structures compatible with Riemannian metrics, is less explored. Below we discuss a few known results. The first global contact geometric result was the following.

Theorem 1.8.22 (Etnyre, Komendarczyk, Massot 2012, [EKM12]). *Let (M, ξ) be a closed contact manifold and g a Riemannian metric compatible with ξ. If there is a constant $C > 0$ such that*

$$\frac{4}{9}C < \kappa_p(\eta) \leq C$$

for all points $p \in M$ and planes η in T_pM, then the pull-back of ξ to the universal cover of M is the tight contact structure on S^3.

The constant 4/9 in the theorem was improved to 1/4 in [GH16]. Recall the classical sphere theorem in Riemannian geometry says that if a simply connected manifold admits a metric whose sectional curvatures are pinched as indicated in the theorem (but with constant 1/4 instead of 4/9), then the manifold must be the sphere. We can think of this as saying the curvature of a metric that a manifold supports can control the topology of the manifold or, conversely, that the topology of a manifold can restrict the types of metrics supported by the manifold. The theorem above says the same thing for metrics compatible with contact structures. In particular, the theorem gives a Riemannian criterion that implies a contact structure must be tight (in fact, universally tight).

The idea behind the proof of this theorem rests on a "Darboux theorem with estimates" and the relation between contact and complex convexity. Given a metric g on a

[5] We note that notation and conventions in this book and the associated literature differ from those that are standard in the contact geometry community. For example, they usually talk about negative contact structures not positive ones.

manifold M the *geodesic ball of radius r about a point p* is

$$B_p(r) = \{\text{union of geodesics of length } r \text{ emanating from } p\}.$$

We note that $B_p(r)$ is not always a ball, but will be for sufficiently small r. In particular the *injectivity radius* at p is

$$inj_p = \sup\{r | \, B_p(r) \text{ is an embedded ball}\}.$$

We can now define the *tightness radius* of (M, ξ) at the point $p \in M$ with respect to any metric g to be

$$\tau_p = \sup\{r < inj_p \mid \xi \text{ restricted to } B_p(r) \text{ is tight}\}.$$

A lower bound on τ_p can be thought of as a quantitative Darboux theorem as it will give the size of a tight (and hence standard) ball about p. To give an estimate on τ_p, we introduce another quantity. We call a domain U bounded by a hypersurface S in a manifold M with a Riemannian metric g *geodesically convex* if any geodesic γ tangent to Σ at a point p locally lies outside of U. That is there is some neighborhood O of p such that $\gamma \cap O \cap U = \{p\}$. We can now define the *convexity radius* at p to be

$$conv_p = \sup\{r < inj_p \mid B_p(r) \text{ is geodesically convex}\}.$$

It is well-known in Riemannian geometry that if the sectional curvatures of a metric are bounded above by $K > 0$ then

$$conv_p \geq \min\left\{inj_p, \frac{\pi}{2\sqrt{K}}\right\}$$

and if the sectional curvatures are non-positive, then $conv_p = inj_p$. We can now state the Darboux theorem with estimates.

Lemma 1.8.23. *If g is a Riemannian metric compatible with the contact structure ξ on M then*

$$\tau_p \geq conv_p.$$

The result follows by using Hofer's pseudo-holomorphic curve techniques to find closed orbits in an overtwisted contact manifold [**Hof93**] together with a relation between Riemannian geodesic convexity and pseudo-holomorphic convexity proven in [**EKM12**]. To prove the "contact sphere theorem above" we need one more ingredient.

Theorem 1.8.24 (Etnyre, Komendarczyk, Massot 2012, [**EKM12**])**.** *Let (M, ξ) be a contact manifold compatible with the Riemannian metric g. If $r < inj_p$ such that ξ restricted to $B_p(r)$ is overtwisted, then one can see a closed leaf in the characteristic foliation of $\partial B_p(r)$.*

Notice that this result says that, while we cannot guarantee ξ on $B_p(r)$ is tight, we can say that if it is not, then it is obviously not tight (that is, we can see the overtwisted disk on $\partial B_p(r)$). This result is proven using facts about compatible metrics and characteristic foliations on families of surfaces that we will be discussing in Section 8.1.

Sketch of the proof of Theorem 1.8.22. By rescalling the metric, we can assume that $C = 1$. Due to the curvature restrictions and the classical Sphere Theorem, we know the universal cover of M is S^3. We pull the contact structure and metric back to S^3 and now need to argue that the contact structure is tight there. To this end, we assume that it is not and derive a contradiction. Let D be an overtwisted disk.

Using arguments similar to those in the classical Sphere theorem we can assume that there are two points p and q in S^3 such that S^3 is the union of $B_p(r_p)$ and $B_q(r_q)$ where r_p the injectivity radius (which is the infimum of inj_x for all $x \in M$) and r_q is less than the convexity radius (which is the infimum of $conv_x$ for all $x \in M$). In particular, we note that $\partial B_q(r_q)$ is contained in the interior of $B_p(r_p)$ and similarly $\partial B_p(r_p)$ is contained on the interior of $B_q(r_q)$. See Figure 1.8.34

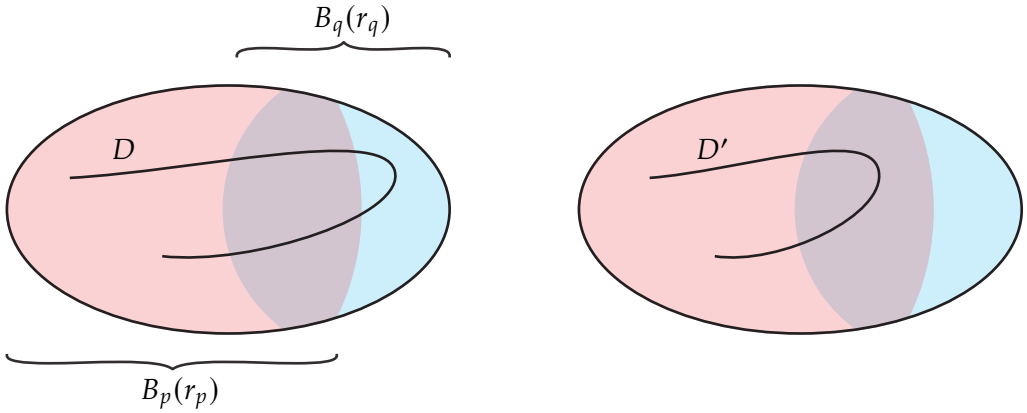

Figure 1.8.34. The decomposition of S^3 into $B_p(r_p)$ and $B_q(r_q)$ and the overtwisted disks D on the left and D' on the right.

From Lemma 1.8.23 we know that the contact structure on $B_q(r_q)$ is tight and hence standard (Eliashberg showed there is a unique tight contact structure, see Chapter 9). In a model for the standard tight 3-ball (see Section 3.2), we can see that there is a vector field whose flow preserves the contact structure and pushes any compact set disjoint from the origin into an arbitrarily small neighborhood of its boundary. As we can isotop the overtwisted disk D to be disjoint from q, we can flow D to an overtwisted disk D' contained in $B_p(r_p)$. Thus the contact structure on $B_p(r_p)$ is overtwisted and Theorem 1.8.24 says that we can see an overtwisted disk on $\partial B_p(r_p)$ which is contained in $B_q(r_q)$, but this contradicts the fact that the contact structure on $B_q(r_q)$ is tight! This disk D could not have existed. □

Using similar ideas as in the proof of Lemma 1.8.23 one can also show.

Theorem 1.8.25 (Etnyre, Komendarczyk, Massot 2012, [EKM12]). *Let (M, ξ) be a contact 3-manifold and g a weakly compatible Riemannian metric. Set*

$$m_g = \sup \|\nabla\rho - \nabla(\ln\theta')^{\perp}\|,$$

where $\rho = \|R_\alpha\|$ is the length of the Reeb field for the contact form α implicated in the definition of compatibility, θ' is the instantaneous rotation of ξ, and $\nabla(\ln\theta')^\perp$ is the component of the gradient $\nabla(\ln\theta')$ that is orthogonal to ξ.

If

$$\kappa_p(\eta) < -m_g^2$$

for all $p \in M$ and η planes in T_pM, then (M, ξ) is universally tight.

We note that this theorem gives a criterion for tightness in terms of a metric that is only weakly compatible with the contact structure. This is important because a negatively curved metric cannot be compatible with a contact structure because for such a metric the Reeb flow traces out geodesics and one cannot foliate a negatively curved manifold by geodesics [**Zeg93**].

ADD MORE

1.8.8. Low-dimensional topology. In this section we will discuss numerous applications of contact geometry to low-dimensional topology and geometry. The first indication that there were subtle connections between contact geometry and low-dimensional topology was in the work of Bennequin and Eliashberg in the 1980s and 1990s. Bennequin established his inequality [**Ben83**] discussed in Section 1.6.1 (see also Section 3.7). This was an effective way to obtain lower bounds on the Seifert genus of a knot, which historically was a difficult problem to understand. Whereas Eliashberg [**Eli90a**] was able to give a proof of the famous Cerf theorem about diffeomorphisms of the 3-sphere extending over the 4-ball, using his classification of tight contact structures on S^3 and holomorphic curve techniques. Add more intro

Cerf's theorem: One of the first indications that contact and symplectic geometry is closely connected to subtle aspects of low-dimensional topology was Eliashberg's proof of Cerf's theorem.

Theorem 1.8.26 (Cerf 1968, [**Cer68**]). *Any diffeomorphism of $S^3 = \partial B^4$ extends over B^4.*

Cerf's theorem is frequently stated as $\Gamma_4 = 0$. Here Γ_n is the group of orientation-preserving diffeomorphisms of S^{n-1} modulo those that extend over B^n.

Cerf's original proof involved a subtle analysis of families of smooth functions on B^4 taking over 100 pages, while Eliashberg's proof [**Eli90a**] is less than a page long! Of course, this is not a fair comparison, as Eliashberg relies on a great deal of work in symplectic and contact geometry. So it is likely that his proof is longer than Cerf's. The amazing thing is that all that other material was already developed to study interesting questions in symplectic and contact geometry, and can then very easily be used to prove this beautiful topological result.

So, how does Eliashberg's proof go? Given a diffeomorphism $f\colon S^3 \to S^3$, one considers the pull-back $f^*\xi_{std}$ of the standard tight contact structure ξ_{std} on S^3. Since there is a unique tight contact structure on S^3, see Theorem 5.1.1, we know that $f^*\xi_{std}$ is isotopic to ξ and hence by Theorem 1.2.10, f is isotopic to a diffeomorphism $g\colon S^3 \to S^3$ that preserves ξ. (Of course, if g can be isotoped to a diffeomorphism that extends over B^4, then so does f).

If N and S are two distinct points in S^3 then $S^3 - \{N, S\}$ is $S^2 \times (0,1)$. After a contact isotopy, we can arrange that g is the identity in a neighborhood of N and S. See Figure 1.8.35.

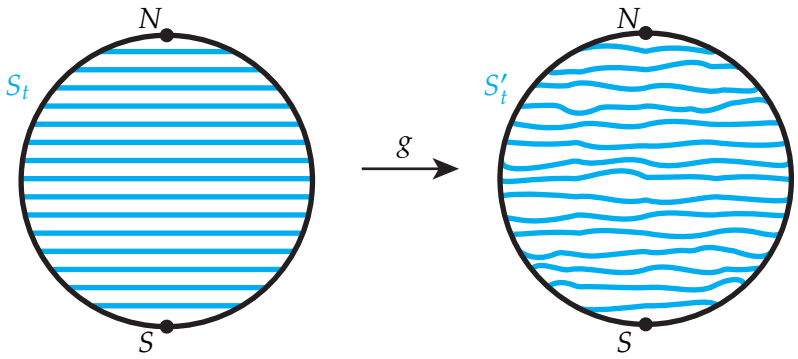

Figure 1.8.35. On the left we see S^3 and the foliation of $S^3 - \{N, S\}$ by spheres S_t. On the right is their image under g.

Exercise 1.8.27. Prove this last statement.
Hint: First, show that there is an isotopy of g through contactomorphisms so that N and S are preserved. This can be done by showing that there is a contact isotopy taking any point in a contact manifold to any other point. To do this, consider a transverse arc between the points, take a standard neighborhood of this arc (as in Section 1.2), and find the isotopy in this neighborhood. This last part might be easier after reading about contact vector fields in Section 3.1.

Now we can arrange that the characteristic foliation on each of the $S_t = S^2 \times \{t\}$ is given as in Figure 1.8.36, see Section 9.1. Note the image $S'_t = g(S_t)$, for $t \in (0,1)$, is a foliation of $S^3 - \{N, S\}$ by spheres and g sends the characteristic foliation of S_t to the characteristic foliation on S'_t. See Figure 1.8.35

Note that the unit ball B^4 in $\mathbb{R}^4$ with its natural symplectic structure is a symplectic filling of (S^3, ξ_{std}). One may now use the theory of holomorphic curves in symplectic manifolds, see Appendix B, to find a map $\Phi\colon (D^2 \times [0,1] \times (0,1)) \to B^4$ such that

(1) $\Phi(\partial(D^2 \times [0,1] \times (0,1))) = S^3 - \{N, S\}$.

(2) Φ is injective on $D^2 \times (0,1) \times (0,1)$.

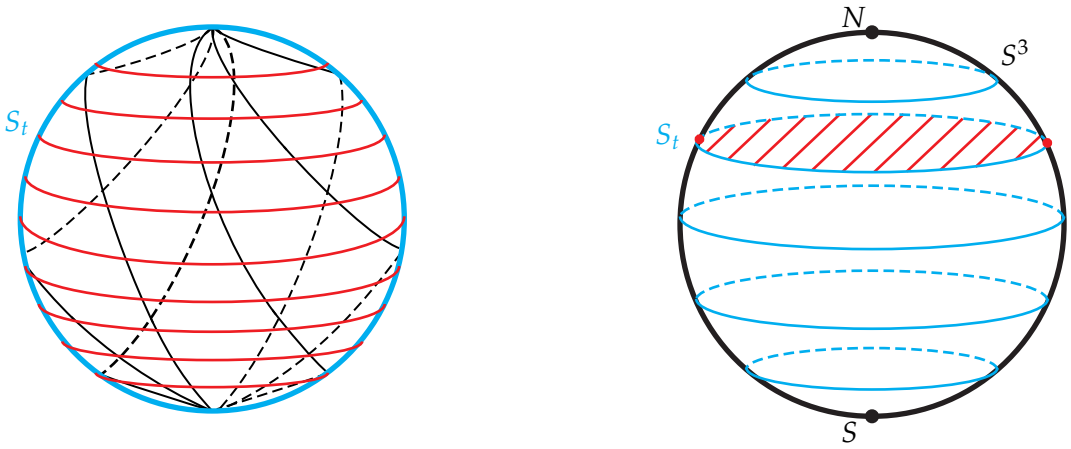

Figure 1.8.36. On the left we see one of the spheres S_t, its characteristic foliation in black, and its foliation by boundaries of holomorphic disks in red. On the right we see a schematic picture of S^3, represented by the black sphere, its foliation by S_t in blue, and the foliation of B^4 by holomorphic disks in red. (We only drew the disks for one S_t so as not to clutter the figure.)

(3) Φ restricted to the interior of its domain is a diffeomorphism to the interior of B^4.

(4) $\Phi(D^2 \times [0,1] \times \{t\})$ is a ball with boundary S_t.

(5) $\Phi(D^2 \times \{i\} \times \{t\})$ is a singular point in the characteristic foliation of S_t for $i = 0, 1$ and $t \in (0,1)$. See Figure 1.8.36.

(6) $\Phi(\partial D^2 \times \{s\} \times \{t\})$ is transverse to the characteristic foliation of S_t for $s \in (0,1)$ and $t \in (0,1)$. See Figure 1.8.36.

(7) $\Phi\colon (D^2 \times \{s\} \times \{t\}) \to B^4$ is a holomorphic map (with respect to a complex structure compatible with the symplectic form on B^4).

Notice that Φ on the interior of $D^2 \times [0,1] \times (0,1)$ foliates the interior of B^4.

We can similarly find $\Phi'\colon (D^2 \times [0,1] \times (0,1)) \to B^4$ with the same properties except with respect to the S'_t.

Notice that the complement of the singular points in the characteristic foliation of each S_t is foliated by leaves of the characteristic foliation and also by the boundaries of holomorphic disks coming from Φ and similar for S'_t. See Figure 1.8.36. One may now argue that g may be isotoped so that the boundaries of holomorphic disks on S_t map to the boundaries of holomorphic disks on S'_t. We know that diffeomorphisms of S^1 extend to diffeomorphisms of D^2 and in fact this is true for families of such diffeomorphism. Thus, we may extend g restricted to each boundary of a holomorphic disk in an S_t to a diffeomorphism of the disk it bounds to the disk its image bounds in S'_t. This extends g over B^4. Of course, one must be careful about smoothness near N and S and the singularities

of the characteristic foliations on the S_t, but an analysis of the behavior of holomorphic curves here will deal with this. See [**GZ10**] for a good, careful exposition of the details.

Bennequin type inequalities: The genus of a knot K in S^3, denoted $g(K)$, is the minimal genus of a Seifert surface for K and the 4-genus of the knot, denoted $g_4(K)$, is the minimal genus of a surface in B^4 with boundary K. Historically, it has been difficult to find the genus of a knot. More recently, there are many techniques, such as the use of Heegaard Floer homology, that can be used to find the genus of a knot, but they can be somewhat complicated. Similarly, finding the 4-genus of a knot is still a very difficult problem. So while understanding the genus and 4-genus of a knot is a subtle topological property, contact geometry can provide insights.

Specifically, we recall from Section 1.6.1 that the Bennequin inequality says that for a Legendrian knot L in the standard tight contact structure on S^3 we have

$$\mathrm{tb}(L) + |\mathrm{rot}(L)| \leq 2g(L) - 1,$$

where $g(L)$ is the minimal genus of a Seifert surface for L. We call $g(L)$ the genus of L. We also saw in Section 1.6.5 that this inequality can be strengthened to show that

$$\mathrm{tb}(L) + |\mathrm{rot}(L)| \leq 2g_4(L) - 1,$$

where $g_4(L)$ is the minimal genus of a surface in B^4 with boudnary L. We call $g_4(L)$ the 4-genus of L.

Now given a knot type K, one can draw front diagrams for Legendrian realizations L of K and $m(K)$ (this is the mirror of K, which is obtained from K by changed all the crossings, and it is easy to see K and $m(K)$ have the same genus and 4-genus) and see which ones maximize the quantity $\mathrm{tb}(L) + |\mathrm{rot}(L)|$. This will give a lower bound on the genus and 4-genus of K, and in many cases it will be sharp.

Here are a few specific applications.

Lemma 1.8.28. *If K or $m(K)$ admits a Legendrian representative L with $\mathrm{tb}(L)+|\mathrm{rot}(L)|+1 > 0$, then K is not smoothly slice (that is $g_4(K) > 0$).*

The proof is immediate from the above inequality.

We now recall the Whitehead double of a knot. Given a knot K, let N be a neighborhood of K. Identify N with the solid torus shown in at the top of Figure 1.8.37 so that the product framing on that torus is mapped to the framing n on N. Then the image of the knot shown in the solid torus is called the *n-twisted Whitehead double of K*, and denoted $W_n(K)$. There is a well-known conjecture about Whitehead doubles.

Conjecture 1.8.29. *A knot K is smoothly slice if and only if its 0-twisted Whitehead double $W_0(K)$ is slice.*

Exercise 1.8.30. Show that if K is slice then $W_0(K)$ is slice.

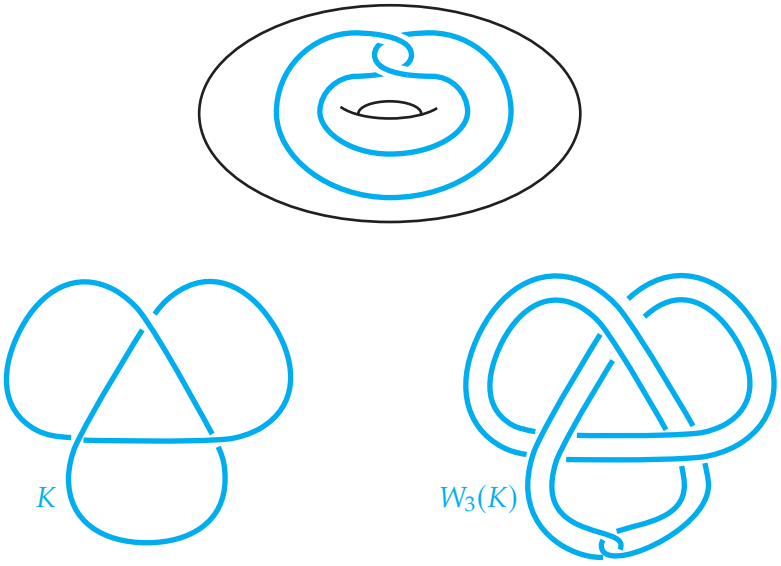

Figure 1.8.37. The solid torus and knot used in the definition of the Whitehead double. On the bottom row we see a knot K and its 3-twisted Whitehead double.

We now note that one can show the other implication also holds under certain contact geometric hypotheses.

Theorem 1.8.31 (Rudolpf 1995, [Rud95]). *If a knot type K admits a Legendrian representative L such that $\mathrm{tb}(L) \geq 0$, then its 0-twisted Whitehead double $W_0(K)$ (and all iterated 0-twisted Whitehead doubles) are not smoothly slice.*

Note the inequality above says that if K is slice then any Legendrian realization of K will have to have Thurston-Bennequin invariant less than 0. So the theorem essentially says that if K is not slice for a contact geometric reason, then none of its iterated 0-twisted Whitehead doubles are either. We sketch the proof in a series of exercises.

Exercise 1.8.32. Given a Legendrian knot L show you can construct a $\mathrm{tb}(L)$-twisted Whitehead double of L using its front diagram. Denote this "Legendrian Whitehead double" by WL.
Hint: Take the front diagram of L and a second copy of the front diagram pushed up slightly. Now replace two parallel strands on the different copies of the diagram by a "Legendrian clasp".

Exercise 1.8.33. Show that $\mathrm{tb}(WL) = 1$ and $\mathrm{rot}(WL) = 0$. Hence the smooth knot $W_{\mathrm{tb}(L)}(L)$ is not slice.

Exercise 1.8.34. If K is the underlying smooth knot of L, then show that $W_n(K)$ is not smoothly slice for any $n \leq \mathrm{tb}(L)$.

Fibered knots and the Harer conjecture: The Harer conjecture postulates a method to build all possible fibered knots in S^3. Recall that an (oriented) link K in a 3-manifold M is called *fibered* if there is a fibration $p\colon (M - K) \to S^1$ such that the closure Σ_θ of $p^{-1}(\theta)$ is an embedded surface with boundary K, that is Σ_θ is a Siefert surface for K. Since all the Σ_θ are diffeomorphic (and even isotopic in M), we can just consider one and call it Σ. We call (K, Σ) a *fibered pair*.

Example 1.8.35. The unknot in S^3 is fibered, since its complement is $S^1 \times \mathbb{R}^2$ and the closure of a fiber is a disk Seifert surface for the unknot.

Example 1.8.36. The Hopf link H in S^3, see Figure 1.8.38, is also fibered. This is easy to see as the complement of H is $T^2 \times \mathbb{R}$, so any fibration of T^2 by circles will give a fibration of the complement of H by open annuli.

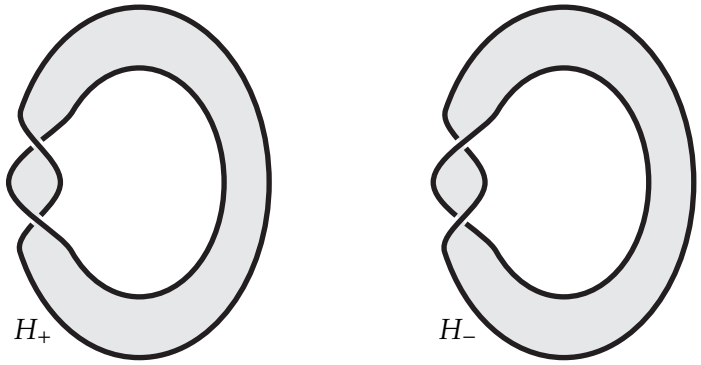

Figure 1.8.38. The two Hopf bands. Note that the linking between the components of $H_\pm$, when the components are oriented as the boundary of the annulus, is ± 1.

Exercise 1.8.37. Show that there are infinitely many distinct fibrations of $S^3 - H$, but only two that give a fibration as described above (that is, whose fibers have closures that are Seifert surfaces for H).

Example 1.8.38. A knot that sits on a Heegaard torus for S^3 is called a *torus knot* See Section 6.5 for more details on torus knots and a construction of a Seifert surface for them.

Exercise 1.8.39. Show that the Seifert surface constructed for torus knots in Section 6.5 is a fiber in the fibration of the complement of the knot.

While there were many constructions of fibered knots in S^3 in 1982, Harer characterized how to construct them all.

Theorem 1.8.40 (Harer 1982, [**Har82**])**.** *Any fibered pair (K, Σ) in S^3 can be obtained from the unknot and disk it bounds by a sequence of "plumbings" and deplumbings of Hopf links and a "twist".*

More specifically, there is a fibered pair (K', Σ') obtained from (K, Σ) by some number of plumbings of Hopf links, a link (U', D') obtained from the unknot and a Seifert disk by some number of plumbings of Hopf links, such that (K', Σ') and (U', D') are related by a twist.

We will describe the plumbing of Hopf links and twists below, but first state Harer's conjecture. To state the conjecture, we use the more recent terminology for "plumbing a Hopf link", and that is *stabilization*.

Conjecture 1.8.41 (Harer conjecture)**.** *Any fibered link in S^3 is obtained from the unknot by a sequence of stabilizations and destabilizations.*

Given two links K_1 and K_2 in S^3 and Seifert surfaces Σ_1 and Σ_2 for them, respectively, we define the plumbing of Σ_1 and Σ_2 as follows. Choose a properly embedded arc γ_i on Σ_i. One may choose a neighborhood N_i of γ_i in Σ_i such that $N_i = [-1,1] \times [-1,1]$ and $\gamma_i = \{0\} \times [-1,1]$ and then isotop Σ_i into a ball B_i such that $\Sigma_i \cap \partial B_i = N_i$ and B_1 and B_2 are disjoint. Finally, one may isotop B_1 so that $B_1 \cap B_2 = N_1 = N_2$ where N_1 is identified with N_2 by switching the interval factors. See Figure 7.2.5. The resulting surface (after the corners are smoothed) is said to be obtained from *plumbing Σ_1 and Σ_2* and we say that its boundary is the link obtained by plumbing K_1 and K_2. (We note that the result of

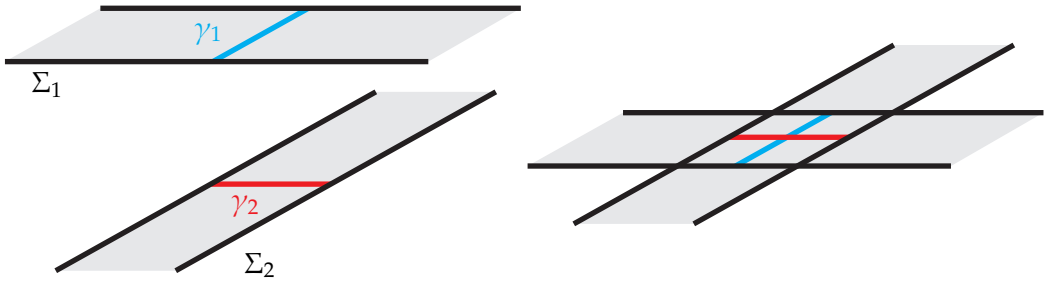

Figure 1.8.39. The plumbing of the surface Σ_1 and Σ_2.

plumbing Σ_1 and Σ_2 depends on the choice of γ_i and the result of plumbing K_1 and K_2 also depends on the choice of the Σ_i.)

We now recall that there are two Hopf links H_+ and H_-. They are shown in Figure 1.8.38. We say that a fibered pair (K', Σ') is obtained from (K, Σ) by *plumbing a Hopf band* if it is obtained by plumbing Σ to either H_+ or H_-. In this situation, also say (K, Σ) is obtained from (K', Σ') by *deplubming a Hopf band*. As noted above, "plumbing a Hopf band" is nowadays typically called *stabilizing* a fibered link. If one plumbs H_+ it is called a *positive stabilization* and if one plumbs H_- it is called a *negative stabilization*.

Given a fibered pair (K, Σ) with an unknot knot U on the interior of Σ such that the framing of U given by Σ is either $2, 0$, or -2, then we say (K', Σ') is obtained from (K, Σ) by a *twist* if it is the image of (K, Σ) under the diffeomorphism from $+1$ surgery on U, if

the framing is -2 or 0, and -1 surgery on U, if the framing is 0 or 2, to S^3. See Figure 1.8.40

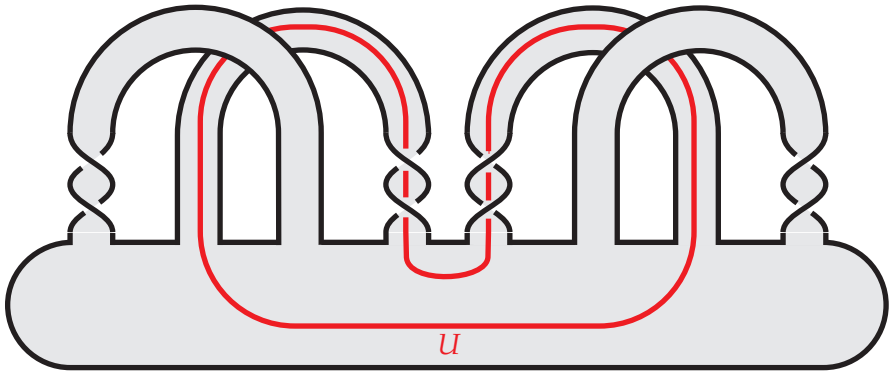

Figure 1.8.40. Twist on a Seifert surface.The framing on U given by the Siefert surface is 0.

These surgeries will be either $+1$ or -1 surgery on the unknot U, and it is easy to see from our discussion in Section 1.5.1 that the resulting manifold is diffeomorphic to S^3. This can be seen by a Rolfsen twist on the surgery curve and this changes K to K'. While it is not obvious, under this operation Σ becomes a Seifert surface Σ' for K' and K' is still fibered.

Example 1.8.42. Prove this last statement.
Hint: If you have not seen this before, it can be difficult to prove this. If you are having difficulties, see Section 12.1.

Exercise 1.8.43. If one performs a $+1$ surgery on the curve U in Figure 1.8.40 one obtains Figure 1.8.41.

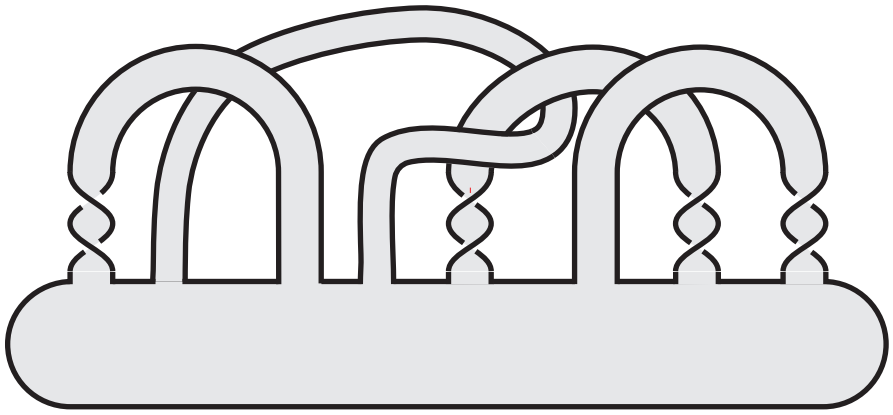

Figure 1.8.41. Twist on a Seifert surface.The framing on U given by the Siefert surface is 0.

The example of a fibered knot in Figure 1.8.41 first appeared in [**Har82**]. A few years later, Melvin and Morton in [**MM86**] showed that it cannot be obtained from the unknot by plumbing Hopf bands.

Using contact topology, Giroux and Goodman prove the Harer conjecture, Conjecture 1.8.41.

Theorem 1.8.44 (Giroux-Goodman 2006, [**GG06**]). *Any two fibered pairs in S^3 are related by a sequence of stabilizations and destabilizations.*

To see how such a theorem could be established, we need to discuss a few results about fibered knots and contact structures. We will more fully discuss this connection in Chapter 12. We first note that fibered pairs are also called *open book decompositions*. We will denote an open book decomposition by the pair (B, π) where B is the fibered link and $\pi\colon (M - B) \to S^1$ is the fibration of the complement of B. Here are some facts about contact structures on open book decompositions:

(1) In [**TW75**], Thurston and Winkelnkemper showed how to associate a contact structure to (B, π).

(2) All of the following statements are due to Giroux [**Gir02**], the contact structure above is uniquely determined by (B, π). Denote the contact structure $\xi_{B,\pi}$. We say $\xi_{B,\pi}$ is supported by (B, π).

(3) Every contact structure on a closed 3-manifold is supported by some open book decomposition.

(4) If (B_+, π_+) is obtained from (B, π) by a positive stabilization, then ξ_{B_+,π_+} is isotopic to $\xi_{B,\pi}$.

(5) If (B_-, π_-) is obtained from (B, π) by a negative stabilization, then ξ_{B_-,π_-} is overtwisted and has d_3-invariant one larger than that of $\xi_{B,\pi}$.

(6) Let ξ and ξ' are associated to the open book decompositions (B, π) and (B', π'), respectively. Then ξ is isotopic to ξ' if and only if (B, π) is related to (B', π') by a sequence of *positive* stabilizations and destabilizations.

The last fact is known as the *Giroux correspondence* and is a cornerstone of modern contact geometry. This is the topic of Chapter 12.

We now sketch the proof of Harer conjecture. Given two fibered pairs (B_0, π_0) and (B_1, π_1) in S^3 (thought of as open book decompositions) we consider the contact structures ξ_{B_i,π_i} associated to them as above. We negatively stabilize (B_i, π_i) to get (B_i', π_i'). The contact structures supported by the new open books are both overtwisted. Without loss of generality we can assume that the d_3-invariant of $\xi_{B_1',\pi_1'}$ is greater than or equal to $\xi_{B_0',\pi_0'}$. Thus we can negatively stabilize (B_0', π_0') some number of times to get an open book (B_0'', π_0'') such that $\xi_{B_0'',\pi_0''}$ has the same d_3-invariant as $\xi_{B_1',\pi_1'}$. According

to our discussion in Section 1.5.4, we know that $\xi_{B_0'',\pi_0''}$ is homotopic to $\xi_{B_1',\pi_1'}$ as a plane field. Now Eliashberg's classification of overtwisted contact structures discussed in Section 1.6.1 tells us that these two contact structures are isotopic. Finally, the Giroux correspondence now says that (B_0'', π_0'') is related to (B_1', π_1') by positive stabilizations and destabilzations. Thus, the original open book decompositions (B_0, π_0) and (B_1, π_1) are related by stabilizations and destabilizations.

Property P: Add section

Heegaard Floer homology and the fiberdness and genus of knots: Add section

Characterizing knot by Floer and Khovanov homologies: Add section

Characterize knots by surgery: Add section

Smooth structures on 4-manifolds with boundary: Add section

Engel structures: Add section

Chapter 2

Characteristic foliations

Characteristic foliations on surfaces will be a key component in our analysis of contact structures on 3-manifolds. In this section, give a detailed analysis of them. In the first section, we define the divergence of a vector field and whether the divergence at a singular point of a singular foliation is zero or not. This is a key component in characterizing which singular foliations can be realized as the characteristic foliation of a surface in a contact manifold. Specifically, we will prove Giroux's result [**Gir91**] that says a singular foliation can be the characteristic foliation of a surface in a contact 3-manifold if and only if its singularities have non-zero divergence.

In Section 2.2, we move to the discussion of generic properties of vector fields and flows. We begin by discussing singular points of a vector field, that is, points where it is zero. Using the linearization of the vector field at a singular point, we define a non-degenerate singular, or more precisely, a hyperbolic singular point, to be one whose linearization has eigenvalues that are not zero or purely imaginary. After noting that "generic" vector fields have non-degenerate singular points, we then discuss the nature of such singular points. More specifically, we discuss nodal and saddle singular points, stable and unstable manifolds, and other useful features of singular points. We then move on to a discussion of periodic orbits in a vector field. These are closed flow lines. A fundamental feature of such flow is determined by its Poincaré return map and its derivative. Using this, we can define when an orbit is degenerate, attracting, or repelling, and then show that vector fields with non-degenerate periodic orbits are "generic". We end this section be discussing general flow lines. We discuss their ω-limit sets, these are then "limits" of the forward trajectory of a flow line, and the α-limit set, which is the "limits" of the backward trajectories of a flow line. We then use these concepts to state the famous Poincaré-Bendixson Theorem for the ω-limit set of points for flows on S^2.

We use this to define the Poincaré-Bendixson Property and notice that this is a "generic" property for vector fields on any compact surface.

In Section 2.3 we prove a theorem of Giroux, **[Gir91]**, that shows any generic property of a vector field is also a generic property of a characteristic foliation of a surface in a contact manifold. So all the results from the previous section tell us that "generic" characteristic foliations are quite nice. In the final section, we show how to understand the twisting of the contact planes along an embedded Legendrian arc in a surface. This will be a key result when studying convex surfaces in the next chapter.

Throughout this section (and the book, unless explicitly said otherwise) we will assume our surfaces are oriented.

2.1. Divergence of vector fields and foliations on surfaces

We want to consider the divergence of vector fields on an orientable surface Σ. To do this we must pick an area form ω on Σ. We can now define the *divergence of the vector field v on Σ, with respect to ω,* to be the unique function $\operatorname{div}_\omega(v)$ satisfying

$$\mathcal{L}_v\omega = (\operatorname{div}_\omega(v))\,\omega,$$

where $\mathcal{L}_v\omega$ denotes the Lie derivative of ω with respect to v. Recall from the definition of the Lie derivative this means that the flow of v is (infinitesimally) scaling ω by the divergence. So for example, $\operatorname{div}_\omega(v) = 0$ if and only if the flow of v preserves ω.

Cartan's formula says

$$\mathcal{L}_v = \iota_v d + d\iota_v,$$

where $\iota_v\omega$ denotes the contraction of ω with v. Since ω is a 2–form on a surface we know $d\omega = 0$ so we can equivalently define the divergence of v to be

$$d\iota_v\omega = (\operatorname{div}_\omega(v))\,\omega.$$

We now make a simple computation to see how the divergence changes as we scale v and ω. To this end let f and g be two functions on Σ and notice that

$$d\iota_{fv}(g\omega) = d(fg\iota_v\omega) = d(fg)\wedge\iota_v\omega + fgd\iota_v\omega,$$

in addition since $d(fg)\wedge\omega$ is a 3–form on a surface it is zero, and hence

$$(\iota_v d(fg))\wedge\omega - d(fg)\wedge\iota_v\omega = 0.$$

Thus, since $\iota_v d(fg) = d(fg)(v)$, we see that

$$d\iota_{fv}(g\omega) = (d(fg)(v) + fg\operatorname{div}_\omega(v))\,\omega = \left(g^{-1}d(fg)(v) + f\operatorname{div}_\omega(v)\right)(g\omega)$$

and in particular

$$\operatorname{div}_{g\omega}(fv) = (df + f\,d\ln g)(v) + f\operatorname{div}_\omega(v). \tag{2.1.9}$$

We have shown the following.

Lemma 2.1.1. *Let v be a vector field on Σ and p a zero of v.*

(1) *The divergence $div_\omega(v)$ at p does not depend on ω.*

(2) *If f is any positive function then*

$$div_\omega(v)(p) = 0 \text{ if and only if } div_\omega(fv)(p) = 0.$$

The lemma above shows that at a zero of a vector field, the divergence is independent of a choice of an area form. However, where the vector field is not zero this is far from the case, the divergence can essentially be anything depending on the choice of the area form.

Lemma 2.1.2. *Let v be a vector field on a surface Σ that is non-zero at the point p. Then given any function g defined near p there is some area form ω on Σ such that in some small neighborhood of p the divergence $div_\omega(v)$ is given by g. In particular, the divergence can be positive or negative or 0 near the point p.*

Proof. The Flow Box Theorem [**dMP80**] from dynamical systems says that there is a coordinate chart for Σ near p in which v is one of the coordinate vector fields. More specifically, there is an open set $U \subset \mathbb{R}^2$, $V \subset \Sigma$, and a diffeomorphism $\phi\colon V \to U$ such that $\phi_* v = \frac{\partial}{\partial x}$, where $\mathbb{R}^2$ has coordinates (x, y). One can find this theorem in most any book on dynamical systems, for example [**dMP80**], but the proof is not hard, and the reader should try to think of their own proof.

Now realizing $\widetilde{g} = g \circ \phi^{-1} : V \to \mathbb{R}$ as the divergence of $\frac{\partial}{\partial x}$ with respect to some area form on V will establish the lemma. To this end, set

$$f(x, y) = \exp \int_0^x \widetilde{g}(t, y)\, dt$$

and $\omega = f(x, y)\, dx \wedge dy$. One easily computes that the divergence of ∂_x with respect to ω is

$$\operatorname{div}_\omega \left(\frac{\partial}{\partial x} \right) = \frac{f_x(x, y)}{f(x, y)} = \widetilde{g}(x, y).$$

□

We recall that in Section 1.3.1 we defined singular line fields on a surface Σ and they are locally flow lines of a vector field up to multiplication by a non-zero function. Thus the divergence of a singular point in a singular foliation is well-defined by Lemma 2.1.1. We now see that this divergence characterizes when a singular foliation can be the characteristic foliation for some contact structure.

Theorem 2.1.3 (Giroux 1991, [Gir91]). *Let $\mathcal{F}$ be a singular foliation on an oriented surface Σ. Then $\mathcal{F}$ is the characteristic foliation induced on Σ for some contact structure if and only if all the singularities of $\mathcal{F}$ have non-zero divergence.*

Proof. We first assume that $\mathcal{F}$ is the characteristic foliation on Σ induced by some contact structure ξ on $\Sigma \times [-1,1]$, where $\Sigma = \Sigma \times \{0\}$. The contact form for ξ can be written

$$\alpha = \beta_t + u_t\, dt$$

where β_t is a 1-form on Σ and u_t is a function on Σ for all $t \in [-1,1]$. Clearly $\mathcal{F} = \Sigma_\xi$ is given by $\ker \beta_0$. We now compute $d\alpha = d\beta_t + dt \wedge \frac{\partial \beta_t}{\partial t} + du_t \wedge dt$ and hence

$$\alpha \wedge d\alpha = -\beta_t \wedge \frac{\partial \beta_t}{\partial t} \wedge dt + \beta_t \wedge du_t \wedge dt + u_t \beta_t \wedge dt.$$

If x is a singularity of Σ_ξ then $(\alpha \wedge d\alpha) = u_0 d\beta_0 \wedge dt$ at x and we see that $d\beta_0$ is not equal to 0 near x. We can let ω be a area form on Σ that agrees with $d\beta_0$ near x. Recall that a area form induces a bijection between vector fields and 1-forms on Σ:

$$\mathfrak{X}(\Sigma) \to \Omega^1(\Sigma) : v \mapsto \iota_v \omega$$

and so there is a vector field v on Σ such that $\iota_v \omega = \beta_0$. Now

$$d\iota_v \omega = d\beta_0 = \omega$$

from which we see that the divergence of v at x is 1. So the divergence of any singular point of $\mathcal{F} = \Sigma_\xi$ is non-zero.

We now assume that the divergence of the singularities of $\mathcal{F}$ is non-zero. We need to construct a contact structure on $\Sigma \times [-1,1]$ such that the characteristic foliation on $\Sigma = \Sigma \times \{0\}$ is $\mathcal{F}$.

We assume for now that $\mathcal{F}$ is orientable so that $\mathcal{F}$ is given as the flow lines of some vector field v on Σ. Now choose a area form ω on Σ and set $\beta = \iota_v \omega$. Let u be the unique function such that $d\beta = u\omega$. We claim there is a 1-form γ on Σ such that $\gamma \wedge \beta \geq 0$ and $\gamma \wedge \beta > 0$ away from the singularities of β. (Recall, a 2 form being greater than or equal to 0 means that it is a non-negative multiple of ω.) We construct γ below. Set $\beta_t = \beta + t(du + \gamma)$ and

$$\alpha = \beta_t + u\, dt,$$

and compute

$$\alpha \wedge d\alpha = (u\, d\beta_t + \beta_t \wedge \gamma) \wedge dt = (u^2 \omega + \beta \wedge \gamma) \wedge dt.$$

Notice that u is the divergence of v so at a singular point of β, we see that $u^2 > 0$ and hence $\alpha \wedge d\alpha > 0$. At a non-singular point of β both terms in $\alpha \wedge d\alpha$ are positive so α is a contact form on $\Sigma \times [-1,1]$ inducing $\mathcal{F}$ as the characteristic foliation on $\Sigma \times \{0\}$.

We are left to find γ.

Exercise 2.1.4. Show there is an almost complex structure J on Σ that is compatible with ω in the sense that for any non-vanishing vector w, we have $\omega(w, Jw) > 0$.

We can now set $\gamma = \iota_{Jv}\omega$. Notice that $(\beta \wedge \gamma)(v, Jv) = (\omega(v, Jv))^2$, and so γ has the desired property.

If $\mathcal{F}$ is not orientable, you can use the above argument to construct local contact forms that define a contact structure on $\Sigma \times [-1, 1]$. □

2.2. Generic properties of vector fields on surfaces

We begin by establishing some notation. If v is a vector field on a surface Σ and p is a point in Σ, then we denote

$$\gamma_p \colon \mathbb{R} \to \Sigma$$

the *flow line of v through p*. That is γ_p satisfies

$$\gamma_p'(t) = v(\gamma(t)), \text{ and}$$
$$\gamma_p(0) = p$$

In general, a flow line might not exist for all time, but we will usually be considering the situation where they do, so our notation above reflects that.

2.2.1. Singular points. Now, consider a zero p of a vector field v on a surface Σ. Recall, we call such a point p a *singular point* of v. We can consider the *linearization* of v at p:

$$Dv_p \colon T_p\Sigma \to T_p\Sigma.$$

We note that since $v \colon \Sigma \to T\Sigma$ the differential of this map is $dv_p \colon T_p\Sigma \to T_{v(p)}(T\Sigma)$. However, if Z is the zero section of $T\Sigma$ then since $v(p) \in Z$ we see that we have the splitting of the tangent space

$$T_{v(p)}(T\Sigma) = T_{v(p)}Z \oplus T_p\Sigma$$

where we are thinking of $T_p\Sigma$ as the kernel of $d\pi \colon T_{v(p)}(T\Sigma) \to T_p\Sigma$ and $\pi \colon T\Sigma \to \Sigma$ is the natural projection. Now the linearization map Dv_p is simply dv_p composed with the projection $T_{v(p)}Z \oplus T_p\Sigma \to T_p\Sigma$.

Exercise 2.2.1. In local coordinates $U \subset \mathbb{R}^2$ around p, we can think of a vector field as a map $f_v \colon U \to \mathbb{R}^2$ since the coordinate system provides a trivialization of TU and sections of a trivial bundle are equivalent to functions from the base to the fiber. Show that Dv_p in these local coordinates is simply the total derivative of f_v.

We call the singular point p *simple* if Dv_p has no zero eigenvalues. It is known that a simple singularity of v is isolated in a strong sense; namely, there are no singular points near p in Σ; but, moreover, there is a neighborhood of v in the space of vector fields containing vector fields that have an isolated singular point near p, see [**dMP80**, Section 2.3].

Exercise 2.2.2. Show p is a simple singularity of v if and only if v is transverse to the zero section of $T\Sigma$ at p.

While simple singularities are somewhat nice, their perturbations can have drastically different behavior, see [**dMP80**, Section 2.3], so we would like to consider even nicer singular points. Specifically, we call a simple singular point p a *hyperbolic singular point* if Dv_p has no purely imaginary eigenvalues. Two important properties of hyperbolic singular points are:

(1) The set of vector fields with only hyperbolic singularities on Σ is open and dense in the set of vector fields on Σ.

(2) The flow of a vector field v near a hyperbolic singular point p is locally equivalent to the flow of its linearization. That is, there is a neighborhood U of p, a neighborhood V of the origin in $\mathbb{R}^2$, and a homeomorphism $\phi\colon U \to V$ such that flow lines of v on U are taken to flow lines of Dv_p on V. (Here we are interpreting the linear map Dv_p as a vector field on $\mathbb{R}^2$.) This fact is a special case of the Hartman-Grobman Theorem.

Need to check regularity. These are all true for C^r vector fields for $r \geq 1$, but what about $r = \infty$? For both of these facts, see [**dMP80**, Chapter 2]. As it is easy to understand linear flows, we can (topologically) understand flows near hyperbolic singular points.

In Section 1.3.2 we gave examples of some special types of singular points, but we now give a more precise definition. If p is a hyperbolic singularity of the vector field v, then we say that p is an *elliptic singular point*, also known as a *nodal singular point*, if the real parts of the eigenvalues of Dv_p have the same sign. If the eigenvalues have real parts with opposite signs, then we call the singular point a *saddle singular point*, or sometimes it is called a *hyperbolic singular point*. This latter terminology, while somewhat common, can be confusing as we see that "elliptic singular points" are "hyperbolic" in the sense of the definition above, but from context it is usually clear what is meant by the term.

Example 2.2.3. In Figure 2.2.1 we see various hyperbolic singular points. The first is a sink, and its linearization has negative real eigenvalues. The middle figure is a spiral sink, and its linearization has complex eigenvalues with negative real parts. The last figure is a saddle singularity, and its linearization has a positive and a negative eigenvalue.

If p is a singular point of the vector field v on a surface Σ then we define its *stable manifold* to be the set of points that "flow to" p

$$W^s(p) = \{q \in \Sigma\colon \lim_{t\to\infty} \gamma_q(t) = p\}$$

and the *unstable manifold* to be the set of points that "flow away from" p

$$W^u(p) = \{q \in \Sigma\colon \lim_{t\to-\infty} \gamma_q(t) = p\}.$$

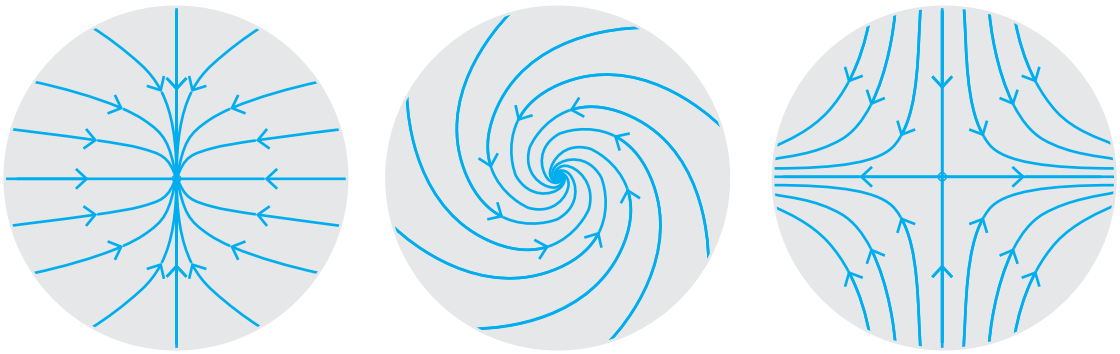

Figure 2.2.1. Examples of hyperbolic singular points.

Given a hyperbolic singular point p of v, we let E^s be the subspace of T_pM spanned by the eigenvectors associated with eigenvalues having positive real part of the linearization of Dv_p, and similarly, E^u is the subspace of T_pM spanned by the eigenvectors associated with eigenvalues having negative real part of the linearization of Dv_p. The Stable/Unstable Manifold Theorem [**Rob99**, Section 5.10] says:

(1) For a hyperbolic singular point p, the stable manifold $W^s(p)$, respectively unstable manifold $W^u(p)$, is the image of an injective immersion of $\mathbb{R}^k$ where k is the dimension of E^s, respectively E^u.

(2) The tangent space $T_pW^s(p) = E^s$ and $T_pW^u(p) = E^u$.

Example 2.2.4. An elliptic point p is called a *source* if all the flow lines are "going away from" p. That is $W^u(p)$ is 2-dimensional and $W^s(p) = \{p\}$. Similarly, p is a *sink* if all the flow lines are "going towards" p. That is $W^s(p)$ is 2-dimensional and $W^u(p) = \{p\}$.

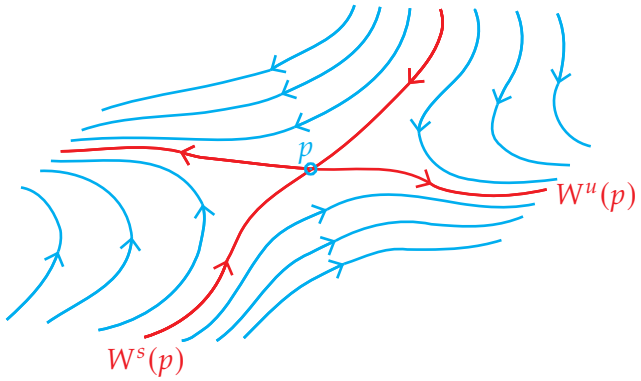

Figure 2.2.2. The stable and unstable manifolds of a saddle singularity.

For a saddle singular point p, both $W^s(p)$ and $W^u(p)$ have dimension 1. See Figure 2.2.2. These manifolds are also sometimes referred to as the stable and unstable *separatrix* of p.

Exercise 2.2.5. Let p be an elliptic point in a characteristic foliation of a surface in a contact manifold. The point p has positive divergence if and only if it is a source. Similarly, the point has negative divergence if and only if it is a sink.

The exercise shows that it is easy to determine if an elliptic point has positive or negative divergence just by looking at the flow. This is not so easy for saddle points.

Exercise 2.2.6. Let p be a saddle point in a characteristic foliation of a surface in a contact manifold. The point p has positive divergence if and only if the sum of the real parts of the eigenvalues of the linearization at p is positive. Similarly, the point p has negative divergence if and only if the sum of the real parts of the eigenvalues of the linearization at p is negative. (Here, by linearization, we mean the linearization of any vector field directing the characteristic foliation.)

Thus, we see that one can "see" the divergence of a saddle point by noting the rate at which flow lines approach the stable manifold versus the rate at which they approach the unstable manifold.

2.2.2. Periodic orbits. We now consider periodic orbits in the flow of a vector field v on a surface Σ. A *periodic orbit* of v is a closed flow line. More precisely, if p is a point such that the flow line γ_p through p is periodic, meaning that there is some t_0 such that $\gamma_p(t_0) = \gamma(0)$, then the image of γ_p is caled a periodic orbit of v. Notice that the condition on γ_p being a periodic orbit implies that $\gamma_p(t + t_0) = \gamma(t)$ for all t. If t_0 is the minimal positive value satisfying this, then we say t_0 is the *period* of the orbit. We also note that if q is any point in the image of γ_p, then γ_q is also a periodic orbit with the same image as γ_p.

Exercise 2.2.7. Show that the image of γ_p is an embedded circle in Σ.

To study periodic orbits further, we need to consider their Poincaré return map. Let I be an embedded interval transverse to v that intersects the image of γ_p at p. By the continuous dependence on the initial conditions to solutions to differential equations, it is easy to see that there is a subset $J \subset I$ such that for any $q \in J$ the flow line γ_q will intersect I. Let t_q be the smallest positive value of t for which $\gamma_q(t) \in I$. We define the *Poincaré return map*

$$\Pi_p \colon J \to I$$

by sending a point $q \in J$ to $\gamma_q(t_q)$ in I. See Figure 2.2.3. If, after possibly shrinking I and J, we parameterize I by $(-\epsilon, \epsilon)$ and J by $(-\delta, \delta)$ for $\delta < \epsilon$ and map 0 to p, then we can think of Π_p as a map $(-\epsilon, \epsilon) \to (-\delta, \delta)$. While this map depends on the choice of transversal I (and the subset J), it is not hard to show that $\Pi'(0)$ does not depend on these choices, as the next exercises show.

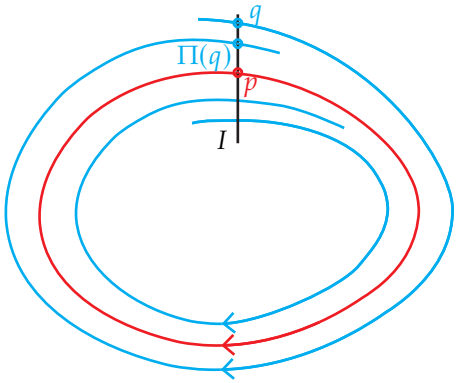

Figure 2.2.3. The Poincaré return map for the periodic orbit γ_p.

Exercise 2.2.8. Show that the conjugacy class of the germ of the Poincaré return map is independent of choices. By this, we mean that if $\bar{I}$ is a different choice of transversal to the flow through p, and $\bar{J}$ is a choice of subset of $\bar{I}$ on which we can define the Poincaré return map $\overline{\Pi}$, then there is a diffeomorphism $\phi\colon \widetilde{I} \to \phi(\widetilde{I})$ of a subset $\widetilde{I}$ of I containing p to a subset of $\bar{I}$ containing p, such that $\Pi = \phi^{-1} \circ \overline{\Pi} \circ \phi$.
Hint: Use the flow of v to identify a neighborhood of the point p in I with a neighborhood of p in $\bar{I}$.

Exercise 2.2.9. Different choices of parameterizations of I by (ϵ, ϵ) affect the map $(-\epsilon, \epsilon) \to (-\delta, \delta)$ by conjugation.

Exercise 2.2.10. Show that $\Pi'(0)$ is independent of all choices made.

We call a periodic orbit γ_p *degenerate* if $\Pi'(0) = 1$ and otherwise we say the periodic orbit is *hyperbolic*, or sometimes *non-degenerate*. If γ_p is a hyperbolic periodic orbit, then we say it is *repelling* if $\Pi'(0) > 1$ and *attracting* if $\Pi'(0) < 1$.

Example 2.2.11. In Figure 2.2.4 we see a degenerate periodic orbit and an attracting periodic orbit. By reversing the direction of the flow in the diagram on the right, we see a repelling periodic orbit.

We now note a few properties of periodic orbits.

(1) For a periodic orbit γ_p of period t_0, one may choose a volume form ω on Σ and compute
$$\log \Pi'(0) = \int_0^{t_0} \operatorname{div}_\omega v(\gamma_p(t))\, dt.$$
See [**HKc91**, Theorem 12.15]. So $\Pi'(0)$, or more properly $\log \Pi'(0)$, is the average divergence of v along the periodic orbit. Thus, $\Pi'(0)$, or more properly $\log \Pi'(0)$, is sometimes referred to as the *divergence of the periodic orbit*.

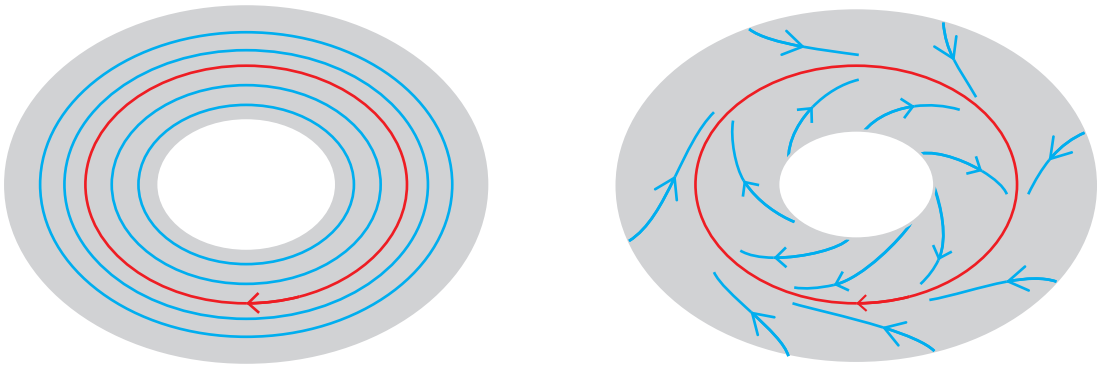

Figure 2.2.4. A degenerate and non-degenerate periodic orbit.

(2) The set of vector fields with only hyperbolic singular points and periodic orbits is residual in the set of all vector fields. That is, they are the intersection of a countable number of open dense sets and are hence dense in the set of all vector fields. See [**dMP80**, Section 3.2].

(3) The set of vector fields with only hyperbolic singular points and periodic orbits, and with the stable and unstable manifolds of saddle singularities being disjoint, is residual in the set of all vector fields. This statement is a simple case of the Kupka-Smale Theorem. See [**dMP80**, Section 3.3].

Turning to characteristic foliations, we say the foliation has a property of a vector field if any vector field directing the foliation has this property. For example, a (non-singular) closed leaf of a characteristic foliation is said to be attracting/repelling if the foliation is directed by a vector field having the leaf as a closed orbit and the closed orbit has this property.

Exercise 2.2.12. Show that a closed (non-singular) leaf in a characteristic foliation is attracting if and only if there is a 1-form β that defines the foliation near the leaf for which $d\beta > 0$. Similarly, show that a closed (non-singular) leaf in the characteristic foliation is repelling if and only if there is a 1-form β that defines the foliation near the leaf for which $d\beta < 0$.

2.2.3. General flowlines. We now discuss general flow lines of the vector field v on a surface Σ. We begin by defining the *ω-limit set* of a point $p \in \Sigma$. The ω-limit set is

$$\omega(p) = \{q \in \Sigma | \text{ there exists } t_n \to \infty \text{ such that } \lim_{n\to\infty} \gamma_p(t_n) = q\}.$$

That is $\omega(p)$ is the set of limit points of $\gamma_p([0,\infty))$. We note that one may similarly define the ω-limit set of γ_p, denoted $\omega(\gamma_p)$, as the ω-limit set of any point on the flow line γ_p.

We can similarly define the *α-limit set* of p to be

$$\alpha(p) = \{q \in \Sigma | \text{ there exists } t_n \to -\infty \text{ such that } \lim_{n\to\infty} \gamma_p(t_n) = q\}.$$

That is $\alpha(p)$ is the set of limit points of $\gamma_p((-\infty, 0])$, or we can also think of $\alpha(p)$ as $\omega(p)$ for the flow of $-v$.

It is clear that on a compact surface the ω-limit set and the α-limit set are non-empty. Some other simple properties of these sets are given in the following exercises.

Exercise 2.2.13. If Σ is compact, show that $\omega(p)$ and $\alpha(p)$ are closed and connected.

Exercise 2.2.14. The sets $\omega(p)$ and $\alpha(p)$ are invariant under the flow of v.

We now state the famous Poincaré-Bendixson Theorem, see [**dMP80**, Section 1.2].

Theorem 2.2.15 (Poincaré-Bendixson)**.** *If v is a vector field on the sphere S^2 with a finite number of singular points, then the ω-limit set of any point p is either*

(1) *a single singular point,*

(2) *a periodic orbit, or*

(3) *the union of critical points $q_0, \ldots, q_k$ and flow lines $\gamma_0, \ldots, \gamma_k$, such that $\omega(\gamma_i) = q_{i+1}$ and $\alpha(\gamma_i) = q_i$, where the indicies are taken modulo k. See Figure 2.2.5.*

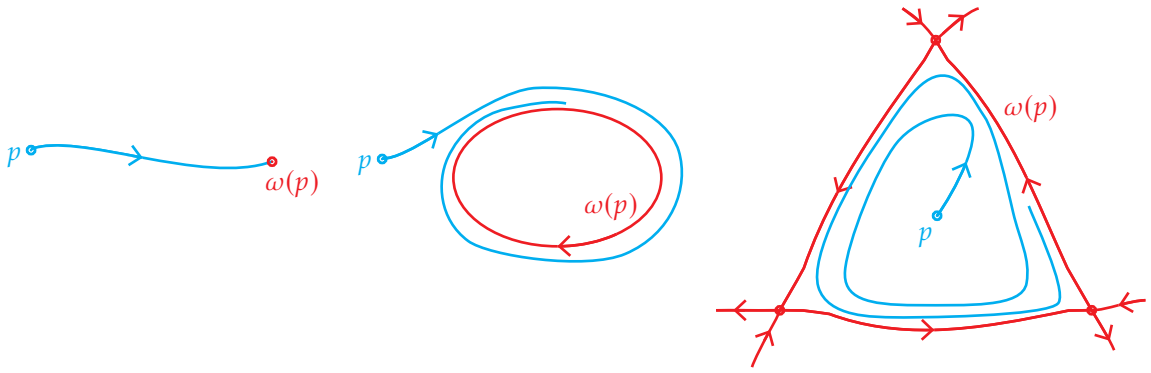

Figure 2.2.5. Limit sets from the Poincaré-Bendixson Theorem.

We note that this result is not true on other surfaces.

Example 2.2.16. Consider a foliation of $\mathbb{R}^2$ by lines of irrational slope. This will descend to a foliation of the torus T^2 with each leaf being dense in T^2. Given any vector field v on T^2 directing this foliation we see that $\omega(p)$

We say a vector field v on any surface Σ has the *Poincaré-Bendixson Property* if the α and ω-limit sets of each point in Σ satisfy the conclusions of the above theorem. Even though surfaces have flows that do not satisfy this property, they are rare.

Theorem 2.2.17. *The set of vector fields on a surface that satisfy the Poincaré-Bendixson Property forms a residual set in the space of all vector fields.*

2.3. Generic properties of characteristic foliations

In the previous section, we saw that a generic vector field had many nice properties. From this, we can see that "most" surfaces in a contact manifold have nice characteristic foliations. This will follow from the following result.

Theorem 2.3.1 (Giroux 1991, [Gir91]). *Let $\mathcal{P}$ be a C^∞ generic property of a vector field on a surface and let Σ be an oriented surface embedded in a contact manifold (M, ξ). Then by a C^∞ small isotopy of Σ we can arrange Σ_ξ is generated by a vector field satisfying $\mathcal{P}$. Moreover, if Σ_ξ already satisfies $\mathcal{P}$ on a closed subset of Σ, then the perturbation can be assumed to fix this subset.*

Proof. On a neighborhood $N = \Sigma \times [-1, 1]$ we can write a contact from for ξ by $\alpha = \beta_s + u_s\, ds$ where the β_s are 1-forms on Σ and u_s are functions on Σ, and s is the coordinate on $[-1, 1]$. If we choose an area form ω on Σ, the just as in the proof of Lemma 1.2.13 we see that ω induces an isomorphisms

$$\mathfrak{X}(\Sigma) \to \Omega^1(\Sigma)\colon\ v \mapsto \iota_v \omega$$

from vector fields on Σ, denoted by $\mathfrak{X}(\Sigma)$, to 1-forms on Σ, denoted by $\Omega^1(\Sigma)$. Thus we have vector field v_s on Σ corresponding to the β_s. We can now find a vector field v_0' that is C^∞ close to v_0 and satisfies $\mathcal{P}$. We can extend this perturbation of v_0' to a perturbation of all the v_s to v_s' so that $v_s' = v_s$ outside a small neighborhood of $s = 0$. Consider the 1-forms β_s' associated to the v_s and let $\alpha' = \beta_s' + u_s\, ds$. Since the β_s' are C^∞ close to the β_s and the contact condition $\alpha \wedge d\alpha > 0$ is an open condition we see that the v_s' can be chosen so that α' is a contact 1-form and $\alpha_t = (1-t)\alpha + t\alpha'$ is a contact form for $t \in [0, 1]$ and agrees with α away from $\Sigma \times \{0\}$. This gives a family of contact structure ξ_t on N and so Gray's theorem, Theorem 1.2.10, says there is an isotopy $\phi_t : N \to N$ that is fixed near the boundary such that $d\phi_t(\xi_0) = \xi_t$. Notice that the characteristic foliation on $\Sigma \times \{0\}$ induced by ξ_1 is generated by a vector field, namely v_0', that satisfies $\mathcal{P}$ and thus so does $\phi_1^{-1}(\Sigma \times \{0\})$ which is an isotopy of $\Sigma \times \{0\}$.

Exercise 2.3.2. Check that this isotopy of $\Sigma = \Sigma \times \{0\}$ is C^∞ small.

We lastly note that wherever v_0 already satisfies $\mathcal{P}$, we could choose v_0' to just be v_0 and thus α_t is fixed here; thus Theorem 1.2.10 says the isotopy is too. □

We note here that by the discussion in the previous section and Theorem 2.3.1 we see that any surface in a contact manifold can be C^∞ perturbed so that its characteristic foliation has only hyperbolic singular points and periodic orbits, the stable and unstable manifolds of the saddle points do not intersect, and the singular foliation satisfies the Poincaré-Bendixson Property

2.4. Families of vector fields on a surface

In Part II of this book, we will be interested in 1-parameter families of vector fields on a surface, so we discuss properties of those here. Maybe move this to Chapter 8 since we do not need this in the Part I

2.5. Twisting along leaves of a characteristic foliation

In our study of convex surfaces it will be important to understand Legendrian arcs in surfaces and how the characteristic foliation behaves near a singular point on the arc.

Lemma 2.5.1. *Let L be a Legendrian arc in a surface $\Sigma \subset (M, \xi)$ and x a point on L that is an isolated singular point of Σ_ξ. If ξ crosses $T\Sigma$ along L at x in a left-handed way then x is a source (respectively, sink) of the characteristic foliation along L if the singular point is positive (respectively negative). If ξ crosses $T\Sigma$ along L at x in a right-handed way then x is a sink (respectively, source) of the characteristic foliation along L if the singular point is positive (respectively negative).*

Proof. Recall the characteristic foliation is the foliation associated with the singular line field $l_x = \xi_x \cap T_x\Sigma$ and the orientation on l_x is given from the intersection of the oriented planes ξ_x followed by the orientation on $T_x\Sigma$. We recall how this orientation is determined. The vector v_1 gives the orientation on l_x if there is a vector $v_2 \in \xi_x$ such that v_1, v_2 orients ξ_x and a vector $v_3 \in T_x\Sigma$ such that v_1, v_3 orients $T_x\Sigma$ and v_1, v_2, v_3 orients T_xM.

We will consider the case of the contact structure passing Σ in a left-handed manner at a positive singular point.

Exercise 2.5.2. Check the other cases.

Now in Figure 2.5.6 we see a positive singularity along a Legendrian arc. So the orientation on ξ_x and $T_x\Sigma$ agree and the singular point. We also see a point on the Legendrian arc

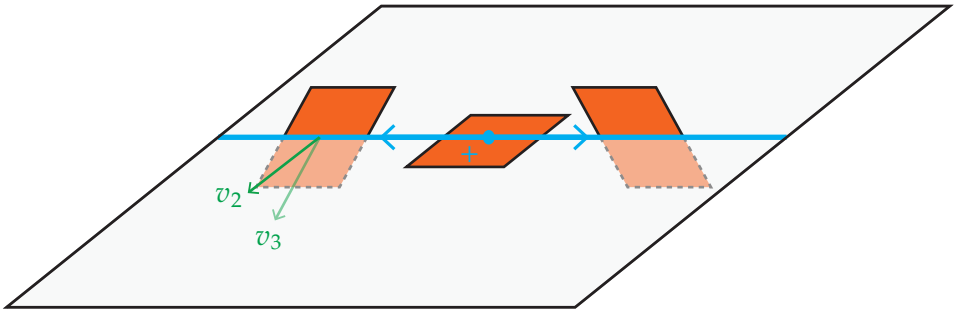

Figure 2.5.6. The characteristic foliation along a Legendrian arc near a positive singular point where the contact planes are twisting past the surface in a left-handed manner.

near the singular point. The vector v_1 is a tangent vector to the arc pointing away from the singularity. The vectors v_2 and v_3 are shown in the figure, verifying that the singular point is a source along the Legendrian arc. We know that v_1, v_2, v_3 orients M because the orientation on M is given by the orientation on ξ followed by the Reeb vector field. This is an easy consequence of $\alpha \wedge d\alpha$ orienting M since ξ is a positive contact structure on M. □

As discussed above, if a singular point is elliptic, then it will be a source if the singularity is positive and a sink if it is negative. Thus we see that if the contact structure is twisting past the surface in a right-handed manner and the singularities are generic, then they must be hyperbolic singularities.

Chapter 3

Convex surfaces

This chapter is the core of this book. Convex surfaces are the main tool we will use to analyze contact structures and Legendrian knots. The reason convex surfaces are so important comes down to the fact that the contact geometry near a convex surface is "more or less" determined by a finite collection of embedded curves on the surface. In many situations, we can cut a manifold along surfaces into simple pieces where we already understand contact structures, and then we can understand the contact structure on the original manifold by gluing these simple pieces together along the surfaces we cut along. To be able to do this, we need to understand the contact structure near the surfaces. Recall that we know the characteristic foliation on a surface determines the contact structure in a neighborhood of the surface (see Theorem 1.3.4). However, singular foliations can be very complicated, so keeping track of these can be quite complicated. This limits the effective use of the above strategy. But if we use convex surfaces instead of other types of surfaces, we only need to keep track of the finite number of curves mentioned above. This is much more tractable! The majority of the results in this section are from the foundational paper [**Gir91**] of Giroux.

A convex surface Σ is simply a surface that has a neighborhood $\Sigma \times [-1,1]$ on which the contact structure is invariant in the $[-1,1]$-direction. Said a different way, Σ is convex if there is a vector field v transverse to Σ whose flow preserves the contact planes. Such a vector field is called a contact vector field. Section 3.1 is devoted to the study of contact vector fields. We then turn to a discussion of convex surfaces in Section 3.2. After defining them, we give criteria in terms of differential forms and also in terms of the characteristic foliation that will imply the surface is convex. The main result of this section says that a surface Σ is convex if and only if its characteristic foliation is "divided" by an embedded 1-manifold Γ_Σ. (We will frequently call an embedded 1-manifold a multi-curve.) This means that Γ_Σ cuts Σ into two surfaces Σ_+ and Σ_-, Γ_Σ is transverse to the characteristic

foliation, and there is a vector field that directs the singular foliation, is pointing out of Σ_+, and its divergence is positive on Σ_+, negative on Σ_-. The multi-curve Γ_Σ is called the dividing set of the convex surface Σ.

In Section 3.3, we prove one of the essential results about convex surfaces. This result says that convex surfaces exist in abundance. Specifically, if Σ is a closed surface, then it can be C^∞ perturbed so that it is convex, and if Σ has Legendrian boundary, then it can also be perturbed to be convex if the twisting of the contact planes along each boundary component is non-positive. This is done by showing that one can construct a dividing set for a "generic" foliation and then apply the work done in the previous section to conclude the surface is convex.

We then turn to the next essential result about convex surfaces. In Section 3.4, we show that it is the dividing curves that essentially determine the contact structure in a neighborhood of a convex surface. Specifically, we show that given any singular foliation that is divided by the dividing curve of the convex surface, it can be realized as the characteristic foliation of the surface after a controlled C^0-small perturbation. Thus, we see that if two convex surfaces are diffeomorphic by a diffeomorphism that takes the dividing curves of one surface to the dividing curves of the other, then after perturbing one of the surfaces (so that its characteristic foliation agrees with the other surface), the surfaces will have contactomorphic neighborhoods. Given this result, we can "normalize" the characteristic foliation on convex tori and other simple surfaces, so we can assume we know exactly what the foliation looks like! In addition, we can show that any curve (or any graph) on a convex surface, satisfying a mild condition, can be made to be part of the characteristic foliation of the surface after a small perturbation.

Now that we know we can find lots of Legendrian curves on a convex surface, we study the classical invariants of these curves in Section 3.5. Specifically, we will see how to compute the Thurston-Bennequin invariant of a Legendrian curve on a convex surface in terms of the number of times the curve intersects the dividing set, and if the curve is the boundary of the convex surface, then we can also compute its rotation number in terms of the Σ_+ and Σ_- regions of the convex surface.

In Section 3.6, we establish the Giroux tightness criterion. This important result states that a closed convex surface has a tight neighborhood if and only if it is either the sphere and the dividing set is connected, or it is not the sphere and the dividing set has no components that bound disks in the surface. With this key result in hand, in Section 3.7, we establish the Bennequin inequality that says in a tight contact manifold for any Legendrian knot L that bounds a surface Σ, we have

$$\mathrm{tb}(L) + |\mathrm{rot}(L)| \leq -\chi(\Sigma).$$

We similarly have a result for closed surfaces if $e(\xi)$ is the Euler class of a tight contact structure on a manifold M and Σ is a closed surface in M, we show that

$$|e(\xi)([\Sigma])| \leq -\chi(\Sigma)$$

if $\Sigma \ncong S^2$, where $[\Sigma]$ is the homology class of Σ. If $\Sigma \cong S^2$, then $e(\xi)([\Sigma]) = 0$.

In the final section of this chapter, we consider how to transfer information from one convex surface to another. More concretely, suppose Σ and Σ' are two convex surfaces, where $\partial\Sigma'$ is a Legendrian knot that is contained in Σ, and Σ and Σ' are otherwise disjoint. We see that the dividing curves on Σ and Σ' interleave along $\partial\Sigma'$. That is, between two adjacent intersections of Γ_Σ with $\partial\Sigma'$, there is exactly one intersection point of $\Gamma_{\Sigma'}$ with $\partial\Sigma'$; and similarly with the roles of Γ_Σ and $\Gamma_{\Sigma'}$ interchanged.

3.1. Contact vector fields

Given a contact manifold (M, ξ), a *contact vector field* v is a vector field whose flow ϕ_t preserves ξ. If α is a contact 1-form for ξ then v is a contact vector field for ξ if and only if

$$L_v\alpha = g\alpha,$$

where $g : M \to \mathbb{R}$ is a function on M. This is easily seen since

$$L_v\alpha = \frac{\partial}{\partial t}\phi_t^*\alpha|_{t=0}$$

and the flow of v preserves ξ if and only if $\phi_t^*\alpha = g_t\alpha$.

Given the contact form α, there is a unique vector field R_α that satisfies

$$\alpha(R_\alpha) = 1, \quad \iota_{R_\alpha} d\alpha = 0.$$

This vector field is called the *Reeb vector field* of α. One easily computes

$$L_{R_\alpha}\alpha = d(\iota_{R_\alpha}\alpha) + \iota_{R_\alpha}(d\alpha) = 0$$

So the Reeb vector field R_α is a contact vector field. Moreover, the condition $\alpha(R_\alpha) = 1$ implies that the vector field is transverse to ξ.

Exercise 3.1.1. Show a vector field v is a Reeb field for some contact 1-form for ξ if and only if v is a contact vector field and transverse to ξ.

Exercise 3.1.2. Show a contact vector field v is always tangent to ξ if and only if it is 0.

While not clear from the definition, the result below shows that there are actually many contact vector fields.

Proposition 3.1.3 (Libermann 1959, [Lib59]). *On a contact manifold (M^3, ξ), contact vector fields are in one-to-one correspondence with sections of the quotient bundle TX/ξ.*

We will consider the transversely orientable case and leave the general case to the reader. We begin by noticing if ξ is transversely orientable, then we may choose a contact form α defining ξ and consider its Reeb vector field R_α. Clearly R_α is a non-zero section of TM/ξ and so $TM/\xi \cong M \times \mathbb{R}$ and sections of TM/ξ are given by HR_α where $H\colon\ M \to \mathbb{R}$ is any function on M. The function H is called a *contact Hamiltonian*.

Proof. With the notation above, assume we are given a contact Hamiltonian H — that is a section of TM/ξ — we will construct a contact vector field v. We begin by setting $v = w - HR_\alpha$ where w is a section of ξ. Notice that $\alpha(v) = -H$ and that $dH - (dH(R_\alpha))\alpha$ is a 1-form on M that vanishes on R_α. Recall from Section 1.2 that if $\Omega^1_\alpha(m)$ is the set of 1-forms that vanish on R_α and $\Gamma(\xi)$ denotes the sections of ξ, then the map

$$\Gamma(\xi) \to \Omega^1_\alpha(M)\colon\ u \mapsto \iota_u d\alpha$$

is a bijection. Noting that $\iota_v d\alpha = \iota_w d\alpha$ we see that there is a unique $w \in \Gamma(\xi)$ such that

$$\iota_w d\alpha = dH - (dH(R_\alpha))\alpha.$$

We note that with this w, the vector field v is contact. Indeed

$$\mathcal{L}_v \alpha = d\iota_v \alpha + \iota_v d\alpha = d(-H) + dH - (dH(R_\alpha))\alpha = -dH(R_\alpha)\alpha.$$

Thus a section of TM/ξ uniquely determines a contact vector field and a contact vector field v clearly gives a section of TM/ξ by setting $H = -\alpha(v)$. □

Exercise 3.1.4. Prove the above proposition in the case that ξ is not transversely orientable.

The above proposition has an immediate useful corollary.

Corollary 3.1.5. *Any locally defined contact vector field can always be extended to a globally defined vector field.*

Proof. Given a contact vector field v defined locally, it gives a section of TM/ξ. Extend this section to a global section and consider the corresponding contact vector field. □

Implicit in the proof of the proposition above is the following statement that we make explicit here.

Lemma 3.1.6. *Given a contact manifold (M, ξ), where ξ is defined as the kernel of the 1-form α. A vector field v is a contact vector field if and only if there is a function $H : M \to \mathbb{R}$ such that*

$$\alpha(v) = -H, \text{ and}$$

$$\iota_v d\alpha = dH - (dH(R_\alpha))\alpha.$$

Given a contact vector field v for a contact manifold (M, ξ) the *characteristic hypersurface* of v is

$$C = \{x \in M | v(x) \in \xi_x\}.$$

We would like to understand when the characteristic hypersurface is a manifold. To this end, we have the following exercises.

Exercise 3.1.7. Show that sections of TM/ξ that are transverse to the zero section are generic in the C^∞ topology (for details on the topology see [**Hir76**]). In particular, if M is compact then such sections are open and dense, while for open M they are residual. Note for a coorientable contact structure, this is equivalent to saying that the set of functions $M \to \mathbb{R}$ that are transverse to zero are generic.

Lemma 3.1.8. *For a generic contact vector field v the characteristic hypersurface is a surface. Moreover, v is tangent to C and directs its characteristic foliation.*

Proof. We consider the case of coorientable contact structures and leave the other case to the reader. With the notation above $C = H^{-1}(0)$. Genericity implies 0 is a regular value of H and hence C is a surface.

Recall $L_v\alpha = g\alpha$ for some function g. Now if $x \in C, w \in T_xC \cap \xi_x$ and $v \neq 0$ then

$$d\alpha_x(v, w) = L_v\alpha(w) - d(\iota_v\alpha)(w) = g\alpha(w) + dH(w) = 0,$$

since $w \in TH^{-1}(0)$ and also in ξ. Thus $v, w \in \xi_x$, and $d\alpha(v, w) = 0$ implies that v is a multiple of w.

Now if $v = 0$ then

$$g\alpha_x = (L_v\alpha)_x = (d\iota_v\alpha)_x = -dH_x = 0$$

for vectors tangent to C. Thus $\alpha = 0$ on vectors tangent to C. (Or $g(x) = 0$ but then $dH_x = 0$ contradicting genericity.) Therefor singularities in C_ξ occur at zeros of v. □

3.2. Convex surface

In this section, we explore the main object of study in this book. A surface Σ in a contact manifold (M, ξ) is a *convex* if there is a contact vector field v that is transverse to Σ. There are several conditions that are equivalent to a surface being convex.

Lemma 3.2.1. *A surface Σ is convex if and only if there is an embedding $\phi : \Sigma \times \mathbb{R} \to M$ such that $\phi(\Sigma \times \{0\}) = \Sigma$ and $d\phi^{-1}(\xi)$ is invariant under translations in the $\mathbb{R}$ direction. We call this a* vertically invariant *contact structure.*

We call the neighborhood of Σ in the lemma above a *vertically invariant neighborhood*.

Proof. If Σ is convex let v be the transverse contact vector field. Set $H = -\alpha(v)$ for some contact 1-form for ξ. Cut off H so that it is zero outside a small tubular neighborhood of Σ (and nonzero in this neighborhood). Let v' be the vector field generated by this new function. The flow of v' gives ϕ. (Note, we needed to cut off H so that we did not have to worry about the flow not existing for all time or having periodic orbits.) Conversely, if t is the coordinate on $\mathbb{R}$ then $d\phi\left(\frac{\partial}{\partial t}\right)$ is a contact vector field for ξ that is transverse to Σ. □

We now state a fairly obvious lemma, but one that will be used frequently later in the book. Recall that for a smooth manifold M, one may use the collar neighborhood theorem to show that adding a product neighborhood to ∂M results in a manifold canonically diffeomorphic to M (meaning that any two choices of the "obvious" diffeomorphism are isotopic). The following lemma is a contact geometric version of this.

Lemma 3.2.2. *Suppose (M, ξ) is a contact manifold with convex boundary Σ. Let ξ' be a contact structure on $\Sigma \times [0,1]$ that is invariant in the $[0,1]$-direction and induces the same characteristic foliation on Σ as ξ does. Gluing $\Sigma \times [0,1]$ to M will result in a manifold that is canonically diffeomorphic to M, up to isotopy, and the result of gluing ξ and ξ' together is contact isotopic to ξ.*

Proof. We begin with a simple exercise.

Exercise 3.2.3. Let η be a contact structure on $\Sigma \times [0,1]$ and η' be one on $\Sigma \times [1,2]$. Assume they are both invariant in the interval direction, and both induce the same characteristic foliation on $\Sigma \times \{pt\}$. Then the contact structure on $\Sigma \times [0,2]$ obtained by gluing η and η' together is isotopic to η (once $\Sigma \times [0,2]$ is identified with $\Sigma \times [0,1]$ via an diffeomorphism that is the identity on Σ).
Hint: While there are several approaches to this exercise, we suggest considering the Reconstruction Lemma, Lemma 1.3.9.

Now we may use the fact that $\Sigma = \partial M$ is convex to find a neighborhood $\Sigma \times [-1,0]$ of Σ in M on which ξ is invariant in the interval direction. Now by the previous exercise we see that the contact structure on $\Sigma \times [-1,1]$ obtained by gluing $\xi|_{\Sigma \times [-1,0]}$ and ξ' together is isotopic to $\xi|_{\Sigma \times [-1,0]}$. The lemma follows. □

Using the coordinates coming from Lemma 3.2.1 there is a contact 1-form α for ξ such that

$$\alpha = \beta + u\, dt,$$

where β is a 1-form on Σ and u is a function on Σ. We note:

(1) $\Sigma_\xi = \ker(\beta)$.

(2) $\Sigma \cap C = \{x \in \Sigma | u(x) = 0\}$.

(3) for α to be a contact form we need

$$\begin{aligned}\alpha \wedge d\alpha &= \beta \wedge (d\beta + du \wedge dt) + u\, dt \wedge d\beta \\ &= (\beta \wedge du + u\, d\beta) \wedge dt > 0.\end{aligned}$$

Lemma 3.2.4. *Let Σ be a surface in a contact manifold (M, ξ), $i\colon \Sigma \to M$ the inclusion map, and α a contact 1-form for ξ. Set $\beta = i^*\alpha$. The surface Σ is convex if and only if there is a function $u\colon \Sigma \to \mathbb{R}$ such that*

$$u\, d\beta + \beta \wedge du > 0. \tag{3.2.10}$$

Proof. If Σ is convex we know such a u exists from the computation above. Conversely, if such a u exists then on $\Sigma \times \mathbb{R}$ we can consider the contact structure $\ker(\beta + u\, dt)$. The characteristic foliation on $\Sigma \times \{0\}$ is the same as the one on $\Sigma \subset M$. Thus by Theorem 1.3.4 we know there is a contactomorphism from a neighborhood of $\Sigma \times \{0\}$ to a neighborhood of Σ. Push the vector field $\frac{\partial}{\partial t}$ to M using the contactomorphism. This is a contact vector field transverse to Σ. □

We will now "dualize" this construction. Let ω be an area form on Σ and define a vector field w on Σ by

$$\iota_w \omega = \beta.$$

Note: w is in the kernel of β so w directs Σ_ξ. That is w is tangent to the foliation at non-singular points and is zero at singular points. If Σ is convex we know

$$\beta \wedge du + u\, d\beta > 0,$$

and hence

$$\beta \wedge du + u(\mathrm{div}_\omega w)\omega > 0,$$

where $\mathrm{div}_\omega w$ is defined in Section 2.1, which implies

$$-du(w)\omega + u(\mathrm{div}_\omega w)\omega > 0.$$

The last line follows because $du \wedge \omega = 0$ (since this is 3-form on a surface) and hence $0 = \iota_w(du \wedge \omega) = du(w)\omega - du \wedge (\iota_w \omega)$. Thus

$$-du(w) + u(\mathrm{div}_\omega w) > 0. \tag{3.2.11}$$

Exercise 3.2.5. Show that the set of functions u on a surface that satisfy Equation (3.2.10), or dually Equation (3.2.11), forms a convex set, and different choices of u correspond to different choices of vertically invariant vector field transverse to Σ.

Shortly we will see that convex surfaces are very common. For the moment let us see that there are surfaces that are not convex.

Example 3.2.6. *Let (r, θ, z) be cylindrical coordinates on $\mathbb{R}^3$. Consider the contact manifold $M = \mathbb{R}^3/\sim$ where $\sim$ is the equivalence relation generated by $z \mapsto z + 1$ and $\xi = ker(dz + r^2 d\theta)$ Let T_c be the torus $\{(r, \theta, z) | r = c\}$. Then the characteristic foliation on T_c is linear. If β is as above it is easy to see that $d\beta = 0$ on T_c. Thus if T_c is convex we need to find a function $u : T_c \to \mathbb{R}$ such that $-du(w) > 0$, where w is pointing along the foliation. Thus u must be decreasing along the flow lines. But this is not possible.*

There is another way a foliation can fail to be convex.

Exercise 3.2.7. Show that if there is a flow line from a negative singularity to a positive singularity then the surface cannot be convex.
Hint: Assume the surface is convex. The contact form can be written $\beta + u\, dt$. At the negative singularity u must be negative at the positive singularity u must be positive.

We will see in Theorem 3.3.6 below that generically a surface is convex if and only if it does not violate either of the two conditions mentioned in the previous two exercises.

We now turn to our last characterization of convex surfaces. Let Σ be a surface and $\mathcal{F}$ be a singular foliation on Σ. A multi-curve Γ is said to divide $\mathcal{F}$ if

(1) $\Sigma \setminus \Gamma = \Sigma_+ \coprod \Sigma_-$,
(2) Γ is transverse to $\mathcal{F}$, and
(3) there is a area form ω on Σ and a vector field w on Σ so that
   (a) $\pm \mathrm{div}_\omega w > 0$ on $\Sigma_\pm$,
   (b) w directs $\mathcal{F}$, and
   (c) w points transversely out of Σ_+ along Γ.

Exercise 3.2.8. Show that if Γ_1 and Γ_2 both divide $\mathcal{F}$ then they are isotopic through dividing curves.

If Σ in (M, ξ) is convex then near Σ write a contact form for ξ as $\beta + u\, dt$. The multi-curve $\Gamma_\Sigma = \{x \in \Sigma | u(x) = 0\}$ (this is the intersection of Σ with the characteristic hypersurface) is called the *dividing set of* Σ.

Theorem 3.2.9 (Giroux 1991, [Gir91]). *Let Σ be an orientable surface in (M, ξ) with Legendrian boundary (possibly empty). Then Σ is a convex surface if and only if Σ_ξ has dividing curves. Moreover, if Σ is convex, then Γ_Σ will divide Σ_ξ.*

Proof. Suppose Σ is convex. Let Γ_Σ be the dividing set of Σ. Let $\beta + u\, dt$ be a vertically invariant contact form for ξ in a neighborhood of Σ. We have $\Gamma_\Sigma = u^{-1}(0)$, thus it is clear that $\Sigma_+ = u^{-1}([0, \infty))$ and $\Sigma_- = u^{-1}(-\infty, 0])$ are the components of $\Sigma \setminus \Gamma_\Sigma$. Moreover, if Γ_Σ is not transverse to Σ_ξ then there would be a vector v tangent to Σ_ξ and Γ_Σ at some point. Thus $v \in \ker \beta$, $du(v) = 0$ and $\iota_v(\beta \wedge du + u\, d\beta) = 0$ at this point (recall $u = 0$ on Γ_Σ),

contradicting the contact condition. (Note: we did not have to assume that the contact vector field is generic. So even though the characteristic hypersurface might not be cut out transversely, we still must have Γ_Σ is transverse to Σ_ξ and hence cut out transversely.)

We are now left to check condition (3) of the definition of dividing curve. The form $\omega' = \beta \wedge du + u d\beta$ is an area form on Σ. Let w be the vector field determined by $\iota_w \omega' = \beta$.

Exercise 3.2.10. Show that w directs the characteristic foliation.
Hint: It is immediate from its definition that w' is tangent to the foliation where it is non-singular and 0 when it is singular. So the main thing to check is that w' induces the correct orientation on the foliation where it is non-singular.

We will now consider Σ away from the dividing curves (that is where $u = 0$). In this region, a simple computation yields $\mathrm{div}_{\omega'}\left(\frac{1}{u}w\right) = \frac{1}{u^2}$. Since $\mathrm{div}_\omega fv = f\mathrm{div}_{f\omega}v$ we see that $\pm\mathrm{div}_{u^{-1}\omega'}(w') = \pm\frac{1}{u^3} > 0$ on $\Sigma_\pm$ (away from the dividing set). Now let A be a small tubular neighborhood of Γ_Σ so that the characteristic foliation on A is by arcs transverse to $\partial A \setminus (\partial\Sigma \cap A)$. Let $\Sigma'_\pm = \Sigma_\pm \cap (\Sigma \setminus A)$. On $\Sigma'_\pm$ let ω by $\pm\frac{1}{u}\omega'$. This defines a (properly oriented) area form on $\Sigma \setminus A$ and a vector field that directs the foliation on $\Sigma \setminus A$ for which $\pm\mathrm{div}_\omega w > 0$ on $\Sigma'_\pm$. We are left to extend ω over A so that $\pm\mathrm{div}_\omega w > 0$ on $\Sigma_\pm$.

Exercise 3.2.11. Show ω can be so extended.
Hint: We have an explicit model for w in A. Write down any area form on A with the desired properties and show that it can be patched into ω near the boundary of A preserving these properties. The proof of Lemma 2.1.2 might be helpful.

Now assume Γ divides Σ_ξ. We want to show that Σ is convex. Let Σ_0 be a small tubular neighborhood of Γ in Σ so that the characteristic foliation on Σ_0 is by arcs running across Σ_0. (Note each component of Σ_0 is an annulus or strip and its core is transverse to Σ_ξ thus it is possible to find Σ_0.) Let $\Sigma'_\pm = \Sigma_\pm \cap (\Sigma \setminus \Sigma_0)$. On $\Sigma'_+ \cup \Sigma'_-$ let $\beta = \iota_v\omega$. On $\Sigma'_\pm$ let $u = \pm 1$. Thus on $\Sigma'_+ \cup \Sigma'_-$ one easily checks that

$$u\,\mathrm{div}_\omega w - du(w) > 0. \tag{3.2.12}$$

Or in other words, $\beta + u\,dt$, is a contact form on $(\Sigma'_+ \cup \Sigma'_-) \times \mathbb{R}$. Of course $\beta = \iota_w\omega$ is well defined on all of Σ. We just need to extend u over Σ_0 so that Equation (3.2.12) is satisfied on all of Σ. To this end, slightly enlarge Σ_0 to Σ'_0 so that Σ'_0 is still foliated by arcs transverse to the boundary and Σ_0 is on the interior of Σ'_0. See Figure 3.2.1. Parameterize an arc in the foliation of Σ'_0 as a flow line of w. Denote the parameterization as $f\colon [0,1] \to \Sigma_0$. Also denote $u|_A$ by u. Thinking of u as a function on $[0,1]$ we see $u(0) = 1$ and $u(1) = -1$. To extend u over Σ'_0 satisfying Equation(3.2.12) we need to solve the equation:

$$u\,\mathrm{div}_\omega w - \frac{du}{dt} > 0.$$

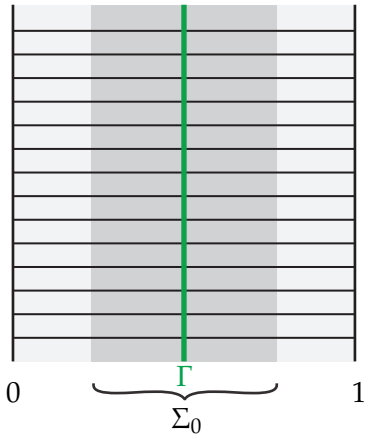

Figure 3.2.1. The region Σ_0'. The curve dividing the foliation Γ is shown in green, the horizontal curves are the leaves of the foliation. The function u is defined in the region shaded in light gray and needs to be extended over the dark gray region.

We can solve this with a function of the form

$$u(t) = g(t)e^{\int_0^t (\mathrm{div}_\omega w)(t)dt},$$

where $g(t)$ satisfies $g'(t) < 0$, and

$$g(t) = \begin{cases} \frac{1}{e^{\int_0^t (\mathrm{div}_\omega w)(t)}} & \text{near } t = 0 \\ -\frac{1}{e^{\int_0^t (\mathrm{div}_\omega w)(t)}} & \text{near } t = 1. \end{cases}$$

It is easy to find such a g. Thus we have extended u over one arc in Σ_0'. One may easily see that we can consistently extend over all arcs in this way. This extended u by construction satisfies Equation (3.2.12) and hence we have a vertically invariant contact form on $\Sigma \times \mathbb{R}$. In addition, the characteristic foliation on $\Sigma \times \{0\}$ is the same as Σ_ξ. Thus a neighborhood of $\Sigma \times \{0\}$ in $\Sigma \times \mathbb{R}$ is contactomorphic to Σ in M. Using this contactomorphism we see Σ is convex. □

Exercise 3.2.12. If Σ is a convex surface in a co-oriented contact manifold (M, ξ) notice that ξ orients Γ_Σ. With this orientation show that $\partial\Sigma_+ = \Gamma_\Sigma$ and $\partial\Sigma_- = -\Gamma_\Sigma$.

Exercise 3.2.13. If Σ is a closed convex surface then the dividing set Γ_Σ cannot be empty.

Example 3.2.14. The unit 2-sphere in $\mathbb{R}^3$ with the contact structure $\xi = \ker(dz + r^2 d\theta)$ is convex as the following exercise verifies. See Figure 3.2.2.

Exercise 3.2.15. Show that $z\frac{\partial}{\partial z} + \frac{1}{2}\frac{\partial}{\partial r}$ is a contact vector field and induces the given dividing set.

Alternatively, we can see the surface is convex as follows. From Section 2.1 we know the divergence of the singular foliation must be positive near the north pole and negative near the south pole. Away from neighborhoods of these poles, we have an annulus as

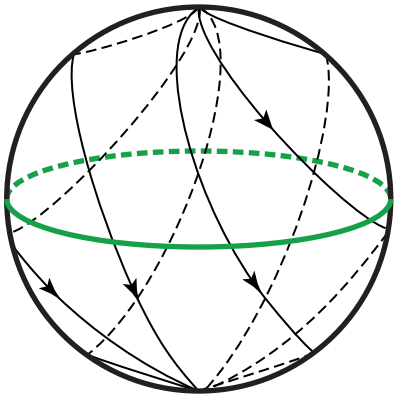

Figure 3.2.2. Convex 2-sphere with dividing curves shown in green.

in the proof of the above theorem. Argue as in that proof to show that the foliation is divided by the curve indicated in the figure.

Example 3.2.16. Here we revisit Example 3.2.6. Let $M = \mathbb{R}^3/\sim$ where $(r, \theta, z) \sim (r, \theta, z + 1)$ have the contact structure $\xi = \ker(dz + r^2 d\theta)$. Consider $T_c = \{(r, \theta, z) : r = c\}$ for a fixed c so that the slope of the characteristic foliation is $\frac{p}{q}$. As discussed in Example 3.2.6, T_c is not a convex torus. Pick two orbits B and C in $(T_c)_\xi$. We have $T_c \setminus (B \cup C) = A_1 \cup A_2$, where A_i is an annulus. Push the interiors of A_1 and A_2 towards the z axis slightly.

Exercise 3.2.17. Check that the foliation is as shown in Figure 3.2.3. From our discussion in Section 2.1 we see that the divergence of the foliation can be assumed to be positive

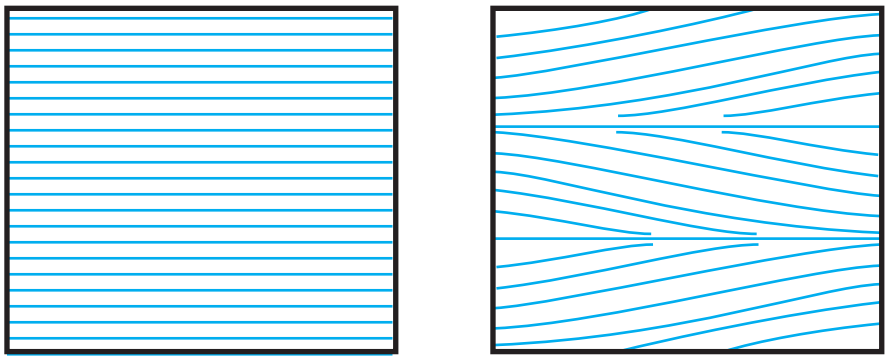

Figure 3.2.3. Non-convex torus, left, is perturbed into a convex torus right.

near the repelling closed orbit and negative near the attracting closed orbit. The complement of these neighborhoods can be assumed to be annuli. Arguing as in the proof of the theorem above, show the foliation can be divided by the curves indicated in the figure and hence the surface is convex.

Note we easily could have arranged that our convex torus had $2n$ periodic orbits and $2n$ components to the dividing curve.

3.3. Finding convex surfaces

We are now ready to see that convex surfaces are plentiful.

Theorem 3.3.1 (Giroux 1991, [Gir91] for the closed case; Kanda 1998, [Kan97] in general)**.** *Any closed surface Σ in a contact manifold (M, ξ) is C^∞-close to a convex surface.*

Any surface with Legendrian boundary satisfying $\mathrm{tw}(\gamma, \Sigma) \leq 0$ *for all boundary components γ may be C^0 small perturbed near the boundary and then C^∞ small perturbed on the interior to become convex. If Σ contains other Legendrian curves L satisfying* $\mathrm{tw}(L, \Sigma) \leq 0$ *then Σ may be made convex after a C^0 small purturbation near the L and the boundary and a C^∞ small perturbation elsewhere.*

To prove this theorem we need a preliminary definition and result.

Definition 3.3.2. A singular foliation $\mathcal{F}$ is called *almost Morse-Smale* if

(1) the singularities are non degenerate,

(2) each close orbit is non degenerate (that is the Poincaré return map is not degenerate), and

(3) there are no flow lines running from a negative singularity to a positive singularity (this could only happen by having a connection between two saddle singularities).

Theorem 3.3.3 (Giroux 1991, [Gir91])**.** *If $\partial\Sigma$ is Legendrian and Σ_ξ is almost Morse-Smale, then Σ is convex.*

Proof. We will show that such Σ_ξ has dividing curves. To this end, along each close leaf put an annulus with boundary transverse to Σ_ξ. Around each elliptic singularity put a small disk with boundary transverse to Σ_ξ. Along the stable (unstable) manifolds of a positive (negative) hyperbolic singularity put a band. Let $\Sigma_\pm$ be the union of the regions just described associated to $\pm$ singularities and periodic orbits. (One should check that these unions define disjoint sets.) One may choose an area form on $\Sigma_\pm$ that agrees with the orientation induced from Σ and so that a vector field w directing the characteristic foliation of $\Sigma_\pm$ has $\pm$ divergence. To do this note that by the discussion in Section 2.1 the divergence near the singularities is independent of the area form and near the periodic points the area form can be chosen to have the desired divergence. Now on Σ_+, say, we know the divergence is positive near the singularities and periodic orbits.

Exercise 3.3.4. Recalling that if $\omega' = e^f \omega$ then $\mathrm{div}_{\omega'} w = \mathrm{div}_\omega w + df(w)$, show that one may choose f so that $\pm\mathrm{div}_{\omega'} w > 0$ on $\Sigma_\pm$.

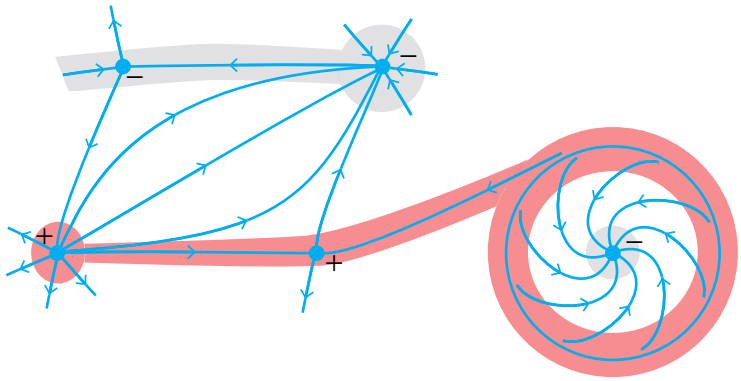

Figure 3.3.4. The regions $\Sigma_\pm$. We see Σ_+ is red and Σ_- in grey. NEED BETTER PICTURE

Hint: Choose a function f that is zero near the elliptic singularities and periodic orbits, K near the hyperbolic singularities and $2K$ near the boundary of Σ_+.

Note $\Sigma' = \Sigma \setminus (\Sigma_+ \cup \Sigma_-)$ is a surface with a non-singular foliation which is transverse to the boundary and without closed leaves (and sitting on an orientable surface). Thus the components of Σ' are annuli or strips foliated by arcs. The vector field directing the foliation on Σ' has $\pm$ divergence near the boundary components touching $\Sigma_\pm$.

Exercise 3.3.5. Extend the area form over Σ' so that the divergence is 0 only near the core of each annulus.

Thus the cores of these annuli form a dividing set for Σ_ξ and by Theorem 3.2.9, Σ is convex. □

Though this theorem suffices for most applications, there is a stronger version. An oriented singular foliation is said to satisfy the Poincaré Bendixson property if the limit set of each flow line (in either positive or negative time) is a singular point, periodic orbit or a union of singular points and connecting orbits.

Theorem 3.3.6 (Giroux 2000, [**Gir00**]). *Let Σ be an oriented surface in (M, ξ) with Legendrian boundary such that Σ_ξ satisfies the Poincaré-Bendixson property. Then Σ is convex if and only if all the closed orbits are non-degenerate and there is no flow from a negative to a positive singularity.*

Exercise 3.3.7. Prove this theorem.
Hint: It is not hard to show that the conditions in the theorem are necessary for convexity, see Example 3.2.6 and Exercise 3.2.7. The proof of sufficiency is very similar to the proof of Theorem 3.3.3.

Proof of Theorem 3.3.1. The closed case is clear by Theorems 2.3.1 and 3.3.3, since (almost) Morse-Smale foliations are generic.

Consider Σ with boundary. Let γ be a boundary component of Σ and N a neighborhood of γ that is contactomorphic to a neighborhood N' of the x-axis in $\mathbb{R}^3/\sim$, where $(x+1, y, z) \sim (x, y, z)$, with the contact structure $\ker(dz - ydx)$. By shrinking the neighborhoods if necessary, the intersection $\Sigma \cap N$ can be assumed to map to an annulus A in N' (prove this if it is not clear to you). The curve $A \cap \partial N'$ wraps around $\partial N'$ some number of times. Let N'' be a smaller neighborhood of the x-axis and let A' be a "uniformly twisting" annulus (by which we mean that the angle formed by the annulus and the xy-plane is changing at a constant rate) in N'' that twists around $\partial N''$ the same number of times as A twists around $\partial N'$. Note the signs of the singularities of A' along γ alternate and can be assumed to be non-degenerate. Now connect $A' \cap \partial N''$ to $A \cap \partial N'$ to get an annulus A''.

Exercise 3.3.8. Show that A is isotopic to A'' by an isotopy fixing the boundary components.

Replace A by A'' to get C^0 isotopy of Σ near γ. Now repeat this construction for the other boundary components.

Recall Lemma 2.5.1 says that if p is a singularity along the x-axis and ξ is twisting past A'' in a right-handed way then p is a positive (negative) singularity of A''_ξ if and only if it is a sink (source) of the flow along γ. The opposite is true if ξ is twisting past A'' in a left handed manner. Thus if $\mathrm{tw}(\gamma, \Sigma) > 0$ then Σ cannot be made convex.

Exercise 3.3.9. If $\mathrm{tw}(\gamma, \Sigma) \leq 0$ then show that we may C^0 isotop Σ in a neighborhood of $\partial\Sigma$, but fixing $\partial\Sigma$, so that Σ_ξ is Morse-Smale near $\partial\Sigma$
Hint: Build a standard neighborhood of $\partial\Sigma$ and see that you can isotop Σ in this neighborhood to have the desired property.

By Theorem 2.3.1 we can C^∞ perturb Σ away from the boundary so that it is almost Morse-Smale on the rest of Σ and thus Σ is convex by Theorem 3.3.3. □

3.4. Convex surfaces and characteristic foliations

We now explore the main property that makes convex surfaces so useful. In particular, the following result will show that the dividing curves of a convex surface essentially determine the contact structure in a neighborhood of the surface.

Theorem 3.4.1 (Giroux 1991, [Gir91]). *Given a compact surface Σ and a contact manifold (M, ξ) let $i : \Sigma \to M$ be an embedding so that $i(\Sigma)$ is a convex surface in (M, ξ), if Σ is not closed then assume $i(\Sigma)$ has Legendrian boundary. Let $\mathcal{F}$ be a singular foliation on Σ such that $\mathcal{F}$ is divided by $\Gamma = i^{-1}(\Gamma_\Sigma)$. Then given any neighborhood U of $i(\Sigma)$ in M, there is an isotopy $\phi_s : \Sigma \to M, s \in [0, 1]$, such that*

(1) $\phi_0 = i$,

(2) ϕ_s *is fixed on* $i^{-1}(\Gamma_\Sigma)$,

(3) $\phi_s(\Sigma) \subset U$ *for all* s,

(4) $\phi_s(\Sigma)$ *is convex with dividing set* Γ_Σ,

(5) $(\phi_1(\Sigma))_\xi = \phi_1(\mathcal{F})$.

This theorem says that any singular foliation that a convex surface could possibly have (that is, one that has the same dividing set), can actually be realized in a C^0 neighborhood of the surface. This is called the *Giroux realization principle* or *Giroux flexibility*. Since Theorem 1.3.5 says the contact structure near the surface is determined by the characteristic foliation, we see that the dividing curves essentially determine the contact structure near the surface.

Exercise 3.4.2. Why do the dividing curves of a convex surface not "determine the contact structure in a neighborhood of the surface"?

Proof. Let $\Psi : \Sigma \times \mathbb{R} \to M$ be a vertically invariant neighborhood of $i(\Sigma)$ in $U \subset M$, so that $\Psi(\Sigma \times \{0\}) = i(\Sigma)$. Such a Ψ clearly exists by Corollary 3.1.5. We will construct the desired isotopy in $X = \Sigma \times \mathbb{R}$ then use Ψ to map it to M.

Since Γ divides both Σ_ξ and $\mathcal{F}$ there is a neighborhood A of Γ in Σ so that both Σ_ξ and $\mathcal{F}$ foliate A by arcs transverse to $\partial A \setminus (\partial\Sigma \cap A)$. Let $\Sigma'_\pm = \Sigma_\pm \cap (\Sigma \setminus A)$ and $X_\pm = \Sigma'_\pm \times \mathbb{R}$. By Exercise 3.2.5 and the discussion in the proof of Theorem 3.2.9 we can find area forms ω_i, vector fields w_i, and functions u_i, $i = 0, 1$, so that $\alpha_0 = \iota_{w_0}\omega_0 + u_0\, dt$ is a contact 1-form for $\xi_0 = \Phi^*(\xi)$, $\alpha_1 = \iota_{w_1}\omega_1 + u_1\, dt$ is a contact form on X that induces $\mathcal{F}$ as the characteristic foliation on $\Sigma \times \{0\}$, and so that $u_i = \pm 1$ on $\Sigma'_\pm$.

We concentrate on X_+ (the same arguments apply to X_-). Note $\omega_1 = f\,\omega_0$, for some positive function f. Referring to Equation (2.1.9) in Section 2.1 we see that

$$f \operatorname{div}_{f\omega_0} w_1 = \operatorname{div}_{\omega_0}(f w_1),$$

Thus $w'_1 = f w_1$ dilates ω_0 on Σ'_+. Now set $w_s = (1-s)w'_1 + s w_0$, $s \in [0, 1]$. All the vector fields w_s dilate ω_0 on Σ'_+. Thus the 1-forms $\alpha_s = \iota_{w_s}\omega_0 + dt$ are all contact forms on X_+.

We have a family of 1-forms α_s on $X_+ \cup X_-$ which we will extend over $A \times \mathbb{R}$. Let B be a small neighborhood of A in Σ. On $X_0 = B \times \mathbb{R}$ we have functions u_s defined near $\partial B \setminus (\partial\Sigma \cap B)$. They are all equal to ± 1 according as the boundary component is in $\Sigma'_\pm$. We can also define the vector fields w_s on $B \times \mathbb{R}$ as a linear combination of w_0 and w_1 as above. Note w_s always generates a foliation by arcs transverse to $\partial B \setminus (\partial\Sigma \cap B)$. We may now extend the u_s's across B as in the proof of Theorem 3.2.9. We can in addition ensure that u_s is 0 on Γ for all s. We now have a one-parameter family of contact forms α_s and vertically invariant contact structures $\xi_s = \ker \alpha_s$ on all of X. Moreover, $(\Sigma \times \{0\})_{\xi_0} = \Sigma_\xi$, $(\Sigma \times \{0\})_{\xi_1} = \mathcal{F}$, and $\Gamma \times \mathbb{R}$ is the characteristic hypersurface for all s. MORE DETAIL?

We apply Moser's method, as in Theorem 1.3.4. One may check that since all the α_t are vertically invariant, the vector field that generates the flow in Moser's method is also vertically invariant. With this observation, it is easy to see that the flow generated by this vector field satisfies all the collusions of the theorem. □

Remark 3.4.3. Convex surfaces are useful for many reasons, but one of the most important ones is the Giroux realization principle. When you have a surface it can be useful to know that you can perturb it to have a generic property (for example, that is how we proved Theorem 3.3.1 that shows convex surfaces are generic), but with convex surfaces, one may isotop them to have very non-generic properties as we will see in the example below. *Adapting these non-generic properties to a given situation is a key to essentially all of the classification results in the coming chapter!*

Example 3.4.4. Recall form Examples 3.2.16 we have convex tori with $2n$ dividing curves, and $2n$ periodic orbits of slope $\frac{p}{q}$. Using Theorem 3.4.1 we can arrange that the characteristic foliation on the torus is as shown in Figure 3.4.5. That is there are $2n$ lines of singularities (n lines of "sources" and n lines of "sinks") with slope $\frac{p}{q}$, called *Legendrian divides*. Between each two adjacent dividing curves there is a line of singularities. Moreover, the rest of the foliation can be assumed to be by lines of slope s where s is any rational number *not equal to* $\frac{p}{q}$. These curves are called *ruling curves*. A torus with such a characteristic foliation is said to be in *standard form*.

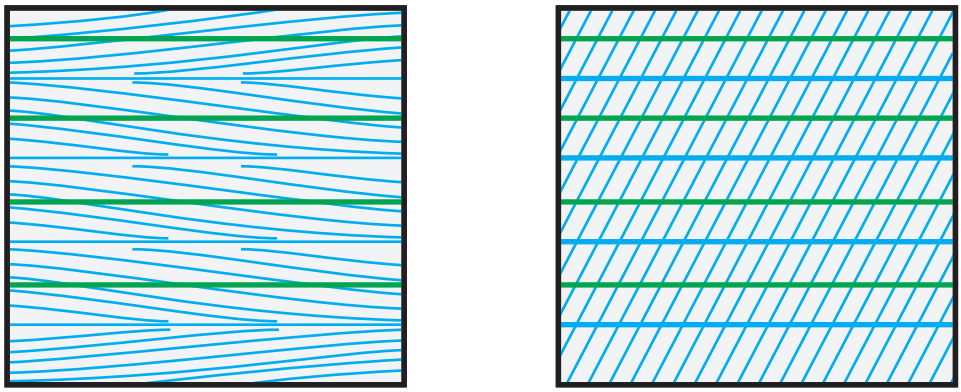

Figure 3.4.5. Two convex tori with the same dividing curves.

Another instance of the idea mentioned in the remark above, and extending the example above, is that one can frequently arrange for a subgraph of the surface to be part of the foliation on a convex surface (not in the example above, we could arrange for a curve of any slope to be part of the characteristic foliation of the torus). This will a key to much of our work in the following chapters. To state the result we need a definition. Say a

properly embedded graph G in a convex surface Σ with fixed dividing set is *non-isolating* if $G \cap \Gamma_\Sigma$ transversely and every component of $\Sigma \setminus G$ intersects Γ_Σ.

Theorem 3.4.5 (Honda 2000, [Hon00a]). *Let Σ be an embedded convex surface in a contact manifold (M, ξ). Let G be a properly embedded graph which is non-isolating. Then there is an isotopy of Σ, rel boundary, as in Theorem 3.4.1 to a surface Σ' so that G is contained in the characteristic foliation of Σ'.*

This theorem is frequently referred to as the *Legendrian realization principle* (or LeRP for short). A particularly useful immediate corollary of the above theorem is the following result.

Corollary 3.4.6 (Kanda 1997, [Kan97]). *Let C be a simple closed curve in a convex surface Σ that intersects the dividing curves transversely and non-trivially. Then Σ may be isotoped so that C is a closed leaf in the characteristic foliation.* □

Proof of Theorem 3.4.5. According to Theorem 3.4.1 we only need to construct a singular foliation on Σ that contains G and is also divided by Γ_Σ. To this end let Σ_0 be a component of $\Sigma \setminus (G \cup \Gamma_\Sigma)$. Assume Σ_0 is in Σ_+ so that all the elliptic points in a foliation must be positive (a similar argument applies if Σ_0 is in Σ_-).

The boundary of Σ_0 contains simple closed curves and arcs (the arcs form circles too, but piecewise-smooth circles). Each can either be in Γ_Σ, G or $\partial\Sigma$. To simplify the discussion we will add $\partial\Sigma$ to G, but to do this we will add a vertex between each pair of intersections of $\partial\Sigma$ and Γ_Σ that does not contain a point of $G \cap \partial\Sigma$. Along the boundary components coming from Γ_Σ we have the foliation flowing out. Along a circle boundary component coming from G, we let the foliation be the circle with the flow nearby flowing away from the circle. See Figure 3.4.6

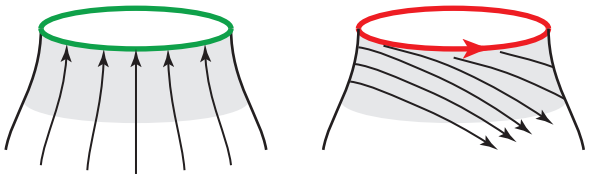

Figure 3.4.6. Building the singular foliation near a boundary component of Σ_0 containing only part of Γ_Σ, left, and G, The shaded grey area is the neighborhood of $\Gamma_\Sigma \cup G$.

Along a boundary component consisting of arcs all coming from G let the foliation have a positive elliptic points at the vertices and a positive hyperbolic point on the interior of each edge. Finally, consider a boundary component c that is made up of arcs from G and Γ_Σ. If an arc in G is adjacent to arcs in Γ_Σ at both endpoints, put a positive hyperbolic singularity in its interior. If there is a series of arcs from G then at each vertex put a positive elliptic point on the interior of an arc from G that has both endpoints on

other arcs from G put a positive hyperbolic point (with the arc being the stable manifolds of the singularity). For any other arc from G just leave as a non singular Legendrian arc.

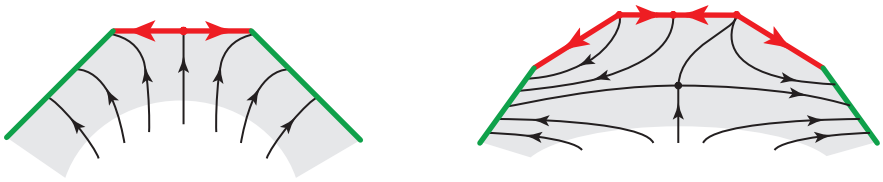

Figure 3.4.7. Building the singular foliation near arcs from G and Γ_G. The shaded grey area is the neighborhood of $\Gamma_\Sigma \cup G$.

See Figure 3.4.7. If you have any "elliptic vertices" use positive hyperbolic singularities to "shield" it from the inside of Σ_0 See Figure 3.4.7.

We have now defined the foliation in a tubular neighborhood A of $\Gamma_\Sigma \cup G$. Moreover, the flow is transverse to the boundary of $\Sigma_0' = \Sigma_0 \setminus A$, and along any boundary component containing a portion of Γ_Σ the flow is pointing out of the surface. Denote such boundary components by ∂_-. Along the other boundary components (which consist of circles in G) it is flowing in, we denote these ∂_+. The non-isolating condition implies that ∂_- is non empty.

It is well-known, see [**Mil65a**], that one may choose a Morse function on Σ_0 with ∂_- a non-critical level set mapping to 0, ∂_+ a non-critical level set mapping to 1, no minima, and only one maxima if ∂_+ is empty and no maxima if ∂_+ is not empty. The gradient flow of this height function gives a foliation of Σ_0' that extends the foliation on A. Note there is at most a single elliptic point that is a source. The other singularities are all hyperbolic and one may always arrange them to have positive divergence. Thus we have constructed a foliation on Σ_0 that has strictly positive divergence. Continuing on the other pieces of $\Sigma \setminus (G \cup \Gamma_\Sigma)$ will eventually yield a foliation on Σ that is divided by Γ_Σ and has G as a union of leaves. □

We now state a useful result that extends the standard Legendrian realization principle. It is sometimes called the *super Legendrian realization principle*.

Lemma 3.4.7. *Suppose γ is a connected curve on a convex surface Σ that is disjoint from the dividing curves Γ_Σ and any component of $\Sigma \setminus \gamma$ that does not intersect Γ_Σ has positive genus, then after a C^0 small isotopy of Σ (not through convex surfaces) one may realize γ as a Legendrian curve in the characteristic foliation of Σ.*

Proof. If γ is a non-separating curve on Σ then $\Sigma \setminus \gamma$ will have one component and since by Exercise 3.2.13 we know Γ_Σ is non-empty, we see that γ is non-isolating and hence by the standard Legendrian realization principle, Theorem 3.4.5, we can realize γ as part of the characteristic foliation of Σ after an isotopy.

Now if γ is separating, then $\Sigma \setminus \gamma$ has two components $\Sigma_1 \cup \Sigma_2$ (we are, of course, assuming that Σ is connected and the general case easily follows) and one of the components, say Σ_1, intersects Γ_Σ non-trivially. If Σ_2 also intersects Γ_Σ non-trivially, then we are done as above, so we assume that $\Gamma_\Sigma \cap \Sigma_2 = \emptyset$. We will C^0 isotop Σ, though non-convex surfaces, to a surface Σ' by an isotopy supported in Σ_2 so that $\Gamma_{\Sigma'}$ intersects both Σ_1 and Σ_2. We can then Legendrian realize γ as above.

To do this, we first choose a non-separating curve c in Σ_2 (we can do this since we assumed that Σ_2 had positive genus). We may apply the Legendrian realization principle to realize c as a circle of singularities in the characteristic foliation of Σ. We now study a neighborhood N of c. We can assume that N is contactomorphic to a neighborhood N' of the x-axis in $\mathbb{R}^3/\sim$, where $(x, y, z) \sim (x + 1, y, z)$, with the contact structure $\xi = \ker(dz - ydx)$ with $\Sigma \cap N$ mapping to the $A = xy -$ plane $\cap N'$. Now replace $A \subset \Sigma$ with A' shown in Figure 3.4.8. Denote the new surface Σ' and notice that Σ' may be constructed

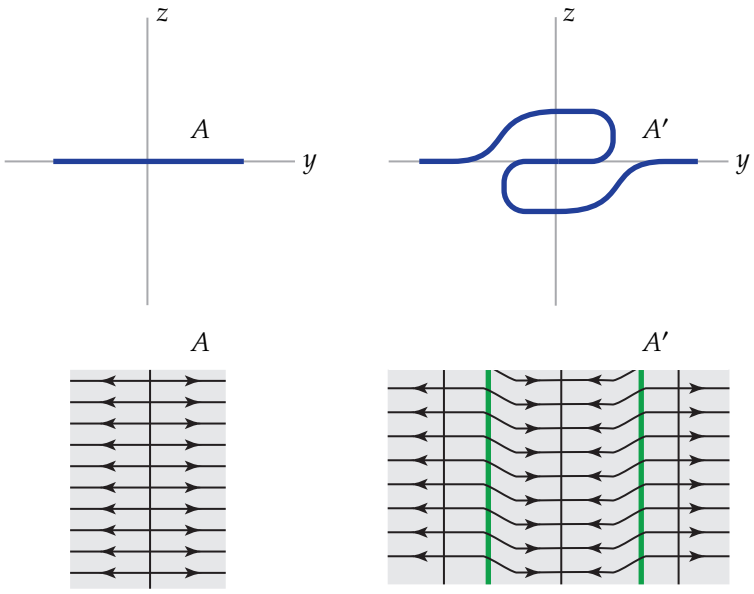

Figure 3.4.8. The annulus A is obtained from the arc in the upper left by crossing with the x-axis, while the annulus A' is obtained by crossing the arc in the upper right with the x-axis. The characteristic foliations on A and A' are shown in the bottom left and right, respectively.

in any open neighborhood of Σ. One may easily see that A' has three parallel circles of singularities and that there are two dividing curves in A'. Thus γ in Σ' is non-isolating and so can be Legendrian realized by Theorem 3.4.5 □

3.5. Legendrian curves on convex surfaces and the relative Euler characteristic.

Now that we know we can have closed curves in the characteristic foliation of a convex surface we wish to see how the contact planes twist along the surface. Recall if L is a Legendrian curve on a surface Σ then $\mathrm{tw}(L,\Sigma)$ denotes the twisting of the contact planes ξ along L measured with respect to the framing on L given by Σ. The following useful theorem is due to Kanda in [**Kan98**].

Theorem 3.5.1. *Let L be a Legendrian curve on a convex surface Σ, then*

$$\mathrm{tw}(L,\Sigma) = -\frac{1}{2}\#(L \cap \Gamma_\Sigma),$$

where # means the number of points in the set. If Σ is a Seifert surface, the the above formula computes the Thurston Bennequin number of L. Moreover, in this case, one has

$$r(L) = \chi(\Sigma_+) - \chi(\Sigma_-)$$

Proof. Let v be a contact vector field for Σ such that the characteristic hypersurface C of v satisfies $\Gamma_\Sigma = C \cap \Sigma$. The twisting of ξ relative to Σ is the same as the twisting of ξ relative to v (since v is transverse to Σ). We claim that ξ always "twists past" v in a left-handed manner. Indeed, let N be a small tubular neighborhood of L. So $N = L \times D^2$ and we can fix the product structure so that the tips of v trace out the curve $L\times\{p\}$ on ∂N where p is a point in ∂D^2. Now ξ can be represented by the 1-form $\beta + u\,dt$, where β is a 1-form on Σ and u is a function on Σ. Note in this set up v is $\frac{\partial}{\partial t}$. Notice that the contact planes intersect $\frac{\partial}{\partial t}$ only when $u = 0$. We will show that each such point contributes $-\frac{1}{2}$ difference in the framing of L coming from ξ relative to v (and hence Σ).

Let us say x is a point on Γ_Σ. Thus $u(x) = 0$. Orient L arbitrarily and let w_1 be vector field along L giving this orientation. Near x we can choose another vector field w_2 along L in $T\Sigma$ such that $\{w_1, w_2\}$ is an oriented basis for Σ and $\beta(w_2) = 1$ (here, of course, we choose the orientation on Σ to agree with the chosen orientation along L). Consider $\widetilde{w} = hw_2 + \frac{\partial}{\partial t}$ so that $\widetilde{w} \in \xi$. Near the dividing set, $\widetilde{w}$ gives the framing on N coming from ξ. Now

$$(\beta + u\,dt)(\widetilde{w}) = h + u = 0,$$

so $h = -u$. Thus at all intersection points of L with Γ_Σ the curve on ∂N coming from v and the curve coming form ξ intersect. Moreover, they intersect in a point with orientation negative (*i.e.* ξ twists past v in a left-handed way). Thus each intersection of L with Γ_Σ contributes a $-\frac{1}{2}$ to $\mathrm{tw}(L,\Sigma)$.

For the computation of $r(L)$ recall the rotation number can be computed from the singularities of the characteristic foliation from Equation (1.4.3). We may use the Giroux

Realization Principal to arrange that the singularities of Σ are all non-degenerate without moving L.

Exercise 3.5.2. Show that $\chi(\Sigma_\pm) = e_\pm - h_\pm$ where $e_\pm$ is the number of $\pm$ elliptic singularities in $\Sigma_\pm$ and $h_\pm$ is the number of $\pm$ hyperbolic singularities of $\Sigma_\pm$.

From this exercise and Equation (1.4.3) we immediately see the desired formula for $r(L)$. □

The rotation number can be thought of a relative Euler characteristic, so we now generalize the above discussion to compute the relative Euler class of a contact structure on any surface. Let ξ be any contact structure (or even simply a plane field) on a manifold M with boundary. Assume $\xi|_{\partial M}$ is trivializable. Given any section s of $\xi|_{\partial M}$ we can define the relative Euler class $e(\xi, s) \in H^2(M, \partial M; \mathbb{Z})$ as follows: Let s' be any extension of s to a section of ξ of all of M. By genericity we can assume the image of s' intersects the zero section of ξ transversely. Denote this intersection by Z. The *relative Euler class* $e(\xi, s)$ is the Poincaré dual of $[Z]$. It is standard to show the relative Euler class depends only on the isotopy (thought non-zero sections) class of s.

Lemma 3.5.3. *Let (M, ξ) be a contact manifold with convex boundary and s a section of $\xi|_{\partial M}$. Let Σ be an oriented connected convex surface properly embedded in M. If a tangent vector field to $\partial\Sigma \subset \partial M$, inducing the correct orientation on $\partial\Sigma$, agrees with s along $\partial\Sigma$ then*

$$e(\xi, s)([\Sigma]) = \chi(\Sigma_+) - \chi(\Sigma_-).$$

The proof of this lemma is almost identical to part of the proof of Theorem 3.5.1. The one difference (which is irrelevant) is that $\partial\Sigma$ might have more than one boundary component.

Suppose ∂M has a convex torus boundary component T. Fix a section of ξ along the other boundary components. By Theorem 3.4.1 we can change the characteristic foliation on T without affecting the contact structure (up to isotopy). Thus we arrange that the characteristic foliation on T is in standard form (Example 3.4.4) with ruling slope r. Now let s be the section of $\xi|_{\partial M}$ that was given on $\partial M \setminus T$, and on T it is tangent to the ruling curves.

Exercise 3.5.4. There are two seemingly different choices for this section along T, depending on the direction we traverse the ruling curves. Show these two choices are isotopic.

Exercise 3.5.5. Suppose we choose a different ruling slope r' and let s' be the corresponding section of ξ along ∂M. Show $e(\xi, s) = e(\xi, s')$.

3.6. Giroux's tightness criterion

Giroux has shown us how to tell if a vertically invariant neighborhood of a convex surface is tight.

Theorem 3.6.1 (Giroux 2001, [Gir01]). *Let Σ be a convex surface in (M, ξ). A vertically invariant neighborhood of Σ is tight if and only if $\Sigma \neq S^2$ and Γ_Σ contains no contractible curves or $\Sigma = S^2$ and Γ_Σ is connected.*

This theorem is known as the *Giroux criterion*.

Proof. If $\Sigma = S^2$ and Γ_Σ is disconnected then we can use Theorem 3.4.5 to Legendrian realize a circle disjoint from the dividing curves that bounds a disk D in S^2. By Theorem 3.5.1 we see that D is an overtwisted disk. If Γ_Σ is connected then the vertically invariant neighborhood of Σ can be identified with the neighborhood of the unit sphere in $\mathbb{R}^3$ with the standard tight contact structure, see Example 3.2.14. Thus the contact structure in the neighborhood is tight.

We now assume $\Sigma \neq S^2$ and there is a simple closed curve $\gamma \subset \Gamma_\Sigma$ that bounds a disk D in Σ. Let D' be a slightly larger disk containing D and not intersecting $\Gamma_\Sigma \setminus \gamma$. If $\Gamma_\Sigma \setminus \gamma \neq \emptyset$ then we may apply the Legendrian realization principle, Theorem 3.4.5, to isotop Σ inside a vertically invariant neighborhood to Σ' so that $\partial D'$ is a Legendrian curve in Σ'_ξ. By Theorem 3.5.1 we have that D' is an overtwisted disk.

If $\Gamma_\Sigma \setminus \gamma = \emptyset$ then since Σ has positive genus we may use the super Legendrian realization principle, Lemma 3.4.7, to realize $\partial D'$ as a Legendrian curve and we can again see that D' is an overtwisted disk.

We are left to see that a surface Σ of positive genus with Γ_Σ having no components bounding a disk has a tight neighborhood. To this end, let U be a vertically invariant neighborhood of Σ. Let $\widetilde{\Sigma} = \mathbb{R}^2$ be the universal cover of Σ. Since no component of Γ_Σ bounds a disk in Σ, Γ_Σ will lift a union of properly embedded lines and arcs in $\widetilde{\Sigma}$. Let V be the universal cover of U. This is simply the vertically invariant "neighborhood" of $\widetilde{\Sigma}$. We claim that the pull back contact structure on V is tight. To see this let G be a graph in Σ that realizes the 1-skeleton of Σ. Clearly G is non-isolating so we may use Theorem 3.4.1 to isotope Σ to Σ' so that G as a Legendrian graph in Σ' and U is a vertically invariant neighborhood of Σ' too. (We now rename Σ', Σ.) Let $\widetilde{G}$ be the graph lifted to $\widetilde{\Sigma}$. If there is an overtwisted disk in V then it lies over some disk D in $\widetilde{\Sigma}$ and we can assume the disk D is a union of regions in $\widetilde{\Sigma} \setminus \widetilde{G}$. Thus we have ∂D is Legendrian. The disk D is convex and its dividing curves are a union of arcs (no closed disk since $\Gamma_{\widetilde{\Sigma}}$ is a union of lines and intervals).

Exercise 3.6.2. Show there is a disk D' in S^2 whose intersection with the equator has the same configuration as Γ_D. See for example Figure 3.6.9.

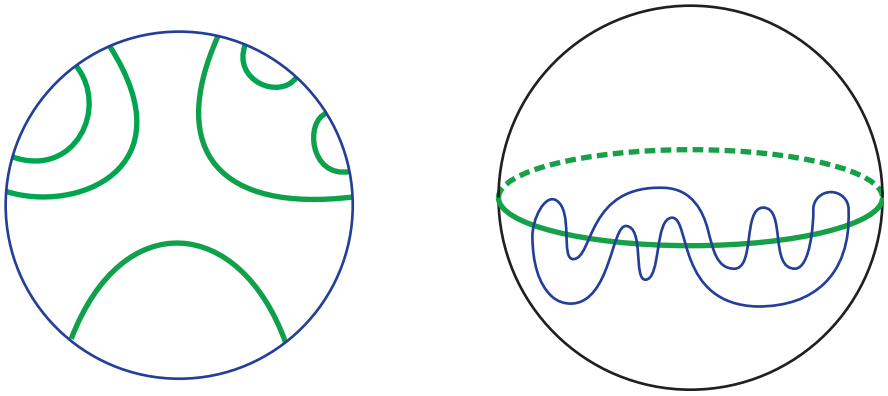

Figure 3.6.9. The annulus A is obtained from the arc in the upper left by crossing with the x-axis, while the annulus A' is obtained by crossing the arc in the upper right with the x-axis. The characteristic foliations on A and A' are shown in the bottom left and right, respectively.

Of course the unit S^2 in the standard tight contact structure on $\mathbb{R}^3$ has the equator as its dividing set so $D' \cap \Gamma_{S^2}$ is the same as $D \cap \Gamma_{\widetilde{\Sigma}}$. Now on S^2 we can draw the foliation $\mathcal{F}$ that on D' agrees with the characteristic foliation on D and on $S^2 \setminus D'$ is the foliation constructed in the proof of Theorem 3.4.5. Since this foliation is divided by Γ_{S^2} we can use Theorem 3.4.5 to realize it in a vertically invariant neighborhood $N = S^2 \times \mathbb{R}$ of S^2 in the standard tight contact structure on $\mathbb{R}^3$. Thus the contact structure on N is tight. Now the contact structure on $D' \times \mathbb{R}$ and $D \times \mathbb{R}$ are contactomorphic, but this contradicts the fact that in $D \times \mathbb{R}$ we assumed there was an overtwisted disk. □

3.7. Bennequin type inequalities

We are now ready to demonstrate the first connection between topology and tight contact structures.

Theorem 3.7.1. *Let (M, ξ) be a tight contact 3-manifold. Any embedded closed surface $\Sigma \neq S^2$ in M satisfies*

$$|e(\xi)([\Sigma])| \leq -\chi(\Sigma),$$

where $e(\xi)$ is the Euler class of the contact structure. If $\Sigma = S^2$ then

$$e(\xi)([\Sigma]) = 0.$$

Remark 3.7.2. There is a similar inequality for the Euler class of a taut foliation (actually one just needs a Reebless foliation), see [**ET98**, **Thu86**].

Remark 3.7.3. The inequality in this theorem implies that only finitely many homology classes in $H^2(M; \mathbb{Z})$ can be realized as the Euler class of a tight contact structure,

in marked contrast to the situation for overtwisted contact structures where any (even) homology class is the Euler class of an overtwisted contact structure.

Exercise 3.7.4. Prove the first claim in the remark.
Hint: Recall that any element in $H_2(M, \mathbb{Z})$ can be realized by an embedded surface. Pick a basis of $H_2(M, \mathbb{Z})$, realize them by surfaces and then think about what the inequality says.

Proof. Given $\Sigma \neq S^2$ in M use Theorem 3.3.1 to make it convex. Since ξ is tight Γ_Σ is a union of S^1's that do not bound disks in Σ. As usual write $\Sigma \setminus \Gamma_\Sigma = \Sigma_+ \cup \Sigma_-$. Clearly

$$\chi(\Sigma) = \chi(\Sigma_+) + \chi(\Sigma_-)$$

since $\chi(\Gamma_\Sigma) = 0$. As in Exercise 1.6.4 one may easily check that

$$e(\xi)(\Sigma) = \chi(\Sigma_+) - \chi(\Sigma_-).$$

Subtracting the first equation form the second yields

$$e(\xi)(\Sigma) - \chi(\Sigma) = -2\chi(\Sigma_-) \geq 0.$$

Thus $-e(\xi)(\Sigma) \leq -\chi(\Sigma)$. By adding the equations together one may similarly show $e(\xi)(\Sigma) \leq -\chi(\Sigma)$, establishing the desired inequality.

If $\Sigma = S^2$ we know $\Sigma \setminus \Gamma_\Sigma$ is the disjoint union of two disks thus $e(\xi)(\Sigma) = 0$. □

Now we state the famous Bennequin inequality.

Theorem 3.7.5 (Bennequin 1983, [Ben83]; Eliashberg 1992, [Eli92])**.** *Let (M, ξ) be a tight contact manifold and K a knot in M bounding the embedded surface Σ. If K is a transverse knot then*

$$\mathrm{sl}(K) \leq -\chi(\Sigma).$$

If K is a Legendrian knot then

$$\mathrm{tb}(K) + |r(K)| \leq -\chi(\Sigma).$$

This theorem was proven for the standard tight contact structure on S^3 and $\mathbb{R}^3$ by Bennequin in [Ben83] and proven for all tight contact structures by Eliashberg in [Eli92]. In fact, it is easy to see that a Bennequin type inequality characterizes whether or not a contact structure is tight.

Exercise 3.7.6. Show that a contact manifold (M, ξ) is overtwisted if and only if there is a Legendrian unknot with $\mathrm{tb} = 0$ if and only if there is a transverse unknot with $\mathrm{sl} = 0$.

Exercise 3.7.7. Show that a contact manifold (M, ξ) is tight if and only if there is some bound on the Thurston-Bennequin invariant of a knot in a fixed knot type if and only if the Bennequin bound holds for all knots.

Proof. Assume K be a Legendrian knot. We will prove $\mathrm{tb}(K)+r(K) \leq -\chi(\Sigma)$ but a similar argument establishes $\mathrm{tb}(K) - r(K) \leq -\chi(\Sigma)$. We may assume that $\mathrm{tb}(K) \leq 0$. Indeed we may negatively stabilize K enough times so that $\mathrm{tb}(K) \leq 0$ (recall each stabilization decreases $\mathrm{tb}(K)$ by 1). Since we are using negative stabilizations $tb(K) + r(K)$ is unchanged. Thus proving the inequality for the stabilized knot will imply the inequality for the original knot.

Since $\mathrm{tb}(K) \leq 0$ Theorem 3.3.1 says we can isotop Σ so that it is convex. By Theorem 3.5.1 we know $r(K) = \chi(\Sigma_+) - \chi(\Sigma_-)$. We claim that

$$\mathrm{tb}(K) + \chi(\Sigma_+) + \chi(\Sigma_-) = \chi(\Sigma).$$

To see this note that by Theorem 3.5.1 there are precisely $tb(K)$ arcs in Γ_Σ, denote their union Γ_a, and so $\chi(\Sigma \setminus \Gamma_a) = \chi(\Sigma) - tb(K)$. But we also know that $\chi(\Sigma \setminus \Gamma_a) = \chi(\Sigma \setminus \Gamma_\Sigma) = \chi(\Sigma_+ \cup \Sigma_-) = \chi(\Sigma_+) + \chi(\Sigma_-)$, since all the components of Γ_Σ not in Γ_a are circles. Thus we have established the above equality.

The Giroux criterion, Theorem 3.6.1, says there are no disk components of $\Sigma \setminus \Gamma_\Sigma$ on the interior of Σ. So any disks in $\Sigma \setminus \Gamma_\Sigma$ must come from an arc in Γ_Σ separating a disk from Σ (unless Σ is a disk). Thus there are at most $-\mathrm{tb}(K)$ disk components in $\Sigma \setminus \Gamma_\Sigma$, and hence there are at most $-\mathrm{tb}(K)$ disk components in Σ_+ (note that this still holds even if Σ is a disk). So $\chi(\Sigma_+)$ equals the number of disk components plus the Euler characteristic of the other components. The Euler characteristic of these other components in non-positive. Thus we have shown

$$\mathrm{tb}(K) \leq -\chi(\Sigma_+).$$

Now we have

$$\begin{aligned}
\mathrm{tb}(K) + r(K) &\leq \mathrm{tb}(K) + r(K) - 2\,\mathrm{tb}(K) - 2\chi(\Sigma_+) \\
&= -\mathrm{tb}(K) + r(K) - 2\chi(\Sigma_+) \\
&= -\mathrm{tb}(K) + \chi(\Sigma_+) - \chi(\Sigma_-) - 2\chi(\Sigma_+) \\
&= -\mathrm{tb}(K) - \chi(\Sigma_+) - \chi(\Sigma_-) = -\chi(\Sigma).
\end{aligned}$$

To prove the inequality for transverse knots we use Lemma 1.4.31 which says if K is a transverse knot then there is a Legendrian knot L such that its positive transverse push off L_+ is transversely isotopic to K. From earlier we know $\mathrm{sl}(K) = \mathrm{tb}(L) - r(L)$. Thus we get $\mathrm{sl}(K) \leq -\chi(\Sigma)$ from the previously established inequality for Legendrian knots □

NEED TO PROVE THE NEXT TWO THEOREMS. Maybe need to put them in a later chapter. Probably need bypasses for the second one... Or do we even need these theorems? They are nice but maybe not essential?

Theorem 3.7.8. *Let ξ_1 and ξ_2 be two tight vertically invariant contact structures on $\Sigma \times \mathbb{R}$. The contact structures are contactomorphic if and only if there is a diffeomorphism $\phi : \Sigma \to \Sigma$ taking the dividing curves Γ_{ξ_1} induced on $\Sigma = \Sigma \times \{0\}$ by ξ_1 to the dividing curves Γ_{ξ_2} induced by ξ_2.*

Theorem 3.7.9. *Let ξ_1 and ξ_2 be two overtwisted vertically invariant contact structures on $\Sigma \times \mathbb{R}$. The contact structures are contactomorphic if and only if*

$$\chi(\Sigma^1_+) - \chi(\Sigma^1_-) = \pm(\chi(\Sigma^2_+) - \chi(\Sigma^2_-)),$$

where $\Sigma \setminus \Gamma_{\xi_i} = \Sigma^i_+ \coprod \Sigma^i_-$.

3.8. Pairs of convex surfaces

Giroux flexibility is one of the key reasons that convex surfaces are so powerful in studying contact structures. Another key feature of convex surfaces is that you can "transfer information" from one convex surface to another if they agree along a Legendrian knot.

Lemma 3.8.1 (Kanda 1997, [Kan97]; Honda 2000, [Hon00a])**.** *Suppose that Σ and Σ' are two convex surfaces and $\partial\Sigma'$ is Legendrian and contained in Σ. Then the dividing curves of Σ and Σ' interlace along $\partial\Sigma'$. More specifically, between any two adjacent points of $\Gamma_\Sigma \cap \partial\Sigma'$ there is a point of $\Gamma_{\Sigma'} \cap \partial\Sigma'$ and vice versa. See Figure 3.8.10.*

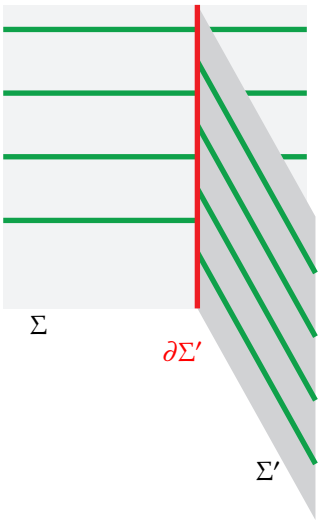

Figure 3.8.10. The interlacing of dividing curves for convex surfaces Σ and Σ' that intersect along a Legendrian knot $\partial\Sigma'$.

Proof. We start by building a standard model for $\partial\Sigma'$. Consider $\mathbb{R}^3/\sim$, where $(x, y, z) \sim (x, y, z + 1)$, with the contact structure $\xi = \ker(\sin(2n\pi z)\, dx + \cos(2n\pi z)\, dy$. Let $\Sigma = \{(x, y, z) : x = 0\}$ and $\Sigma' = \{(x, y, z) : y = 0, x \geq 0\}$. Note both these surface are convex

and the boundary of Σ' is a Legendrian curve in Σ. In Figure 3.8.10 we see the situation for $n = 2$. The choice of n in this model is clearly determined by $\mathrm{tw}(\partial\Sigma', \Sigma')$.

Exercise 3.8.2. Show that the situation described in Lemma 3.8.1 can always be modeled as described above.

One may easily see in the model that the conclusion of the lemma holds. □

Not only can we compare dividing curves using the lemma above, we can use the model built in the proof to "round the edge" and get a new convex surface.

Lemma 3.8.3 (Honda 2000, [**Hon00a**]). *Suppose that Σ and Σ' are convex surfaces and $\partial\Sigma' = \partial\Sigma$ is Legendrian. We may isotope Σ and Σ' in an arbitrarily small neighborhood of $\partial\Sigma$ so that the union of the surfaces is a smooth surface. Moreover, the surface will be convex with dividing curves shown in Figure 3.8.11.*

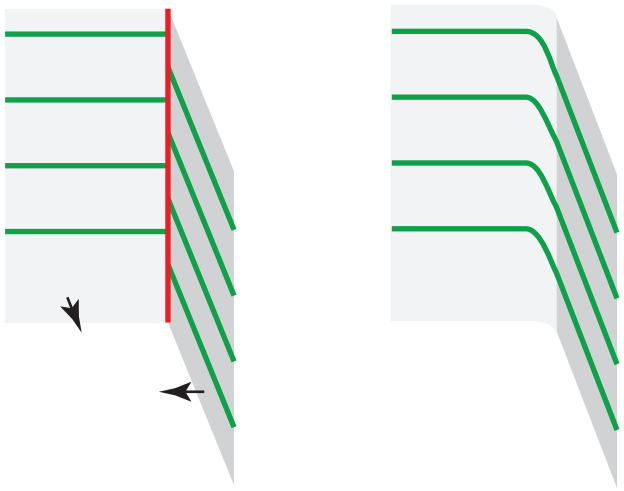

Figure 3.8.11. On the left are two convex surfaces that intersect along a Legendrian knot in their boundary. On the right, the edge between the surfaces has been rounded forming a new convex surface. The arrows on the left show the co-orientation on the surfaces.

Proof. Given Σ and Σ' in the model constructed in the previous proof, we define a new surface Σ'' obtained by "rounding the edge". Specifically, Σ'' is formed from $\Sigma \cap \Sigma'$ by replacing $\Sigma \cap \Sigma'$ intersect a small neighborhood N of $\partial\Sigma$ (thought of as the z-axis) with the intersection of N with $\{(x, y, z) : (x - \delta)^2 + (y - \delta)^2 = \delta^2\}$ For a suitably chosen δ. The surface Σ'' will be a smooth surface (actually just C^1, but it can then be smoothed by a C^1 small isotopy which of course does not change the characteristic foliation) with dividing curve as shown in Figure 3.8.11. □

Chapter 4

Continued fractions and the Farey graph

In later chapters, it will be essential to keep track of embedded curves on a torus. When we mention curves on a torus, we mean maps from the circle S^1 to the torus T^2. In this chapter, we will extensively study curves on tori. In the first section, we discuss how, after choosing a basis for the first homology of a torus, to represent any embedded curve as an ordered pair of relatively prime numbers and as elements of the rational numbers together with infinity. We also discuss how to compute the intersection number of curves in terms of these representations.

In Section 4.2 we introduce the Farey graph. This is a convenient way to describe all embedded curves on the torus and to see various interactions between them. For example, curves correspond to vertices of the Farey graph, and two curves form a basis for the first homology of the torus if and only if they are connected by an edge in the Farey graph.

We discuss continued fraction expansions of rational numbers in the next section. We will see that the continued fraction of a rational number is closely connected to where the number sits in the Farey graph. We can also use the continued fraction of a rational number to find other curves on the torus that form a basis with a given curve. We expand on the relation between continued fractions and the Farey graph in Section 4.4. More specifically, we show that for a rational number r less than -1, its continued fraction expansion describes a minimal path in the Farey graph from 0, anti-clockwise, to r. Along the way, we define the notion of a continued fraction block in the Farey graph. These are the basic building blocks in the minimal path mentioned above and will be central to many of our classification results.

In Section 4.5, we give estimates on the intersection number between two curves in terms of their representation as rational numbers. In the last section, we discuss the relation between continued fractions and the integer lattice in $\mathbb{R}^2$.

For much more on the Farey graph and continued fractions, we highly recommend Hatcher's excellent book [**Hat22**].

4.1. Curves on the torus

Before discussing a systematic way to describe embedded curves on a torus, we first make a few simple observations that will be useful later. Notice that given a curve γ on T^2 then it represents a homology class $[\gamma]$ in $H_1(T^2)$. We will study curves through their homology class (and sometimes abuse notation referring to γ and $[\gamma]$ as both the curve and its homology class).

Exercise 4.1.1. Given two embedded curves γ_1 and γ_2, then $[\gamma_1]$ and $[\gamma_2]$ form a basis for $H_1(T^2)$ if and only if γ_1 and γ_2 can be isotoped so that they intersect in exactly one point.

Exercise 4.1.2. A curve γ on T^2 is embedded if and only if $[\gamma]$ is part of a basis for $H_1(T^2)$.

Exercise 4.1.3. Any automorphism of $H_1(T^2)$ is induced by a unique, up to isotopy, diffeomorphism of T^2.

Since $\pi_1(T^2) = H_1(T^2) \cong \mathbb{Z}^2$ the homotopy class of a curve on the torus is the same as its homology class. To represent curves on the torus we will choose a basis for $H_1(T^2)$ and denote it by λ and μ.

Exercise 4.1.4. Show that λ and μ can be represented by embedded curves on T^2.

Now given any curve γ on T^2 its homology class can be written

$$[\gamma] = a\lambda + b\mu.$$

We will denote this by $\begin{pmatrix} a \\ b \end{pmatrix}$. So with the basis chosen, homology classes of curves are in one-to-one correspondence with ordered pairs.

Exercise 4.1.5. Show that $\begin{pmatrix} a \\ b \end{pmatrix}$ can be represented by an embedded curve if and only if a and b are relatively prime.

Summarizing, given an embedded curve γ we can represent it by the relatively prime ordered pair $\begin{pmatrix} a \\ b \end{pmatrix}$, and hence the pair is uniquely determined by $b/a \in \mathbb{Q}^*$, where $\mathbb{Q}^*$ is the extended rational numbers $\mathbb{Q} \cup \{\infty\}$.

Once we choose an orientation on T^2 then we have the intersection pairing

$$H_1(T^2) \times H_1(T^2) \to \mathbb{Z}$$

defined by taking the algebraic intersection number between two curves representing the two homology classes. That is given curves γ_1 and γ_2 on the torus we can compute their intersection number $I(\gamma_1, \gamma_2) = \gamma_1 \cdot \gamma_2$, see [**GP10**], which roughly counts the number of intersection points between the curves with a sign determined by the orientation on the curves and the orientation on T^2. It is well-known that this defines a skew-symmetric, bi-linear pairing on $H_1(T^2)$ (that is dual to the cup product pairing).

When choosing the basis λ, μ for $H_1(T^2)$ we will always choose them so that

$$\lambda \cdot \mu = -\mu \cdot \lambda = 1,$$

and clearly we have $\lambda \cdot \lambda = 0 = \mu \cdot \mu$. Thus for two curves γ_1 and γ_2 represented by $\begin{pmatrix} a \\ b \end{pmatrix}$ and $\begin{pmatrix} c \\ d \end{pmatrix}$, respectively, we have

$$[\gamma_1] \cdot [\gamma_2] = ad - bc.$$

Exercise 4.1.6. Show that if γ_1 and γ_2 are embedded curves then the minimal number of intersections between is $|ad - bc|$.

Since γ_1 and γ_2 can also be represented by b/a and d/c we will also use the notation

$$b/a \cdot d/c = ad - bc.$$

From Exercise 4.1.1 we see that two numbers b/a and c/d correspond to curves that form a basis for $H_1(T^2)$ if and only if $b/a \cdot d/c = \pm 1$.

4.2. The Farey graph

Warning: *There are different conventions for the construction of the Farey graph. They all contain the same information and are related by a simple homeomorphism of the graph. So some of the discussion below might appear different than in some of the published literature.*

The Farey graph is a convenient way to understand curves on a torus and relations between curves. To define the Farey graph, let $\mathbb{D}$ be the unit disk in $\mathbb{R}^2$. We will think of this as the hyperbolic plane with the circle at ∞ adjoined. This interpretation is not so important. The main thing is when we say two points on the boundary of $\mathbb{D}$ are connected by a geodesic, we mean they are connected by a segment of a circle (or line) that is orthogonal to $\partial\mathbb{D}$. With this understood, we can ignore the fact that $\mathbb{D}$ is the hyperbolic plane.

Label the point $(1, 0)$ on $\partial\mathbb{D}$ by $0 = \frac{0}{1}$, the point $(0, \pm 1)$ by $\pm\infty = \frac{\pm 1}{0}$, and joint them by a geodesic. If two points on $\partial\mathbb{D}$ with non-negative x-coordinate have been labeled by

$\frac{p}{q}$, $\frac{p'}{q'}$ and are joined by an edge, then label the point on $\partial\mathbb{D}$ halfway between them (with non-negative x-coordinate) by $\frac{p+p'}{q+q'}$. Then connect this point to $\frac{p}{q}$ by a geodesic and also connect this point to $\frac{p'}{q'}$ by a geodesic. Below we will see that if we continue this process then all positive fractions will appear as labels on vertices in the graph. Now repeat this process for the points on $\partial\mathbb{D}$ with non-positive x-coordinate except start with $\infty = \frac{-1}{0}$. See Figure 4.2.1.

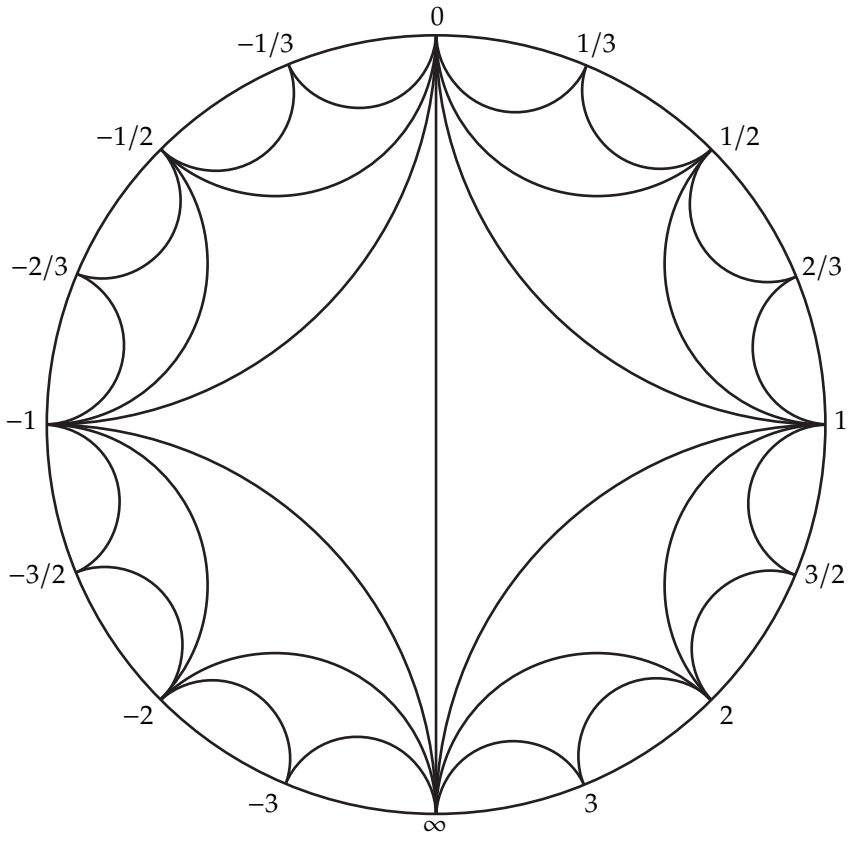

Figure 4.2.1. A finite portion of the Farey graph.

Let us examine the construction of the Farey graph more closely to make clear its relation to curves on a torus and several of its basic properties. First, recall that an element of $\mathbb{Q}^*$ corresponds to an embedded curve in T^2. In particular, $p/q \in \mathbb{Q}^*$ corresponds to the curve γ in the homology class $q\lambda + p\mu$ which we represent by the ordered pair $\begin{pmatrix} q \\ p \end{pmatrix}$. Thus when given the labels $\frac{p}{q}$ and $\frac{p'}{q'}$ as in the construction above, then $\frac{p+p'}{q+q'}$ corresponds to the homology class in $H_1(T^2)$ that is the sum of the homology classes corresponding to the curves given by the first two fractions. We denote $\frac{p+p'}{q+q'}$ by $\frac{p}{q} \oplus \frac{p'}{q'}$ and call this the

Farey sum of $\frac{p}{q}$ and $\frac{p'}{q'}$, this is also known as the *mediant* of the fractions. We will also use the notation $\frac{p}{q} \oplus k\frac{p'}{q'}$ to mean $\frac{p+kp'}{q+kq'}$, that is the result of Farey summing $\frac{p'}{q'}$ to $\frac{p}{q}$, k times. From our discussion above, thinking of fractions as curves on T^2, the Farey sum is just the curve representing the sum of their homology classes. We will now prove:

(1) If the pairs of integers p, q and p', q' are relatively prime, then so is $p + p', q + q'$. That is the Farey sum of fractions in lowest common terms is a fraction in lowest common terms, and all the points in the Farey graph correspond to embedded curves in the torus.

(2) If two vertices in the Farey graph are connected by an edge, then their labels correspond to curves on T^2 that form an integral basis for $H_1(T^2)$.

We prove these two facts at the same time and inductively. We start with the positive rational numbers (that is labels on the Farey graph with positive x-coordinate). The start of the construction only has the points $0 = \frac{0}{1}$ and $\infty = \frac{1}{0}$ labeled. The next point to be labeled is the point $(1, 0)$ and it is labeled $\frac{1}{1} = \frac{1}{0} \oplus \frac{0}{1}$. Now clearly in $H_1(T^2)$ the curve $\frac{1}{1}$ is the sum of the other two curves and since the sum of two basis elements is another basis element we see from Exercises 4.1.2 and 4.1.5 that $\frac{1}{1}$ corresponds to an embedded curve and hence its fraction consists of relatively prime integers. Moreover, the sum of two basis elements forms a basis with either of the two summands. Thus both items claimed above are true for $\frac{1}{0} \oplus \frac{0}{1}$. One may now easily see that if we inductively assume that $\frac{p}{q}$ and $\frac{p'}{q'}$ satisfy the items above and are connected by an edge then their Farey sum does as well. The argument for negative rationals is similar.

We next notice that

(3) The numbers appear in order as one moves clockwise from $-\infty$ to ∞. (Here of course $-\infty = \infty$.)

To see this we again start with the positive rationals. If the statement is true for $\frac{p}{q}$ and $\frac{p'}{q'}$, say $\frac{p}{q} < \frac{p'}{q'}$, then $pq' < qp'$. Now consider $\frac{p+p'}{q+q'}$. We clearly see that $(q + q')p < (p + p')q$ and hence $\frac{p}{q} < \frac{p+p'}{q+q'}$. We similarly see that $\frac{p+p'}{q+q'} < \frac{p'}{q'}$. Thus we inductively see that the claim holds. One may argue similarly for the negative rationals.

We also note that

(4) All numbers in the extended rationals $\mathbb{Q}^*$ appear as labels in the Farey graph.

There are several ways to see that this is true, but we will give a simple proof in the next section. Finally, improving on Item (2) above we have the following observation.

Lemma 4.2.1. *Two points in $\mathbb{Q}^*$ correspond to an integral basis of $\mathbb{Z}^2 = H_1(T^2)$ if and only if there is an edge in the Farey graph connecting them.*

Exercise 4.2.2. Proof this lemma.
Hint: If $\begin{pmatrix} q \\ p \end{pmatrix}$ and $\begin{pmatrix} s \\ r \end{pmatrix}$ form an integral basis for $\mathbb{Z}^2$ then the matrix with columns given by these vectors has determinant ± 1. Show you can just consider the case when all the terms are non-negative. Consider the case when either p or r is 0, then consider the case when $p = r \neq 0$ and argue that there is an edge in the Farey graph between the corresponding rational numbers. Finally if $p \neq r$ and neither is 0, then form a new matrix by subtracting the column with smaller second entry from the other one. Note that this matrix will have the same determinant and if there is an edge between the rational numbers corresponding to these two columns then there will be an edge for the original two columns. Continue this process until you have reduced to a previously studied case.

Exercise 4.2.3. Suppose that $\frac{p}{q}$ and $\frac{r}{s}$ are connected by an edge in the Farey graph. Then show that $\frac{p}{q} \cdot \frac{r}{s} = -1$ if and only if $\frac{p}{q}$ is clockwise of $\frac{r}{s}$. (Of course, on $\partial\mathbb{D}^2$ every point is clockwise of every other point, but here we mean that if you look at the shorter arc that the points divide $\mathbb{D}^2$ into, then along that segment $\frac{p}{q}$ is clockwise of $\frac{r}{s}$.) **Note.** If either $\frac{p}{q}$ and $\frac{r}{s}$ is 0 or ∞ then one must use the convention that $\infty = \frac{-1}{0}$ and $0 = \frac{0}{-1}$ and for negative fractions the denominator is negative. Of course, the statement has no meaning if one of the fractions is 0 and the other is ∞.

We will denote by (a, b) the vertices in the Farey graph that are strictly clockwise of the vertex labeled a and strictly anticlockwise of the vertex labeled b. Notice that if $a < b$ then this notation agrees with the standard notation for intervals in the real line, but if $a > b$ then the interval will contain numbers larger than a, less than b, and ∞. The interval $[a, b]$ will denote the same region, except it will contain the endpoints a and b. We similarly will use the notation $(a, b]$ and $[a, b)$.

At various times it will be convenient to have another view of the Farey graph. Recall there is an isometry of the hyperbolic metric on $\mathbb{D}^2$ to the hyperbolic metric on upper half space in $\mathbb{R}^2$. On the circle at infinity, this will be stereographic projection from $S^1 - \{\infty\}$ to $\mathbb{R}^1$. So we can think of the vertices of the Farey graph as being in $\mathbb{R}$ and the edges of the graph as being in the upper half-plane. See Figure 4.2.2. We will use both models for the Farey graph depending on context.

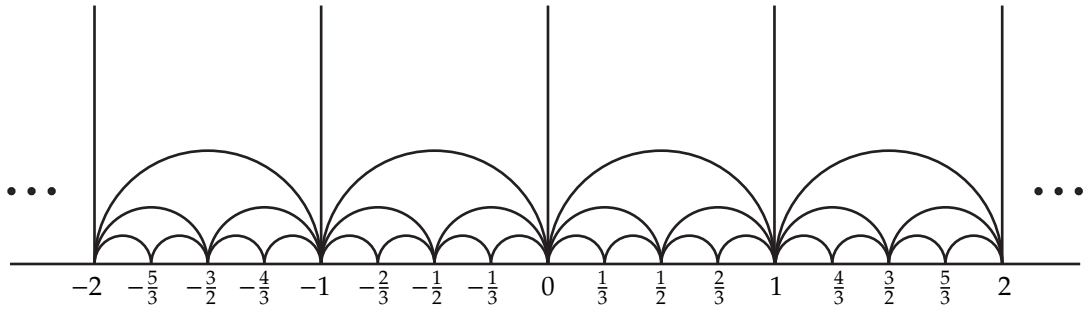

Figure 4.2.2. An alternate view of a finite portion of the Farey graph.

4.3. Continued fractions

A rational number r may be represented as a continued fraction

$$r = a_0 - \cfrac{1}{a_1 - \cfrac{1}{a_2 - \cfrac{1}{\ldots - \cfrac{1}{a_n}}}}$$

with $a_0 \in \mathbb{Z}$ and the other $a_i \leq -2$. We will denote this by $r = [a_0; a_1, \ldots, a_n]$.

In later chapters, we will frequently consider fractions r of the form $r < -1$, and in that case in their continued fraction we can take all the $a_i \leq -2$, and to emphasize this we will drop the semicolon and use $[a_0, a_1, \ldots, a_n]$.

It is not hard to find continued fractions. Below we add a few examples and exercises for completeness.

Example 4.3.1. Consider $-21/8$. We note that the greatest integer less than $-21/8$ is $\lfloor -21/8 \rfloor = -3$ so we can write $-21/8 = -3 - 1/a$. Solving for a we get $a = -8/3$ and $\lfloor -8/3 \rfloor = -3$. So $-8/3 = -3 - 1/b$. Solving for be we find $b = -3$. From this we see that $-21/8 = [-3, -3, -3]$.

Arguing as above we easily see $19/2 = [9; -2]$.

Exercise 4.3.2. Compute the continued fraction expansion of $-\frac{p^2}{p^2-p+1}$ where $p > 1$.

Exercise 4.3.3. Compute the continued fraction expansion of $-\frac{pqn-1}{(pq-1)n-1}$ where $n \geq 1$ and $1 < p < q$ are relatively prime integers.

Exercise 4.3.4. Give an algorithm to compute the continued fraction expansion of any $r \in \mathbb{Q}^*$.

If we know that $r = \frac{p}{q} = [a_0; a_1, \ldots, a_n]$ then we define

$$r^a = [a_0; a_1, \ldots, a_{n-1}],$$

with the convention that if $n = 0$ then $r^a = \infty$; we also define

$$r^c = [a_0; a_1, \ldots, a_n + 1]$$

if r is not a positive integer and equals ∞ if it is a positive integer. In the next lemma we explain how to describe r^c and r^a via the Farey graph. See Figure 4.3.3.

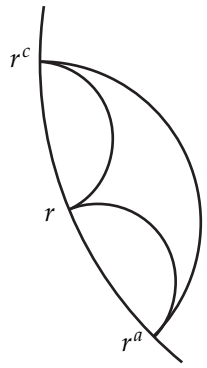

Figure 4.3.3. The rational numbers r^a and r^c.

Lemma 4.3.5. *Suppose that $r = \frac{p}{q}$ is not a non-negative integer. The number r^a is the largest rational number bigger than r with an edge to r in the Farey graph and r^c is the smallest rational number less than r with an edge to r in the Farey graph. Moreover, there is an edge in the Farey graph between r^a and r^c, and r is the Farey sum of r^a and r^c, that is if $r^a = \frac{p^a}{q^a}$ and $r^c = \frac{p^c}{q^c}$ then*

$$r = \frac{p^a + p^c}{q^a + q^c}.$$

If r is a positive integer then $r^c = \infty$ and $r^a = r - 1$.

In preparation for the proof of this lemma, we start with a couple of exercises, but first given $r = [a_0; a_1, \ldots, a_n]$ we set

$$\frac{p_k}{q_k} = [a_0; a_1, \ldots, a_k]$$

for $k = 0, \ldots, n$ and $p_{-1} = 1, p_{-2} = 0, q_{-1} = 0$, and $q_{-2} = 1$. In particular $\frac{p_n}{q_n} = r$

Exercise 4.3.6. Inductively show that

$$p_{k+1} = a_{k+1}p_k - p_{k-1} \text{ and } q_{k+1} = a_{k+1}q_k - q_{k-1}.$$

Exercise 4.3.7. If $\frac{p}{q}$ and $\frac{p'}{q'}$ satisfy $\frac{p}{q} \cdot \frac{p'}{q'} = p'q - q'p = \pm 1$, then $\frac{pr-q}{p} \cdot \frac{p'r-q'}{p'} = \pm 1$

Proof of Lemma 4.3.5. We assume for now that $\frac{p_n}{q_n} = [a_0, \dots a_n]$ is negative. Using the notation established after the statement of the lemma we see that

$$\frac{p_0}{q_0} = \frac{a_0}{1} \text{ and } \frac{p_1}{q_1} = \frac{a_0a_1 - 1}{a_1}$$

and so

$$\frac{p_0}{q_0} \cdot \frac{p_1}{q_1} = q_0p_1 - p_0q_1 = -1.$$

From Exercise 4.3.6 we clearly see that

$$\frac{p_{k+1}}{q_{k+1}} \cdot \frac{p_k}{q_k} = p_k(a_{k+1}q_k - q_{k-1}) - q_k(a_{k+1}p_k - p_{k-1}) = \frac{p_k}{q_k} \cdot \frac{p_{k-1}}{q_{k-1}}$$

and hence we can conclude that $\frac{p}{q} \cdot \frac{p_{n-1}}{q_{n-1}} = -1$ and hence from Exercise 4.2.3 we see that $\frac{p_{n-1}}{q_{n-1}}$ is anticlockwise of $\frac{p}{q}$ and there is an edge in the Farey graph between them.

Now notice that $\frac{a_n}{1} \cdot \frac{a_n+1}{1} = 1$ and thus by Exercise 4.3.7 we can inductively see that if we set $\frac{p^c}{q^c} = [a_0, a_1, \dots, a_n + 1]$ then $\frac{p}{q} \cdot \frac{p^c}{q^c} = 1$. Thus Exercise 4.2.3 tells us that $\frac{p^c}{q^c}$ is clockwise of $\frac{p}{q}$ and there is an edge in the Farey graph between them.

Finally since $[a_0, \dots, a_{n-1}]$ is obtained from $[a_0, \dots, a_{n-1}, a_n + 1]$ by dropping the last term, we see from the first paragraph of the proof that $\frac{p^c}{q^c} \cdot \frac{p_{n-1}}{q_{n-1}} = -1$. Thus $\frac{p^c}{q^c}$ is clockwise of $\frac{p_{n-1}}{q_{n-1}}$ and there is an edge in the Farey graph between them. Setting $\frac{p^a}{q^a} = \frac{p_{n-1}}{q_{n-1}}$ and combining the above results says that one sees the numbers $\frac{p^a}{q^a}$, $\frac{p}{q}$, and $\frac{p^c}{q^c}$ moving clockwise on the Farey graph and there is an edge in the Farey graph between any pair of the numbers.

Exercise 4.3.8. Show that the absolute value of the numerators (and the denominators) of $\frac{p^a}{q^a}$ and $\frac{p^c}{q^c}$ are less than the absolute value of the numerator (and the denominator) of $\frac{p}{q}$.

Exercise 4.3.9. Show that $\frac{p}{q} = \frac{p^a}{q^a} \oplus \frac{p^c}{q^c}$.
Hint: If two numbers r and s share an edge in the Farey graph, then there are exactly two other numbers that have an edge to both r and s. One will be $r \oplus s$.

This completes the proof of the lemma for negative $\frac{p}{q}$. If $\frac{p}{q}$ is positive but not an integer, then the same arguments hold. If $\frac{p}{q}$ is an integer then one may easily check that the claimed result is true. (Notice the difference between this case and the others is that a_0 will be a positive number.) □

We are now ready to give a simple proof of Item (4) from the previous section that claims that all elements of $\mathbb{Q}^*$ appear as labels on vertices in the Farey graph. We induct on the absolute value of the denominator. It is clear from construction that all fractions with denominator 0 or ±1 appear. So now we assume that all fractions with denominators

having absolute value less than k appear in the Farey graph. If $\frac{p}{q}$ has $|q| = k$, then from Exercise 4.3.8 we know that $\frac{p^a}{q^a}$ and $\frac{p^c}{q^c}$ satisfy $|q^a|, |q^c| < k$. Thus they appear as labels on vertices in the Farey graph and then so must $\frac{p^a}{q^a} \oplus \frac{p^c}{q^c} = \frac{p}{q}$.

Here we list some useful facts regarding continued fractions where . As before, let $a_0, a_1, \cdots, a_n$ be positive integers and $[a_0, \ldots, a_i] = \frac{p_i}{q_i}$. Then

Lemma 4.3.10.

(1) *If $a_i \geq 2$ for all i, then $p_i > p_{i-1}$, $q_i > q_{i-1}$ and $p_i > q_i$. In particular, $\frac{p_i}{q_i} > 0$ for all i.*
(2) *If $a_i \geq 2$ for all i and $a_1 \geq k$, then $p_i > (k-1)q_i + 1$.*
(3) *If $[a_i, \ldots, a_0] = \frac{p_i}{p_{i-1}}$.*
(4) $\frac{p_i - p_{i-1}}{q_i - q_{i-1}} = [a_0, \ldots, a_i - 1]$
(5) $\frac{p_i - q_i}{p_{i-1} - q_{i-1}} = [a_i, \ldots, a_0 - 1]$

Exercise 4.3.11. Prove the lemma above.

4.4. Paths in the Farey graph

In the next chapter, and the rest of the book, we will be interested in minimal paths between vertices in the Farey graph. We review soem basic properties of such paths in this section. By a path in the Farey graph we mean a sequence of vertices $v_0, \ldots, v_n$ (we will use the same notation to refer to a vertex and its label) such that $v_i \cdot v_{i-1} = -1$ for each i. Notice that this means that we have a sequence of edges starting at v_0 and moving clockwise to v_n (notice our path moves monotonically in one direction. That is, it is not allowed to go back and forth). We call the path *minimal* if there is no subset of the vertices that satisfy the same condition; or said another way, a path is minimal if it is the shortest path in the Farey graph starting at v_0 and moving clockwise to v_n. If a path is not minimal then there is some i such that $v_{i-1} \cdot v_{i+1} = -1$. In this case, we can shorten the path by removing v_i. Clearly, any path can be shortened to a minimal path. One may similarly discuss paths and minimal paths that move anticlockwise, for example for a path as above $v_n, \ldots, v_0$ would be an anticlockwise path with $v_i \cdot v_{i-1} = 1$.

A key type of minimal path is a *continued fraction block*. While we normally consider clockwise paths, it will be convenient to describe continued fraction blocks as anticlockwise paths. We say the path $v_0, \ldots, v_n$ is a continued fraction block if there is a vertex t such that $t \cdot v_0 = 1$ and

$$v_k = v_{k-1} \oplus t = v_0 \oplus kt$$

for $k = 1, \ldots n$. See Figure 4.4.4.

Here are a few other ways to think about a continued fraction block. A path $v_0, \ldots, v_n$ is a continued fraction block if it is a minimal path and each vertex v_i, for $i > 1$, is the

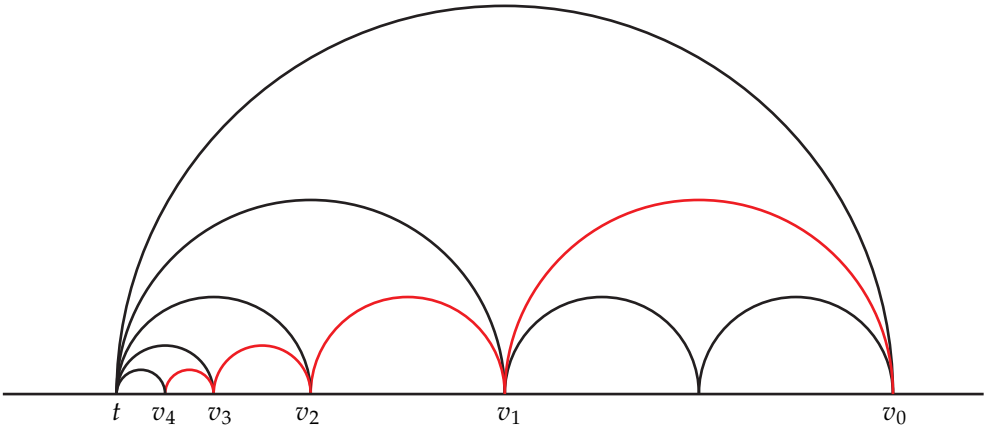

Figure 4.4.4. A continued fraction block.

farthest anticlockwise jump that can be made from v_{i-1} and the path still be minimal. So we can say that a continued fraction block is a sequence of maximal anti-clockwise jumps for a minimal path. To see that this is equivalent to the first definition we start by considering v_0 and v_1 with $v_0 \cdot v_1 = 1$. From Exercise 4.3.9 there are two vertices with an edge to v_0 and v_1. One is the Farey sum of the two the other we will denote as t.

Exercise 4.4.1. Check that $v_1 = v_0 \oplus t$.

Clearly $v_1 \oplus t$ is another step in the path and since there is an edge from v_1 to t and from $v_1 \oplus t$ to t it is easy to see that $v_1 \oplus t$ is the largest jump that one can make from v_1 and still have a minimal path. Thus we must have $v_2 = v_1 \oplus t$. One can inductively check that $v_i = v_{i-1} \oplus t$, so both ways to think of a continued fraction block are the same.

Given the above description, one sometimes says that a continued fraction block is a sequence of "half-maximal jumps". This makes sense because a maximal jump from v_i would go to the vertex t and then the path would be able to be shortened. So a "maximal jump" among minimal paths is a"half-maximal jump" among all paths.

We have another way to think of a continued fraction block, which is sometimes given as the actual definition. We will explore that in the following exercise.

Exercise 4.4.2. A path $v_0, \ldots, v_n$ is a continued fraction block if there is a change of basis for $H_1(T^2)$ that takes $v_0, \ldots, v_n$ to $-1, -2, \ldots, -n+1, -n$. (Recall, to associate curves on a torus to elements of $\mathbb{Q}^*$, one must choose a basis.)

We will now see that any minimal path can be thought of as a composition of continued fraction blocks. Indeed suppose $v_0, \ldots, v_m$ is a minimal anticlockwise path in the Farey graph. There is some k such that $v_0, \ldots, v_k$ is a continued fraction block (notice that any two vertices sharing an edge can be thought of as a continued fraction block).

We now consider the possibilities for v_{k+1}. Suppose v' would have been the next vertex in a continued fraction block if $v_0, \ldots, v_k$ were extended. We know that v_{k+1} must have an edge to v_k and we know that there is an edge between v_k and v'. Thus all the possible "next" vertices in the path must be in $[v', v_k]$ and have an edge to v_k. Thus the possibilities are

$$w_l = v' \oplus l v_k.$$

If $v_{k+1} = w_l$ then we say that the next continued fraction block is l *down* from the previous one. So there will be some k' such that $v_{k+1}, \ldots, v_{k'}$ is a continued fraction block. We can continue in this manner to see that any minimal path in the Farey graph is a sequence of continued fraction blocks.

Suppose we are given a rational number $\frac{p}{q} < -1$ with continued fraction

$$\frac{p}{q} = [a_0, a_1, \ldots, a_n].$$

We can build a minimal path in the Farey graph by starting with the vertex $[a_0, a_1, \ldots, a_n]$, going to $[a_0, a_1, \ldots, a_{n-1}, a_n + 1]$ and adding the edge between these two vertices (that exists by Lemma 4.3.5), then we have the vertex $[a_0, a_1, \ldots, a_{n-1}, a_n + 2]$ and add the edge back to the previous vertex. We can continue "adding 1 to the last element in the continued faction", with the understanding that $[a_0, a_1, \ldots, a_k, -1] = [a_0, a_1, \ldots, a_k + 1]$, until we reach -1. By Lemma 4.3.5 we see that this process creates a minimal path in the Farey graph that goes from $\frac{p}{q}$ clockwise to -1.

give an example or two, add figures and maybe some exercises

We now analyze this path more thoroughly. Consider the vertices

$$v_{|a_n|-1} = [a_0, a_1, \ldots, a_n], v_{|a_n|-2} = [a_0, \ldots, a_{n-1}, a_n + 1], \ldots,$$

$$v_0 = [a_0, \ldots, a_{n-1}, a_n + (|a_n| - 1)] = [a_0, \ldots, a_{n-2}, a_{n-1} + 1].$$

These are the first $|a_n|$ vertices in the path we just constructed. We note that they are part of a continued fraction block. To see this notice that if we let $t = [a_0, a_1, \ldots, a_{n-1}]$, then according to Lemma 4.3.5 there is an edge in the Farey graph between t and all the v_i. Notice that since there is an edge between v_0 and t and there is also an edge between v_1 and both v_0 and t, that $v_1 = v_0 \oplus t$.

Exercise 4.4.3. Prove the last statement and more generally that $v_k = v_0 \oplus kt$.

This observation explains the terminology "continued fraction block" defined above.

To continue the path from $[a_0, a_1, \ldots, a_{n-1} + 1]$ we obtain another continued fraction block from $[a_0, a_1, \ldots, a_{n-1} + 1]$ to $[a_0, a_1, \ldots, a_{n-2} + 1]$ and so on until our last continued fraction block $[a_0 + 1]$ to -1. Notice that whenever $a_k = -2$ then there is no corresponding continued fraction block.

Summarizing what we have proven about the path above: we have k continued fraction blocks where $k-1$ is the number of a_i not equal to -2 for $i < n$ (notice that there will always be at least one edge for a_n, but not for the $a_i = -2$). The continued fraction block associated to $[a_0, a_1, \ldots, a_l + 1]$ has length $|a_l| - 1$ and $|a_l| - 2$ edges while the continued fraction associated to $[a_0, a_1, \ldots, a_n]$ has $|a_n|$ vertices and $|a_n| - 1$ edges.

We would now like to consider building the path from -1 to $\frac{p}{q} < -1$ starting from -1. We have the continued fraction expansion $\frac{p}{q} = [a_0, \ldots, a_n]$ with $a_i \leq -2$.

Exercise 4.4.4. Show that $\frac{p}{q}$ is in the interval $[r_i, s_i]$ for all i where $r_i = [a_0, \ldots, a_{i-1} + 1]$ for $s_i = [a_0, \ldots, a_{i-1}]$.
Hint: Consider Lemma 4.3.5

Given the above exercise, the start of the path from -1 anticlockwise to $\frac{p}{q}$ is

$$-1, -2, \ldots, a_0 + 1.$$

We will now inductively see how to proceed. That is suppose we have created our path from -1 to $[a_0, \ldots, a_k + 1]$ for $k < n$ and a_{k+1} to a_{k+l} are all -2 with $k + l < n$ and $a_{k+l+1} < -2$. Then the next part of the path is a continued fraction block from $[a_0, \ldots, a_{k+l} + 1]$ to $[a_0, \ldots, a_{k+l+1} + 1]$ that is $l + 1$ down from the previous continued fraction block.

Exercise 4.4.5. Prove this last statement.
Hint: Consider the path from $[a_0 + 1]$ to $[a_0, -2, \ldots, -2, a_{k+1}]$ where there are k, -2s and $a_{k+1} \neq -2$. Show this continued fraction block is $k + 1$ down from $-1, \ldots, a_0 + 1$. Then use a change of basis to prove this in the general case.

This process will create the path from -1 to $\frac{p}{q}$ except for the last continued fraction block will go from $[a_0, \ldots, a_{n-1} + 1]$ to $[a_0, \ldots, a_n]$.

Exercise 4.4.6. We now consider paths that do not begin at -1 and go to $\frac{p}{q} < -1$. Given any path from $\frac{a}{b}$ clockwise to $\frac{p}{q}$, show that there is a change of basis for $H_1(T^2)$ that will make $\frac{a}{b} = -1$ and $\frac{p}{q} < -1$.

With the above exercise in hand, we can use the above discussion to create any path in the Farey graph from a continued fraction.

4.5. Intersection of curves on the torus

In future sections, it will be useful to have bounds on the intersection number between curves on a torus (this is particularly useful when applying the Imbalance Principle, Theorem 5.4.18). To state our results, we recall that our conventions for vertices in the Farey

graph require all denominators to be positive (so any negative fraction has a negative numerator). In addition, recall that

$$\frac{b}{a} \cdot \frac{d}{c} = ad - bc.$$

We first make a simple observation about the sign of intersections between two curves.

Lemma 4.5.1. *Given any rational numbers $\frac{p}{q}$ and $\frac{p'}{q'}$, then we have*

$$\frac{p'}{q'} \cdot \frac{p}{q} \leq 0$$

if $\frac{p}{q} \leq \frac{p'}{q'}$ and

$$\frac{p'}{q'} \cdot \frac{p}{q} > 0$$

if $\frac{p}{q} > \frac{p'}{q'}$.

Proof. If $\frac{p'}{q'} \geq \frac{p}{q}$ we clearly have $p'q \geq q'p$ and so $p'q - q'p \geq 0$. Hence $\frac{p'}{q'} \cdot \frac{p}{q} \leq 0$. We have a similar computation if $\frac{p'}{q'} < \frac{p}{q}$. □

We are now ready for our first bound on intersection numbers.

Lemma 4.5.2. *Suppose k and l are integers such that $k < l < \frac{p}{q}$. Then*

$$\left| k \cdot \frac{p}{q} \right| > \left| l \cdot \frac{p}{q} \right|.$$

In addition if $\frac{p'}{q'} \in (k-1, k)$ and $\frac{p}{q} > k$, then

$$\left| \frac{p}{,} q' \cdot \frac{p}{q} \right| > \left| (k-1) \cdot \frac{p}{q} \right| > \left| k \cdot \frac{p}{q} \right|.$$

Proof. Write $p = mq + r$ with $r \in [0, q-1]$. Now

$$k \cdot \frac{p}{q} = mq + r - qk = (m-k)q + r > (m-l)q + r = l \cdot \frac{p}{q}$$

By Lemma 4.5.1 we know the left and right numbers are positive, thus establishing the first inequality of the lemma.

Now since $\frac{p'}{q'}$ is strictly between $k-1$ and k, we know from the construction of the Farey graph that there are positive integers a and b such that

$$\frac{p'}{q'} = a\frac{k-1}{1} \oplus b\frac{k}{1}.$$

Thus we see

$$\left|\frac{p'}{q'} \cdot \frac{p}{q}\right| = a\left|(k-1)\cdot\frac{p}{q}\right| + b\left|k\cdot\frac{p}{q}\right| > \left|(k-1)\cdot\frac{p}{q}\right| > \left|k\cdot\frac{p}{q}\right|.$$

The first equality follows since the sign of the intersection of $\frac{p}{q}$ with k and with $k-1$ is the same by Lemma 4.5.1, the first inequality follows from the fact that a and b are positive integers, and the last inequality was proven above. □

Our last estimate on intersection numbers handles the case when there is no integer between $\frac{p'}{q'}$ and $\frac{p}{q}$.

Lemma 4.5.3. *Suppose $a_0 = \left\lfloor \frac{p}{q} \right\rfloor, a_1, \ldots, a_n = \frac{p}{q}$ is the shortest clockwise path from $\left\lfloor \frac{p}{q} \right\rfloor$ to $\frac{p}{q}$. Then*

$$\left|a_{i-1}\cdot\frac{p}{q}\right| < \left|a_i\cdot\frac{p}{q}\right|$$

and if $\frac{p'}{q'} \in (a_{i-1}, a_i)$ then

$$\left|\frac{p'}{q'}\cdot\frac{p}{q}\right| < \left|a_{i-1}\cdot\frac{p}{q}\right|.$$

Exercise 4.5.4. Adapt the proof of Lemma 4.5.2 to prove the last lemma.

4.6. The integer lattice $\mathbb{Z}^2$

Chapter 5

Tight contact structures

All classification results that we explain here rely on Eliashberg's fundamental theorem that the 3-ball has a unique contact structure up to isotopy.

Theorem 5.0.1 (Eliashberg 1992, [Eli92]). *Any two tight contact structures on the* 3*-ball,* B^3*, that induce the same characteristic foliation on* ∂B^3 *are isotopic through contact structures. Moreover, if the contact structures agreed near* ∂B^3*, then the isotopy can be taken to be the identity near* ∂B^3*.*

This theorem will be proven in Section 9.1 using an argument due to Giroux [Gir00], but for now, we explore how to use convex surface theory to classify contact structures on other manifolds using this theorem. Though not mentioned in the theorem, it is clear that there is indeed a tight contact structure on B^3 as we can take B^3 to be the unit ball in $\mathbb{R}^3$ with its standard contact structure and this latter contact structure is tight by the Bennequin inequality, see Section 1.6. Moreover, this contact structure on B^3 has convex boundary, see Example 3.2.14, and the dividing set consists of a single circle. Thus, using Giroux flexibility, that is Theorem 3.4.1, we can arrange that the characteristic foliation on ∂B^3 is any singular foliation that is divided by a single curve.

In Section 5.1, we will show how to classify tight contact structures on S^3 and $S^1 \times S^2$. We will carefully go through the steps of both proofs. Classification on S^3 is quite simple, but the classification on $S^1 \times S^2$ is a bit more complicated. The latter result is the paradigm for subsequent classification results, so we will first give a proof of this result with all the details spelled out, but then give a second proof where some of the "well-known" parts are left out. It is the second proof that will resemble the proofs we give for other manifolds, so the reader is encouraged to convince themselves that the second proof is indeed equivalent to the first proof. The second proof focuses on the "main ideas" and leaves out some details that should be easy for the reader to fill in. The

subsequent classification results focus on these main ideas as if all the minor details are presented, the main thread of the argument can be lost. Nonetheless, if the reader has gotten comfortable that the second proof of the classification of tight contact structures on $S^1 \times S^2$ is equivalent to the first, then they should have no trouble following the proofs later in the book.

We then, in Section 5.2, turn to notation for the set of tight contact structures up to isotopy on a given manifold, with special attention paid to manifolds with boundary.

A key feature in our classification results are basic slices and bypass attachments, which are discussed in Sections 5.3 and 5.4, respectively. More specifically, in Section 5.3 we show that there are exactly two basic slices. That is, there are exactly two tight, minimally twisting contact structures on $T^2 \times [0,1]$ with two dividing curves on each boundary component such that the homology class of the dividing curves on $T^2 \times \{0\}$ and on $T^2 \times \{1\}$ form a basis for the first homology of T^2. Here, minimally twisting is a technical condition indicating that convex tori parallel to the boundary in $T^2 \times [0,1]$ have dividing slope "between" the dividing slopes on the boundary. In the following section, we discuss bypasses. These are the fundamental way that one goes from one convex surface to another, through surfaces that are not (necessarily) convex. More specifically, a bypass is a convex disk in a contact manifold intersecting a convex surface in a single arc intersecting the dividing set 3 times, having Legendrian boundary with contact twisting -1, and a few other technical conditions. Given a bypass for a convex torus with two dividing curves (and other technical conditions), a "one-sided neighborhood" of the torus and bypass disk forms a basic slice. So basic slices and "attaching" a bypass to a convex torus (in a nice way) are very closely related. We also discuss how pushing a convex surface past a dividing curve on a general convex surface affects the dividing curves.

Sections 5.5, 5.6, and 5.7 are devoted to the classification of tight contact structures on $T^2 \times [0,1]$ (here we only consider minimally twisting ones), solid tori, and lens spaces. These sections should be considered together, as their proofs are intertwined. Specifically, we show a upper bound on the number of minimally twisting contact structures on $T^2 \times [0,1]$ with certain boundary conditions, which is an upper bound on the number of tight contact structures on solid tori with certain boundary conditions, which is a upper bound on tight contact structures on a certain lens space, and we then provide a lower bound on the number of tight contact structures on this lens space which agrees with the first established upper bound. So the proof of any of these results relies on results from all three sections. We also note that these three sections is our first use of our "executive summary of main results" and "proofs of main results" format discussed in the Introduction. Recall the "executive summary of main results" is meant to be a survey of the main results about the classification of tight contact structures on the relevant manifolds. Proofs are not presented in this subsection as they might detract from a clear picture of

the classification results and their corollaries. The proofs are then collected in the "proofs of main results" subsection. We hope this makes the presentation helpful as a research reference and as a learning reference.

In Section 5.8 we give the complete classification of tight contact structures on the 3-torus T^3 up to isotopy and contactomoprhism. Finally, in Section 5.9 we consider tight contact structures on $T^2 \times [0,1]$ again. This time, we consider contact structures that are not minimally twisting, but still have only two dividing curves on their boundary.

5.1. Simple classification results

In this section, we will give three classification results that indicate how to use Eliashberg's theorem above to classify contact structures on other 3-manifolds. The proofs will become progressively more complicated with the last one being the prototype of how one uses convex surfaces to classify contact structures on a given manifold. We begin by considering tight contact structures on the 3-sphere.

Theorem 5.1.1 (Eliashberg 1992, [**Eli92**])**.** *Up to contact isotopy there is exactly one tight contact structure on S^3.*

Proof. The existence of a tight contact structure on S^3 follows from Bennequin's theorem, Theorem 1.6.6, and also from Theorem 1.6.13 since S^3 is the convex boundary of a symplectic ball.

Let ξ and ξ' be two tight contact structures on S^3. Given a point $p \in S^3$ there is a smooth isotopy of S^3 that will take ξ' at p to ξ at p. Pushing ξ' forward by this isotopy gives a contact isotopy of ξ' so that ξ and ξ' agree at p. Now the proof of Darboux's theorem, Theorem 1.2.2, shows that we may further isotop ξ' so that ξ and ξ' agree in a neighborhood N of p. Now let B' be a closed 3-ball centered at p and contained in N and $B = S^3 \setminus B'$. Now ξ and ξ' restricted to B are two tight contact structures on the 3-ball B that agree along ∂B. Thus by Theorem 5.0.1 we see that ξ' is isotopic to ξ on B through contact structures and this isotopy is fixed near ∂B. Thus we still have that ξ' and ξ agree on B' and we have found our isotopy from ξ' to ξ on S^3. □

The next simplest classification result is for tight contact structures on $S^1 \times S^2$.

Theorem 5.1.2. *Up to contact isotopy there is a unique tight contact structure on $S^1 \times S^2$.*

Proof. The existence of a tight contact structure on $S^1 \times S^2$ follows from Theorem 1.6.13 since it is the convex boundary of a symplectic structure on $S^1 \times D^3$ (that is a Weinstein domain with a single 0-handle and a single 1-handle).

Let ξ and ξ' be two tight contact structures on $S^1 \times S^2$. Fixing a point $p \in S^1$ we can consider the spheres $S = \{p\} \times S^2$ in $(S^1 \times S^2, \xi)$ and $S' = \{p\} \times S^2$ in $(S^1 \times S^2, \xi')$. We can

isotopy both spheres to make them convex by Theorem 3.3.1 and by the Giroux criterion, Theorem 3.6.1, we know the dividing curve Γ on S is a single circle as is the dividing curves Γ' on S'. Since Γ divides S_ξ we know there is some identification of S with S' so that S_ξ is divided by Γ' on S'. Now by the Giroux realization principle, Theorem 3.4.1, we can isotop S' so that S'_ξ, is this foliation. Now there is a smooth isotopy of $S^1 \times S^2$ that takes S' to S and under the isotopy S'_ξ, is taken to S_ξ. Pushing ξ' forward by this isotopy results in a contact structure (that we still call ξ') such that ξ and ξ' induce the same characteristic foliation on S. Since we know the characteristic foliation determines the contact structure in a neighborhood of a surface, Theorem 1.3.4, we see that we can isotopy ξ' in a neighborhood of S so that ξ and ξ' agree in a neighborhood $N = (-\epsilon, \epsilon) \times S^2$ of S.

Now let γ be a circle in $S^1 \times S^2$ that is isotopic to $S^1 \times \{q\}$ for some point $q \in S^2$ and intersects N in a Legendrian arc that is transverse to S. We may isotop γ, relative to $\gamma \cap N$, so that it is Legendrian in ξ and isotop γ, relative to $\gamma \cap N$, to a curves γ' that is Legendrian in ξ'. After possibly stabilizing these Legendrian curves, we can assume that they both have the same contact framing.

Exercise 5.1.3. Show that there is an isotopy of $S^1 \times S^2$ relative to N that takes γ' to γ and if we push ξ' forward by this isotopy, then ξ and ξ' agree along $\gamma = \gamma'$.

Theorem 1.2.6 says Legendrian knots have unique neighborhoods, but the proof actually shows that we may isotop ξ', relative to N, so that ξ and ξ' agree in a neighborhood $N' = S^1 \times D^2$ of γ.

We now note that $S^1 \times S^2 \setminus (N \cup N')$ is B^3

Exercise 5.1.4. Prove this last statement.

Let S^2 be a 2-sphere in $N \cup N'$ so that S^2 bounds a 3-ball B^3 and $S^1 \times S^2 = N \cup N' \cup B^3$. Since $S^2 \subset N \cup N'$ we know that ξ and ξ' induce the same characteristic foliation on S^2 and hence by Eliashberg's classification of tight contact structures on B^3, Theorem 5.0.1, we know that we can isotop ξ' on B^3 to ξ through contact structures by an isotopy fixed near the boundary. This completes the isotopy of ξ' to ξ on $S^1 \times S^2$. □

The previous proofs already demonstrated how to use convex surfaces to classify contact structures on a manifold, but our next result will give a prototype of the convex surface theory techniques and another important building block for many of the classification results we will see in the rest of this section (and the rest of the book).

Theorem 5.1.5 (Kanda 1997, [Kan97]). *Let $\mathcal{F}$ be a singular foliation on the boundary of $S^1 \times D^2$ that is divided by two parallel curves of slope n (that is each curve is in the homology class of $[S^1 \times \{p\}] + n[\{q\} \times D^2]$). Then up to contact isotopy there is a unique tight contact structure on $S^1 \times D^2$ that induces $\mathcal{F}$ on the boundary.*

We will give the proof of this theorem twice. The first time we will include all the details, and the second time we will give a quick proof that any expert in convex surfaces would understand and could easily turn into the detailed proof if necessary. As we progress in the book, the proofs will start to look more like the second proof, so we encourage the reader to make sure they understand how to unpack the second proof to recreate the first proof.

First Proof. We first establish the existence of a tight contact structure satisfying the hypothesis of the theorem. To this end recall the standard contact structure on $\mathbb{R}^3$ is tight because the Bennequin inequality holds, see Section 1.6, and thus any of its contact submanifold will be tight. Now let N be a neighborhood of any Legendrian knot, to be specific, we consider the maximal Thurston-Bennequin invariant Legendrian unknot given in Example 1.4.16. We know that the contact structure on this neighborhood is tight; moreover, by Theorem 1.2.6 we know that any two Legendrian circles have contactomorphic neighborhoods. Thus we can assume N is a neighborhood of the x axis in $\mathbb{R}^3/\sim$ where $(x, y, z) \sim (x + 1, y, z)$ and we equip this space with the contact structure $\ker(dz - y\,dx)$. Notice that $y\frac{\partial}{\partial y} + z\frac{\partial}{\partial z}$ is a contact vector field and if N is of the form $S^1 \times D^2$ where D^2 is a round disk in the yz-plane, then ∂N is convex. One may easily compute that the dividing set on ∂N consists of two dividing curves of slope 0. We can apply a diffeomorphism to N to get a new tight contact structure with any integral dividing slope. Finally, using Giroux realization principle, Theorem 3.4.1, we know that we can realize any singular foliation as the characteristic foliation on ∂N that is divided by the given dividing curves.

Let ξ and ξ' be two tight contact structures on $S^1 \times D^2$ as in the statement of the theorem. Since they both induce the same characteristic foliation on $\partial(S^1 \times D^2)$ we can use Theorem 1.3.4 to isotop ξ' to agree with ξ in a neighborhood N of the boundary. Moreover, since the characteristic foliation on the boundary admits dividing curves, we know by Theorem 3.2.9 it is convex and so we can assume the neighborhood on which the contact structures agree is vertically invariant. Using the Giroux realization principle, that is Theorem 3.4.1, we may arrange that a torus T in N that is parallel to $\partial(S^1 \times D^2)$ has characteristic foliation that is in standard form, see Example 3.4.4, with ruling curves of slope ∞ (that is the ruling curves are meridians). See Figure 5.1.1.

Let D be a disk in $S^1 \times D^2$ with boundary a ruling curve on T (and intersecting T only in its boundary). Note that ∂D intersects the dividing curves on $\partial(S^1 \times D^2)$ exactly twice and hence by Theorem 3.5.1 we know that $\mathrm{tw}(\partial D, T) = -1$. Since the framing given to ∂D by T and by D is the same we see that $\mathrm{tw}(\partial D, D) = -1$. Since the twisting is negative we can apply Theorem 3.3.1 to isotop D to be convex in ξ and isotop it to D' so that it is convex in ξ'. We know by Theorem 3.5.1 that the dividing curves on these disks intersect the boundary exactly twice and by Theorem 3.6.1 that there are no closed curves in the

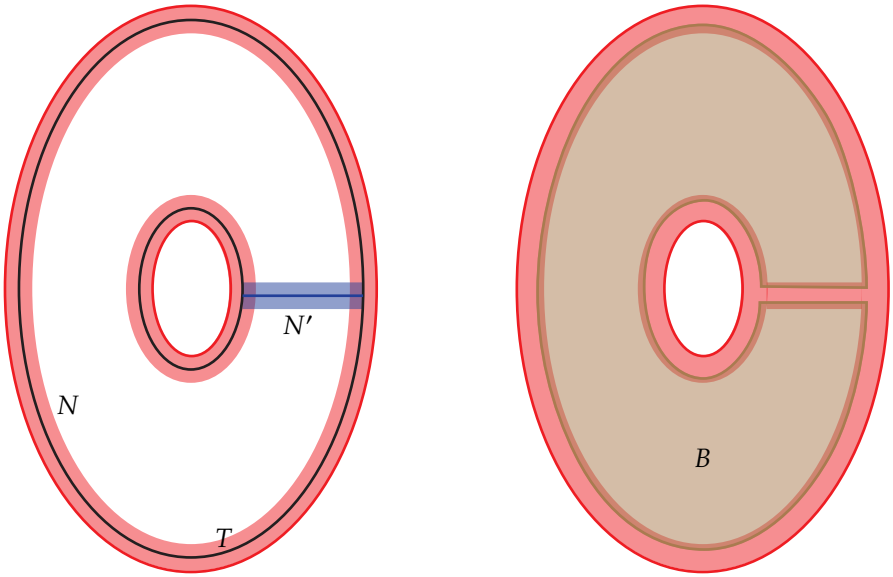

Figure 5.1.1. A cross-section of $S^1 \times D^2$. On the left, the neighborhood N is shown in red and the neighborhood N' is shown in blue. The torus T is shown in black. On the right, $N \cup N'$ is shown in red while the ball B is shown in brown.

dividing set. Thus the dividing set on both disks consists of a single arc. Thus using the Giroux realization principle, that is Theorem 3.4.1, we may arrange that the characteristic foliation on D' is the same as the foliation on D. Now there is a smooth isotopy of $S^1 \times D^2$ that is fixed on N and takes D' to D and the image of the characteristic foliation on D' agrees with the characteristic foliation on D. Pushing ξ' forward by this isotopy gives an isotopy of ξ' so that ξ and ξ' induce the same characteristic foliation on D. Once again we can use Theorem 1.3.4 to isotop ξ' to agree with ξ in a neighborhood N' of D, by an isotopy that is fixed on N. Thus we see that ξ' can be isotoped to agree with ξ on $N \cup N'$.

Now notice that there is a sphere S embedded in $N \cup N'$ that bounds a ball B in $S^1 \times D^2$ so that $N \cup N' \cup B = S^1 \times D^2$. Moreover ξ and ξ' agree in a neighborhood of the boundary of B and thus by Eliashberg's classification of tight contact structures on the 3-ball, that is Theorem 5.0.1, we know that ξ' can be isotoped to agree with ξ on B by an isotopy fixed near the boundary of B. This final isotopy makes ξ' agree with ξ on all of $S^1 \times D^2$ and completes the proof. □

In the first paragraph of the above proof, we constructed a neighborhood N of any Legendrian knot L such that ∂N is convex with two dividing curves of slope equal to the contact framing. As in Example 3.4.4 we can assume that the characteristic foliation on ∂N consists of two Legendrian divides parallel to the dividing curves and ruling curves of any slope not equal to the dividing slope. Such a neighborhood of L will be called a *standard neighborhood of* L.

We are now ready for the "streamlined" proof.

Second Proof. The existence of a tight contact structure as in the theorem is established as in the previous proof.

Given two tight contact structures ξ and ξ' on $S^1 \times D^2$ as in the statement of the theorem, we know that we can isotopy ξ' to ξ in a neighborhood of the boundary since they induce the same characteristic foliation. We can assume that a meridional curve μ is Legendrian by Giroux flexibility. Since μ intersects the dividing curves two times (since the dividing curves are longitudinal) we know its twisting relative to the boundary is -1. Let D be the disk μ bounds. The twisting of the contact planes relative to D is also -1 so we can make D convex in both ξ and ξ'. We know the dividing set of D contains no closed curves, by Giroux's tightness criterion, and that they intersect ∂D two times. Thus the dividing curves on D for both ξ and ξ' consist of a single arc and we can isotop so that the dividing curves agree and by Giroux flexibility, we can also assume their characteristic foliations are the same. Thus we can isotop ξ' so that so that it agrees with ξ in a neighborhood of D too. Now ξ and ξ' agree on the complement of a ball in $S^1 \times D^2$, thus we can isotope one to the other by Eliashberg's classification of tight contact structures on the 3-ball. □

Exercise 5.1.6. Review the above two proofs to make sure you are comfortable that if you read the second proof, you could quickly understand how to create the first proof. In other words, that you see the second proof is rigorous.

We end this section by noting an important consequence of the previous theorem.

Corollary 5.1.7. *Given a tight contact structure on $S^1 \times D^2$ for which the boundary is convex with two dividing curves of slope n, then one can find a convex torus T in $S^1 \times D^2$ that is isotopic to $\partial(S^1 \times D^2)$ and has two dividing curves of slope s if and only if $s \in (-\infty, n]$.*

Proof. If we can prove the corollary for any n then it is true for all n as there is a diffeomorphism of $S^1 \times D^2$ taking any longitude to any other longitude. To prove the theorem we consider a model contact structure. On $S^1 \times \mathbb{R}^2$, with angular coordinate ϕ on S^1 and polar coordinates (r, θ) on $\mathbb{R}^2$, consider the contact structure $\xi' = \ker(d\phi + r^2\, d\theta)$. Notice that as a goes increases in the interval $(0, \infty)$, the tori $T_a = \{(\phi, r, \theta) : r = a\}$ have linear characteristic foliation of slope $-1/r^2$. Thus the slopes range from $-\infty$ to 0 (not including the endpoints). So we may choose a such that T_a has slope n for some negative integer n. We may now perturb the torus T_a to a convex torus T as in Example 3.2.6 so that T has two dividing curves of slope n. Thus if S is the solid torus in $S^1 \times \mathbb{R}^2$ that T bounds and $\xi = \xi'|_S$, then by Theorem 5.1.5 (S, ξ) is the unique tight contact structure on the solid torus with two dividing curves of slope n. We can see from the model and the perturbation of T_a from Example 3.2.6, that T_b for $b < a - \epsilon$ sits inside of (S, ξ), for some small ϵ.

We can then perturb T_b to be convex with two dividing curves of slope $-1/b^2$. As ϵ can be assumed to be arbitrarily small in Example 3.2.6, we see that any slope in $(-\infty, n]$ is realized as the dividing slope of a convex torus.

To see that slopes outside $(-\infty, n]$ cannot be realized by convex tori in (S, ξ) we will need to develop a little more theory. We will prove this at the end of Section 5.5. □

5.2. Isotopy classes of contact structures

We will denote the set of isotopy classes of tight contact structures on a manifold M by

$$\text{Tight}(M).$$

With this notation Theorem 5.1.1 and 5.1.2 can be restated as

$$|\,\text{Tight}(S^3)| = 1 \text{ and } |\,\text{Tight}(S^1 \times S^2)| = 1,$$

respectively.

If the manifold M has boundary and $\mathcal{F}$ is a singular foliation on ∂M, then the set of isotopy classes of tight contact structures on M inducing the foliation $\mathcal{F}$ on ∂M is denoted by

$$\text{Tight}(M; \mathcal{F}).$$

If Γ is a collection of curves on ∂M and $\mathcal{F}$ is a singular foliation on ∂M that is divided by Γ then we denote the set of isotopy classes of tight contact structures on M inducing the foliation $\mathcal{F}$ on ∂M is denoted by

$$\text{Tight}(M; \Gamma).$$

The notation indicates that this set does not depend on $\mathcal{F}$ and that is indeed the case.

Lemma 5.2.1. *Suppose that $\mathcal{F}_i, i = 0, 1$, are two singular foliations on ∂M that are both divided by the multi-curve Γ. Then there is a one-to-one correspondence between* $\text{Tight}(M; \mathcal{F}_0)$ *and* $\text{Tight}(M; \mathcal{F}_1)$.

So when we use the notation $\text{Tight}(M; \Gamma)$ this will always mean $\text{Tight}(M; \mathcal{F})$ for any fixed singular foliation $\mathcal{F}$ on ∂M that is divided by Γ.

Proof. □

Using the notation established above we can rephrase Theorems 5.0.1

$$|\,\text{Tight}(B^3; \Gamma)| = 1$$

where Γ is a simple closed curve on ∂B^3. And Theorem 5.1.5 is equivalent to

$$|\,\text{Tight}(S^1 \times S^2; \Gamma)| = 1$$

where Γ consists of two longitudinal curves on $\partial S^1 \times D^2$.

If M is a manifold with a torus boundary and there is a preferred basis for $H_1(\partial M)$ then the dividing curves on ∂M are determined by the slope of the curves which is given by an element in $\mathbb{Q}^*$, see Section 4.1, and the number of dividing curves, which is an even number. We will use the notation

$$\text{Tight}(M; s)$$

to denote $\text{Tight}(M;\Gamma)$ where Γ consists of two curves of slope s on ∂M. Using this notation Theorem 5.1.5 can be stated

$$|\,\text{Tight}(S^1 \times S^2; n)| = 1$$

where we are using longitude-meridian coordinates on $\partial S^1 \times D^2$ and the longitude is given by the product structure.

5.3. Basic slices

In this section we will discuss a basic building block for all the classification results to come in the rest of this chapter.

5.3.1. Executive summary of the main results. The contact manifold $(T^2 \times [0,1], \xi)$ is called a *basic slice* if

(1) ξ is tight.

(2) $T_i = T^2 \times \{i\}$ is convex with $\#\Gamma_{T_i} = 2$, for $i = 0, 1$.

(3) v_0, v_1 form an oriented integral basis for $H_1(T^2 \times \{0\}; \mathbb{Z})$, where v_i is a minimal length integral vector with slope equal to the slope s_i of the dividing curves Γ_{T_i}.

(4) the slope of the dividing curves on any convex torus T in M parallel to the boundary is in $[s_0, s_1]$ (see the end of Section 4.2 for this notation) this condition is called *minimal twisting*.

As a reminder about the last bullet point, a slope being in $[s_0, s_1]$ means that if we view slopes on the Farey graph, then the slope is clockwise of s_0 and counterclockwise of s_1.

Theorem 5.3.1 (Giroux 2000, [Gir00]; Honda 2000, [Hon00a]). *For each pair of slopes s_0 and s_1 connected by an edge in the Farey graph, there are exactly two basic slices with dividing slopes s_0 and s_1. Moreover, their relative Euler classes are given by*

$$\pm(v_1 - v_0) \in H_1(T^2; \mathbb{Z}) \cong H^2(T^2 \times [0,1], \partial(T^2 \times [0,1]); \mathbb{Z}),$$

where the v_i are as in Item (3) above.

MIGHT need to say something about which components of v_i are negative to get the right formula

We will denote the isotopy classes of minimally twisting, tight contact structures on $T^2 \times [0,1]$ with T_i being convex with two dividing curves of slope s_i, for $i = 0, 1$, by

$$\text{Tight}_{min}(T^2 \times [0,1]; s_0, s_1).$$

So the theorem above can be paraphrased as

$$|\,\text{Tight}_{min}(T^2 \times [0,1]; s_0, s_1)| = 2$$

if s_0 and s_1 share an edge in the Farey graph.

Once we have classified basic slices we can also observe the sorts of convex tori that can be realized inside them.

Corollary 5.3.2. *Let $(T^2 \times [0,1], \xi)$ be a basic slice with dividing slopes s_0 and s_1 in its back and front boundary components, respectively. A slopes can be realized as the dividing slope on a convex torus T parallel to the boundary of $T^2 \times [0,1]$ if and only if $s \in [s_0, s_1]$. A slope s can be realized as the slope of a linearly foliated torus parallel to the boundary of $T^2 \times [0,1]$ if and only if $s \in (s_0, s_1)$.*

5.3.2. Proof of the main results. We start with the classification of basic slices.

Proof of Theorem 5.3.1. Note that given any basic slice there is a diffeomorphism of $T^2 \times [0,1]$ taking s_0 to ∞ and s_1 to -1. So we will assume these are our slopes. With that the proof clearly follows from Lemmaa 5.3.3 and 5.3.7 below. □

We first establish an upper bound on the number of basic slices with the given dividing slopes.

Lemma 5.3.3. *There are at most two basic slices with $s_0 = \infty$ and $s_1 = -1$.*

Proof. Arguing as in the proof of Theorem 5.1.5, we will show that given a contact structure on $T^2 \times [0,1]$ we can cut $T^2 \times [0,1]$ along convex surfaces until we obtain a 3-ball with a unique tight contact structure on it. The number of possible tight contact structures will then be determined by the number of choices we had for the dividing curves on the surfaces we cut along. Our proof below will be in the style of the second, more succinct, proof of Theorem 5.1.5. The reader is encouraged to expand this proof to be in the style of the first proof of Theorem 5.1.5.

Let $(T^2 \times [0,1], \xi)$ be a basic slice. So T_i is convex with two dividing curves, $i = 0, 1$, and the slope of the dividing curves on T_0, T_1 is $\infty, -1$, respectively. We can assume the characteristic foliation on $T_0 \cup T_1$ is standard (see Exercise 3.2.16) with ruling slope 0 (that is the ruling curves are vertical). Now take a vertical annulus $A = S^1 \times [0,1]$ the boundary component $S_i = S^1 \times \{i\}$ a ruling curve in T_i, and $A \cap \partial(T^2 \times [0,1]) = \partial A$. Note the twisting number of S_i with respect to A is -1. This is because the twisting with respect to A is the same as with respect to T_i, and the twisting on T_i is computed to be -1, using

Theorem 3.5.1, as the curve S_i intersects the dividing curves twice. Using Theorem 3.3.1 we can now perturb A to be convex with standard boundary.

Since ξ is tight and the dividing curves on A intersect each boundary component twice we know that Γ_A is either two boundary parallel arcs (that is, each cobounds a disk with the boundary of A) or two arcs running from one boundary component of A to the other. See Figure 5.3.2

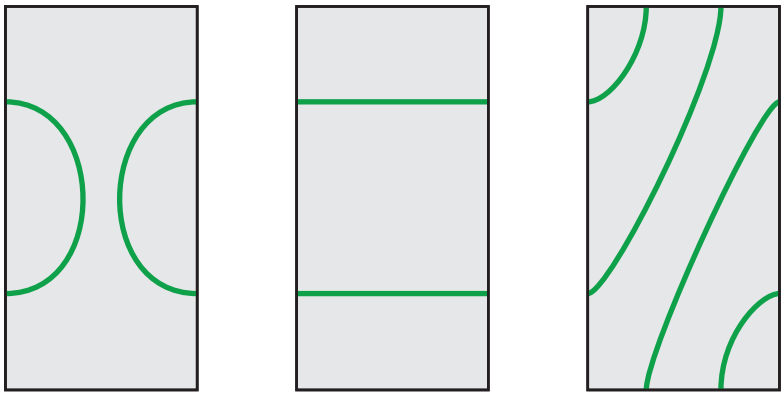

Figure 5.3.2. Three possible dividing curves on the annulus A. (The top and bottom of each rectangle are identified to form the annulus.)

If the components of Γ_A were boundary parallel then we could Legendrian realize a vertical simple close curve L on A with twisting number 0. We could then find a torus T in $T^2 \times [0,1]$ that contained L and was convex. Since the twisting of L with respect to T is 0, we know the dividing curves must also be vertical. This contradicts the fact that ξ has minimal twisting. Thus the dividing curves must run from one boundary component of A to the other.

We can fix an identification of the boundary components of A so that for each curve c in Γ_A, $c \cap S_0$ is taken to $c \cap S_1$. After identifying the boundary components of A, Γ_A with consist of two simple closed curves of slope h for some integer h. We call $h = h(A)$ the holonomy of A. In Figure 5.3.2, with the natural identifications of the right and left side of the rectangles, the holonomy is 0 and 1 for the two rightmost pictures. (Note we never really identify the boundary components of A we are just using the identification to define h.)

We now show that we can isotop A so as to increase or decrease $h(A)$ by 1 (and hence after further isotopy we can increase or decrease the holonomy by any integer). Thus, once this is achieved, up to isotopy, there is only one possible configuration for the dividing curves on A. To see how to change the slope of the dividing curves on A Let T_i' be a parallel copy of T_i in a vertically invariant neighborhood of T_i. Now let A' be a parallel copy of A in a vertically invariant neighborhood of A with boundary on the

$T_0' \cup T_1'$. Consult Figure 5.3.3 throughout this construction. Notice that $A \cup A'$ cut T_i' into

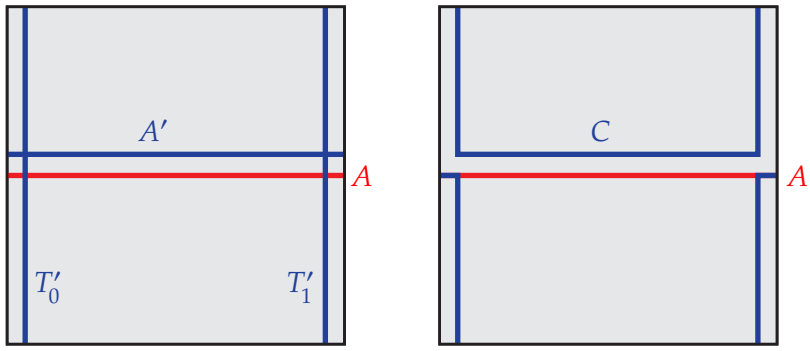

Figure 5.3.3. Both figures are $S^1 \times [0,1]$ cross sections of the basic slice (identify the top and bottoms of the squares). On the left are the tori and annuli used in the isotopy of A. On the right is C before edge rounding

two annuli, one of which, denoted T_i'', is disjoint from a vertically invariant neighborhood of A. Now $A' \cup T_0'' \cup T_1''$ is an annulus with boundary on A, we can add two sub-annuli of A to $A' \cup T_0'' \cup T_1''$ to construct an annulus C that has the same boundary as A.

Exercise 5.3.4. Show the pieces that make up C can be assumed to be convex surfaces with Legendrian boundary.

We now round the corners on C, as discussed in Section 3.8, to create a smooth convex annulus (which we still denote by C).

Exercise 5.3.5. Show C is isotopic, rel boundary, to A and $h(C) = h(A) \pm 1$ where the ± 1 depends on which side of A the annulus A' sits. For the latter consult Figure 5.3.4.

Thus up to isotoping A rel boundary, there is only one possibility for Γ_A. Now if we cut $T^2 \times [0,1]$ open along A and round the corners we get solid torus S with convex boundary.

Exercise 5.3.6. Show that the dividing curves on ∂S consist of two curves each of slope $-\frac{1}{2}$.

Should we do this? It is the first time we are doing this and will be used many times in the rest of the book!

Using Theorem 3.4.1 we can assume the characteristic foliation on ∂S is standard with ruling slope 0. Thus we can find a meridional disk D with ∂D a ruling curve in ∂S. The twisting along ∂D is -2 so we can make D convex. There are two possibilities for the dividing curves on D. See Figure 5.3.5. After cutting S along D we get the 3-ball which has a unique tight contact structure. Thus there are only two possible basic slices corresponding to the different possibilities for the dividing curves on D. □

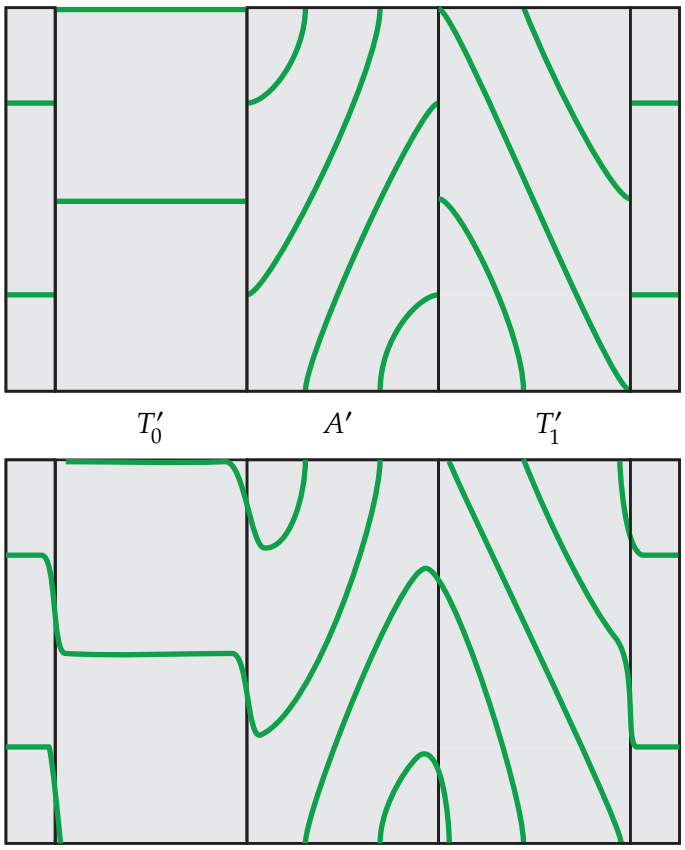

Figure 5.3.4. The piecewise smooth annulus C is shown on the top and the annulus with edges rounded is shown on the bottom. In this example the original annulus A had holonomy 1 and the new annulus C has holonomy 0.

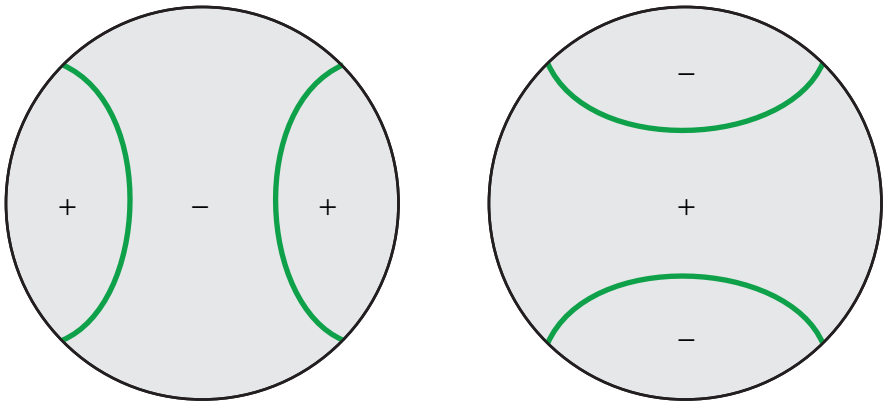

Figure 5.3.5. Possible dividing curves on D.

We are now left to prove that two basic slices exist and compute the relative Euler class.

Lemma 5.3.7. *There are two basic slices with $s_0 = \infty$ and $s_1 = -1$ and they are distinguished by relative Euler classes which are given by* $\begin{pmatrix} \pm 1 \\ 0 \end{pmatrix} \in H^2(T^2 \times [0,1]; \mathbb{Z}) \cong H_1(T^2; \mathbb{Z})$.

Proof. Consider $T^2 \times \mathbb{R}$ with the contact structure $\xi = \ker(\sin(2\pi z)\, dx + \cos(2\pi z)\, dy)$, where (x, y) are coordinates on T^2 and z is the coordinate on $\mathbb{R}$. When this contact structure is pulled back to the universal cover $\mathbb{R}^3$ it is contactomorphic to the standard contact structure, and hence it is tight (see Exercise 1.1.17). Thus the contact structure on $T^2 \times \mathbb{R}$ and any subset of it is tight. Consider $T^2 \times [0, \frac{1}{8}] \subset T^2 \times \mathbb{R}$. The foliation on $T^2 \times \{0\}$ is linear of slope ∞ and the foliation on $T^2 \times \{\frac{1}{8}\}$ is linear of slope -1. Thus we can perturb the boundary (as in Example 3.2.16) to be convex with two dividing curves on each boundary component of slope ∞ and -1 respectively. Denote this contact manifold $(T^2 \times [0,1], \xi)$. To show $(T^2 \times [0,1], \xi)$ is a basic slice we only need to check that it is minimally twisting (the other properties are clear from the construction). We note that in $T^2 \times [0,1]$ the $[0,1]$ factor just represents an interval and is not the z-coordinate on $T^2 \times \mathbb{R}$ (though it is a rescaling of it).

For this, we need a basic result about linear twisting of characteristic foliations. To this end, let $M_{r,r'} = T^2 \times [a,b]$ with the contact structure $\xi = \ker(\sin(2\pi z)\, dx + \cos(2\pi z)\, dy)$, where the slope of the characteristic foliation on $T^2 \times \{a\}$ and $T^2 \times \{b\}$ is r and r', respectively, and $0 < b - a < 1/2$. Note, the characteristic foliations on $T^2 \times \{t\}$ is linear and moving from r to r' in a left-handed manner as t goes from a to b.

Lemma 5.3.8. *If s is a slope not in the interval $[r, r']$ then there is no convex torus in $(M_{r,r'}, \xi)$ with dividing slope s.*

Remark 5.3.9. There is also no such linearly foliated torus as we could perturb it to be convex with dividing curves having the same slope.

Proof. If the lemma is not true then there is a convex torus T parallel to each boundary component of $M_{r,r'}$ with slope s not between r and r'. There is another (abstract) slope s' such that $s' < s < r' < r$ and the minimal integral vectors v and v' corresponding to slopes s and s' from an oriented basis of T^2. By "abstract" slope we just mean a slope of a curve on T^2 not necessarily related to dividing curves on a torus in $M_{r,r'}$ in any way.

Exercise 5.3.10. Prove such a slope s' exists
Hint: Consider the Farey graph, Section 4.2.

There is a linear diffeomorphism of T^2 taking s to 0 and s' to ∞.

Exercise 5.3.11. Show that this diffeomorphism sends r and r' to some negative slope.

Let ϕ be the corresponding diffeomorphism of $M_{r,r'}$. Note $\phi_* \xi$ is a subset of the contact structure $\ker(\sin(2\pi z)\, dx + \cos(2\pi z)\, dy)$, on $T^2 \times (0, \frac{1}{4})$.

Exercise 5.3.12. Prove this assertion.
Hint: The map ϕ is a linear map on the torus and hence $\phi_*\xi$ is a contact structure on $T^2 \times [0,1]$ that induces linear foliations on $T^2 \times \{\text{point}\}$ whose slopes rotate from $\phi(r)$ to $\phi(r')$. Now use Theorem 1.3.7.

Exercise 5.3.13. Show that $(T^2 \times (0, \frac{1}{4}), \ker(\sin(2\pi z)\, dx + \cos(2\pi z)\, dy))$ embeds in S^3 with the standard tight contact structure such that the x-direction maps to a meridian of an unknot and the y-direction maps to a longitude for the same unknot.
Hint: See Exercise 1.1.19.

From the previous two exercises we see that $\phi(M_{r,r'})$ with $\phi_*\xi$ embeds in S^3 with the standard contact structure. Moreover the slope of the characteristic foliation on $\phi(T)$ is 0. But from the construction of this embedding $\phi(T)$ bounds a solid torus such that the curve of slope 0 is a meridian for the torus. Thus a meridional disk for this solid torus with boundary a leaf in the characteristic foliation is an overtwisted disk, contradicting the tightness of the standard contact structure on S^3. □

We now return to the proof of Lemma 5.3.7. We left off trying to show that $(T^2 \times [0,1], \xi)$ is minimally twisting. Recall $(T^2 \times [0,1], \xi)$ is obtained from $(T^2 \times [0, \frac{1}{8}], \xi = \ker(\sin(2\pi z)\, dx + \cos(2\pi z)\, dy))$ by perturbing the boundary to be convex. We discuss the perturbation of $T^2 \times \{0\}$ more carefully (a similar discussion holds for $T^2 \times \{\frac{1}{8}\}$). There is some function $f : T^2 \to [-\delta, \delta]$ such that the graph of f in $T^2 \times \mathbb{R}$ is the perturbation of $T^2 \times \{0\}$ that makes it convex. Note that $f_t(p) = tf(p)$ for any $t \in (0,1]$ is also a function whose graph is a perturbation of $T^2 \times \{0\}$ making it convex. Let (M_t, ξ_t) be the contact manifold obtained from $T^2 \times [0, \frac{1}{8}]$ by perturbing $T^2 \times \{0\}$ by f_t (and similarly for $T^2 \times \{\frac{1}{8}\}$). Notice that M_t is contained in $T^2 \times [-t\delta, \frac{1}{8} + t\delta]$ and hence Lemma 5.3.8 shows that there are no convex tori (parallel to the boundary) in (M_t, ξ_t) with slope outside $[\frac{1}{\epsilon_t}, -1 + \epsilon_t]$ where ϵ_t is some small number depending on t and going to zero as t goes to zero (to see this recall the slope of the characteristic foliation on $T^2 \times \{0\}$ is ∞ and so for $T^2 \times \{r\}$ for r just less than 0 will have very large positive slope, and we have an analogous statement when r is just larger than $\frac{1}{8}$). Note there is a canonical way (up to isotopy) to identify M_t with $T^2 \times [0,1]$, we use t only to make precise the physical subset of $T^2 \times \mathbb{R}$ that we are talking about.

We now claim that for any $t \in (0,1]$ we can think of (M_1, ξ_1) as a subset of (M_t, ξ_t). More specifically there is a contactomorphism of (M_1, ξ_1) onto a subset of (M_t, ξ_t) that does not change the slopes of curves on the T^2 factor of M_t. Once this is proven we will see that $(M, \xi) = (M_1, \xi_1)$ is minimally twisting since if there were a convex torus T parallel to the boundary with slope s not in $[\infty, -1]$ then we could find such a torus (with slope s) inside (M_t, ξ_t) for any t contradicting our discussion in the previous paragraph.

To prove our claim we use a simple version of an important technique called "discretization of isotopy" (see Section 8.2 for the full description). For each $t \in (0,1]$ there is a vertically invariant neighborhood U_t of the graph of f_t in $T^2 \times \mathbb{R}$. For each t let $O'_t = \{t' \in (0,1] : \text{the graph of } f_{t'} \subset U_t\}$ and O_t be an open connected interval in O'_t containing t. Fixing t_0 we want to show that (M_1, ξ_1) is a subset of (M_{t_0}, ξ_{t_0}). If t_0 is in O_1 then the graph of f_{t_0} is in U_1 the vertically invariant neighborhood of T_1, the graph of $f = f_1$. Thus we can use the invariant neighborhood structure to find two tori T'_1 and T''_1 that are translates of T_1 in the product neighborhood structure such that the graph of f_{t_0} separates T'_1 and T''_1. See Figure 5.3.6. As in the proof of Lemma 5.2.1 we see that whether

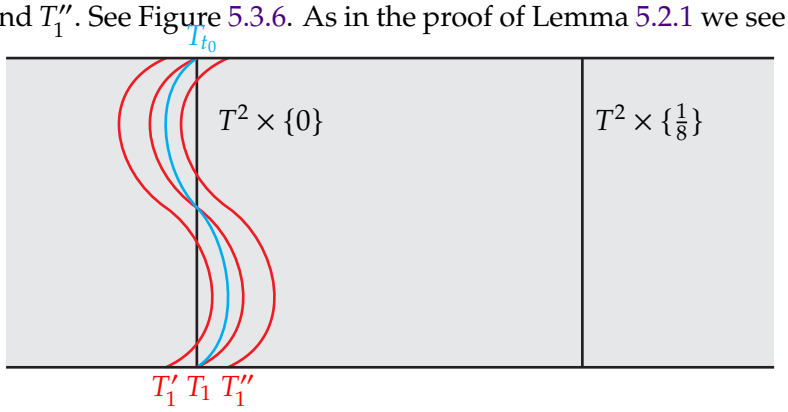

Figure 5.3.6. Part of $T^2 \times \mathbb{R}$ showing T_{t_0} is contained in an invariant neighborhood of T_1.

we cut $T^2 \times \mathbb{R}$ along T_1, T'_1 or T''_1 we will get contact manifolds isotopic to (M_1, ξ_1). Since one of T'_1 or T''_1 is inside (M, ξ_{t_0}) we see that (M, ξ_1) can be thought of as a subset of (M_{t_0}, ξ_{t_0}). We can also think of (M_{t_0}, ξ_{t_0}) as a subset of (M_1, ξ_1) since one of T'_1 or T''_1 will be outside of M_{t_0}. (Recall, we are only discussing altering one boundary component but we must alter the other one in a similar fashion.) Now suppose t_0 is not in O_1 but that $O_{t_0} \cap O_1 \neq \emptyset$. Let t_1 be a point in the intersection. As above (M_1, ξ_1) can be thought of as a subset of (M_{t_1}, ξ_{t_1}) and (M_{t_1}, ξ_{t_1}) can be though of as a subset of (M_{t_0}, ξ_{t_0}).

Exercise 5.3.14. Finish this line of argument to show that for any fixed $t_0 \in (0,1]$ we may always think of (M, ξ) as a subset of (M_{t_0}, ξ_{t_0}).
Hint: For a fixed t_0 the interval $[t_0, 1]$ is compact so it can be covered by a finite number of the O_t's.

Exercise 5.3.15. Show that given any subset $T^2 \times [a,b]$ of $(T^2 \times \mathbb{R}, \xi = \ker(\sin(2\pi z)\,dx + \cos(2\pi z)\,dy))$ where $b - a < 1$ and the slopes of the characteristic foliations on $T^2 \times \{a\}$ and $T^2 \times \{b\}$ form a basis for $\mathbb{Z}^2$, one can perturb the boundary components to be convex to obtain a basic slice.

We now compute the Euler class of (M, ξ). Let A be a vertical annulus. That is A is a vertical curve in the torus T^2 times $[0,1]$. We can assume the boundary of L are Legendrian ruling curves in ∂M. Perturb A to be convex. From the proof of Lemma 5.3.3 we

know that there are two dividing curves on A that run from one boundary component to the other. Thus Lemma 3.5.3 implies that $e(\xi)(A) = 0$. Now if A' is a horizontal annulus we can assume that $A' \cap (T^2 \times \{0\})$ is a Legendrian divide and the other boundary component is a Legendrian ruling curve that intersects the dividing curves on $\partial(T^2 \times [0,1])$ twice. Now make A' convex. From the discussion in Section 3.8 and the Giroux tightness criterion for convex surfaces, Theorem 3.6.1, we see that A' has exactly one dividing curve beginning and ending on $A' \cap (T^2 \times \{1\})$. Thus from Lemma 3.5.3 we see that $e(\xi)(A') = \pm 1$. From this we can conclude that the Poincaré dual of $e(\xi)$ is $\begin{pmatrix} \pm 1 \\ 0 \end{pmatrix} \in H_1(T^2; \mathbb{Z})$ and we note that $\begin{pmatrix} \pm 1 \\ 0 \end{pmatrix} = \mp \left(\begin{pmatrix} -1 \\ 1 \end{pmatrix} - \begin{pmatrix} 0 \\ 1 \end{pmatrix} \right) = \mp(v_1 - v_0)$. We do not actually need to know the sign here. To see this consider the map $\Psi(x, y, t) = (-x, -y, t)$ of $T^2 \times [0,1]$ to itself. The map Ψ preserves the dividing curves on $\partial(T^2 \times [0,1])$ and $\Psi_* \xi$ is minimally twisting, thus $\Psi_* \xi$ is a basic slice. Also note that acting on $H_1(T^2; \mathbb{Z})$ we see $\Psi_* \begin{pmatrix} \pm 1 \\ 0 \end{pmatrix} = \begin{pmatrix} \mp 1 \\ 0 \end{pmatrix}$. Thus $(T^2 \times [0,1], \xi)$ and $(T^2 \times [0,1], \Psi_*(\xi))$ are distinct (up to isotopy) basic slices realizing the claimed relative Euler classes. □

Exercise 5.3.16. Identify the exact relative Euler class of $(T^2 \times [0,1], \xi)$ in the proof above.

Exercise 5.3.17. Show that the basic slice you get from perturbing the boundary of $(T^2 \times [\frac{1}{2}, \frac{5}{8}], \xi = \ker(\sin(2\pi z)\, dx + \cos(2\pi z)\, dy))$ to be convex will give the basic slice $(T^2 \times [0,1], \Psi_* \xi)$ from the proof.

Examining our model (M, ξ) for a basic slice we can prove our corollary about the slopes that can be realized by dividing slopes in a basic slice.

Proof of Corollary 5.3.2. All the existence statements are clear from the model for the basic slice constructed at the end of the proof of the previous lemma. The non-existence part follows from Lemma 5.3.8 except for the case of a linear foliation of slope s_0 or s_1. □

5.4. Bypasses and basic slices again

Bypasses are the fundamental way of going from one convex surface to another and we will see that a "bypass attachment" to a convex torus with the appropriate dividing curves will yield a basic slice.

Let Σ be a convex surface and α a Legendrian arc in Σ that intersects the dividing curves Γ_Σ in 3 points p_1, p_2, p_3 (where p_1, p_3 are the end points of the arc). Then a *bypass for Σ (along α)*, see Figure 5.4.7, is a convex disk D with Legendrian boundary such that

(1) $D \cap \Sigma = \alpha$,

(2) $\mathrm{tb}(\partial D) = -1$,

(3) $\partial D = \alpha \cup \beta$,

(4) $\alpha \cap \beta = \{p_1, p_3\}$ are corners of D and elliptic singularities of D_ξ.

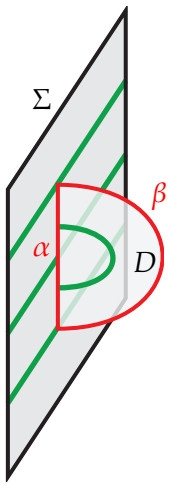

Figure 5.4.7. A piece of Σ and the bypass D.

After isotopy we can assume (by Giroux flexibility theorem 3.4.1) that the characteristic foliation on D is given in Figure 5.4.8.

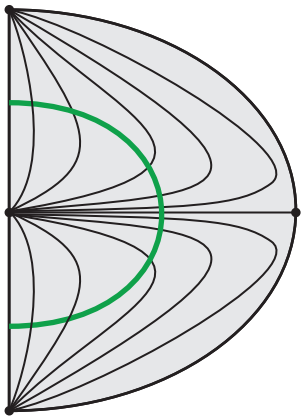

Figure 5.4.8. Standard foliation on a bypass.

If there is a natural orientation on the disk D then the sign of the singularity on the interior of α is called the *sign of the bypass*.

Theorem 5.4.1 (Honda 2000, [**Hon00a**]). *Let Σ be a convex surface and D a bypass for Σ along $\alpha \subset \Sigma$. Inside any open neighborhood of $\Sigma \cup D$ there is a (one sided) neighborhood $N = \Sigma \times [0,1]$ of $\Sigma \cup D$ with $\Sigma = -\Sigma \times \{0\}$ (where N is oriented as the product of Σ and $[0,1]$) such that Γ_Σ*

is related to $\Gamma_{\Sigma\times\{1\}}$ *as shown in Figure 5.4.9. We say* $\Sigma' = \Sigma \times \{1\}$ *is* obtained from Σ by attaching a bypass from the front.

If we have the same setup except that $\Sigma = \Sigma \times \{1\}$ *then* Γ_Σ *is related to* $\Gamma_{\Sigma\times\{1\}}$ *as shown in Figure 5.4.9. We say* $\Sigma' = \Sigma \times \{1\}$ *is* obtained from Σ by attaching a bypass from the back.

If one says that Σ' is obtained from Σ by attaching a bypass, it is assumed that the bypass is attached from the front.

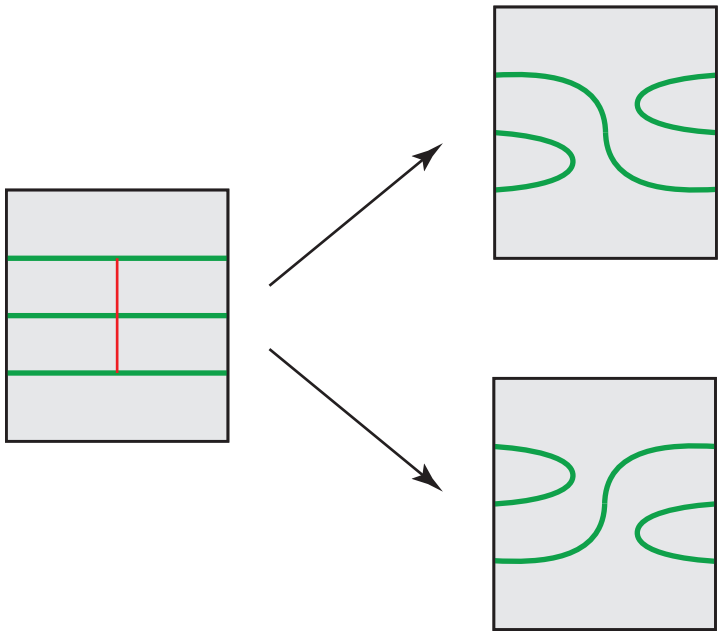

Figure 5.4.9. Result of a bypass attachment. The original surface Σ with attaching arc α, left. The surface Σ' obtained from a bypass attachment from the front is shown on the upper right, and the attachment from the back is shown on the lower right.

Remark 5.4.2. If the endpoints of the attaching arc agree, that is $p_1 = p_3$, then the bypass is called *degenerate*.

Exercise 5.4.3. Show a degenerate bypass can be attached to a surface and have a similar effect on the dividing curves as a regular bypass. What exactly is the effect on the dividing curves? (Maybe read the following proof first.)

Proof. There are many ways to try to prove this theorem and the reader is encouraged to think about their own way of showing this. The main idea is to use the Edge Rounding Lemma 3.8.3. With that said, we give an argument for the theorem. Though it might seem a bit convoluted, the goal of this proof is to try to only round one edge at a time. (If the reader pursues the most obvious proof they will have to deal with three surfaces coming together in a triple point like three coordinate planes in $\mathbb{R}^3$.)

Using the transverse contact vector field v we get by definition of Σ being convex, we can construct a vertically invariant (one-sided) neighborhood $\Sigma \times [0, \epsilon]$ of Σ with D attached to $\Sigma \times \epsilon$. To achieve this we push D forward using the flow of v. Now extend α in $\Sigma \times \{\epsilon\}$ to the simple closed curve in Figure 5.4.10 and let A be a neighborhood of α' in

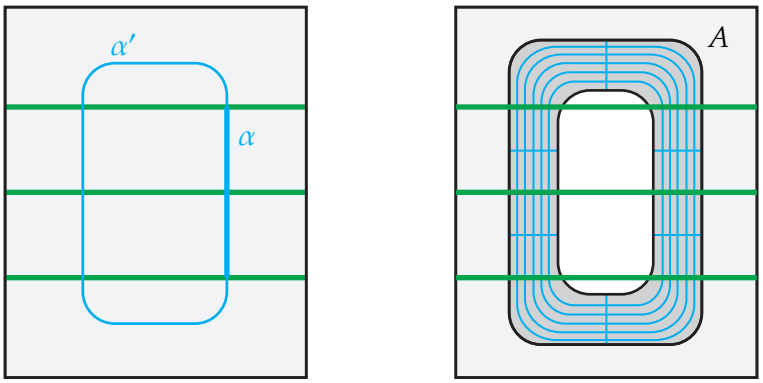

Figure 5.4.10. The arc α', left. The shaded region on the right is the annulus A.

$\Sigma \times \{\epsilon\}$ that is standardly ruled by curves parallel to α'. Use v to flow α' forward to get an annulus A' and flowing D by v again we can assume that D is attached to the top of A' to obtain the annulus A'' seen in Figure 5.4.11.

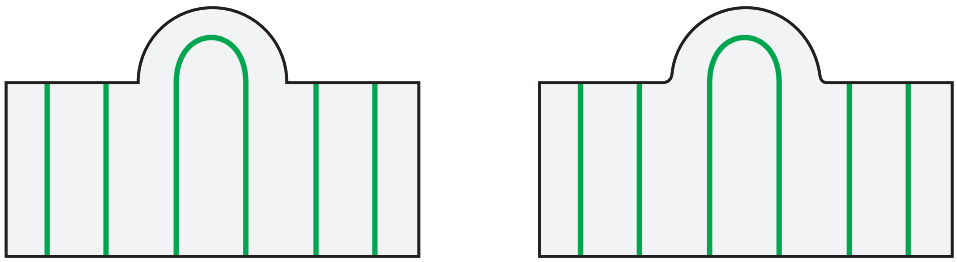

Figure 5.4.11. The annulus A'', left, and the annulus B, right. (The right and left sides of each picture are identified.)

Exercise 5.4.4. Show we can round the corners of A'' by a C^0 small isotopy to obtain the annulus B that has smooth Legendrian boundary. See Figure 5.4.11.
Hint: Show this situation can be modeled as follows: Let Q be three quadrants in the xy-plane in $\mathbb{R}^3$. Consider the radially symmetric tight contact structure on $\mathbb{R}^3$. Show, after possibly perturbing A'' rel boundary, a neighborhood of the corner of A'' is contactomorphic to a neighborhood of the origin in $\mathbb{R}^3$ so that a neighborhood of the corner in A'' is taken to Q. Now in this explicit model prove the corner can be rounded.

The annulus B is convex so there is a contact vector field w for B. Moreover, we can assume that w is tangent to $\Sigma \times \{\epsilon\}$ along A and the flow of α' by w produces the Legendrian ruling of A.

Exercise 5.4.5. Show we can find a w with such properties.

Let $C = B \times [-\delta, \delta]$ be a vertically invariant neighborhood of B obtained from B by the flow of w. The boundary of C not identified with part of the boundary of $\Sigma \times [0, \epsilon]$ (this is called the *upper boundary*) is shown on the left in Figure 5.4.12. When the corners on

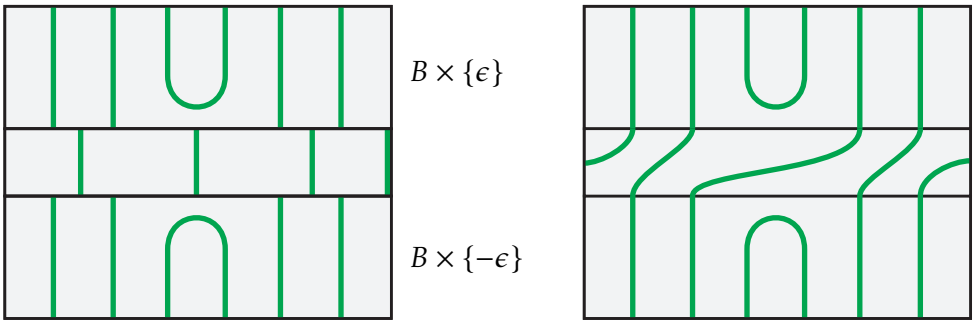

Figure 5.4.12. The upper boundary of ∂C, left. Upper boundary of C after corners are rounded, right. (The left and right sides of each picture are identified. The middle strip in both pictures is the upper boundary of ∂B times an interval.

these boundary components are rounded you get the picture on the right in Figure 5.4.12. Let $N' = \Sigma \times [0, \epsilon] \cup C$. Figure 5.4.13 shows the upper boundary of N'. Let N be N' with

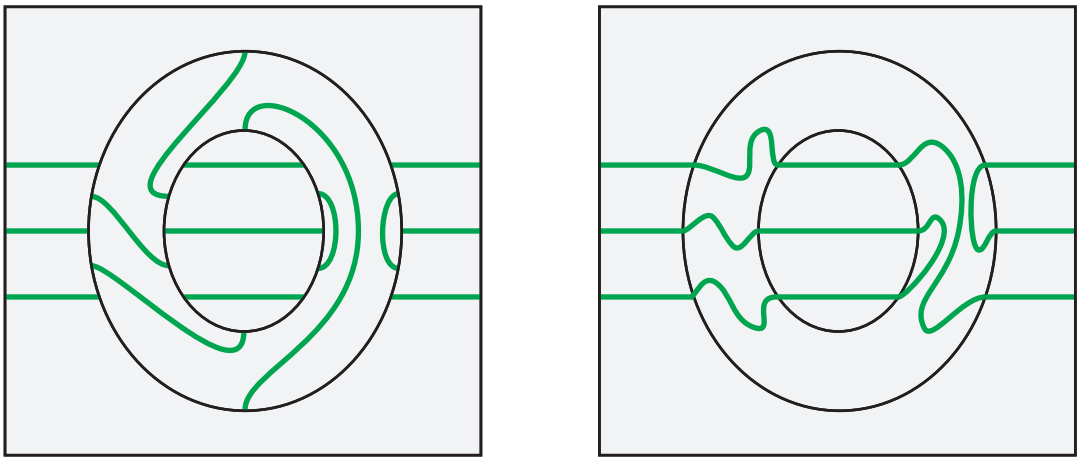

Figure 5.4.13. Top view of N', left. Top view of N, right.

corners rounded. Then the upper boundary of N is shown in Figure 5.4.13 and N is a neighborhood of $\Sigma \cup D$. This completes the proof the theorem. □

Exercise 5.4.6. If Σ' be obtained from Σ by a bypass attachment then show

$$\chi(\Sigma'_+) - \chi(\Sigma'_-) = \chi(\Sigma_+) - \chi(\Sigma_-).$$

Theorem 5.4.7 (Honda 2002, [Hon02]). *Let Σ be a convex surface and Σ' be obtained from Σ by a bypass attachment in a tight contact manifold. Then*

(1) $\Gamma_{\Sigma'} = \Gamma_\Sigma$ *(this is called a trivial bypass attachment),*

(2) $|\Gamma_{\Sigma'}| = |\Gamma_\Sigma| + 2$,

(3) $|\Gamma_{\Sigma'}| = |\Gamma_\Sigma| - 2$,

(4) $\Gamma_{\Sigma'}$ *is obtained from* Γ_Σ *by a positive Dehn twist about some curve in* Σ,

(5) $\Gamma_{\Sigma'}$ *is obtained from* Γ_Σ *by a "mystery move", see Figure 5.4.14.*

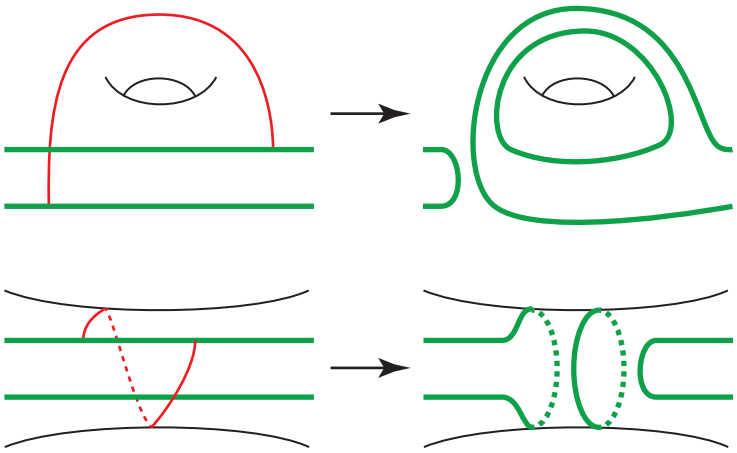

Figure 5.4.14. The Mystery Moves.

Proof. Let α be the arc of attachment and p_1, p_2, p_3 the points where α intersects the dividing curves. As above we take the end points of α to be p_1 and p_3. Let γ_i be the component of the dividing set in which p_i sits.

Case (I): all the γ_i's are distinct. In this case it is easy to see that γ_1 is joined to γ_2, γ_2 is joined to γ_3 and γ_3 is joined to γ_1. So in Σ all the γ_i's are distinct but on Σ' they have all been joint. Thus Conclusion (3) of the theorem holds.

Case (II): all the γ_i's are the same. There are six possible configurations for the bypass here. See Figure 5.4.15. In Configurations 2., 3. and 4. we see that we have increased the number of dividing curves by two so the Conclusion (2) of the theorem holds. The figure shows regions where there might be topology, if there were no topology in any of these regions (by which we mean that the red and green arcs cobound a disk) then a contractible dividing curve is formed. Thus this cannot happen in a tight contact structure so we will never see such bypasses. In Configurations 1., 5. and 6. if all regions do not

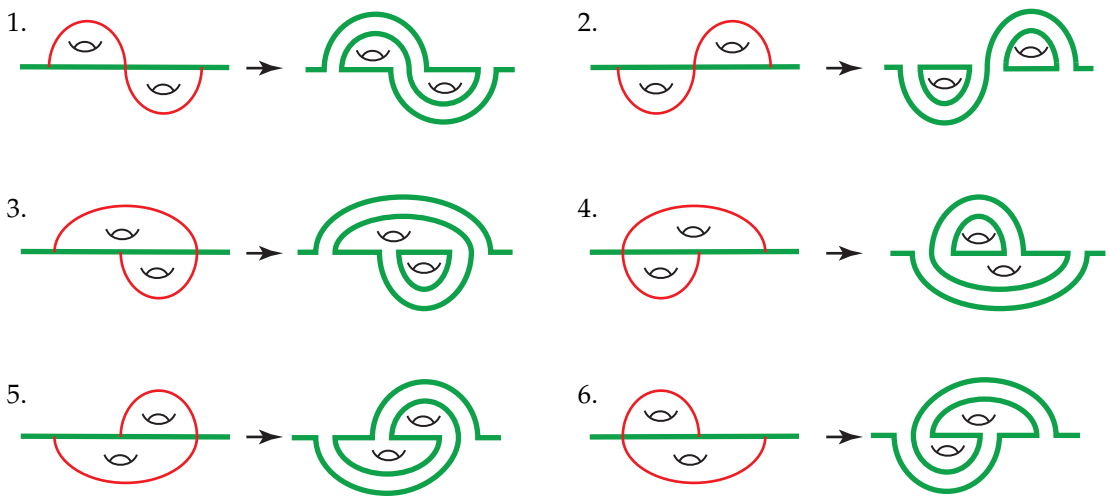

Figure 5.4.15. The six configurations in Case (II).

have topology in them, then the dividing curves after the bypass attachment are isotopic to the dividing curves before the attachment. So we have a trivial bypass attachment and Conclusion (1) of the theorem holds. Finally, if all the regions have topology, then attaching the bypass is the same as applying a Dehn twist to the dividing curves. That is Conclusion (4) of the theorem holds.

Exercise 5.4.8. Show Conclusion (4) of the theorem holds in these cases.
Hint: See Figure 5.4.16 for Configuration (1). The other configurations are similar.

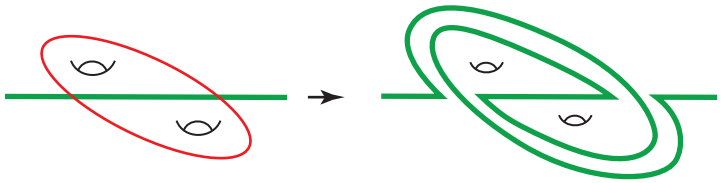

Figure 5.4.16. A right-handed Dehn twist along the curve on the left changes the dividing curves as shown.

Case (III): $\gamma_1 = \gamma_3$ but γ_2 is distinct. In this situation one easily sees conclusion (4) of the theorem holds. See Figure 5.4.17. If the endpoints of the attaching arc are switched from what is shown in Figure 5.4.17 then we see conclusion (5).

Case (IV): If $\gamma_1 \neq \gamma_3$ but γ_2 agrees with γ_1 or γ_2. As similar analysis as to Case (II) show either conclusion (1), (4) or (5) happens. □

We now apply the above theorem to see what happens when we attach bypasses to low genus surfaces.

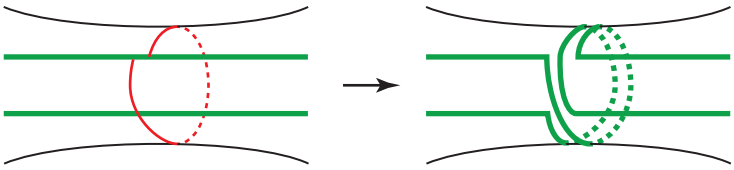

Figure 5.4.17. The configuration in Case (III).

Example 5.4.9. If $\Sigma = S^2$ is a convex sphere in a tight contact manifold then any bypass attachment must be trivial! This is clear since Γ_Σ has only one component. See Figure 5.4.15.

Example 5.4.10. If $\Sigma = T^2$ is a convex torus in a tight contact manifold then the situation in Theorem 5.4.7 also simplifies. Specifically, we can have:

(1) Trivial bypass attachment (if the bypass attaching arc intersects only one dividing curve on Σ and does not wind around any topology).

(2) Attachment that increases the number of dividing curves (if the bypass attaching arc intersects only one dividing curve on Σ and winds around some topology).

(3) Attachment that decreases the number of dividing curves (if the bypass attaching arc intersects three different dividing curves on Σ)

(4) Attachment that performs a right-handed Dehn twist (if the attaching arc involves only two dividing curves of Σ). *Note:* This can only happen when $|\Gamma_\Sigma| = 2$.

We note that in the first two cases, the attaching arc from the bypass must have consecutive intersections with a single dividing curve more than once. When this does not happen, we say the intersections of the bypass with the dividing curves are *efficient* and in this case, only the last two cases can happen.

5.4.1. Basic slices again. The last case in the example above is going to be very important for our use of convex surfaces to classify contact structures so we elaborate on this further in the following theorem which we will generalize shortly.

Theorem 5.4.11 (Honda 2000, [**Hon00a**])**.** *Let T be a convex torus in a tight contact structure. Assume that T is standardly foliated with dividing slope ∞ and ruling slope r with $-1 \leq r < 0$. Assume there is a bypass D attached to T along a ruling curve. There is a (one-sided) neighborhood $N = T^2 \times [0,1]$ of $T \cup D$ with $T \times \{0\} = T$ such that*

(1) *If $|\Gamma_T| > 2$ then $|\Gamma_{T^2\times\{1\}}| = |\Gamma_T| - 2$ and the dividing slope is unchanged.*

(2) *If $|\Gamma_T| = 2$ then the dividing slope on $T^2 \times \{1\}$ is -1 and $|\Gamma_{T^2\times\{1\}}| = 2$.*

Moreover in Case (2), N is a basic slice.

Proof. Part (1) is immediate from Theorem 5.4.7. Part (2) is also obvious if $r > -1$, see Figure 5.4.18.

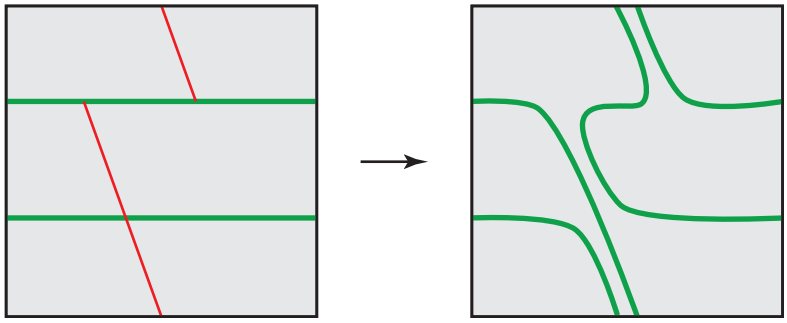

Figure 5.4.18. A bypass attached along a ruling curve slope r with $-1 \leq r < 0$.

All conditions for a basic slice are clearly satisfied except for minimal twisting. To show minimal twisting we embed N into a standard model where we know the twisting is minimal. To this end consider $T^2 \times \mathbb{R}$ with the contact structure $\xi = \ker(\sin(2\pi z)\, dx + \cos(2\pi z)\, dy)$, used in the proof of Lemma 5.3.7 concerning basic slices. We can perturb $T_0 = T^2 \times \{0\}$ and $T_{\frac{1}{8}} = T^2 \times \{\frac{1}{2}\}$ to be convex with two dividing curves each and having slope ∞ and -1, respectively. We further perturb these tori so that the characteristic foliations are standard with both having ruling slope $-\frac{q}{p}, p > q > 0$. Let A be a convex annulus between these two tori whose boundary is a ruling curve on each of the tori. So $\partial A \cap T_i$ is a $(p, -q)$-curve on T_i. The dividing curves on T_0 are $(0, 1)$-curves. So by the discussion in Section 4.1 concerning curves on tori we know

$$\partial A \cap \Gamma_{T_0} = 2 \left| \frac{-q}{p} \cdot \frac{1}{0} \right| = 2p.$$

Similarly

$$\partial A \cap \Gamma_{T_{\frac{1}{8}}} = 2 \left| \frac{-q}{p} \cdot \frac{-1}{1} \right| = 2(p - q).$$

Since $q \neq 0$, we see that $\partial A \cap T_0$ intersects Γ_A more times than $\partial A \cap T_{\frac{1}{8}}$. From Lemma 3.8.1 we know that the dividing curves Γ_A intersect the boundary component of $\partial_0 A = \partial A \cap T_0$, $2p$ times, and the other boundary component $\partial_1 A = \partial A \cap T_1$, $2(p-q)$ times. Since we are in a tight contact structure Γ_A consists of arcs and possibly circles parallel to the boundary of A. Since $p > p - q$ we see that at least one arc with one boundary component on $\partial_0 A$ must have its other endpoint on $\partial_0 A$ too. Thus this arc a, together with an arc on $\partial_0 A$ bounds a disk D in A. If this disk contains no other components of Γ_A then we may use the Giroux Flexibility, Theorem 3.4.1, to realize a characteristic foliation on A that on a disk slightly larger than D is the foliation shown in Figure 5.4.8. Thus we have a bypass on A for T_0; moreover, this bypass is entirely contained in the region $T^2 \times [0, 1/8]$. Attaching this bypass to T_0 will result in a region contactomorphic to N contained in $T^2 \times [0, 1/8]$.

Exercise 5.4.12. Prove this last statement.

By Lemma 5.3.8 this is minimally twisting so N must also be minimally twisting.

We are left to consider the case when $r = -1$. In this case the argument is as above except the bypass is *degenerate*. As indicated via Exercise 5.4.3 this makes no difference and thus the conclusions of the proof still hold. □

We now state a generalization of the previous theorem that tells us how to attach bypasses to arbitrary tori with two dividing curves. While this is clearly a corollary of the previous theorem, it is important enough in its own right to be called a theorem.

Theorem 5.4.13. *Let T be a convex torus with two dividing curves of slope s and characteristic foliation in standard form, see Example 3.4.4, and ruling slope $r \neq s$. Suppose D is a bypass for T that can be attached from the front side along a ruling curve. If T' is the convex surface that results after attaching the bypass D to T, then T is convex with two dividing curves of slope s' where s' is the point in the interval $[s, r]$ (in the Farey graph) that is closest to r connected to s by an edge.*

Given the same setup with D attached to the back side of T, then the conclusion is the same except s' is the point in the interval $[r, s]$ that is closest to r connected to s by an edge.

Proof. We will only consider the case when $s = \infty$ and the bypass is attached from the front, with the other cases immediately following by a change of basis (and for bypasses attached from the back, an orientation reversing change of basis).

For $r \in [-1, 0)$ notice that Theorem 5.4.11 gives the desired result as -1 is the point in $[\infty, r]$ closest to r with an edge to ∞. Now suppose $r \in [n, n+1)$ for some integer n. There is a change of basis that fixes ∞ and sends n to -1. It is easy to see that $n+1$ goes to 0 under this change of basis. In this basis r is in $[-1, 0)$. So from the case already considered, we know attaching the bypass will result in a convex torus with dividing slope -1. Changing back to the original basis the next dividing set has slope n and it is clear that n is the point closest to r in $[\infty, r]$ with an edge to ∞ (note the only points in the Farey graph with an edge to ∞ are the integers). This completes the proof. □

5.4.2. Finding bypasses. We have seen that bypasses allow you to understand how convex surfaces change. In the proof of Theorem 5.4.11 we saw how to find a bypass in a specific situation. We now discuss how to formalize this as a way to find bypasses in other particular situations.

Lemma 5.4.14. *Let Σ be a convex surface and Σ' be a convex surface with Legendrian boundary such that one component of $\partial\Sigma'$ a subset of Σ. Moreover, assume $\Sigma' \cap \Sigma \subset \partial\Sigma'$. If $\Gamma_{\Sigma'}$ has an outermost "boundary parallel" dividing curve γ and $|\Gamma_{\Sigma'}| \neq 1$ then Σ' may be isotoped rel boundary so that γ is isotopic in Σ' to a Legendrian curve β such that the disk β cuts off from Σ' is a bypass for Σ along part of $\partial\Sigma'$.*

An arc properly embedded in a surface with boundary is called *boundary parallel* if one of the components of the complement of the arc is a disk. If the arc is part of a dividing set then we say it is *outermost* if the disk it separates off contains no other components of the dividing set.

Remark 5.4.15. Because of this lemma, boundary parallel dividing curves are frequently called bypasses. This is an abuse of language, but should not cause confusion if one is careful. One should be careful as there are extra hypotheses in the lemma (that is $|\Gamma_{\Sigma'}| \neq 1$), but this is not essential as long as Σ' is not a disk or an annulus due to the Super Legendrian Realization Principle, that is Lemma 3.4.7.

Exercise 5.4.16. Use the Legendrian Realization Principle to prove Lemma 5.4.14.
Hint: See the proof of Theorem 5.4.11.

We now consider two of the most used versions of the above lemma.

Lemma 5.4.17. *Suppose Σ and Σ' are surfaces as in Lemma 5.4.14. Assume further that Σ' is a disk. If $tb(\partial\Sigma') < -1$ then there is a bypass for Σ.*

Proof. If $\mathrm{tb}(\partial\Sigma') = -n$ then there will be n arcs in $\Gamma_{\Sigma'}$. At least one of them must be boundary parallel and outermost. So if $n > 1$ Lemma 5.4.14 finishes the proof. □

The following lemma formalizes the argument we made at the end of the proof of Theorem 5.4.11.

Lemma 5.4.18 (Imbalance Principle: Honda 2000, [**Hon00a**])**.** *Suppose Σ and Σ' are surfaces as in Lemma 5.4.14. Moreover, assume that $\Sigma' = S^1 \times [0,1]$ with $S^1 \times \{0\} \subset \Sigma$ (and of course $\partial\Sigma'$ Legendrian). If $tw(S^1 \times \{0\}, \Sigma') < tw(S^1 \times \{1\}, \Sigma') < 0$ then there is a bypass for Σ.*

Proof. It is clear that $\Gamma_{\Sigma'}$ will have more than one component. The dividing set $\Gamma_{\Sigma'}$ will intersect $S^1 \times \{i\}$, $-2tw(S^1 \times \{i\}, \Sigma')$ times. Thus not all arc starting at $S^1 \times \{0\}$ can run to $S^1 \times \{1\}$. So at least one must be boundary parallel and outermost. Thus Lemma 5.4.14 finishes the proof. □

5.5. Contact structures on thickened tori

In this section we classify minimally twisting contact structures on $T^2 \times [0,1]$ and discuss many of their properties.

5.5.1. Executive summary of main results. Recall a contact structure on $T^2 \times [0,1]$ with convex boundary is called minimally twisting if the slope of the dividing curves on any convex torus parallel to the boundary is between s_0 and s_1, the slopes of the dividing curves on $T_0 = T \times \{0\}$ and $T_1 = T \times \{1\}$, respectively. Also recall $Tight_{min}(T^2 \times [0,1], s_0, s_1)$

is the set of minimally twisting tight contact structures on $T^2 \times [0,1]$ with convex boundary and each boundary component having two dividing curves with slope s_0 on T_0 and s_1 on T_1. We have the following two cases for minimally twisting contact structures. The first theorem considers thickened tori with the same dividing slope on the back and front boundary components.

Theorem 5.5.1 (Giroux 2000, [Gir00]; Honda 2000, [Hon00a]). *There is a bijection*

$$h : Tight_{min}(T^2 \times [0,1], s_0, s_0) \to \mathbb{Z}.$$

The map h is called the "holonomy map". Moreover, up to contactomorphism, there is a unique tight contact structure on $T^2 \times [0,1]$ with the given boundary data.

Recall from Section 4.3 that we can write a rational number r in terms of its continued fraction

$$r = [a_0; a_1, \dots, a_n] = a_0 - \cfrac{1}{a_1 - \cfrac{1}{\dots - \cfrac{1}{a_n}}},$$

where the $a_i \leq -2$ are integers for $i > 0$ and a_0 can be any integer. Also, recall that the semicolon is replaced by a comma if $a_0 \leq -2$.

Theorem 5.5.2 (Giroux 2000, [Gir00]; Honda 2000, [Hon00a]). *Suppose that $r < -1$ and has continued fraction expansion $[a_0, \dots, a_n]$. Then*

$$|Tight_{min}(T^2 \times [0,1]; r, -1)| = |(a_0+1)(a_1+1)\cdots(a_{n-1}+1)a_n|.$$

That is there are $|(a_0+1)(a_1+1)\cdots(a_{n-1}+1)a_n|$ contact structures up to isotopy in $Tight_{min}(T^2 \times [0,1]; r, -1)$. Moreover, these contact structures are also distinct up to contactomorphism and are distinguished by their relative Euler classes, see Corollary 5.5.13 for the computation of the Euler classes.

In Section 4.3 we discussed continued fraction expansions, so it is easy to apply this theorem.

Example 5.5.3. To compute the number of elements in $\text{Tight}_{min}(T^2 \times [0,1]; -21/8, -1)$ we note that $-21/8 = [-3,-3,-3]$ so

$$|\,\text{Tight}_{min}(T^2 \times [0,1]; -21/8, -1)| = 2 \cdot 2 \cdot 3 = 12.$$

If we have a thickened torus with dividing curves having slopes not satisfying the hypothesis of this theorem, we can still determine, as explained in the next examples, the number of minimally twisting contact structures.

Example 5.5.4. We determine the number of elements in $\text{Tight}_{min}(T^2 \times [0,1]; (n+1)/n, 2)$. To this end, we note that the linear diffeomorphism

$$\begin{pmatrix} -1 & 1 \\ -1 & 0 \end{pmatrix}$$

sends $(n+1)/n$ to $-n$ and 2 to -1. This diffeomorphism induces a diffeomorphism of $T^2 \times [0,1]$ that identifies $Tight_{min}(T^2 \times [0,1]; (n+1)/n, 2)$ with Tight$(T^2 \times [0,1]; -n, -1)$. So the theorem tells us that

$$|Tight_{min}(T^2 \times [0,1]; (n+1)/n, 2)| = n - 1.$$

Example 5.5.5. As another example, we determine the number of elements in Tight$_{min}(T^2 \times [0,1]; -(2+3n)/(3+4n), -1/2)$. Note that the linear diffeomorphism

$$\begin{pmatrix} -1 & -1 \\ 0 & -1 \end{pmatrix}$$

sends $-(2+3n)/(3+4n)$ to $-(2+3n)(1+n)$ and $-1/2$ to -1. Thus as above we can identify Tight$_{min}(T^2 \times [0,1]; -(2+3n)/(3+4n), -1/2)$ with Tight$_{min}(T^2 \times [0,1]; -(2+3n)/(1+n), -1)$. One may easily compute that $-(2+3n)/(1+n) = [-3, -(n+1)]$ and so we know

$$|Tight_{min}(T^2 \times [0,1]; -(2+3n)/(3+4n), -1/2)| = 2(n+1).$$

Exercise 5.5.6. Compute the number of elements in Tight$_{min}(T^2 \times [0,1]; 7/5, 2)$
Hint: Find a linear diffeomorphism of T^2 that sends ∞ to 1 and -1 to 2, then invert it and proceed as in the previous examples. It is clear why -1 goes to -2 by why did we send ∞ to 1?

Exercise 5.5.7. Given any two sets of curves Γ_0 and Γ_1 with distinct slopes we can find a linear diffeomorphism of T^2 inducing a diffeomorphism of $T^2 \times [0,1]$ that arranges their slopes to satisfy the hypothesis of the theorem.

Remark 5.5.8. This exercise shows that the previous two theorems classify all minimally twisting contact structures on $T^2 \times [0,1]$. Non-minimally twisting contact structures on $T^2 \times [0,1]$ will be considered in Section 5.9. In Section 8.4 we will consider the situation when the dividing curves on the boundary components have more than two dividing curves.

Exercise 5.5.9. Show that if ξ is a tight contact structure on $T^2 \times [0,1]$ with convex boundary that is not minimally twisting, then any slope can be realized as the slope of a convex torus parallel to the boundary.
Hint: It might help to read the proof of Theorem 5.5.2 first.

Before moving on we rephrase Theorem 5.5.2 in a way that can be useful in applications. To do so we need to discuss decorated paths in the Farey graph. Given a minimal path in the Farey graph, see Section 4.4, we call it a *decorated path* if each edge has been given a + or − sign. We say two decorations of a path P differ by *shuffling in continued fraction blocks* if they have the same number of + signs (and hence − signs) in each continued fraction block. Notice that this means that the ordering of the signs in a continued faction block is unimportant. Shuffling in continued fraction blocks gives an equivalence relation on decorated paths.

Theorem 5.5.10. *The contact structures in* $\text{Tight}_{min}(T^2 \times [0,1]; s_0, s_1)$ *are in one-to-one correspondence with equivalence classes of decorations in a minimal path in the Farey graph from* s_0 *clockwise to* s_1.

It can sometimes be much easier to use this theorem than to change coordinates and use Theorem 5.5.1.

Example 5.5.11. We use Theorem 5.5.10 to compute the number of elements in $\text{Tight}_{min}(T^2 \times [0,1]; 5/19, 1)$. To this end, we locate 5/19 and 1 on the Farey graph and construct a minimal path. See Figure 5.5.19. Notice that there are two continued fraction blocks in the

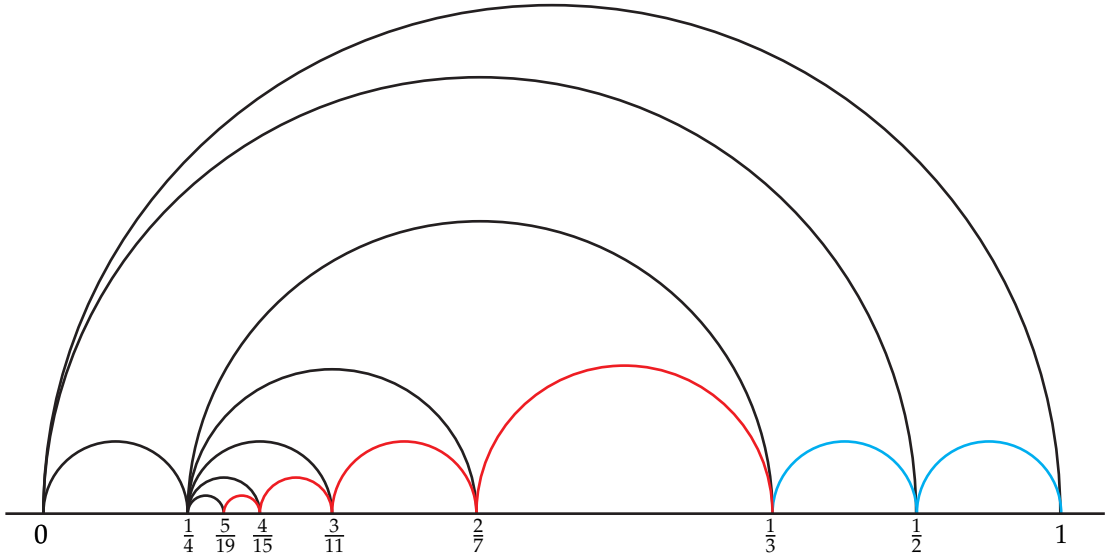

Figure 5.5.19. A minimal path in the Farey graph from 5/19 clockwise to 1. The continued fraction blocks are represented in different colors. (Some of the distances are not to scale.)

path from 5/19 to 1, with the first having 4 edges and the second having 2. Since there are 5 ways to decorate the edges of a continued fraction block with 4 edges and 3 ways for the one with 2 edges, we see that

$$|Tight_{min}(T^2 \times [0,1]; 5/19, 1)| = 15.$$

Maybe give a few homework problems on this too?

Given any decorated path P in the Farey graph from s_0 clockwise to s_1 one can construct a contact structure on $T^2 \times [0,1]$. Indeed, suppose the path P has n edges, denoted $e_1, \cdots, e_n$ as we move from s_0 to s_1, and the vertices of e_i are e_i^0 and e_i^1 (moving clockwise from the first vertex to the second). Now on $T^2 \times [(i-1)/n, i/n]$ consider the basic slice with boundary data e_i^0 and e_i^1 and having relative Euler class $\pm(e_i^1 - e_i^0)$ where the sign is determined by the sign on the edge. See Section 5.3 for the discussion of basic slices. The union of these basic slices gives a contact structure ξ_P on $T^2 \times [0,1]$.

Recall, in Section 4.4 we discussed shortening a non-minimal path in the Farey graph. We can a shortening of a decorated path *consistent* if the two edges that are replaced by a single edge have the same sign, and in this case we label the new edge with the sign of the two edges that are removed. The theorems above tell us when a, possibly non-minimal, path P in the Farey graph corresponds to a tight contact structure.

Corollary 5.5.12. *Let P be a decorated path in the Farey graph. The contact structure ξ_P on $T^2 \times [0,1]$ constructed above is tight if and only if the path can be consistently shortened to a minimal decorated path.*

In the proof of Theorems 5.5.2 and 5.5.10 we will see that given an element in $\xi \in \text{Tight}_{min}(T^2 \times [0,1]; s_0, s_1)$ there is a minimal decorated path P in the Farey graph from s_0 clockwise to s_1 such that $\xi = \xi_P$, and P is unique upto shuffling in continued fraction blocks. With this notation in hand, we can compute the relative Euler class of a minimally twisting contact structure.

Corollary 5.5.13. *Given a contact structure ξ_P in $\text{Tight}_{min}(T^2 \times [0,1]; s_0, s_1)$ described by the decorated path P with edges e_i as above, then the relative Euler class of ξ_P is Poincaré dual to*

$$\sum_{i=1}^{n} \epsilon_i (e_i^1 - e_i^0),$$

where recall the e_i^j are the end points of the edge e_i thought of as elements in $H_1(T^2)$, and ϵ_i is the sign on e_i.

With this in mind, we can discuss gluing two contact structures on thickened tori together.

Corollary 5.5.14. *Let $\xi \in \text{Tight}_{min}(T^2 \times [0,1]; s_0, s_1)$ and $\xi' \in \text{Tight}_{min}(T^2 \times [0,1]; s_1, s_2)$ be associated to the decorated paths P and P', respectively. Then the result of gluing the front boundary of $(T^2 \times [0,1], \xi)$ to the back boundary of $(T^2 \times [0,1], \xi')$ results in a tight contact structure if and only if the path $P \cup P'$ can be consistently shortened to a minimal decorated path from s_0 to s_2.*

Remark 5.5.15. We note that in this last corollary, the contact structure obtained by gluing ξ and ξ' together does not have to be minimally twisting. It will be if and only if s_2 is not in the interval $[s_0, s_1]$.

Next, we state a very useful corollary of the classification result for minimally twisting contact structures on thickened tori.

Corollary 5.5.16. *Suppose $\xi \in \text{Tight}_{min}(T^2 \times [0,1]; s_0, s_1)$ then a slope s can be realized as the dividing slope on a convex torus parallel to the boundary if and only if $s \in [s_0, s_1]$. Moreover, if it can be realized, then it can be realized by a convex torus with only two dividing curves and such a convex torus is unique up to contactomorphism.*

Should we state the same theorem for prelagranian tori? it is a bit more complicated...

We finally consider when a minimally twisting contact structure is universally tight.

Corollary 5.5.17. *Given a minimal decorated path P in the Farey graph from s_0 clockwise to s_1, the contact structure ξ_P is universally tight if and only if all the signs in P are the same.*

5.5.2. Proofs of the main results. We are now ready to start proving our main theorems about minimally twisting contact structures on thickened tori. We begin when there is no twisting at all.

Proof of Theorem 5.5.1. Set $M = T^2 \times [0,1]$. We assume that we have a minimally twisting contact structure on M and ∂M has a standard foliation with ruling slope $s_0 = s_1 = \infty$. Let A be a vertical annulus (that is $S^1 \times [0,1]$ with S^1 a curve of slope 0 on T^2) with boundary ruling curves on ∂M. Make A convex. First note that all the dividing curves on A run from one boundary component to the other. In other words, there are no boundary parallel dividing curves, because if there were we would have a bypass on A which when attached to ∂N would produce a convex torus with dividing slope not equal to -1.

Exercise 5.5.18. Show that if we cut M along A and round the corners we get $S^1 \times D^2$ with boundary having dividing curves of slope -1.

There is a unique such tight contact structure on $S^1 \times D^2$. Thus the contact structure on M is determined by the dividing curves on A.

Now pick an identification $\phi : S^1 \times \{0\} \to S^1 \times \{1\}$ of the boundary components of A (for example, use the product structure on A). Given a contact structure on M we can always isotop A so that $\phi(\Gamma_A \cap (S^1 \times \{0\})) = \Gamma_A \cap (S^1 \times \{1\})$. So a component of Γ_A becomes a $(k,1)$ curve on $A/\sim = T^2$, where $\sim$ is induced by ϕ. Define $h(A) = k$. From the above discussion if two contact structures on M have the same $h(A)$ then they are isotopic.

Below we will show that any annulus isotopic to A must realize the same k, so that k is an invariant of the contact structure; but first, we show that any integer can be $h(A)$ for some tight contact structure. Indeed let ξ_0 be a tight contact structure on an $[0,1]$-invariant neighborhood of a convex torus with dividing slope ∞. Then $k(A)$ for this contact structure is clearly 0. Now set $\phi_k(x,y,t) = (x, y + tk, t)$. (Here (x,y) are the obvious coordinates on T^2 and t is the coordinate on $[0,1]$.) This is a diffeomorphism of M. Moreover, it is clear that $h(A) = k$ for the contact structure $\xi_k = (\phi_k)_*(\xi_0)$.

Exercise 5.5.19. Show that ξ_0 is minimally twisting since it is $[0,1]$-invariant. Thus conclude that all the ξ_k are minimally twisting.

We have model contact structures realizing all possible $k \in \mathbb{Z}$ and our discussion above shows that any tight minimally twisting contact structure is isotopic to one of these. Note that all these contact structures are contactomorphic by definition.

We now show that ξ_k is not isotopic to $\xi_{k'}$ if $k \neq k'$. We do this by showing that if A' is any annulus in (M, ξ_k) isotopic to A then $h(A') = k$. This shows that h is a map on contact structures not just on the pairs (A, ξ). Assume in ξ_0 there is an annulus A' isotopic to A, rel boundary, such that $h(A') = k \neq 0$. Let $\widetilde{M} = \mathbb{R} \times S^1 \times [0,1]$ be a covering space of N. There is a lift $\widetilde{A'}$ of A' to $\widetilde{N}$. The annulus $\widetilde{A'}$ splits $\widetilde{M}$ into two pieces M_1 and M_2. Form one of M_1 or M_2 the slope on $\widetilde{A'}$ looks negative, suppose it is M_1. Let $\widetilde{A}$ be a lift of A to M_1 (note this implies $\widetilde{A'}$ and $\widetilde{A}$ are disjoint). Let N be the region between $\widetilde{A'}$ and $\widetilde{A}$. It is easy to see N is a solid torus. Let C_1 and C_2 be the two components of $\partial\widetilde{M} = \mathbb{R}^1 \times S^1 \times \{0,1\}$ between $\widetilde{A'}$ and $\widetilde{A}$.

Exercise 5.5.20. Show that (after rounding the edges of N) ∂N is convex with two dividing curves of slope $\frac{1}{|h(A')|-1}$.
Hint: this is very similar the discussion surrounding Figure 5.3.4.

Notice that if $|h(A')| > 1$ then we can assume the ruling curves of ∂N are meridional and take a meridional disk D with boundary a ruling curve. Moreover, ∂D intersects the dividing curves $2(|h(A')| - 1)$ times and thus there is more than one component to the dividing curves on D when it is made convex. From this we know there is a boundary parallel dividing curve and we can Legendrian realize a bypass for ∂N on D. When we attach this bypass, Lemma 5.4.13 says that we get a convex torus in N with dividing slope 0. That is there is a solid torus N' in N with convex boundary having two dividing curves of slope 0. We know from Theorem 5.1.5 that there is a unique tight contact structure on N', and N' is a standard neighborhood of a Legendrian knot with the contact planes twisting 0 times relative to the product structure on N.

Let $\widetilde{A}_2$ be a lift of A to N_2 and set N_2 equal to the region between $\widetilde{A}$ and $\widetilde{A}_2$. This is a solid torus containing N (and N'). Moreover, arguing as in the exercise above, the slope of the dividing curves on N_2 is -1. There is a contactomorphism of N_2 to a standard neighborhood of a maximal Thurston-Bennequin unknot in S^3 with the standard contact structure that sends the product framing on N_2 to the 0 framing on the unknot (since the Thurston-Bennequin of the unknot is -1). But from the above construction inside this neighborhood of the Legendrian unknot, there is a neighborhood N' of a Legendrian knot (in the same knot type) with twisting equal to 0. This contradicts the Bennequin inequality. Thus the annulus A' could not have existed in the first place. □

We are now ready to prove half of our main theorem about minimally twisting contact structure on thickened tori.

Proof of half of Theorem 5.5.2 and Corollary 5.5.13. Here we will prove that

$$|Tight_{min}(T^2 \times [0,1]; r, -1)| \leq |(a_0 + 1)(a_1 + 1) \cdots (a_{n-1} + 1)a_n|$$

the other inequality necessary to prove the theorem will be established in Section 5.7.

Consider the manifold $M = T^2 \times [0,1]$. We wish to get an upper bound on the number of tight minimally twisting contact structures on M such that $T_i = T^2 \times \{i\}, i = 0,1$, is convex with two dividing curves Γ_i of slope $s_0 = -\frac{p}{q}, p > q > 0$, and slope $s_1 = -1$. Given such a contact structure on M the strategy will be to break M into pieces on which any contact structure under consideration will restrict to basic slices. From this, we get an upper bound since each basic slice admits only two possible contact structures. This first upper bound is not good enough, so we introduce "shuffling" which will give the desired upper bound.

We begin by taking the characteristic foliation on ∂M to be standard with dividing slope s_i on the respective boundary components and ruling slope 0. Let $A = S^1 \times [0,1]$ where S^1 is a circle on T^2 with slope 0. We also take ∂A to be Legendrian ruling curves on ∂M. Note

$$tw(S^1 \times \{0\}, A) = -\frac{1}{2}(S^1 \times \{0\} \cap \Gamma_0) = -\left|\frac{-1}{1} \cdot \frac{0}{1}\right| = -p$$

$$tw(S^1 \times \{1\}, A) = -\frac{1}{2}(S^1 \times \{1\} \cap \Gamma_1) = -\left|\frac{-p}{q} \cdot \frac{0}{1}\right| = -1.$$

Thus the Imbalance Principle, Lemma 5.4.18, gives a bypass D for T_1 along $S^1 \times \{0\}$. Attaching D to T_0 we get a neighborhood of $T_0 \cup D$ that we denote $T^2 \times [0,1/2]$. Hence by Theorem 5.4.13 we can write M as

$$M = \left(T^2 \times [0,1/2]\right) \cup \left(T^2 \times [1/2,1]\right),$$

where $T^2 \times [0,1/2]$ is a basic slice; moreover, we know that the dividing slopes on $T^2 \times \{1/2\}$ is the slope in $[-p/q, 0]$ closest to 0 with an edge to $-p/q$. From the discussion in Section 4.4 we know that this slope is $[a_0, \ldots, a_{n-1}, a_n + 1]$.

As above we can find a bypass for the back face of $T^2 \times \{1/2\}$ along the annulus A and with this create another basic slice. Now continuing in this manner we can break $T^2 \times [0,1]$ into a collection of basic slices and the edges in the Farey graph corresponding to the basic slices will form a minimal path from $-p/q$ to -1. From our discussion in Section 4.4 we know there are

$$k = |a_n + 1| + |a_{n-1} + 2| + \ldots + |a_0 + 2|$$

edges in this minimal path. So we have broken $T^2 \times [0,1]$ into basic slices denoted $B_i = T^2 \times [\frac{i-1}{k}, \frac{i}{k}]$ for $i = 1, \ldots n$. (Note what we called $T^2 \times [0,1/2]$, we now are calling $T^2 \times [0,1/k]$.) Moreover, if the dividing slope on the back face of B_i has continued fraction expansion $[t_0, \ldots, t_l]$ then on its front face the dividing curves have expansion $[t_0, \ldots, t_l + 1]$. Since each basic slice has only two possible contact structures we have proven the upper bound of 2^k for the number of possible tight minimally twisting contact structures on M. This number is much larger than the upper bound for which we are looking. To improve the upper bound we recall from Section 4.4 that the B_i's can be grouped into

natural "continued fraction blocks". That is we can break M up into $k'+1$ pieces M_i where k' is the number of a_i that are not equal to -2 (when $i < n$, that is when $i = n$ we will count that a_n whether or not it is -2). The slopes of the dividing curves on the front face and back face of M_i is $[a_0, \dots, a_{i'}+1]$ and respectively $[a_0, \dots, a_{i'+1}+1]$, for $i = 2, \dots, k'-1$, where i' is the i^{th}, a_i that is not -2. For $i = 1$ we have $-\frac{p}{q} = (a_0, \dots, a_k)$ and $(a_0, \dots, a_{n-1}+1)$, respectively, and for $i = k'$ we have a_0+1 and -1, respectively. We now find a better upper bound on the number of tight contact structures on a continued fraction block.

Lemma 5.5.21. *A continued fraction block of length m has at most $m+1$ tight minimally twisting contact structures.*

From Section 4.4 we know that the continued fraction blocks M_i have length $|a_{i'}| - 2$ except for the first one that will have length $|a_n| - 1$. Thus the lemma says the basic slices will have at most $|a_{i'}+1|$ minimally twisting contact structures except for the first one which has $|a_n|$. For all the a_i that are equal to -2 notice that $|a_i+1| = 1$ so we conclude that

$$|Tight_{min}(T^2 \times [0,1]; r, -1)| \leq |(a_0+1)(a_1+1)\cdots(a_{n-1}+1)a_n|.$$

Proof of Lemma 5.5.21. As shown in Excercise 4.4.2 we can assume that the dividing slopes for our continued fraction block are $s_0 = -1$ and $s_1 = -m-1$. Arguing as in the previous proof we can break $T^2 \times [0,1]$ into m pieces $B_i = T^2 \times [\frac{i-1}{m}, \frac{i}{m}], i = 1, \dots, m$, each of which is a basic slice. Moreover the dividing slope on $T_{\frac{i-1}{m}}$ is $-i$. By Theorem 5.3.1 each B_i admits two tight minimally twisting contact structures which we denote ξ_+ and ξ_-. We immediately get the upper bound of 2^m. To improve this upper bound we notice that we can "shuffle the basic slice layers". That is any contact structure on $T^2 \times [0,1]$ is isotopic to one in which all the ξ_+'s, say, come first, followed by all the ξ_-'s. Thus there is an integer $k = 0, \dots, m$ that counts the number of say ξ_+ regions, and the contact structure on $T^2 \times [0,1]$ is completely determined by this integer. If we can establish this, then the upper bound on the contact structures on this continued fraction block follows.

It is clearly sufficient to show that adjacent layers can be shuffled. That is the continued fraction block $B_1 \cup \cdots \cup B_m$ is isotopic to the continued fraction block with B_i and B_{i+1} exchanged for any i. If the adjacent layers have the same sign there is nothing to prove. So we assume B_i and B_{i+1} have signs $-$ and $+$ respectively. Let A be an annulus running from $T^2 \times \{i-1\}$ to $T^2 \times \{i+1\}$ such that $T^2 \times \{j\} \cap A$ is a Legendrian ruling curve of slope 0 for $j = i-1, i, i+1$. Make A convex. There are two essentially distinct possibilities for the dividing curves on A, either the bypasses can be nested or not. See Figure 5.5.20.

If the bypasses are not nested then we can clearly attach them in any order. That is we can attach the $+$ one first then the $-$ one. This would make B_i have sign $+$ and B_{i+1} have sign $-$. So the only difficulty is shuffling the layer is when the bypasses are nested.

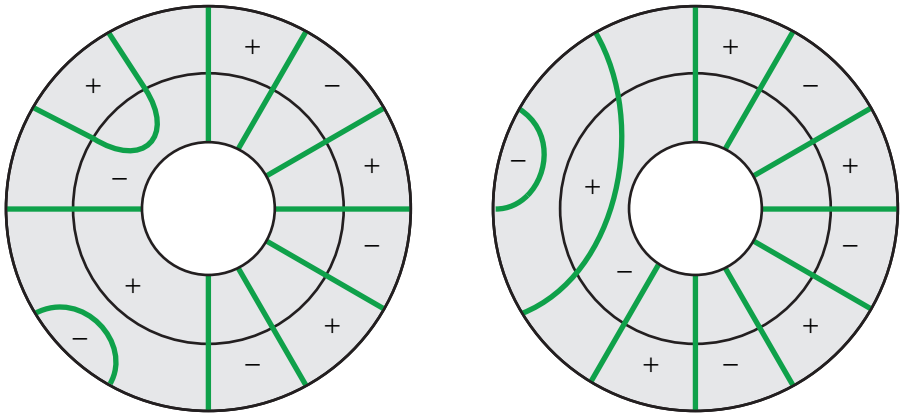

Figure 5.5.20. Two possible configurations of dividing curves. Nested bypasses on the right and non-nested on the left.

Supposing the bypasses are nested we isotop A to A' by "adding copies of T_{i-1} and T_i". See Figure 5.5.21. This isotopy is essentially the same as the one we did in the proof of

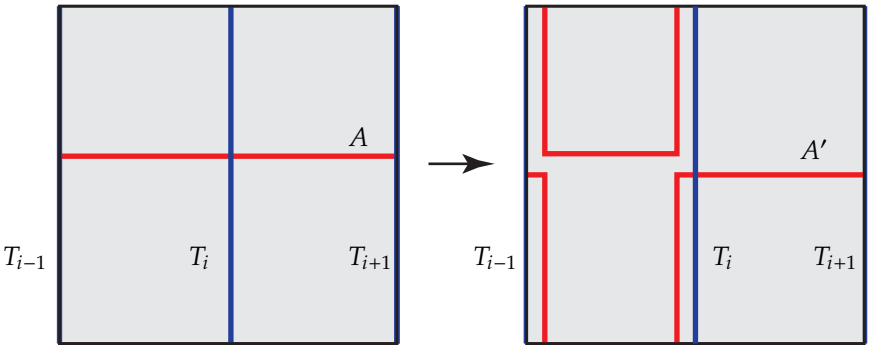

Figure 5.5.21. Isotoping A, left, to A', right. This is a cross section of $T^2 \times [0,1] = B_i \cup B_{i+1}$, so the top and bottom of the figures should be identified.

Lemma 5.3.3 to change the holonomy when classifying basic slices, so if the isotopy is not clear from the figure, please see the proof of that lemma for the details of the isotopy. The slope of the dividing curves on T_{i-1} is $-\frac{1}{i-1}$ and the slope of the dividing curves on T_i is $-\frac{1}{i}$. Thus the dividing curves on A' are as shown in Figure 5.5.22. In particular, the bypasses are no longer nested and we can shuffle the layers.

We cannot shuffle layers between different continued fraction blocks. This will follow from the computation of the relative Euler class below, but you should think about what goes wrong with the above proof. □

As noted above, this completes the proof of (half of) our theorem except for the fact that the relative Euler class distinguishes the contact structures in $\text{Tight}_{min}(T^2 \times [0,1]; r, -1)$. Before we do this we give a proof of Corollary 5.5.13.

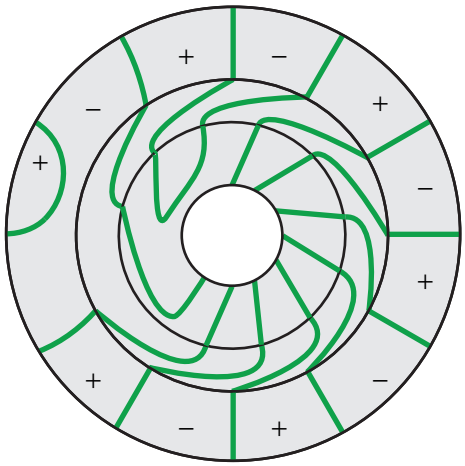

Figure 5.5.22. Dividing curves on A'. The middle annulus corresponds to T_i. We did not draw T_{i-1} in the figure since it does not affect the nesting of the bypasses. NEW PICTURE! also check rounding!

To this end, we notice that in the proof above we saw that any contact structure in $|Tight_{min}(T^2 \times [0,1]; r, -1)|$ is the union of basic slices and we know what the relative Euler class of a basic slice is from Theorem 5.3.1. Thus the corollary follows immediately from the following exercise.

Exercise 5.5.22. Suppose we have contact manifolds (M_1, ξ_1) and (M_2, ξ_2) that can be glued together on one of their boundary components. Also, assume that a section σ_i of the contact planes has been chosen along the boundary of each manifold and that the sections agree on the component they are glued along. Let σ be the section of the boundary of the glued manifold $M_1 \cup M_2$. Then the relative Euler class satisfies

$$e(\xi_1 \cup \xi_2, \sigma) = e(\xi_1, \sigma_1) \oplus e(\xi_2, \sigma_2)$$

in $H^2(M_1 \cup M_2, \partial(M_1 \cup M_2))$ which is a quotient of $H^2(M_1, \partial M_1) \oplus H^2(M_2, \partial M_2)$, which is where the sum on the left-hand side of the equality takes place.

We now must show that the contact structures on $T^2 \times [0,1]$ that come as the union of basic slices corresponding to a decorated minimal path in the Farey graph from $-p/q$ to -1 have different relative Euler classes unless they differ by shuffling in a continued fraction block.

To see this, consider the continued fraction blocks $M_i, i = 1 \dots k$ that make up such a contact structure. For convenience of notation, k is not the same as the k in the discussion above and we label the continued fraction block in reverse order from above. That is M_1 has a front fact having dividing slope -1. We will show that all the relative Euler classes are different by seeing how they evaluate on the annulus with slope 0.

We start by considering a general continued fraction block. Recall, that the vertices in the continued faction block are formed as follows. We start with a vertex v_0 and t such that $t \cdot v_0 = 1$. Then the other vertices are $v_i = v_0 \oplus it$. Notice that the basic slice corresponding to v_i and v_{i+1} has relative Euler class Poincaré dual to $\pm t = \pm(v_{i+1} - v_i)$. Thus if there are m basic slices in the continued fraction block then evaluating its relative Euler class on the annulus of with slope 0 will result in numbers between $-m|0 \cdot t|$ and $m|0 \cdot t|$. Applying this observation to the continued fraction block M_1 which corresponds to the path with vertices $-1, -2, \ldots, a_0 + 1$ so the block has $|a_0| - 1$ basic slices. Thus our observation says that the relative Euler class evaluated on the 0 sloped annulus will result in numbers between $-|a_0 + 1|$ and $|a_0 + 1|$. Now suppose the continued fraction block M_2 was one down from M_1, see Section 4.4 for the terminology. Then the vertices in the continued fraction block are of the form $(a_0 + 1) \oplus ia_0$ and hence the relative Euler class of each basic slice in this continued fraction block evaluates to $\pm a_0$ on the 0 sloped annulus. Notice that this number is larger than those coming from all possible configurations of bypasses for M_1. If M_2 is further a continued fraction block that is more than one down from M_1 then each of its basic slices will have an even larger (in absolute value) evaluation on the annulus of slope 0.

Exercise 5.5.23. Prove the last claim in the proof above.

Exercise 5.5.24. Show that the evaluation of the relative Euler class of each basic slice in M_i on the 0 sloped annulus will have an absolute value larger than the corresponding quantity for all the other previous continued fraction blocks combined.

Given the previous exercise, the following exercise should be fairly clear.

Exercise 5.5.25. If two elements of $\text{Tight}_{min}(T^2 \times [0,1]; r, -1)$ have the same relative Euler classes then they must correspond to the same decorated paths in the Farey graph from $-p/q$ to -1, upto shuffling in continued fraction blocks.

Since two decorated minimal paths in the Farey graph from $-p/q$ to -1 correspond to the same contact structure if they differ by shuffling in continued faction blocks, the previous exercise shows that contact structures determined by a decorated minimal path will have the same relative Euler class if and only if the paths are related by shuffling in continued fraction blocks. So once we prove that all such paths give elements of $\text{Tight}_{min}(T^2 \times [0,1]; r, -1)$ in Section 5.7, the proof will be complete. □

The rephrasing of Theorem 5.5.2 in terms of the Farey graph follows immediately from the proof of Theorem 5.5.2.

Proof of Theorem 5.5.10. When $s_0 = -p/q$ and $s_1 = -1$ the proof of Theorem 5.5.2 shows that any contact structure in $\text{Tight}_{min}(T^2 \times [0,1]; s_0, s_1)$ can be broken into basic slices corresponding to the edges in a minimal path in the Farey graph from $-p/q$ to -1 and hence

is determined by decorations on the path; moreover, if two decorations differ by shuffling in a continued fraction block, then they correspond to the same contact structure. Lastly, if they do not differ by shuffling, then their relative Euler classes will be different. Thus Theorem 5.5.10 follows in this case. The general case follows from a change of basis, see Exercise 5.5.7. □

We now explain when a general path in the Farey graph represents a tight minimally twisting contact structure.

Proof of Corollary 5.5.12. Let P be a decorated path in the Farey graph from s_0 to s_1 that is not minimal. Suppose that some shortening of the path is inconsistent. We will show that the contact structure ξ_P corresponding to this path (see the definition of ξ_P just before the statement of Corollary 5.5.12) is overtwisted. More precisely, given such a path P, there are two adjacent edges with opposite signs that can be shortened. We will show that the union of the basic slices that correspond to these two edges is overtwisted. Notice that after changing the basis we can assume that the first basic slice is in $\text{Tight}_{min}(T^2 \times [0,1/2]; -2, -3/2)$ and the second is in $\text{Tight}_{min}(T^2 \times [1,2]; -3/2, -1)$. Let us say the first basic slice is positive so has relative Euler class Poincaré dual to $\begin{pmatrix} 1 \\ -1 \end{pmatrix}$ and the second basic slice has relative Euler class Poincaré dual to $\begin{pmatrix} 1 \\ -2 \end{pmatrix}$. Now consider a convex annulus A of slope ∞ in $T^2 \times [0,2]$ that has boundary ruling curves on the boundary of $T^2 \times [0,2]$. We can moreover assume that A intersects $T^2 \times \{1\}$ in a ruling curve. Thus A is split into two convex annuli A_1 and A_2. Evaluating the relative Euler class of the first basic slice on A_1 will yield

$$\begin{pmatrix} 1 \\ -1 \end{pmatrix} \cdot \begin{pmatrix} 0 \\ 1 \end{pmatrix} = 1$$

and evaluating the relative Euler class of the second basic slice on A_2 will yield

$$\begin{pmatrix} 1 \\ -2 \end{pmatrix} \cdot \begin{pmatrix} 0 \\ 1 \end{pmatrix} = 1.$$

We also know that ∂A_1 intersects the dividing curves on $T^2 \times \{0\}$ two times, and the dividing curves on $T^2 \times \{1/2\}$ four times. Similarly A_2 intersects the dividing curves on $T^2 \times \{1/2\}$ four times, and the dividing curves on $T^2 \times \{1\}$ two times. Given this, and the fact that there cannot be contractible dividing curves (by the Giroux tightness criterion, Theorem 3.6.1) and some dividing curves must go from one boundary component to the other (or the basic slices would not be minimally twisting, see the proof of Lemma 5.3.3) we see that the dividing curves on A_1 and A_2 must be as shown in Figure 5.5.23. If Γ_{A_2} is as shown in the middle of the figure, then on $A_1 \cup A_2$ there is a dividing curve that bounds a disk and thus the contact structure is overtwisted by the Giroux criterion,

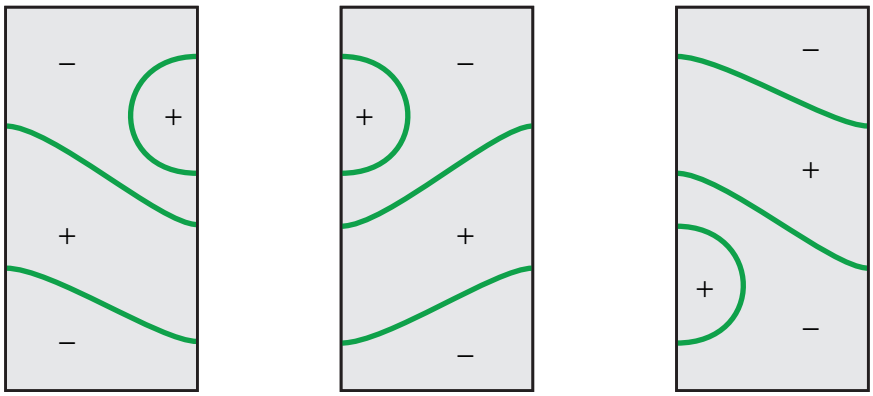

Figure 5.5.23. On the left is the only possibility for the dividing set Γ_{A_1}, up to holonomy (see the proof of Lemma 5.3.3 for the definition of holonomy) which will not be relevant for our discussion. The middle and right annuli show the only two possible configurations for the dividing set Γ_{A_2}, up to holonomy. (The top and bottom of each rectangle are identified to form the annulus.)

Theorem 3.6.1. If Γ_{A_2} is as shown on the right of the figure, then one may "isotop A_2 along $T_{1/2}$ and T_1" as in the proof of Lemma 5.3.3 where we showed how to change holonomy, so that the dividing curves on A_2 are as in the middle annulus in Figure 5.5.23. Thus we see that ξ_P is overtwisted.

To prove that a path that can be consistently shortened corresponds to a tight minimally twisting contact structure we will need the following simple lemma.

Lemma 5.5.26. *Given a basic slices* $(T^2 \times [0,1/2], \xi) \in \text{Tight}_{min}(T^2 \times [0,1/2]; -2, -3/2)$ *and* $(T^2 \times [1/2,1]; \xi') \in \text{Tight}_{min}(T^2 \times [1/2,1]; -3/2, -1)$ *with the same sign* $\pm$*. Then the contact manifold* $(T^2 \times [0,1], \xi \cup \xi')$ *is a basic slice with sign* $\pm$*.*

Proof. We start with a basic slice $(T^2 \times [0,1], \xi'') \in \text{Tight}_{min}(T^2 \times [0,1]; -2, -1)$ with sign $\pm$. From Corollary 5.3.2 we can find a convex torus T parallel to the boundary of $T^2 \times [0,1]$ that has two dividing curves of slope $-3/2$. We can assume that $T = T^2 \times \{1/2\}$.

Exercise 5.5.27. Show that T will break $T^2 \times [0,1]$ two to two basic slices one on $T^2 \times [0,1/2]$ and the other on $T^2 \times [1/2,1]$.

Exercise 5.5.28. Show that ξ'' restricted to $T^2 \times [0,1/2]$ and to $T^2 \times [1/2,1]$ is a $\pm$ basic slice.
Hint: Consider the relative Euler classes and how they glue together to give the relative Euler class of ξ''.

It is clear now that ξ'' restricted to $T^2 \times [0,1/2]$ is ξ and restricted to $T^2 \times [1/2,1]$ is ξ'. Thus gluing ξ and ξ' together yields ξ'' as claimed in the lemma. □

Notice whenever a decorated path P can be consistently shortened, the lemma says that we can replace P with a shorter decorated path P' such that ξ_P and $\xi_{P'}$ are the same contact structure. Consistently shortening P to a minimal decorated path P'' will yield an element of $\text{Tight}_{min}(T^2 \times [0,1]; s_0, s_1)$ by Theorem 5.5.2 and thus ξ_P is tight. □

Next up is the proof of Corollary 5.5.14. Recall this says when we can glue two minimally twisting contact structures on a thickened torus, the result a tight contact structure.

Proof of Corollary 5.5.14. Let ξ_P and $\xi_{P'}$ be two minimally twisting contact structures corresponding to the minimal decorated paths P and P' with the dividing slope on the front face of ξ_P agreeing with the dividing slope on the back face of ξ_Q. Then the result of gluing ξ_P and $\xi_{P'}$ is the contact structure described by the path $P \cup P'$. The tightness of this contact structure is now determined by Corollary 5.5.12. □

We now consider the slopes that can be realized by convex tori in a thickened torus.

Proof of Corollary 5.5.16. Suppose $\xi \in \text{Tight}_{min}(T^2 \times [0,1]; s_0, s_1)$. Since ξ is minimally twisting we know that no slope outside $[s_0, s_1]$ can be realized by a convex torus parallel to the boundary. On the other hand, since $(T^2 \times [0,1], \xi)$ can be broken into basic slices with slopes corresponding to the vertices of the minimal path from s_0 clockwise to s_1, we can appeal to Corollary 5.3.2 concerning the realization of convex tori with certain slopes in basic slices to see that we can realize any slope in $[s_0, s_1]$ as a convex torus parallel to the boundary with two dividing curves.

Given a convex torus T with two dividing curves of slope s in ξ. Notice that T cuts $T^2 \times [0,1]$ into two thickened tori, so we obtain an element of $\text{Tight}_{min}(T^2 \times [0,1]; s_0, s)$ and an element of $\text{Tight}_{min}(T^2 \times [0,1]; s, s_1)$. Each of these corresponds to decorated paths in the Farey graph, say P_1 and P_2. When we glue these two contact structures together we obtain ξ which is tight. Thus the decorated path $P_1 \cup P_2$ can consistently be shortened to a minimal decorated path from s_0 to s_1 by Corollary 5.5.14.

Exercise 5.5.29. Show that P_1 and P_2 are uniquely determined by ξ and the slope s.

So we see that if we had two convex tori T and T' with two dividing curves each of slope s, then they would both break $(T^2 \times [0,1], \xi)$ into two minimally twisting contact structures on thickened tori ξ_1 and ξ_2, and ξ_1' and ξ_2' respectively, corresponding to the decorated paths P_1 and P_2. But since the decorated paths are the same there is a contactomorphism from ξ_1 to ξ_1' and from ξ_2 to ξ_2'. We can combine these contactomorphism to get a contactomorphism form ξ to itself taking T to T'. □

We are finally ready to determine which minimally twisting contact structures on thickened tori are universally tight.

Proof of Corollary 5.5.17. ADD PROOF! □

We end this section by tying up a loose end and proving the last half of Corollary 5.1.7.

Proof of half of Corollary 5.1.7. We are left to see that given the unique tight contact structure ξ on $S^1 \times D^2$ with convex boundary having two dividing curves of slope integral slope n, then any slope $s \notin (-\infty, n]$ cannot be realized by a convex torus isotopic to the boundary of $S^1 \times D^2$. Suppose such a torus T exists. Then T splits $S^1 \times D^2$ into two pieces. The first is a solid torus S with convex boundary having dividing slope s and the second is a thickened torus $T^2 \times [0,1]$ with dividing slopes $s_0 = s$ and $s_1 = n$. We know that the contact structure on the latter piece must be minimally twisting, or by Exercise 5.5.9 we could realize any slope as the dividing slope of a convex torus. In particular, we can find a torus T' with dividing slope ∞. A Legendrian divide on T' will bound a meridional disk in $S^1 \times D^2$ and since the twisting of the contact planes relative to the disk is 0 (since the twisting is the same as the twisting relative T'). So this is an overtwisted disk, contradicting the fact that ξ is tight. Thus the contact structure on the thickened torus is minimally twisting as claimed. From Corollary 5.5.16 we know that in the thickened torus we can find a torus parallel to the boundary that has any dividing slope in $[s, n]$. Since s is not in $(-\infty, n]$ we see that we can choose this slope to be ∞ and as above this gives an overtwisted disk. Since ξ is tight we see that the torus T cannot exist. □

5.6. Contact structures on solid tori

In this section we will discuss a useful way to think about solid tori. We will then classify tight contact structures on solid tori and discuss several useful properties.

5.6.1. Executive summary of main results. We begin by discussing a way to think about solid tori that will be useful for discussing surgery and other constructions. We first recall a simple fact.

Exercise 5.6.1. Show that the quotient space of the annulus by one of its boundary components is diffeomorphic to the disk.
Hint: It should be easy to prove that the quotient space is homeomorphic to the disk, so the difficulty is understanding the smooth structure on the quotient space.

We now consider a parametric version of this exercise. That is we start with $T^2 \times [0,1]$ and fix some basis of $H_1(T^2)$ so that we can discuss curves on T^2 as elements of $\mathbb{Q}^*$, see Section 4.1. We can now foliate $T^2 \times \{0\}$ by curves of slope $r \in \mathbb{Q}^*$. Let S_r be the quotient space of $T^2 \times [0,1]$ where each of the leaves of the foliation on $T^2 \times \{0\}$ are collapsed to a point.

Exercise 5.6.2. Show that S_r is diffeomorphic to the solid torus.
Hint: One can change coordinates on T^2 so that T^2 is $S^1 \times S^1$ where the second S^1 factor is the slope r curve. Now $T^2 \times [0,1]$ is $S^1 \times (S^1 \times [0,1])$ and we see that this exercise is the same as the previous exercise we have crossed everything by S^1.

Notice that the slope on ∂S_r that bounds the meridional disk of the solid torus is r. We say that S_r is the *solid torus with lower meridian* r. Notice that S_∞ is what one would naturally call $S^1 \times D^2$. The reason for making this definition is that we will see many situations where there is a natural coordinate system on the boundary of a solid torus and in this coordinate system the meridian has some slope other than ∞, so instead of having to make a change of coordinates that might complicate an argument, we simply use the preferred coordinate system and just explicitly say that the meridian has slope r.

We can similarly foliate $T^2 \times \{1\}$ by curves of slope r and let S^r be the quotient space of $T^2 \times [0,1]$ that collapses each of the leaves to a point. We say S^r is the *solid torus with upper meridian* r.

We note that for the torus S_r the co-orientation on ∂S_r (induced from the orientation on ∂S_r) points out of the solid torus, while for S^r it points into the solid torus.

We are now ready to state the main classification result for solid tori.

Theorem 5.6.3 (Giroux 2000, [Gir00]; Honda 2000, [Hon00a]). *Let $-p/q < -1$ have continued fraction expansion $[a_0, \dots, a_n]$, then*

$$\left|\mathrm{Tight}(S^0; -p/q)\right| = |(a_0+1)(a_1+1)\cdots(a_{n-1}+1)a_n|.$$

Moreover, these contact structures are also distinct up to contactomorphism and are distinguished by their relative Euler classes.

Since the solid torus $S^1 \times D^2$ is S_∞ we would like to have a formula for the tight contact structures on S_∞. To this end, we define a function $\Phi : \mathbb{Q} \to \mathbb{Z}$ as follows. If $r \in (-1, 0)$ then set

$$\Phi(r) = |(b_0+1)(b_1+1)\cdots(b_{n-1}+1)b_n|$$

where $1/r = [b_0, \dots, b_n]$. For other rational numbers, we set

$$\Phi(r) = \begin{cases} 1 & r \in \mathbb{Z} \\ \Phi(r - \lceil r \rceil) & r \notin \mathbb{Z}, \end{cases}$$

where $\lceil r \rceil$ is the smallest integer greater than r. Notice that the function is 1-periodic: $\Phi(r \pm 1) = \Phi(r)$.

Theorem 5.6.4 (Giroux 2000, [Gir00]; Honda 2000, [Hon00a]). *For any rational number r we have*

$$\left|\mathrm{Tight}(S_\infty; r)\right| = \Phi(r).$$

Moreover, these contact structures are also distinct up to contactomorphism and are distinguished by their relative Euler classes.

Give formula for other lower meridians

Exercise 5.6.5. Give a formula for $|\text{Tight}(S^m, r)|$ for any $r \in \mathbb{Q}^*$.
Hint: read the proof of Theorem 5.6.4 first.

Give some examples and homeworks

Just as for thickened tori, we can interpret our classification result in terms of paths in the Farey graph.

Theorem 5.6.6. *Let P be a minimal path in the Farey graph from m clockwise to r. The contact structures in $\text{Tight}(S_m; r)$ are in one-to-one correspondence with equivalence classes of decorations on P with all but the first edge decorated. Here, two decorations are equivalent if they differ by shuffling signs in a continued fraction block (and doing nothing with the non-decorated edge), see the discussion before Theorem 5.5.10 for shuffling in continued fraction blocks.*

Similarly, if P is a minimal path in the Farey graph from r clockwise to m, then the contact structures in $\text{Tight}(S^m; r)$ are in one-to-one correspondence with equivalence classes of decorations on P with all but the last edge decorated.

Give some examples and homeworks

Given our classification results, we can determine when we can glue a tight structure on a solid torus to a tight structure on a thickened torus to obtain a tight structure on the new solid torus.

Corollary 5.6.7. *Given a tight contact structure $\xi \in \text{Tight}(S_m; r)$ corresponding to the decorated path P and a minimally twisting contact structure $\xi' \in \text{Tight}_{min}(T^2 \times [0,1]; r, s)$ corresponding to the decorated path P', then the result of gluing ξ and ξ' along their boundaries with the same dividing slope will give a tight structure in $\text{Tight}(S_m; s)$ if and only if $m \notin [r, s]$ and $P \cup P'$ can be consistently shortened to a minimal path.*

Consistently shortening a non-minimal decorated path in the Farey graph was discussed just before Corollary 5.5.12. We have the same definition here when two adjacent edges with a sign can be shortened; however, for the path P the first edge does not have a sign so if this edge is part of a pair of edges that can be shortened, then it is always consistent and the new edge created after shortening has no sign. Sometimes, one labels the unlabeled edge with a 0, and when shortening an edge with a 0 the sign on the other edge is "absorbed" by the 0 (0 times anything is 0).

Exercise 5.6.8. State and prove a version of the corollary for gluing solid tori with upper meridians to thickened tori.

Just as for thickened tori, we can determine which dividing slopes can be realized by convex tori parallel to the boundary of a solid torus.

Corollary 5.6.9. *Given a tight contact structure $\xi \in \text{Tight}(S_m; s)$ then a slope can be realized as the slope r of a convex torus parallel to the boundary of the solid torus if and only if $r \in (m, s]$. And if the slope can be realized, then it can be realized by a convex torus with two dividing curves.*

Unlike for thickened tori, we do not have a uniqueness statement for convex tori with a given dividing slope. We will illustrate this in a context that will be useful later when studying Legendrian knots.

Corollary 5.6.10. *Suppose $\xi \in \text{Tight}(S_\infty; s)$. Given a slope $s \in (\infty, s]$ there is some integer n such that $r \in [n, n+1)$ and there are exactly $|n - \lfloor s \rfloor| + 1$ distinct convex tori in (S_∞, ξ) with two dividing curves of slope s, up to contactomorphism.*

Exercise 5.6.11. State and prove a version of the corollary for solid tori with any lower meridian or any upper meridian.

Lastly, we observe that we can determine when a tight contact structure on a solid torus is universally tight.

Corollary 5.6.12. *Given a minimal decorated path P in the Farey graph from m clockwise to s with the first edge left unsigned, the contact structure ξ_P on S_m is universally tight if and only if all the signs in P are the same.*

5.6.2. Proofs of the main results. We begin with the proof of our main classification result on solid tori from which all other results will follow.

Proof of half of Theorem 5.6.3. We will show that

$$\left|\text{Tight}(S^0; -p/q)\right| \leq |(a_0+1)(a_1+1)\cdots(a_{n-1}+1)a_n|$$

and the other inequality will be proven in Section 5.7.

Let C be the core of the solid torus. By Lemma 1.4.34 we can realize C as a Legendrian knot L with very negative twisting. Using the framing on L coming from the product structure on the solid torus we can say the contact twisting is $-m$. Let N be a standard neighborhood of L (See the end of Section 5.1 for the definition of a standard neighborhood).

Exercise 5.6.13. In the basis for $H_1(T^2)$ we are using to measure slopes on tori parallel to ∂S^0, show that the slope of the dividing curves on ∂N is $-1/m$

Now let $M = S^0 \setminus N$. We have a tight contact structure on the thickened torus M with boundary slopes $s_0 = -1/m$ and $s_1 = p/q$.

Exercise 5.6.14. Show that the contact structure on M is minimally twisting.

Notice that -1 is in the interval $[-1/m, p/q]$ so by Corollary 5.5.16 we know that there is a convex torus T parallel to the boundary of M with two dividing curves of slope -1. We can use T to split S^0 into two pieces. One N' is a solid torus with upper meridian 0 and the other M' is a thickened torus with a minimally twisting contact structure having dividing slope -1 on its back face and p/q on its front face. Notice that N' has a unique tight contact structure by Theorem 5.1.5. Thus the number if possible tight contact structures on S^0 with dividing slope p/q is bounded above by the number of tight structures on N' and the minimally twisting contact structures on M'. That is

$$\left|\text{Tight}(S^0; p/q)\right| = \left|\text{Tight}_{min}(T^2 \times [0,1]; -1, p/q)\right|$$

which gives the claimed upper bound by Theorem 5.5.2.

We are left to prove the claim about the relative Euler classes distinguishing the contact structures. Recall in the proof of Theorem 5.5.2 about minimally twisting contact structures on thickened tori, we distinguished the contact structures by the relative Euler characteristic evaluated on an annulus of slope 0. In our current context that annulus can be extended to a meridional disk for S^0 and thus all of the contact structures on M' are distinguished by evaluating on the meridional disk intersected with M'. Thus all of the potential tight contact structures on S^0 are distinguished by evaluating the relative Euler class on the meridional disk. That is, the relative Euler class of tight contact structures on S^0 distinguishes them. □

We now turn to the case of classifying tight contact structures on solid tori with lower meridian ∞.

Proof of Theorem 5.6.4. We begin by noticing that $h\colon\ T^2 \times [0,1] to T^2 \times [0,1]\colon\ (\theta, \phi, t) \mapsto (\phi, \theta, 1-t)$ is an orientation preserving diffeomorphism. Moreover, h will send curves of slope ∞ on $T^2 \times \{0\}$ to curvse of slope 0 on $T^2 \times \{1\}$ and curves of slope r on $T^2 \times \{1\}$ to curves of slope $1/r$ on $T^2 \times \{0\}$. Thus h induces a bijection

$$\text{Tight}(S_\infty; r) \to \text{Tight}(S^0; 1/r).$$

This establishes the theorem for $1/r \in (-1, 0)$ by appealing to Theorem 5.6.3.

Recall S_∞ is naturally identified with $S^1 \times D^2$ and we can use the angular coordinate ϕ on S^1, and polar coordinates (r, θ) on D^2. Now observe that the diffeomorphism $g_n\colon\ S_\infty \to S_\infty\colon\ (\phi, r, \theta) \mapsto (\phi, r, \theta + n\phi)$ will send a slope r on ∂S_∞ to $r + n$.

Exercise 5.6.15. Prove this last statement.

Thus g_n induces a bijection

$$\text{Tight}(S_\infty; r) \to \text{Tight}(S_\infty; r + n),$$

which establishes the theorem for any $r \notin \mathbb{Z}$ from the above observation. Finally, for $r \in \mathbb{Z}$ we see that the dividing curves on S_∞ are longitudinal, and thus by Theorem 5.1.5 we see that $|\text{Tight}(S_\infty; r)| = 1$ in this case. Thus completing the proof. □

We now move to the proof of the classification of tight contact structures on solid tori in terms of decorated paths in the Farey graph.

Proof of Theorem 5.6.6. Using the diffeomorphisms discussed in the last proof it suffices to check the theorem for $\text{Tight}(S^0; r)$ with $r < -1$. In this case given any $\xi \in \text{Tight}(S^0; r)$ the proof of Theorem 5.6.3 shows that we can split ξ into a minimally twisting tight contact structure on $T^2 \times [0, 1]$ with dividing slopes r and -1 on the back and front boundaries, respectively, and a tight contact structure in $\text{Tight}(S^0; -1)$. Since $\text{Tight}(S^0; -1)$ contains a unique isotopy class of contact structure and elements in $\text{Tight}_{min}(T^2 \times [0, 1]; r, -1)$ are determined by a decorated path in the Farey graph from r to -1 up to shuffling in continued fraction blocks, we see that any contact structure in $\text{Tight}(S^0; r)$ is given by a path as claimed. Moreover, given such a path we can glue the corresponding unique contact structure on S^0 with dividing curves of slope -1 to the thickened torus given by truncating the path to go from r to -1, and the result must be tight or there would be too few contact structures in $\text{Tight}(S^0; r)$. So contact structures in $\text{Tight}(S^0; r)$ are given by decorated paths from r to 0 and any such path gives an element in $\text{Tight}(S^0; r)$. Finally, the Euler class computation in the proof of Theorem 5.6.3 shows that contact structures given by two such paths are isotopic if and only if they differ by shuffling in continued fraction blocks. □

We now consider gluing tight contact structures on the solid torus to tight contact structures on the thickened torus.

Proof of Corollary 5.6.7. Given a tight contact structure $\xi \in \text{Tight}(S_m; r)$ corresponding to the decorated path P and a minimally twisting contact structure $\xi' \in \text{Tight}_{min}(T^2 \times [0, 1]; r, s)$ corresponding to the decorated path P'. We may split P into a path P_0 and P_1 where P_0 have two vertices m and m^c while P_1 is a minimal path from m^c to r. From the last proof, we know that we can split ξ into a tight contact structure ξ_{P_0} on S_m with dividing curves of slope m^c and a minimally twisting tight contact structure ξ_{P_1} on $T^2 \times [0, 1]$ with dividing slopes m^c and r. Now gluing the contact structure ξ_{P_1} and ξ' corresponding to P' will result in an overtwisted contact structure if $P_1 \cup P'$ cannot be consistently shortened. Moreover, if $P_1 \cup P'$ can be shortened but $m \in [r, s]$ then we can realize a convex torus T in the thickened torus with dividing slope m and a Legendrian divide on this torus will bound a meridional disk in the solid torus. Since the twisting of the contact planes with respect to this disk will be zero (since it is zero on the torus T) we see that we have an overtwisted disk. Thus one implication of the corollary follows.

Now assume that $P_1 \cup P'$ can consistently be shortened, and $m \notin [r, s]$. We are left to show that ξ glued to ξ' is tight. For this, we need a lemma.

Lemma 5.6.16. *Given a tight contact structure on a solid torus $S^1 \times D^2 = S_\infty$ with dividing slope $n \in \mathbb{Z}$ and any integer $m < n$ then we find a convex torus T_m parallel to the boundary of the solid torus with two dividing curves of slope m. The torus T_m separates $S^1 \times D^2$ into a smaller solid torus with a convex boundary having dividing slope m and a contact structure on a thickened torus in $\text{Tight}_{min}(T^2 \times [0,1]; m, n)$. Moreover, T_m may be chosen so that any decorated minimal path from m clockwise to n is realized by this splitting.*

Notice that the lemma says that if you glue a solid torus with longitudinal divides to a thickened torus whose upper boundary has dividing curves that are also longitudes for the solid torus then the resulting contact structure will be the unique tight contact structure on the solid torus. With this in hand, we note that we can split P_1 into P_1' and P_1'' where P_1' has vertices that have an edge to m and only the first vertex in P_1'' does. Now $P_0 \cup P_1'$ describes a unique tight contact structure on a solid torus with longitudinal divides, while $P_1'' \cup P'$ can be consistently shortened to a path P''. Thus the result of gluing ξ to ξ' is the same as the result of gluing the contact structure given by $P_0 \cup P_1'$ on the solid torus (that is the unique contact structure with the given dividing curves) to the contact structure given by P'' and this is tight by the proof of Theorem 5.6.4. □

We now prove the lemma above to complete the proof of Corollary 5.6.7.

Proof of Lemma 5.6.16. ADD PROOF □

We would now like to determine which dividing slopes can be realized by a convex torus parallel to the boundary of a solid torus with a tight contact structure.

Proof of Corollary 5.6.9. As in the proof of Corollary 5.6.7 we may split S_m into two solid tori S_m' with dividing slope l where l is a longitude for S_m and a thickened torus $T^2 \times [0,1]$ with dividing slopes $s_0 = l$ adn $s_1 = s$. We know from Corollary 5.1.7 that any slope in $(m, l]$ can be realized by a convex torus with two dividing curves isotopic to the boundary of the solid torus. And by Corollary 5.5.16 we know that any slope in $[l, s]$ can be realized by a convex torus isotopic to the boundary with two dividing curves. Thus we can realize any slope in $(m, s]$ as the dividing slope of a convex torus isotopic to the boundary of S_m.

It is easy to argue that slopes outside $(m, s]$ cannot be realized by convex tori.

Exercise 5.6.17. Prove this.

Hint: If this exercise is not easy, then see the second half of the proof of Corollary 5.1.7 at the end of Section 5.5 where is similar argument is given. □

We will now classify, up to contactomorphism, how many convex tori of a given slope exist in a solid torus with a tight contact structure.

Proof of Corollary 5.6.10. ADD PROOF □

We end by proving which tight contact structures on a solid torus are universally tight.

Proof of Corollary 5.6.12. ADD PROOF □

5.7. Contact structures on lens spaces

In this section we recall the definition of lens spaces and interpret them in terms of tori with upper and lower meridians as discussed in the previous section. We then give the classification of tight contact structures on lens spaces and discuss their properties.

5.7.1. Executive summary of main results. Recall a *lens space* $L(p,q)$ is the 3-manifold obtained from S^3 by performing $-\frac{p}{q}$ surgery on the unknot. Using Rolfsen twists (see Section 1.5), we may assume that $-\frac{p}{q} < -1$. As discussed in Section 1.5, performing $-\frac{p}{q}$ surgery on a knot is the result of removing a tubular neighborhood of the knot and gluing in a solid torus so that the meridian maps to the $-\frac{p}{q}$ curve on the boundary of the complement of the neighborhood (we are using longitude-meridian coordinates to identify curves on a torus with elements of $\mathbb{Q}^*$). Using our notation from the previous section, we could also say that this surgery is obtained by removing the neighborhood N of the knot and replacing it with a solid torus with lower meridian $-\frac{p}{q}$, that is $S_{-\frac{p}{q}}$.

Exercise 5.7.1. Show that the complement of a neighborhood of the unknot in S^3 is a solid torus with upper meridian 0.

Thus we see that $L(p,q)$ can be thought of as the union of two solid tori S^0 and $S_{-\frac{p}{q}}$.

Another way to say this is $L(p,q)$ is obtained from $T^2 \times [0,1]$ by collapsing the slope $-\frac{p}{q}$ curves on $T^2 \times \{0\}$ and the slope 0 curves on $T^2 \times \{1\}$.

Theorem 5.7.2 (Giroux 2000, [Gir00]; Honda 2000, [Hon00a]). *Let $-\frac{p}{q} < -1$. Given the continued fraction expansion $-\frac{p}{q} = [a_0, \dots, a_n]$ with $a_i \leq -2$, the classification of tight contact structures on $L(p,q)$ is given by*

$$\left|\text{Tight}(L(p,q))\right| = |(a_0+1)(a_1+1)\cdots(a_n+1)|$$

Moreover, all these structures are distinguished by their Γ-invariant.

Recall that the Γ-invariant, discussed in Section 1.6, can be thought of as a "half Euler class". In fact, when p is odd, tight contact structures on $L(p,q)$ are distinguished by their

Euler class, but for even p one sometimes needs the full power of the Γ-invariant. We also note that a simple case of this theorem was originally proven by the first author in [Etn00].

Example 5.7.3. It is known that two lens spaces $L(p, q_1)$ and $L(p, q_2)$ are homotopy equivalent if and only if

$$q_1 q_2 \cong \pm n^2 \mod p$$

for some $n \in \mathbb{Z}$, [Whi41].

So, $L(7,1)$ and $L(7,2)$ are homotopy equivalent since $4^2 \cong 2 \cdot 1 \bmod 7$. However, notice that

$$-7 = [-7] \text{ and } -7/2 = [-4,-2],$$

so according to the classification above $L(7,1)$ has 6 contact structures while $L(7,2)$ has 3. Thus we see that $L(7,1)$ and $L(7,2)$ are not diffeomorphic. So tight structures on lens spaces are sensitive enough to distinguish distinct homotopy equivalent 3-manifolds! The fact that $L(7,1)$ and $L(7,2)$ are not diffeomorphic was, of course, already known since we know that $L(p, q_1)$ and $L(p, q_2)$ are diffeomorphic if and only if

$$q_1 q_2 \cong \pm 1 \mod p \quad \text{or} \quad q_1 \cong \pm q_2 \mod p,$$

see [Bro60], but this example shows that tight contact structures can see subtle distinctions in the topology of 3-manifolds.

Let us consider $L(11,2)$ and $L(11,5)$. By the above fact we know that these lens spaces are diffeomorphic since $10 \cong -1 \bmod 11$. However,

$$-11/2 = [-6,-2] \text{ and } -11/5 = [-3,-2,-2,-2,-2],$$

so the classification of tight contact structures says that $L(11,2)$ has 5 tight contact structures while $L(11,5)$ has 2. While this seems to contradict the above classification of lens spaces it turns out that $L(11,2)$ and $L(11,5)$ are orientation *reversing* diffeomorphic, but not orientation *preserving* diffeomorphic and contact structures are sensitive to the orientation of a manifold (recall by "contact structure" we mean "positive contact structure"). So again, we see that tight contact structures can distinguish the oriented diffeomorphism type of some 3-manifolds.

Refining the above statement about the diffeomorphism type of lens spaces $L(p, q_1)$ and $L(p, q_2)$ are orientation preserving diffeomorphic if and only if

$$q_1 q_2 \cong 1 \mod p,$$

here we are assuming that $q_i < p$ is positive, see [Rol76, Chapter 9]. So again we see that $L(11,2)$ and $L(11,5)$ not being orientation preserving diffeomorphic was known, but this example does point out the subtle features that tight contact structures can detect.

Exercise 5.7.4. Show that the number of tight contact structures on a lens space can distinguish the oriented diffeomorphism types of the lens spaces $L(p,q)$ for a fixed $p \leq 11$. Hint: For $p = 11$ you will need to use the fact that if M and N are diffeomorphic then the number of tight contact structures on M and N are the same and the number of tight contact structures on $-M$ and $-N$ are the same.

While tight contact structures can distinguish many homotopy equivalent, non-diffeomorphic lens spaces, it cannot distinguish them all. For example, if we consider $L(16,7)$ and $L(16,9)$, we see that $7 \cdot 9 = 63 \cong -1 \bmod 16$ so these lens spaces are orientation reversing diffeomorphic, but not orientation preserving diffeomorphic. We have $-16/7 = [-3,-2,-2,-3]$ and $-16/9 = [-2,-5,-2]$, so each lens space has 4 tight contact structures and when you reverse orientations on both they also have 4 tight contact structures.

Just like for the classification of minimally twisting contact structures on thickened tori and tight contact structures on solid tori, we can also state the classification in terms of paths in the Farey graph. We will call a minimal path in the Farey graph *partially decorated*, if each edge in the path, except for the first and last edge, has a sign.

Theorem 5.7.5. *The contact structures in* $\mathrm{Tight}(L(p,q))$ *are in one-to-one correspondence with equivalence classes of partial decorations on a minimal path in the Farey graph from* $-p/q$ *clockwise to* 0*. Here equivalence is up to shuffling signs in continued fraction blocks.*

In the next two exercises, we note that this last theorem can be particularly useful if one has a non-standard description of a lens space.

Exercise 5.7.6. Let L^s_r be the quotient space of $T^2 \times [0,1]$ where the curves of slope r are collapsed on $T^2 \times \{0\}$ and the curves of slope s are collapsed on $T^2 \times \{1\}$. Show that L^s_r is a lens space and in terms of r and s find p and q such that L^s_r is diffeomorphic to $L(p,q)$. Hint: Find a change of basis for $H_1(T^2)$ that takes s to 0 and r to some number less than -1 (recall when we say number we mean an element of $\mathbb{Q}^*$ so r can be taken to $-\infty$).

Exercise 5.7.7. Describe the classification of tight contact structures on L^s_r in terms of paths in the Farey graph.

Let T be the Heegaard torus for $L(p,q)$, that is the torus that separates $L(p,q)$ into two solid tori. From the classification of tight contact structures on lens spaces we note that possible dividing slopes on a convex realization of T are constrained.

Corollary 5.7.8. *Given any tight contact structure* ξ *on* $L(p,q)$*, the Heegaard torus* T *in* $L(p,q)$ *can be realized as a convex torus with dividing slope* s *if and only if* $s \in (-p/q, 0)$*. Moreover, if the slope* s *can be realized by a convex torus isotopic to* T*, then it can also be realized by one with two dividing curves.*

Exercise 5.7.9. Rephrase the corollary for tight contact structures on L^s_r.

Remark 5.7.10. The 3-sphere S^3 can be thought of as the lens space $L(1,0)$ which is obtained as $-\infty$ surgery on the unknot. The main theorem, Theorem 5.7.2 does not apply since we do not have a continued fraction expansion of $-\infty$, but the statement in Theorem 5.7.5 does hold. One may verify that the proofs of these two theorems may be adapted to show that S^3 has a unique contact structure, thus giving another (more complicated) proof of Theorem 5.1.1. However, from this perspective we can see that Corollary 5.7.8 holds for S^3. As this result is important for us later on, we will state it as its own corollary.

Corollary 5.7.11. *One can realize a slope as the dividing slope on a convex Heegaard torus for S^3 if and only if it is negative. (Here we are thinking of S^3 as $L(1,0) \cong L^0_{-\infty}$.)*

We end by noting that we can determine which tight contact structures on $L(p,q)$ are universally tight.

Corollary 5.7.12. *A tight contact structure on $L(p,q)$ is universally tight if and only if it corresponds to a partially decorated path in the Farey graph with all signs the same.*

In particular, $L(p,q)$ for $q \neq p-1$ has exactly two universally tight contact structures, that are the same plane field but with opposite orientations, and $L(p,p-1)$ has exactly one.

5.7.2. Proofs of the main results. We begin by proving our main classification result for lens spaces, Theorem 5.7.2, and this will in turn complete the proof of our classification of tight structures on solid tori and thickened tori.

Proof of Theorem 5.7.2 and completing the proofs of Theorems 5.5.2 and 5.6.3. We begin by recalling that in Lemma 1.6.30 we used Legendrian surgery and the Γ-invariant to show that

$$\left|\mathrm{Tight}(L(p,q))\right| \geq |(a_0+1)(a_1+1)\cdots(a_n+1)|.$$

Thus once we prove the inequality

$$\left|\mathrm{Tight}(L(p,q))\right| \leq |(a_0+1)(a_1+1)\cdots(a_n+1)|$$

in a manner similar to the partial proofs of Theorems 5.5.2 and 5.6.3 above, the proof of Theorem 5.7.2 will be done.

For the second inequality we will show below that there is a torus T in $L(p,q)$ such that $L(p,q) \setminus T$ is the union of two solid tori $V_0 \cup V_1$, where V_0 is a solid torus with lower meridian $-p/q$ and convex boundary with two dividing curves of slope $r^c = [a_0,\ldots,a_{n-1},a_n+1]$ while V_0 is a solid torus with upper meridian 0 and convex boundary having dividing slope r^c. Given this, we note that by Lemma 4.3.5 the dividing curves on ∂V_0 are longitudinal and hence there is a unique tight contact structure on V_0 by Theorem 5.1.5. So all the possible contact structures on $L(p,q)$ come from the possible contact

structures on V_1 and by Theorem 5.6.3 that satisfies

$$\left|\text{Tight}(L(p,q))\right| \leq \left|\text{Tight}(S^0; r^c)\right| \leq |(a_0+1)(a_1+1)\cdots(a_n+1)|$$

establishing our second inequality.

We now show the claimed torus T above exists. Let C be the core of the torus $S_{-\frac{p}{q}} \subset L(p,q)$. We can realize C as a Legendrian knot, by Lemma 1.4.34, and let N be a standard neighborhood of it. Let s be the slope of the dividing curves on ∂N. From Corollary 5.6.9 we know that any slope in $(-p/q, s]$ can be realized by a convex torus parallel to the boundary of N. From Lemma 4.3.5 we know that r^c is clockwise of $-p/q$ so we can find some s' in $(-p/q, r^c]$ that can be realized as the dividing slope on a convex torus T' in N that is parallel to ∂N. Now T' will cut $L(p,q)$ into two solid tori. One, V_0', is contained in N and the other, V_1', has upper meridian 0. So V_1' is a torus with upper meridian 0 that supports a tight contact structure and has convex boundary with two dividing curves of slope r. Once again, appealing to Corollary 5.6.9 we see that there is a convex torus T in V_1' that is parallel to the boundary and has dividing slope r^c. This proves the existence of T and establishes the second inequality above.

The proofs of Theorems 5.5.2 and 5.6.3 are also complete since in the previous two sections we saw that

$$\begin{aligned}\left|\text{Tight}(S^0; p/q)\right| &\leq \left|\text{Tight}_{min}(T^2\times[0,1]; -p/q, -1)\right| \\ &\leq |(a_0+1)(a_1+1)\cdots(a_{n-1}+1)a_n|\end{aligned}$$

and we have just shown that

$$\begin{aligned}|(a_0+1)(a_1+1)\cdots(a_{n-1}+1)a_n| &\leq \left|\text{Tight}(L(p',q'))\right| \\ &\leq \left|\text{Tight}(S^0; p/q)\right|\end{aligned}$$

where $-p'/q' = [a_0, \ldots, a_{n-1}, a_n - 1]$. □

We now turn to the description of tight contact structure on lens space in terms of partially decorated paths in the Farey graph.

Proof of Theorem 5.7.5. In the proof of Theorem 5.7.2 we saw that we can uniquely break any tight contact structure on $L(p,q)$ into three pieces. Specifically, a tight contact structure on S^0 with dividing slope -1, a tight structure on $S_{-p/q}$ with dividing slope $(-p/q)^c$, and a tight contact structure on the thickened torus $T^2\times[0,1]$ with dividing slopes $(-p/q)^c$ and -1. (We are using the notation for solid tori with upper and lower meridians established at the beginning of Section 5.6.) The contact structure on the thickened torus must be minimally twisting or else the contact structure on $L(p,q)$ would be overtwisted since by Exercise 5.5.9 we know that any slope can be realized as a dividing slope in a non-minimally twisting contact structure. Thus Theorem 5.5.10 says that the contact structure on $T^2\times[0,1]$ is determined by a decorated path from $(-p/q)^c$ to -1 up to shuffling in

continued fraction blocks. Theorem 5.6.4 tells us that the contact structures on the two solid tori are unique. Thus the contact structure on $L(p,q)$ is given by a partially decorated path from $-p/q$ to 0, and from the proof of Theorem 5.7.2 we know each such path gives a tight contact structure. □

We now move to the proof of Corolloary 5.7.8 and Corollary 5.7.11 about the slopes that can be realized as the dividing slope of Heegaard tori in lens spaces.

Proof of Corollary 5.7.8 and Corollary 5.7.11. We will consider the case when $L(p,q)$ is not S^3 and leave the S^3 case as an exercise.

Given a tight contact structure ξ on $L(p,q)$ we use the decomposition into two solid tori and a thickened torus from the proof of Theorem 5.7.5. Theorem 5.5.16 tells us that any slope in $[(-p/q)^c,-1]$ can be realized by a convex torus with two dividing curves in the $T^2\times[0,1]$ and Theorem 5.6.9 allows us to realize any slope in $(-p/q,(-p/q)^c]$, respectively $[-1,0)$, by a convex torus with two dividing curves in $S_{-p/q}$, respectively S^0. Thus we see that any slope in $(-p/q,0)$ can be realized as the dividing slope on a convex torus isotopic to the Heegaard torus.

Now suppose that there is a convex torus T in $L(p,q)$ with dividing slope $s\notin(-p/q,0)$.

Exercise 5.7.13. Show that we can assume that the torus has only two dividing curves.

Notice that T breaks $L(p,q)$ into two solid tori. One is $S_{-p/q}$ with dividing slope s and the other is S^0 with dividing slope s. Theorem 5.6.9 tells us that in $S_{-p/q}$ we can realize any slope in $(-p/q,s)$ as the dividing slope of a torus parallel to the boundary of the solid torus and similarly in S^0 we can realize any slope in $(s,0)$. Since $s\notin(-p/q,0)$ it is easy to see that we can realize any slope by a convex torus in $L(p,q)$. In particular, we can find a convex torus of slope 0. A Legendrian divide on this torus will bound an embedded (meridional) disk in S^0 and have twisting 0, that is it will bound an overtwisted disk. This contradicts the fact that ξ is tight and hence any $s\notin(-p/q,0)$ cannot be realized by a convex torus isotopic to the Heegaard torus in $L(p,q)$. □

We end with determining which contact structures on $L(p,q)$ are universally tight.

Proof of Corollary 5.7.12. GIVE PROOF OF FIRST PART

We now observe that a path from $-p/q<-1$ clockwise to 0 will have at least two edges and it will have exactly two edges if and only if $-p/q=-p/(p-1)$.

Exercise 5.7.14. Prove the last statement.

When there are only two edges, there is a unique partially decorated path (since there is no sign on the first or last edge). Thus there is a unique tight contact structure on $L(p,p-1)$, and from above it is universally tight. On the other hand, if a path has more

than two edges there will be an edge with a sign. If the contact structure is universally tight all the signs must be the same. Thus there are exactly two universally tight contact structures. □

5.8. Contact structures on the 3-torus

In this section we will construct an infinite family of tight contact structures on the 3-torus and prove that these are all tight contact structures up to contactomorphism. We will also give the classification of tight contact structures on the manifold, up to isotopy.

5.8.1. Executive summary of main results. We begin by constructing some tight contact structures on T^3. For each positive integer n we have the following tight contact structures on $T^3 = \mathbb{R}^3/\sim$, where $\sim$ is the equivalence relation generated by unit translation in each coordinate direction:

$$\xi_n = \ker(\sin(2\pi nz)\,dx + \cos(2\pi nz)\,dy).$$

We will refer to "directions" in T^3 by their corresponding directions in $\mathbb{R}^3$.

Theorem 5.8.1 (Kanda 1997, [Kan97]; Giroux 2000, [Gir00])**.** *If ξ is a tight contact structure on T^3 then it is contactomorphic to ξ_n for exactly one n. All tight contact structures on T^3 have Euler class 0 and are universally tight.*

While Kanda's paper appeared before Giroux's paper, Kanda acknowledges in his paper that Giroux also had a proof that was presented in talks prior to the publication of [Kan97]. That proof appeared in [Gir00]. We also note that another proof of this theorem was given by Honda in [Hon00b].

We can also classify tight contact structures on T^3 up to isotopy.

Theorem 5.8.2. *There is a one-to-one correspondence between* Tight(T^3) *and*

$$\{(A, k) | A \in H_2(T^3) \text{ is primitive and } k \text{ is a negative integer}\}.$$

Recall that $H_2(T^3)$ is isomorphic to $\mathbb{Z}^3$ and we call an element in $H_2(T^3)$ primitive if it is part of a basis for $H_2(T^3)$.

Exercise 5.8.3. Show that $A \in H_2(T^3)$ is primitive if it can be realized as the homology class of a linear incompressible torus in T^3, where linear means that it will lift to copies of $\mathbb{R}^2$ in the universal cover of T^3.

In the proof of the previous theorem we will see that there is a unique linear torus T^2 in any tight contact structure ξ on T^3 such that every linear homology class on T^2 admits a Legendrian representative with twisting 0. We will call this the *base torus*. Given the base torus T^2, any Legendrian knot isotopic to a linear closed curve that intersects T^2 one time will have twisting k for some positive integer k. We say that the contact structure

has *Giroux torsion* $k-1$ in this case. See Section 9.3 for more on Giroux torsion (we note that the definition of Giroux torsion is not in terms of the twisting mentioned above, but is a consequence of it).

Corollary 5.8.4. *Two tight contact structures on T^3 are isotopic if and only if they have the same base tori and Giroux torsion.*

5.8.2. Proofs of the main results. We begin the proof of Theorem 5.8.1 by showing that all the contact structures ξ_n are distinct.

Proposition 5.8.5. *The contact structures ξ_n are distinct.*

The proof of this proposition shows that the different ξ_n have Legendrian knots with different contact framings for different n.

Proof. Identify $H_1(T^3)$ with $\mathbb{Z}^3$ by picking as a basis the loops in each of the coordinate directions.

Lemma 5.8.6. *Any Legendrian knot L in (T^3, ξ_n) (with $tw(L) \leq 0$) isotopic to the linear simple closed curve in the homology class (a, b, c), where a, b, c are all prime to one another, satisfies*

$$tw(L) \leq -n|c|,$$

where the twisting of L is measured with respect to any incompressible torus containing L. Moreover, there is a linear Legendrian knot with $tw(L) = -n|c|$.

For $|c| \neq 0$ the assumption that $tw(L) \leq 0$ is not necessary because if there were a Legendrian knot as in the lemma with $tw(L) > 0$ then one could stabilize the knot until it had twisting 0 which would then contradict the inequality in the lemma. Moreover, one can show that the hypothesis that $tw(L) \leq 0$ is never necessary but it requires extra work and we do not need that result for the proof of Theorem 5.8.5.

Exercise 5.8.7. Show that the assumption that $tw(L) \leq 0$ is not needed.
Hint: If this is difficult read the rest of this section first.

Notice that this lemma says that the ξ_n can be distinguished by the fact that the smooth knot realizing the linear simple closed curve in the homology class $(0, 0, 1)$ has different Legendrian representatives. For example, ξ_n admits a Legendrian representative with $tw = -n$ while for ξ_k with $k < n$ all Legendrian representatives must have $tw < -n$. Hence all the ξ_n are distinct and are distinguished by the "Legendrian knot theory they support". It turns out that all contact structures can be "distinguished by their Legendrian or transverse knot theory", see [**EV10**]. □

We are now left to prove the lemma.

Proof of Lemma 5.8.6. We begin by considering the case where L is in the homology class $(0, 0, \pm 1)$. We will prove this result by contradiction. Assume L is a Legendrian knot isotopic to the linear simple closed curve in the homology class $(0, 0, 1)$ with $tw(L) = -n + 1$ (note if the inequality in the lemma is violated we can always find such a Legendrian knot by stabilization). Let A be the T^2 in T^3 corresponding to the xz-plane and let B be the torus corresponding to the yz-plane.

Exercise 5.8.8. Show that A and B are convex and compute that each torus A and B has a dividing set with $2n$ dividing curves running in the $(1, 0, 0)$ and $(0, 1, 0)$ direction, respectively.
Hint: Consider the explicit model we have for ξ_n above.

There is a finite cover of T^3 that unwraps the xy directions (but not the z direction) in T^3 in which there are lifts $\widetilde{L}$, $\widetilde{A}$, and $\widetilde{B}$ of L, A, and B so that $\widetilde{L}$ is disjoint from $\widetilde{A} \cup \widetilde{B}$. Note $tw(\widetilde{L})$ (measured in the cover) is equal to $tw(L)$. Furthermore $\widetilde{A}$ and $\widetilde{B}$ are convex each having $2n$ dividing curves running in the $(1, 0, 0)$ and $(0, 1, 0)$ direction, respectively.

Exercise 5.8.9. Prove the claims about $\widetilde{L}$, $\widetilde{A}$, and $\widetilde{B}$.

Let S be the manifold obtained by removing small vertically invariant neighborhoods of $\widetilde{A}$ and $\widetilde{B}$ and rounding the resulting corners. Clearly $S = S^1 \times D^2$ and using the edge rounding lemma (Lemma 3.8.3) we see that there are two dividing curves on ∂S with slope $-n$.

Exercise 5.8.10. Prove this.
Hint: Consider how the dividing curves intersect a meridian and a longitude on S.

We know the contact structure ξ_n is universally tight since when pulled back to the universal cover we have the standard contact structure on $\mathbb{R}^3$, see Examples 1.1.11. Thus the contact structure on S is tight. By Theorem 5.1.5 there is a unique tight contact structure on S. Note $\widetilde{L}$ is the core of S and with respect to the product structure on S the twisting of $\widetilde{L}$ is one greater than the slope of the dividing curves. Let $S' \subset (S^3, \xi_{std})$ be a standard neighborhood of the Legendrian unknot U with $tb(L) = -1$. Since there is a diffeomorphism from S to S' taking the dividing curves on S to the dividing curves on S' we know (again by Theorem 5.1.5) the contact structure on S is contactomorphic to the one on S'. Now $\widetilde{L}$ is a Legendrian knot in S' with twisting number equal to 0. But in S^3 this is an unknot with $tb = 0$ and hence violates the Bennequin inequality (Theorem 3.7.5). Thus our hypothesized L cannot exist.

For the case $(a, b, \pm 1)$ we need the following lemma, which we prove later.

Lemma 5.8.11. *Let $A \in SL(3, \mathbb{Z})$ and $\Psi_A : T^3 \to T^3$ be the induced diffeomorphism of T^3. Assume Ψ_A preserves the xy-plane in T^3 then Ψ_A is isotopic to a contactomorphism of ξ_n.*

Given this lemma we can clearly apply a contactomorphism to (T^3, ξ_n) taking $(a, b, \pm 1)$ to $(0, 0, \pm 1)$ and thus this case is reduced to the first case considered above.

Now consider the case with (a, b, c), and $|c| > 1$. Let L be a Legendrian knot isotopic to a linear simple closed curve in the homology class (a, b, c). Denote by $\Phi : T^3 \to T^3$ the $|c|$ fold covering map of T^3 that unwraps the z-direction. Clearly $\Phi^* \xi_n = \xi_{n|c|}$. Let $\widetilde{L}$ be a lift of L.

Exercise 5.8.12. Show that $tw(\widetilde{L}) = tw(L)$ (recall the twisting is measured with respect to any incompressible torus containing the Legendrian knot and the incompressible torus can also be lifted to the cover.)
Hint: See Figure 5.8.24.

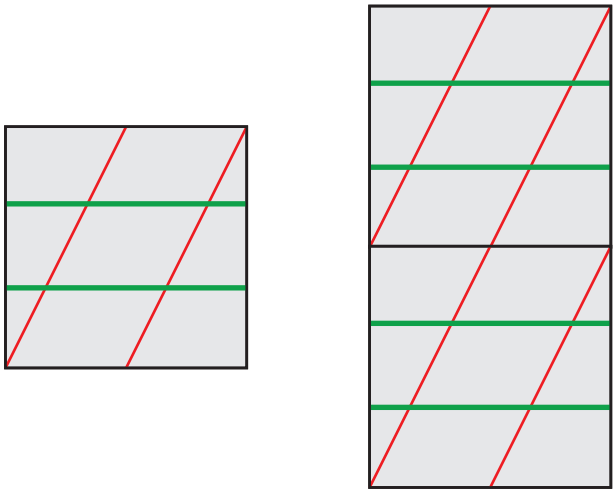

Figure 5.8.24. On the left is the knot L sitting in the xz-plane (or an isotopic copy of it). On the right is the two fold cover of the xz-plane. Note there are two lifts of L we have chosen one to be $\widetilde{L}$. As always, dashed lines are dividing curves.

So we have

$$tw(L) = tw(\widetilde{L}) \leq -n|c|.$$

Exercise 5.8.13. In all the above cases find a Legendrian knot realizing the corresponding upper bound.

We are finally left to consider the case $(a, b, 0)$. It is easy to see that for any such homology class there is a constant k such that the torus $\{(x, y, z)|z = k\}$ in T^3 is foliated by (a, b) curves. Thus any leaf in this foliation is a Legendrian simple closed curve with $tw = 0$. □

Proof of Lemma 5.8.11. Under the hypothesis that Ψ_A preserves the xy-plane we can write

$$A = \begin{pmatrix} a & b & e \\ c & d & f \\ 0 & 0 & g \end{pmatrix},$$

where $g(ad - bc) = 1$. Note this implies $g = \pm 1$ and we assume $g = 1$. The other case is handled similarly. Let

$$\begin{pmatrix} a(t) & b(t) \\ c(t) & d(t) \end{pmatrix} \in SL(2, \mathbb{R}), t \in [0, 1],$$

be a path a matrices from the identity matrix to

$$\begin{pmatrix} a & b \\ c & d \end{pmatrix}.$$

In addition let $e(t)$ and $f(t)$ be two functions on the unit interval starting at e and f, respectively and ending at 0. Finally set

$$A(t) = \begin{pmatrix} a(t) & b(t) & e(t) \\ c(t) & d(t) & f(t) \\ 0 & 0 & g \end{pmatrix},$$

and note that $A(t)$ is a path of matrices in $SL(3, \mathbb{R})$ from the identity to A. The matrices $A(t)$ do not necessarily induce diffeomorphisms of T^3 but we can pull back the 1-form on $\mathbb{R}^3$ defining ξ_n with $A(t)$ to get

$$\begin{aligned} \alpha_t =& [a(t)\cos(2n\pi z) + c(t)\sin(2n\pi z)]\, dx \\ &+ [b(t)\cos(2n\pi z) + d(t)\sin(2n\pi z)]\, dy \\ &+ [e(t)\cos(2n\pi z) + f(t)\sin(2n\pi z)]\, dz. \end{aligned}$$

Note all these forms are invariant under the unit translations in the coordinate directions. So they all define 1-forms on T^3. Also, α_0 is the 1-form α defining ξ_n and $\alpha_1 = \Psi_A^* \alpha$. Thus we have a one-parameter family of contact structures from ξ_n to $\Psi_A^* \xi_n$. Thus using Gray's theorem,Theorem 1.2.10, we can find an isotopy of Ψ_A so that it preserves ξ_n. □

We are now ready for the classification of contact structures on T^3 up to contactomorphism.

Proof of Theorem 5.8.1. We are given a contact structure ξ on T^3. We would like to find two incompressible tori T_0 and T_1 such that

(1) T_i is convex for $i = 0, 1$,

(2) $T_0 \cap T_1 = L$ a Legendrian simple closed curve and

(3) $-2tw(L) = \#\Gamma_{T_i}$, for $i = 0, 1$.

If we find such tori then we can construct a contactomorphism to (T^3, ξ_n), where $n = -tw(L)$. Indeed, from Theorem 3.5.1 we see that $tw(L) = -\frac{1}{2}\#(\Gamma_{T_i} \cap L)$ so each component of Γ_{T_i} intersects L once. Let h_i be the homology class of L on T_i and h_i' the homology class of a component of Γ_{T_i}, then h_i, h_i' form a basis for $H_1(T_i)$. Thus we can find a diffeomorphism f from T^3 to $T^3 = \mathbb{R}^3/\sim$ taking L to the z axis, h_0' to the homology class of the x-axis and h_1' to the homology class of the y-axis. By isotoping f we can assume f takes the dividing curves on T_0 to the dividing curves on the xz-plane (we are giving $T^3 = \mathbb{R}^3/\sim$ the contact structure ξ_n) and the dividing curves on T_1 to the dividing curves on the yz-plane. There is a further isotopy of f so that f takes the characteristic foliations of T_0 and T_1 to the characteristic foliations on the xz- and yz-planes, respectively. Thus we can isotop f to be a contactomorphism on a neighborhood of $T_0 \cup T_1$. Now the complement of this neighborhood is a solid torus S.

Exercise 5.8.14. Show that there are two dividing curves on ∂S and they have slope $-n$. Hint: Work in $R^3/\sim$.

We can now use Theorem 5.1.5 to further isotop f so that it is a contactomorphism from (T^3, ξ) to (T^3, ξ_n).

So the proof is done once we find the tori T_0 and T_1 satisfying the conditions above. To this end, we choose:

(1) a convex linear torus T with the minimal number of dividing curves among all such tori, and

(2) a Legendrian knot L' isotopic to a linear simple closed curve that intersects T transversely one time, and that has maximial possible twisting $tw(L')$ (but non-positive).

By a linear torus in T^3 we mean one that lifts to linear $\mathbb{R}^2$ in the universal cover. We also note that T will have 2 dividing curves, but we only know this *a postiori*. Let γ be a linear non-homologous simple closed curve in T which has intersection with each connected component of Γ_T equal to 1. Using Theorem 3.4.5, we can Legendrian realize γ on T.

Exercise 5.8.15. There is a convex torus S that contains L' and γ as Legendrian curves. Moreover, we can assume that $S \cap T = \gamma$.
Hint: This argument is identical to the one used in Theorem 3.3.1. Basically, find nice strips containing the arcs that could be convex. Extend them to a torus in any way you can. Then C^∞ perturb this torus away from the strips to make it convex.

If the dividing curves of S are not homotopic to $S \cap T$ then S and T will be the desired tori T_0 and T_1. Indeed, note that the number of dividing curves on S and T are the same, since

$$tw(\gamma) = -\frac{1}{2}\#(\Gamma_S \cap \gamma) \leq -\frac{1}{2}\#\Gamma_S,$$

and

$$tw(\gamma) = -\frac{1}{2}\#(\Gamma_T \cap \gamma) = -\frac{1}{2}\#\Gamma_T.$$

However, we chose T so that $\#\Gamma_T$ is minimal thus we must have $\#\Gamma_T = \#\Gamma_S$. Moreover, the above inequality must be an equality, and thus S and T satisfy all the conditions necessary for T_0 and T_1.

Now suppose that dividing curves of S are homotopic to $S \cap T$. We will then choose a linear closed curve γ' on T that intersects each component of Γ_T once and also intersects γ once. We can assume that $\gamma \cap \gamma'$ is the point where L' intersects T. We can Legendrian realize γ' on T and as above construct a torus S' that is convex, contains L' and γ' and $S' \cap T = \gamma'$. Also as above if the dividing curves on S' are not homotopic to $S' \cap T$ then S' and T will be desired tori T_0 and T_1.

Exercise 5.8.16. Show that in the previous two cases, T is not the base torus of the contact structure.

We are left to consider the case where the dividing curves on S are homotopic to $S \cap T$ and the dividing curves on S' are homotopic to $S' \cap T$. Notice that in the constructions above, we can assume that $S \cap S' = L'$. We now claim that S and S' can be taken to be T_0 and T_1. To see this we only need to verify Property (3). To this end we first note that homologically each dividing curve in Γ_S (and $\Gamma_{S'}$) intersects L' one time, because the dividing curves are homotopic to $S \cap T$ (and $S' \cap T$). The actual number of intersection points between each dividing curve in Γ_S (and $\Gamma_{S'}$) and L' is one. We see this as follows: if this were not the case then there would be an arc c in $\Gamma_S \setminus (\Gamma_S \cap L')$ that cobounded a disk D in $S \setminus L'$ with an arc on L'. See Figure 5.8.25. Thus there is a simple closed curve L''

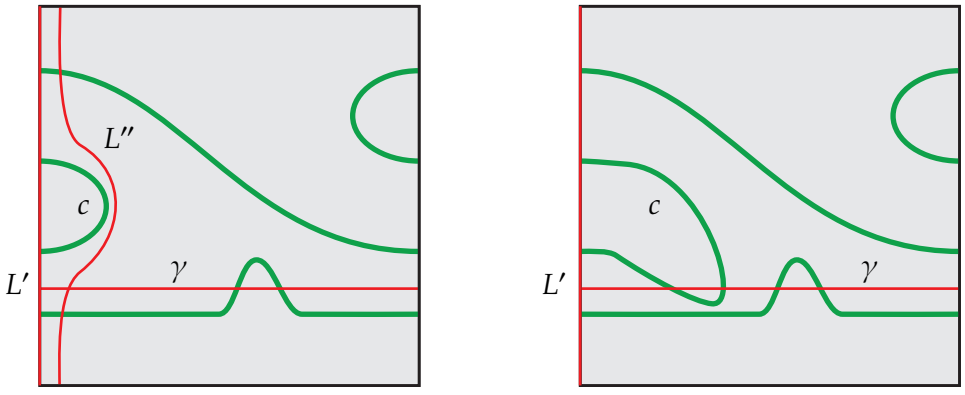

Figure 5.8.25. On the left, dividing curves on S that intersect L' more than once. On the right, we see a case where c intersects γ.

on S that intersects Γ_S two fewer times than L' and is homotopic to L'. By the Legendrian

realization principal, Theorem 3.4.5, we can assume L'' is a Legendrian simple closed curve on an isotoped copy of S. Moreover, Theorem 3.5.1 says that

$$tw(L'') = -\frac{1}{2}\#(\Gamma_S \cap L'') > -\frac{1}{2}\#(\Gamma_S \cap L') = tw(L')$$

contradicting the choice of L', if L'' intersects T once. The only way for L'' to intersect T more than once is for D to intersect γ. The simplest case of this is shown on the right of Figure 5.8.25. If this happens we have a bypass for T along S. Notice that γ intersected the dividing curves of T efficiently, so we understand how attaching a bypass to T will affect Γ_T, see Example 5.4.10. If Γ_T has more than two components, then pushing T across the bypass will decrease the number of components in the dividing set of T which contradicts our choice of T. Thus we must have that $\#\Gamma_T$ is 2 and when we push T past the bypass we change the slope of Γ_T but not the number of curves. Once we push T across the bypass we can not realize L'' so that it intersects the new T exactly once and thus contradicts the choice of L' completing the proof. (We note that the disk D might intersect T in many arcs, so we will have to attach several bypasses to T before we can realize L'', but this does not change the conclusion.) □

We now turn to the classification of tight contact structures on T^3 up to isotopy.

Proof of Theorem 5.8.2 and Corollary 5.8.4. Given any tight contact structure ξ on T^3 we can use Theorem 5.8.1 to get a contactomorphism $\phi : T^3 \to T^3$ taking ξ_n to ξ for some n, where ξ_n is defined just before Theorem 5.8.1. Let T be the image of the torus in T^3 given by the xy-plane (see the beginning of the section for our convention of T^3 as the quotient of $\mathbb{R}^3$ by $\mathbb{Z}^3$). This is clearly a base torus in (T^3, ξ), and ξ has a unique base torus. By Lemma 5.8.6 we know that any Legendrian knot isotopic to a linear closed curve and intersecting T one time has twisting $-n$ and no larger. So the map

$$\Phi : \text{Tight}(T^3) \to \{(A, k) | A \in H_2(T^3) \text{ is primitive and } k \text{ is a negative integer}\}$$

sending ξ to $(T, -n)$ is well-defined.

We first claim that this map is surjective.

Exercise 5.8.17. Given any linear torus T in T^3 show that there is a diffeomorphism from $T^3 = \mathbb{R}^3/\mathbb{Z}^3$ to T^3 sending the torus corresponding to the xy-plane to T.

Given the exercise, we can find a tight contact structure with base torus any pre-assigned linear torus in T^3 and realizing any negative k as the maximal twisting of Legendrian knots isotopic to a linear closed curve intersecting the base torus one time. Thus Φ is surjective.

We now show that if $\Phi(\xi) = \Phi(\xi') = (A, k)$ then ξ is isotopic to ξ which will complete the proof of the theorem and corollary. By hypothesis, ξ and ξ' have homologous base tori in T^3.

Exercise 5.8.18. Show that the base tori are isotopic (that is if two incompressible tori in T^3 are homologous then they are isotopic).

We can assume the base tori in ξ and ξ' have the same characteristic foliation. Thus there is an isotopy of T^3 taking the base torus of ξ to that of ξ' so that the characteristic foliation is preserved. Push ξ forward by this isotopy to get a contact structure, which we still call ξ, that has the exact same base torus T. Let L and L' be isotopic linear closed curves that intersect the base torus T one time each, in the same point of T, and such that L is Legendrian in ξ and L' is Legendrian in ξ' with both having twisting k. We can smoothly isotopy L to L', relative to T, and then push ξ forward by this isotopy so $L = L'$ is Legendrian in both ξ and ξ'. A further isotopy of ξ near L will result in ξ agreeing with ξ' along L. Take linear curves γ and γ' on T that intersect each dividing curve of T exactly once and intersect each other once where L intersects T. Now let T_0, respectively T_1, be tori in (T^3, ξ) that contain L and γ, respectively L and γ'. Let T_0' and T_1' be similar tori in (T^3, ξ'). (Actually, we can take $T_i = T_i'$ but we want to emphasize that they are in different contact structures and will be isotoping them independently.) We can make T_i convex relative to L and similarly for T_i'.

Looking at the proof of Theorem 5.8.1 we know that T_i has $2|k|$ dividing curves homotopic to $T_i \cap T$ and T_i' also has $2|k|$ dividing curves homotopic to $T_I' \cap T$ (this is because T is the base torus in both cases, see Exercise 5.8.16). We can now realize the characteristic foliation on T_i' on T_i using Giroux flexibility. Thus there is a smooth isotopy taking T_i to T_i' (relative to L) and the characteristic foliation on T_i to the characteristic foliation on T_i'. Pushing forward ξ by this isotopy we see that $T_i = T_i'$ and ξ and ξ' induce the same foliation on these tori. Since we know the characteristic foliation determines the contact structure in a neighborhood of a surface, Theorem 1.3.4, we see that we can isotopy ξ in a neighborhood of $T_0 \cup T_1$ so that ξ and ξ' agree in that neighborhood. The complement of this neighborhood of a solid torus, so arguing as in the first paragraph of the proof of Theorem 5.8.1 we see that ξ is isotopic to ξ'. □

5.9. Contact structures on thickened tori again

We would now like to classify non-minimally twisting contact structures on $T^2 \times [0, 1]$.

5.9.1. Executive summary of main results. To state the classification result, we first construct various model contact structures. Let $(N_0 = T^2 \times [0, 1], \overline{\xi})$ be the basic slice with dividing slopes $s_0 = -\infty$ and $s_1 = 0$ and having relative Euler class Poincaré dual to $\begin{pmatrix} 1 \\ 1 \end{pmatrix}$.

Let $N_{\frac{n\pi}{2}}$ be $(N_0, \overline{\xi})$ rotated anticlockwise by $\frac{n\pi}{2}$. [1] Now set

$$\xi_1^- = N_\pi \cup N_{\frac{3\pi}{2}},$$

$$\xi_2^- = N_\pi \cup N_{\frac{3\pi}{2}} \cup N_{2\pi} \cup N_{\frac{5\pi}{2}}$$

and similarly define $\xi_k^- = N_\pi \cup \cdots \cup N_{\frac{(2k+1)\pi}{2}}$ for all positive integers k. Also define

$$\xi_1^+ = N_0 \cup N_{\frac{\pi}{2}}$$

and for each $k > 1$ set $\xi_k^+ = \xi_1^+ \cup \xi_{k-1}^-$. Intuitively, $\xi_k^\pm$ goes through k half twists as you go from the back fact of $T^2 \times [0,1]$ to the front face. The structures ξ_k^+ and ξ_k^- differ in that the orientation on the contact planes along the back face of $T^2 \times [0,1]$ is opposite.

Exercise 5.9.1. Show that all the contact structures $\xi_k^\pm$ contact embed in $T^2 \times \mathbb{R}$ with the contact structure $\ker(\sin(2\pi z)\, dx + \cos(2\pi z)\, dy)$ and thus are universally tight.

We are now ready for the first classification result.

Theorem 5.9.2 (Honda 2000, [**Hon00a**])**.** *A complete non-repeating list of non-minimally twisting tight contact structures on $T^2 \times [0,1]$ with convex boundary, and each boundary component having two dividing curves of slope ∞, is given by $\xi_k^\pm$ where k runs through all positive integers.*

The relative Euler class of these contact structures is

$$P.D.(e(\xi_{2m}^\pm, s)) = \begin{pmatrix} 0 \\ 0 \end{pmatrix}$$

$$P.D.(e(\xi_{2m-1}^\pm, s)) = \pm \begin{pmatrix} 2 \\ 0 \end{pmatrix}$$

Remark 5.9.3. As there is a diffeomorphism from $T^2 \times [0,1]$ to $T^2 \times [0,1]$ that takes the ∞ sloped curve to a curve of any slope s, the above theorem gives a complete classification of non-minimally twisting contact structures on $T^2 \times [0,1]$ with both boundaries having the same pair of dividing curves.

We now consider non-minimally twisting contact structures on thickened tori with distinct dividing slopes.

Theorem 5.9.4. *Let ξ be a tight contact structure on $T^2 \times [0,1]$ with convex boundary having minimal number of dividing curves with dividing slopes s_0 and s_1, then we may isotop ξ so that ξ restricted to $T^2 \times \left[\frac{1}{2}, 1\right]$ is minimally twisting with dividing slopes $s_{\frac{1}{2}} = s_0$ and s_1 and ξ restricted*

[1] Note we are denoting the manifold and the contact structure by $N_{\frac{n\pi}{2}}$. In this section we will frequently blur the line between contact manifold and contact structure. This should not cause any confusion since all manifolds in this section are $T^2 \times [0,1]$.

to $T^2 \times \left[0, \frac{1}{2}\right]$ is non-minimally twisting with dividing slopes s_0 and $s_{\frac{1}{2}} = s_0$. In addition, the contact structures on the pieces are uniquely determined by ξ.

Moreover, if ξ is a minimally twisting contact structure on $T^2 \times \left[\frac{1}{2}, 1\right]$ with dividing slopes $s_{\frac{1}{2}} \neq s_1$ and $\xi' = \xi_k^{\pm}$ on $T^2 \times \left[0, \frac{1}{2}\right]$, then the result of gluing ξ' and ξ together is tight if and only if the path describing ξ has only one sign on all the edges and that sign agrees, respectively disagree, with $\xi_k^{\pm}$ if k is odd, respectively even.

We can factor non-minimally twisting contact structures in another way too.

Exercise 5.9.5. In the theorem above we factored the minimally twisting contact structure off of the front boundary of $T^2 \times [0,1]$, but one could also factor it off of the back boundary of $T^2 \times [0,1]$. Prove this and give the criteria for the result of gluing a minimally twisting contact structure to the back boundary of a non-minimally twisting contact structure to be tight. should we say what the gluing criteria is just so it is in print?

We end with the easy observation from the above results.

Corollary 5.9.6. *Any non-minimally twisting tight contact structure on $T^2 \times [0,1]$ with convex boundary having two dividing curves each, is universally tight.*

5.9.2. Proofs of the main results. We begin by classifying the non-minimally twisting contact structures on $T^2 \times [0,1]$ with the same dividing slope on both boundary components.

Proof of Theorem 5.9.2. We break the proof into two pieces.

Lemma 5.9.7. *Let ξ be a non-minimally twisting tight contact structure on $T^2 \times [0,1]$ satisfying the hypothesis of Theorem 5.9.2. Then ξ is isotopic to $\xi_k^{\pm}$ for some choice of sign and some k.*

Lemma 5.9.8. *The contact structures $\xi_k^{\pm}$ are all distinct.*

This theorem clearly follows from these lemmas. □

We now turn to the proofs of the lemmas.

Proof of Lemma 5.9.7. Given ξ, set $N = T^2 \times [0,1]$ and assume ∂N is standard with ruling slope 0. Let A be a vertical annulus in N (*i.e.* $A = S^1 \times [0,1]$ with S^1 a curve on T^2 of slope 0) with boundary ruling curves. Assume $|\Gamma_A|$ is minimal among all annuli isotopic rel boundary to A. Orient A so that $S^1 \times \{0\}$ is oriented up (that is $\frac{\partial}{\partial y}$ is positively tangent to $S^1 \times \{0\}$). Note A must have boundary parallel dividing curves.

Exercise 5.9.9. Prove that if A did not have boundary parallel dividing curves then the contact structure is minimally twisting (and hence invariant in the $[0,1]$-direction).

Cut N open along A and round corners to get M a solid torus. Let D be a meridianal disk to the solid torus. Note the boundary of D is broken into four pieces; two α_0 and α_1 that run along A, one that runs along T_0, and one that runs along T_1. We can choose D so that the parts of ∂D that run along T_0 and T_1 do not intersect any dividing curves. In this case all the dividing curves on D run from α_0 to α_1.

Exercise 5.9.10. Show that if a dividing curve on D began and ended on α_0, say, then you could find a bypass for A and decrease $|\Gamma_A|$.
HINT: You need to be careful if the outermost boundary parallel dividing curve is adjacent to the boundary of one of the α_i's.

Thus there is only one possible configuration for the dividing curves on D. Since cutting M along D yields the unique tight contact structure on the 3-ball we see that the contact structure on N is determined by the dividing curves on A. The topological type of the dividing curves on A is determined by the number of simple closed curves k in Γ_A and the signs of the bypasses on the front and back face.

Exercise 5.9.11. Show that the sign of the bypass on the front face of N is determined by k and the sign of the bypass on back face of N.

Exercise 5.9.12. Given a fixed k show that ξ_k^+ and ξ_k^- have a vertical annulus with k simple closed dividing curves.

Exercise 5.9.13. Show that no vertical annulus in ξ_k^+ has fewer that k simple closed curves.
HINT: Recall all the ξ_k's embed in various tight contact structures on T^3. Use the classification of contact structures on T^3. If you are stuck read the next proof.

These exercises and the above discussion clearly finish the proof of the lemma. □

We now turn to distinguishing all the $\xi_k^\pm$.

Proof of Lemma 5.9.8. We begin by observing that all the ξ_{2m}^+'s are distinct up to isotopy. Indeed note that

$$(T^2 \times [0,1], \xi_{2m}^+)/\sim$$

is contactomorphic to (T^3, ξ_m), where $\sim$ glues the front and back face by the identity.

Exercise 5.9.14. Prove this last statement.

Since the ξ_m's on T^3 are distinct for distinct m's so are the ξ_{2m}^+'s.

Note ξ_{2m}^- is contactomorphic to ξ_{2m}^+ via a diffeomorphism that rotates the T^2 by π. Thus all the ξ_{2m}^- are distinct up to isotopy too. If we glue $N_{\frac{\pi}{2}}$ to the front of ξ_{2m-1}^+ we get a contact manifold contactomorphic to ξ_{2m}^+. Thus all the ξ_{2m-1}^+ are distinct up to isotopy. We can similarly see that all the ξ_{2m-1}^- are distinct up to isotopy.

We are left to show the four sets of contact structures $\mathcal{S}_{o+}, \mathcal{S}_{o-}, \mathcal{S}_{e+}$ and $\mathcal{S}_{e-}$ are non-overlapping, where $\mathcal{S}_{o+}$ is the set of ξ^+_{2m-1}'s, $\mathcal{S}_{o-}$ is the set of all ξ^-_{2m-1}'s and similarly for the $\mathcal{S}_{e+}$ and $\mathcal{S}_{e-}$. The key to this is to observe that the annulus A from the previous proof will have a positive bypass on the back face of any element in $\mathcal{S}_{e+}$ or $\mathcal{S}_{o+}$ and a negative bypass otherwise. Similarly, A will have a positive bypass on the front face of $\mathcal{S}_{o+}$ and $\mathcal{S}_{e-}$ and a negative one otherwise. CHECK the signs of the bypasses.

Exercise 5.9.15. Check these assertions.
HINT: Recall the relative Euler class of N_0 is Poincaré dual to $\begin{pmatrix}1\\1\end{pmatrix}$.

We are not done yet since we have only shown the bypasses on the obvious annulus in contact structures form the various sets have different signs. To really show these sets are disjoint we do the following: if we glue $N_{-\frac{\pi}{2}}$ to the back of any element in $\mathcal{S}_{e+}$ or $\mathcal{S}_{o+}$ we see the resulting contact structure is contactomorphic to an element in $\mathcal{S}_{o-}$ or $\mathcal{S}_{e-}$, respectively. In particular, the contact structure is tight after gluing. However if we glue $N_{-\frac{\pi}{2}}$ to the back of any element of $\mathcal{S}_{e-}$ or $\mathcal{S}_{o-}$ then we get overtwisted contact structures.

Exercise 5.9.16. Find the overtwisted disk
HINT: Look on the annulus A.

Thus the sets $\mathcal{S}_{e+} \cup \mathcal{S}_{o+}$ and $\mathcal{S}_{e-} \cup \mathcal{S}_{o-}$ are disjoint. Similarly, by gluing N_0 to the font of various contact manifolds you see the sets $\mathcal{S}_{o+} \cup \mathcal{S}_{e-}$ and $\mathcal{S}_{o-} \cup \mathcal{S}_{e+}$ are disjoint. This completes the proof. □

We now consider the case of non-minimally twisting contact structures with different dividing slopes on the front and back faces of $T^2 \times [0,1]$.

Proof of Theorem 5.9.4. Let ξ be a tight contact structure on $T^2 \times [0,1]$ with convex boundary having minimal number of dividing curves with dividing slopes s_0 and s_1. Without loss of generality, we can assume that $s_0 = \infty$. Assume the boundary components are in standard form and T_1 has ruling slope ∞. Consider the annulus A of slope ∞ with one boundary component a Legendrian divide on T_0 and the other a ruling curve on T_1. We can make A convex and we note that the dividing set does not intersect $A \cap T_0$ so all the non-closed dividing curves have boundary on $A \cap T_1$. Thus by the Imbalance Principle, Theorem 5.4.18, we can find a bypass for T_1 along A unless $|\partial A \cap \Gamma_{T_1}| = 2$ and A has no closed dividing curves (since in this case there is only one dividing curve and we cannot realize a bypass). Below we will show that this latter case cannot happen. Thus be have a bypass for T_1 along A. When we attach the bypass we will create a basic slice, see Theorem 5.4.11, and the dividing slope on the new torus will have an edge to s_1, be anticlockwise of a_1, and be as close to ∞ as possible. If we continue attaching bypasses we will have broken $T^2 \times [0,1]$ into a sequence of basic slices, which we denote $T^2 \times \left[\frac{1}{2}, 1\right]$,

and $T^2 \times \left[0, \frac{1}{2}\right]$ that has dividing curves on the front and back boundaries of slope ∞. The former case is clearly a minimally twisting contact structure as claimed in the theorem and the latter is a non-minimally twisting contact structure. We prove the uniqueness of the contact structures on these pieces later.

We now verify the claim above that A cannot have a dividing curve with one component (which implies that $|A \cap \Gamma_{T_1}| = 2$ and A has no closed dividing curves). Since A is an annulus of slope ∞ the dividing slope of T_1 must be an integer n (since it must have an edge to ∞ in the Farey graph). Consider an annulus A' of slope $n+2$ with boundary ruling curves on T_0 and T_1. The Imbalance Principle implies that there is a bypass for T_1 on A' and attaching this bypass will result in a basic slice with the slope of the new torus ∞. Thus we have split $T^2 \times [0,1]$ into two pieces: a sequence of basic slices, which we denote $T^2 \times \left[\frac{1}{2}, 1\right]$ and a tight contact structure on $T^2 \times \left[0, \frac{1}{2}\right]$ with dividing slope on both boundary components having slope ∞. The latter contact structure cannot be minimally twisting, or the original ξ would be minimally twisting. Since it is not minimally twisting then we know that there is an annulus A as above that has closed dividing curves on it. Thus we can assume that we were never in this case in the first place.

We now consider gluing a minimally twisting contact structure ξ on $T^2 \times \left[\frac{1}{2}, 1\right]$ corresponding to a decorated path P from ∞ to r (see Theorem 5.5.10) to $\xi_k^{\pm}$ on $T^2 \times \left[0, \frac{1}{2}\right]$. We assume, for now, that $r > 0$. Recall from the proof of Lemma 5.9.7 that the vertical annulus A has a bypass on $T_{\frac{1}{2}}$ of a fixed sign depending on $\pm$ and k. Consider the last basic slice used to build $\xi_k^{\pm}$ (recall their definition from the beginning of this section). We note that it has a slope 0 dividing curve on its back boundary and slope ∞ on its front boundary. Thus we can find a torus T with dividing slope slope r^c (recall this is the furthest clockwise vertex in the Farey graph with an edge back to r, see Section 4.3) in this basic slice. So T will divide $T^2 \times \left[0, \frac{1}{2}\right]$ into $T^2 \times \left[0, \frac{1}{4}, \frac{1}{2}\right]$ and $T^2 \times \left[\frac{1}{4}, \frac{1}{2}\right]$, where the contact structure on the latter is a minimally twisting contact structure with dividing slope on its back boundary 0 and on its front boundary is r^c. Notice that since this minimally twisting contact structure is obtained by splitting a basic slice all the signs in the decorated path P' determining the contact structure are the same and agree with that of the basic slice. Gluing $T^2 \times \left[\frac{1}{4}, \frac{1}{2}\right]$ to $T^2 \times \left[\frac{1}{2}, 1\right]$ results in a contact structure given by the decorated path $P' \cup P$. Since there is an edge from r^c to r we know that the contact structure will be tight if and only if the path can consistently be shortened to a single edge, see Theorem 5.5.14. Thus all the signs in P must be the same.

Now suppose that all the signs of P are the same and are consistent with $\xi_k^{\pm}$.

Exercise 5.9.17. Show that the result of gluing $T^2 \times \left[0, \frac{1}{2}\right]$ to $T^2 \times \left[\frac{1}{2}, 1\right]$ can be embedded in $T^2 \times \mathbb{R}$ with the contact structure $\ker(\sin(2\pi z)\, dx + \cos(2\pi z)\, dy)$ and hence are universally tight.

Exercise 5.9.18. Prove the above gluing result in the case when $r < 0$.
Hint: You might need to consider Exercise 5.3.15 since you will need to consider the last two basis slices in the definition of $\xi_k^{\pm}$.

This completes the proof. □

We finally prove that all the non-minimally twisting contact structures on $T^2 \times [0, 1]$ are universally tight.

Proof. The corollary is an immediate consequence of the discussion in the last two paragraphs of the previous proof. □

Chapter 6

Legendrian knots

In this chapter, we investigate some essential elements of contact geometric knot theory– that is, the theory of Legendrian and transverse knots. The study of Legendrian and transverse knots is an extremely rich and still highly active research area in both low and high-dimensional contact geometry. There are many remarkable combinatorial, analytical, and topological tools to study these objects. Legendrian contact homology, various Floer homologies, and (microlocal) sheaf theoretic invariants are a few that one can mention. Our focus here will be on the topological side of Legendrian and transverse knots. In particular, we would like to explain a strong interplay between convex surfaces and the theory of Legendrian and transverse knots in 3-dimensions.

We begin in Section 6.1 by discussing neighborhoods of Legendrian and transverse knots. The key result in this section is that understanding Legendrian knots is equivalent to understanding their standard neighborhoods. In particular, we can use standard neighborhoods to understand stabilizations and destabilizations of Legendrian knots.

Surgery on Legendrian knots is the prime focus of Section 6.2. Recall from Section 1.5 that one can construct contact structures in every homotopy class of plane field by simple surgeries on transverse knots, and in Section 1.6 we saw that one could construct many tight contact structures by Legendrian surgery on Legendrian knots in the standard tight contact structure on S^3. In Section 6.2, we will see how to perform general "contact surgeries" on any Legendrian knot and show that any contact structure on any closed 3-manifold can be obtained as a sequence of contact surgeries on Legendrian knots in the standard tight contact structure on S^3. We also give several algorithms to understand these surgeries in terms of simpler surgeries; specifically, contact (± 1)-surgeries on Legendrian knots. We also discuss ways to understand Lutz twists (and half-Lutz twists) in terms of contact surgery and also relations between contact surgery diagrams related

to handle slides in the smooth category, as discussed in Section 1.5.1. Finally, we discuss how to compute the "standard invariants", see Section 1.5.4, for contact structures obtained via contact (± 1)-surgery.

Section 6.3 we discuss the relation between the classification of Legendrian knots in a given knot type and the classification of transverse knots in that knot type.

In Section 6.4 and 6.5, we classify Legendrian (and transverse) realizations of the unknot and torus knots, respectively. We show that these knot types are Legendrian simple — meaning that they are determined by their rotation number and Thurston-Bennequin invariant — and we determine their mountain ranges.

Finally, in Section 6.6, we consider Legendrian knots in overtwisted contact structures. In an overtwisted contact structure, one has two types of Legendrian knots: loose, which are knots whose complement is overtwisted, and non-loose, whose complement is tight. We will see that loose knots are determined by their classical invariants up to contactomorphism smoothly isotopic to the identity, and that they realize all possible pairs of integers as rotation number and Thurston-Bennequin invariants. On the other hand, we see that these classical invariants for non-loose knots are restricted. We also give a classification of non-loose Legendrian unknots. More specifically, we see that they only exist in one of the infinitely many overtwisted contact structures on S^3 and have a somewhat surprising mountain range.

6.1. Neighborhoods of Legendrian and transverse knots

In this section, we will see that one can study Legendrian knots by studying their "standard neighborhoods" and that transverse knots do not have such canonical neighborhoods.

6.1.1. Executive summary of main results. Recall from Theorem 1.2.6, that any Legendrian knot L in a contact manifold (M, ξ) has a neighborhood contactomorphic to a neighborhood of the x-axis in $(\mathbb{R}^3, \xi_{std})/\sim$ where $(x, y, z) \sim (x+1, y, z)$. This neighborhood can be chosen to have convex boundary with two dividing curves whose slope is given by the twisting of the contact planes (just take the neighborhood of the x-axis to be a round disk about the origin in the yz-plane times S^1). This is called a *standard neighborhood* of a Legendrian knot L. Conversely any such solid torus is a standard neighborhood of a unique Legendrian knot.

Lemma 6.1.1. *If S is a solid torus in a contact manifold (M, ξ) with convex boundary having two dividing curves with longitudinal slope, then S is a standard neighborhood of a unique Legendrian knot and the contact framing is given by the slope of the dividing curves.*

A simple corollary of this says that studying Legendrian knots in a contact manifold is equivalent to studying their standard neighborhoods.

Lemma 6.1.2. *Two Legendrian knots are Legendrian isotopic if and only if their standard neighborhoods are ambiently contact isotopic.*

In Section 1.4.3 we defined stabilization for Legendrian knots in $(\mathbb{R}^3, \xi_{std})$ in terms of their front diagram. Notice that the stabilization can be done in an arbitrarily small neighborhood of the Legendrian knot. Thus given an oriented Legendrian knot L in (M, ξ) it has a standard neighborhood $N(L)$ contactomorphic to a standard neighborhood $N(L')$ of a Legendrian knot L' in $(\mathbb{R}^3, \xi_{std})$ so that the orientation on L and L' agree under the contactomorphism. We now define the *±-stabilization* of L to the image of the ±-stabilization $S_\pm(L')$ under this contactomorphism. We denote this by $S_\pm(L)$. We now interpret stabilization in terms of standard neighborhoods. Let $N(L)$ be a standard neighborhood of a Legendrian knot. We can identify $N(L)$ with $S^1 \times D^2$ and use this identification to talk about slopes on $\partial N(L)$ (in the language set up in Section 5.6, $N(L)$ is being identified with a solid torus S_∞ with lower meridian ∞). In these coordinates the slope of the dividing curves is some integer n given by the contact twisting (if the framing on $N(L)$ is given by a Seifert surface, then $n = \mathrm{tb}(L)$). We can stabilize L in this neighborhood and thus take a standard neighborhood $N(S_\pm(L))$ inside of $N(L)$. Notice that $N(S_\pm(L))$ has convex boundary having two dividing curves with slope $n-1$ since stabilization decreases the the contact framing. Thus the region $R_\pm = \overline{N(L) - N(S_\pm(L))}$ is diffeomorphic to $T^2 \times [0,1]$ with convex boundary having dividing slopes $n-1$ and n. This is a basic slice. Thus there are two possible contact structures on $R_\pm$ (see Section 5.3). From Section 5.3 we know that the relative Euler class of basic slices with the given dividing curves is $\begin{pmatrix} 0 \\ \pm 1 \end{pmatrix}$. To make sense of this we need an oriented basis for T^2, we orient the longitude in the same direction as L and the meridian so that the longitude followed by the meridian is an oriented basis of T^2 thought of as the boundary of $N(L)$. Given this, we call R_+ with relative Euler class $\begin{pmatrix} 0 \\ 1 \end{pmatrix}$ the positive basic slice and R_- the negative basic slice. We have now mostly proven the following result.

Lemma 6.1.3. *The difference between a standard neighborhood of the stabilized Legendrian $S_+(L)$ and the standard neighborhood of L is a positive basic slice and similarly the difference between the standard neighborhoods of $S_-(L)$ and L is a negative basic slice.*

Exercise 6.1.4. Prove this lemma.

We can turn the above discussion around to see when Legendrian knot L *destabilizes*, that is when there is a Legendrian knot L' such that L is a stabilization of L'. We say L

positive destabilizes if $L = S_+(L')$ and negatively destabilizes if $L = S_-(L')$. This will be very helpful in our classification of Legendrian representatives of certain knot types.

Theorem 6.1.5. *The following are equivalent for a Legendrian knot L with contact twisting n (here we have fixed a framing on L to describe the contact framing as an integer).*

(1) *L $\pm$-destabilizes.*

(2) *The standard neighborhood $N(L)$ is contained in a solid torus S with convex boundary having two dividing curves of slope $n+1$ such that $\overline{S - N(L)}$ is a $\pm$ basic slice.*

(3) *There is a $\pm$-bypass for $\partial N(L)$ that is outside of $N(L)$ and attached along a ruling curve of slope larger than $n+1$.*

(4) *There is a $\pm$-bypass for L on a convex surface containing L that induces a framing larger than $n+1$.*

To summarize, any Legendrian knot can be stabilized as many times as desired, but destabilization is much more difficult and one must find a bypass or a suitable "thickening" of its standard neighborhood to say that it can be destabilized.

We note a useful corollary of the above theorem.

Corollary 6.1.6. *If $N(L)$ is a standard neighborhood of a Legendrian knot L, then any Legendrian knot L' in $N(L)$ that is smoothly isotopic to L is obtained from L by some number of stabilizations.*

Exercise 6.1.7. Prove this corollary.

It can sometimes be useful to consider neighborhoods of Legendrian knots where the coordinates describing the slopes on the boundary are not the "standard" ones discussed above. We can understand this by a simple coordinate change. Suppose we have a solid torus S_m in a contact manifold (we are using the notation of a solid torus with lower meridian m from Section 5.6). If S_m has convex boundary with two dividing curves of slope r, where r and m share an edge in the Farey graph, then S_m is a standard neighborhood of a Legendrian knot L. A stabilization of L will have a standard neighborhood with dividing slope r' where r' is the first slope anti-clockwise of r with an edge to m in the Farey graph. Similarly, a destabilization of L will have a standard neighborhood with dividing slope r'' where r'' is the first slope clockwise of r with an edge to m in the Farey graph.

We can also consider solid tori S^m with upper meridian m. Again S^m has convex boundary with two dividing curves of slope r where r has an edge in the Farey graph to m, then S^m is a standard neighborhood of a Legendrian knot L. A stabilization of L will have a standard neighborhood with dividing curves of slope r' where r' is the first slope clockwise of r with an edge to m and a destabilization of L will have a standard neighborhood with dividing slope r'' where r'' is the first slope anti-clockwise of r with an edge to m.

Exercise 6.1.8. Verify the statements above about standard neighborhoods of Legendrian knots with lower or upper meridian m.

We now consider the boundary of a standard neighborhood of a Legendrian knot.

Theorem 6.1.9. *Let $N(L)$ be a standard neighborhood of a Legendrian knot L. Assume that $\partial N(L)$ is in standard form (see Section 3.4.4).*

(1) *Both Legendrian divides are Legendrian isotopic to L.*

(2) *If the ruling slope is integral and greater than the dividing slope, then a ruling curve is Legendrian isotopic to L.*

(3) *If the ruling slope is integral and less than the dividing slope, then the ruling curve is Legendrian isotopic to $(S_+ \circ S_-)^k(L)$ where k is the difference between the dividing slope and the ruling slope.*

We now turn to transverse knot. Theorem 1.2.4 guarantees that any transverse knot T in a contact manifold (M, ξ) is contactomorphic to a neighborhood of the z-axis in $(\mathbb{R}^3, \xi_{std})/\sim$, where $(x, y, z) \sim (x, y, z + 1)$ where ξ_{std} is give by $\ker(dz - r^2\, d\theta)$. Notice that the neighborhoods of the z-axis has neighborhoods $N_{r_0} = \{(r, \theta, z) : r \leq r_0\}$ and the characteristic foliation on ∂N_{r_0} is a linear foliation with slopes increasing as r_0 increases. It is not hard to see that most of these neighborhoods with different radii are not contactomorphic, and if we ask the contactomorphism to preserve the framing on the z-axis, then none of them are contactomorphic. Thus, unlike for Legendrian knots, it is not easy to study transverse knots via their "standard neighborhoods", since there really is no "standard neighborhood". In Section 6.3 we will see that one can study transverse knots by studying their Legendrian approximations (see Section 1.4.4), this gives an avenue to classify and study transverse knots.

6.1.2. Proofs of main results. In order to prove Lemma 6.1.1 concerning solid tori with convex boundary having two longitudinal dividing curves uniquely determining a Legendrian knot that is a standard neighborhood, we need to study the space of contact structures on such a torus. We know that there is a unique $\xi \in \text{Tight}(S^1 \times D^2; n)$ from Theorem 5.1.5. Let $\Xi(S^1 \times D^2, \xi)$ be the space of contact structures on $S^1 \times D^2$ that are isotopic to ξ (and agree with ξ near the boundary).

Lemma 6.1.10. *The space $\Xi(S^1 \times D^2, \xi)$ is simply connected.*

This lemma will be proven in Section **??**, make sure to add proof but given the lemma we are ready to prove Lemma 6.1.1.

Proof of Lemma 6.1.1. Given Lemma 6.1.10 we can use Lemma 1.2.19 to see that classifying Legendrian knots in $(S^1 \times D^2, \xi)$ up to Legendrian isotopy is the same as classifying

them up to contactomorphism (where the contactomorphisms are smoothly isotopic to the identity). Now suppose that L and L' are two Legendrian knots in $(S^1 \times D^2, \xi)$ that are both smoothly isotopic to the core of the torus and have contact twisting n (relative to the framing on the core coming from the product structure on the solid torus) where n is the slope of the dividing curves on $\partial(S^1 \times D^2)$. Then by Theorem 1.2.6 there is a framing preserving contactomorphism ϕ from a standard neighborhood N of L to a standard neighborhood N' of L' that takes L to L'. Notice that both $(S^1 \times D^2) \setminus N$ and $(S^1 \times D^2) \setminus N'$ are diffeomorphic to $T^2 \times [0,1]$ and both have minimally twisting contact structures and dividing slope n on both boundary components. Thus by Theorem 5.5.1 we can extend ϕ to all of $S^1 \times D^2$. Thus we have constructed a contactomorphism of $(S^1 \times D^2, \xi)$ that takes L to L' and is smoothly isotopic to the identity (since it preserves the framing). □

We are now ready to show that two Legendrian knots are Legendrian isotopic if and only if their standard neighborhoods are ambiently contact isotopic.

Proof of Lemma 6.1.2. We first clarify that when we say that two standard neighborhoods are ambiently contact isotopic, we of course mean that the standard neighborhoods have been arranged to have the same characteristic foliation on their boundary. With this understood, we suppose that L and L' are Legendrian isotopic knots in any contact manifold. Let N and N' be standard neighborhoods of L and L', respectively, and arrange that the characteristic foliation on their boundaries are the same. Lemma 1.2.17 gives us an ambient contact isotopy taking L to L'. Thus after a contact isotopy we can think of N and N' as two standard neighborhoods of a fixed Legendrian knot $L = L'$. Let N'' be a standard neighborhood of L contained in the interior of $N \cap N'$ for which the characteristic foliation on $\partial N''$ agrees with the characteristic foliation on ∂N. Notice that $N'' \setminus N$ is $T^2 \times [0,1]$ and the contact structure is invariant in the $[0,1]$-direction (assuming we have chosen the correct product structure on $T^2 \times [0,1]$, see Theorem 5.5.1). Thus there is a contact vector field transverse to $\partial N''$ and ∂N whose flow takes $\partial N''$ to ∂N and we see there is an ambient contact isotopy taking N'' to N. We may similarly construct an ambient contact isotopy from N' to N'' and hence we have a contact isotopy taking N to N'.

Now suppose we have two Legendiran knots L and L' with standard neighborhoods N and N', respectively, that are ambiently contact isotopic. Thus there is a Legendrian isotopy of L to a Legendrian knot in N'. But now L and L' are two Legendrian knots in N' with the same contact twisting and that twisting agrees with the slope of the dividing curves on $\partial N'$. Now Lemma 6.1.1 gives a further Legendrian isotopy of L taking it to L'. □

Turning to destabilizations of Legendrian knots we are ready to prove Theorem 6.1.5. Recall this theorem says that the following are equivalent for a Legendrian knot L with contact twisting n:

(1) L $\pm$-destabilizes.

(2) The standard neighborhood $N(L)$ is contained in a solid torus S with convex boundary having two dividing curves of slope $n+1$ such that $\overline{S - N(L)}$ is a $\pm$ basic slice.

(3) There is a $\pm$-bypass for $\partial N(L)$ that is outside of $N(L)$ and attached along a ruling curve of slope larger than $n+1$.

(4) There is a $\pm$-bypass for L on a convex surface containing L that induces a framing larger than $n+1$.

Proof of Theorem 6.1.5. We first show that Item (1) implies Item (2). So, suppose that L positively destabilizes. That is there is some L' such that $L = S_+(L')$. Let $N(L')$ be a standard neighborhood of L'. Notice that the contact twisting of L' is $n+1$ (since stabilization reduces contact twisting by 1 and so the dividing curves on $\partial N(L')$ have slope $n+1$. Clearly, if we set $S = N(L')$ then this solid torus has the properties needed in Item (2) by Lemma 6.1.3. The same argument works when L negatively destabilizes.

We can easily see that Item (2) implies Item (1) since the solid S torus given in Item (2) will be the neighborhood of a Legendrian knot L', and the fact that L is the appropriate stabilization of L' follows from Lemma 6.1.3.

Item (3) clearly implies Item (2) since Theorem 5.4.13 tells us how the slope of dividing curves changes when we attach a bypass and the other implication is also clear as we can find a bypass attached along the claimed slope in a basic slice.

Now if we have a solid torus S as in Item (2) then we can find an annulus A with one boundary component a ruling curve of slope $n+2$ on ∂S and the other boundary component on L. The twisting of the contact planes along L relative to A is -2 and the twisting along the other boundary component is -1. Thus we can make A convex. The dividing curves of A intersect L four times and the other boundary component two times. Thus there must be a dividing curve on A that co-bounds a disk with an arc on L. We may now use Giroux Flexibility, Theorem 3.4.1, to create a bypass for L on A.

We note that in the last argument, assuming Item (2) is true, we created a bypass for the neighborhood of L on an annulus, thus we have also shown Item (2) implies Item (4).

Finally, we assume that we have a bypass for L along a surface Σ such that the framing Σ induces on L is greater than the contact framing. We may use Giroux Flexibility again to arrange that a neighborhood of L on Σ is foliated by copies of L (that is the annular neighborhood of L will look like a neighborhood of a ruling curve on a convex torus).

We can now take a standard neighborhood N of L that intersects Σ in one of the curves parallel to L. Notice that $\Sigma \setminus (\Sigma \cap N)$ is still a convex surface and we have a bypass for ∂N attached along a ruling curve of slope larger than n. Thus we see that Item (4) implies Item (3). □

We end this section by proving Theorem 6.1.9 that tells us about various knots on the boundary of a standard neighborhood of a Legendrian knot.

Proof of Theorem 6.1.9. Let L be a Legendrian knot and $N(L)$ a standard neighborhood of L. Recall the model for a standard neighborhood given at the start of this section. Specifically, $N(L)$ is contactomorphic to $S^1 \times D^2_\epsilon$ in $(\mathbb{R}^3, \xi_{std})/\sim$ where $(x, y, z) \sim (x+1, y, z)$ where D^2_ϵ is the disk of radius ϵ in the yz-plane. Notice that $A = \{y = 0\} \cap N(L)$ is an annulus whose characteristic foliation is by circles parallel to L and of course L is the core of this annulus. It is clear that we can take ∂A to be the two Legendrian divides on $\partial N(L)$. Thus we see that either Legendrian divide on $\partial N(L)$ is Legendrian isotopic to L (via the leaves in the characteristic foliation of A).

Fix a framing on L so that the dividing curves on $\partial N(L)$ have slope 0. Let L' be a ruling curve on $\partial N(L)$ with integral slope $n > 0$. Let A be an annulus with one boundary component on L and the other on L'. Notice that A induces the framing n on L and thus the contact twisting along L is $-n$. Similarly, the contact twisting along L' relative to A is $-n$. So we can make A convex. Note that all the dividing curves of A must go from one boundary component of A to the other. This is true since if not, there would be a bypass for L along A and Theorem 6.1.5 would say L destabilizes to some Legendrian L''. But now if $N(L'')$ is a standard neighborhood of L'' then $N(L) \setminus N(L'')$ is $T^2 \times [0, 1]$ with dividing slope 1 on $T^2 \times \{0\}$ and 0 on $T^2 \times \{1\}$. This says that in $T^2 \times [0, 1]$ we can realize any slope in $[1, 0]$. Since ∞ is in this interval the contact structure is overtwisted (a Legendrian divide on a convex torus with this slope would bound a disk, which would thus be an overtwisted disk). Now we can use Giroux Flexibility to arrange that the characteristic foliation of A has $2n$ lines of singularities going from one boundary component to the other and then the rest of A is foliated by "ruling curves". These ruling curves provide a Legendrian isotopy from L to L'.

As above we suppose the dividing curves on $\partial N(L)$ have slope 0. Let L' be a ruling curve on $\partial N(L)$ with integral slope $n < 0$. Notice that L' is smoothly isotopic to L.

Exercise 6.1.11. Show that the framing induced on L' from $\partial N(L)$ differs from the framing on L' induced from L (that is from the framing on L) is $-n$

Notice that from Theorem 3.5.1 we know that the twisting of the contact planes along L' relative to $\partial N(L)$ is $-n$. Thus the contact twisting of L' in the framing of L is $-2n$. Thus if we consider L' pushed into the interior of $N(L)$ we see from Corollary 6.1.6 that it is

simply L stabilized $2n$ times. We are left to see that L' is L stabilized positively n times and negatively n times. This will follow if L and L' have the same rotation number (or if L is a non-null-homologous knot then the relative rotation number between L and L' is 0). This will easily follow from a more general description of rotation numbers for curves on convex tori discussed in Section 6.5. □

6.2. Contact surgery

In this section we will discuss surgery on Legendrian knots and see that one can construct all contact structures on a manifold by such surgeries. We will also see how to describe such surgeries in terms of the Farey graph as well in terms of surgeries on Legendrian knots described in terms of their front diagrams.

6.2.1. Executive summary of main results. Recall that the contact structure gives a Legendrian knot $L \subset (M, \xi)$ natural framing. Using this framing we can identify slopes on the boundary of a neighborhood of L by an extended rational number $r \in \mathbb{Q}^*$ (see Section 4.1). We say $(M_L(r), \xi_L(r))$ is the result of *contact* (r)*-surgery* on L if it is obtained from (M, ξ) by removing a standard neighborhood $N(L)$ of L, then gluing in a solid torus so that the boundary of the meridional disk of the torus is glued to the r slope curve on $\partial\overline{M - N(L)}$, and finally extending $\xi|_{M\setminus N(L)}$ over the torus by a tight contact structure on the torus.

If L is null-homologous, then it is the boundary of a surface Σ and inherits a framing from Σ. Dehn surgery on L is described in terms of the framing coming from Σ and we know that $\mathrm{tb}(L)$ is simply the contact framing minus the framing coming from Σ (see Section 1.5.1 for a discussion of Dehn surgery). Thus the 3-manifold obtained from contact (r)-surgery on L is the same is the result of Dehn $r + \mathrm{tb}(L)$ surgery on L. When writing contact surgery on a Legendrian knot in a front diagram we will always put the r in parentheses and a surgery coefficient without parentheses will always denote a Dehn surgery coefficient (that is in terms of the Seifert framing). See Figure 6.2.1.

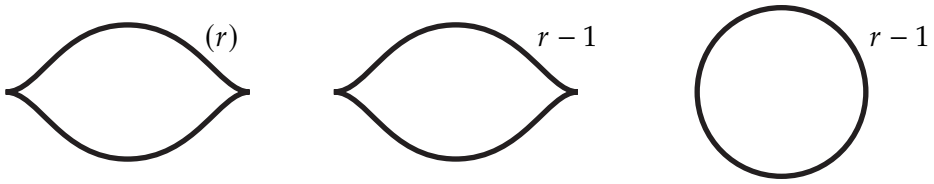

Figure 6.2.1. On the left is contact (r)-surgery on the Legendrian unknot. In the middle, the Dehn surgery coefficient is shown on the Legendrian unknot. On the right is a smooth representation of the unknot with this the Dehn surgery coefficient corresponding to the contact surgery described on the left.

Remark 6.2.1. Notice that this definitely does not describe a unique tight contact structures for all r since there might be many choices for the extension of $\xi|_{M\setminus N(L)}$ over the solid torus.

To better understand this, we describe the surgery differently. Recall, as discussed in the previous section, that the standard neighborhood $N(L)$ can be thought of as a solid torus S_∞ with lower meridian ∞ and having convex boundary with two dividing curves of slope 0 (the slope is 0 since we are using the framing on L coming from the contact planes). The result of contact (r)-surgery is removing S_∞ from M and replacing it with S_r with a contact structure in Tight$(S_r; 0)$. We classified contact structures in Tight$(S_r; 0)$ in Section 5.6. In particular, if $r = 1/n$ for any integer n, then there is a unique tight contact structure in Tight$(S_r; 0)$ and contact (r)-surgery is completely well-defined. For $r = 0$ we see that Tight$(S_0, 0)$ is empty since a meridional disk can have boundary a dividing curve and hence the contact structure is overtwisted. Thus contact (0)-surgery is not defined. For other r, there are choices for contact (r)-surgery and one must specify what choice is made in a given situation. In Section 5.6 we saw how to compute the number of contact structures in Tight$(S_r; 0)$ in terms of the continued fraction of r and also in terms of paths in the Farey graph from r clockwise to 0 with $\pm$ decorations on the all the edges except the first.

We saw in Section 1.6.3 that if L was a Legendrian knot in (S^3, ξ_{std}), or more generally any Stein fillable contact manifold, then contact (-1)-surgery produced a contact structure that was also Stein fillable. So we see that such a contact surgery holds a special place among all contact surgeries. Contact (-1)-surgery is usually called *Legendrian surgery*. One can show that some other contact surgeries that preserve Stein fallibility.

Lemma 6.2.2. *For any $r < 0$, contact (r)-surgery on L is equivalent to contact (-1)-surgeries on all components of a link obtained from L by a sequence of stabilizations and Legendrian push-offs of L.*

Moreover, if (M, ξ) is symplectically fillable in any sense, then contact (r)-surgery is also symplectically fillable in the same sense.

We note here that a Legendrian push-off of L is a copy of L obtained by pushing L slightly in the direction of a Reeb vector field.

The second part of the lemma follows immediately from the first and the fact that Legendrian surgery preserves all types of symplectic fillability. The latter fact will be explained in Chapter 7.

We cannot effect contact (r)-surgery for any r by a sequence of Legendrian surgeries, but if we consider both $(+1)$ and (-1) contact surgeries we can achieve any contact (r)-surgery.

Lemma 6.2.3. *Any contact (r)-surgery on a Legendrian knot L is equivalent of contact (± 1)-surgery on the components of a link obtained from L by a sequence of stabilizations and Legendrian push-offs of L.*

In the next subsection we will give an explicit algorithm to convert a given contact surgery into a sequence of contact (± 1)-surgery and to convert a description of a contact surgery in terms of the Farey graph (recall from above that a contact surgery can be described by a decorated path in the Farey graph) into one in terms of contact (± 1)-surgeries on the Legendrian and its Legendrian push-offs and stabilizations.

We now state two useful lemmas about contact surgery. The first is "cancellation result".

Lemma 6.2.4 (Ding and Geiges 2001, [DG01])**.** *For any Legendrian knot L in a contact manifold (M, ξ) performing contact (± 1)-surgery on L and contact (∓ 1)-contact surgery on a Legendrian push-off of L results in (M, ξ). That is contact $(+1)$ and contact (-1)-surgery on the same knot cancel.*

Our second useful observation is that Lutz twists can be performed via contact surgery.

Lemma 6.2.5. *Let L be an oriented Legendrian knot in a contact manifold (M, ξ). Let L' be a Legendrian push-off of L negatively stabilized twice. Performing a half-Lutz twist on the transverse push-off L_+ of L results in the same contact structure obtained from contact $(+1)$-surgery on both L and L'. See Figure 6.2.11.*

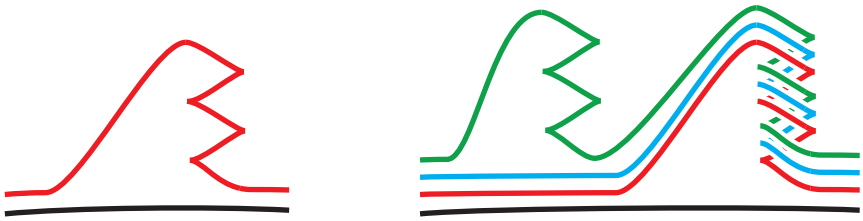

Figure 6.2.2. The black arc is a portion of the Legendrian knot L, while the other components are Legendrian push-offs and stabilizations of L. Contact $(+1)$-surgery on the link on the left link is equivalent to a half-Lutz twist on the transverse push-off of L while contact $(+1)$-surgery on the right link is equivalent to a full-Lutz twist.

It was first observed in [EH02a] that one can "undo" a half-Lutz twist via contact (-1)-surgeries which implies this lemma given the previous lemma. The lemma was first explicitly stated in [DG04]. Since a Lutz twist is the same as two half-Lutz twists, it is clear that one can obtain a full-Lutz twist by a sequence of four contact $(+1)$-surgeries. See Figure 6.2.11.

The operation of contact surgery, in principle, captures the entire complexity of contact geometry of closed, oriented 3-manifolds. This is via the following extension of the Lickorish-Wallace theorem for 3-manifolds.

Theorem 6.2.6 (Ding-Geiges 2004, [DGS04]). *Every closed, co-oriented, contact 3-manifold (M, ξ) can be obtained by contact (± 1) surgery along a Legendrian link in (S^3, ξ_{std}).*

Compare with [EH02a]. We note that the proof of this theorem will show that one can choose that only one of the contact surgery coefficients is positive and the rest are negative. As mentioned above, if a contact surgery diagram only involves negative coefficients, the resulting contact structure will be Stein fillable. However, there exist tight but not Stein fillable contact structures, and in particular, such a contact structure must contain positive coefficients in any contact surgery description.

Just as for smooth 3-manifolds, a given contact structure can be described by more than one contact surgery diagram. For example, one can use Lemma 6.2.4 to add canceling $(+1)$ and (-1)-contact surgery pairs to a diagram. Here, we discuss other useful modifications of contact surgery diagrams that are the contact geometric analog of "handle slides" in smooth topology.

Lemma 6.2.7. *The contact surgery diagrams in Figure 6.2.3 and Figure 6.2.4 represent the same contact manifold.*

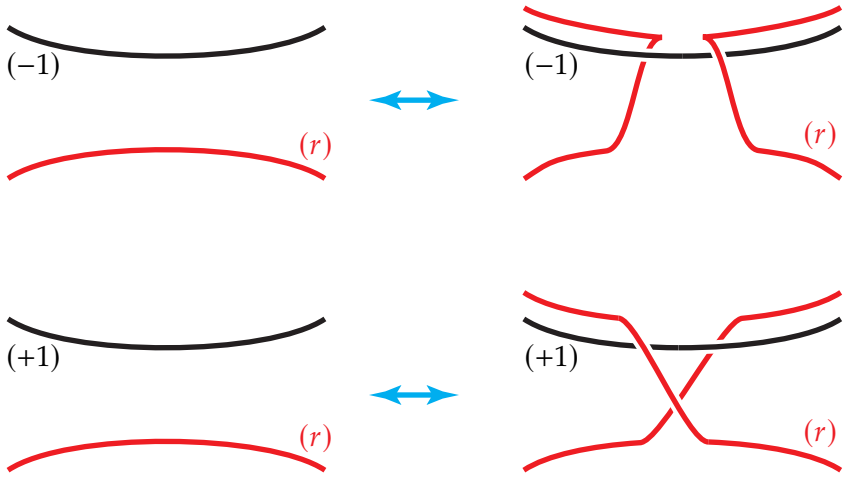

Figure 6.2.3. Equivalent contact surgery diagrams. The red curves above the black curves on the left are copies of the black curves shifted up outside the region shown.

The next alteration one can make to a contact surgery diagram is analogous to converting a 1-handle into "dotted circle notation", [GS99].

Lemma 6.2.8. *One may replace a 1-handle used in the description of a contact manifold with a $(+1)$-surgery on a maximal Thurston-Bennequin invariant unknot as shown in Figure 6.2.5.*

We note that these results seem to have been known for some time, and implicitly used in some papers, but a version of them was first written down with careful proofs in [DG09], thought there the handle slides were actually different.

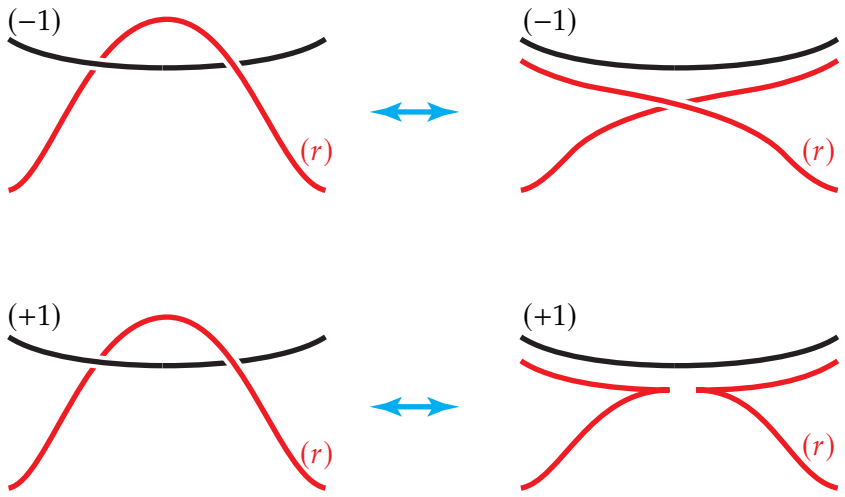

Figure 6.2.4. Equivalent contact surgery diagrams. The red curves near the black curves on the left are copies of the black curves shifted up outside the region shown.

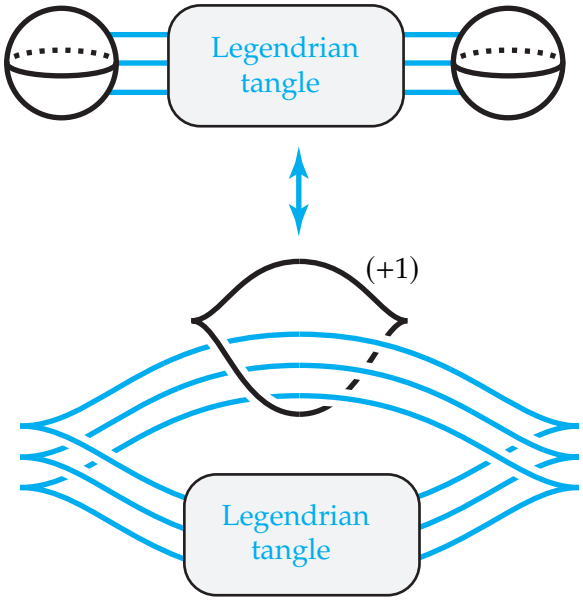

Figure 6.2.5. Equivalent contact surgery diagrams. The blue tangle has arbitrary surgery coefficients.

It will be useful to be able to compute the invariants of the homotopy class of a contact structure, see 1.5.2, obtained from contact surgery on a Legendrian link. Given the above results, we will restrict to the case of contact (± 1)-surgery on a Legendrian link[1]. Recall these homotopy invariants are the Euler class $e(\xi)$, its refinement: Γ-invariant $\Gamma(\xi)$, and

[1] We note that there are (more complicated) formulas to compute these invariants for any contact surgeries as was shown in [EKO24].

the d_3-invariant $d_3(\xi)$. We first compute the first and last invariants as they are more straightforward. Recall that the d_3-invariant is only defined when the Euler class of the plane field is torsion (and a similar invariant can be defined when the Euler class is not torsion, see [Gom98]).

Theorem 6.2.9. *Suppose that the contact structure ξ on M is obtained from (S^3, ξ_{std}) by contact surgery on the link $L_1 \cup \cdots \cup L_{n+m}$ where contact (-1)-surgery is performed on the first n components of the link and contact $(+1)$-surgery is performed on the last m components.*

(1) *The Poincaré dual of the Euler class of ξ is given by*

$$P.D.(e(\xi)) = \sum_{i=1}^{n+m} \mathrm{rot}(L_i)[\mu_i],$$

where $[\mu_i]$ is the homology class of the meridian to L_i in M.

(2) *If $e(\xi)$ is torsion then we have that*

$$d_3(\xi) = \frac{1}{4}(c^2 - 3\sigma(M) - 2(\chi(X) - 1)) + m,$$

where X is the 4-manifold obtained from B^4 by attaching 2-handles to the L_i with the given framings, M is its intersection form, $\sigma(M)$ is the signature of M, and c^2 is computed as follows. Let $\mathbb{r}$ be the column vector whose i^{th} entry is $\mathrm{rot}(L_i)$, then

$$c^2 = \mathbb{r}^T M^{-1} \mathbb{r},$$

where $\mathbb{r}^T$ is the transpose of $\mathbb{r}$.

This theorem is due to Gompf in [Gom98] in the case of contact (-1)-surgeries and was generalized to the above theorem by Ding, Geiges, and Stipsicz in [DGS04].

We now turn to the Γ-invariant which is a refinement of the Euler class and is determined by it if $H_1(M)$ has no 2-torsion. We recall that Γ is a map from the set of spin structures on M to the set of elements in $H_1(M)$ which, when multiplied by 2, are Poincaré dual to $e(\xi)$ (that is the set of "half-Euler classes"). We will represent spin structures in a surgery diagram for M using characteristic sublinks, see Appendix 1.4.

Theorem 6.2.10. *Suppose that the contact structure ξ on M is obtained from (S^3, ξ_{std}) by contact (± 1)-surgery on the link $L_1 \cup \cdots \cup L_n$. Let I be the matrix with i, j entry $\mathrm{link}(L_i, L_j)$ where $\mathrm{link}(L_i, L_i)$ is the smooth surgery coefficient on L, and $\mathbb{m}$ be the column vector with i^{th} entry the homology class of the meridian μ_i. If the spin structure $\mathfrak{s}$ is represented by the characteristic sub-link $(L_i)_{i\in J}$, then*

$$\Gamma(\xi, \mathfrak{s}) = \frac{1}{2}\left(\sum_{i=1}^{n} \mathrm{rot}(L_i)[\mu_i] + \sum_{i\in J} (I\mathbb{m})_i\right),$$

where $(I\mathbb{m})_i$ is the i^{th} entry in the vector $I\mathbb{m}$.

This theorem is again due to Gompf in [Gom98] in the case of contact (-1)-surgeries and was generalized to the above theorem by Kegel, Onaran, and the first author in [EKO24].

6.2.2. Proofs of main results. We begin by describing an algorithm to turn any contact (r)-surgery L, for $r < 0$, into a sequence of contact (-1)-surgeries on L (recall this is also called Legendrian surgery) and its Legendrian push-offs and stabilizations. To this end, we first note that if $N(L)$ is a standard neighborhood of L where, as a solid torus, we think of it as $S^1 \times D^2 = S_\infty$ and the contact structure on it is the unique element in $\text{Tight}(S_\infty; 0)$, then Legendrian surgery on L is the result of removing $S_\infty = N(L)$ and replacing it with S_{-1} with the unique tight contact structure in $\text{Tight}(S_{-1}; 0)$. We would like to reinterpret this if we are using "non-standard" coordinates on $\partial N(L)$. Suppose we have chosen coordinate on $\partial N(L)$ so that the meridional slope is m. Then $N(L)$ is a solid torus with lower meridian m, that is S_m and the dividing curves on $\partial N(L)$ must be longitudinal with respect to m. That is their slope s has an edge to m in the Farey graph. Notice that this is a unique slope m' in (m, s) that has an edge to both m and s (for example if m and s are both negative then $m' = s \oplus m$). Then Legendrian surgery on L is the result of removing $S_m = N(L)$ and replacing it with $S_{m'}$ with the unique tight contact structure in $\text{Tight}(S_{m'}; r)$.

Before describing the algorithm, we first consider some examples of converting a contact (r)-surgery where the contact structure on the solid torus is described by a path in the Farey graph to a sequence of Legendrian surgery on L and its Legendrian push-offs and stabilizations.

Example 6.2.11. Suppose we want to perform contact (-4)-surgery on L where the contact structure on the solid torus glued in during the surgery is given by the path in the Farey graph shown on the left in Figure 6.2.6. We note that $N(L)$ is S_∞ with the unique contact structure in $\text{Tight}(S_\infty; 0)$. This corresponds to the path shown in the middle of Figure 6.2.6. Recall our discussion of stabilization of Legendrian knots in terms of their standard neighborhoods from the previous section. If we stabilize L positively twice and negatively once then we have the standard neighborhood $N(S^2_+ \circ S_-(L))$ inside of $N(L)$, its boundary has dividing slope -3 and its complement in $N(L)$ is a tight contact structure on $T^2 \times [0, 1]$ given by the path shown on the right of Figure 6.2.6. If we perform Legendrian surgery on $S^2_+ \circ S_-(L)$, then, as discussed above, we will remove $N(S^2_+ \circ S_-(L))$ and replace it with the solid torus S_{-4}. Thus after this Legendrian surgery, the original $N(L)$ has been replaced by the solid torus with the contact structure given on the left of Figure 6.2.6. That is we have effected the contact (-4)-surgery on L by Legendrian surgery on $S^2_+ \circ S_-(L)$. See the top row of Figure 6.2.7

From this example, it is easy to see that any contact (-4)-surgery on L can be achieved by Legendrian surgery on some three-fold stabilization of L and moreover any negative

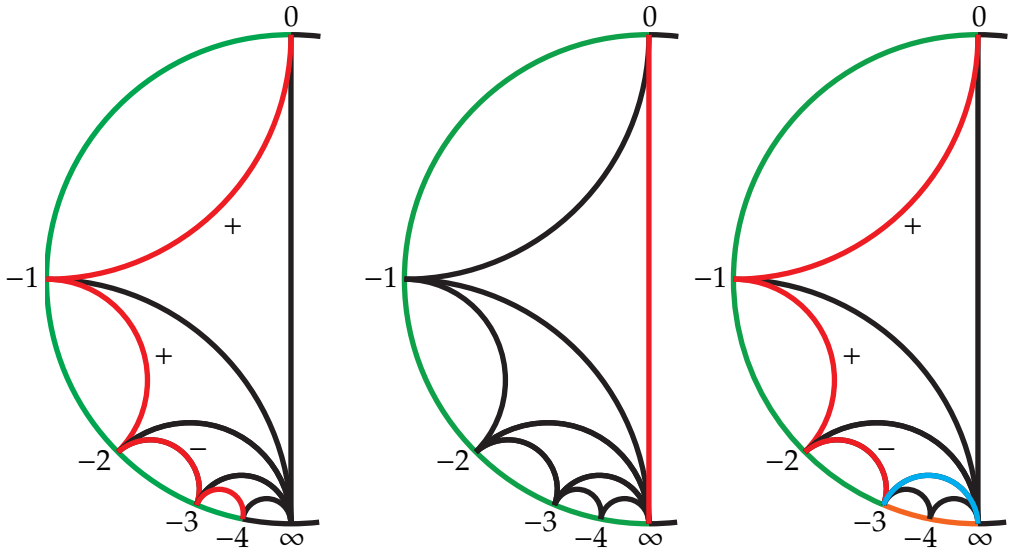

Figure 6.2.6. On the left is a path shown in red that describes the contact structure on a solid torus used to perform a contact (-4)-surgery on L. (The arc in green shows the slopes that can be realized by convex tori in this solid tori.) In the middle we see the contact structure on $N(L)$. On the right we see in red the path corresponding to the contact structure on the complement of $N(S^2_+ \circ S_-(L))$ in $N(L)$ and in blue the solid torus $N(S^2_+ \circ S_-(L))$.

integer surgery can be similarly achieved. This proves a special case of the first part of Lemma 6.2.2.

Example 6.2.12. We now consider contact $(-1/2)$-surgery on L. Recall that this contact surgery is unique, but we note that it is represented by replacing the standard neighborhood of $N(L)$, thought of as S_∞, by a solid torus with lower meridian $-1/2$ with its unique tight contact structure. If we perform Legendrian surgery on L we remove $N(L)$ and replace it with S_{-1}. The contact structure on S_{-1} is shown in Figure 6.2.8. We note that the contact structure on S_{-1} has convex boundary with dividing slope 0. That is, it is a neighborhood of a unique Legendrian knot L'. If we perform Legendrian surgery on L' we remove S_{-1} and, according to our discussion above, replace it with $S_{-1/2}$. That is contact $(-1/2)$-surgery on L can be achieved by Legendrian surgery on L followed by Legendrian surgery on L'. We would now like to identify L'. According to Theorem 6.1.9 L' is Legendrian isotopic to a dividing curve on ∂S_{-1}, but ∂S_{-1} is also ∂S_∞ so this Legendrian divide is also Legendrian isotopic to L and can be thought of as a Legendrian push-off of L along the Reeb vector field. See Figure 6.2.7

Thus we see that contact $(-1/2)$-surgery can be achieved by Legendrian surgery on L and a Legendrian push-off of L. It is clear that any contact $(1/n)$-surgery, for a negative integer n can similarly be achieved. This proves a special case of the first part of Lemma 6.2.2.

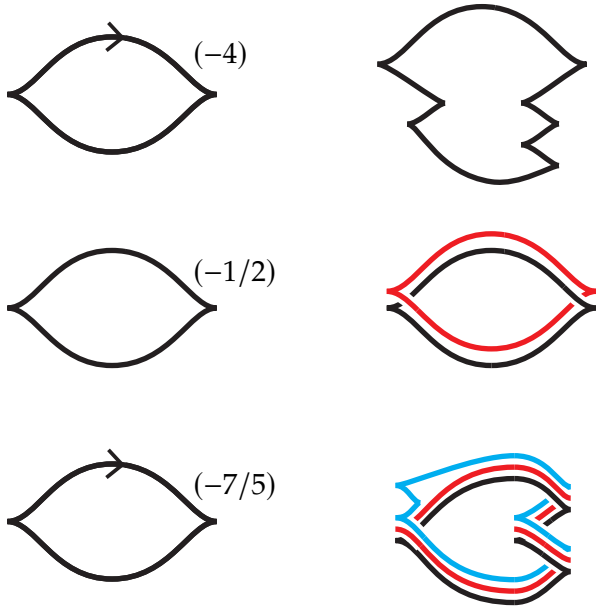

Figure 6.2.7. Converting contact surgery into a sequence of Legendrian surgeries. Rows 1, 2, and 3 illustrate Examples 6.2.11, 6.2.12, and 6.2.13, respectively, in the case that L is the maximal Thurston-Bennequin Legendrian unknot. The contact surgeries on the left are realized by Legendrian surgery on the links shown on the left.

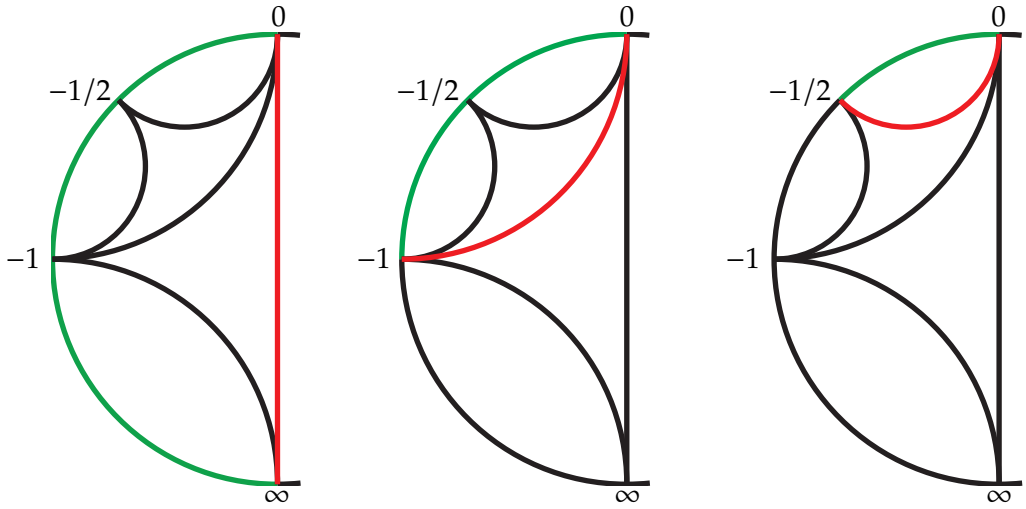

Figure 6.2.8. On the left is we see in red the path corresponding to the contact structure on the complement of $N(L)$ (The arc in green shows the slopes that can be realized by convex tori in this solid tori.) In the middle we see the contact structure on S_{-1} which is a standard neighborhood of a Legendrian knot L'. On the right we see in red the path corresponding to the contact structure $S_{-1/2}$ that is glued to the complement of $N(L) = S_\infty$ when performing contact $(-1/2)$-surgery.

We consider one more example, combining elements of the above two examples, before giving the general algorithm.

Example 6.2.13. Suppose we want to perform contact $(-7/5)$-surgery on L where the contact structure on the solid torus glued in during the surgery is given by the path in the Farey graph shown on the left in Figure 6.2.9. We note that $N(L)$ is S_∞ with the unique

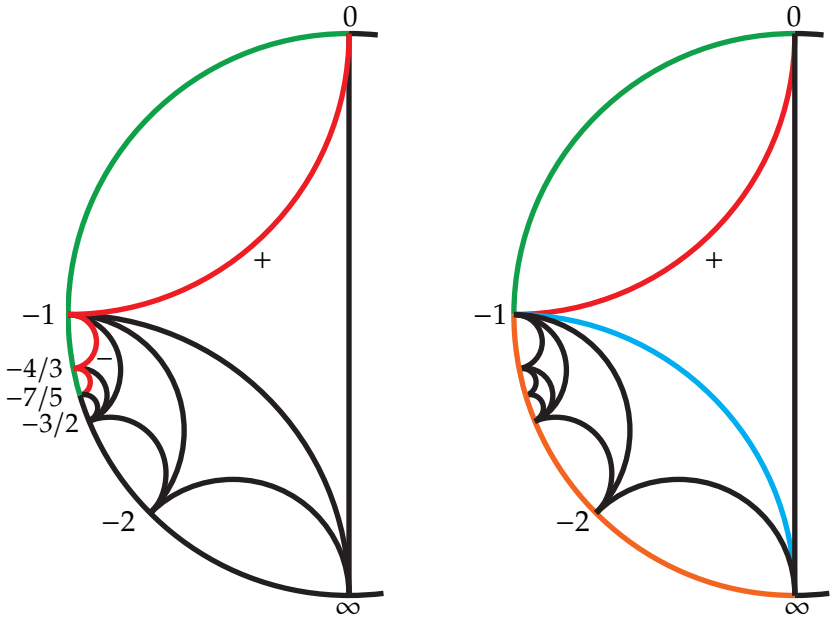

Figure 6.2.9. On the left is a path shown in red that describes the contact structure on a solid torus used to perform a contact $(-7/5)$-surgery on L. (The arc in green shows the slopes that can be realized by convex tori in this solid tori.) On the right we see the region between $N(L)$ and $N(S_+(L))$ in red and the neighborhood $N(S_+(L))$ in blue.

contact structure in Tight$(S_\infty; 0)$. Recall our discussion of stabilization of Legendrian knots in terms of their standard neighborhoods from the previous section. If we stabilize L positively once then we have the standard neighborhood $N(S_+(L))$ inside of $N(L)$, its boundary has dividing slope -1 and its complement in $N(L)$ is a tight contact structure on $T^2 \times [0, 1]$ given by the path shown on the middle of Figure 6.2.9.

Performing Legendrian surgery on $S_+(L)$ will remove $N(S_+(L))$, thought of as S_∞ with convex boundary having dividing slope -1 and replacing it with S_{-2} with convex boundary having dividing slope -1. This is a standard neighborhood of a Legendrian knot L' and is shown on the left in Figure 6.2.10. As discussed above, we we perform Legendrian surgery on L' we will remove its standard neighborhood and replace it with $S_{-3/2}$. The contact structure on $S_{3/2}$ has convex boundary with dividing slope -1 and is a standard neighborhood of some Legendrian knot L''. The contact structure on $S_{-3/2}$ is shown in the middle of Figure 6.2.10. If we stabilize L'' negatively and consider its standard neighborhood $N(S_-(L''))$ we see the dividing slope on $\partial N(S_-(L''))$ is $-4/3$ (notice that in the consistent coordinates we use to describe slopes on all our tori, the meridional slope of $N(S_-(L''))$ is $-3/2$). The complement of $\partial N(S_-(L''))$ in $S_{3/2}$ (thought of as the standard

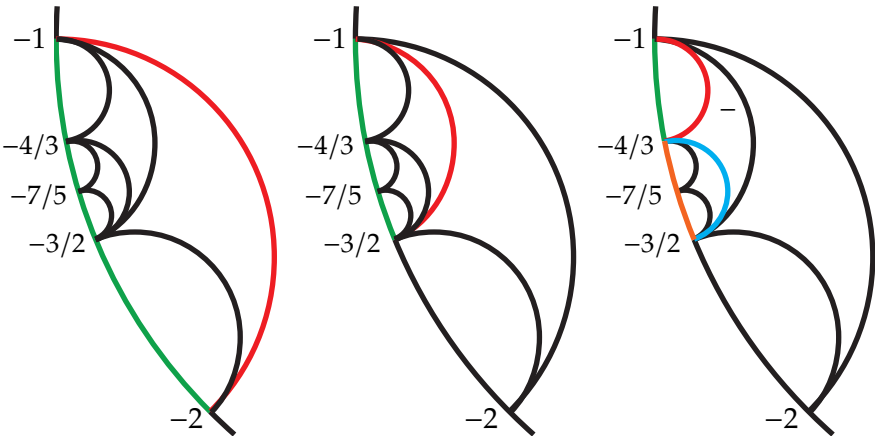

Figure 6.2.10. On the left, shown in red, is the contact structure on S_{-2} that is the result of Legendrian surgery on $S_+(L)$. In the middle is the result of surgery on L' determined by the solid torus S_{-2} which is a solid torus $S_{-3/2}$ that is a standard neighborhood of a Legendrian L''. On the right we see the $T^2 \times [0,1]$ in red that is the result of negatively stabilizing L'' and in blue we see the standard neighborhood of the stabilized knot.

neighborhood of L'') is $T^2 \times [0,1]$ and the contact structure is shown on the right of Figure 6.2.10. Performing Legendrian surgery on $S_-(L'')$ will remove $N(S_-(L''))$ and replace it with $S_{-7/5}$ with its unique tight contact structure. Notice that this sequence of surgeries has had the effect of removing $N(L)$ and replacing it with the desired contact structure.

We are left to identify L' and L'' in terms of L. As argued in the previous examples, we see that L' is a Legendrian push-off of $S_+(L)$ and so is L''. Thus the contact $(-7/5)$-surgery is achieved by Legendrian surgery on the link obtained by positively stabilizing L, taking two Legendrian push-offs of the stabilization and negatively stabilizing the second Legendrian push-off. One can clearly do any contact $(-7/5)$-surgery on L in a similar manner. See Figure 6.2.7.

We are now ready to present the general algorithm for turning a negative contact surgery on a Legendrian knot into a sequence of Legendrian surgeries on an associated link. To this end, it will be helpful to consider arbitrary coordinates on a solid torus. So a Legendrian knot L can have standard neighborhood $N(L)$ which is a torus with lower meridian m and dividing slope s where s and m are connected by an edge in the Farey graph. In these coordinates a contact surgery with a negative coefficient will correspond to a smooth surgery slope r where $r \in (m, s)$. (Recall our conventions for discussing intervals of slopes on the Farey graph from the end of Section 4.2.)

Algorithm to convert contact surgery into a sequence of Legendrian surgeries. Given a Legendrian knot L and surgery slope r as above, we first produce a sequence of slopes in the interval $[m, s]$ as follows.

(1) Let $s_0 = s$ and $m_0 = m$.

(2) Given s_{i-1} and m_{i-1} consider the points $c_0 = s_i, c_1, \dots c_{l_i}$ in $(m_i, s_i]$ so that they form a continued fraction block and $r \in (c_{l-1}, c_l]$. (For example, if both s_{i-1} and m_{i-1} are negative, or both positive, then $c_j = s_{i-1} \oplus jm_{i+1}$.) Notice that each c_j has an edge to m_{i-1}
   (a) If $l_i = 1$, then let $s_i = s_{i-1}$ a and $m_i = c_1$.
   (b) If $l_i \neq 1$, then let $s_i = c_{l-1}$ and $m_i = m_{i-1}$.

(3) If $r = m_i$, then stop, otherwise repeat the above step to get the next s_j and m_j.

Note the above procedure produces a sequence of slopes $s_0, \dots, s_k$ that start at s and move anti-clockwise towards r (but not necessarily strictly anti-clockwise) and a sequence of slopes $m_0, \dots, m_k$ that start at m and move clockwise with $m_k = r$.

Let N_i be the solid torus with meridional slope m_i and dividing slope s_i. By the definition of the s_i and m_i it is clear that each N_i is a solid torus with longitudinal dividing curves and hence is a standard neighborhood of a Legendrian knot L_i.

By construction, N_0 is the original $N(L)$. We now see how N_i is obtained from N_{i-1}. If s_i and m_i are obtained from s_{i-1} and m_{i-1} as in Item (2a), then N_i is the result of Legendrian surgery on L_{i-1} in N_{i-1}. We also notice that in this case, L_i is Legendrian isotopic to a dividing curve on ∂N_i, and since $\partial N_i = \partial N_{i-1}$ it is also isotopic to L_{i-1}. In particular, it is a Legendrian push-off of L_{i-1}. If s_i and m_i are obtained from s_{i-1} and m_{i-1} as in Item (2b), then N_i is the standard neighborhood of L_{i-1} after it has been stabilized $l_i - 1$ times and thus L_i is this stabilized knot. Notice for the construction of the m_i and s_i to terminate, we must have that the final torus N_k is obtained from N_{k-1} by Legendrian surgery on L_{k-1}.

We note that if we perform all of these stabilizations and surgeries in $N(L)$ then this will result in a solid torus with lower meridian r. That is, if L is in M then this is equivalent to removing $N(L)$ from M and replacing it with S_r. We now consider the contact structure on S_r. Let $A_i = N_i \setminus N_{i-1}$. Notice that the torus S_r is $A_0 \cup \dots \cup A_{k-1} \cup N_k$. Note that $A_i = \partial N_i$ will be empty if the i^{th} slopes are obtained from the $(i-1)^{st}$ slopes as in Item (1a) and A_i will be a $T^2 \times [0, 1]$ in the other case. In this latter case, the contact structure on A_i will be a continued fraction block determined by the stabilizations done to get from L_{i-1} to L_i. Thus the path in the Farey graph given by $A_0 \cup \dots \cup A_{k-1} \cup N_k$ will be a minimal path from $s = s_0$ anti-clockwise to r and any decorations on this path determining a contact structure in Tight$(S_r; s)$ can be achieved by some choice of stabilizations. That is we have shown that any negative contact surgery on L that corresponds to a sequence of Legendrian surgeries on L and its Legendrian push-offs and stabilizations.

Exercise 6.2.14. Consider the three examples above and see how they were constructed from this algorithm.

Exercise 6.2.15. Suppose that L is a Legendrian knot with Thurston-Bennequin invariant 3. Describe how to do contact $\left(\frac{1}{n} - 3\right)$ surgery on L in terms of Legendrian surgery and similarly for contact $\left(-\frac{1}{n} - 3\right)$-surgery.

Exercise 6.2.16. Suppose that L is a Legendrian knot with Thurston-Bennequin invariant 2. Describe how to do contact $\left(\frac{13}{49} - 2\right)$ surgery on L in terms of Legendrian surgery.

Proof of Lemma 6.2.2. The first part of the lemma follows from the above algorithm and the second follows from Lemma 7.4.27. □

We are now ready to show that any contact surgery on L can be achieved by a sequence of contact (± 1)-surgeries on a link L and its Legendrian push-offs and stabilizations.

Proof of Lemma 6.2.3. Recall that if $N(L)$ is a standard neighborhood of L in (M, ξ), thought of using standard coordinates on $\partial N(L)$ (so that $N(L)$ is S_∞), then contact $(+1)$-surgery on L is the result of removing $N(L)$ form M and replacing it with S_1 with its unique tight contact structure. We would like to interpret this for $N(L)$ with any coordinates on its boundary. So if $N(L)$ is S_m for some slope m and the dividing slope on $\partial N(L)$ is s for some slope with an edge to m in the Farey graph, then notice that there is a unique slope m' with an edge to s and m that is not contained in $[m, s]$. Contact $(+1)$-surgery on L is the result of removing $N(L)$ from M and replacing it with $S_{m'}$ with its unique tight contact structure.

We now return to $N(L)$ with standard coordinates on $\partial N(L)$ such that the dividing slope is 0 (that is we are using the contact framing on L). Performing contact $(+1)$-surgery on L will result in a solid torus S_1 and S_1 has dividing slope 0. So S_1 is a standard neighborhood of a Legendrian knot L'. As observed above, we know that L' is Legendrian isotopic to a ruling curve on $\partial S_1 = \partial N(L)$ and hence Legendrian isotopic to L. In fact, L' is a Legendrian push-off of L. Contact $(+1)$-surgery on L' we will result in a solid torus $S_{1/2}$. Continuing we see that if we perform contact $(+1)$-surgery on L and $n-1$ Legendrian push-offs of L then this is the same as removing $N(L)$ from M and replacing it with $S_{1/n}$ with its unique tight contact structure.

Suppose we wish to perform contact (r)-surgery on L for some $r > 0$. Notice that there is a unique k such that $\frac{1}{k+1} \leq r < \frac{1}{k}$. Perform contact (1)-surgery on L and n Legendrian push-offs of L. This will result in a solid torus $S_{1/(k+1)}$ with convex boundary having dividing slope 0. This is a standard neighborhood of a Legendrian knot L', which as above is simply a Legendrian push-off of L. Notice that $r \in [1/(k+1), 0]$ so contact r surgery on L' is a negative contact surgery and from the algorithm above can be achieved by a sequence of Legendrian surgeries on L' and its Legendrian push-offs and stabilizations. □

We now turn to the proof of the "cancellation lemma".

Proof of Lemma 6.2.4. From the above discussion, it is clear that if we use the contact framing on L then its standard neighborhood $N(L)$ is S_∞ with convex boundary having dividing curves of slope 0. Contact (+1)-surgery removes S_∞ and replaces it with S_1 with the same dividing curves on the boundary. Now S_1 is a standard neighborhood of some Legendrian knot L' and contact (-1)-surgery on L' removes S_1 and replaces it with S_∞. That is it undoes the previous surgery. Now we observe, as we did above. that L' is a Legendrian push-off of L. Thus concluding the proof in this case. The case where we initially perform contact (-1)-surgery on L is analogous. □

With the above discussion of contact surgery in terms of the Farey graph, the proof that one can perform a half-Lutz twist via contact surgery is relatively simple.

Proof of Lemma 6.2.5. We recall and reformulate how to perform a Lutz twist. Let T be a transverse knot in (M, ξ). We take a standard neighborhood $N(T)$ of T. Recall this means that $N(T)$ is $D^2_\epsilon \times S^1$ in $\mathbb{R}^3/\sim$, where $(x, y, z) \sim (x, y, z + 1)$, with the contact structure $\xi_{std} = \ker(\cos r\, dz + r \sin r\, d\theta)$, where D^2_t is the disk of radius t about the origin in the xy-plane. Notice that the characteristic foliation on $\partial N(T)$ is a linear foliation of some negative slope a, after possibly shrinking $N(T)$ and changing the framing on $N(T)$ we can assume that $a = 0$. We consider $\partial(D^2_t \times S^1)$ as t decreases from ϵ to 0 the slopes of the linear characteristic foliations go from 0 to $-\infty$ (though never make it to $-\infty$). A half-Lutz twist removes $N(T)$ from M and replaces it with a torus with the same meridian, but where the slopes of the foliations on the tori range from 0 to $-\infty$ continue to twist to 0 and finally twist from 0 to $-\infty$ (though this time making it to $-\infty$). See Section 1.5.3 for more details.

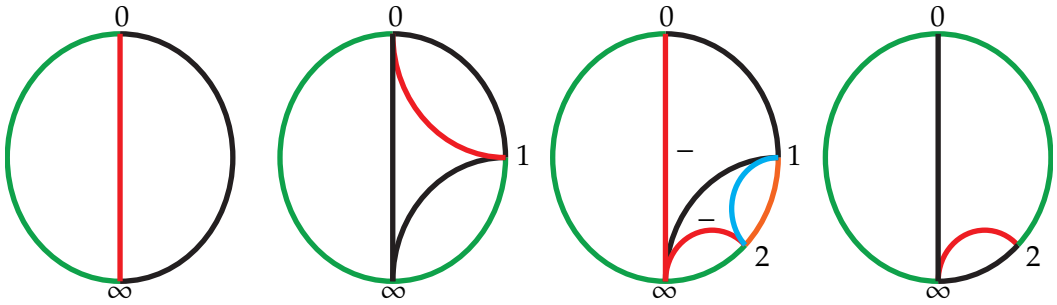

Figure 6.2.11. The first diagram shows the neighborhood $N(L)$ and the green indicates that the slopes realized by linear characteristic foliations are in $(\infty, 0]$ and when perturbed to S is a standard neighborhood of L. The second diagram shows the torus S'' that we replace S by in the first stop of our two step Lutz twist. The third diagram shows the torus S' shown in blue and $S'' - S'$ is shown in red. The final diagram shows S''' the result of contact (+1)-surgery on L'.

We note that we could make this a two step process. See Figure 6.2.11. We could first remove a neighborhood $N(T)$ of the transverse knot T and replace it with a solid torus with lower meridian 1 and where the contact structure induces characteristic foliations on the concentric tori that go from 0 anti-clockwise to 1 (but not reaching 1). The core of this solid torus is a transverse knot T' and we could take a neighborhood $N(T')$ of it with boundary having linear foliation of slope 2. Notice that the characteristic foliations on the concentric tori range from 2 anti-clockwise to 1 (but not reaching 1). We could then replace a neighborhood of this transverse knot by one with lower meridian ∞ so we see that the characteristic foliations on this new torus range from 2 anti-clockwise to $-\infty$. It is clear that these two steps replicate the half-Lutz twist.

Notice that we would get the same result if we perturbed the boundary of $N(T)$ to get a new solid torus S with convex boundary having two dividing curves of slope 0 (all convex tori will have standard foliation on the boundary, see Example 3.4.4), removed this and replaced with a solid torus S'' with meridional slope 1 and then perturbed the boundary of $N(T')$ to get a new solid torus S' with convex boundary having two dividing curves of slope 2, removed this and replaced with a solid torus S''' with meridional slope $-\infty$. But S is a neighborhood of a Legendrian knot L and the replacement of S by S'' is contact (+1)-surgery on L. The second perturbed neighborhood S' is a standard neighborhood of a Legendrian knot L' and the replacement of S' by S''' is a contact (+1)-surgery on L'. We are left to see that T is the transverse push-off of L and L' is a Legendrian push-off of L that has been negatively stabilized twice. The first statement is clear from Lemma 1.4.31 that shows transverse knots can be Legendrian approximated. For the second statement note that the Legendrian defined by S'' and by S are the same since these two standard neighborhoods share the same boundary and hence the same Legendrian divides, and we know the Legendrian divides are isotopic to the Legendrian curve defined by the neighborhood, see Theorem 6.1.9. Now S' is contained in S'' and is a standard neighborhood of the Legendrian L'. From Corollary 6.1.6 we know that L' is a stabilization of L, and from Section 6.1 it is clear that it is two-fold stabilization. In the next section, we will see that two Legendrian knots with the same transverse push-off must be related by negative stabilization. Thus L' is obtained from L by two negative stabilizations. □

It is sometimes convenient not to use the Farey graph to convert general contact surgeries into a sequence of contact $(\pm)$-surgeries. An algorithm for doing this was first described in work of Ding, Geiges, and Stipsicz [**DGS04**].

The DGS Algorithm. Let L be a Legendrian knot in (M, ξ). We consider contact (r)-surgery along L. There are two cases:

When $r < 0$. Write r as a continued fraction

$$r = [a_0, a_1, \cdots, a_n]$$

where $a_0 \leq -1$ and the other $a_i \leq -2$. Then contact (r)-surgery along L can be described as Legendrian surgery along the link $L_0 \cup L_1 \cup \cdots \cup L_n$ where

- L_0 is the Legendrian represented by the original Legendrian knot L with $|a_0 + 1|$ additional stabilizations,
- for $i \geq 2$, L_i is obtained from a Legendrian push-off of L_{i-1} with $|a_1+2|$ additional stabilizations,

When $r > 0$. Write $r = \frac{p}{q}$ where p, q are relatively prime integers. Let $k \in \mathbb{Z}$ be the smallest positive integer such that $\frac{p}{p-kp}$ is negative. Then contact (r)-surgery along L can be described as contact $(+1)$-surgery on k Legendrian push-offs of L followed by contact $(p/(p - kp))$-surgery on L and this last surgery can be written as a sequence of contact (-1)-surgeries as described above. More specifically, if

$$\frac{p}{p - kp} = [b_0, , b_1 \cdots, b_n]$$

where $b_0 \leq -1$ and the other $b_i \leq -2$. Then contact (r)-surgery along L can be described as contact surgery along a Legendrian link $(L^1 \cup \cdots L^k) \cup (L_0 \cup \cdots \cup L_n)$ where

- for $i = 1, \ldots, k$, L^i are parallel Legendrian push-offs of the Legendrian knot L,
- L_0 is obtained from a Legendrian push-off of L^k by $|a_1 + 1|$ additional stabilizations.
- for $j \geq 2$, L_j is obtained from a Legendrian push-off of L_{j-1} with $|a_j+2|$ additional stabilizations,
- the contact surgery coefficient on each L^i, $i = 1, \cdots, k$, is 1 and the coefficient is -1 on each L_j, $j = 1, \cdots, n$.

Exercise 6.2.17. Show that the above algorithm does achieve $\mathrm{tb}(L) - r$ Dehn surgery on L.
Hint: It might be easier to consider some of the exercises below first.

We note that there is another way to realize contact (r)-surgery on L for $r < 0$ which we now discuss as it can sometimes make computing invariants of the contact structure, like the d_3-invariant, easier. Indeed let

$$p/q = \mathrm{tb}(L) + r = [c_0; c_1, \ldots, c_n]$$

where $c_0 < \mathrm{tb}(L)$ because $r < 0$, and the other $c_i \leq -2$. Consider the link in Figure 6.2.12. Legendrian realizes the component K_i as a Legendrian knot with $\mathrm{tb}(K_i) = c_i + 1$. Legendrian surgery on this link is the same as some contact (r)-surgery on L. Moreover, any contact (r)-surgery can be so realized.

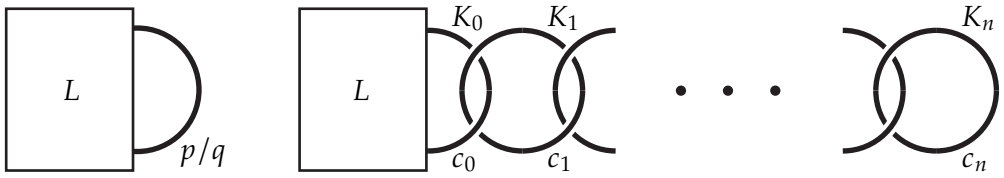

Figure 6.2.12. Two surgery pictures representing p/q Dehn surgery on L. (Here $K_0 = L$.)

Exercise 6.2.18. Show that the smooth surgery is equivalent to $\mathrm{tb}(L) + r$ Dehn surgery on L.
Hint: This can easily be done with slam dunk moves. See Section 1.5.1.

Exercise 6.2.19. Show that any contact (r)-surgery on L for $r < 0$ can be achieved by the above construction.
Hint: The link in Figure 6.2.12 is contained in a standard neighborhood of L. Show that after surgery, you can realize all possible relative Euler classes of contact structures on the solid torus that results from the surgery.

Exercise 6.2.20. Show that the two algorithms for performing contact (r)-surgery on L via Legendrian surgeries are equivalent as smooth surgery diagrams and one must perform the same number of stabilizations in each algorithm.
Hint: Start with Figure 6.2.12 and handle slide (see Section 1.5.1 for handle slides) K_2 over K_1, the K_3 over the knot K_2 became after its slide. Continue with the other K_i.

We now turn to the proof that every contact structure can be obtained by contact surgery on some link in (S^3, ξ_{std}).

Proof of Theorem 6.2.6. We first notice that if we perform contact $(+1)$-surgery on the unknot in (S^3, ξ_{std}) with Thurston-Bennequin invariant -2 we get an overtwisted contact structure ξ' on S^3. Indeed, the smooth surgery coefficient is -1 so the smooth manifold will be S^3 and contact $(+1)$-surgery will replace the standard neighborhood $N(L)$ with S_{-1} and ∂S_{-1} will have dividing curves of slope -2. Thus the slopes realizable by convex tori parallel to the boundary of the solid torus will be in $(-1, -2]$, and in particular, there is a torus T with dividing slope 0. A Legendrian dividing curve on T will bound a disk in the complement of a neighborhood of L, and thus the contact structure is overtwisted.

We now claim that given two overtwisted contact manifolds (M_1, ξ_1) and (M_2, ξ_2) one can find a Legendrian link in (M_1, ξ_1) on which contact (-1)-surgery will give (M_2, ξ_2). The theorem clearly follows. To see this we first recall from Section 1.5 that any smooth, closed 3-manifold is obtained from S^3 by Dehn surgery on a link, and thus it is easy to see that one can obtain M_2 from M_1 by Dehn surgery on a link in M_1. Let L_i be the components of this link and r_i be the surgery coefficients (recall by using the slam dunk operation we can assume that all the r_i are integers). In Section 6.6 we will see that we

can Legendrian realize the link so that the L_i have Thurston-Bennequin invariant $r_i + 1$. Thus contact $(+1)$-surgery on this link will produce a contact structure ξ_1' on M_2.

Recall from the proof of Theorem 1.5.22 that one can get from one homotopy class of plane field on M_2 to another by a sequence of half-Lutz twists. Combining Lemmas 6.2.4 and 6.2.5 show that we can then get from one to the other by a sequence of contact (-1)-surgeries. Since an overtwisted contact structure is determined by its homotopy class of plane field, this says we can get from (M_2, ξ_1') to (M_2, ξ_2) by contact (-1)-surgery. □

We will not establish our lemmas showing how one may manipulate a surgery diagram. In particular, we will prove Lemma 6.2.7 by establishing the moves in Figures 6.2.3 and 6.2.4. To this end, we first need some preliminary results.

Lemma 6.2.21. *The red curve on the left, respectively right, of Figure 6.2.13 is an unknot with Thurston-Bennequin invariant* -1 *in the manifold obtained by contact* (-1)*-surgery, respectively contact* $(+1)$*-surgery, on* L*.*

Figure 6.2.13. Legendrian knot L shown in black. The curves in red are maximal Thurston-Bennequin invariant Legendrian unknots in the surgered manifolds. (Outside the region of L shown, the red curves are copies of the black curves shifted slightly up.)

Proof. We consider the picture on the left first. Notice that before surgery, the red curve, which we denote L', links L exactly $\mathrm{tb}(L) - 1$ times. We will begin by showing that we may assume that L' is a ruling curve on the boundary of a standard neighborhood of L.

We clearly see that $\mathrm{tb}(L') = \mathrm{tb}(L) - 2$. Let T be the torus boundary of a neighborhood of L.

Exercise 6.2.22. Show that the framing of L' given by T and given by the Seifert surface for L' differ by $\mathrm{tb}(L) - 1$.
Hint: If you are having trouble, see our discussion of framings on torus knots in the proof of Lemma 6.5.3.

From the exercise, we see that the contact twisting of L' with respect to T is -1 and hence we can make T convex by the Legendrian realization principle, Theorem 3.4.5. Notice that we could have assumed that L' and hence T were contained in a standard neighborhood of L and also outside a smaller standard neighborhood of L. Thus T is contained in $T^2 \times I$ with an I-invariant contact structure on it. Thus, when we make T convex, it must have dividing slope $\mathrm{tb}(L)$. Moreover, since the contact twisting along L'

is -1, L' can only intersect the dividing curves 2 times (see Theorem 3.5.1). So we see that T has 2 dividing curves. In other words, T can be taken to be the boundary of a standard neighborhood N of L. We can arrange for T to be in standard form with ruling curves parallel to L'.

When we perform contact (-1)-surgery on L, we remove N and then glue in a new solid torus S so that the meridian is mapped to a curve of slope $\mathrm{tb}(L) - 1$; that is, to L'. Now we can take S to have a contact structure with convex boundary and ruling curves of slope ∞ (that is, the ruling curves bound meridional disks in S). Now it is clear that the meridional ruling curves in S are Legendrian unknots with Thurston-Bennequin invariant -1.

Exercise 6.2.23. If this last statement is not clear, then prove it!
Hint: compare the framing on the ruling curve coming from ∂S and from the meridional disk it bounds. Also, recall how to compute the contact twisting of the curve on ∂S.

This completes the claim for contact (-1)-surgery on L. The proof for contact $(+1)$-surgery is very similar and left as an exercise to the reader. □

Lemma 6.2.24. *Suppose L is a Legendrian unknot with $\mathrm{tb}(L) = -1$ and L is the union of two arcs $L = a \cup b$ such that $a \cap b = \partial a = \partial b$, then L maybe be C^0 isotoped near ∂a so that a is Legendrian isotopic to b so that ∂a is fixed and the tangent vectors at ∂a are fixed. The specific modification is described in the proof.*

Proof. We begin by letting D be a disk that L bounds. We may isotop the disk so that along L it is tangent to the contact planes only at a and b. Using a local model, a neighborhood of L, we can arrange he characteristic foliation of D near L to be as shown on the left-hand side of Figure 6.2.14.

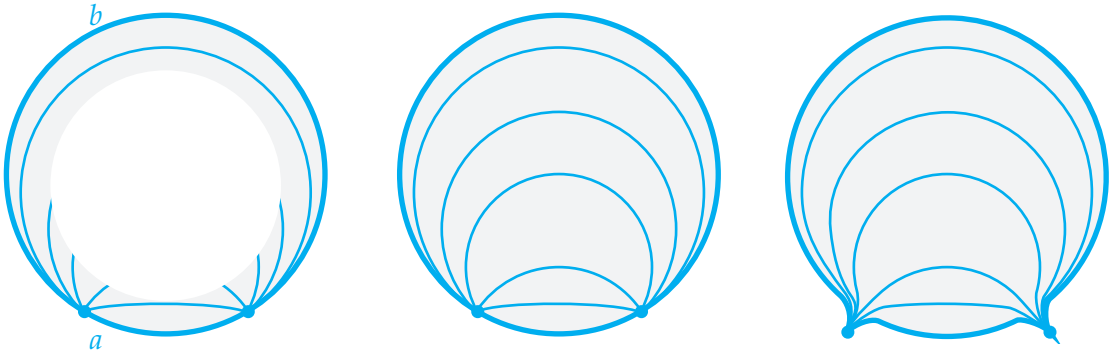

Figure 6.2.14. On the left, we see the characteristic foliation on D near L. The points ∂a are elliptic singularities. In the middle, we see the characteristic foliation on D, and on the right, we see the deformation of D to D' in an arbitrarily small neighborhood of ∂a.

Exercise 6.2.25. Provide the details of the claim above.

Now one can make the disk convex, by Theorem 3.3.1, without moving D near L. We can now use Giroux realization, Theorem 3.4.1, to arrange that the characteristic foliation on D is shown in the middle of Figure 6.2.14. Finally, in any arbitrarily small neighborhood of ∂a we may alter D to a disk D' so that the characteristic foliation on D' is as shown on the right-hand side of Figure 6.2.14.

Exercise 6.2.26. Use a local model for a point to show that this can be done.

The characteristic foliation on D' now gives the claimed isotopy. □

Remark 6.2.27. In the proof above, one can see that if ∂a consists of cusps in a front diagram for L, then the isotopy from D to D' is "squeezing" the cusps so that they become more tangent.

We are now ready to establish the moves in Figures 6.2.3 and 6.2.4.

Proof of Lemma 6.2.7. The proof that the diagrams in Figure 6.2.3 represent the same contact manifold is given in Figure 6.2.15. More specifically, focus on the upper row. On

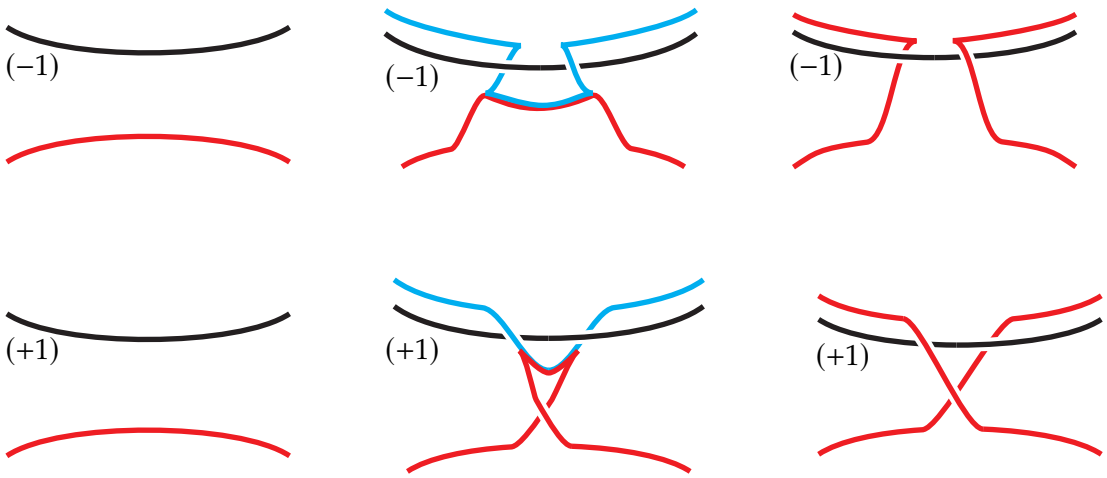

Figure 6.2.15. On the upper left, we see contact (-1)-surgery on L and another Legendrian curve in red. In the upper middle, we see that the red Legendrian curve has been isotoped, and we see the blue curve, which is a meridian of the surgered Legendrian L. On the upper right, we see the result of isotoping the red curve across the blue unknot. We have a similar isotopy in the lower row, except here one performs a Type 1 Legendrian Reidemeister move in the center figure.

the left, we see a black Legendrian knot on which contact (-1)-surgery has been done, and another Legendrian knot represented in red. If we can show that the red knot on the left is Legendrian isotopic to the red curve on the right, then any Legendrian surgery on the red curve on the right will be equivalent to the same surgery on the right. The

isotopy is given in the figure. Since the blue curve in the middle is a maximal Thurston-Bennequin invariant unknot by Lemma 6.2.21, we may isotop the middle red curve to the red curve on the left by Lemma 6.2.24. The isotopy in the second row is similar.

We turn to Figure 6.2.4. The proof of the top handle slide in that figure is given in Figure 6.2.16. Once again, we see the blue curve in the upper left is a maximal Thurston-

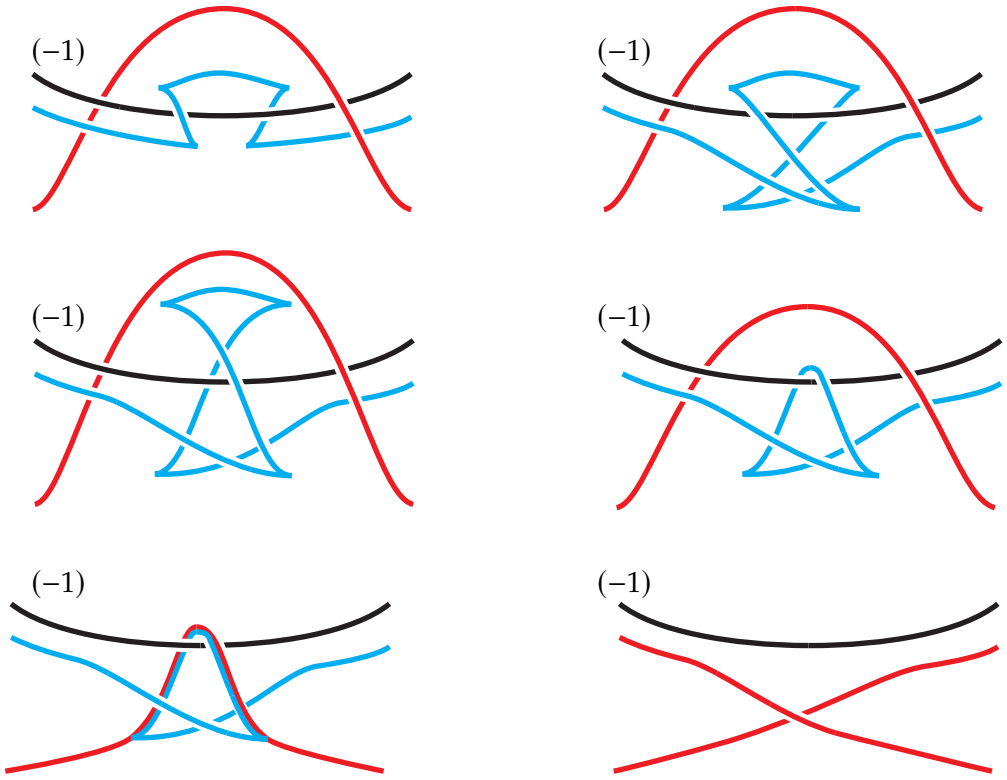

Figure 6.2.16. In the upper left corner, we see contact (-1)-surgery on the black Legendrian knot L, its blue meridional curve, and another Legendrian knot in red. In the next four diagrams (moving right to left and top to bottom) we see Legendrian isotopies of the blue and red curves. In the bottom right corner, we see the result of sliding the red knot over the blue unknot.

Bennequin invariant Legendrian uknot after contact (-1)-surgery on the black Legendrian knot L. The majority of the figure consists of Legendrian isotopies of this blue curve given by Legendrian Reidemeister moves, see Theorem 1.4.22. Then at the end we isotop the red curve over the blue unknot as we did above.

The proof of the bottom handle slide in Figure 6.2.4 is left to the reader. It is very similar to, but easier than, the last argument (and involves two Type 1 Legendrian Reidermester moves). □

We now turn to our last "surgery manipulation" lemma, that is Lemma 6.2.8 that tells us how to replace a Stein 1-handle with contact (+1)-surgery on the maximal Thurston-Bennequin unknot. Before we begin the proof, we give a few exercises that we will need in the proof.

Exercise 6.2.28. Show that contact (+1)-surgery on the maximal Thurston-Bennequin unknot in (S^3, ξ_{std}) is the unique tight contact structure on $S^1 \times S^2$.
Hint: Consider our description of contact surgery earlier in the section and a concrete model for the tight contact structure on $S^1 \times S^2$.

Exercise 6.2.29. Let L be any Legendrian representative of $S^1 \times \{pt\}$ in $S^1 \times S^2$ with its tight contact structure. Show that Legendrian surgery on L gives (S^3, ξ_{std}).
Hint: First verify that any smooth integeral surgery on $S^1 \times \{pt\}$ in $S^1 \times S^2$ gives S^3. Now consider our discussion of contact surgery above.

Proof of Lemma 6.2.8. We need to see that the two diagrams in Figure 6.2.5 represent the same contact manifold. We begin by taking the black Legendrian representative of $S^1 \times \{pt\}$ shown in Figure 6.2.17. a Legendrian push-off of it, shown in red, and performing

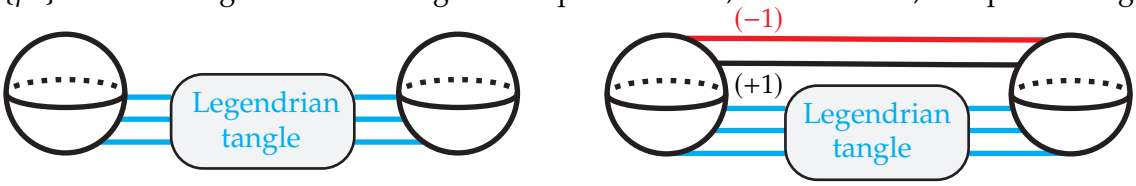

Figure 6.2.17. On the left is a presentation of a contact manifold, and on the right is a presentation giving the same contact manifold.

contact (-1)-surgery on the red curve and contact $(+1)$-surgery on the black curve. By the cancellation lemma, Lemma 6.2.4, we see that this does not affect the resulting contact manifold.

We get the top diagram in Figure 6.2.18 from the right-hand diagram in Figure 6.2.17 by performing the handle slide shown on the top of Figure 6.2.3. The bottom diagram in Figure 6.2.18 is obtained from the top by a Legendrian isotopy (this can be seen since the contact structure on $S^1 \times S^2$ is invariant in the S^1 direction). Now the Stein 1-handle and red curve may be isotoped away from the rest of the diagram, and we see that they may then be removed from the diagram using Exercise 6.2.29. This results in the diagram at the bottom of Figure 6.2.5, thus completing the proof. □

We now turn to the computation of the homotopy class invariants of a contact structure produced by surgery on a link in (S^3, ξ_{std}).

Proof of Theorem 6.2.9. PROVE! □

Proof of Theorem 6.2.10. PROVE! □

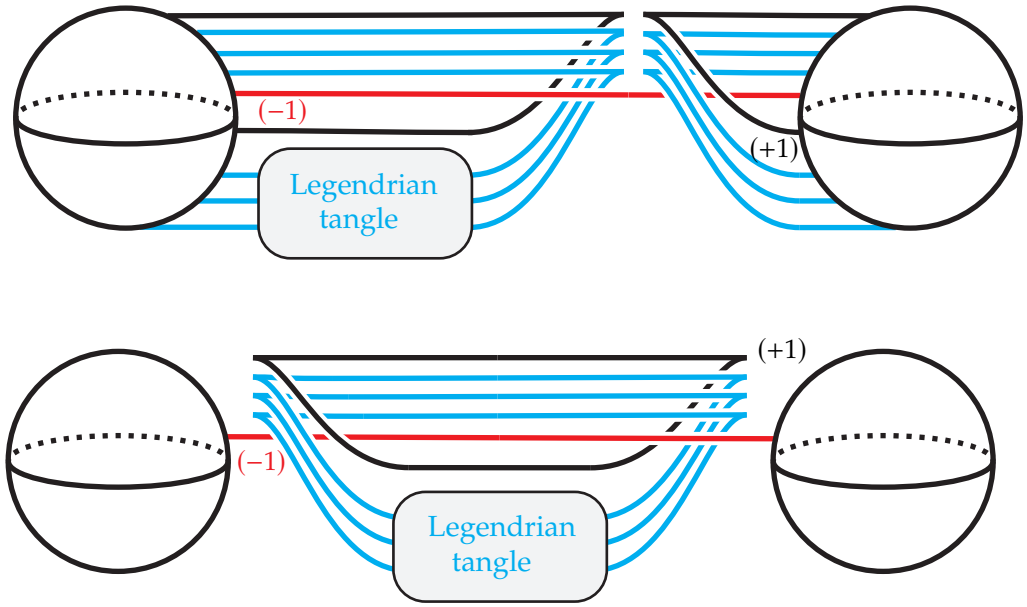

Figure 6.2.18. The top diagram shows the result of handle sliding the curves in Figure 6.2.17 over the red curve. The bottom diagram is obtained by a Legendrian isotopy.

6.3. Classification of Legendrian and transverse knots

In this section we will discuss the relation between the classification of Legendrian and transverse knots as well as a general strategy to classify them. In the following few sections we will implement this strategy for the unknot and torus knots.

6.3.1. Executive summary of main results. We begin by noting the relation between the classification of smooth, transverse, and Legendrian knots.

Theorem 6.3.1. *Two Legendrian knots L_1 and L_2 are smoothly isotopic if and only if they are related by stabilizations. The same is true for two transverse knots.*

It is obvious that two Legendrian knots that are Legendrian isotopic must be smoothly isotopic, so the real content of this theorem is that any two Legendrian knots in the same smooth knot type are Legendrian isotopic after some number of stabilizations. We will give a proof of this in any contact manifold using convex surfaces below, but note that in (R^3, ξ_{std}) there is a "simpler" proof using the Legendrian Reidemeister moves discussed in Section 1.4.

Exercise 6.3.2. Proof that two Legendrian knots in $(\mathbb{R}^3, \xi_{std})$ that are smoothly isotopic are Legendrian isotopic after sufficiently many stabilizations. This result was originally proven by Fuchs and Tabachnikov [**FT97**].

Hint: Show that after sufficiently many stabilizations any smooth Reidemeister move can be done by Legendrian Reidemeister moves.

We now consider the relation between transverse and Legendrian knots.

Theorem 6.3.3 (In $(\mathbb{R}^3, \xi_{std}$. Epstein, Fuchs, and Meyer 2001, [EFM01]; In a general contact manifold, Etnyre and Honda 2001, [EH01a]). *Two Legendrian knots L_1 and L_2 have transversely isotopic positive transverse push-off if and only if they are Legendrian isotopic after some number of negative stabilizations.*

Note that this theorem says the classification of transverse knots up to transverse isotopy in a knot type K is equivalent to the classification of Legendrian knots in the knot type K up to Legendrian isotopy and negative stabilization. Thus if one can determine the mountain range for Legendrian knots in the knot type K (that is understand the set of Legendrian knots $\mathcal{L}(K)$) then one may easily write down the classification of transverse knots in the knot type K, by looking at the asymptotic behavior of the mountain range as one approaches negative infinity along lines of slope 1 in the mountain range.

Example 6.3.4. Here we illustrate how to determine the transverse classification of knots in a knot type from the Legendrian classification. In Figure 6.3.19 we see the mountain range for Legendrian representatives of the $(2,3)$-cable of the right-handed trefoil and at the bottom of the figure we see the self-linking numbers of transverse representatives of this knot type and the number of representatives for each self-linking number. We

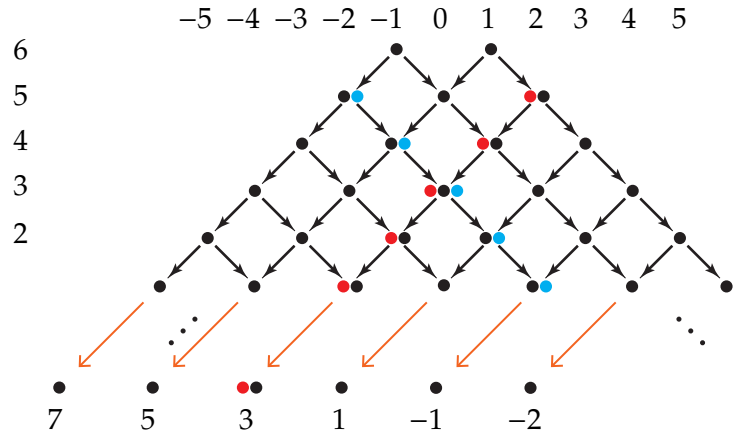

Figure 6.3.19. The mountain range for the $(3,2)$-cable of the right-handed trefoil and along the bottom are the self-linking numbers of transverse representatives of the cable.

will show that this is indeed the classification of Legendrian knots in this knot type in Section 10.2. If we look at the line with slope 1 passing through the point $(6,-1)$ we see that there is only one Legendrian knot for each integer point on the line when the

second entry is very negative. From the above theorem, that means that there is only one transverse push-off of Legendrian knots on this line. That is, there is a unique transverse knot in this knot type with self-linking 7 (recall the self-linking of a transverse push-off of L is $\mathrm{tb}(L) - \mathrm{rot}(L)$). We see the same for the line of slope 1 through the point $(6, 1)$, but when considering the line of slope 1 through the point $(5, 2)$ we see that there are two Legendrian knots for each integer point on this line. So the above theorem says there are two distinct transverse knots that are transverse push-offs of these Legendrian knots. That is, there are two transverse knots with self-linking number 3. Continuing we see that for each odd integer less than or equal to 7 there is exactly one transverse representative of this knot having this as its self-linking number, except there are two when the self-linking number of 3.

Here is the standard way in which we will classify Legendrian knots in a given knot type K.

- **Step 1.** Identify the maximal Thurston-Bennequin invariant in the knot type of K and classify Legendrian knots realizing this.
- **Step 2.** Identify and classify the non-maximal Thurston-Bennequin Legendrian knots in the knot type of K that do not destabilize.
- **Step 3.** Prove that all other Legendrian knots destabilize to one of the identified Legendrian knots in Step 1. and 2.
- **Step 4.** Determine which stabilizations of the maximal Thurston-Bennequin invariant knots and non-destabilizable knots are Legendrian isotopic.

Later in this chapter we will classify Legendrian knots in the knot types of the unknot and torus knots. Here we will see that the second step in the process above is not relevant as there are no non-destabilizable knots that do not have maximal Thurston-Bennequin invariant. We will see an example where Step 2 is essential in Section 10.2.

In our study of Legendrian knots, it will frequently be useful to know the maximal possible Thurston-Bennequin invariant of Legendrian representatives of a knot type. We will denote this quantity $\overline{\mathrm{tb}}(K)$ for the knot K. Notice that this is an invariant of the smooth knot K. In our results below we will use $\mathcal{K}$ to denote the set of smooth knots in the knot type K, and we will use $\mathcal{L}(\mathcal{K})$ to denote the set of all Legendrian representatives in the knot type of K.

Recall from Lemmas 1.2.17 and 1.4.1 that the classification of Legendrian knots up to Legendrian isotopy is equivalent to the classification up to ambient contact isotopy and for Legendrian knots in (S^3, ξ_{std}) and (B^3, ξ_{std}) this is also equivalent to the classification up to contactomorphisms that are smoothly isotopic to the identity. We end this section by noting one other equivalence type of classification that can be useful when trying to classify Legendrian knots.

Theorem 6.3.5. *Two Legendrian knots in (S^3, ξ_{std}) are Legendrian isotopic if and only if the complements of their standard neighborhoods are contactomorphic.*

This result was implicit in much of the early literature on the classification of Legendrian knots, e.g. [**EH01a**], but was first stated in [**Etn05**] and a careful proof was given in [**Keg18**].

6.3.2. Proofs of main results. We begin with the proof of Theorem 6.3.1 that says that two Legendrian knots are smoothly isotopic if and only if they are Legendrian isotopic after sufficiently many stabilizations.

Proof of Theorem 6.3.1. Can't find in the literature for a general contact manifold! We can prove with state transition, so we need to put off proof till Part II. □

We are not ready to prove that the transverse classification of knots in a knot type is equivalent to the Legendrian classification up to negative stabilization.

Proof of Theorem 6.3.3. We first note that if L and L' are related by negative stabilization then their positive transverse push-offs are transversely isotopic. We first observe that the transverse push-off L_+ has a neighborhood N with boundary convex and containing L as a Legendrian divide. Notice that by Lemma 6.1.1 we know that N is a standard neighborhood of L. We choose a framing on N so that the dividing curves have slope 0. Now inside of N we know there is a torus T whose characteristic foliation is linear of slope -1. Let L'' be a leaf in this foliation. We note that the positive transverse push-off of L'' is the same as L_+ (see the definition of transverse push-off in Section 1.4.4). The contact framing of L'' relative to T is 0 and with respect to the framing on N it is -1 (if this is not clear see the exercise in the proof of Theorem 6.1.9). Thus L'' is a Legendrian knot in the standard neighborhood N of L with contact twisting one less than L. From Corollary 6.1.6 we know that L'' is a stabilization of L. Since L'' and L' have the same transverse push-off, they must be the same stabilization of L (since the self-linking of the transverse push-off is $\mathrm{tb}(L) - \mathrm{rot}(L)$). Thus L and L' have the same transverse push-off.

Now assume that L and L' are two Legendrian knots with the same positive transverse push-off. Let $N(L)$ and $N(L')$ be standard neighborhoods of L and L' respectively. The transverse push-off of L and L' can be assumed to be inside of $N(L)$ and $N(L')$, respectively. Since the transverse push-offs are transversely isotopic we know there is an ambient contact isotopy taking one to the other, see Exercise 1.2.18. Thus, after a contact isotopy, we can assume that $N(L)$ and $N(L')$ contain the same transverse knot T that is a transverse push-off of both L and L'. Take a neighborhood N of T inside $N(L) \cap N(L')$. We can choose N small enough so that its boundary has linear characteristic foliation with slope some very negative integer. Let L'' be a leaf in that foliation. From the definition of Legendrian approximation it is clear that T is the transverse push-off of L''. Since L'' is

in $N(L)$ we know by Corollary 6.1.6 that it is a stabilization of L and since the transverse push-offs of L and L'' are the same L'' must be a negative stabilization of L. The same argument shows that L'' is a negative stabilization of L' as well. □

Turning to the proof that a Legendrian knot in (S^3, ξ_{std}) is determined by its complement we first note the following simple result.

Lemma 6.3.6. *Given two Legendrian knots L_0 and L_1 in a contact manifold (M, ξ) and a contactomorphism ϕ from the complement of a standard neighborhood of L_0 to the complement of a standard neighborhood of L_2 that sends the meridian of L_0 to the meridian of L_1, then ϕ can be extended to a contactomorphism of (M, ξ) that sends L_0 to L_1.*

Proof. Since ϕ sends the meridian of one knot to the meridian of the other, one can smoothly extend ϕ over the neighborhoods of the knots to get a diffeomorphism from M to M.

Exercise 6.3.7. Proof that ϕ can be so extended.

Since there is a unique tight contact structure on a solid torus with longitudinal dividing curves, by Theorem 5.1.5, the extension of ϕ can be isotoped to be a contactomorphism on neighborhoods of the knots without changing the fact that it is a contactomorphism in the complements of the neighborhoods. Thus we have arranged that ϕ is extended to a contactomorphism of (M, ξ) that takes a standard neighborhood of L_0 to a standard neighborhood of L_1. Now Lemma 6.1.1 says we can further isotope ϕ so that it takes L_0 to L_1. □

Proof of Theorem 6.3.5. Let L_0 and L_1 be Legendrian knots in (S^3, ξ_{std}) with standard neighborhoods $N(L_0)$ and $N(L_1)$. Suppose that $\phi\colon (S^3 \setminus N(L_0)) \to (S^3 \setminus N(L_1))$ is a contactomorphism. A result of Gordon and Luecke [**GL89**] says that any diffeomorphism of the complement of a knot to the complement of another knot must take the meridian to the meridian. Thus the previous lemma tells us that ϕ can be extended to a contactomorphism of (S^3, ξ_{std}) taking L_0 to L_1. Since any diffeomorphism of S^3 is smoothly isotopic to the identity we know by Lemma 1.4.1 that L_0 and L_1 are Legendrian isotopic.

The implication that Legendrian isotopic knots have contactomorphic complements easily follows from the fact that Legendrian isotopy between knots implies ambient contact isotopy, see Lemma 1.2.17. □

6.4. Classification of Legendrian and transverse unknots

The main theorem here is the following result of Eliashberg and Fraser [**EF98**, **EF09**].

Theorem 6.4.1 (Eliashberg and Fraser, 1998 and 2009, [EF98, EF09]). *If $\mathcal{U}$ is the unknot in any tight contact manifold (M, ξ), then there is a unique element $L \in \mathcal{L}(\mathcal{U})$ with* $\mathrm{tb}(L) = -1$ *(and L will have* $\mathrm{rot} = 0$*) and all other elements of $\mathcal{L}(\mathcal{U})$ are stabilizations of L. See Figure 6.4.20 for a front diagram of L.*

From the theorem it is clear that the mountain range for $\mathcal{U}$ is given in Figure 6.4.20

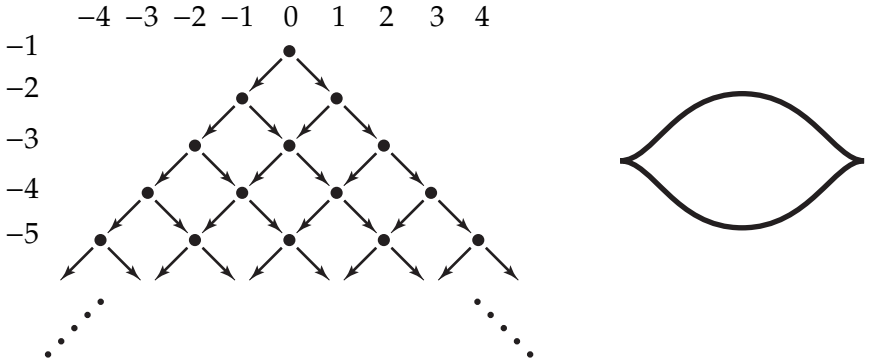

Figure 6.4.20. The mountain range for the unknot is shown on the left and a front diagram for the Legendrian unknot with tb = −1 is shown on the right.

We will use convex surfaces to give a quick proof of this theorem, which is quite different than the original proof due to Eliashberg and Fraser and also holds in any tight contact manifolds.

Proof. The Bennequin inequality, Theorem 3.7.5, tells us that

$$\mathrm{tb}(L) + \mathrm{rot}(L) \leq -\chi(D^2) = -1$$

for all Legendrian unknots. Thus we know that $\mathrm{tb}(L)$ must always be less than or equal to -1. We will show

(1) any $L \in \mathcal{L}(\mathcal{U})$ with $\mathrm{tb}(L) < -1$ destabilizes, and

(2) there is a unique element $L \in \mathcal{L}(\mathcal{U})$ with $\mathrm{tb}(L) = -1$.

The theorem then clearly follows.

For Item (1) let $L \in \mathcal{L}(\mathcal{U})$ with $\mathrm{tb}(L) < -1$. Let D be a disk that L bounds. Notice that $tw(L, D) = \mathrm{tb}(L) < -1$ so we can use Theorem 3.3.1 to make D convex. Then by Theorem 3.5.1 we know that the dividing set on D intersects the boundary $-2\,\mathrm{tb}(L) > 2$ time. Thus we see there must be a boundary parallel arc. Thus Lemma 5.4.14 gives a bypass for L along D and since the framing of L given by D is larger than the framing given by ξ we see that L destabilizes (see Theorem 6.1.5).

Turning to Item (2) we will first consider the case of (S^3, ξ_{std}). We suppose $L, L' \in \mathcal{L}(\mathcal{U})$ both have $\mathrm{tb} = -1$. Let N and N' be standard neighborhoods of L and L' respectively. Set $C = S^3 \setminus N$ and $C' = S^3 \setminus N'$. Notice that C and C' are solid tori that

are naturally S^0 (that is have upper meridian 0, see Section 5.6) and dividing slope -1. There is a unique tight contact structure on S^0 with convex boundary having two dividing curves of slope -1 (see Theorem 5.1.5) and so there is a contactomorphism from C to C' and thus L and L' are Legendrian isotopic by Theorem 6.3.5.

Exercise 6.4.2. Give a direct proof that L and L' are isotopic by either using front diagrams or the characteristic foliations on disks L and L' bound. (Or, better, try to give arguments using both.)

We now consider an arbitrary tight contact manifold (M, ξ).

Exercise 6.4.3. Show that two Legendrian knots in (B^3, ξ_{std}) are Legendrian isotopic in B^3 if and only they are Legendrian isotopic in (S^3, ξ_{std}).

Given $L, L' \in \mathcal{L}(\mathcal{U})$ in (M, ξ) with both have tb $= -1$. Let D and D' be the disks that L and L' bound, respectively. We note that we can use Giroux flexibility, Theorem 3.4.1, to arrange that the characteristic foliation on D and D' are as shown in Figure 6.4.21.

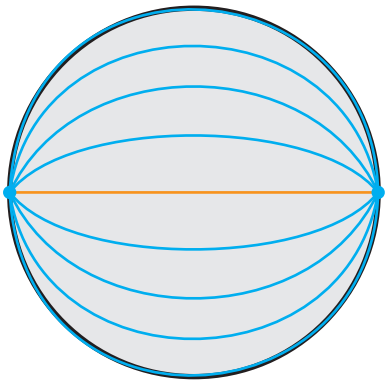

Figure 6.4.21. Characteristic foliation on D and D'. The orange line is just a leaf in the foliation and should be considered when trying to solve the exercise.

Exercise 6.4.4. Use the characteristic foliation on D and D' to show that L and L' can be Legendrian isotoped to be in a small neighborhood of distinct Legendrian arcs.

In particular, we can assume that D and D' are disjoint. Given this, we can find a B^3 containing D and D', and hence L and L'. From above we know that L and L' are Legendrian isotopic in B^3. □

6.5. Classification of Legendrian and transverse torus knots

Next we provide a complete classification, due to the first author and Honda [**EH01a**], of Legendrian knots in the knot types of torus knots in any tight contact manifold.

6.5.1. Executive summary. We start by establishing notation for torus knots. Let N be a neighborhood of the unknot in a manifold M, μ be the curve on ∂N that bounds a disk in N, and λ be the curves on ∂N that bounds a disk in $M \setminus N$. Using this basis for $H_1(\partial N)$ we can represent any embedded curve γ by its homology class $p[\lambda] + q[\mu]$ for relatively prime integers p and q, see Section 4.1. An embedded curve on ∂N realizing $p[\lambda] + q[\mu]$ is called a (p,q)-*torus knot* and is denoted $T_{p,q}$. We say $T_{p,q}$ is a *positive torus knot* if $pq > 0$ and a *negative torus knot* if $pq < 0$. For convenience, one might want to just consider the case of $M = S^3$ in which case ∂N is a Heegaard torus of S^3.

Example 6.5.1. In Figure 6.5.22 we see on the left the torus knot $T_{1,0}$ which is clearly the unknot, and on the right we see the torus knot $T_{2,3}$ which is easy to see is the right-handed trefoil.

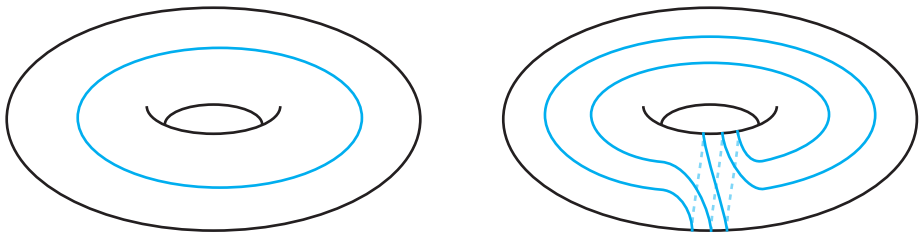

Figure 6.5.22. The torus knots $T_{1,0}$ and $T_{2,3}$.

We note note some important facts about torus knots.

Exercise 6.5.2. Show that $T_{p,q}$ is isotopic to $T_{q,p}$ and that $T-p,-q$ is isotopic to $T_{p,q}$.
Hint: Notice that the unknot U is isotopic to $-U$ and if U' is a meridian to the unknot then U and U' are isotopic.

Lemma 6.5.3. *The torus knot $T_{p,q}$ bounds a Seifert surface of genus*

$$\frac{(p-1)(q-1)}{2}$$

and if $\mathcal{F}_T$ is the framing of $T_{p,q}$ given by the torus ∂N and $\mathcal{F}_A$ is the framing given to $T_{p,q}$ by the Seifert surface then

$$\mathcal{F}_T - \mathcal{F}_S = pq.$$

We begin with a simple statement about all torus knots.

Theorem 6.5.4 (Etnyre and Honda, 2001, **[EH01a]**)**.** *Torus knots are Legendrian simple, that is two Legendrian knots in the knot type $\mathcal{T}_{p,q}$ are Legendrian isotopic if and only if they have the same Thurston-Bennequin invariants and rotation numbers.*

This theorem is an immediate corollary of the two theorems below that completely classify Legendrian torus knots. We begin with positive torus knots.

Theorem 6.5.5 (Etnyre and Honda, 2001, [EH01a]). *If $\mathcal{T}_{p,q}$ is a positive torus knot, then there is a unique Legendrian knot $L \in \mathcal{L}(\mathcal{T}_{p,q})$ with*

$$\mathrm{tb}(L) = pq - p - q.$$

Moreover, $\mathrm{rot}(L) = 0$ *and any other element in $\mathcal{L}(\mathcal{T}_{p,q})$ is a stabilization of L.*

The front diagram of the maximal Thurston-Bennequin invariant Legendrian (p, q)-torus knot in $(\mathbb{R}^3, \xi_{std})$ is shown in Figure 6.5.23.

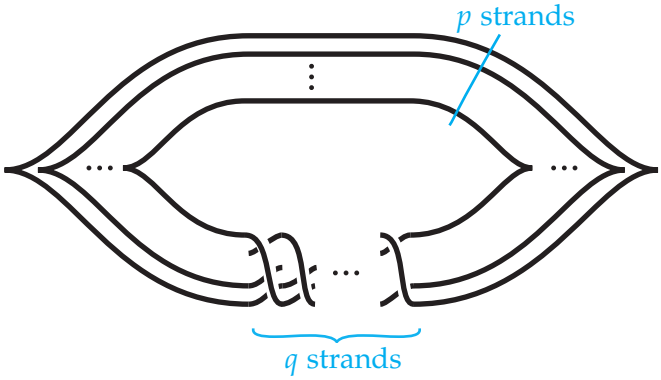

Figure 6.5.23. The positive (p, q)-torus knot with $\mathrm{tb} = pq - p - q$. All other Legendrian representatives of this knot are stabilizations of this knot.

Exercise 6.5.6. Compute the Thurston-Bennequin invariant and rotation number of the knot in Figure 6.5.23.

Exercise 6.5.7. Find a Legendrian isotopy between the front diagram for the maximal Thurstong-Bennequin invariant (p, q)-torus knot and the $(q.p)$-torus knot. (We know from the theorem above that these are isotopic, but try to find a sequence of Legendrian Reidemeister moves, see Theorem 1.4.22.)

The above theorem completely classifies Legendrian representatives of positive (p, q)-torus knots. In particular, we can easily write down the mountain range for $\mathcal{L}(\mathcal{T}_{p,q})$, see Figure 6.5.24. We note that the mountain range for any positive (p, q)-torus knot saturates the Bennequin bound, that is any pair of integers allowable by the Bennequin bound (and the fact that their sum must be odd) is realized as the rotation number and Thurston-Bennequin invariant of a (p, q)-torus knot.

Notice that the symmetry of (p, q)-torus knots from Exercise 6.5.2 when talking about negative (p, q)-torus knots we may assume that $-q > p > 1$ without any loss of generality.

Theorem 6.5.8 (Etnyre and Honda, 2001, [EH01a]). *If $T_{p,q}$ is a negative torus knot with $-q > p > 1$, then*

(1) *The maximal Thurston-Bennequin invariant of $\mathcal{T}_{p,q}$ is pq.*

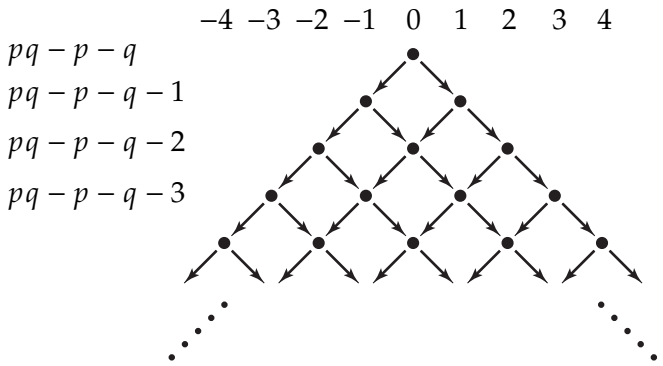

Figure 6.5.24. The mountain range for the positive (p, q)-torus knots.

(2) *Any knot in* $\mathcal{L}(\mathcal{T}_{p,q})$ *is a stabilization of one with* $\mathrm{tb} = pq$.

(3) *If* k *is a positive integer such that* $-k - 1 < \frac{q}{p} < -k$ *then there are exactly* $2k$ *knots in* $\mathcal{L}(\mathcal{T}_{p,q})$ *with* $\mathrm{tb} = pq$ *and they are determined by their rotation numbers which are*

$$\left\{ \pm(q - p + 2pn) : 0 \leq n < \frac{q-p}{p} \right\}$$

(4) *The knot* $T_{p,q}$ *is Legendrian simple, that is two knots in* $\mathcal{L}(\mathcal{T}_{p,q})$ *are Legendrian isotopic if and only if they have the same* tb *and* rot.

We will explore the mountain ranges for negative torus knots in the examples below and in particular parse the expression in the theorem for rotation numbers in the examples below, but first we consider the front diagrams for negative torus knots in $(\mathbb{R}^3, \xi_{std})$ with $\mathrm{tb} = pq$. To this end, write $-q = (n_1 + n_2 + 1)p + e$ where $0 < e < p$ and the n_i are positive integers. Then Figure 6.5.25 shows the desired front diagrams.

Exercise 6.5.9. Compute the Thurston-Bennequin invariant and rotation numbers of the Legendrian knots depicted in Figure 6.5.25. Show that the possible rotation numbers realized agree with those in Item (3) of the theorem.

Example 6.5.10. Consider the torus knot $T_{2,-3}$. From the theorem above we know the maximal Thurston-Bennequin invariant of Legendrian representatives is -6 and the rotation numbers are

$$\pm(3 - 2 - 2 \cdot 2n) \qquad \text{for} \quad 0 \leq n < \frac{3-2}{2} = \frac{1}{2}.$$

That is the rotation numbers for Legendrian representatives of $T_{2,-3}$ with $\mathrm{tb} = -6$ are $-1, 1$. So the mountain range for $\mathcal{L}(\mathcal{T}_{2,-3})$ is shown in Figure 6.5.26.

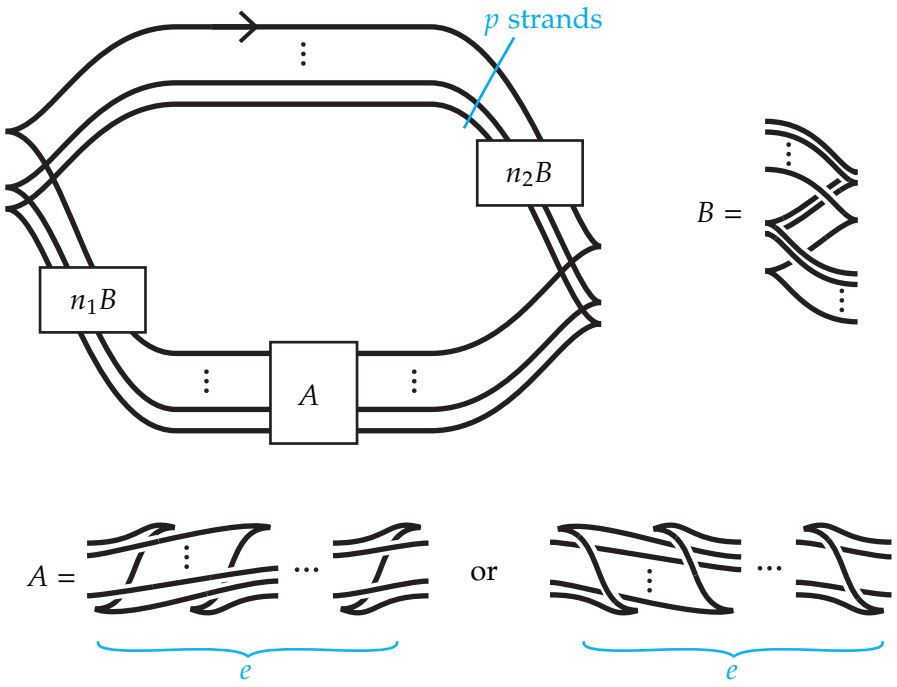

Figure 6.5.25. The negative (p, q)-torus knots with tb $= pq$ is shown in the upper right, where the boxes are replaced with copies of B or A as indicated. All other Legendrian representatives of this knot are stabilizations of these knots.

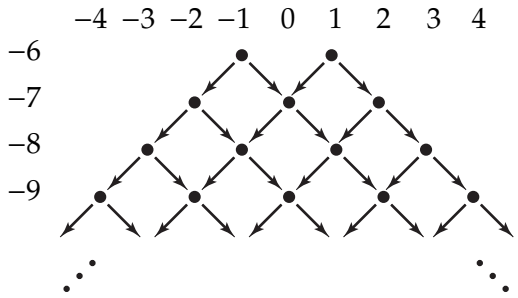

Figure 6.5.26. The mountain range for the positive $(2, -3)$-torus knots.

More generally, consider $T_{2,-(2k+1)}$, The maximal Thurston-Bennequin invariant of Legendrian representatives is $-4n - 2$. The possible rotation numbers for such representatives are

$$\pm(2k + 1 - 2 - 2 \cdot 2n) \qquad \text{for} \quad 0 \leq n < \frac{2k + 1 - 2}{2} = k - \frac{1}{2}.$$

One easily sees that this yields all odd numbers between $-2k + 1$ and $2k - 1$. Thus the mountain range for $\mathcal{L}(\mathcal{T}_{2,-(2k+1)})$ is shown in Figure 6.5.27.

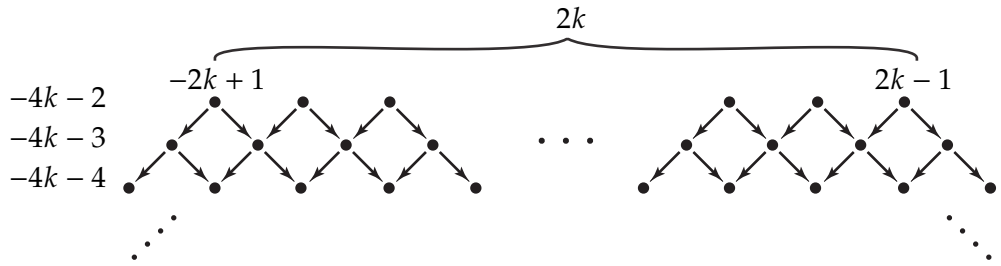

Figure 6.5.27. The mountain range for the positive $(2, -(2k+1))$-torus knots.

Example 6.5.11. Consider the torus knot $T_{3,-10}$. From the theorem above we know the maximal Thurston-Bennequin invariant of Legendrian representatives is -30 and the rotation numbers for such knot are

$$\pm(10 - 3 - 2 \cdot 3n) \qquad \text{for} \quad 0 \leq n < \frac{10-3}{3} = \frac{7}{3}.$$

This gives possible rotation numbers of

$$-7, -5, -1, 1, 5, 7$$

Thus we see that the mountain range for $\mathcal{L}(\mathcal{T}_{3,-10})$ is shown in Figure 6.5.28.

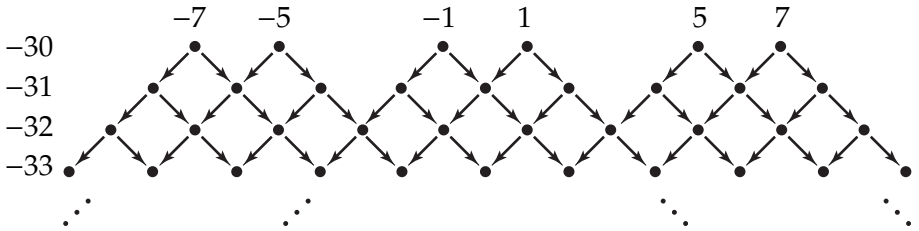

Figure 6.5.28. The mountain range for the positive $(3, -10)$-torus knots.

One can see the mountain range of the $(4, -9)$-torus knot in Example 1.4.38.

Exercise 6.5.12. Draw front diagrams for all the examples discussed above.

Exercise 6.5.13. Given positive integers m and n, show there exist negative torus knots $T_{p,q}$ with mountain ranges having exactly $2n$ "peaks" and "valleys" of depth m.
Hint: Read the proof of the classification result first.

One might wonder why the classification of Legendrian positive torus knots and negative torus knots is so different. This really comes down to slopes that can be realized as dividing slopes on certain convex tori. Specifically, we will see in the proofs of these results that the following simple result is key.

Lemma 6.5.14. *Let (M, ξ) be any tight contact manifold and S a solid torus in M whose core is in the knot type of the unknot. The boundary of S can be made convex with slope r if and only if $r \in (-\infty, 0)$, and in addition we may assume that ∂S has two dividing curves. Moreover, if S has convex boundary of slope r then for any $s \neq r$ we can find a convex torus T disjoint from and isotopic to ∂S with two dividing curves of slope s.*

In particular, in (S^3, ξ_{std}) we can find a convex Heegaard torus of slope r if and only if $r \in (-\infty, 0)$.

We end this section by discussing transverse torus knots.

Theorem 6.5.15. *The torus knot $T_{p,q}$ is transversely simple. Any odd integer less than or equal to*

$$\begin{aligned} pq - p - q \quad & \text{for } pq > 0 \\ pq + q - p \quad & \text{for } -q > p > 0, \end{aligned}$$

can be realized as the self-linking number of a transverse (p, q)-torus knot.

While this theorem is a simple corollary of the classification of Legendrian torus knots, it was originally proven for positive torus knots by the first author in [**Etn99**] using different techniques.

Exercise 6.5.16. Prove this theorem.

6.5.2. Proofs of main results. We begin by constructing Seifert surfaces for torus knots and comparing the framings coming from the Seifert surface and the torus containing the knot.

Proof of Lemma 6.5.3. Let T be a torus bounding a solid torus S in the knot type of the unknot. Let μ be the curve in T bounding a disk D_μ in S and λ the curve bounding a disk D_λ outside of S. Then we can construct a (p, q) torus knot by first taking p disjoint copies of λ and q disjoint copies of μ and then at replacing each of the pq intersection point between the curves with a "resolved curves". See Figure 6.5.29.

To construct the Seifert surface for $T_{p,q}$ we take p disjoint copies of the disk D_λ and q disjoint copies of D_μ. We now resolve their intersection points as follows: remove a small neighborhood of each intersection point from the disks and replace it with a strip having part of its boundary on the disk and the other part is the "resolving arcs" used to create the torus knot above. See Figure 6.5.30 for this construction near a single intersection point. We now compute the Euler characteristic of this surface. Notice the surface constructed is homotopy equivalent to a 1-complex with a vertex for each disk and an edge for each strip. That is the Euler characteristic is $p + q - pq$. From this, it is easy to see that the genus of the surface is as claimed.

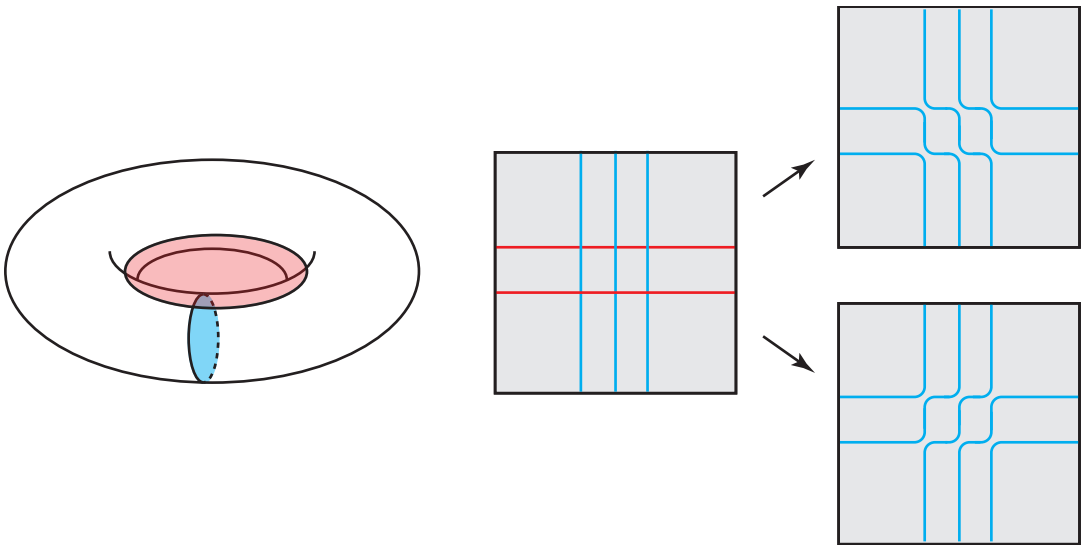

Figure 6.5.29. On the left we see the disks D_λ and D_μ. In the middle, we see the torus represented by a square with opposite edges identified and on the torus two copies of λ and three copies of μ. Note they intersect in 6 points. On the top right we see a resolution of the intersection points leading to the positive (p, q)-torus knot and on the bottom right we see the resolution leading to the negative $(p, -q)$-torus knot.

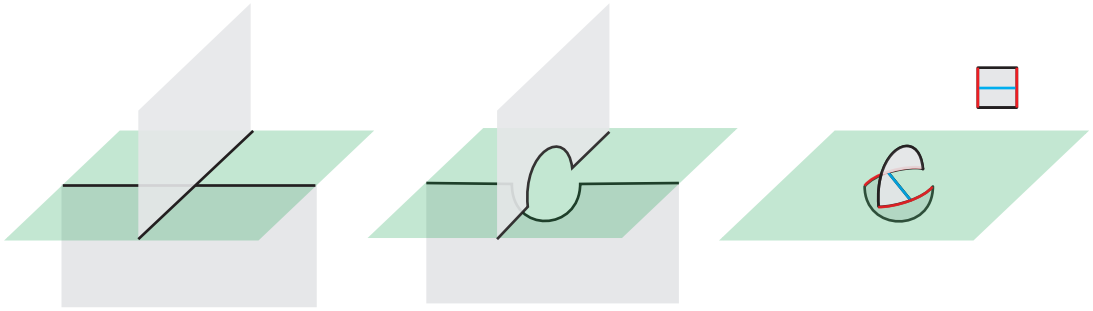

Figure 6.5.30. On the left we see two disks near an intersection point on T (shown in green). In the middle diagram, we see the result of removing a neighborhood of the intersection point from each disk. On the right, we see a disk thought of as $[0, 1] \times [0, 1]$ that can be glued to the middle figure. On the top we see the strip and below that we see it mapped into the neighborhood of the intersection point.

Turning to the framing induced on the torus knot from T and the Seifert surface we can take a vector normal to the knot and tangent to T. This is the framing given by T. Rotate the vectors giving this framing in the normal bundle to the knot by $\pi/2$. Notice that away from the resolved double points. This agrees with the framing given by the Seifert surface.

Exercise 6.5.17. Show that in a neighborhood of the resolved double point the framing given by T and by the Seifert surface differ by ± 1 depending on whether one did the resolution to get a positive torus knot or a negative torus knot.

Since there were pq double-points that were resolved we see that the difference between the two framings is pq. □

We are now ready for the classification of Legendrian positive torus knots.

Proof of Theorem 6.5.4. Suppose $pq > 0$. We first note that the Bennequin inequality, Theorem 3.7.5, and the Seifert surface for a (p, q)-torus knot constructed in Lemma 6.5.3 tells us that any $L \in \mathcal{L}(\mathcal{T}_{p,q})$ has $\mathrm{tb}(L) \leq pq - p - q$. The theorem clearly follows once the following two items are verified.

(1) any element of $\mathcal{L}(\mathcal{T}_{p,q})$ destabilizes to an element with $\mathrm{tb} = pq - p - q$, and

(2) there is a unique element in $\mathcal{L}(\mathcal{T}_{p,q})$ with $\mathrm{tb} = pq - p - q$.

To prove Item (1) let L be any element in $\mathcal{L}(\mathcal{T}_{p,q})$ with $\mathrm{tb}(L) < pq - q - q$. Let T be any torus containing L and bounding a solid torus with core in the knot type of the unknot. By Lemma 6.5.3 we know that the twisting of the contact planes relative to T is less than $-p - q$ and hence we can isotop T relative to L to make T convex by Theorem 3.3.1. Using Lemma 6.5.14 we can find a torus T' isotopic to T that has two dividing curves of slope -1. Assume that the ruling slope of T' is q/p. Let A be an annulus with one boundary component on L and the other on a ruling curve of T'. We note that $\partial A \cap T'$ intersects the dividing curves on T', $2(p + q)$ times and the dividing curves on T, $2|tw(L, T)| > 2(p + 2)$ times. Thus the contact twisting along each boundary component relative to A is negative. So we may make A convex. Notice that the dividing set on A must contain an arc parallel to the boundary component L. Thus Lemma 5.4.14 says there is a bypass for L on A and Theorem 6.1.5 says that L destabilizes.

We now turn to the proof of Item (2). In this case assume that we have two Legendrian representatives L and L' in $\mathcal{L}(\mathcal{T}_{p,q})$ with $\mathrm{tb} = pq - p - q$. Then as above we can put L and L' on convex tori T and T'.

Exercise 6.5.18. Show that any curve γ on a torus with a negative slope not equal to -1 will intersect the curve of slope q/p more than $p + q$ times.

Given the exercise, we see that both T and T' must have two dividing curves of slope -1 (since otherwise their tb would be less than $pq - p - q$). We can use Giroux flexibility to arrange that T and T' are in standard form with ruling curves of slope q/p and L and L' are among the ruling curves. Now T and T' bound solid tori S and S', respectively, in the knot type of the unknot; in fact, they are standard neighborhoods of Legendrian unknots with $\mathrm{tb} = -1$. From Theorem 6.4.1 we know these Legendrian unknots are isotopic and

hence Lemma 6.1.2 says there is an ambient contact isotopy that takes S to S' and, in particular, T to T'. After this isotopy L and L' are ruling curves on the same convex torus and hence Legendrian isotopic through ruling curves on $T = T'$. □

We now turn to the classification of Legendrian negative torus knots. We start with determining the maximal Thurston-Bennequin invariant of negative torus knots.

Lemma 6.5.19. *If $pq < 0$ then $\overline{\text{tb}}(T_{p,q}) = pq$.*

Proof. Note that Figure 6.5.25 describes a negative Legendrian torus knot with tb $= pq$. So. it will be enough prove that there is no negative Legendrian torus knot with $tb > pq$. Suppose not. That is, we suppose there exists a Legendrian negative torus knot L with $tb(L) = pq + 1$. Now by attaching a Stein 2-handle to $D^4 = \partial S^3$ along L, we obtain a Stein manifold W. It is easy to check that the boundary 3-manifold is $\partial W = S^3_L(pq) = L(p, q*)\#L(q, p*)$ where $p*, q*$, modulo p, q, are multiplicative inverses of p, q, respectively, and which obviously includes a 2–sphere S. On the other hand, a theorem of Eliashberg in [**Eli90a**] says, under this circumstances, that there must be an embedded 3–ball D in W such that $\partial D = S$. We prove now that this is not possible, and hence get the desired contradiction. Assume there is such a ball, then there are essentially two possibilities for W. Either W has a 1-handle, i.e. $W = W' \cup$ 1-handle or W is the boundary sum of two 4– manifolds, say $W = W_1 \natural W_2$. The former possibility is impossible as this would imply that our simply connected W has $H_1(W) \neq 0$. The latter possibility of $W = W_1 \natural W_2$, after using a Mayer-Vietoris type argument, will lead one of the summands to be an integral homology sphere which cannot happen as ∂W is a connected sum of non-trivial lens spaces. □

Proof of Theorem 6.5.8. We are assuming that $-q > p > 0$ and we recall the items claimed in the theorem.

(1) The maximal Thurston-Bennquin invariant of $T_{p,q}$ is pq.

(2) Any knot in $\mathcal{L}(\mathcal{T}_{p,q})$ is a stabilization of one with tb $= pq$.

(3) If k is a positive integer such that $-k - 1 < \frac{q}{p} < -k$ then there are exactly $2k$ knots in $\mathcal{L}(\mathcal{T}_{p,q})$ with tb $= pq$ and they are determined by their rotation numbers which are
$$\left\{\pm(q - p + 2pn : 0 \leq n < \frac{q-p}{p}\right\}$$

(4) The knot $T_{p,q}$ is Legendrian simple, that is two knots in $\mathcal{L}(\mathcal{T}_{p,q})$ are Legendrian isotopic if and only if they have the same tb and rot.

Item (1) was proven in Lemma 6.5.19, so we start with the proof of Item (2). Suppose $L \in \mathcal{L}(\mathcal{T}_{p,q})$ and $\text{tb}(L) < pq$. Let T be a torus containing L that bounds a solid torus with core an unknot. According to Lemma 6.5.3 we know that $\text{tw}(L, T) < 0$, thus we

can isotop T, relative to L, so that it is convex by Theorem 3.3.1. From Lemma 6.5.14, we can find a torus T' isotopic to T with dividing slope q/p. Let A be an annulus with one boundary component L and the other a dividing curve on T'. It is easy to see that A can be made convex (see the argument in the previous proof, if this is not clear). Notice that the dividing set of A must contain an arc that is parallel to L. Thus Lemma 5.4.14 says there is a bypass for L on A and Theorem 6.1.5 says that L destabilizes.

Turning to Item (3) let $L \in \mathcal{L}(\mathcal{T}_{p,q})$ have $\mathrm{tb}(L) = pq$. As above we can put L on a convex torus T that bounds a solid torus S in the knot type of an unknot. By Lemma 6.5.3 we know $\mathrm{tw}(L,T) = 0$, and thus the dividing slope of T must be q/p and L will be one of the Legendrian divides on T. Recall that we are assuming there is a positive integer k such that $-k-1 < q/p < -k$, so by Lemma 6.5.14 there are convex tori T' and T'' isotopic to, and disjoint from T, with two dividing curves of slope $-k$ and $-k-1$ respectively. Let S' and S'' be the solid tori that T' and T'' bound (if we are in S^3 then T' and T'' bound solid tori on both sides, one is S_∞ and one is S^0, we choose the one with lower meridian ∞ and the torus S was also chosen this way, see Section 5.6 for terminology). We note that we must have $S'' \subset S \subset S'$ since if any of the inclusions were reversed then the $T^2 \times [0,1]$ difference between two of the tori would contain a convex torus with dividing slope ∞ and its Legendrian divide would bound an overtwisted disk. Notice that S' is a standard neighborhood of a Legendrian unknot L' with $\mathrm{tb} = -k$ and S'' is a standard neighborhood of a Legendrian knot L'' that is a stabilization of L' (by Lemma 6.1.3).

We claim that L is determined by L' and L''. (By this we mean that if $\widetilde{L}$ is another Legendrian (p,q)-torus knot with $\mathrm{tb} = pq$ having unknots $\widetilde{L'}$ and $\widetilde{L''}$ associated to it as above and L' is Legendrian isotopic to $\widetilde{L'}$ and L'' is Legendrian isotopic to $\widetilde{L''}$ then L and $\widetilde{L}$ are Legendrian isotopic.) Assuming this for a moment we note that there are k possibilities for L', that is there are k Legendrian unknots with $\mathrm{tb} = -k$. This follows easily from the classification of Legendrian unknots in Theorem 6.4.1. Moreover, there are 2 possibilities for L'' since there are exactly two ways to stabilize L'. Thus there are at most $2k$ possible elements in $\mathcal{L}(\mathcal{T}_{p,q})$ with $\mathrm{tb} = pq$, but in Exercise 6.5.9 it was shown that there are at least $2k$ such knots. Thus there are exactly $2k$ such knots and, in addition, it was verified in that exercise that the the possible rotation numbers are as claimed. This completes the proof of Item (3). We will give a different computation of the rotation numbers below.

We now verify the claim that L is determined by L' and L''. Let $\widetilde{L}$ be another Legendrian (p,q)-torus knot with $\mathrm{tb} = pq$ having unknots $\widetilde{L'}$ and $\widetilde{L''}$ associated to it as above, let $\widetilde{S'}$ and $\widetilde{S''}$ be their associated solid tori, and let $\widetilde{T}$ be the convex torus on which $\widetilde{L}$ sits. We assume that L' is Legendrian isotopic to $\widetilde{L'}$ and L'' is Legendrian isotopic to $\widetilde{L''}$. Thus by Lemma 6.1.2 we know there is an ambient contact isotopy taking S' to $\widetilde{S'}$. Since L'' and $\widetilde{L''}$ are the same stabilization of $L = \widetilde{L}$ they are isotopic in $S' = \widetilde{S'}$ and hence Lemma 6.1.2

says there is an abient contact isotopy of S' taking S'' to $\widetilde{S''}$. Thus we can assume that L and $\widetilde{L}$ (and T and $\widetilde{T}$) are contained in the basic slice $T^2 \times [0,1] = S' \setminus S''$.

We will show that there is a torus $\overline{T}$ in $T^2 \times [0,1]$ that has a linear characteristic foliation of slope q/p and the Legendrian dividing curves on T and $\widetilde{T}$ agree with $T \cap \overline{T}$ and $\widetilde{T} \cap \overline{T}$, respectively. Given this, we can Legendrian isotop L to $\widetilde{L}$ through leaves of the characteristic foliation of $\overline{T}$ and thus completing the proof of our claim. This follows from the following lemma that will be useful later.

Lemma 6.5.20. *Suppse $(T^2 \times [0,1], \xi)$ is a basic slice with dividing slopes s_0 and s_1. Let r be any slope in (s_0, s_1). Given any convex torus T in $T^2 \times [0,1]$ with dividing slope r (and any even number of dividing curves), there is a torus $\overline{T}$ in $T^2 \times [0,1]$ that has linear characteristic foliation of slope r and $T \cap \overline{T}$ are the Legendrian dividing curves on T.*

Proof. We note that we can find convex tori T' and T'' (these are not related to the similarly denoted tori in the proof above) in $T^2 \times [0,1]$ with each having two dividing curves of slope r and that cobound a thickened torus containing T. If T has two dividing curves then we can take T' and T'' to be copies of T in an invariant neighborhood of T. If T has more than two dividing curves then we proceed as follows. Suppose T' is closer to $T^2 \times \{0\}$ than T'', then we can find T' by taking an annulus A with one boundary component a Legendrian divide on $T^2 \times \{0\}$ and the other a ruling curve on T. We can make A convex and find a bypass for T along A. From Theorem 5.4.11 we know attaching this bypass will reduce the number of dividing curves on T by two. Continuing to attach bypasses we arrive at T'. We may similarly find T''.

We can break $T^2 \times [0,1]$ into four pieces using the above tori

$$T^2 \times [0,1] = R_1 \cup R_2 \cup R_3 \cup R_4,$$

where $\partial R_1 = (T^2 \times \{0\}) \cup T'$, $\partial R_2 = T' \cup T$, $\partial R_3 = T \cup T''$, and $\partial R_4 = T'' \cup (T^1 \times \{1\})$. The contact structure on R_1 is given by a path in the Farey graph from s_0 to r with all edges decorated by the sign of the basic slice and similarly for R_4 except the path goes from r to s_1. Notice that $R_2 \cup R_3$ is an invariant neighborhood from T' to T''. Choose a slope r' that had an edge to r in the Farey graph and consider the annulus A_1 in R_2 and A_2 in R_3 with boundary ruling curves of slope r' on the tori T' and T for A_1 and T and T'' for A''.

Exercise 6.5.21. Prove we can make these annuli convex and the contact structure on R_2 and R_3 is completely determined by the dividing curves on A_1 and A_2, respectively.

Let ξ' be the contact structure on $T^2 \times [0,1]$ constructed in the proof of the existence of a basic slice with slopes s_0 and s_1 (if we choose the correct model this is of course contactomorphic to ξ, but we will build a particular contactomorphism between ξ and ξ'). Note from Corollary 5.3.2 we know that in $(T^2 \times [0,1], \xi')$ there is a torus $\overline{T}$ that has

linear characteristic foliation of slope r. We will now see how to decompose $(T^2\times[0,1],\xi')$ into pieces that are contactomorphic to the R_i above.

Exercise 6.5.22. Show that one can perturb $\overline{T}$ into three tori $\widehat{T}$, $\widehat{T'}$, and $\widehat{T''}$ in $(T^2\times[0,1],\xi')$ that are all convex with dividing slope r and such that

(1) $\widehat{T'}$ and $\widehat{T''}$ have two dividing curves and cobound a thickened torus containing $\widehat{T}$,
(2) $\widehat{T}$ has the same number of dividing curves as T,
(3) the Legendrian dividing curves on $\widehat{T}$, $\widehat{T'}$, and $\widehat{T''}$ are exactly their intersection with $\overline{T}$,
(4) the tori split $T^2\times[0,1]$ into four regions $\widehat{R}_1,\widehat{R}_2,\widehat{R}_3,\widehat{R}_4$ in the same way the R_i were constructed above, and there are annuli $\widehat{A}_1$ and $\widehat{A}_2$ in the $\widehat{R}_2$ and $\widehat{R}_3$ respectively that have slope r' have boundary ruling curves and the dividing set on $\widehat{A}_i$ is the same as on A_i.

Hint: Show $\widehat{R}_2\cup\widehat{R}_3$ can be thought of as $\widehat{A}\times S^1$ where $\widehat{A}$ is an annulus of slope r' and the contact structure is S^1-invariant. The dividing curves on A consist of two arcs going from one boundary component of A to the other. Find an arc γ in $\widehat{A}$ that splits $\widehat{A}$ into $\widehat{A}_1$ and $\widehat{A}_2$.

Note that there is a contactomorphism taking $\widehat{R}_i$ to R_i for each i and they together give a contactomorphism from $(T^2\times[0,1],\xi')$ to $(T^2\times[0,1],\xi)$ and the image of $\overline{T}$ will be the torus claimed in the lemma. □

We now turn to the proof of Item (4).

Exercise 6.5.23. Show that if r and r' are adjacent rotation numbers for a maximal Thurston-Bennequin invariant (p,q)-torus knot then $|r-r'|$ is either $2e$ or $2(p-e)$ where we recall that $-q=np+e$ and n and e are positive integers.

Suppose L and L' are the maximal Thurston-Bennequin invariant Legendrian knots with rotation numbers r and r', respectively. We know that we can write $-q=(n_1+n_2+1)p+e$ and $-q=(n_1'+n_2'+1)+e$ and L is given by the front project in Figure 6.5.25 for some choice of A and L' is also give by this front projections but where the n_i are replaced by n_i' and some choice for A is made.

Show that if $|r-r'|=2e$ then $n_i=n_i'$ and the choice for A in the two front diagrams is opposite for L and L'. If $|r-r'|=2(p-e)$ then, assuming $r>r'$ show that $n_1'=n_1+1$ while $n_2'=n_2-1$ and the choice of A for L on the left of the figure while the choice of A for L' is on the right.

Using Legendrian Reidemeister moves, see Theorem 1.4.22, show that if $r=r'+2e$ then $S^e_-(L)$ is Legendrian isotopic to $S^e_+(L')$ and similarly if $r=r'+2(p-e)$.

This exercise completes the proof of Item (4) and hence the theorem, but we will give another proof below that is more in the spirit of convex surfaces and will be useful when studying cabled knots. □

We now give an alternate computation of the rotation numbers of maximal Thurston-Bennequin invariant (p, q)-torus knots as well as showing they become Legendrian isotopic as soon as they have been stabilized enough for their rotation numbers to be the same. Given a null-homologous convex torus T in a contact manifold (M, ξ) let N be an invariant neighborhood of T.

Exercise 6.5.24. Since T is null-homologous, show that $\xi|_N$ can be trivialized.

Let $\mathcal{T}$ be a trivialization of ξ on N. If T is in standard form then define a section s of ξ along T as follows: s will be tangent to the Legendrian divides and agreeing COME BACK TO THIS!

6.6. Classification of non-loose Legendrian unknots

Since Eliashberg's seminal result classifying overtwisted contact structures on 3–manifolds [**Eli89**], there has been very little study of Legendrian and transverse knots in an overtwisted contact structure [**CEMM23**, **EF09**, **Etn13**, **EMM22**]. But some recent advances [**EMT24**] suggest that the study of Legendrian and transverse knots in overtwisted contact structures is essential for our understanding of the geometry of tight contact structures and that their classification can be subtle and surprising [**EMM22**]. In this section we will introduce the basic facts about Legendrian and transverse knots in overtwisted contact structures.

6.6.1. Executive Summary. There are two kinds of Legendrian knots in an overtwisted contact structure: *loose* Legendrian knots, whose standard neighborhood has an overtwisted complement, and *non-loose* Legendrian knots, whose standard neighborhoods have a tight complement. Similarly we say a transverse knot is *loose* if its complement is overtwisted and *non-loose* otherwise. We note that in the literature some authors use the term *exceptional* instead of non-loose.

In most contact structures, and in particular most overtwisted contact structures, it is not true that two Legendrian knots are Legendrian isotopic if and only if they are contactomorphic (by a contactomorphism smoothly isotopic to the identity) as is the case in (S^3, ξ_{std}) by Lemma 1.4.1. We will see a specific case where this fails below. Thus in this section we will classify Legendirian knots up to co-orientation preserving contactomorphism, smoothly isotopic to the identity. We call this a *coarse classification* of Legendrian knots and make a similar definition for transverse knots.

Theorem 6.6.1. *Null-homologous loose Legendrian knots are coarsely classified by their classical invariants (that is knot type, Thurston-Bennequin invariant, and rotation number) and any pair of integers whose sum is odd can be realized as the Thurston-Bennequin invariant and rotation number of a loose Legendrian knot in any knot type. Loose transverse knots are coarsely classified by their classical invariants (that is, knot type and self-linking number) and any odd integer can be realized as the self-linking number of a loose transverse knot.*

Remark 6.6.2. A similar theorem should hold for non-null-homologous knots too, but there is no rotation number in that case and the contact framing does not correspond to the integers (in fact, the framings on the knot might be finite if there are $S^1\times S^2$ summands in the manifolds)

So we have a complete, course, classification of loose Legendrian and transverse knots. It turns out that non-loose Legendrian knots are much interesting and have applications to the construction of tight contact structures, see for example [**EMT24**, **Mat22**]. We discuss the little that is known about their classification below. For now we make a few general observations. The first is that non-loose Legendrian knots obey a version of Bennequin bound.

Theorem 6.6.3 ([Świątkowski 1992, [**Ś92**]). *Let (M,ξ) be an overtwisted contact manifold and L a non-loose Legendrian knot in (M,ξ) with a Seifert surface Σ. Then*

$$-|\operatorname{tb}(L)| + |\operatorname{rot}(L)| \leq -\chi(\Sigma).$$

See Figure 6.6.31.

Unlike for Legendrian knots in general, a given knot in a contact manifold might not be approximable by a non-loose Legendrian knot. In particular, we have the following result.

Theorem 6.6.4 (Chatterjee, Etnyre, Min, Mukherjee 2023, [**CEMM23**]). *If M is an irreducible 3-manifold then a knot K in M has a non-loose Legendrian representative in some overtwisted contact structure on M if and only if M admits a tight contact structure. If K admits a non-loose Legendrian representative and K is not the unknot, then K admits such representatives in at least two overtwisted contact structures.*

The knot K admits non-loose transverse representatives in some overtwisted contact structure on M if and only if K is not the core of a Heegaard torus for a lens space and M admits a tight contact structure. If K admits non-lose transverse representatives then it admits such representatives in at least two overtwisted contact structures.

In general, it is not well-understood how many contact structures support non-loose representatives of a given knot K, but from the examples we understand (see below) it

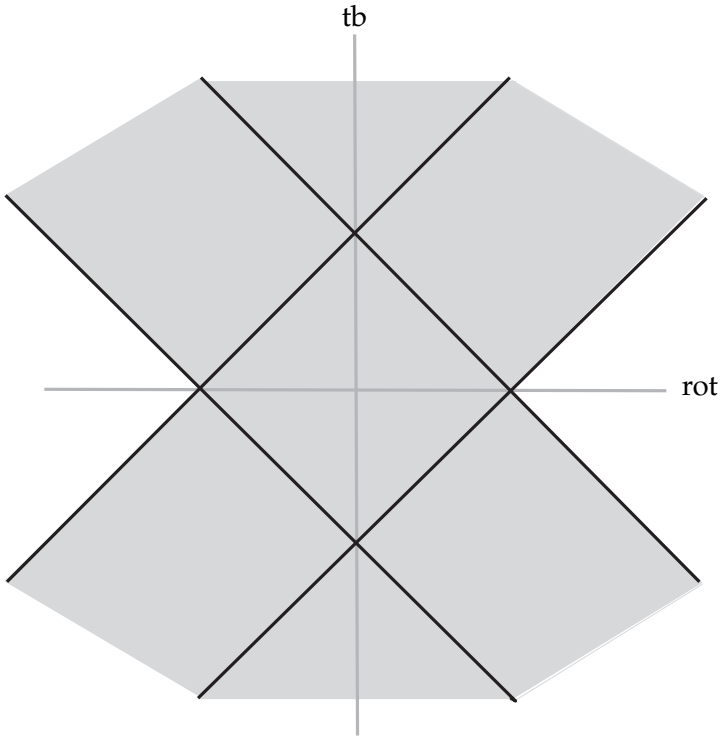

Figure 6.6.31. Possible (rot, tb) numbers for non-loose Legendrian knots in a fix knot type $\mathcal{K}$. The solid lines corresponds to $-|\operatorname{tb}(\mathcal{K})| + |\operatorname{rot}(\mathcal{K})| = -\chi(\Sigma)$

seems that there are very few contact structures in which K will admit non-loose representatives. We note that in [CEMM23] a version of the above theorem was proven that did not require M to be irreducible. We will not give the proof of this result here, but refer the interested reader to [CEMM23]. In the above theorem we see that the criteria for a knot to have a non-loose Legendrian representative and a non-loose transverse representative is different. The distinction between non-loose Legendrian and transverse knots is further highlighted by the next result.

Lemma 6.6.5. *Any Legendrian approximation of a non-loose transverse knot is non-loose, but the transverse push-off of non-loose Legendrian knots need not be non-loose.*

We now turn to the first classification of non-loose Legendrian and transversal knots.

Theorem 6.6.6 (Eliashberg and Fraser 1998, [EF98])**.** *The contact manifold (S^3, ξ_n) admits a non-loose Legendrian representative of the unknot if and only if $n = 1$. In (S^3, ξ_1) the complete list of non-loose Legendrian unknots is $L_k^{\pm}$ for $i > 1$ and L_1 where*

$$\operatorname{tb}(L_k^{\pm}) = k, \operatorname{rot}(L_k^{\pm}) = \pm(k-1), \operatorname{tb}(L_1) = 1, \text{ and } \operatorname{rot}(L_1) = 0.$$

In addition $S_{\mp}(L_k^{\pm}) = L_{k-1}^{\pm}$ for $k > 2$, $S_{\mp}(L_2^{\pm}) = L_1$ and $S_{\pm}(L_1)$ is loose. See Figure 6.6.32.

There are no non-loose transverse unknots.

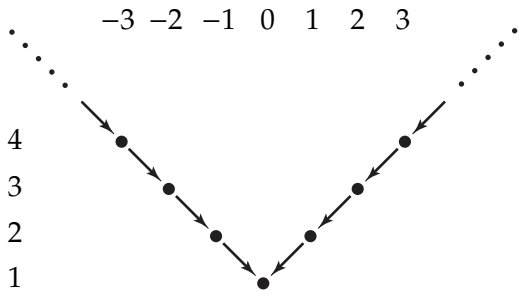

Figure 6.6.32. The mountain range for non-loose unknots in (S^3, ξ_1).

We can exhibit the non-loose unknots in (S^3, ξ_1) by a contact surgery diagram. See Figure 6.6.33. To see this one may easily see that the surgery in the figure gives S^3 and

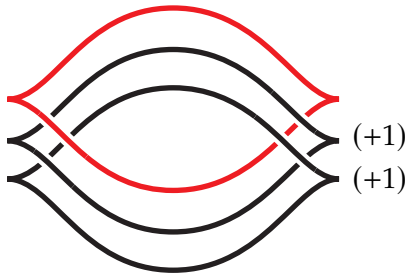

Figure 6.6.33. The non-loose Legendrian unknot with tb = 1 is shown in red.

compute that the d_3-invariant of the surgery manifold is 1. To see that the red curve is a non-loose unknot with tb = 1 we note that Legendrian surgery on the red curve cancels one of the contact (+1)-surgeries, see Lemma 6.2.4, leaving the tight contact structure on $S^1 \times S^2$.

Exercise 6.6.7. Prove that contact (+1)-surgery on the maximal Thurston-Bennequin invariant Legendrian unknot gives the tight contact structure on $S^1 \times S^2$.

Exercise 6.6.8. Show that if L is a Legendrian knot in an overtwisted manifold on which Legendrian surgery produces a tight contact manifold, then L is non-loose.

A simple corollary of the above result is that there are no non-loose transverse unknots.

Corollary 6.6.9. *Any transverse unknot in any overtwisted contact structure is loose.*

We now recall work of Vogel that classifies Legendrian unknots up to Legendrian isotopy. We point out that this is only such result that pushes classification beyond "coarse classification".

Theorem 6.6.10 (Vogel 2018, [Vog18]). *In* (S^3, ξ_1) *for each* $(k, \pm(k-1))$ *with* $k \geq 1$ *there are exactly two non-loose Legendrian knots up to Legendrian isotopy with* $\mathrm{tb} = k$ *and* $\mathrm{rot} = \pm(k-1)$.

Loose Legendrian unknots in (S^3, ξ_n) *are uniquely determined by their* tb *and* rot *unless* $n = 1$ *and* $\mathrm{tb} > 0$*, in which case there are exactly two representatives that are not Legendrian isotopic for each realizable* tb *and* rot.

We will not prove this theorem, but not the proof involves studying the contactomorphism group of overtwisted contact structures. See [Vog18] for details. We will also not further discuss Legendrian and transverse knots in overtwisted contact structures but refer the reader to [Dym01, Etn13] for general results about non-loose Legendrian knots and [EMM22] for the classification of non-loose Legendrian torus knots, see also [GO20, Mat22] for previous work on non-loose torus knots.

6.6.2. Proof of the main results. We begin with a sketch of the proof that loose Legendrian (and transverse) knots are "simple".

Sketch of the proof of Theorem 6.6.1. Eliashberg's classification of overtwisted contact structures, Theorem 1.6.2, also holds for contact manifolds with boundary and we can analyze homotopy classes of plane field on a manifold with boundary (and plane field fixed near the boundary) just as we did on a closed manifold in Section 1.5.2. Recall, that they are determined by the Euler class (or a slight refinement if the homology has 2-torsion) and a d_3 invariant. Given two null-homologous loose Legendrian knots L and L' in the same knot type we can consider complements C and C', respectively, of their standard neighborhoods. If $\mathrm{tb}(L) = \mathrm{tb}(L')$ then the characteristic foliation on their boundaries can be assumed to be the same. One can show that the Euler class of the contact structure on C and C' is determined by that of the ambient contact manifold and the rotation numbers of L and L'. Lastly, the d_3-invariant of the contact structure on C and C' is determined by that of the ambient contact manifold. Thus if all the classical invariants of L and L' are the same, then Eliashberg's classification of overtwisting contact structures says C is contactomorphic to C' (and we can assume that this contactomorphism takes the meridian of L to the meridian of L'). Thus we can extend this contactomorphism over the neighborhoods of the knots to get an ambient contactomorphism taking L to L'.

For details of the study of plane fields on a 3-manifold with boundary and the above proof, see [Etn13]. □

We now turn to a version of the Bennequin bound for non-loose Legendrian knots.

Proof of Theorem 6.6.3. The inequality in the theorem will hold if the following two inequalities hold

$$\begin{aligned} \mathrm{tb}(L) \pm \mathrm{rot}(L) &\leq -\chi(\Sigma) \qquad \text{if } \mathrm{tb}(L) \leq 0 \\ -\mathrm{tb}(L) \pm \mathrm{rot}(L) &\leq -\chi(\Sigma) \qquad \text{it } \mathrm{tb}(L) > 0, \end{aligned}$$

for any surface Σ with $\partial\Sigma = L$.

To verify these inequalities, let $N(L)$ be a standard neighborhood of L with ruling curves of slope 0. Note each ruling curve is null-homologous in the complement of $N(L)$ which is tight. In the case that $\mathrm{tb}(L) < 0$ then from Theorem 6.1.9 we know that a ruling curve is isotopic to L and we get the desired inequality from the standard Bennequin inequality, Theorem 3.7.5. We obtain the same conclusion if $\mathrm{tb}(L) = 0$ except this time we use a Legendrian divide. Finally, if $\mathrm{tb} > 0$ then Theorem 6.1.9 says the 0 sloped ruling curve is $S_+^{\mathrm{tb}(L)} \circ S_-^{\mathrm{tb}(L)}(L)$ and thus has $\mathrm{tb} = -\mathrm{tb}(L)$ and $\mathrm{rot} = \mathrm{rot}(L)$. Thus again, the standard Bennequin inequality yields the desired result. □

Recall Lemma 6.6.5 says that any Legendrian approximation of a non-loose transverse knot is non-loose, but it need not be true that a transverse push-off of a non-loose Legendrian knot is non-loose.

Proof of Lemma 6.6.5. Let T be a non-loose transverse knot and L some Legendrian approximation. If L can an overtwisted disk in its complement, then there is such a disk in the complement of a small standard neighborhood of L. But the transverse push-off L_+ of L is contained in the standard neighborhood. Thus L_+ is loose, but L_+ is transversely isotopic to T, and thus T is loose. This contradicts our hypothesis and thus L is non-loose.

From the classification of non-loose Legendrian unknots in Theorem 6.6.6 and the fact that there are no non-loose transverse unknots, we see that the transverse push-off of a non-loose Legendrian knot can be loose. □

We end this section with the (coarse) classification of non-loose Legendrian unknots.

Proof of Theorem 6.6.5. We will study Legendrian unknots via their complements. Given a Legendrian unknot L with $\mathrm{tb} = n$ its complement C of the standard neighborhood $N(L)$ is a solid torus with upper meridian 0 and convex boundary with two dividing curves of slope n (all slopes are described by longitude-meridian coordinates on the standard neighborhood of L).

Recall from Theorem 5.6.3 we know that $\mathrm{Tight}(S^0; n)$ has $|n|$ elements if $n < 0$, 0 elements if $n = 0$, 1 element if $n = 1$, and 2 elements if $n > 1$. We note that in (S^3, ξ_{std}) there are $|n|$ Legendrian unknots with $\mathrm{tb} = n < 0$. Thus all the tight contact structures on C in this case come from the complement of Legendrian knots in the tight S^3 and hence do not correspond to non-loose Legendrian unknots. However, all the contact structures

with $n > 0$ do not occur in the tight S^3 and we see that when we glue the standard neighborhood of L to any one of these we obtain an overtwisted contact structure because C will contain a convex torus with dividing slope ∞ and a Legendrian divide on this torus will bound a disk, and hence an overtwisted disk, in $N(L)$.

The paths in the Farey graph for the two contact structures in Tight$(S^0; n)$ when $n > 1$ are shown in Figure 6.6.34 as is the one in Tight$(S^0; 1)$. Let $L_n^{\pm}$ be the Legendrian unknot

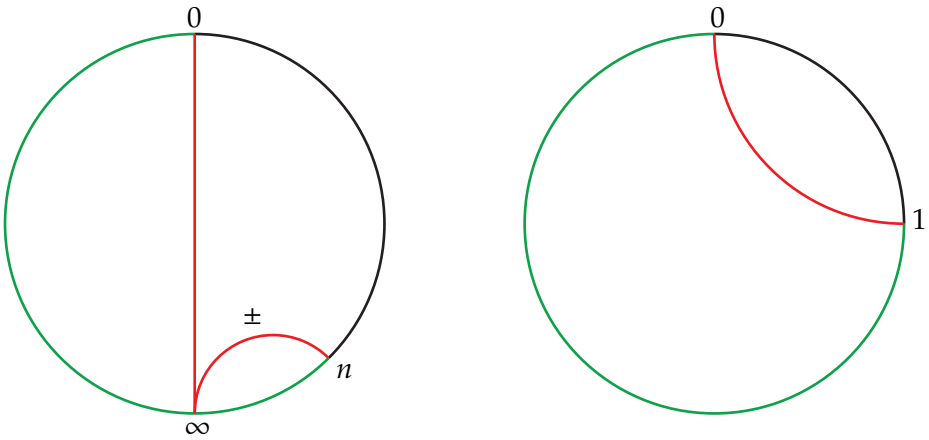

Figure 6.6.34. Farey graphs for the contact structures on the complement of non-loose Legendrian unknots with tb > 1 on the left and tb = 1 on the right.

with complement the contact structure in Tight$(S^0; n)$ corresponding to the path in the Farey graph with a $\pm$ sign and let L_1 be the one with complement having the unique contact structure on Tight$(S^0; 1)$. We now set $C_n^{\pm}$ to be the complement of the standard neighborhood of $N(L_n^{\pm})$ and similarly C_1 is the complement of $N(L_1)$.

We note that the meridional disk for $C_n^{\pm}$ is a Seifert surface for $L_n^{\pm}$ and thus we can compute the rotation number of $L_n^{\pm}$ using this disk by Theorem 3.5.1. More specifically, if $\partial C_n^{\pm}$ has ruling slope 0, then Theorem 6.1.9 says that a ruling curve will have the same rotation number as $L_n^{\pm}$ and if D is the disk in C that this ruling curves bounds then we can make it convex and $\text{rot}(L_n^{\pm}) = \chi(D_+) - \chi(D_-)$.

Exercise 6.6.11. The contact structure on $C_n^{\pm}$ from the complement of $N(L_n^{\pm})$ is the union of the unique tight contact structure in Tight(S^0, ∞) and a basic slice in Tight$_{min}(T^2 \times [0,1]; \infty, n)$. Use the formula for the Euler class of basic slices in Theorem 5.3.1 to show that $\text{rot}(L_n^{\pm}) = \pm(n-1)$. Similarly, $\text{rot}(L_1) = 0$.

We now see that $S_{\mp}(L_n^{\pm}) = L_{n-1}^{\pm}$ for $n > 3$ and $S_{\mp}(L_2^{\pm}) = L_1$. Given this, we see that all the non-loose unknots are in one overtwisted contact structure on S^3. Recall that if $N(S_{\mp}(L_n^{\pm})$ is a standard neighborhood of $S_{\mp}(L_n^{\pm})$ then its complement in $N(L_n^{\pm})$ is a $\mp$ basic slice. If we add this basic slice to $C_n^{\pm}$ then we get $C_{n-1}^{\pm}$.

Exercise 6.6.12. Check this last statement. Note that as you move the basic slice from the neighborhood of the knot to the complement the sign changes (since the orientation on the manifold changes!).

We have a similar result for $L_2^{\pm}$ and this completes the claim.

We are left to see that the overtwisted contact structure containing these non-loose knots in ξ_1, that is has $d_3 = 1$. To this end consider Figure 6.6.33.

Exercise 6.6.13. Show that the red curve in the figure has tb $= 1$ and compute the d_3-invariant.

This completes the classification of non-loose Legendrian knots. The fact that there are no non-loose transverse unknots follows since as one negatively stabilizes a Legendrian knot its transverse push-off is unchanged and after some number of negative stabilizations any non-loose Legendrian unknot becomes loose and hence its transverse push-off is also loose. □

Chapter 7

Symplectic fillings

This chapter focuses on various types of symplectic fillings of contact manifolds, symplectic cobordisms between contact manifolds, and various constructions. In Section 7.1 we review and expand on our discussion in Section 1.6.2 about various types of symplectic fillings of contact manifolds. The next section discusses toric 4-manifolds as a convenient way to build symplectic fillings and symplectic caps for lens spaces (we will also use toric geometry in Section 13.3 to build symplectic 4-manifolds and show that contact manifolds with positive Giroux torsion do not admit strong symplectic fillings). In Section 7.3 we will show how to glue a symplectic filling of a contact manifold to a symplectic cap to build closed symplectic manifolds. We will then use this construction to show that there are contact structures that are weakly but not strongly fillable. We will also show that Fintushel and Stern's important smooth construction of rational blow-down can be done in the symplectic category. In Section 7.4, we turn to another important construction of symplectic manifolds. Specifically, we will discuss attaching Weinstein handles to symplectic manifolds with convex boundary. The last section of this chapter will show that there are tight contact structures that are not fillable.

7.1. Types of symplectic convexity (and concavity)

Here we consider several types of fillability and discuss how they are related. We first recall from Section 1.6.2 that a compact symplectic manifold (X, ω) is a *weak symplectic filling* of a contact manifold (M, ξ), also simply called a *weak filling*, if

- $\partial X = M$ as oriented manifolds, and
- $\omega|_\xi$ is an area form

Remark 7.1.1. We note that the compactness assumption in the definition above is essential. Indeed, for any $(M, \xi = \ker\alpha)$, the (non-compact) symplectic manifold $(Y \times$

$[0,\infty), d(e^t\alpha))$ satisfies the listed properties above forms a weak symplectic filling of (M,ξ) .

If ξ is an oriented contact structure (so we have chosen a preferred orientation on ξ), then in the second bullet above, we would require that $\omega|_\xi$ be an area form defining the given orientation. If (M,ξ) admits such an (X,ω), then we say that it is *weakly symplectically fillable* or just *weakly fillable*.

We now move on to a stronger form of symplectic fillability. We say that a compact symplectic manifold (X,ω) is a *strong symplectic filling* of a contact manifold (M,ξ), also called a *strong filling*, if

- $\partial X = M$ as oriented manifolds,
- there is a vector field v defined near ∂X and transverse to ∂X such that
$$\mathcal{L}_v\omega = \omega,$$
- v points out of X along ∂X, and
- $\alpha = (\iota_v\omega)|_M$ is a contact form for ξ

A vector field v satisfying the second bullet point above is called a *symplectic dilation*. See Figure 7.1.1 Recall that $\mathcal{L}_v$ is the Lie derivative in the direction of v and ι_v is the contraction of v into a differential form. If (M,ξ) admits such an (X,ω), then we say that it is *strongly symplectically fillable* or just *strongly fillable*. It is common to refer to a strong symplectic filling as simply a *symplectic filling* and only add the word "strong" when trying to contrast with a weak symplectic filling. We also say that (M,ξ) is the *convex boundary* of (X,ω) and that (X,ω) is a *convex symplectic filling* of (M,ξ). So a convex symplectic filling is the same thing as a strong symplectic filling of a contact manifold.

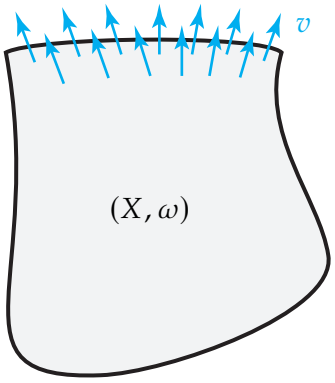

Figure 7.1.1. A symplectic manifold (X,ω) with convex boundary.

We now remind two examples of strong symplectic fillings from Section 1.6.2 for the convenience of the reader.

Example 7.1.2. Consider $\mathbb{C}^2$ with the symplectic form $\omega = dx_1 \wedge dy_1 + dx_2 \wedge dy_2$. The radial vector field $v = \frac{1}{2}\left(x_1\frac{\partial}{\partial x_1} + y_1\frac{\partial}{\partial y_1} + x_2\frac{\partial}{\partial x_2} + y_2\frac{\partial}{\partial y_2}\right)$ satisfies $\mathcal{L}_v\omega = \omega$ and is transverse to the unit sphere S^3. Moreover, our discussion in Example 1.1.18 shows that ξ_{std} on S^3 is the kernel of $\iota_v\omega$. Thus, the unit ball B^4 is a strong symplectic filling of (S^3, ξ_{std}).

Example 7.1.3. Consider the symplectic manifold $(\mathbb{C} - \{0\}) \times \mathbb{C}$ with symplectic form $dr \wedge d\theta + dx \wedge dy$ where (r, θ) are polar coordinates on $\mathbb{C} - \{0\}$ and (x, y) are Cartesian coordinates on $\mathbb{C}$. Let $v = (r-1)\frac{\partial}{\partial r} + \frac{1}{2}\left(x\frac{\partial}{\partial x} + y\frac{\partial}{\partial y}\right)$ and $S^1 \times S^2$ be the boundary of a small tubular neighborhood $S^1 \times D^2$ of $S^1 = \{(r, \theta, x, y) | r^2 + x^2 + y^2 < \epsilon^2\}$. Notice that v is transverse to $S^1 \times S^2$ and dilates ω. Thus $(S^1 \times D^3, \omega)$ is a strong symplectic filling of $(S^1 \times S^2, \xi_{std})$ where $\xi_{std} = \ker(\iota_v\omega)$.

It is easy to see how weak and strong convexity are related.

Lemma 7.1.4. *If (X, ω) is a strong symplectic filling of (M, ξ), then it is also a weak filling of (M, ξ).*

Proof. This is clear as $d\alpha$ is positive on $\ker \alpha$ and $\omega = d\alpha$ on M. □

We will show in Section 7.3 that there are weakly fillable contact structures that are not strongly fillable, but in some cases they are the same.

Theorem 7.1.5. *If (X, ω) is a weak symplectic filling of a contact structure ξ on M and ω is exact near M, then ω may be deformed near M to a new symplectic form ω' such that (X, ω') is a strong symplectic filling of (M, ξ) and agrees with ω away from M.*

This was originally proven by Ohta and Ono in [**OO99**], but the main part of the argument, on which our argument below is based, appeared first in the work of Eliashberg in [**Eli91**].

Proof. Using the collar neighborhood theorem from differential topology, we can consider the neighborhood $(0, 1] \times M$ of M in X. We denote by β a primitive for ω on $(0, 1] \times M$. We also take α to be a contact form for ξ such that $d\alpha = \omega$ on ξ.

Exercise 7.1.6. Show such an α exists.
Hint: what happens to $d\alpha$ restricted to ξ when α is rescaled.

Given any $C > 0$ we can find a $K > 0$ such that there is a function $f\colon (0, 1] \to \mathbb{R}$ such that

- $f = 0$ on $(0, 1/8]$
- $f = Kt$ on $[7/8, 1]$,
- f is non-decreasing and strictly increasing on $(1/8, 1]$, and

- $f'(t) > C$ for $t \in [1/4, 3/4]$.

We also choose $g\colon (0,1] \to \mathbb{R}$ such that

(1) $g = 1$ on $(0, 1/4]$,

(2) $g = 0$ on $[3/4, 1]$,

(3) g is strictly decreasing on $(1/4, 3/4)$, and

(4) $g'(t) > -3$ for all t.

We will determine the constants C and K later, but for now consider the form

$$\omega' = d(f\alpha) + d(g\beta).$$

It is clear that on $(0, 1/8) \times M$, $\omega' = \omega$ so ω' can be extended to all of X by ω. On $(7/8, 1] \times M$ the vector field $v = t\frac{\partial}{\partial t}$ is a dilation of ω, is transverse to $\{t\} \times M$, and $\iota_v \omega'$ is a contact form for ξ. Thus, if ω' is a symplectic form on X, then it is the form claimed in the theorem.

We note that $\omega' = f'\, dt \wedge \alpha + f\, d\alpha + g'\, dt \wedge \beta + g\, d\beta$ and so

$$\omega' \wedge \omega' = g^2\, d\beta \wedge d\beta + 2ff'\, dt \wedge \alpha \wedge d\alpha + 2f'g\, dt \wedge \alpha \wedge d\beta + 2fg\, d\alpha \wedge d\beta$$
$$2fg'\, d\alpha \wedge dt \wedge \beta + 2gg'\, dt \wedge \beta \wedge d\beta.$$

We have dropped any term with $dt \wedge dt$ or $d\alpha \wedge d\alpha$ (since we are thinking of α as pulled back to $(0, 1] \times M$ from M and hence essentially a 1-form on a 3-manifold).

Exercise 7.1.7. Show that the first four terms are all non-negative multiples of $\omega \wedge \omega$ and at any point of $(0, 1] \times M$ at least one of them is positive.
Hint: Notice that $d\beta = \omega$ and $d\alpha$ agree on ξ. At any point, try evaluating the form on the vectors $\frac{\partial}{\partial t}$, X_α, v_1, and v_2 where R_α is the Reeb vector field of α and v_1, v_2 is an oriented basis for ξ.

We do not know anything about the last two terms, but notice that each has g' in it. Whenever g' is non-zero, observe that if K and C are chosen large enough, then ff' is larger than fg' or gg' by any desired amount. Thus, the second term in the whole expression will always dominate the last two terms so that the whole expression will be a positive multiple of $\omega \wedge \omega$ and hence ω' is a symplectic form. □

The above theorem is most commonly used in the following form, which is an immediate corollary of the theorem.

Corollary 7.1.8. *Let M be a rational homology sphere, that is it has the rational homology of S^3. If (X, ω) is a weak symplectic filling of a contact structure ξ on M, then we may alter ω near M to obtain a strong symplectic filling of (M, ξ).*

Strengthening strong symplectic fillability, consider Liouville domains. A *Liouville manifold* is a symplectic manifold (X, ω) with a chosen primitive λ for ω, that is $d\lambda = \omega$. Notice that ω induces an isomorphism

$$\phi_\omega \colon \Gamma(TX) \to \Omega^1(X) \colon v \mapsto \iota_v \omega$$

where $\Gamma(TX)$ is the space sections of TX, that is vector fields on X, and $\Omega(X)$ is the space of 1-forms on X.

Exercise 7.1.9. Prove that ϕ_ω is an isomorphism.
Hint: This is very similar to the proof of Lemma 1.2.13 in the contact setting.

We can now define the *Liouville vector field* associated to λ to be $v_\lambda = \phi_\omega^{-1}(\lambda)$.

Exercise 7.1.10. Show that the flow of v_λ expands ω, that is

$$\mathcal{L}_{v_\lambda} \omega = \omega.$$

That this last exercise makes it clear that we can alternatively define a Liouville manifold X to be a symplectic manifold (X, ω) together with a vector field v such that $\mathcal{L}_v \omega = \omega$. The primitive for ω will be $\iota_v \omega$, and v will be its Liouville vector field.

Exercise 7.1.11. Show that a Liouville manifold cannot be closed.

If the Liouville manifold (X, λ) is compact, then we say it is a *Liouville domain* if the Liouville vector field v_λ is transverse to the boundary of X and pointing out of X.

Exercise 7.1.12. Show that if (X, λ) is a Liouville domain, then $\lambda|_{\partial X}$ is a contact form on ∂X and $(X, d\lambda)$ is a strong symplectic filling of $(\partial X, \ker(\lambda|_{\partial X}))$.

If the contact manifold (M, ξ) is contactomorphic to the contact manifold on the boundary of a Liouville domain (X, ω), then we say that (M, ξ) is *exactly symplectically fillable*.

Example 7.1.13. Recall in Section 1.8.4 we defined a 1-form λ on the cotangent bundle T^*M of any manifold M such that $d\lambda$ is a symplectic form. The form λ is frequently called the *Liouville form* for T^*M and it clearly gives T^*M the structure of a Liouville manifold. If we take a Riemannian metric M and let $U^*M = \{\beta \in T_x^*M : \|\beta\| \leq 1\}$ be the unit disk bundle in T^*M, then one may check that the Liouville vector field associated to λ points out of ∂U^*M. Thus, U^*M is a Liouville domain and $\ker \lambda|_{\partial U^*M}$ is a contact structure on ∂U^*M that admits an exact symplectic filling.

There is a particularly nice type of Liouville domain called a Weinstein manifold. A Weinstein manifold is a Liouville domain (X, λ) together with a function $\phi \colon X \to \mathbb{R}$ satisfying:

- ϕ is a Morse function,
- ϕ is bounded below,
- ∂X is a regular level set of ϕ, and
- the Liouville vector field v_λ is gradient-like for ϕ.

Here we say v_λ is gradient-like for ϕ if the zeros of v_λ are non-degenerate and agree with the critical points of $d\phi$, and $d\phi(v_\lambda) > 0$ away from the critical points of ϕ. While we will not consider this situation here, one can consider non-compact Liouville manifolds; in this case, one also requires that ϕ be proper (that is, the preimage of compact sets are compact).

Example 7.1.14. Let $f\colon M \to \mathbb{R}$ be a Morse function on a compact manifold. As discussed in the example above, we have the symplectic structure $\omega = d\lambda$ on T^*M. We now let $\phi\colon T^*M \to \mathbb{R}$ be $\phi(x) = f \circ \pi(x) + \|x\|^2$ where $\pi\colon T^*M \to M$ is the projection map and $\|x\|$ the the norm of an element in T^*M with respect to some Riemannian metric g on M. We note that ϕ is a Morse function on T^*M. Now let ∇f be the gradient of f with respect to g. We can consider the flow of ∇f in M. This induces a flow on T^*M. Let v_f be the corresponding vector field on T^*M. Finally, let $v = v_f + v_r$ where v_r is the radial vector field in T^*M. It is easy to check that v is gradient-like for ϕ and v is dilating for $d\lambda$. Thus $(T^*M, d\lambda, \phi, v)$ is a Weinstein manifold.

Recall in Section 1.6.2 we defined Stein manifolds and Stein fillings of contact structures. For convenience, we recall those definitions here. A *Stein manifold* is a complex manifold X with a J-convex function $\phi\colon X \to \mathbb{R}$ that is bounded below and proper. Recall that if J is the almost complex structure on X associated to the complex structure, then ϕ is J-convex if $d\lambda(v, Jv) > 0$ for non-zero vectors v where $\lambda(v) = -d\phi(Jv)$.

A *Stein domain* is a sub-level set of ϕ for a Stein manifold (X, ϕ) and a contact manifold (M, ξ) is called *Stein fillable* if (M, ξ) is contactomorphic to a regular level set of ϕ. As noted in Section 1.6.2 a Stein filling of (M, ξ) is also a strong filling, but we can say more.

Lemma 7.1.15. *If (X, ϕ) is a Stein filling of a contact manifold (M, ξ), then there is a Morse function ϕ' arbitrarily close to ϕ so that $(X, -d\phi \circ J, \phi')$ is a Weinstein filling of (M, ξ).*

Proof. Given the Stein domain (X, ϕ) with associated almost complex structure J, we can find a Morse function ϕ' that is C^k-close to ϕ for any k. For $k > 1$ it is easy to check that ϕ' is also J-convex (since J-convexity is an open condition on functions with the C^2 topology, but for this we recall that what we are calling J-convex, some would call *strictly* J-convex). The form $\omega = d(-d\phi' \circ J)$ is a symplectic structure on X (this follows directly from the fact that ϕ' is J-convex). We can now let $g(v, w) = \omega(v, Jw)$.

Exercise 7.1.16. Show that g is a Riemannian metric on X and that is $g(Jv, Jw) = g(v, w)$.

We can now let $\nabla\phi'$ be the gradient of ϕ with respect to g. That is $\nabla\phi'$ is a vector field on X such that $\iota_{\nabla\phi'}g = d\phi'$. Clearly $\nabla\phi'$ is gradient-like for ϕ', since it is actually the gradient. We now claim

$$\mathcal{L}_{\nabla\phi'}\omega = \omega$$

which shows that (X, ω, ϕ') is a Weinstein filling of (M, ξ). To see this, we note that for any tangent vector v we have

$$\begin{aligned}(\iota_{\nabla\phi'}\omega)(v) = \omega(\nabla\phi', v) &= -g(\nabla\phi', Jv)\\ &- (J^*\iota_{\nabla\phi'}g)(v) = -(J^*d\phi')(v),\end{aligned}$$

That $\iota_{\nabla\phi'}\omega = -d\phi' \circ J$ and therefore we have

$$\mathcal{L}_{\nabla\phi'}\omega = d(\iota_{\nabla\phi'}\omega) = -d(d\phi' \circ J) = \omega,$$

as claimed. □

Exercise 7.1.17. Show that a Stein domain must have connected boundary.

It is subtle to determine if a given smooth manifold admits a complex structure (here we mean an honest complex structure, not an almost complex structure), so the following result of Eliashberg is quite spectacular.

Theorem 7.1.18 (Eliashberg [**Eli90b**], 1990)**.** *If (X, λ, ϕ) is a Weinstein filling of a contact manifold (M, ξ), then after composing ϕ with a diffeomorphism of $\mathbb{R}$ it is J-convex for some complex structure on X, thus giving a Stein filling of (M, ξ).*

The proof of this result is well beyond what we will cover in this book and is only stated here for completeness. In addition, there are many more precise statements one can make about the connection between Weinstein and Stein manifolds. For a comprehensive look at this connection, the reader should consult the standard book [**CE12**] on the topic. Given the last two theorems, constructing Weinstein fillings of contact manifolds is essentially equivalent to constructing Stein fillings. While we will not prove how one can construct Stein fillings in this book, we will see how to construct Weinstein fillings in Section 7.4.

We now collect the results relating to various fillings of contact manifolds. For a contact manifold (M, ξ) being

$$\text{Stein fillable} = \text{Weinstein fillable} \tag{7.1.13}$$

$$\Rightarrow \text{exactly fillable} \tag{7.1.14}$$

$$\Rightarrow \text{strongly fillable} \tag{7.1.15}$$

$$\Rightarrow \text{weakly fillable} \tag{7.1.16}$$

$$\Rightarrow \text{tight} \tag{7.1.17}$$

The equality follows from Lemma 7.1.15 and Theorem 7.1.18. None of the implications can, in general, be inverted, though Implication 7.1.16 can be inverted for rational homology spheres by Theorem 7.1.5. Implication 7.1.16 cannot always be inverted. This was shown by Eliashberg in [**Eli96**] and we will give his argument for this in Section 7.3 Implication 7.1.17 cannot be inverted. This was originally shown by Honda and the first author in [**EH02b**]. We will prove this in Section 7.5 using an argument of Lisca and Stipsicz [**LS04**].

In [**Ghi05a**], Ghiggini showed that there are strongly fillable contact structures that are not Stein fillable and so Implication 7.1.15 cannot be reversed. Bowden showed that there are exact but not Stein fillable contact structures in [**Bow12**]. Thus, Implication 7.1.13 cannot be reversed. We will discuss Ghiggini's and Bowden's examples in Section 13.2.

When discussing symplectic fillings, one sometimes hears about *semi-fillings*. For example, one might say (X, ω) is a *strong symplectic semi-filling* of a contact manifold (M, ξ) to indicate that (X, ω) has convex boundary, but M is, possibly, only one component of the boundary. So the word "semi" allows for the symplectic filling to have more than one boundary component. This will be further discussed in Section 12.4 where we will see that for contact structures supported by planar open books (the terminology will be defined in that section) any symplectic semi-filling is actually a symplectic filling (that is, the boundary must be connected). A famous early example of this is McDuff's proof, following Gromov, that any symplectic filling of the standard tight contact structure on S^3 has connected boundary.

Theorem 7.1.19 (Gromov 1984, [**Gro85**] and McDuff 1991, [**McD91**])**.** *If (X, ω) is a symplectic semi-filling of (S^3, ξ_{std}), then X has connected boundary.*

We end this section by discussing the opposite of a symplectic filling. A symplectic manifold (X, ω) is said to have *concave boundary* if there is a vector field v defined near ∂X such that

$$\mathcal{L}_v \omega = \omega$$

and v points into X along ∂X. We say that a compact (X, ω) is a *symplectic cap* for the contact manifold (M, ξ) if

- (X, ω) has concave boundary where v is the vector field showing the boundary is concave,
- $\partial X = -M$ (where $-M$ is M with its opposite orientation), and
- $\iota_v \omega$ is a contact from for ξ.

See Figure 7.1.2. The condition that $\partial X = -M$ might seem strange at first, but we notice that since v is pointing into X along ∂X, the contact 1-form $\iota_v \omega$ is a *negative* contact

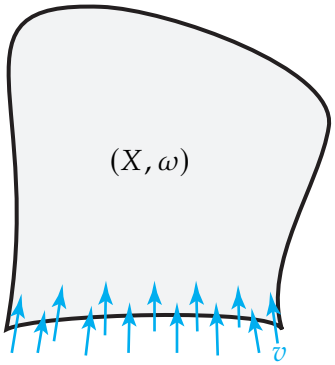

Figure 7.1.2. A symplectic manifold (X, ω) with cocave boundary.

form on ∂X (recall ∂X is oriented using the standard "outward normal first" rule from differential topology, [**Lee13**, Chapter 15]) and since we always are interested in positive contact structures, $\ker \iota_v \omega$ is a *positive* contact structure on $M = -\partial X$. (Recall our discussion about positive and negative contact structures on Page 10.)

Example 7.1.20. We will see in Chapter 13 that all contact 3-manifolds have many symplectic caps, but we give many simple examples of symplectic caps for (S^3, ξ_{std}) here. Just as there is a Darboux theorem for contact manifolds, see Theorem 1.2.2, there is a Darboux theorem for symplectic manifolds [**MS95**, Theorem 3.2.2]. Specifically, if (X, ω) is any symplectic $2n$-manifold, then any point $x \in X$ has a neighborhood U that is symplectomorphic to an open ball about the origin in $\mathbb{R}^{2n}$ with its standard symplectic form $\omega = \sum_{i=1}^{n} dx_i \wedge dy_i$. Now let X° be the result of removing a small open ball about the origin in U from X. Since the radial vector field on $\mathbb{R}^{2n}$ is a symplectic dilation and transverse to round spheres about the origin, we see that if X is compact and without boundary, then $(X^\circ, \omega|_{X^\circ})$ is a symplectic cap for (S^3, ξ_{std}).

Remark 7.1.21. One can also talk about a *weak symplectic cap*, but they do not currently have practical applications, so they have not been studied. We will reserve the term "symplectic cap" as we defined above, but sometimes say "strong symplectic cap" to emphasize that the cap has a concave boundary.

7.2. Toric manifolds and building symplectic fillings and caps

We will now discuss a convenient way to describe some symplectic manifolds and, in particular, for our purposes, construct some symplectic fillings and symplectic caps that will be useful later in the book. Specifically, we will discuss toric manifolds. We will just discuss the basics here, but refer the interested reader to Symington's excellent discussion of toric geometry in dimension 4, [**Sym03**].

We begin with a simple example of a symplectic manifold. Consider $X = T^2 \times \mathbb{R}^2$ equipped with the symplectic form

$$\omega = dp_1 \wedge dq_1 + dp_2 \wedge dq_2,$$

where (q_1, q_2) are angular coordinates on T_2 and (p_1, p_2) are coordinates on $\mathbb{R}^2$. (Notice that this is just the standard symplectic structure on T^*T^2.) We have the projection map

$$\pi : X \to \mathbb{R}^2.$$

Each fiber of this trivial bundle is a Lagrangian torus. In general, a *Lagrangian submanifold* L of a symplectic manifold is a submanifold of half the dimension of the symplectic manifold on which the symplectic form restricts to be the zero form.

We will now build more interesting manifolds by considering quotients of subspaces of X. Let l be a line in $\mathbb{R}^2$ with rational slope r/s. Consider $C_l = \pi^{-1}(l)$. Clearly, this is just $T^2 \times \mathbb{R}$, but we now examine ω on C_l. One may easily check that the vector

$$K = r\frac{\partial}{\partial q_1} - s\frac{\partial}{\partial q_2}$$

at any point $x \in C_l$ is in the kernel of $\omega|_{C_l}$. Moreover,

$$S_1 = s\frac{\partial}{\partial p_1} + r\frac{\partial}{\partial p_2} \text{ and } S_2 = s\frac{\partial}{\partial q_1} + r\frac{\partial}{\partial q_2}$$

span a symplectic subspace of $T_x C_l$.

Exercise 7.2.1. The flow of the vector field K generates a circle action on C_l. Show that the quotient of C_l by this action is $S^1 \times \mathbb{R}$.
Hint: It is easy to check that the quotient of any torus fiber in C_l by this action is a circle.

Exercise 7.2.2. Show that ω induces a symplectic form on the quotient space $S^1 \times \mathbb{R}$.
Hint: The quotient map sends the span of S_1 and S_2 to a basis for the tangent space of $S^1 \times \mathbb{R}$.

Now consider h_l, which is the half-space in $\mathbb{R}^2$ that is on one side or the other of l (and includes l), and let $H_l = \pi^{-1}(h_l)$ be its preimage in X.

Exercise 7.2.3. Show that the quotient of H_l by the action of S^1 on C_l is a symplectic manifold diffeomorphic to $S^1 \times \mathbb{R}^3$.
Hint: Let $f\colon\ : X \to \mathbb{R}$ be the composition of π with a linear map on $\mathbb{R}^2$ that has l as its zero set and $H_l = f^{-1}([0, \infty))$. Notice that C_l is the preimage of the regular value 0. We also have an S^1 action on H_l that is given by extending the one above from C_l to all of H_l. Now let $\widehat{f}\colon X \times \mathbb{C} \to \mathbb{R}$ be the funtion $\widehat{f}(x, z) = f(x) + |z|^2$. Show that $\widehat{f}^{-1}([0, \infty)) = (f^{-1}(0) \times S^1) \cup f^{-1}(0)$. Extend the S^1 action above to this manifold by the diagonal action on the first part. Show that the qotient of $\widehat{f}^{-1}([0, \infty))$ by the S^1 action is $f^{-1}((0, \infty)) \cup (f^{-1}(0)/S^1)$ which in turn is the quotient of H_l by the S^1 action on C_l.

The construction in this exercise is a simple case of a (positive) *symplectic cut*. For the more general symplectic cut, see [**Ler95**].

We now investigate the region R between two rays, as shown in Figure 7.2.3 (ignore the blue arc for now). Let X_R be $\pi^{-1}(R)$ after one quotients C_{l_i} by the action on C_{l_i} by the

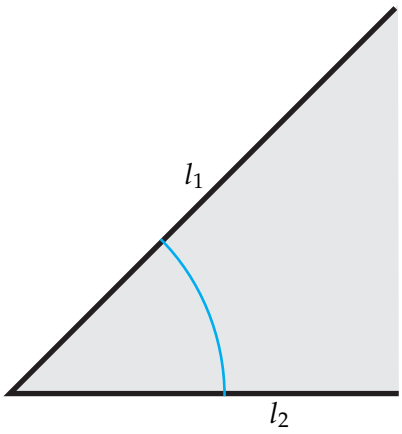

Figure 7.2.3. A region R in $\mathbb{R}^2$ between two rays l_1 and l_2.

action discussed above.

Lemma 7.2.4. *Translate R so that the intersection of l_1 and l_2 is at the origin. If l_1 and l_2 are spanned by integral vectors, then X_R is a manifold if and only if the vectors form an integral basis for $\mathbb{Z}^2$.*

Remark 7.2.5. The proof of this lemma will show that when X_R is a manifold, it will be diffeomorphic to $\mathbb{R}^4$.

Proof. One should try to prove this directly in terms of the quotient space involved, but we give a simple workaround. We first notice that from our discussion above, X_R is a manifold at any point except possibly the point above the vertex where the rays l_1 and l_2 meet. Thus we only need to prove that that point has a neighborhood that is Euclidean.

We claim that X_R is a manifold for the region in Figure 7.2.3, where l_1 is spanned by the vector $\begin{bmatrix}1 & 1\end{bmatrix}^t$ and l_2 is spanned by $\begin{bmatrix}1 & 0\end{bmatrix}^t$. Once this is done, we will see that X_R is a manifold for any l_1 and l_2 spanned by integral vectors that form a basis for $\mathbb{Z}^2$, since there will be a diffeomorphism of X that takes l_1 and l_2 to the lines in Figure 7.2.3. To establish our claim, consider the blue arc in Figure 7.2.3. Let M be the manifold in X_R above the blue arc. We claim that this is S^3. If we see this is true, then it is clear that the compact region cut off from X_R by the blue arc is a cone on S^3 and hence the 4-ball. Thus, the point in X_R above the vertex has a B^4 neighborhood, showing that X_R is indeed a manifold.

If we consider the points in X above the blue arc, before we take any quotients, then we have $[0,1]\times T^2$. If $\{0\}\times T^2$ is above the line l_1, then we need to collapse the circles of slope -1 and in $\{1\}\times T_2$, we will need to collapse the curves of slope 0. In our notation from Section 5.6, this means M is the union of a solid torus with lower meridian -1, which we denoted S_{-1} and a solid torus with upper meridian 0, which we denoted S^0. We will denote this union by S^0_{-1}.

Exercise 7.2.6. Show S^0_{-1} is S^3.

We are left to see that if the integral vectors that span l_1 and l_2 do not form a basis for $\mathbb{Z}^2$, then X_R is not a manifold. As discussed above, the only way that X_R is not a manifold is that the point in X_R above the vertex of $l_1\cup l_2$ does not have a neighborhood that is Euclidean. As above, we can assume that l_2 is spanned by $\begin{bmatrix}1 & 0\end{bmatrix}^t$ and then l_1 will be spanned by $\begin{bmatrix}q & p\end{bmatrix}^t$ for some relatively prime p and q where $p\neq 1$. The manifold M above the analog of the blue arc in R will be $S^0_{-p/q}$.

Exercise 7.2.7. Show $S^0_{-p/q}$ is the lens space $L(p,q)$.

Thus, the neighborhood of the point above the vertex in X_R is a cone on $L(p,q)$ and so that point does not have Euclidean neighborhood. □

We would now like to see when X_R has a symplectic structure. To this end, take any point $\mathbf{q}=(a,b)\in\mathbb{R}^2$ consider the radial vector field based at $\mathbf{q}$

$$v_{\mathbf{q}} = (q_1-a)\frac{\partial}{\partial q_1}+(q_2-b)\frac{\partial}{\partial q_2}.$$

Exercise 7.2.8. Show that this vector field on X dilates the symplectic form ω.

Now consider a curve c in $\mathbb{R}^2$ that is transverse to the radial vector field $v_{\mathbf{q}}$. The manifold $X_c=\pi^{-1}(c)$ is a thickend torus $c\times T^2$ and $\iota_{v_{\mathbf{q}}}\omega = -(q_1-a)\,dp_1-(q_2-b)\,dq_2$ is a contact form on X_c. We notice that, if $\mathbf{q}'$ is a point in c, then the characteristic foliation on $\pi^{-1}(\mathbf{q}')$ is a linear foliation of slope given by minus the reciprocal of the angle of $v_{\mathbf{q}}$ with the positive q_1-axis.

Exercise 7.2.9. If l_1 is a line in $\mathbb{R}^2$ and $v_{\mathbf{q}}$ is tangent to l_1, the $v_{\mathbf{q}}$ induces a vector field on H_l that expands the symplectic form on H_l induced by ω.

We are now ready to see when the manifold X_R above admits a symplectic form.

Lemma 7.2.10. *Let R be the region bounded by two rays l_1 and l_2 that are defined by vectors that form an integral basis for $\mathbb{Z}^2$. The manifold X_R is a symplectic manifold if and only if the angle in R formed by l_1 and l_2 is convex.*

Proof. If the angle is convex, we will use the model given in Figure 7.2.3 for R since there is a symplectomorphism of X taking any other such region to this one.

From our discussion at the beginning of this section, we know that X_R admits a symplectic structure at every point except possibly the point above the vertex of $l_1 \cup l_2$.

Exercise 7.2.11. Consider the radial vector field $v_{\mathbf{q}}$ where $\mathbf{q}$ is the vertex of $l_1 \cup l_2$. If M is the manifold above the blue arc in Figure 7.2.3, then $\iota_{v_{\mathbf{q}}}\omega$ induces the tight contact structure on M.

Exercise 7.2.12. Show that $X_R - \{\mathbf{x}\}$, where $\mathbf{x}$ is the point above the vertex of $l_1 \cup l_2$, is symplectomoprhic to $\mathbb{R}^4 - \{(0,0,0,0)\}$ with its standard symplectic structure.

From the exercises above, we see that the symplectic structure on $X_R - \{\mathbf{x}\}$ clearly extends to X_R. So X_R is a symplectic manifold.

Now consider the case when the angle is not convex.

Exercise 7.2.13. Show that the contact structure induced on M (defined analogously to M in the convex case) is overtwisted.

Given this, the manifold X_R cannot be symplectic since it would give a filling of the contact structure on M, but overtwisted contact structures cannot be fillable by Theorem 1.6.13. □

From our above discussion, we can now form many symplectic manifolds with convex and concave boundaries. We begin by discussing regions bounded by 3 line segments and an arc as shown in Figure 7.2.4. For these to be manifolds, we need the vectors span-

Figure 7.2.4. Two regions in $\mathbb{R}^2$.

ning adjacent arcs to be spanned by vectors that form an integral basis for $\mathbb{Z}^2$, and for them to be symplectic, we need that each angle between two edges is convex. After applying a diffeomorphism to X we can assume that the first edge is spanned by $\begin{bmatrix}0 & 1\end{bmatrix}^t$, the second edge is spanned by $\begin{bmatrix}1 & 0\end{bmatrix}^t$, and the third is spanned by $\begin{bmatrix}n & 1\end{bmatrix}^t$. Then the arc c, shown in blue in the figure, connects the endpoints of the union of the arcs. Denote the region just described by R_n.

Exercise 7.2.14. Show that the symplectic manifold X_{R_n} is diffeomorphic to a disk bundle over S^2 with Euler number $-n$. (See Appendix A for the Euler number of disk bundles

over surfaces.)
Hint: The middle arc is clearly an S^2. If one chooses a point in the middle arc and a line segment connecting it to the blue arc, show that the part of X_{R_n} above the line segment is $S^1 \times D^2$ and that the interior of the region is "foliated" by such arcs. From this, one can conclude that X_{R_n} is a disk bundle over the sphere. To determine the Euler number, consider the Euler number of the boundary (which is an S^1-bundle over S^2 and has the same Euler number). From above we know ∂X_{R_n} is $L(n, 1)$.

Exercise 7.2.15. Given R_n for $n \neq 0$, show that if there is a radial vector field $v_{\mathbf{q}}$ that is transverse to the blue arc and tangent to the first and third edges of R_n. If $n > 0$, show that X_{R_n} has convex boundary and if $n < 0$ then it has concave boundary.

Now consider a region R bounded by line segments $l_1, \ldots, l_n$ and an arc c, such that each line segment intersects only the line segments with adjacent indices and only in their endpoints. See Figure 7.2.5 for the case when $n = 3$. For X_R to be a manifold, two adjacent edges must be spanned by integral vectors that form a basis for $\mathbb{Z}^2$, and for X_R to have a symplectic structure induced from X, all the corners must be convex. To identify

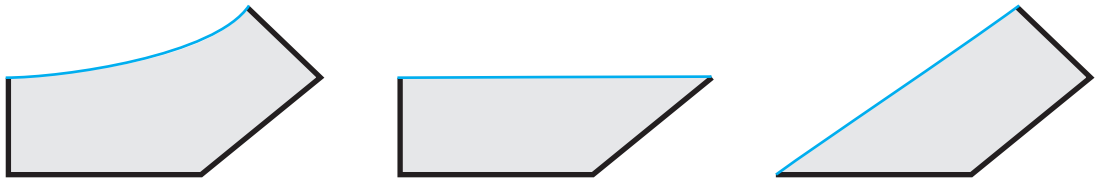

Figure 7.2.5. Plumbing two disk bundles.

X_R we need to define the plumbing of disk bundles. Given two disk bundles E_1 and E_2 over surfaces S_1 and S_2 we can choose disks D_i in S_i, then the bundle restricted to D_i is trivial. That is $E_i|_{D_i} = D_i \times D^2$. The result of identifying $E_1|_{D_1}$ with $E_2|_{D_2}$ by interchanging the disk factors, is called *plumbing* E_1 and E_2. Figure 7.2.6 shows a handle presentation for the result of plumbing disk bundles over spheres.

Figure 7.2.6. Plumbing disk bundles over spheres.

Exercise 7.2.16. Show that X_R as described above is the result of plumbing $n - 2$ disk bundles over spheres together.
Hint: See Figure 7.2.5 where the two disk bundles that are plumbed to obtain X_R are shown in the middle and on the right.

Exercise 7.2.17. Show that if X_R is the result of plumbing disk bundles with negative Euler number, then X_R has a convex boundary. If one of the disk bundles has a positive Euler number, then show X_R can be taken to have concave boundary.

Lemma 7.2.18. *Any lens space admits a contact structure with a symplectic filling and a symplectic cap coming from the construction above.*

Exercise 7.2.19. Prove this lemma.
Hint: Recall our discussion of Rolfsen twists from Section 1.5.1.

We note that by changing the lengths of the line segments in R one can construct many different symplectic structures on X_R, but this will not affect the contact geometry of ∂X_R.

7.3. Symplectic cut-and-paste

In this section, we will see that one may use strong symplectic fillings and symplectic caps to perform symplectic cut-and-paste operations. We will then use this construction to prove that weakly symplectically fillable contact structures need not be strongly symplectically fillable, and also prove that the important smooth 4-dimensional construction of rational blowdowns can be done in the symplectic category.

7.3.1. A symplectic cut-and-paste construction. The main construction in this section is the following gluing result.

Theorem 7.3.1. *Suppose that (X_1, ω_1) has a strongly convex boundary component M_1 and (X_2, ω_2) has a strongly concave boundary component M_2. If there is a diffeomorphism $f\colon M_1 \to M_2$ that is isotopic to a contactomorphism of the contact structure induced on M_1 by ω_1 to the contact structure induced on M_2 by ω_2, then there is a symplectic structure ω on the result of gluing X_1 to X_2 using f:*

$$X = X_1 \cup_f X_2 = \frac{(X_1 \coprod X_2)}{\{(x \in M_1) \sim (f(x) \in M_2)\}}.$$

The manifold X will consist of 3 pieces, X_1, X_2, and a product $U = M_1 \times [0,1]$. One can arrange that ω agrees with ω_1 on X_1 and a constant rescaling of ω_2 on X_2.

Remark 7.3.2. Clearly, after a constant rescaling ω from the theorem, we can assume that ω agrees with ω_2 on X_2 and a constant rescaling of ω_1 on X_1.

A weaker version of the theorem can be paraphrased by saying that a strong symplectic filling and and strong symplectic cap can be glued together by a contactomorphism of their boundaries.

For the proof of this theorem, we will need to use the *symplectization* of a contact manifold. Given a contact manifold (M, ξ) consider the subset of the cotangent bundle consisting of forms that vanish on ξ:

$$\{\beta \in T_p^*M : \beta(\xi_p) = 0\}.$$

One may easily check that there are two components to this set. Recall ξ is oriented, and we call a vector $v \in T_pM$ positive with respect to ξ if it is positively transverse to ξ. We denote by $\mathrm{Symp}(\xi)$ the component of the above set consisting of elements that evaluate positively on vectors that are positive with respect to ξ. Recall that in Section 1.8.4 we defined the Liouville form λ on T^*M that was the primitive for the canonical symplectic form $d\lambda$ on T^*M.

Exercise 7.3.3. Show that $d\lambda$ is a symplectic form on $\mathrm{Symp}(\xi)$.

We call $(\mathrm{Symp}(\xi), d\lambda)$ the *symplectization of* (M, ξ). This is a nice description because it does not involve making any choices, but we have another description of the symplectization if we choose a contact form for ξ. Specifically, let α be a contact form for ξ and consider the map

$$F\colon (0,\infty) \times M \to T^*M\colon (t, p) \mapsto t\alpha(p).$$

Exercise 7.3.4. Show that the image of F is $\mathrm{Symp}(\xi)$ and F induces a symplectomorphism from $((0,\infty) \times M, d(t\alpha))$ to $(\mathrm{Symp}(\xi), d\lambda)$.
Hint: Recall properties of λ discussed in Section 1.8.4.

Given this exercise, one frequently see the symplectization of (M, ξ) defined to be $((0,\infty) \times M, d(t\alpha))$.

Exercise 7.3.5. If α and α' are two contact forms for ξ show directly that $((0,\infty)\times M, d(t\alpha))$ is symplectomorphic to $((0,\infty) \times M, d(t\alpha'))$.
Hint: Recall there is some positive function $h\colon M \to \mathbb{R}$ such that $\alpha' = h\alpha$.

An important property of the symplectization is that there is a dilating vector field.

Exercise 7.3.6. Show that the vector field $v = t\frac{\partial}{\partial t}$ is a symplectic dilation of $((0,\infty) \times M, d(t\alpha))$.

For the sake of completeness, we mention one last way that people think about the symplectization.

Exercise 7.3.7. Show that $(\mathbb{R} \times M, d(e^t\alpha))$ is symplectomorphic to $((0,\infty) \times M, d(t\alpha))$. Moreover, show that the vector field $v = \frac{\partial}{\partial t}$ is a symplectic dilation of $(\mathbb{R} \times M, d(e^t\alpha))$.

We note in Figure 7.3.7, the symplectization is usually drawn so that it is expanding as you move up and contracting as you move down. This is because of the symplectic dilation v expands volume as you move in the positive t direction.

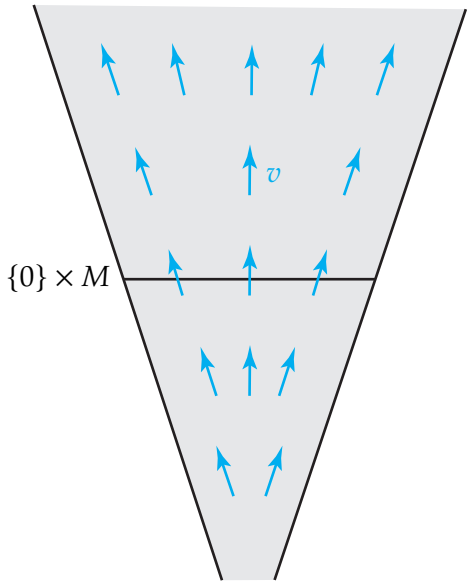

Figure 7.3.7. The symplectization $(\mathbb{R} \times M, d(e^t \alpha))$ and the symplectic dilation v.

Proof of Theorem 7.3.1. Since M_1 is a convex boundary component of (X_1, ω_1), there is a symplectic dilation v_1 of ω_1 defined near M_1 and pointing out of X_1. Similarly, there is a symplectic dilation v_2 of ω_2 defined near the boundary component M_2 of X_2. Let $\alpha_i = \iota_{v_i} \omega_i$.

Consider the symplectization $((0, \infty) \times M_1, d(t\alpha_1))$.

Exercise 7.3.8. Find an open set U containing M_1 in X_1 that is symplectomorphic to $U' = [1, 1 - \epsilon) \times M_1$ in $(0, \infty) \times M_1$ for $\epsilon > 0$ sufficiently small.
Hint: Extend the identity map from $M_1 \subset \partial X_1$ to $\{1\} \times M_1 \subset \mathbb{R} \times M_1$ by the negative flow of v_1 on X_1 and the negative flow of $t \frac{\partial}{\partial t}$ on $(0, \infty) \times M_1$. See Figure 7.3.8.

Now, since $f \colon M_1 \to M_2$ is isotopic to a contactomorphism, we assume that we have performed the isotopy so that it is a contactomorphism. (Note that this does not change X as gluing manifolds via isotopic diffeomorphisms of the boundary results in diffeomorphic manifolds.) Thus, $f^* \alpha_2$ is also a contact form for $\xi_1 = \ker \alpha_1$ and we must have some positive function $h \colon M_1 \to \mathbb{R}$ such that $f^* \alpha_2 = h \alpha_1$. Notice that we can scale ω_2 by a large constant (which rescales α_2 by the same constant) so that h is always bigger than 1. Consider the map

$$F \colon M_2 \to \mathbb{R} \times M_1 \colon x \mapsto (h \circ f^{-1}(x), f^{-1}(x)).$$

We can compute the pull-back

$$F^*(t\alpha_1) = (h \circ f^{-1}(x))(f^{-1})^* \alpha_1 = \alpha_2,$$

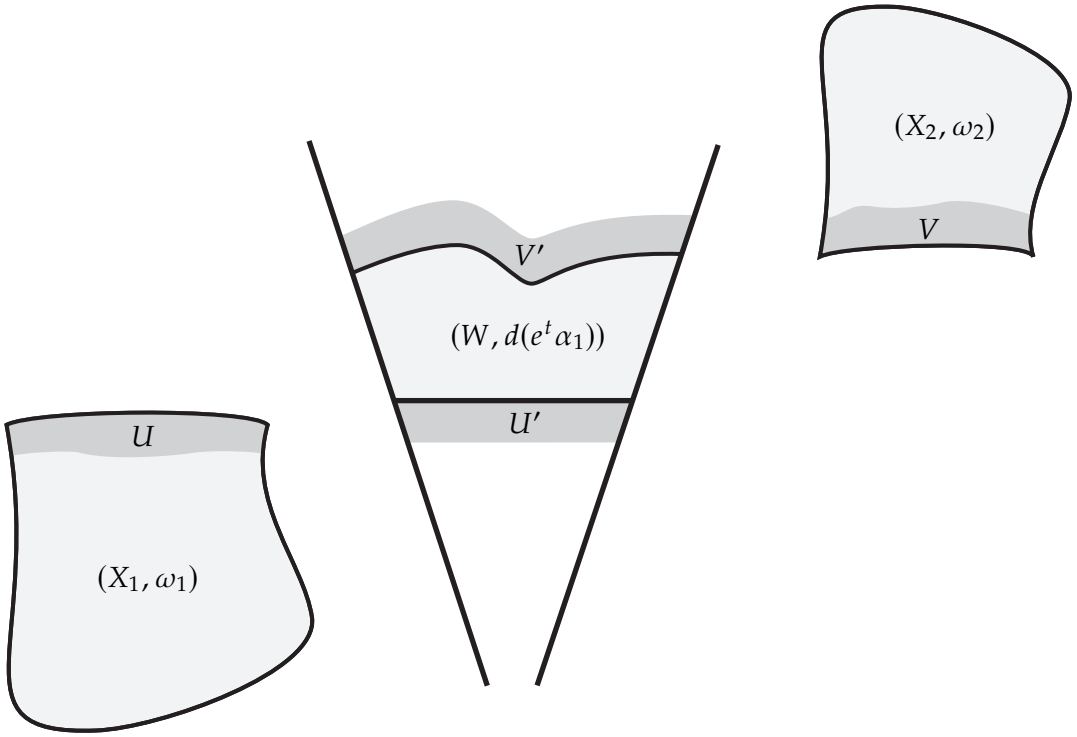

Figure 7.3.8. The pieces used to construct a symplectic form on X.

where the last equality follows by applying the pull-back by f^{-1} to $f^*\alpha_2 = h\alpha_1$.

Since we chose h to be larger than 1 everywhere we see that $g(x) = h \circ f^{-1}(x) > 1$ for all x. Thus, the image of F is disjoint from the set $\{1\} \times M_1$.

Exercise 7.3.9. Find an open set V containing M_2 in X_2 that is symplectomorphic to $V' = \{(t, x) \in (0, \infty) \times M_1 \colon\ g(x) \leq t < g(x) + \epsilon\}$ for $\epsilon > 0$ small enough.
Hint: Extend the map F using the flow of v_2 on X_2 and of $t\frac{\partial}{\partial t}$ on $\mathbb{R} \times M_1$.

Finally, let $W = \{(t, x) \in (0, \infty) \times M_1 \colon\ 1 - \epsilon < t < g(x) + \epsilon\}$. We can glue X_1 to W using the symplectomorphism from the first exercise and W to X_2 using the symplectomorphism in the second exercise, to obtain a symplectic manifold diffeomorphic to X whose properties are as claimed in the theorem. □

7.3.2. Weakly but not strongly fillable contact structures. As a first application of our gluing theorem, we prove that there are weakly fillable contact structures that are not strongly fillable. To this end, consider the unit disc bundle in the cotangent bundle of T^2

$$U^*T^2 = \{\beta \in T^*T^2 \colon\ \|\beta\| \leq 1\}$$

where the length is measured with respect to some Riemannian metric on T^2. As we noted in Example 7.1.13 U^*T^2 together with the Liouville form λ on T^*T^2 is a Liouville

domain and, in particular, a strong symplectic filling of its boundary (T^3, ξ), where $\xi = \ker \lambda|_{\partial U^*T^2}$.

In Section 5.8, we classified all tight contact structures on T^3. According to Theorem 5.8.1 the contact structures

$$\xi_n = \ker(\cos(2\pi nz)\, dx + \sin(2\pi nz)\, dy).$$

for $n \in \mathbb{Z}_{\geq 0}$ constitute all tight contact structures on T^3, up to contactomorphism.

Exercise 7.3.10. Show that the contact structure ξ on $T^3 = \partial U^*T^2$ is ξ_1. Moreover, show that the fiber direction in ∂U^*T^2 corresponds to the z coordinate in the definition of ξ_1 from Section 5.8.

Exercise 7.3.11. Let $\pi_n \colon T^3 \to T^3$ be the n-fold covering map that restricts to the n-fold cover of each fiber in $T^3 = \partial U^*T^2$. Show that $\xi_n = (\pi_n)^*\xi_1$.

We now consider another description of ξ_n. Consider the forms

$$\alpha_n^{s,t} = s\, dz + t(\cos(2\pi nz)\, dx + \sin(2\pi nz)\, dy).$$

For any $s \geq 0$ and any $t > 0$, this is a positive contact form on T^3. Of course, $\alpha_n^{0,1} = \alpha_n$, and it defines the contact structures ξ_n. Thus ξ_n is contact isotopic to $\ker \alpha_n^{1,1}$ and we find a further contact isotopy to $\xi_n^\epsilon = \ker \alpha_n^{1,\epsilon}$ for any small $\epsilon > 0$. Notice that as $\epsilon > 0$ approaches 0, the contact planes ξ_n^ϵ approach the tangent planes to the tori $T^2 \times \{z\}$ for any fixed $z \in S^1$.

If we let $X = T^2 \times D^2$ with the symplectic from $\omega = dx \wedge dy + r\, dr \wedge d\theta$, where x and y are angular coordinates on T^2 and (r, θ) are polar coodinates on D^2, then for small ϵ it is clear that (X, ω) is a weak symplectic filling of ξ_n^ϵ. We have proven the following lemma.

Lemma 7.3.12. *The contact structure ξ_1 on T^3 is strongly symplectically filled by $(U^*T^2, d\lambda)$ and ξ_n , for $n \geq 1$, is weakly filled by $(T^2 \times D^2, \omega)$, for ω above.*

We are now ready for the main result about the fillings of ξ_n.

Theorem 7.3.13 (Eliashberg 1996, [**Eli96**])**.** *For $n \geq 2$, the contact manifold (T^3, ξ_n) is not strongly fillable by any symplectic manifold.*

Proof. Consider the symplectic structure $\omega = dx \wedge dy$ on $\mathbb{R}^2$. It is easy to see that the unit circle S^1 in $\mathbb{R}^2$ is Lagrangian.

Exercise 7.3.14. Show that $T^2 = S^1 \times S^1$ in $R^4 = \mathbb{R}^2 \times \mathbb{R}^2$ (where each S^1 is the unit circle in the corresponding $\mathbb{R}^2$) is Lagrangian with respect to the product symplectic form Ω on $\mathbb{R}^2 \times \mathbb{R}^2$. Or more generally, show that the product of any two Lagrangian submanifolds is a Lagrangian submanifold of the product symplectic manifold.

We now consider the symplectic manifold (B^4, Ω) in $(\mathbb{R}^4, \Omega)$, where B^4 is a ball of radius larger than 1 centered at the origin. Notice that the Lagrangian torus T^2 from the exercise is contained in B^4. Notice that ∂B^4 is convex. In fact, Ω is exact, so (B^4, Ω) is an exact symplectic filling of the standard contact structure on S^3.

Just as we proved that Legendrian knots have standard neighborhoods in Theorem 1.2.6, it is also true that any two diffeomorphic Lagrangian submanifolds of symplectic manifolds have symplectomorphic neighborhoods. The reader is encouraged to try to adapt our proof of Theorem 1.2.6 to establish this, or consult [**MS98**, Theorem 3.4.13]. Thus, there is a neighborhood U of T^2 in (B^4, Ω) that it symplectomorphic to the rescaling $\epsilon U^* T^2$ of $U^* T^2$.

Let $X = \overline{B^4 - U}$. Clearly $\partial X = S^3 \cup T^3$, with S^3 being a convex boundary component of X and T^3 being a concave boundary component (since T^3 is a convex boundary of U). Moreover, the induced contact structure on T^3 is ξ_1 and the induced contact structure on S^3 is the unique tight contact structure.

Exercise 7.3.15. Show that $\pi_1(X) \cong \mathbb{Z}$ and S^1 fiber in $T^3 = \partial(\epsilon U^* T^2)$ generates the fundamental group.

We can now consider the n-fold cover of X: $p_n \colon X_n \to X$.

Exercise 7.3.16. Show that ∂X_n consists of T^3 and n disjoint S^3.
Hint: Since S^3 is simply connected, $p_n(\partial B^4)$ must be the trivial n-fold cover of S^3.

Since we can lift the dilating vector fields near the boundary of X to X_n, we see that the T^3 component of ∂X_n is concave while the S^3 components are convex.

Exercise 7.3.17. Show the contact structure on the concave boundary T^3 of X_n is ξ_n and the contact structure on the convex boundary components of X_n is the standard tight contact structure on S^3.

Now if there was a strong symplectic filling (W, ω') of (T^3, ξ_n) for $n > 1$, then we could use Theorem 7.3.1 to glue X_n and W together to obtain a symplectic 4-manifold X_n' with n convex S^3 boundary components. We now recall an amazing theorem of Gromov and McDuff, see Appendix B.

Theorem 7.3.18 (Gromov 1985, [**Gro85**] and McDuff 1991, [**McD91**])**.** *If (X, ω) is a semi-symplectic filling of $(S^3.\xi_{std})$, then X is diffeomorphic to a blowup of B^4.*

Notice that the above theorem says that any filling of the standard tight contact structure on S^3 must have connected boundary. Thus, X_n' cannot exist and there is no strong symplectic filling of (T^3, ξ_n) for $n > 1$. □

We note that the above theorem can be greatly generalized. In Section 13.3, we will discuss a result of Gay [**Gay06**] that shows any contact structure with positive Giroux torsion (see Section 9.3 for the definition of Giroux torsion) cannot be strongly symplectically fillable. As observed when we classified tight contact structures on T^3 in Section 5.8, ξ_n has Giroux torsion $n-1$.

7.3.3. Rational blow-downs. In the late 1990s, Fintushel and Stern defined an operation on 4-manifolds called a rational blow-down, [**FS97**]. We will define this operation below, but discuss its significance first. We recall that in dimension 4 there are infinite families of homeomorphic but not diffeomorphic manifolds. We call these "exotic" 4-manifolds (technically, one of them is just a smooth manifold and the others are "exotic" copies of it). One of the first standard ways to construct exotic smooth 4-manifolds was to perform "log transforms" [**GS99**] in embedded tori in the 4-manifold. Fintushel and Stern proved that, in many situations, a log transform can be performed by a sequence of standard operations called blow-ups followed by a single rational blow-down. So the rational blow-down generalized log transforms, and it could be used to construct other exotic 4-manifolds too. One could see the exotic nature of the manifolds constructed through this process by seeing the effect of a rational blow-down on the Donaldson invariants of the manifold (nowadays, one more often uses Seiberg-Witten invariants or Heegaard Floer invariants). A natural question arose as to whether or not the rational blow-down could be done in the symplectic category; that is, if one started with a symplectic manifold, could one guarantee the result was also symplectic? It was shown in one case that the rational blow-down could be done in the symplectic category by the first author in [**Etn96**], and then the general case was settled by Symington in [**Sym98**]. Below, we present a combination of these two arguments to prove that the rational blow-down can be done symplectically.

We define two 4-manifolds with boundary. The first, denoted $C(p)$ for any $p \geq 2$, is the plumbing of disk bundles over S^2 shown in Figure 7.3.9. It is a simple exercise to see

Figure 7.3.9. The manifold $C(p)$. There are $p-2$, -2 spheres in the plumbing.

that $\partial C(p)$ is the lens space $L(p^2, p-1)$.

The second manifold, denoted $B(p)$, is shown in Figure 7.3.10.

Exercise 7.3.19. Show that $\partial B(p)$ is diffeomorphic to $L(p^2, p-1)$.

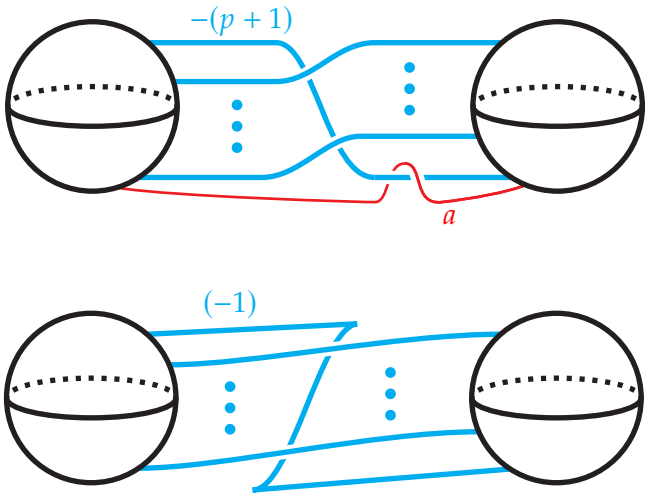

Figure 7.3.10. A smooth description of the manifold $B(p)$ is shown on the top (the curve a will be used later, but is not part of the surgery diagram). There are p strands going over the 1-handle. On the bottom, we see a Stein description of $B(p)$. The framing shown is a contact (-1)-framing, so it is a smooth $-(p+1)$ framing.

Given a 4-manifold X that contains $C(p)$, a *rational blowdown* of X is the result of removing $C(p)$ from X and gluing in $B(p)$.

Exercise 7.3.20. Show that this is well-defined. Specifically, show that the choice of identification of $\partial B(p)$ with $\partial C(p)$ does not affect the diffeomorphism type of the rational blowdown.
Hint: Diffeomorphisms of lens spaces are well-understood, see [**Bon83**]. Show any diffeomorphism of $L(p^2, p-1)$ extends over $B(p)$.

The main result we would like to establish is the following.

Theorem 7.3.21 (Symington 1998, [**Sym98**]). *If (X, ω) is a symplectic 4-manifold and there are symplectic spheres $S_0, \dots, S_{p-2}$ in X such that S_0 has self intersection $-(p+2)$, the other spheres have self-intersection -2 and each sphere only intersects the spheres with adjacent indicies (that is the spheres intersect according to the plumbing diagram in Figure 7.3.9), then a neighborhood of the spheres can be chosen to be $C(p)$ and one may perform the rational blowdown so that the result is a symplectic manifold.*

Here we only present the proof of Symington's theorem, but note that similar arguments also work for generalization of rational blow-downs. See [**PS14**].

Proof. We note that we can use the constructions of toric manifolds in Section 7.2 to find a region R in $\mathbb{R}^2$ so that X_R is diffeomorphic to $C(p)$.

Exercise 7.3.22. By adjusting the lengths of the line segments that define R, show that we may arrange that the areas of the spheres in X_R agree with the symplectic areas of the sphere S_i in X.

We can now take a diffeomorphism from the union of spheres in X to those in X_R that restricts to a symplectomorphism on each sphere. We can further extend this to a diffeomorphism of a neighborhood of the spheres in X to a neighborhood of the spheres in X_R. There is a symplectic version of Theorem 1.2.1 that uses the Moser trick, similar to the one we used in the proof Gray's theorem (Theorem 1.2.10), to prove that the above diffeomorphism can be isotoped to be a symplectomorphism in a neighborhood of the spheres. See [**MS95**, Chapter 3]. Now observe that in any neighborhood of the spheres in X_R, one can find a smaller neighborhood N of the spheres that has a convex boundary.

If we remove the interior of N from X, we will have a manifold X' with concave boundary. Notice that the bottom diagram in Figure 7.3.10 shows that $B(p)$ is a symplectic manifold with convex boundary. So, according to our gluing theorem, Theorem 7.3.1, we can glue X' to $B(p)$ to obtain a closed symplectic manifold if the contact structures on ∂N and $\partial B(p)$ are contactomorphic.

We are left to show that ∂N and $\partial B(p)$, with the obvious contact structures are contactomorphic. But since we have a classification of tight contact structures on the lens space $L(p^2, p-1)$, this should be straightforward. Let the contact structure on the boundary of N be denoted by ξ_1 and the one on the boundary of $\partial B(p)$ be denoted by ξ_2. According to the classification of tight contact structures in Theorem 5.7.2, we know that they will be isotopic if their Γ-invariants are the same. We recall from Section 1.5.4, where we defined the Γ-invariant, that the Γ-invariant of the contact structure is determined by the Euler class of the contact structure if p is odd. So we begin with the slightly simpler computation of the Euler class.

To this end, we begin with $\partial N = \partial C(p)$. Since there are no 1-handles in $C(p)$ we know that the CW-homology chain groups are generated by the cores of the 2-handles $c_0, \cdots, c_{p-2}$ (where c_0 is the 2-handle with framing $-(p+2)$ and the rest have framing -2). Or more precisely, the homology classes are represented by the core of the handle union a disk, each attaching sphere bounds (that is, the spheres S_i in each of the disk bundles). If the reader is unfamiliar with the algebraic topology of handlebodies, we refer them to [**GS99**, Page 111]. We write

$$C_2(N;\mathbb{Z}) = \mathbb{Z}\langle c_0, \cdots, c_{p-2}\rangle.$$

Thus, the co-chain group is generated by the duals c_i^* of the c_i. Finally, we note that the relative homology chain group is generated by the co-cores $k_0, \cdots, k_{p-2}$ of the 2-handles and the Poincaré dual of c_i^* is k_i. We can now use the adjunction formula in Symplectic

geometry [MS98] to compute the first Chern class $c_1(N)$. The adjunction formula gives

$$\langle c_1(N), S_i \rangle = \chi(S_i) + S_i \cdot S_i,$$

where $S_i \cdot S_i$ is the self-intersection of S_i with itself and $\chi(S_i)$ is the Euler characteristic of S_i. Thus we see

$$\langle c_1(N), S_i \rangle = \begin{cases} -p & \text{for } i = 0 \\ 0 & \text{for } i \neq 0 \end{cases}.$$

That is the Poincaré dual of $c_1(N)$ is given by $-pk_0$. Now the Euler class of ξ_1 is simply the restriction of $c_1(N)$ to the boundary, and the Poincaré dual wil be the image of $-pk_0$ under the connecting map in the long exact sequence of the pair $(N, \partial N)$. Thus the Poincaré dual of $e(\xi)$ is $PD(e(\xi_1)) = -p[a]$, where a is the meridian to the attaching sphere of the handle h_0 and is a generator of $H_1(L(p^2, p-1))$. (Here we use brackets to indicate the homology class of the curve.)

We now turn to ξ_2. Theorem 6.2.9 gives a formula for $e(\xi_2)$. If we let m be the meridian to the attaching sphere of the 2-handle in Figure 7.3.10, then the Poincaré dual of $e(\xi_2) = -[m]$. Here we have chosen the orientation on the Legendrian attaching sphere so that its rotation number is -1.

Exercise 7.3.23. Show that under a diffeomorphism from $\partial C(p)$ to $\partial B(p)$, the curve a maps to the curve shown in Figure 7.3.10.

Exercise 7.3.24. In $H_1(L(p^2, p-1))$ show that $-[m]$ is the same as $-p[a]$.

Thus, we see that the Euler classes of ξ_1 and ξ_2 are the same, and if p is odd, the contact structures are isotopic.

Now, when p is even, we need to compute the Γ-invariant. We will use the formula in Theorem 6.2.10 for this. We will need to represent spin structures on M using characteristic sub-links as discussed in Appendix 1.4. For $C(P)$, we note that there is a unique way we can Legendrian realize the link if Figure 7.3.9 so that Legendrian surgery on it will give a symplectic manifold with $c_1(C(p))$ computed above. Specifically, the first unknot in the figure will have tb $= -p-1$ and rotation number $-p$, while all the others will have tb $= -1$ and rotation number 0. Denote the components of the link by $L_1, \cdots, L_{p-1}$ so that the indices are increasing from left to right. There are two spin structures on $L(p^2, p-1)$ given by the characteristic sub-links $\emptyset$ and $\{L_1, \cdots, L_{p-1}\}$. Evaluating Γ on one of these is enough to determine Γ. We choose the spin structure $\mathfrak{s}$ corresponding to the empty characteristic sub-link. This spin structure is characterized by the fact that it will extend over a 2-handle attached to a with even framing. We have

$$\Gamma(\xi_1, \mathfrak{s}) = \frac{1}{2}\left(\sum_{i=1}^{n} \text{rot}(L_i)[\mu_i] + \sum_{i \in J} (M\mathbb{m})_i\right),$$

where J is the indices on the components in the characteristic sub-link. Thus, in our case, we have

$$\Gamma(\xi_1, \mathfrak{s}) = -\frac{1}{2}p[a],$$

recall that a is the meridian to the $-(p+1)$-framed unknot in Figure 7.3.9

We now turn to ξ_2 on the boundary of $B(p)$. To use the formula above for Γ, we need to turn the Weinstein 1-handle into a contact (+1)-surgery on the maximal Thurston-Bennequin invariant unknot as discussed in Lemma 6.2.8.

Exercise 7.3.25. In an exercise above, it was shown that the diffeomorphism from $\partial C(p)$ to $\partial B(p)$ sends a to the curve a in Figure 7.3.10. Show that this diffeomorphism preserves the parity of a framing on a.

From this exercise, we see that the spin structure $\mathfrak{s}$ on $\partial B(p)$ will extend over a handle attached to a with odd framing. Thus, this spin structure corresponds to the characteristic sub-link $\{K_2\}$ where K_1 is the unknot with tb $= -1$ coming from the 1-handle and K_2 is the other component of the link. If we let μ_i be the meridian to K_i then we see that

$$\Gamma(\xi_2, \mathfrak{s}) = \frac{1}{2}([\mu_2] - (p+1)[\mu_2] - p[\mu_1]).$$

Recall from above that $[\mu_2] = p[a]$ (above μ_2 was called m).

Exercise 7.3.26. Show that $[\mu_1] = (p+1)[a]$

From the above, we see that $\Gamma(\xi_2, \mathfrak{s}) = \frac{1}{2}(-p^2[a] - p(p+1)[a]) = -\frac{1}{2}p[a] - p^2[a]$. But since $H_1(L(p^2, p-1)) \cong \mathbb{Z}/p^2\mathbb{Z}$ we see that the Γ invariant of ξ_2 agrees with that of ξ_1 and hence they are isotopic. □

Remark 7.3.27. Symington's proof of the above theorem in [**Sym98**] did not use the classification of tight contact structures on lens spaces or the Γ-invariant, but instead gave a direct argument using toric geometry — as discussed above — and almost toric geometry — a generalization of toric geometry that we do not cover here. Another proof of this theorem could be done by directly proving that ξ_1 and ξ_2 are universally tight contact structures and then recalling that (up to orientation on the plane fields) there is only one of these on any lens space (there are actually two up to isotopy, but they differ by reversing the orientation on one of the plane field). With this observation, we can now employ the gluing theorem to build the symplectic structure on the rational blowdown.

7.4. Symplectic cobordisms

We will now study Weinstein handle attachments. To this end, we will begin with a simple observation. For this observation, we recall that a linear subspace L of a symplectic vector space (V, ω) is called *isotropic* if $\omega|_L$ is the zero 2-form.

Exercise 7.4.1. Show that an isotropic subspace of a symplectic vector space of dimension $2n$ has dimension at most n.
Hint: Consider the symplectic orthogonal $L^{\perp_\omega} = \{w \in V : \omega(w,u) = 0 \text{ for all } u \in L\}$. Show that $\dim(L) + \dim(L^{\perp_\omega}) = \dim V$ and then note that if L is isotopic then $L \subset L^{\perp_\omega}$.

Lemma 7.4.2. *Let v be a dilating vector field for the symplectic form ω on X. Let $p \in X$ be a non-degenerate 0 of v. The negative eigenspace of v at p is isotropic.*

We recall that if p is a non-degenerate zero of v, then the flow of v has a fixed point at p and the derivative of the flow at p will be a symplectic automorphism of T_pX. The derivative will split the tangent space into a positive eigenspace and a negative eigenspace.

Proof. Let $\phi_t \colon X \to X$ be the time t flow of v. Since $\mathcal{L}_v\omega = \omega$ we see that $\phi^*\omega = e^t\omega$. Thus

$$e^t\omega(w,u) = (\phi_t^*\omega)(w,u) = \omega(d\phi_t(w), d\phi_t(u)).$$

If w, u are in the negative eigenvectors of v at p then $d\phi_t \colon T_pX \to T_pX$ and w and u are being scalled by a number smaller than 1, so $\omega(d\phi_t(w), d\phi_t(u))$ is bounded for $t \geq 0$ and we see that $\omega(w,u)$ must be 0. That is the negative eigenspace must be isotopic. □

Corollary 7.4.3. *If (X, ω, ϕ, v) is a Weinstein manifold, and p is a critical point of ϕ, then the index of p is at most $\frac{1}{2}\dim X$. So in our case, the index is at most 2.*

Exercise 7.4.4. Prove this corollary.
Hint: Relate the index of the critical point p of ϕ with the dimension of the negative eigenspace for a vector field v that is gradient-like for ϕ.

We will now discuss attaching Weinstein handles of index i for $i \leq 2$ to a symplectic manifold. All of these arguments are essentially special cases of Weinstein's original discussion of symplectic handle addition [**Wei91**], though we need to slightly alter the arguments when discussing adding handles to weak symplectic fillings, and our discussion of extending the Morse function on a Weinstein manifold over an attached handle is different as well. See also [**CE12**]. The main theorem is the following.

Theorem 7.4.5. *If (X, ω) is a weak, strong, exact, or Weinstein symplectic filling of a contact manifold, then attaching a Weinstein k-handle, for $k = 0, 1, 2$, will result in a new symplectic manifold that is also a symplectic filling of its boundary of the same type.*

Later, we will see that by definition, a Weinstein 2-handle, has an attaching sphere that is a Legendrian knot in ∂X.

This is an immediate corollary of Lemmas 7.4.7, 7.4.16, and 7.4.27. The theorem is also true for Stein manifolds, but is beyond the scope of this book.

7.4.1. Index 0 Weinstein handles. We begin with a model for the handle. Consider $\mathbb{R}^4$ with coordinates p_1, q_1, p_2, q_2 and the standard symplectic from $\omega_{std} = dp_1 \wedge dq_1 + dp_2 \wedge dq_2$. We define the function

$$f_0 = \frac{1}{4}\left(p_1^2 + q_1^2 + p_2^2 + q_2^2\right)$$

and the vector field

$$v_0 = \frac{1}{2}\left(p_1\frac{\partial}{\partial p_1} + q_1\frac{\partial}{\partial q_1} + p_2\frac{\partial}{\partial p_2} + q_2\frac{\partial}{\partial q_2}\right).$$

Exercise 7.4.6. Show that v_0 is a dilating vector field for ω_{std}:

$$\mathcal{L}_{v_0}\omega_{std} = \omega_{std},$$

and that v_0 is gradient like for f_0:

$$df_0(v_0) > 0$$

away from the origin and v_0 and df_0 vanish at the origin.

The above exercises have established the following result.

Lemma 7.4.7. *If (X, ω) is a weak, strong, exact, or Weinstein symplectic filling of a contact manifold, then attaching a Weinstein 0-handle will result in a new symplectic manifold that is also a symplectic filling of its boundary of the same type.*

Proof. If we let B^4 be the unit ball in $\mathbb{R}^4$ then the symplectic manifold (B^4, ω_{std}) with the vector field v_0 and function f_0 is a Weinstein manifold. We say $(B^4, \omega_{std}, f_0, v_0)$ is a Weinstein 0-handle. Attaching a 0-handle to (X, ω) is just taking the disjoint union with (B^4, ω_{std}). The result clearly follows. □

7.4.2. Index 1 Weinstein handles. We consider the same symplectic form ω_{std} on $\mathbb{R}^4$ as in the previous section, but now consider the function

$$f_1 = \frac{1}{4}\left(p_1^2 + q_1^2\right) + \left(p_2^2 - \frac{1}{2}q_2^2\right)$$

and the vector field

$$v_1 = \frac{1}{2}\left(p_1\frac{\partial}{\partial p_1} + q_1\frac{\partial}{\partial q_1}\right) + \left(2p_2\frac{\partial}{\partial p_2} - q_2\frac{\partial}{\partial q_2}\right).$$

Exercise 7.4.8. Show that that v_1 is a dilating vector field for ω_{std}:

$$\mathcal{L}_{v_1}\omega_{std} = \omega_{std},$$

and that v_1 is gradient like for f_1:

$$df_1(v_1) > 0$$

away from the origin and v_1 and df_1 vanish at the origin.

Let $H_- = f_1^{-1}(-1)$ and $S_- = H_- \cap (\{(0,0,0)\} \times \mathbb{R})$. Notice that S_- consists of two points and that v_1 is transverse to H_-. See the left-hand side of Figure 7.4.11. We now consider

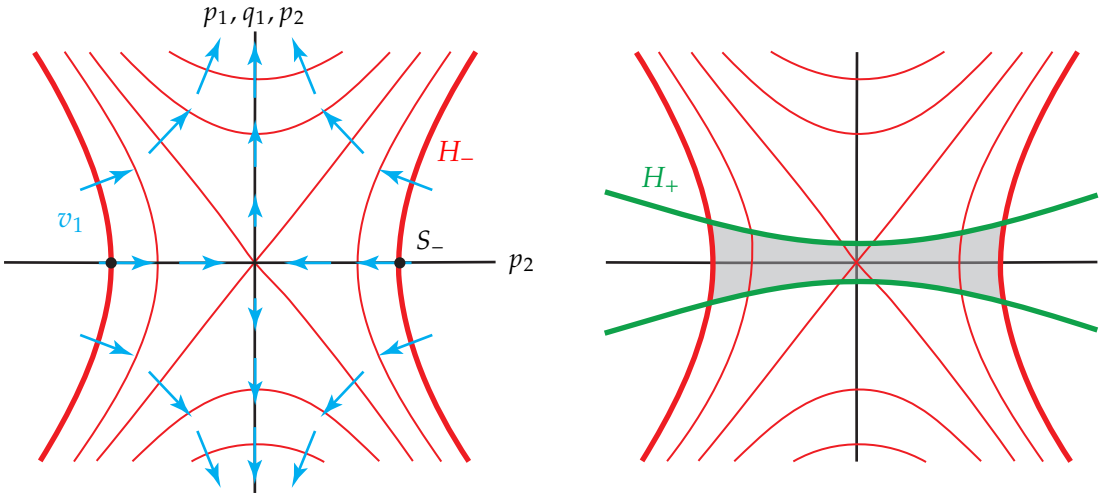

Figure 7.4.11. On the left we see some level sets of f_1 and $H_- = f_1^{-1}(1)$ in a thicker line. The vector field v_1 is also indicated as is the 0-sphere S_-. On the right, we see H_+ and the 1-handle h_1 is highlighted.

a function

$$g_1 = a_1 p_1^2 + a_2 q_1^2 + a_3 p_2^2 - a_4 q_2^2,$$

with $a_i > 0$ for all i.

Exercise 7.4.9. Show that for any positive c, the vector field v_1 is transverse to $g_1^{-1}(c)$.

Exercise 7.4.10. Show that for any $\epsilon > 0$ we can choose a_4 very large and the other a_i small positive numbers so that the intersection of H_- and $H_+ = g_1^{-1}(1)$ is contained in an ϵ-neighborhood of S_-.

Let A_- be the compact region in H_- bounded by $H_- \cap H_+$ and B_+ be the compact region in H_+ bounded by $H_- \cap H_+$. Notice that by construction, A_- is contained in an ϵ-neighborhood of S_-. Let h_1 be the region bounded by $A_- \cup B_+$. A Weinstein 1-handle is $(h_1, \omega_{std}, f_1, v_1)$. See the right-hand side of Figure 7.4.11. (Technically, this is not quite right. We will see below that we can attach this handle to weak, strong, and exact fillings of a contact manifold, but in order to attach this to a Weinstein manifold and extend the Weinstein structure, we will need to modify the handle. As this is a little technical, we ignore this until we need to address the matter.) We notice that v_1 points into h_1 along A_- and out of h_1 on B_+.

Lemma 7.4.11. *If (X, ω) is any symplectic manifold with convex boundary and S is an embedding of S^0 in ∂X, then there is a neighborhood N_X of S in X and a neighborhood N_H of S_- in $f_1^{-1}((-\infty, -1))$ that are symplectomorphic. Moreover, since ω is exact near S, we can assume*

there is a dilating vector field v for ω near S. For any such v, we can assume that the symplectomorphism takes v to v_1.

Remark 7.4.12. Notice that we did not specify if ∂X had a weakly or strongly convex boundary. The theorem holds in either case, and in the latter case, we can take v to be the dilating vector field defined near ∂X.

Proof. We begin by considering the case of a strong symplectic filling (the exact case will also follow) and then consider the weakly fillable case later. Let v be the dilating vector field for ω defined near ∂X and $\alpha = \iota_v\omega$ on ∂X be the induced contact from and ξ its kernel. Similarly let $\alpha_1 = \iota_{v_1}\omega_{std}$ restricted to H_- be the contact form induced from v_1 and ω, and ξ_1 its kernel.

We begin by showing that there is a neighborhood U_X of S in ∂X, a neighborhood U_H in H_-, and a contactomorphism $\phi\colon U_X \to U_H$ such that $\phi^*\alpha_1 = \alpha$. Notice that this is stronger than the Darboux theorem we discussed in the introduction, as the contactomorphism preserves not only the contact structure but also the two given contact forms.

To this end, we let Σ_X be two small disks with centers on two points of S.

Exercise 7.4.13. Show that Σ_X can be chosen so that

(1) Σ_X is tangent to ξ at the points in S,

(2) Σ_X is transverse to ξ away from S, and

(3) $d\alpha$ is symplectic on Σ_X.

One can find a similar surface Σ_H in H_- centered on the two points of S_-. After possibly shrinking Σ_X and Σ_H we can find a symplectomoprhism $\phi_1\colon (\Sigma_X, d\alpha) \to (\Sigma_H, d\alpha_1)$. This is the symplectic version of Darboux's theorem. The proof is quite similar to the contact version of Darboux's theorem given in the introduction and is a nice exercise for the reader or consult [**MS98**, Chapter 3].

Extend ϕ_1 to a diffeomorphism ϕ_2 from a neighborhood U_X of S in ∂X to a neighborhood U_H of S_- in H_- by using the Reeb flow of α and α_1.

Exercise 7.4.14. Prove that $\phi_2^* d\alpha_1 = d\alpha$
Hint: The Reeb flow preserves $d\alpha_1$ and $d\alpha$, and these agree on the surfaces Σ_X because their kernels (spanned by the Reeb vector field) agree, and they agree on $T\Sigma_X$.

We also note that $\phi_2^*\alpha_1 = \alpha$ at the two points of S.

We will now construct a diffeomorphism $\phi_3\colon \ : U_X \to U_X$ such that $\phi_3^*(\phi_2^*\alpha_1) = \alpha$. To do this, we consider

$$\beta_t = \alpha + t(f_2^*\alpha_1 - \alpha).$$

Exercise 7.4.15. Show that, after possibly shrinking U_X, β_t is a contact form for U_X. Hint: Notice that all the $\ker \beta_t$ agree on S and $d\beta_t$ is symplectic on $\ker \beta_t$ near S.

Now since $d(\phi_2^*\alpha_1 - \alpha) = 0$ and $f_2^*\alpha_1 - \alpha = 0$ on S, we know there is a function h such that $-(\phi_2^*\alpha_1 - \alpha) = dh$ and $h = 0$ on S. Set $w_t = hR_{\beta_t}$. (Recall R_{β_t} is the Reeb field fo β_t.) Let ψ_t be the flow of w_t and note that

$$\begin{aligned}\frac{d}{dt}\psi_t^*\beta_t &= \psi_t^*\left(\mathcal{L}_{w_t}\beta_t + \frac{d}{dt}\beta_t\right)\\ &= \psi_t^*\left(\iota_{w_t}\beta_t + \iota_{w_t}d\beta_t - dh\right) = \psi_t^*(dh + 0 - dh) = 0,\end{aligned}$$

Where the first equality follows from the formula for $\frac{d}{dt}\psi_t^*\beta_t$ developed in the proof of Theorem 1.2.10, the second equality is Cartan's formula for the Lie derivative, and the last equality follows from the definition of the Reeb vector field and w_t. Thus $\psi_t^*\beta_t = \beta_0$ and if we set $\psi_3 = \psi_1$ then we have our desired diffeomorphism. Now setting $\phi = \phi_2 \circ \phi_3$ we see that $\phi^*\alpha_1 = \alpha$ as claimed.

We can now extend ψ to a diffeomorphism Ψ of a neighborhood N_X of S in X and a neighborhood N_H in $f_1^{-1}((-\infty, -1))$ by the backwards flow of v and v_1. By construction Ψ is a symplectomorphism from (N_X, ω) to (N_H, ω_{std}) and takes v to v_1. This completes the proof of the lemma in the case that (X, ω) is a strong or exact filling of its boundary.

We now turn to the case where (X, ω) is a weak filling of its boundary. ADD THIS! □

We are now ready to attach a Weinstein 1-handle to symplectic fillings.

Lemma 7.4.16. *If (X, ω) is a weak, strong, exact, or Weinstein symplectic filling of a contact manifold, then attaching a Weinstein 1-handle will result in a new symplectic manifold (X', ω') that is also a symplectic filling of its boundary of the same type.*

Moreover, if the attaching sphere lies on one component of ∂X, then $\partial X'$ will be the connected sum of ∂X with the standard tight contact structure on $S^1 \times S^2$; otherwise, $\partial X'$ will be ∂X with the two components containing the attaching sphere connected summed. (See Section 9.2 for a discussion of the connected sum of contact manifolds.)

Proof. We consider the case of weak, strong, and exact fillings first. Let S be the attaching sphere for the 1-handle in ∂X. By Lemma 7.4.11 we know there are neighborhoods N_X of S in X and N_H of S_- in $f_1^{-1}((-\infty, -1))$ that are symplectomorphic by a symplectomorphism that takes the dilating vector field v for ω to the dilating vector field v_1.

Consider the subset R of $\mathbb{R}^4$ the union of N_H and h_1. We can use the symplectomorphism to identify N_H in R and N_X in X. This will give a new manifold X' with a 1-handle attached. Since the gluing map was a symplectomorphism, there is a symplectic structure on X', and the vector field v on X can be extended over X' by v_1. One may easily check that in the case that X was a strong or exact filling, this will make X' a strong or exact

filling of its boundary. If X were a weak filling of its boundary, then X' will be a weak filling away from the boundary coming from h_1, and along that part of the boundary, it will have a dilating vector field and hence be a weak filling there too.

Exercise 7.4.17. After reviewing the definition of the connected sum of contact manifolds in Section 9.2 prove that $\partial X'$ is related to ∂X as claimed in the lemma.

If (X, ω) were a Weinstein manifold, then we must also see how to extend the function defining the Weinstein structure over the attached handle. This requires a modification of the handle h_1 so that we can extend a Morse function of the handle in the "standard way". We briefly describe this process.

Consider $H_- = f_1^{-1}(-1)$ as before, but now let $H_+ = f_1^{-1}(c)$ for any fixed positive c. Now given a Weinstein manifold (X, ω, f, v) and an attaching sphere S in ∂X, let N_X and N_H be the neighborhoods of S and S_1, respectively, in X and $f_1^{-1}((-\infty, -1))$ from Lemma 7.4.11. Recall that means there is a symplectomorphism ϕ between these neighborhoods that takes the dilating vector field v to the dilating vector field v_1. We can now choose a small disk bundle neighborhood D of S_1 in H_1 that is contained in N_H. Now consider the image F of ∂D under the flow of v_1. See Figure 7.4.12. Now consider the compact region in $\mathbb{R}^4$ bounded by H_-, H_+, and F. Call this $\widehat{h}_1$. This will be our model for the refined handle attachment. We can assume that $N_H \cap H_1$ is a larger disk bundle D'

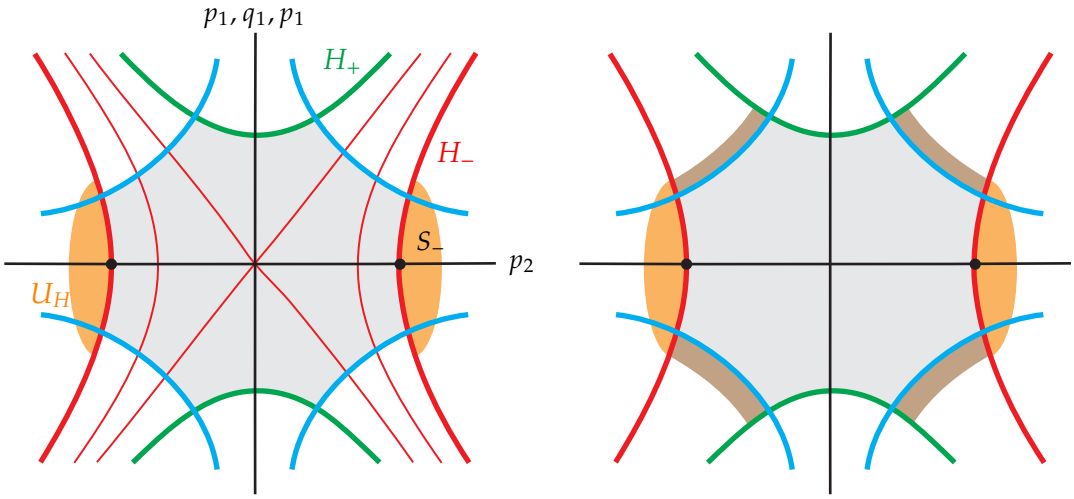

Figure 7.4.12. On the left, we see the handle $\widehat{h}_1$ in grey as well as the neighborhood N_H in orange. On the right, we see the same handle together with the image a larger disk bundle in H_1 under the flow of v_1 shown in brown.

over S_-. Let E be the image of the flow of $\overline{D' - D}$ under v_1 that lies between H_- and H_+. We note that E will be given by the time $t \in [0, k]$ flow of $\overline{D' - D}$ for some fixed $k > 0$. See the right-hand side of Figure 7.4.12. Let $\widehat{h}_1'$ denote the union of $\widehat{h}_1$ and E.

We now consider (X, ω). Let C be the complement of the $\phi(D)$ in ∂X. We can consider the symplectization of $(\partial X, \xi)$, defined by the contact 1-form $\alpha = \iota_v \omega$. We use the model for the symplectication $(\mathbb{R} \times \partial X, d(e^t \alpha))$. Notice that we can add $([0, k] \times \partial M, d(e^t \alpha))$ to (X, ω) to obtain a new Weinstein manifold (the extension of f should be obvious). We do not do this. Instead, we add $([0, k] \times C, d(e^t \alpha))$ to X to obtain a symplectic manifold with corners that we denote by X_e. See Figure 7.4.13. We can now glue $\widehat{h}_1'$ to X_e by identifying

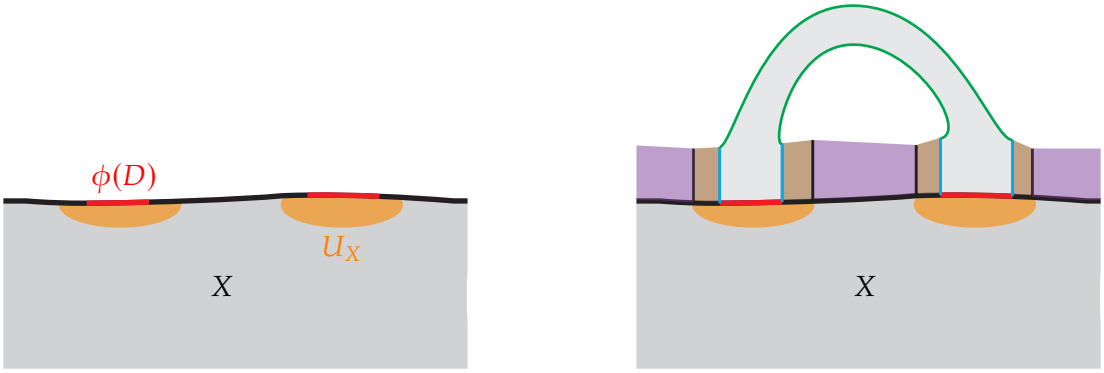

Figure 7.4.13. On the left, we see X and the neighborhood N_X in orange. On the right, we see the region X_e, which is the dark grey, brown, and purple parts. The light grey is the handle $\widehat{h}_1'$.

N_H with N_X via ϕ and the region E in $\widehat{h}_1'$ with part of $([0, k] \times C, d(e^t \alpha))$ using the flow if the dilating vector fields.

Exercise 7.4.18. This gives a smooth manifold that we denote X' with a symplectic form ω'. Moreover, the dilating vector field v on X can be extended over X' by v_1 on $\widehat{h}_1'$ and by the vector field in the symplectization on $([0, k] \times C, d(e^t \alpha))$. Call this vector field v'.

We are left to extend f on X to X' so that we have a Weinstein structure on X'. We can do this by using f_1, after adding some constant, on $\widehat{h}_1'$ and by projection onto $[0, k]$ on (again, after adding some constant). Denote this function f'.

Exercise 7.4.19. Show X' is obtained from X by attaching a 1-handle to S and, in addition, that (X', ω', f', v') is a Weinstein manifold.

This completes the proof in the Weinstein case. □

7.4.3. Index 2 Weinstein handles. We consider the same symplectic form ω_{std} on $\mathbb{R}^4$ as in the previous section, but now consider the function

$$f_2 = (q_1^2 + q_2^2) - \frac{1}{2}(p_1^2 + p_2^2)$$

and the vector field

$$v_2 = 2\left(q_1\frac{\partial}{\partial q_1} + q_2\frac{\partial}{\partial q_2}\right) - \left(p_1\frac{\partial}{\partial p_1} + p_2\frac{\partial}{\partial p_2}\right).$$

Exercise 7.4.20. Show that that v_2 is a dilating vector field for ω_{std}:

$$\mathcal{L}_{v_2}\omega_{std} = \omega_{std},$$

and that v_2 is gradient like for f_2:

$$df_2(v_2) > 0$$

away from the origin and v_2 and df_2 vanish at the origin.

Let $H_- = f_2^{-1}(-1)$ and $S_- = H_- \cap (\{p_1p_2\text{-plane}\})$. Notice that S_- is a circle and that v_1 is transverse to H_-. See the left-hand side of Figure 7.4.11 (but label the horizontal axis by p_1, p_2 and the vertical axis by q_1, q_2). We now consider the function

$$g_2 = a_1q_1^2 + a_2q_2^2 - a_3p_1^2 - a_4p_2^2,$$

with $a_i > 0$ for all i.

Exercise 7.4.21. Show that for any positive c, the vector field v_2 is transverse to $g_2^{-1}(c)$.

Exercise 7.4.22. Show that for any $\epsilon > 0$ we can choose a_3 and a_4 very large and the other a_1, a_2 small positive numbers so that the intersection of H_- and $H_+ = g_2^{-1}(1)$ is contained in an ϵ-neighborhood of S_-.

Let A_- be the compact region in H_- bounded by $H_- \cap H_+$ and B_+ be the compact region in H_+ bounded by $H_- \cap H_+$. Notice that by construction, A_- is contained in an ϵ-neighborhood of S_-. Let h_2 be the region bounded by $A_- \cup B_+$. A Weinstein 2-handle is $(h_2, \omega_{std}, f_2, v_2)$. See the right-hand side of Figure 7.4.11. (Technically, this is not quite right. We will see below that we can attach this handle to weak, strong, and exact fillings of a contact manifold, but in order to attach this to a Weinstein manifold and extend the Weinstein structure, we will need to modify the handle. As this is a little technical, we ignore this until we need to address the matter.) We notice that v_2 points into h_2 along A_- and out of h_2 on B_+. So we have a contact structure ξ_- on A_- and ξ_+ on B_+ induced from the contact form $\iota_{v_2}\omega_{std}$ restricted to A_- and B_+.

Exercise 7.4.23. Show that S_- is a Legendrian circle in (A_-, ξ_-), the contact twisting along S_- relative to the product framing is +1, and that A_- is a standard neighborhood of S_-.

We are now ready for a neighborhood lemma that we will need to attach a Weinstein 2-handle.

Lemma 7.4.24. *If (X, ω) is any symplectic manifold with convex boundary and S is an embedding of S^1 in ∂X, then there is a neighborhood N_X of S in X and a neighborhood N_H of S_- in $f_2^{-1}((-\infty, -1))$ that are symplectomorphic. Moreover, since ω is exact near S, we can assume there is a dilating vector field v for ω near S, and for any such v, we can assume that the symplectomorphism takes v to v_2.*

Remark 7.4.25. Notice that we did not specify if ∂X had a weakly or strongly convex boundary. The theorem holds in either case, and in the latter case, we can take v to be the dilating vector field defined near ∂X.

Exercise 7.4.26. Prove this lemma.
Hint: The proof is nearly identical to the proof of Lemma 7.4.24 for Weinstein 1-handles. The only difference is that the surfaces Σ_X and Σ_H will be annuli containing S and S_-, respectively.

Lemma 7.4.27. *If (X, ω) is a weak, strong, exact, or Weinstein symplectic filling of a contact manifold, then attaching a Weinstein 2-handle will result in a new symplectic manifold $(X', \omega'$ that is also a symplectic filling of its boundary of the same type.*

Moreover, if the attaching sphere is a Legendrian knot L in ∂X, then $\partial X'$ will be the result of Legendrian surgery (recall this is contact (-1)-surgery) on L in ∂X.

Proof. The first part of this proof is almost identical to the proof of Lemma 7.4.16.

Exercise 7.4.28. Prove the result in the first paragraph of the lemma.

We are left to see that attaching a Weinstein 2-handle affects the boundary by Legendrian surgery on the attaching sphere L. Notice that when the handle is attached, we remove the image of the solid torus A_- from ∂X and glue B_+ to the resulting manifold. Recall from Exercise 7.4.23 that A_- is just a standard neighborhood of S_- and S_- is identified with L.

Exercise 7.4.29. Show that B_+ is also a standard neighborhood of a Legendrian knot.

So when we glue B_+ in the place of A_-, we are gluing in a solid torus with a tight contact structure. That is, we are performing some contact surgery on L; we just need to determine which contact surgery we are performing. Clearly, the meridian for B_+ is the same as the product longitude for A_-. In Exercise 7.4.23 it was shown that the contact framing of S_- is one larger than the product framing. Thus, the meridian of B_+ is glued to a framing curve that is one less than the contact framing. In other words, we are performing a contact (-1)-surgery. □

7.5. Tight but not fillable contact structures

In this section, we construct a tight but not symplectically fillable contact structure. The first such example appeared in [EH02b] based on the work of Lisca in [Lis99]. There the authors verified that the result of smooth two surgery on the $(2,3)$-torus knot admits a tight structure that is tight but has no symplectic filling. This result was generalized by Lisca and Stipsicz. Specifically, we show the following.

Theorem 7.5.1 (Lisca and Stipsicz 2004, [LS04]). *Let M_n be $2n$ surgery on the $(2,2n+1)$-torus knot. Then M admits a contact structure ξ that is tight but has no symplectic filling.*

Remark 7.5.2. In [LS04], they actually show that smooth r-surgery on the torus knot $T_{2,2n+1}$, where $r \in [2n-1, 4n)$, has a tight contact structure that is not fillable. Technically for the existence of tight contact structures one needs [MT15] for when $r \in (2n-1, 2n)$. This result was later generalized by Owens and Strle [OS12] to all positive torus knots $T_{p,q}$ where $0 < p < q$ are relatively prime.

Their argument in this generality in terms of both surgery coefficients and the torus knots considered is quite similar to the one we present below, but requires slightly more work. We leave it as an exercise to generalize the argument below to this general case. Given this remark, it is clear there are many tight but not fillable contact structures.

Proof. Recall from Section 6.5 that there is a unique Legendrian L_n in the knot type of the $T_{2,2n+1}$ torus knot with $\mathrm{tb}(L) = 2n-1$. Let ξ_n be the contact structure on $M_n = S^3_L(2n)$ obtained from contact $(+1)$-surgery on L_n. We have the following two lemmas.

Lemma 7.5.3. *The contact manifold (M_n, ξ_n) is tight.*

Lemma 7.5.4. *The contact manifold (M_n, ξ_n) is not symplectically fillable.*

The theorem clearly follows from these two lemmas. □

We now establish the tightness of (M, ξ).

Proof of Lemma 7.5.3. From Appendix C we know that the contact invariant in Heegaard Floer homology is functorial under contact $(+1)$-surgery. That is if W_n is the cobordism from S^3 to $M_n = S^3_{L_n}(2n)$ obtained from attaching a 2-framed 2-handle to $S^3 \times [0,1]$ then

$$F_{\overline{W_n}}(c(\xi_{std}) = c(\xi_n)$$

where ξ_{std} is the standard contact structure on S^3. We claim the map $F_{\overline{W_n}}$ is injective and thus $c(\xi_n) \neq 0$ and so ξ_n is tight.

To see that $F_{\overline{W_n}}$ is injective, we first note that $T_{2,2n+1}$ is an L-space knot. Recall from Appendix C that this means some positive surgery $T_{2,2n+1}$ is an L-space. See Definition 1.6.38.

Exercise 7.5.5. Show that $4n+1$ surgery on $T_{2,2n+1}$ is a lens space, which, of course, is an L-space.

Since $T_{2,2n+1}$ is a L-space knots we know that for any $r \geq 2n-1$ the manifold $S^3_{T_{2,2n+1}}(r)$ is an L-space [**LS04**]. (Here $2n-1$ is minus the Euler characteristic of the minimal genus Seifert surface of $T_{2,2n+1}$.) Thus $M_n = S^3_{L_n}(2n)$ is an L-space as is $S^3_{L_n}(2n+1)$. We now recall the exact triangle in Heegaard Floer theory

$$\begin{array}{ccc} \widehat{\mathrm{HF}}(-S^3) & \longrightarrow & \widehat{\mathrm{HF}}(-M_{L_n}(2n)) \\ & \nwarrow \quad \swarrow & \\ & \widehat{\mathrm{HF}}(-M_{L_n}(2n+1)) & \end{array}$$

Which gives us

$$\begin{array}{ccc} \mathbb{Z} & \longrightarrow & \mathbb{Z}^{2n} \\ & \nwarrow \quad \swarrow & \\ & \mathbb{Z}^{2n+1} & \end{array}$$

Thus, the lower left map must be the zero map, and the top map, which is F_{W_n}, must be injective, as claimed. □

Proof of Lemma 7.5.4. We will prove that (M_n, ξ_n) is not symplectically fillable by showing that if it were, we can construct a closed 4-manifolds with an intersection form that violates Donaldson's diagonalization theorem, which we will recall below.

We first note that $-M_n$ bounds a 4-manifold X_n with intersection which is of the form

$$\begin{bmatrix} -2 & 1 & 1 & 1 & 0 \\ 1 & -2 & 0 & 0 & 0 \\ 1 & 0 & -2 & 0 & 0 \\ 1 & 0 & 0 & -2 & 1 \\ 0 & 0 & 0 & 1 & -(n+1) \end{bmatrix}.$$

To see this, consider Figure 7.5.14 that gives a sequence of surgery diagrams describing M_n. The bottom drawing describes M_n as a small Seifert fibered space. To obtain $-M_n$, one reverses all the crossings in the surgery diagram and changes the sign on each surgery coefficient. Then, after a few Rolfsen twists, one sees that $-M_n$ is given by the diagram in Figure 7.5.15. One may now perform inverse slam-dunk movers to obtain a

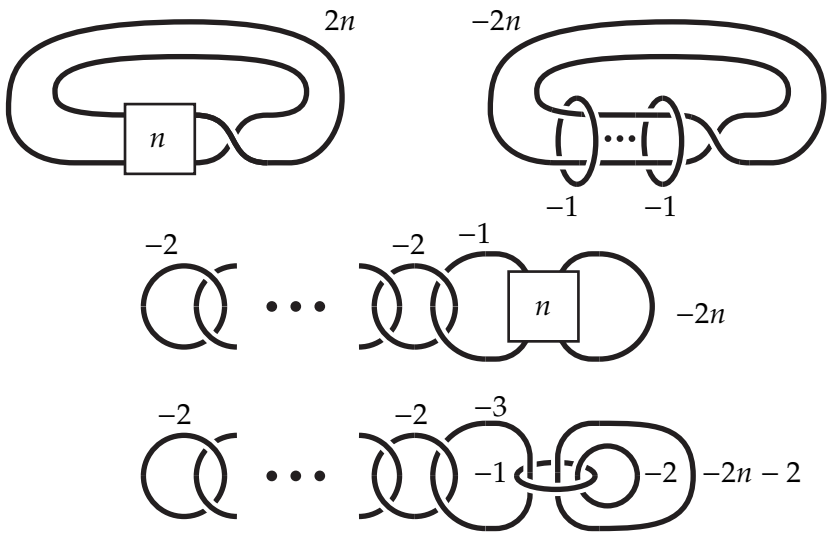

Figure 7.5.14. The manifold M_n. The first diagram on the top left is the definition of M_n. The second diagram on the top row is obtained by blowing up n times. The second row is obtained from the upper right diagram by sliding the -1-framed unknots over the one to its right and then isotoping the diagram. The bottom diagram is obtained from the middle one by blowing up twice and doing a handle slide.

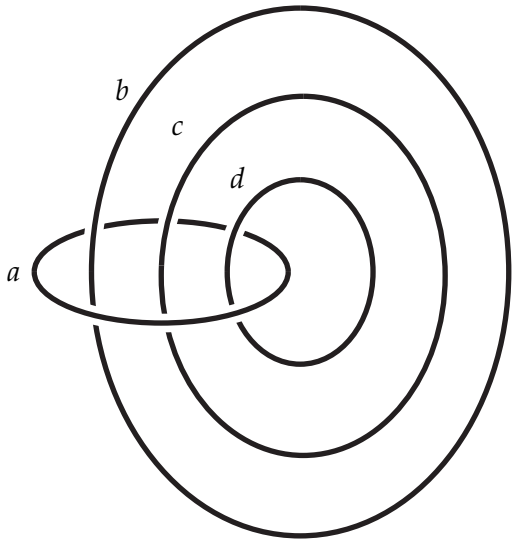

Figure 7.5.15. The diagram for M_n when $a = -1$, $b = -2$, $c = -2n - 2$ and $d = -\frac{2n+1}{n}$. The diagram for $-M_n$ when $a = -2$,$b = -2$, $c = -\frac{2n+2}{2n+1}$, and $d = -\frac{2n+1}{n+1}$

surgery diagram with integer coefficients and hence a diagram for a 4-manifold X_n with $\partial X_n = -M_n$ and intersection form containing the one indicated above.

Exercise 7.5.6. Show that the intersection form of X_n is negative definite.

Now suppose that (M_n, ξ_n) bounds a symplectic manifold (Y_n, ω_n). As discussed in the proof of Lemma 7.5.3, we know that M_n is an L-space. In Appendix C we see that any symplectic filling of an L-space must be negative definite. Thus, we may glue Y_n and X_n together to obtain a closed 4-manifold Z_n with a negative definite intersection form (since X_n and Y_n are negative definite and M_n is a rational homology sphere). We now recall Donaldson's famous diagonalization theorem.

Theorem 7.5.7 (Donaldson 1983, [Don83])**.** *If X is a smooth, closed, oriented four-manifold with definite intersection form, then the intersection form of X is diagonalizable over $\mathbb{Z}$.*

Remark 7.5.8. In [Don83], the above theorem was proven under the additional hypothesis that X was simply connected. This extra hypothesis was removed a few years later in [Don87].

From the above, we see that the intersection form for Z_n, and in particular the part of it given by the matrix above, will need to embed in some diagonal intersection form D. Suppose $e_1, \dots, e_k$ span D. Let $f_1, \dots, f_5$ be the elements in the intersection form of Z_n that give the matrix above. Notice that since $f_i^2 = -1$, for $i = 1, \dots, 4$, and the only elements in D that have square -2 are $\epsilon_1 e_i + \epsilon_2 e_j$ for some $i \neq j$ and $\epsilon_l = \pm 1$. So, up to composing our embedding of the intersection form of Z_n into D we can assume that f_1 map to $e_1 - e_2$, Since $f_1 \cdot f_2 = 1$ we see that f_2 must map to something that contains either $-e_1$ or e_2, so again, up to composing with an automorphism of D we can assume that f_2 maps to $e_2 - e_3$ and similarly f_3 maps to $e_4 - e_1$.

Exercise 7.5.9. Show that we can assume that f_4 maps to $e_2 + e_3$.

But now f_5 must map to something, an element e that satisfies

$$e \cdot (e_2 + e_3) = 1, \text{and } e \cdot (e_2 - e_3) = 0.$$

However, this is not possible since $(e_2 + e_3) + (e_2 - e_3) = 2e_2$ so we need $2e \cdot e_2 = 1$ and there is no such e. Thus Z_n cannot exist, and (M_n, ξ_n) is not symplectically fillable. □

Part II: Advanced topic in convex surface theory

Chapter 8

Convex surfaces II

Chapter 9

Tight contact structures II

Chapter 10

Legendrian knots II

Chapter 11

Convex surfaces and tight contact structures III

Some of Emmanuel's results. Tightness of the standard 3-ball.

Chapter 12

Open book decompositions

Chapter 13

Symplectic fillings II

Chapter 14

Overtwisted contact structures

Appendix A

Constructing and classifying bundles

1.1. Structure groups

1.2. Obstruction theory

1.3. Characteristic classes

Euler class

If $E \to M$ is an oriented k-dimensional vector bundle over an n-manifold M. Then the *Euler class* of E is defined to be the Poincaré dual of $\sigma^{-1}(\mathbf{0})$ where σ is a section of E that is transverse to the zero section $\mathbf{0}$ of E. We denote this by $e(E)$ and it is a cohomology class in $H^?(M)$

1.4. Spin and Spin^c structures

Appendix B

Holomorphic curves in contact geometry

Theorem 2.0.1 (Gomov 1985, [Gro85] and McDuff 1991, [McD91]). *If (X, ω) is a semi-sympmlectic filling of $(S^3.\xi_{std})$, then X is diffeomorpic to a blowup of B^4.*

Appendix C

Heegaard Floer Homology

Index

Bibliography

[AMR88] R. Abraham, J. E. Marsden, and T. Ratiu. *Manifolds, tensor analysis, and applications*, volume 75 of *Applied Mathematical Sciences*. Springer-Verlag, New York, second edition, 1988.

[Arn66] V. Arnold. Sur la géométrie différentielle des groupes de Lie de dimension infinie et ses applications à l'hydrodynamique des fluides parfaits. *Ann. Inst. Fourier (Grenoble)*, 16:319–361, 1966.

[BEM15] Matthew Strom Borman, Yakov Eliashberg, and Emmy Murphy. Existence and classification of overtwisted contact structures in all dimensions. *Acta Math.*, 215(2):281–361, 2015.

[Ben83] Daniel Bennequin. Entrelacements et équations de Pfaff. In *Third Schnepfenried geometry conference, Vol. 1 (Schnepfenried, 1982)*, volume 107 of *Astérisque*, pages 87–161. Soc. Math. France, Paris, 1983.

[BGMZ24] Jonathan Bowden, Fabio Gironella, Agustin Moreno, and Zhengyi Zhou. Tight contact structures without symplectic fillings are everywhere, 2024.

[Bla02] David E. Blair. *Riemannian geometry of contact and symplectic manifolds*, volume 203 of *Progress in Mathematics*. Birkhäuser Boston Inc., Boston, MA, 2002.

[Bon83] Francis Bonahon. Difféotopies des espaces lenticulaires. *Topology*, 22(3):305–314, 1983.

[Bou02] Frédéric Bourgeois. Odd dimensional tori are contact manifolds. *Int. Math. Res. Not.*, (30):1571–1574, 2002.

[Bow12] Jonathan Bowden. Exactly fillable contact structures without Stein fillings. *Algebr. Geom. Topol.*, 12(3):1803–1810, 2012.

[Bre93] Glen E. Bredon. *Topology and geometry*, volume 139 of *Graduate Texts in Mathematics*. Springer-Verlag, New York, 1993.

[Bro60] E. J. Brody. The topological classification of the lens spaces. *Ann. of Math. (2)*, 71:163–184, 1960.

[Cas13] Meredith Casey. *Branched covers of contact manifolds*. PhD thesis, Georgia Institute of Technology, 2013.

[CE12] Kai Cieliebak and Yakov Eliashberg. *From Stein to Weinstein and back*, volume 59 of *American Mathematical Society Colloquium Publications*. American Mathematical Society, Providence, RI, 2012. Symplectic geometry of affine complex manifolds.

[CEMM23] Rima Chatterjee, John B. Etnyre, Hyunki Min, and Anubhav Mukherjee. Existence and construction of non-loose knots, 2023.

[Cer68] Jean Cerf. *Sur les difféomorphismes de la sphère de dimension trois* ($\Gamma_4 = 0$), volume No. 53 of *Lecture Notes in Mathematics*. Springer-Verlag, Berlin-New York, 1968.

[CH85] S. S. Chern and R. S. Hamilton. On Riemannian metrics adapted to three-dimensional contact manifolds. In *Workshop Bonn 1984 (Bonn, 1984)*, volume 1111 of *Lecture Notes in Math.*, pages 279–308. Springer, Berlin, 1985. With an appendix by Alan Weinstein.

[Che02] Yuri Chekanov. Differential algebra of Legendrian links. *Invent. Math.*, 150(3):441–483, 2002.

[CM20] James Conway and Hyunki Min. Classification of tight contact structures on surgeries on the figure-eight knot. *Geom. Topol.*, 24(3):1457–1517, 2020.

[CMP19] Roger Casals, Emmy Murphy, and Francisco Presas. Geometric criteria for overtwistedness. *J. Amer. Math. Soc.*, 32(2):563–604, 2019.

[Col97] Vincent Colin. Chirurgies d'indice un et isotopies de sphères dans les variétés de contact tendues. *C. R. Acad. Sci. Paris Sér. I Math.*, 324(6):659–663, 1997.

[CPP15] Roger Casals, Dishant M. Pancholi, and Francisco Presas. Almost contact 5-manifolds are contact. *Ann. of Math. (2)*, 182(2):429–490, 2015.

[Dar82] G. Darboux. Sur le problème de pfaff. *Bull. Sci. Math.*, 6:14–36, 49–38, 1882.

[DG01] Fan Ding and Hansjörg Geiges. Symplectic fillability of tight contact structures on torus bundles. *Algebr. Geom. Topol.*, 1:153–172, 2001.

[DG04] Fan Ding and Hansjörg Geiges. A Legendrian surgery presentation of contact 3-manifolds. *Math. Proc. Cambridge Philos. Soc.*, 136(3):583–598, 2004.

[DG09] Fan Ding and Hansjörg Geiges. Handle moves in contact surgery diagrams. *J. Topol.*, 2(1):105–122, 2009.

[DGS04] Fan Ding, Hansjörg Geiges, and András I. Stipsicz. Surgery diagrams for contact 3-manifolds. *Turkish J. Math.*, 28(1):41–74, 2004.

[dMP80] W. de Melo and J. Palis. Moduli of stability for diffeomorphisms. In *Global theory of dynamical systems (Proc. Internat. Conf., Northwestern Univ., Evanston, Ill., 1979)*, volume 819 of *Lecture Notes in Math.*, pages 318–339. Springer, Berlin, 1980.

[Don83] S. K. Donaldson. An application of gauge theory to four-dimensional topology. *J. Differential Geom.*, 18(2):279–315, 1983.

[Don87] S. K. Donaldson. The orientation of Yang-Mills moduli spaces and 4-manifold topology. *J. Differential Geom.*, 26(3):397–428, 1987.

[Dym01] Katarzyna Dymara. Legendrian knots in overtwisted contact structures on S^3. *Ann. Global Anal. Geom.*, 19(3):293–305, 2001.

[EF98] Yakov Eliashberg and Maia Fraser. Classification of topologically trivial Legendrian knots. In *Geometry, topology, and dynamics (Montreal, PQ, 1995)*, volume 15 of *CRM Proc. Lecture Notes*, pages 17–51. Amer. Math. Soc., Providence, RI, 1998.

[EF09] Yakov Eliashberg and Maia Fraser. Topologically trivial Legendrian knots. *J. Symplectic Geom.*, 7(2):77–127, 2009.

[EFM01] Judith Epstein, Dmitry Fuchs, and Maike Meyer. Chekanov-Eliashberg invariants and transverse approximations of Legendrian knots. *Pacific J. Math.*, 201(1):89–106, 2001.

[EG91] Yakov Eliashberg and Mikhael Gromov. Convex symplectic manifolds. In *Several complex variables and complex geometry, Part 2 (Santa Cruz, CA, 1989)*, volume 52 of *Proc. Sympos. Pure Math.*, pages 135–162. Amer. Math. Soc., Providence, RI, 1991.

[EG00a] John Etnyre and Robert Ghrist. Contact topology and hydrodynamics. I. Beltrami fields and the Seifert conjecture. *Nonlinearity*, 13(2):441–458, 2000.

[EG00b] John Etnyre and Robert Ghrist. Contact topology and hydrodynamics. III. Knotted orbits. *Trans. Amer. Math. Soc.*, 352(12):5781–5794 (electronic), 2000.

[EG01] John Etnyre and Robert Ghrist. An index for closed orbits in Beltrami fields. *Phys. D*, 159(3-4):180–189, 2001.

[EG02] John Etnyre and Robert Ghrist. Contact topology and hydrodynamics. II. Solid tori. *Ergodic Theory Dynam. Systems*, 22(3):819–833, 2002.

[EG05] John Etnyre and Robert Ghrist. Generic hydrodynamic instability of curl eigenfields. *SIAM J. Appl. Dyn. Syst.*, 4(2):377–390 (electronic), 2005.

[EGH00] Y. Eliashberg, A. Givental, and H. Hofer. Introduction to symplectic field theory. *Geom. Funct. Anal.*, (Special Volume, Part II):560–673, 2000. GAFA 2000 (Tel Aviv, 1999).

[EH01a] John B. Etnyre and Ko Honda. Knots and contact geometry. I. Torus knots and the figure eight knot. *J. Symplectic Geom.*, 1(1):63–120, 2001.

[EH01b] John B. Etnyre and Ko Honda. On the nonexistence of tight contact structures. *Ann. of Math. (2)*, 153(3):749–766, 2001.

[EH02a] John B. Etnyre and Ko Honda. On symplectic cobordisms. *Math. Ann.*, 323(1):31–39, 2002.

[EH02b] John B. Etnyre and Ko Honda. Tight contact structures with no symplectic fillings. *Invent. Math.*, 148(3):609–626, 2002.

[EH05] John B. Etnyre and Ko Honda. Cabling and transverse simplicity. *Ann. of Math. (2)*, 162(3):1305–1333, 2005.

[EKM12] John B. Etnyre, Rafal Komendarczyk, and Patrick Massot. Tightness in contact metric 3-manifolds. *Invent. Math.*, 188(3):621–657, 2012.

[EKO24] John Etnyre, Marc Kegel, and Sinem Onaran. Contact surgery numbers. *Journal of Symplectic Geometry*, to appear, 2024.

[Eli89] Y. Eliashberg. Classification of overtwisted contact structures on 3-manifolds. *Invent. Math.*, 98(3):623–637, 1989.

[Eli90a] Yakov Eliashberg. Filling by holomorphic discs and its applications. In *Geometry of low-dimensional manifolds, 2 (Durham, 1989)*, volume 151 of *London Math. Soc. Lecture Note Ser.*, pages 45–67. Cambridge Univ. Press, Cambridge, 1990.

[Eli90b] Yakov Eliashberg. Topological characterization of Stein manifolds of dimension > 2. *Internat. J. Math.*, 1(1):29–46, 1990.

[Eli91] Yakov Eliashberg. On symplectic manifolds with some contact properties. *J. Differential Geom.*, 33(1):233–238, 1991.

[Eli92] Yakov Eliashberg. Contact 3-manifolds twenty years since J. Martinet's work. *Ann. Inst. Fourier (Grenoble)*, 42(1-2):165–192, 1992.

[Eli96] Yasha Eliashberg. Unique holomorphically fillable contact structure on the 3-torus. *Internat. Math. Res. Notices*, (2):77–82, 1996.

[EMM22] John B. Etnyre, Hyunki Min, and Anubhav Mukherjee. Non-loose torus knots, 2022.

[EMT24] John B. Etnyre, Hyunki Min, and Bülent Tosun. Surgeries on torus knots, 2024.

[ENV13] John B. Etnyre, Lenhard L. Ng, and Vera Vértesi. Legendrian and transverse twist knots. *J. Eur. Math. Soc. (JEMS)*, 15(3):969–995, 2013.

[ET98] Yakov M. Eliashberg and William P. Thurston. *Confoliations*, volume 13 of *University Lecture Series*. American Mathematical Society, Providence, RI, 1998.

[Etn96] John Boyd Etnyre. *Symplectic constructions on 4-manifolds*. ProQuest LLC, Ann Arbor, MI, 1996. Thesis (Ph.D.)–The University of Texas at Austin.

[Etn98] John B. Etnyre. Symplectic convexity in low-dimensional topology. *Topology Appl.*, 88(1-2):3–25, 1998. Symplectic, contact and low-dimensional topology (Athens, GA, 1996).

[Etn99] John B. Etnyre. Transversal torus knots. *Geom. Topol.*, 3:253–268, 1999.

[Etn00] John B. Etnyre. Tight contact structures on lens spaces. *Commun. Contemp. Math.*, 2(4):559–577, 2000.

[Etn05] John B. Etnyre. Legendrian and transversal knots. In *Handbook of knot theory*, pages 105–185. Elsevier B. V., Amsterdam, 2005.

[Etn13] John B. Etnyre. On knots in overtwisted contact structures. *Quantum Topol.*, 4(3):229–264, 2013.

[EV10] John B. Etnyre and Jeremy Van Horn-Morris. Fibered transverse knots and the Bennequin bound. *Int. Math. Res. Not.*, page 27, 2010. arXiv:0803.0758v2.

[FF16] Anatoly Fomenko and Dmitry Fuchs. *Homotopical topology*, volume 273 of *Graduate Texts in Mathematics*. Springer, [Cham], second edition, 2016.

[FS97] Ronald Fintushel and Ronald J. Stern. Rational blowdowns of smooth 4-manifolds. *J. Differential Geom.*, 46(2):181–235, 1997.

[FT97] Dmitry Fuchs and Serge Tabachnikov. Invariants of Legendrian and transverse knots in the standard contact space. *Topology*, 36(5):1025–1053, 1997.

[Gay06] David T. Gay. Four-dimensional symplectic cobordisms containing three-handles. *Geom. Topol.*, 10:1749–1759, 2006.

[Gei91] Hansjörg Geiges. Contact structures on 1-connected 5-manifolds. *Mathematika*, 38(2):303–311, 1991.

[Gei93] Hansjörg Geiges. Contact structures on $(n-1)$-connected $(2n+1)$-manifolds. *Pacific J. Math.*, 161(1):129–137, 1993.

[Gei08] Hansjörg Geiges. *An introduction to contact topology*, volume 109 of *Cambridge Studies in Advanced Mathematics*. Cambridge University Press, Cambridge, 2008.

[GG06] Emmanuel Giroux and Noah Goodman. On the stable equivalence of open books in three-manifolds. *Geom. Topol.*, 10:97–114 (electronic), 2006.

[GH16] Jian Ge and Yang Huang. 1/4-pinched contact sphere theorem. *Asian J. Math.*, 20(5):893–901, 2016.

[Ghi05a] Paolo Ghiggini. Strongly fillable contact 3-manifolds without Stein fillings. *Geom. Topol.*, 9:1677–1687 (electronic), 2005.

[Ghi05b] Paolo Ghiggini. Tight contact structures on Seifert manifolds over T^2 with one singular fibre. *Algebr. Geom. Topol.*, 5:785–833, 2005.

[Ghi08] Paolo Ghiggini. On tight contact structures with negative maximal twisting number on small Seifert manifolds. *Algebr. Geom. Topol.*, 8(1):381–396, 2008.

[GHVHM] Paolo Ghiggini, Ko Honda, and Jeremy Van Horn-Morris. The vanishing of the contact invariant in the presence of torsion. arXiv:0706.1602v2.

[Gir91] Emmanuel Giroux. Convexité en topologie de contact. *Comment. Math. Helv.*, 66(4):637–677, 1991.

[Gir00] Emmanuel Giroux. Structures de contact en dimension trois et bifurcations des feuilletages de surfaces. *Invent. Math.*, 141(3):615–689, 2000.

[Gir01] Emmanuel Giroux. Structures de contact sur les variétés fibrées en cercles audessus d'une surface. *Comment. Math. Helv.*, 76(2):218–262, 2001.

[Gir02] Emmanuel Giroux. Géométrie de contact: de la dimension trois vers les dimensions supérieures. In *Proceedings of the International Congress of Mathematicians, Vol. II (Beijing, 2002)*, pages 405–414, Beijing, 2002. Higher Ed. Press.

[GL89] C. McA. Gordon and J. Luecke. Knots are determined by their complements. *J. Amer. Math. Soc.*, 2(2):371–415, 1989.

[GLS06] Paolo Ghiggini, Paolo Lisca, and András I. Stipsicz. Classification of tight contact structures on small Seifert 3-manifolds with $e_0 \geq 0$. *Proc. Amer. Math. Soc.*, 134(3):909–916 (electronic), 2006.

[GLS07] Paolo Ghiggini, Paolo Lisca, and András I. Stipsicz. Tight contact structures on some small Seifert fibered 3-manifolds. *Amer. J. Math.*, 129(5):1403–1447, 2007.

[GM88] Mark Goresky and Robert MacPherson. *Stratified Morse theory*, volume 14 of *Ergebnisse der Mathematik und ihrer Grenzgebiete (3) [Results in Mathematics and Related Areas (3)]*. Springer-Verlag, Berlin, 1988.

[GO20] Hansjörg Geiges and Sinem Onaran. Exceptional Legendrian torus knots. *Int. Math. Res. Not. IMRN*, (22):8786–8817, 2020.

[Gom98] Robert E. Gompf. Handlebody construction of Stein surfaces. *Ann. of Math. (2)*, 148(2):619–693, 1998.

[GP10] Victor Guillemin and Alan Pollack. *Differential topology*. AMS Chelsea Publishing, Providence, RI, 2010. Reprint of the 1974 original.

[Gra59] John W. Gray. Some global properties of contact structures. *Ann. of Math. (2)*, 69:421–450, 1959.

[Gro85] M. Gromov. Pseudoholomorphic curves in symplectic manifolds. *Invent. Math.*, 82(2):307–347, 1985.

[GS99] Robert E. Gompf and András I. Stipsicz. 4-*manifolds and Kirby calculus*, volume 20 of *Graduate Studies in Mathematics*. American Mathematical Society, Providence, RI, 1999.

[GT98] H. Geiges and C. B. Thomas. Contact topology and the structure of 5-manifolds with $\pi_1 = Z_2$. *Ann. Inst. Fourier (Grenoble)*, 48(4):1167–1188, 1998.

[GZ10] Hansjörg Geiges and Kai Zehmisch. Eliashberg's proof of Cerf's theorem. *J. Topol. Anal.*, 2(4):543–579, 2010.

[Har82] John Harer. How to construct all fibered knots and links. *Topology*, 21(3):263–280, 1982.

[Har88] J. Harrison. C^2 counterexamples to the Seifert conjecture. *Topology*, 27(3):249–278, 1988.

[Hat22] Allen Hatcher. *Topology of numbers*. American Mathematical Society, Providence, RI, [2022] ©2022.

[HH58] Friedrich Hirzebruch and Heinz Hopf. Felder von Flächenelementen in 4-dimensionalen Mannigfaltigkeiten. *Math. Ann.*, 136:156–172, 1958.

[Hir76] Morris W. Hirsch. *Differential topology*, volume No. 33 of *Graduate Texts in Mathematics*. Springer-Verlag, New York-Heidelberg, 1976.

[HKc91] Jack K. Hale and Hüseyin Ko¸cak. *Dynamics and bifurcations*, volume 3 of *Texts in Applied Mathematics*. Springer-Verlag, New York, 1991.

[HKM03] Ko Honda, William H. Kazez, and Gordana Matić. Tight contact structures on fibered hyperbolic 3-manifolds. *J. Differential Geom.*, 64(2):305–358, 2003.

[Hof93] H. Hofer. Pseudoholomorphic curves in symplectizations with applications to the Weinstein conjecture in dimension three. *Invent. Math.*, 114(3):515–563, 1993.

[Hon00a] Ko Honda. On the classification of tight contact structures. I. *Geom. Topol.*, 4:309–368 (electronic), 2000.

[Hon00b] Ko Honda. On the classification of tight contact structures. II. *J. Differential Geom.*, 55(1):83–143, 2000.

[Hon02] Ko Honda. Gluing tight contact structures. *Duke Math. J.*, 115(3):435–478, 2002.

[Hua13] Yang Huang. A proof of the classification theorem of overtwisted contact structures via convex surface theory. *J. Symplectic Geom.*, 11(4):563–601, 2013.

[Kan97] Yutaka Kanda. The classification of tight contact structures on the 3-torus. *Comm. Anal. Geom.*, 5(3):413–438, 1997.

[Kan98] Yutaka Kanda. On the Thurston-Bennequin invariant of Legendrian knots and nonexactness of Bennequin's inequality. *Invent. Math.*, 133(2):227–242, 1998.

[Keg18] Marc Kegel. The Legendrian knot complement problem. *J. Knot Theory Ramifications*, 27(14):1850067, 36, 2018.

[Kir89] Robion C. Kirby. *The topology of* 4*-manifolds*, volume 1374 of *Lecture Notes in Mathematics*. Springer-Verlag, Berlin, 1989.

[KK96] Greg Kuperberg and Krystyna Kuperberg. Generalized counterexamples to the Seifert conjecture. *Ann. of Math. (2)*, 143(3):547–576, 1996.

[KM63] Michel A. Kervaire and John W. Milnor. Groups of homotopy spheres. I. *Ann. of Math. (2)*, 77:504–537, 1963.

[Kro08] Vladimir Krouglov. The curvature of contact structures on 3-manifolds. *Algebr. Geom. Topol.*, 8(3):1567–1579, 2008.

[Kup94] Krystyna Kuperberg. A smooth counterexample to the Seifert conjecture. *Ann. of Math. (2)*, 140(3):723–732, 1994.

[Kup96] Greg Kuperberg. A volume-preserving counterexample to the Seifert conjecture. *Comment. Math. Helv.*, 71(1):70–97, 1996.

[Lee13] John M. Lee. *Introduction to smooth manifolds*, volume 218 of *Graduate Texts in Mathematics*. Springer, New York, second edition, 2013.

[Ler95] Eugene Lerman. Symplectic cuts. *Math. Res. Lett.*, 2(3):247–258, 1995.

[Lib59] Paulette Libermann. Sur les automorphismes infinitésimaux des structures symplectiques et des structures de contact. In *Colloque Géom. Diff. Globale (Bruxelles, 1958)*, pages 37–59. Librairie Universitaire, Louvain, 1959.

[Lis99] Paolo Lisca. On symplectic fillings of 3-manifolds. In *Proceedings of 6th Gökova Geometry-Topology Conference*, volume 23, pages 151–159, 1999.

[LM97] P. Lisca and G. Matić. Tight contact structures and Seiberg-Witten invariants. *Invent. Math.*, 129(3):509–525, 1997.

[LP87] John M. Lee and Thomas H. Parker. The Yamabe problem. *Bull. Amer. Math. Soc. (N.S.)*, 17(1):37–91, 1987.

[LS04] Paolo Lisca and András I. Stipsicz. Ozsváth-Szabó invariants and tight contact three-manifolds. I. *Geom. Topol.*, 8:925–945 (electronic), 2004.

[LS07] Paolo Lisca and András I. Stipsicz. Ozsváth-Szabó invariants and tight contact three-manifolds. II. *J. Differential Geom.*, 75(1):109–141, 2007.

[Lut77] Robert Lutz. Structures de contact sur les fibrés principaux en cercles de dimension trois. *Ann. Inst. Fourier (Grenoble)*, 27(3):ix, 1–15, 1977.

[Lut79] Robert Lutz. Sur la géométrie des structures de contact invariantes. *Ann. Inst. Fourier (Grenoble)*, 29(1):xvii, 283–306, 1979.

[Mar71] J. Martinet. Formes de contact sur les variétés de dimension 3. In *Proceedings of Liverpool Singularities Symposium, II (1969/1970)*, pages 142–163. Lecture Notes in Math., Vol. 209, Berlin, 1971. Springer.

[Mas61] W. S. Massey. Obstructions to the existence of almost complex structures. *Bull. Amer. Math. Soc.*, 67:559–564, 1961.

[Mas08] Patrick Massot. Geodesible contact structures on 3-manifolds. *Geom. Topol.*, 12(3):1729–1776, 2008.

[Mat18] Irena Matkovič. Classification of tight contact structures on small Seifert fibered L-spaces. *Algebr. Geom. Topol.*, 18(1):111–152, 2018.

[Mat22] Irena Matkovič. Non-loose negative torus knots. *Quantum Topol.*, 13(4):669–689, 2022.

[McD91] Dusa McDuff. Symplectic manifolds with contact type boundaries. *Invent. Math.*, 103(3):651–671, 1991.

[Mil65a] John Milnor. *Lectures on the h-cobordism theorem*. Princeton University Press, Princeton, NJ, 1965. Notes by L. Siebenmann and J. Sondow.

[Mil65b] John W. Milnor. *Topology from the differentiable viewpoint*. Based on notes by David W. Weaver. The University Press of Virginia, Charlottesville, Va., 1965.

[MM86] P. M. Melvin and H. R. Morton. Fibred knots of genus 2 formed by plumbing Hopf bands. *J. London Math. Soc. (2)*, 34(1):159–168, 1986.

[MN23] Hyunki Min and Isacco Nonino. Tight contact structures on a family of hyperbolic l-spaces, 2023.

[MNW13] Patrick Massot, Klaus Niederkrüger, and Chris Wendl. Weak and strong fillability of higher dimensional contact manifolds. *Invent. Math.*, 192(2):287–373, 2013.

[Mos65] Jürgen Moser. On the volume elements on a manifold. *Trans. Amer. Math. Soc.*, 120:286–294, 1965.

[MS74] John W. Milnor and James D. Stasheff. *Characteristic classes*. Princeton University Press, Princeton, N. J.; University of Tokyo Press, Tokyo, 1974. Annals of Mathematics Studies, No. 76.

[MS95] Dusa McDuff and Dietmar Salamon. *Introduction to symplectic topology*. Oxford Mathematical Monographs. The Clarendon Press Oxford University Press, New York, 1995. Oxford Science Publications.

[MS98] Dusa McDuff and Dietmar Salamon. *Introduction to symplectic topology*. Oxford Mathematical Monographs. The Clarendon Press Oxford University Press, New York, second edition, 1998.

[MT15] T. E. Mark and B. Tosun. Naturality of Heegaard Floer invariants under positive rational contact surgery. *ArXiv e-prints: 1509.01511*, September 2015.

[Mur12] E. Murphy. Loose Legendrian Embeddings in High Dimensional Contact Manifolds. *ArXiv e-prints*, January 2012.

[Ni09] Yi Ni. Link Floer homology detects the Thurston norm. *Geom. Topol.*, 13(5):2991–3019, 2009.

[Nie06] Klaus Niederkrüger. The plastikstufe—a generalization of the overtwisted disk to higher dimensions. *Algebr. Geom. Topol.*, 6:2473–2508, 2006.

[Nov65] S. P. Novikov. The topology of foliations. *Trudy Moskov. Mat. Obšč.*, 14:248–278, 1965.

[OO99] Hiroshi Ohta and Kaoru Ono. Simple singularities and topology of symplectically filling 4-manifold. *Comment. Math. Helv.*, 74(4):575–590, 1999.

[OS03] Peter Ozsváth and Zoltán Szabó. Knot Floer homology and the four-ball genus. *Geom. Topol.*, 7:615–639 (electronic), 2003.

[OS04a] Burak Ozbagci and András I. Stipsicz. *Surgery on contact 3-manifolds and Stein surfaces*, volume 13 of *Bolyai Society Mathematical Studies*. Springer-Verlag, Berlin, 2004.

[OS04b] Peter Ozsváth and Zoltán Szabó. Holomorphic disks and genus bounds. *Geom. Topol.*, 8:311–334 (electronic), 2004.

[OS04c] Peter Ozsváth and Zoltán Szabó. Holomorphic disks and knot invariants. *Adv. Math.*, 186(1):58–116, 2004.

[OS04d] Peter Ozsváth and Zoltán Szabó. Holomorphic disks and three-manifold invariants: properties and applications. *Ann. of Math. (2)*, 159(3):1159–1245, 2004.

[OS04e] Peter Ozsváth and Zoltán Szabó. Holomorphic disks and topological invariants for closed three-manifolds. *Ann. of Math. (2)*, 159(3):1027–1158, 2004.

[OS05] Peter Ozsváth and Zoltán Szabó. Heegaard Floer homology and contact structures. *Duke Math. J.*, 129(1):39–61, 2005.

[OS12] Brendan Owens and Sašo Strle. Dehn surgeries and negative-definite four-manifolds. *Selecta Math. (N.S.)*, 18(4):839–854, 2012.

[Pet16] Peter Petersen. *Riemannian geometry*, volume 171 of *Graduate Texts in Mathematics*. Springer, Cham, third edition, 2016.

[Pla04a] Olga Plamenevskaya. Bounds for the Thurston-Bennequin number from Floer homology. *Algebr. Geom. Topol.*, 4:399–406, 2004.

[Pla04b] Olga Plamenevskaya. Contact structures with distinct Heegaard Floer invariants. *Math. Res. Lett.*, 11(4):547–561, 2004.

[PS97] V. V. Prasolov and A. B. Sossinsky. *Knots, links, braids and 3-manifolds*, volume 154 of *Translations of Mathematical Monographs*. American Mathematical Society, Providence, RI, 1997. An introduction to the new invariants in low-dimensional topology, Translated from the Russian manuscript by Sossinsky [Sosinskiĭ].

[PS14] Heesang Park and András I. Stipsicz. Smoothings of singularities and symplectic surgery. *J. Symplectic Geom.*, 12(3):585–597, 2014.

[Ras03] Jacob Rasmussen. *Floer homology and knot complements*. PhD thesis, Harvard University, 2003.

[Rob99] Clark Robinson. *Dynamical systems*. Studies in Advanced Mathematics. CRC Press, Boca Raton, FL, second edition, 1999. Stability, symbolic dynamics, and chaos.

[Rol76] Dale Rolfsen. *Knots and links*. Publish or Perish Inc., Berkeley, Calif., 1976. Mathematics Lecture Series, No. 7.

[Rud95] Lee Rudolph. An obstruction to sliceness via contact geometry and "classical" gauge theory. *Invent. Math.*, 119(1):155–163, 1995.

[Ś92] Jacek Świątkowski. On the isotopy of Legendrian knots. *Ann. Global Anal. Geom.*, 10(3):195–207, 1992.

[Sav12] Nikolai Saveliev. *Lectures on the topology of 3-manifolds*. De Gruyter Textbook. Walter de Gruyter & Co., Berlin, revised edition, 2012. An introduction to the Casson invariant.

[Sch74] Paul A. Schweitzer. Counterexamples to the Seifert conjecture and opening closed leaves of foliations. *Ann. of Math. (2)*, 100:386–400, 1974.

[Sym98] Margaret Symington. Symplectic rational blowdowns. *J. Differential Geom.*, 50(3):505–518, 1998.

[Sym03] Margaret Symington. Four dimensions from two in symplectic topology. In *Topology and geometry of manifolds (Athens, GA, 2001)*, volume 71 of *Proc. Sympos. Pure Math.*, pages 153–208. Amer. Math. Soc., Providence, RI, 2003.

[Thu82] William P. Thurston. Three-dimensional manifolds, Kleinian groups and hyperbolic geometry. *Bull. Amer. Math. Soc. (N.S.)*, 6(3):357–381, 1982.

[Thu86] William P. Thurston. A norm for the homology of 3-manifolds. *Mem. Amer. Math. Soc.*, 59(339):i–vi and 99–130, 1986.

[Tos20] Bülent Tosun. Tight small Seifert fibered manifolds with $e_0 = -2$. *Algebr. Geom. Topol.*, 20(1):1–27, 2020.

[TW75] W. P. Thurston and H. E. Winkelnkemper. On the existence of contact forms. *Proc. Amer. Math. Soc.*, 52:345–347, 1975.

[Vog18] Thomas Vogel. Non-loose unknots, overtwisted discs, and the contact mapping class group of S^3. *Geom. Funct. Anal.*, 28(1):228–288, 2018.

[Wei91] Alan Weinstein. Contact surgery and symplectic handlebodies. *Hokkaido Math. J.*, 20(2):241–251, 1991.

[Whi41] J. H. C. Whitehead. On incidence matrices, nuclei and homotopy types. *Ann. of Math. (2)*, 42:1197–1239, 1941.

[Wu06] Hao Wu. Legendrian vertical circles in small Seifert spaces. *Commun. Contemp. Math.*, 8(2):219–246, 2006.

[Zeg93] A. Zeghib. Sur les feuilletages géodésiques continus des variétés hyperboliques. *Invent. Math.*, 114(1):193–206, 1993.